Chemoecological investigations of predator-prey relationships in New Zealand nudibranchs for the discovery of new natural products

A thesis

submitted in fulfilment

of the requirements for the degree

of

Doctor of Philosophy in Chemistry

at

The University of Waikato

by

Lauren Gris

THE UNIVERSITY OF
WAIKATO
Te Whare Wānanga o Waikato

2025

Abstract

This study describes chemical ecology investigations of predator-prey relationships in New Zealand nudibranchs for the discovery of new natural products. Three predator-prey relationships were established, and twenty secondary metabolites were isolated and characterised from various New Zealand marine organisms, including five new compounds.

Predator-prey relationships were established for three nudibranch species, *Polycera hedgpethi, Ceratosoma amoenum* and *Goniobranchus aureomarginatus* by means of field studies and laboratory-based feeding-choice experiments. Results indicated that *P. hedgpethi* prefers the bryozoan *Bugula neritina*, while *C. amoenum* and *G. aureomarginatus* prefer feeding on the marine sponges *Dysidea teawnui* and *Dictyodendrilla* cf. *dendyi*, respectively. For two of the predator-prey relationships, common metabolites were found in both predator and prey. As such, *Dysidea teawanui* and *C. amoenum* both contain a sterol peroxide, while *G. aureomarginatus* and *D*. cf. *dendyi* both contain dictyodendrins C (**209**) and F (**212**). *P. hedgpethi* and *B. neritina* specimens were also chemically investigated but common metabolites were not found. Additionally, three nudibranch species, *Dendrodoris krusensternii*, *Dendrodoris nigra* and *Aphelodoris luctuosa*, were chemically investigated and yielded a range of secondary metabolites previously reported from marine invertebrates. A polymeric 3-alkyl pyridinium salt (**146**) was found in high concentration within *A. luctuosa* and its eggs. Moreover, an endemic bryozoan, *Amathia gracei*, was chemically investigated and yielded a known brominated alkaloid.

Investigation of *G. aureomarginatus* samples by LC-MS screening, to determine metabolite distribution and any ecological role of the compounds isolated, indicated that dictyodendrins C (**209**) and F (**212**) were present in the digestive glands, while a norditerpene, gracilin was only present in the mantle. Quantitative NMR spectroscopy indicated that the polymeric 3-alkyl pyridinium salt (**146**) was present in higher concentration in the mantle of *Aphelodoris luctuosa*, consistent with a defensive purpose and with its presence in high concentration within the egg masses of *A. luctuosa*. Morphological analysis revealed oxea spicules within the digestive gland of *Aphelodoris luctuosa*, suggesting that it is possibly feeding on haplosclerid sponges.

An additional seven known polyaromatic alkaloids and five new sulphated denigrins alkaloids, denigrins H-L (**262**-**266**) were isolated and characterised from the sponge *D.* cf. *dendyi* by means of NMR spectroscopy and HR-ESI-MS guided isolation. The new and known metabolites isolated in this research were assessed in a general cytotoxicity assay against HeLa cells. Results indicated that the compounds were not particularly active (IC_{50} > 57 µM).

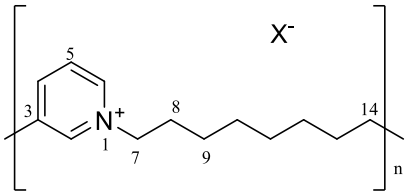

146

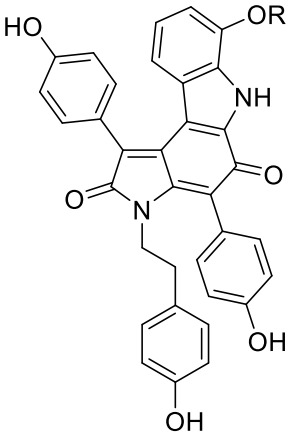

209 R = OSO_3Na
212 R = OH

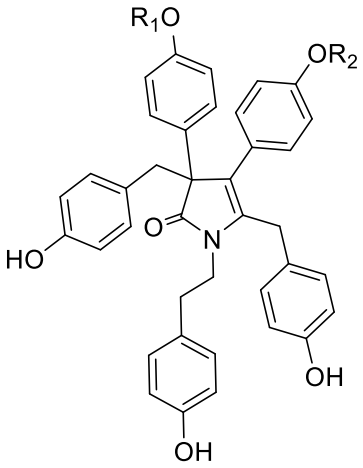

262 R_1 = H, R_2 = OSO_3Na
263 R_1 = OSO_3Na, R_2 = H

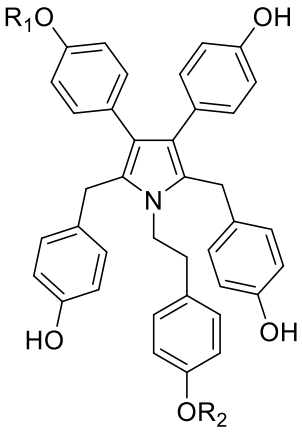

264 R_1 = H, R_2 = OSO_3Na
265 R_1 = OSO_3Na, R_2 = H
266 R_1 = R_2 = OSO_3Na

Acknowledgments

First and foremost, I am extremely grateful to my chief supervisor Professor Michèle Prinsep for her expertise, encouragement, support, constant enthusiasm and dedication, which were all invaluable during this journey. Working under your supervision has been rewarding in countless ways and allowed me to progress as an independent scientist as the years went by. I cannot imagine having done a PhD under anyone else and will remain ever grateful.

I would also like to express my gratitude to my secondary supervisor Professor Christopher Battershill. I am grateful to have benefited from your expertise and enthusiasm, which has been of great help during this study. I would like to thank Dr. Linda Peters for her knowledge and guidance in cell culture work. Even though you were not one of my supervisors, I am thankful for the opportunity to have worked with you and for all the knowledge I gained. I am also grateful to have benefited from the proofreading expertise of Kim Pritchard during the last stages of this journey.

The past and current technical staff have been of great assistance, and I would like to specifically thank Karla, Jenny and Annie for their help, along with Atiga and Hayden for their support and expertise in NMR spectroscopy and LC-MS. Special mention also to Kirsty for her microscope expertise, and to Judith and Geetanjali for their help upon starting work in the physical containment laboratories. Also, many thanks to the University diving team, specifically to Holly, Warrick, Bonnie and Katherine who were instrumental in assisting me with sample collection and identification. I would also like to thank Rebecca Hull from the University of Melbourne for collection of Australian samples.

I am thankful to the academic staff of the Department of Chemistry and Applied Physics for their support and for contributing to the pleasant work environment. I wish you all the best in your future endeavours.

In addition, I would also like to acknowledge the University of Waikato for providing me with financial support by means of a Doctoral scholarship and a Student Research Trust Grant, without which I would not have been able to fulfil this journey.

I am thankful to the past and current students of the Prinsep research group, namely Caitlin, Chloé and Nikki for their great company, warmth and for the interesting discussions we had. I very much enjoyed the countless coffee catch-ups we shared Nikki and I wish you all the best in the future! Also, my best wishes to all the past and current graduate students, specifically to Amber, Kavitha and William. I wish you all the best with your further endeavours.

I would also like to greatly thank my wonderful parents for their encouragement and financial support and for being one of my drives into pursuing this journey. Many thanks to my sisters Audrey and Kathleen for their helpful encouragement, and to Claire, Noémie, Adeline and Pauline for their precious friendship.

Last but not least, the support, advice and encouragement I received from my partner have been inestimable during this journey far from home and I would not be where I am today without it. Thank you very much for everything you have done for me, and no doubts that the list is long.

Contents

Abstract ii

Acknowledgments iv

Contents vi

List of Abbreviations x

List of Figures xii

List of Tables xvi

List of Equations xviii

Publications included in this thesis xix

Chapter 1 Introduction 20

1.1 Marine natural products in drug discovery – a brief historical overview 20
1.1.1 The emergence of natural products 20
1.1.2 The rise of marine natural products chemistry 2
1.1.3 Marine natural products and derivatives in clinical use 4

1.2 Marine invertebrates 7
1.2.1 Chemical defence in marine invertebrates 7

1.3 Sponges 9
1.3.1 Sponge-microorganism associations 10

1.4 Nudibranchs 12
1.4.1 Nudibranch defence mechanisms 13

1.5 Sequestration and biotransformation of diet-derived natural products by nudibranchs 18
1.5.1 Sequestration and biotransformation from sponges 19
1.5.2 Sequestration from bryozoans 34
1.5.3 Sequestration from ascidians and soft corals 38

1.6 Research aims 40

Chapter 2 Chemical analysis of New Zealand marine invertebrates 41

2.1 The New Zealand marine ecosystem 42

2.2 *Amathia gracei* 43
2.2.1 Isolation procedure 44
2.2.2 Convolutamine L 45
2.2.3 Occurrence of brominated alkaloids within the *Amathia* genus 46
2.2.4 Concluding remarks 51

2.3 New Zealand nudibranchs 52
2.3.1 Cytotoxicity screening 53

2.4 *Dendrodoris krusensternii* 54
2.4.1 Cytotoxic activity of crude extracts 55

2.4.2 Isolation procedure 55
2.4.3 Cinnamolide 56
2.4.4 Metabolite distribution 58
2.4.5 Investigation of the diet 59
2.4.6 Concluding remarks 60

2.5 *Dendrodoris nigra* 61
2.5.1 Cytotoxic activity of crude extracts 62
2.5.2 Isolation procedure 63
2.5.3 7-Deacetoxy-olepupuane 63
2.5.4 Drimane esters 65
2.5.5 Metabolite distribution 67
2.5.6 Investigation of the diet 68
2.5.7 Occurrence and origin of drimane sesquiterpenes within Dendrodorididae nudibranchs 69
2.5.8 Concluding remarks 72

2.6 *Aphelodoris luctuosa* 73
2.6.1 Cytotoxic activity of crude extracts 74
2.6.2 Isolation procedure 75
2.6.3 Polymeric 3-alkyl-pyridinium salt 75
2.6.4 Metabolite distribution investigation by qNMR spectroscopy 79
2.6.5 Occurrence of 3-alkyl pyridinium salt 83
2.6.6 Investigation of the diet 85
2.6.7 Concluding remarks 88

2.7 Summary 89

Chapter 3 Investigation of predator-prey relationships by feeding-choice experiments 90

3.1 Establishment of the feeding-choice experiments configuration 92
3.1.1 Methodology development 92
3.1.2 Selected configuration 95

3.2 *Polycera hedgpethi* 97
3.2.1 Collection and field study 98
3.2.2 Feeding-choice experiments 99
3.2.3 Discussion 101

3.3 *Ceratosoma amoenum* 102
3.3.1 Collection and field study 103
3.3.2 Feeding-choice experiments 104
3.3.3 Discussion 105

3.4 *Goniobranchus aureomarginatus* 107
3.4.1 Collection and field study 108
3.4.2 Feeding-choice experiments 108
3.4.3 Discussion 111

3.5 Summary 112

Chapter 4 Investigation of predator-prey relationships by chemical analysis 113

4.1 *Polycera hedgpethi* and *Bugula neritina* 115
4.1.1 Sample collection and extraction 115
4.1.2 *Bugula neritina* 115
4.1.3 *Polycera hedgpethi* and its eggs 117

4.1.4 Concluding remarks 121

4.2 *Ceratosoma amoenum* and *Dysidea teawanui* 122
4.2.1 Cytotoxicity of crude extracts 122
4.2.2 *Dysidea teawanui* 123
4.2.3 *Ceratosoma amoenum* and its eggs 127
4.2.4 Concluding remarks 130

4.3 *Goniobranchus aureomarginatus* and *Dictyodendrilla* cf. *dendyi* 131
4.3.1 Sample collection and dissection 131
4.3.2 Cytotoxicity of crude extracts 132
4.3.3 *Dictyodendrilla* cf. *dendyi* 133
4.3.4 Discussion 152
4.3.5 *Goniobranchus aureomarginatus* 153
4.3.6 *Goniobranchus aureomarginatus* eggs 169
4.3.7 Concluding remarks 170

4.4 Summary 172

Chapter 5 New denigrin alkaloids from further analysis of the marine sponge *Dictyodendrilla* cf. *dendyi* 174

5.1 Occurrence and bioactivities of denigrin alkaloids 176

5.2 Further denigrin alkaloids from *Dictyodendrilla* cf. *dendyi* 178
5.2.1 Isolation procedure for denigrins H-K 178
5.2.2 Denigrin H 180
5.2.3 Denigrin I 185
5.2.4 Denigrin J 188
5.2.5 Denigrin K 191
5.2.6 Isolation procedure for denigrin L 194
5.2.7 Denigrin L 195
5.2.8 Oxidative rearrangement of denigrin E derivatives 198
5.2.9 Occurrence, bioactivities and biogenesis of polyaromatic pyrrole and pyrrolidone alkaloids 199

5.3 Cytotoxic activity 205
5.3.1 Cytotoxic activity of eleven polyaromatic alkaloids 205

5.4 Concluding remarks 208

Chapter 6 Conclusion and Future Recommendations 209

Chapter 7 Experimental 212

7.1 General experimental procedures 212
7.1.1 Solvents 212
7.1.2 Nudibranch dissection 212
7.1.3 Morphological analysis 213
7.1.4 Extraction 213
7.1.5 Thin layer chromatography 213
7.1.6 Reversed phase C18 bench column chromatography 214
7.1.7 Size exclusion chromatography 214
7.1.8 Normal phase bench column chromatography 214
7.1.9 Sample preparation for high performance liquid chromatography and liquid chromatography mass spectrometry analysis 215

7.1.10 High performance liquid chromatography 215
7.1.11 Liquid chromatography mass spectrometry screening 215
7.1.12 High resolution mass spectrometry 216
7.1.13 Nuclear magnetic resonance spectroscopy 216
7.1.14 Infrared spectroscopy 217
7.1.15 Ultraviolet spectroscopy 217
7.1.16 Optical rotation 217

7.2 Sample collection, identification, maintenance and extraction 218
7.2.1 Collection sites 218

7.3 Feeding choice experiments 220
7.3.1 Methodology development 220
7.3.2 Selected no-flow configuration - general protocol 221
7.3.3 *Polycera hedgpethi* 222
7.3.4 *Ceratosoma amoenum* 222
7.3.5 *Goniobranchus aureomarginatus* 222

7.4 Sample extraction for predator-prey investigation 223
7.4.1 *Polycera hedgpethi* and *Bugula neritina* 223
7.4.2 *Ceratosoma amoenum* and *Dysidea teawanui* 223
7.4.3 *Goniobranchus aureomarginatus* and *D.* cf. *dendyi* 224

7.5 Isolation of secondary metabolites 225
7.5.1 Isolation of two brominated alkaloids from *Amathia gracei* 225
7.5.2 Isolation of cinnamolide from *Dendrodoris krusensternii* 226
7.5.3 Isolation of two drimane sesquiterpenes from *Dendrodoris nigra* 226
7.5.4 Isolation of polymeric 3-alkyl pyridinium salt from *Aphelodoris luctuosa* 227
7.5.5 Isolation of 5α,8α-epidioxy-24-methylcholesta-6-diene-3β-ol from *Dysidea teawanui* 227
7.5.6 Isolation of metabolites from *Dictyodendrilla* cf. *dendyi* 228
7.5.7 Isolation of metabolites from *Goniobranchus aureomarginatus* 234

7.6 Quantitative NMR spectroscopy 237

7.7 Cell culture and bioassay 239
7.7.1 Reviving HeLa cervical cancer cells 239
7.7.2 Culturing of cells 239
7.7.3 Subculturing of cells 240
7.7.4 Cell counting and cell viability 240
7.7.5 Cytotoxic activity of eleven arylpyrrole alkaloids 241
7.7.6 Cytotoxicity screening of the crude extracts 246

Appendices 248

Appendix A. ^{1}H NMR spectra relevant to Chapter 2 250

Appendix B. Complementary data for the feeding-choice experiments described in Chapter 3 255

Appendix C. NMR spectra and separation trees relevant to Chapter 4 258

Appendix D. Separation trees, NMR and HR-ESI-MS spectra relevant to Chapter 5 271

References 304

List of Abbreviations

3-APS	3-Alkyl Pyridinium Salt
ACN	Acetonitrile
BACE	β-site Amyloid precursor protein Cleaving Enzyme
BCE	Before the Common Era
^{13}C NMR	Carbon-13 Nuclear Magnetic Resonance
C18	Octadecyl derivatised silica gel
Chloroform-*d*	Deuterated Chloroform
DOPA	3,4-dihydroxyphenylalanine
DCM	Dichloromethane
COSY	Correlation Spectroscopy (^{1}H to ^{1}H correlations)
d	Doublet
δ	Chemical shift (ppm)
DG	Digestive Glands
DMSO-d_6	Deuterated DMSO
DMSO	Dimethyl Sulfoxide
ED_{50}	Median Effective Dose
EEZ	Exclusive Economic Zone
EGF	Epidermal Growth Factor
EMA	European Medicines Agency
ESI-MS	Electrospray Ionisation-Mass Spectrometry
EtOAc	Ethyl acetate
FA	Formic Acid
FDA	United States Food and Drug Administration
^{1}H NMR	Proton Nuclear Magnetic Resonance
HMBC	Heteronuclear Multiple-Bond Correlation (^{1}H to ^{13}C correlations)
HPLC	High Performance Liquid Chromatography
HR-ESI-MS	High Resolution Electrospray Ionisation-Mass Spectrometry
IC_{50}	Half maximal Inhibitory Concentration
IR	Infrared
gHSQC	Gradient Heteronuclear Single-Quantum Coherence
J	Coupling constant
LC-MS	Liquid Chromatography-Mass Spectrometry
LH-20	Crosslinked dextran-based size exclusion resin
m	Multiplet
m/z	Mass to charge ratio
MNP	Marine Natural Product
MDFs	Mantle Dermal Formations
MEM	Minimum Essential Medium
Methanol-d_4	Deuterated Methanol
MIC	Minimum Inhibitory Concentration
mult.	Multiplicity

MTT assay	Colourimetric cytotoxicity assay using 3-(4,5-dimethylthiazol-2-yl)-2,5-diphenyltetrazolium bromide
3-PAPS	Polymeric 3-Alkyl Pyridinium Salt
PDA	Photo Diode Array
ppm	Parts Per Million
q	Quartet
s	Singlet
SDS	Sodium Dodecyl Sulphate
SEM	Scanning Electron Microscope
SCUBA	Self-Contained Underwater Breathing Apparatus
t	Triplet
TGA	Therapeutic Goods Administration
TLC	Thin Layer Chromatography
UV	Ultraviolet
US	United States
WoRMS	World Register of Marine Species

List of Figures

Figure 1: Taxonomic classification of sponges according to the World Register of Marine Species (WoRMS).[9] Orders examined in this study are highlighted in blue. 9
Figure 2: General anatomy of dorid nudibranchs (A- *Goniobranchus aureomarginatus*, 5 cm long courtesy of Warrick Powrie. B- *Aphelodoris luctuosa,* 7 cm long) and aeolid nudibranchs (C- *Antiopella novozealandica*, 1 to 2 cm long, courtesy of Warrick Powrie. D- *Glaucus atlanticus*, 4 cm long, courtesy of Yanika Reiter). 12
Figure 3: Taxonomic classification of nudibranchs according to the World Register of Marine Species (WoRMS).[9] The order examined in this study is highlighted in blue. 13
Figure 4: Colour code utilised for sections 1.4 and 1.5. 15
Figure 5: Sequestration of sponge metabolites by *Felimare picta.* 15
Figure 6: Sequestration and biotransformation of secondary metabolites by *Hypselodoris orsini*..... 16
Figure 7: *De novo* biosynthesis of polygodial by *Dendrodoris limbata*. 17
Figure 8: Sequestration of fennebricins by the nudibranch *Jorunna funebris*. 20
Figure 9: Sequestration of secondary metabolites by *Doriprismatica atromarginata*. 21
Figure 10: Sequestration of secondary metabolites by *Doriprismatica stellata*. 22
Figure 11: Sequestration of secondary metabolites by *Chromodoris strigata* and *Goniobranchus albonares*..... 23
Figure 12: Sequestration and biotransformation of dietary secondary metabolites by *Glossodoris* nudibranchs. 24
Figure 13: Sequestration and biotransformation of metabolites by *Goniobranchus sinensis*..... 25
Figure 14: Sequestration of secondary metabolites by *Phyllidia varicosa*. 25
Figure 15: Sequestration of secondary metabolites by *Felimare* and *Hypselodoris* species..... 26
Figure 16: Sequestration of secondary metabolites by *Felimare fontandraui*. 27
Figure 17: Sequestration of dendrolasin (**58**) by *Chromodoris lochi*. 27
Figure 18: Sequestration and *de novo* biosynthesis of secondary metabolites by *Cadlina luteomarginata*. 29
Figure 19: Sequestration of latrunculin by *Chromodoris* nudibranchs. 30
Figure 20: Sequestration and biotransformation of secondary metabolites by *Hexabranchus sangineus*. 31
Figure 21: Sequestration of secondary metabolites by *Peltodoris nobilis*. 33
Figure 22: Sequestration of secondary metabolites by *Peltodoris atromaculata*. 33
Figure 23: Sequestration of tambjamines by *Tambja* and *Tyrannodoris* nudibranchs. 36
Figure 24: Sequestration of tripeptides (**88**) and (**89**) by the nudibranch *Antiopella novozealandica.*.. 37
Figure 25: Sequestration of diterpenes by the nudibranch *Tritoniopsis elegans*..... 39
Figure 26: The New Zealand Exclusive Economic Zone.[205] Available under Creative Commons Attribution 4.0 license (CC BY 4.0 License), https://www.marineregions.org/. Latitude 42° 45' 58.1" S (-42.76615°), longitude 71° 43' 45.6" E (71.72934°)..... 42
Figure 27: *Amathia gracei* specimen. 43
Figure 28: Taxonomic classification of *Amathia gracei* according to the World Register of Marine Species (WoRMS).[209] 44
Figure 29: The isolation procedure for convolutamine L (**94**)..... 45
Figure 30: Selected COSY (blue) and HMBC (purple) correlations for convolutamine L (**94**)..... 46
Figure 31: A- *Dendrodoris krusensternii* (7 cm long) crawling in a tank. B- *Dendrodoris krusensternii* spawning in a tank..... 54

Figure 32: Taxonomic classification of *Dendrodoris krusensternii* according to the World Register of Marine Species (WoRMS).[236] 54
Figure 33 : The isolation procedure for cinnamolide (**122**) from *Dendrodoris krusensternii.* 56
Figure 34: Selected COSY (blue) and HMBC (purple) correlations for cinnamolide (**122**). 57
Figure 35: Extracted ion mode (235.2) LC-MS chromatogram (positive ion mode) of the four *Dendrodoris krusensternii* crude extracts showing the presence of cinnamolide (**122**). 58
Figure 36: A- *Dendrodoris nigra* (5 cm long) in a sea grass bed at Pahoia beach. B- Pahoia beach collection site. C- Bright yellow egg masses found alongside *Dendrodoris nigra*. D- Bright yellow egg mass spawned in the laboratory. 61
Figure 37: Taxonomic classification of *Dendrodoris nigra* according to the World Register of Marine Species (WoRMS).[243] 61
Figure 38: The isolation procedure for 7-deacetoxy-olepupuane **(124)** and drimane esters (**125**) from *Dendrodoris nigra.* 63
Figure 39: Selected COSY (blue) and HMBC (purple) correlations for 7-deacetoxy-olepupuane (**124**).. 64
Figure 40: Extracted ion mode (*m/z* 279 and 524) LC-MS chromatogram (positive ion mode) of different *Dendrodoris nigra* crude extracts (whole-body, digestive glands, mantle and eggs) showing the presence of compounds (**124**) (black LC-MS trace) and (**125**) (green LC-MS trace). 67
Figure 41: A- *Aphelodoris luctuosa* (7 cm long) crawling in a tank. B- One of the egg masses spawned in a tank by *Aphelodoris luctuosa.* 73
Figure 42: Taxonomic classification of *Aphelodoris luctuosa* according to the World Register of Marine Species (WoRMS).[269] 73
Figure 43: Cytotoxicity of the crude extracts of *Aphelodoris luctuosa* (whole-body, mantle and digestive gland) and its eggs on HeLa cells using an MTT assay. 74
Figure 44: Isolation procedure for 3-PAPS (**146**) from *Aphelodoris luctuosa* and its eggs. 75
Figure 45: Selected COSY (blue) and HMBC (purple) correlations for compound (**146**) 76
Figure 46: MS/MS fragmentation pattern of compound (**146**) on ESI-MS (positive ion mode). 78
Figure 47: Concentration of compound (**146**) in *Aphelodoris luctuosa* tissues (mantle and digestive organs). Values quantified by ^{1}H NMR spectroscopy and presented as means of duplicate analyses of five nudibranchs 82
Figure 48: A- *Haliclona* sp. collected at Salisbury Wharf (Courtesy of Caitlin Berquist). B- *Haliclona* sp. displaying oxea spicules observed under a stereo microscope. 86
Figure 49: A and B – Digestive glands of *Aphelodoris luctuosa* digested in nitric acid and observed under a stereo microscope. C and D - Digestive glands of *Aphelodoris luctuosa* digested in nitric acid and observed under a compound microscope. 87
Figure 50 : A- Scheme of the initial Atema flume chamber (30 cm long) used for the feeding-choice experiments, adapted from the configuration used by Munday *et al.*[309] The water inflow is represented with red arrows. B- Initial experimental configuration built for the feeding-choice experiments. 93
Figure 51: A- General set-up for the colouring trial. Dimensions of the tank: 45 cm x 23 cm x 4.5 cm. B– Dual single inflow. C- Dual Y-type inflow. D– Dual 4-inflow. 94
Figure 52: Scheme of the selected feeding-choice configuration (45 cm x 23 cm x 4.5 cm) with the cross representing the starting point of the nudibranch and both prey placed on opposite sides of the tank. 95
Figure 53: *Polycera hedgpethi* (3 cm long) crawling in a tank. 97
Figure 54: Taxonomic classification of *Polycera hedgpethi* according to the World Register of Marine Species (WoRMS).[8] 97

Figure 55: A- *Bugula neritina* (left) and unidentified hydrozoan (right). B- Egg cases found on *Bugula neritina* in the wild (circled in red). C- *Polycera hedgpethi* spawning in a tank. D- Eggs (0.5 cm thick) spawned by *Polycera hedgpethi*. 98
Figure 56: Time spent on prey for each *Polycera hedgpethi* specimen across the feeding-choice experiments (n = 5)..... 100
Figure 57: *Polycera hedgpethi* (3 cm long) feeding on *Bugula neritina*. 101
Figure 58: Two *Ceratosoma amoenum* specimens (each 4 to 5 cm long) crawling in a tank. 102
Figure 59: Taxonomic classification of *Ceratosoma amoenum* according to the World Register of Marine Species (WoRMS).[8] 102
Figure 60: A- Underwater photograph of *Dysidea teawanui*[251] (reproduced with permission from the copyright holder), B- *Dictyodendrilla dendyi* (courtesy of the Victoria University of Wellington Marine Natural Products group). 103
Figure 61: Time spent on prey for each *Ceratosoma amoenum* specimen across the feeding-choice experiments (n = 4)..... 105
Figure 62: *Dysidea teawanui* fragments (3 to 4 cm long) before (left) and after (right) feeding-choice experiments with *Ceratosoma amoenum.* Published open access under Creative Commons licenses (CC BY-NC-ND and CC BY) by Gris *et al*.[315] 106
Figure 63: Underwater photograph of two *Goniobranchus aureomarginatus* individuals (each 5 cm long), courtesy of Warrick Powrie). 107
Figure 64: Taxonomic classification of *Goniobranchus aureomarginatus* according to the World Register of Marine Species (WoRMS).[8] 107
Figure 65: A- *Goniobranchus aureomarginatus* (5 cm long) spawning during an experiment. B- *Goniobranchus aureomarginatus* (5 cm long) crawling on *Dictyodendrilla* cf. *dendyi* during the feeding-choice experiments (published open access under Creative Commons licenses (CC BY-NC-ND and CC BY) by Gris *et al.*[315] 109
Figure 66: Time spent on prey for each *Goniobranchus aureomarginatus* specimen across the feeding-choice experiments (n = 6). 110
Figure 67: Cytotoxicity of the crude extracts of *Polycera hedgpethi* and its eggs on HeLa cells using an MTT assay. 118
Figure 68: LC-MS chromatogram (extracted ion mode) to screen for the presence of bryostatins and diacylguanidines (**169**) and (**170**). 120
Figure 69: Cytotoxicity of the crude extracts of *Ceratosoma amoenum*, its eggs and *Dysidea teawanui* against HeLa cells using an MTT assay. 122
Figure 70: The isolation procedure for ergosterol peroxide (**186**) from *Dysidea teawanui*. 125
Figure 71: Cytotoxicity of the crude extracts of *Goniobranchus aureomarginatus* (whole-body and dissected) and its eggs, and *Dictyodendrilla* cf. *dendyi* on HeLa cells using an MTT assay.. 133
Figure 72: Thin layer chromatography (EtOAc/MeOH 5:1) of early eluting *Dictyodendrilla* cf. *dendyi* fractions after initial C18 reversed phase purification. 137
Figure 73: The isolation procedure for dictyodendrins C (**209**) and D (**210**) from *Dictyodendrilla* cf. *dendyi*. 137
Figure 74: ^{1}H NMR spectrum (methanol-d_4, 600 MHz) of dictyodendrin C (**209**)..... 139
Figure 75: COSY (blue) and selected HMBC (purple) correlations for dictyodendrin C (**209**). 140
Figure 76: An example of the TLC plates obtained for the *Dictyodendrilla* cf. *dendyi* fractions after initial C18 purification. A- visible light. B- under UV light at 254 nm. 143
Figure 77: A- TLC plate (EtOAc/MeOH 5:1) of early eluting *Goniobranchus aureomarginatus* fractions after initial C18 purification. B- TLC plate (EtOAc 100%) of one *Goniobranchus aureomarginatus* fraction (left) and three *Dictyodendrilla* cf. *dendyi* fractions after initial C18 purification. 158

Figure 78: The isolation procedure for dictyodendrins C (**209**), F (**212**), gracilin A (**244**) and 6α,15 α,16α -triacetoxyspongian (**236**) from *Goniobranchus aureomarginatus*. 159
Figure 79: LC-MS chromatogram of fraction 13 (positive ion mode). 161
Figure 80: Isolation procedure for the study of metabolite distribution within *Goniobranchus aureomarginatus*. 164
Figure 81: LC-MS chromatogram of the viscera crude extract displaying dictyodendrin F (**212**, blue trace) and 6α,15α,16α-triacetoxyspongian (**236**, black trace). 165
Figure 82: Representation of the aromatic section of the ^{1}H NMR spectrum of a fraction of the viscera extract containing dictyodendrins C (**209**) and F (**212**). 166
Figure 83 : Structures assigned to the previously reported denigrins with the general structure of denigrin type compounds displayed in blue. 177
Figure 84: A- ^{1}H NMR spectrum of denigrin H (**262**). B- ^{1}H NMR spectrum of the mixture of denigrins H (**262**) and I (**263**). C- ^{1}H NMR spectrum of denigrin I (**263**). 179
Figure 85: ^{1}H NMR spectrum (methanol-d_4) of denigrin H (**262**). 180
Figure 86: ^{13}C NMR spectrum (methanol-d_4) of denigrin H (**262**). 181
Figure 87: COSY (blue) and HMBC (purple) correlations for the construction of rings A, D and E of denigrin H (**262**). 182
Figure 88: COSY (blue) and HMBC (purple) correlations for the construction of rings B and C of denigrin H (**262**). 183
Figure 89: COSY (blue) and selected HMBC (purple) correlations for denigrin H (**262**). 183
Figure 90: ^{1}H NMR spectrum (methanol-d_4) of denigrin I (**263**). 186
Figure 91: ^{1}H NMR spectrum (methanol-d_4) of denigrin J (**264**). 189
Figure 92: COSY (blue) and selected HMBC (purple) correlations for denigrin J (**264**). 190
Figure 93: ^{1}H NMR spectrum (methanol-d_4) of denigrin K (**265**). 192
Figure 94: Isolation procedure for denigrin L (**266**). 194
Figure 95: TLC (EtOAc/MeOH 5:1) of several fractions containing denigrin L (**266**) as a pink spot in fractions 19 to 25. Solvent front displayed as the pencil lines. 195
Figure 96: ^{1}H NMR spectrum (methanol-d_4) of denigrin L (**266**). 196
Figure 97: Oxidative conversion of compound (**265**) to compound (**267**). 199
Figure 98: Toxicity of denigrins H-L (**262-666**) to HeLa cells with the lower end of the concentrations tested displayed. 206
Figure 99: Toxicity of dictyodendrins C (**209**), D (**210**), F (**212**), denigrin E (**226**), dactylpyrrole A (**225**) and lamellarin O1 (**228**) to HeLa cells with the lower end of the concentrations tested displayed. 207
Figure 100: Scanning electron microscope (SEM) images of the radula of *Goniobranchus aureomarginatus*. 211
Figure 101: Gradient of both organic and aqueous mobile phases for standard LC-MS analysis. 216
Figure 102: Gradient of both aqueous (Type 1 water) and organic (acetonitrile) mobile phases used for the analysis of the fraction of *Amathia gracei.* 225
Figure 103: A- LC-MS chromatogram showing the resolution of both peaks corresponding to denigrin H (**262**) (right) and I (**263**) (left). B- PDA chromatogram at 220 nm for the separation of denigrin H (**262**) (right) and I (**263**). 232

List of Tables

Table 1: ^{1}H and ^{13}C NMR data for convolutamine L **(94)** compared with literature values (DMSO-d_6).[212] 46
Table 2: IC_{50} values of the crude extracts of *Dendrodoris krusensternii* (whole-body and dissected) and its eggs on HeLa cells using an MTT assay. 55
Table 3: ^{1}H and ^{13}C NMR data for cinnamolide (**122**) compared with literature values (chloroform-*d*).[237,238] 57
Table 4: IC_{50} values of the crude extracts of *Dendrodoris nigra* (whole-body and dissected) and its eggs on HeLa cells using an MTT assay. 63
Table 5: ^{1}H and ^{13}C NMR data for 7-deacetoxy-olepupuane (**124**) compared with literature values (chloroform-*d*).[244] 64
Table 6: ^{1}H and ^{13}C NMR data for drimane esters (**125**) compared with literature values (chloroform-*d*).[247] 66
Table 7: ^{1}H and ^{13}C NMR data for 3-PAPS (**146**) compared with literature values (methanol-d_4).[272] 77
Table 8: MS/MS Fragmentation of 3-PAPS (**146**) in ESI-MS positive ion mode. 78
Table 9: Concentration of compound **(146**) within *Aphelodoris luctuosa* crude extracts. 81
Table 10: Comparison of sponge spicule length between several New Zealand *Haliclona* species[291] and the spicules found in the digestive gland of *Aphelodoris luctuosa.* 88
Table 11: *Polycera hedgpethi* feeding-choice experiments with two potential prey species. Number of choices considering the first choice and the total number of choices. 99
Table 12: *Polycera hedgpethi* feeding-choice experiments with two potential prey species. Frequency of the total time spent on prey considered. 100
Table 13: *Ceratosoma amoenum* feeding-choice experiments with two sponge species as offered prey. Number of choices considering the first choice and the total number of choices. 104
Table 14: *Ceratosoma amoenum* feeding-choice experiment with two sponge species as offered prey. Frequency of the total time spent on prey considered. 105
Table 15: *Goniobranchus aureomarginatus* feeding-choice experiments with two sponge species as offered prey. Number of choices considering the first choice and the total number of choices. 109
Table 16: *Goniobranchus aureomarginatus* feeding-choice experiment with two sponge species as offered prey. Frequency of the total time spent on prey considered. 110
Table 17: ^{1}H and ^{13}C NMR data for 5α,8α-epidioxy-24-methylcholesta-6,22-dien-3β-ol (**186**) compared with literature values (chloroform-*d*).[366] 126
Table 18: Collection and extraction of samples for the investigation of the predator-prey relationship between *Goniobranchus aureomarginatus* and *Dictyodendrilla* cf. *dendyi.* 131
Table 19: IC_{50} values of the crude extracts of *Goniobranchus aureomarginatus* (whole-body and dissected) and its eggs, and *Dictyodendrilla* cf. *dendyi* on HeLa cells using an MTT assay. .. 132
Table 20: ^{1}H and ^{13}C NMR assignments determined for dictyodendrin C (**209**) compared with literature values (methanol-d_4).[382] 140
Table 21: ^{1}H and ^{13}C NMR assignments determined for dictyodendrin D (**210**) compared with literature values (methanol-d_4).[382] 142
Table 22: ^{1}H and ^{13}C NMR assignments determined for dictyodendrin F (**212**) compared with literature values (methanol-d_4).[391] 144

Table 23: ^{1}H NMR assignments determined for dictyodendrin B (**208**) compared with literature values (methanol-d_4).[382] 146
Table 24: ^{1}H NMR assignment determined for dactylpyrrole A (**225**) compared with literature values (methanol-d_4).[2] 147
Table 25: ^{1}H and ^{13}C NMR assignments for denigrin E (**226**) in methanol-d_4 148
Table 26: ^{1}H and ^{13}C NMR assignments determined for denigrin G (**227**) compared with literature values (methanol-d_4).[392] 149
Table 27: ^{1}H and ^{13}C NMR assignments determined for lamellarin O1 (**228**) compared with literature values (methanol-d_4).[393] 151
Table 28: ^{1}H NMR assignments determined for dictyodendrin C (**209**) compared with literature values (methanol-d_4) and to compound (**209**) isolated from *Dictyodendrilla* c.f. *dendyi*.[2] 159
Table 29: ^{1}H NMR assignments determined for dictyodendrin F (**212**) compared with literature values (methanol-d_4) and to compound (**212**) isolated from *Dictyodendrilla* c.f. *dendyi*.[2] 160
Table 30: The MS^2 fragments of gracilin A (**244**) and 6α,15α,16α-triacetoxyspongian (**236**) (positive ion mode). 161
Table 31: ^{1}H NMR assignments (methanol-d_4) of characteristic signals determined for gracilin A (**244**) and 6α,15α,16α-triacetoxyspongian (**236**) compared with literature values (chloroform-*d*).[423,414] 162
Table 32: IC_{50} values of the crude extracts of *Goniobranchus aureomarginatus* (whole-body and dissected) from Tauranga and Otago collections. 167
Table 33: ^{1}H and ^{13}C NMR assignments determined for denigrin H (**262**) 184
Table 34: ^{1}H and ^{13}C NMR assignments determined for denigrin I (**263**). 187
Table 35: ^{1}H and ^{13}C NMR assignments determined for denigrin J (**264**). 190
Table 36: ^{1}H and ^{13}C NMR assignments determined for denigrin K (**265**). 193
Table 37: ^{1}H and ^{13}C NMR assignments determined for denigrin L (**266**). 197
Table 38: IC_{50} values for denigrins H-L (**262-266**), dictyodendrins C (**209**), D (**210**), and F (**212**), denigrin E (**226**), dactylpyrrole A (**225**) and lamellarin O1 (**228**) against HeLa cells. 206
Table 39: GPS coordinates for the sample collection sites for this research. 219
Table 40: Table of the voucher specimens kept for this research 219
Table 41: Collection and extraction of samples for the investigation of a predator-prey relationship between *Polycera hedgpethi* and *Bugula neritina.* 223
Table 42: Collection and extraction of samples for the investigation of a predator-prey relationship between *Ceratosoma amoenum* and *Dysidea teawanui.* 223
Table 43: Collection and extraction of samples for the investigation of a predator-prey relationship between *Goniobranchus aureomarginatus* and *Dictyodendrilla* cf. *dendyi.* 224
Table 44: Masses of *Aphelodoris luctuosa* samples and resulting crude extracts. 237
Table 45: Sample preparation and concentration of compound (**146**) within *Aphelodoris luctuosa* samples 238
Table 46: Calculations of dilutions for dictyodendrin C (**209**). 242
Table 47: Preparation of the stock solutions for each of the compounds tested in the MTT assay. 243
Table 48: Dilution preparations for each pure compound tested in the MTT assay. 244
Table 49: Dilution preparations for each crude extract and pure compound tested in the MTT assay. 247

List of Equations

Equation 1 : Formula for the purity of the analyte (P_s) calculation.[258] 80
Equation 2 : Formula to calculate the concentration of cells using a haemocytometer. 240
Equation 3 : Calculation of the percentage of cell viability using trypan blue. 241
Equation 4 : Formula for the calculation of the percentage of inhibition for the MTT assay. 245

Publications included in this thesis

Chapters 3 and 4

L. Gris, C. N. Battershill and M. R. Prinsep, Investigation of the Dietary Preferences of Two Dorid Nudibranchs by Feeding-Choice Experiments and Chemical Analysis. *J. Chem. Ecol.*, 2023, **49**, 599-610.

Author contributions: Conceptualization, M.R.P.; sample collection, L.G. and C.N.B.; methodology, L.G., M.R.P. and C.N.B; feeding-choice experiments, L.G.; data analysis, L.G. and M.R.P; investigation, L.G., C.N.B. and M.R.P.; writing—original draft preparation, L.G.; writing—review and editing, M.R.P., and C.N.B.; supervision, M.R.P. and C.N.B.; project administration, M.R.P.; funding acquisition, M.R.P.

Chapter 5

L. Gris, M. R. Prinsep, L. M. Peters and C. N. Battershill, Denigrins H–L: Sulfated Derivatives of Denigrins D and E from a New Zealand Dictyodendrilla c.f. *dendyi* Marine Sponge. *Mar. Drugs*, 2024, **22**, 231.

Author contributions: Conceptualization, M.R.P.; methodology, L.G., M.R.P. and L.M.P.; data analysis, L.G., M.R.P. and L.M.P.; investigation, L.G., C.N.B. and M.R.P.; writing—original draft preparation, L.G.; writing—review and editing, M.R.P., L.M.P. and C.N.B.; supervision, M.R.P. and C.N.B.; project administration, M.R.P.; funding acquisition, M.R.P.

Chapter 1

Introduction

1.1 Marine natural products in drug discovery – a brief historical overview

1.1.1 The emergence of natural products

Throughout history, humans have depended on Nature to meet their basic needs, including remedies for the treatment of a wide range of diseases.[1] As early as 2600 BCE in Mesopotamia, plants were the predominant source of traditional remedies, including oils of *Commiphora* species (myrrh), which are still presently in use to treat coughs, colds and inflammation.[2] Knowledge of natural product use from medicinal plant sources ultimately improved as a result of trial and error across an extended period of time, by means of palatability trials or untimely deaths.[2] Although evidence about the uses of marine organisms in traditional medicines is scarce,[3] it is worth mentioning that marine invertebrates were frequently used for their digestive properties during the Ancient Greek period, with reports from Xenocrates mentioning the healing effect of the broth of the bivalve mollusc *Callista chione* for abdominal bloating and pain.[4] Historically, marine organisms were widely used as food sources[3] and occasionally as dyes, especially by the ancient Phoenicians who utilised chemical secretions from marine molluscs to create dyes for woollen textiles, such as Tyrian purple.[1]

Later in the 19th century, chemical and pharmacological studies of plant traditional remedies led to the isolation of several early drugs which include morphine (1826) and codeine (1832) from poppy seeds, along with quinine (1820) from *Cinchona* bark, all of which are still in wide use.[5,6]

The early 20th century saw the discovery of the first widely used antibiotic by Fleming (penicillin from fungi, 1928), which sparked great interest by drug companies and research groups to focus on microorganisms as sources of new medicines.[7] This led to a prolific period for antibiotic research, which saw the discovery of streptomycin, chloramphenicol and chlortetracycline, to cite a few examples.[7]

While the search for bioactive natural products from microorganisms was at its peak during the second World War, numerous researchers and pharmaceutical companies started to focus on alternate, non-microbial natural sources of pharmaceuticals and began to turn their attention to the ocean and its unique biodiversity.[2]

1.1.2 The rise of marine natural products chemistry

Despite the ocean covering over 70% of the Earth's surface, its reputation as a hostile and inhospitable place, along with difficulties accessing it, explain its delayed exploration.[2] Due to its extensive range of temperature, pressure, light, and nutritional conditions, the ocean has been considered as one of the most complex biospheres on Earth, displaying favourable conditions for the discovery of unique natural products, which have long evolved to aid marine organisms' survival in these harsh conditions.[8] Among the thirty six animal phyla reported so far,[9] thirty four of these are found in the ocean and fifteen exclusively so, corroborating its extensive biodiversity.[10,11]

Initially, the study of marine organisms was limited to those easily attainable by hand at low tide or by breath-hold diving.[11] The publication of three reports by Bergmann and Feeney in the early 1950s, describing unusual bioactive nucleosides from the sponge *Tectitethya* (formerly *Cryptotethya*)[12] *crypta* inhabiting the shallow waters of Florida, is regarded as one of the earliest chemical studies of marine natural products.[13-15] Notably, analogues of these nucleosides, spongothymidine (**1**) and spongouridine (**2**), were later synthesised and led to the development of the first two approved marine-derived drugs by the United States Food and Drug Administration (US FDA).[16,17]

It is worth mentioning for this review that several other early studies by Bergmann *et al.* reported on the isolation of several sterols from sponge species, with the initial structures proposed often revised in later studies.[18-20]

Marine natural products research began to emerge as a full discipline in its own right in the 1970s, with the refinement of SCUBA diving techniques, followed by the introduction of manned submersibles (1980s) and remotely operated vehicles (1990s), with their subsequent utilisation by natural products chemists and biologists.[2] Exploration of a wide range of marine organisms (sponges, algae, tunicates, bryozoans) became possible, leading to 2,500 new metabolites reported during the decade from 1977–1987, and over 840 novel metabolites just for the year 1998 alone, with numerous compounds displaying biological activity.[1,21] These studies demonstrated that the marine environment is a rich source of bioactive compounds, many of which belong to unique chemical classes not found in terrestrial sources.[1]

Initially, marine toxins were a subject of focus,[22] leading to the isolation of saxitoxin (**3**) from the dinoflagellate *Gonyaulax catanella,*[23,24] the well-known tetrodotoxin (**4**)[25] from a pufferfish, along with aplysiatoxin (**5**) and debromoaplysiatoxin (**6**) from the Hawaiian sea hare *Stylocheilus longicauda.*[26] Notably, the period between 1970 and 1990 was also prolific for the isolation of terpenoids from algae, including brominated, nitrogenated and oxygenated heterocycles, sterols and amines, with reports of antitumour, antibacterial and antifungal activity.[2,21,27,28] As such, dictyolides A (**7**), B (**8**) and nordictyolide (**9**), displaying antitumour activities, were isolated from the brown alga *Dictyota dichotoma*.

In the early 2000s, the field benefitted from a renaissance, driven by technological progress in analytical chemistry and spectroscopy, and also partly, a broad realisation that competing technologies, such as combinatorial chemistry, failed to deliver new drug leads in significant numbers.[16] As such, the marine environment was still seen as an attractive source of bioactive compounds and this led to the success story of several natural products in the first decade of the 21st century.

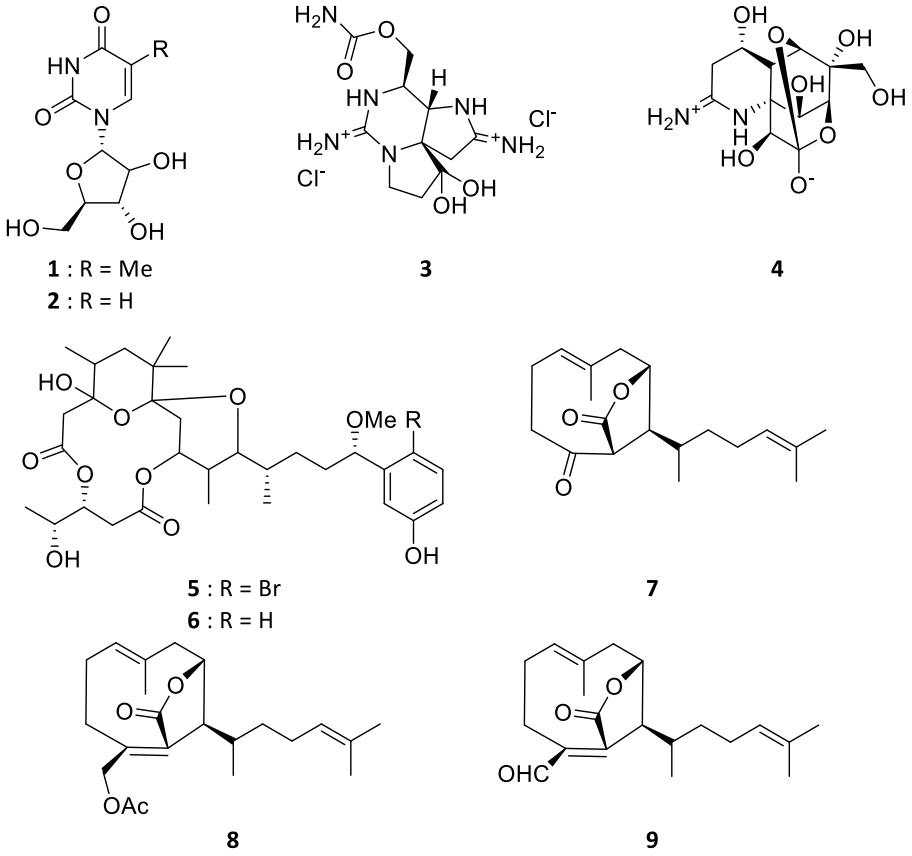

1.1.3 Marine natural products and derivatives in clinical use

Even though the search for so called "Drugs from the Sea" began as early as the 1950s, the first approval of marine natural product (MNP) derivatives occurred in the 1970s with US FDA approval of two synthetic analogues of (**1**) and (**2**). The anticancer agent Ara-C (cytarabine) (**10**) was approved in 1969, followed by the antiviral drug Ara-A (vidarabine) (**11**) in 1976.[16,17] Both have now been in clinical use for decades, although the FDA currently lists Ara-A as discontinued.[16,17]

It was not until 2004 that the first true marine natural product was approved by the FDA. As such, the approval of the non-narcotic analgesic ziconotide (**12**) (ω-conotoxin MVIIA, marketed as Prialt), gave a second wind to the discipline. This linear 25 amino acid peptide, isolated from the venom of a tropical cone snail, is used for the treatment of chronic pain in spinal cord injury and must be delivered via an intrathecal injection route. [1,16] The venom of the Pacific piscivorous *Conus magus* contains an array of toxic peptides, or conotoxins, that target the neuromuscular system, resulting in prey immobilisation.[16]

In 2004, omega-3-acid ethyl esters (P-OM3) (**13**), sourced mainly from fish, then extracted and *trans*-esterified, also gained FDA approval as anti-hypertriglyceridemia agents.[29]

Shortly afterwards in October 2007, the antitumour trabectedin (**14**) (Yondelis/ecteinascidin-743/ET-743), from the tropical tunicate (*Ecteinascidia turbinata*), was approved by the European Medicines Agency (EMA) for the treatment of soft-tissue sarcoma.[16] The extremely low amount of the active components from the extract prevented their full structure elucidation for many years, but this was finally achieved in 1990.[30] Interestingly, the structures of these ecteinascidins display similarities with the safracins and saframicins from various *Streptomyces* spp., as well as from the sponge-derived renieramycins and xestomycin.[30]

Several years later, in 2010, eribulin mesylate (**15**) was approved by the FDA as an intravenous treatment of metastatic breast cancer.[31] Eribulin mesylate is a synthetic analogue of Halichondrin B which was isolated in minimal quantity from two unrelated sponges, *Halichondria okadai* and *Axinella* sp,[32,33]and from the New Zealand sponge *Lissodendoryx* sp.[34]

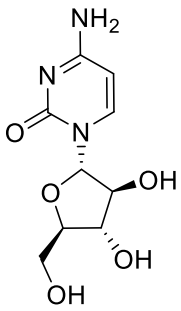

10

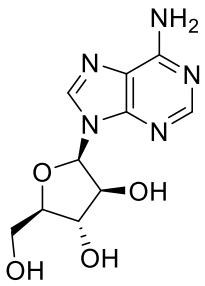

11

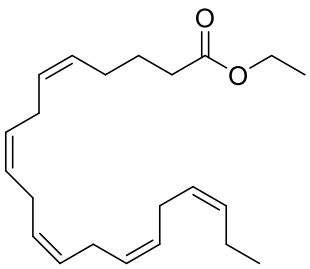

13

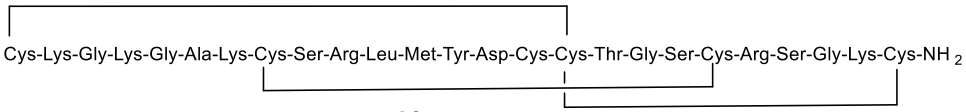

12

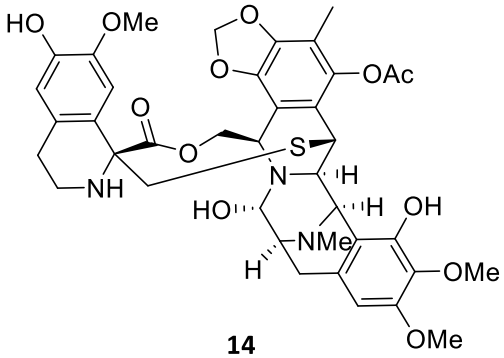

14

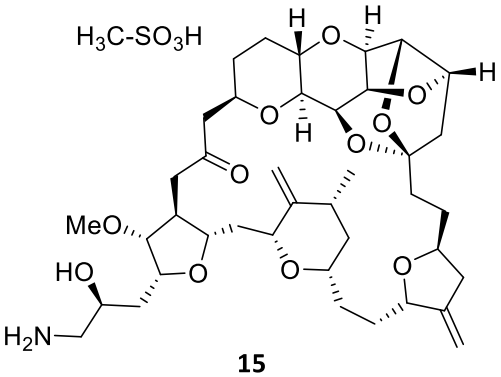

15

In 2011, the FDA approved brentuximab vedotin (Adcetris®), the first commercially available antibody-drug conjugate incorporating a payload derived from MNPs, for the treatment of Peripheral T-Cell Lymphoma.[35-37] The "warhead", composed of monomethyl auristatin E (MMAE) (**16**), is derived from dolastatin-10, a secondary metabolite from the sea hare *Dolabella auricularia* and cyanobacteria *Symploca hynoides* and *Lyngbya majuscula.*[37]

In 2018, Australia's Therapeutic Goods Administration (TGA) approved the use of pliditepsin (Aplidin®) (**17**), a depsipeptide isolated from the Mediterranean tunicate *Aplidium albicans,* as an anti-cancer agent for the treatment of multiple myeloma.[38] While the FDA and EMA initially refused to approve its use, the European Commission revoked this decision and requested a re-assessment of the application for Aplidin by the EMA in June 2024.[39]

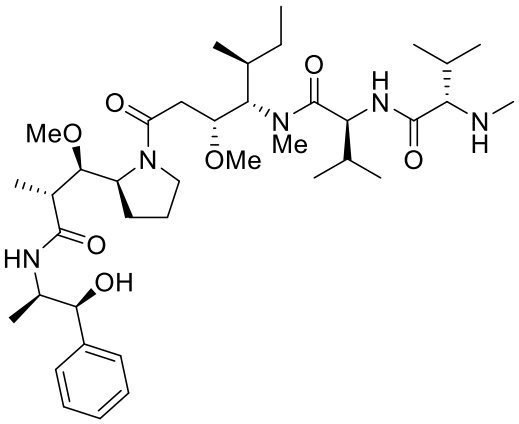

16

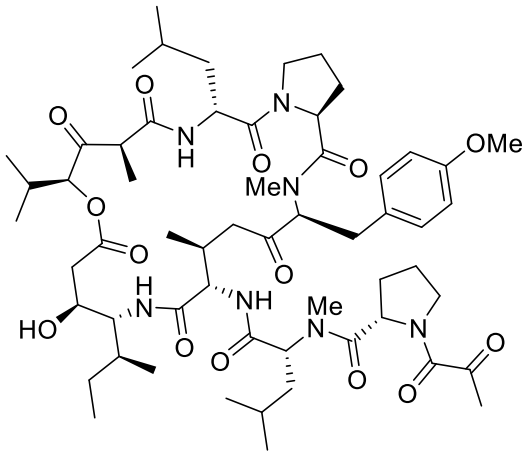

17

Overall, eight drugs from MNPs and derivatives have been clinically approved by at least one of the most representative medical agencies (FDA, EMA and TGA).[29,40] Interestingly, six out of the eight approvals occurred in the 21st century, despite several compounds being isolated decades earlier, demonstrating the long-term endeavour required before widespread approval. More than twenty other candidate compounds are presently in the pipeline and are being evaluated in Phase I–III clinical trials in the United States and Europe for the treatment of various diseases,[29] including pliditepsin (Aplidin®) (**17**), in clinical trial as an antiviral agent.[41]

1.2 Marine invertebrates

Among the huge biodiversity inhabiting our oceans, invertebrates account for approximately 60% of reported species,[8] most belonging to the phyla Annelida, Arthropoda, Bryozoa, Cnidaria, Porifera, and Mollusca.[42] Marine invertebrates have been considered as one of the most prolific sources of new natural products, with over 15 000 new MNPs reported over the last thirty years.[43] This considerable attention is driven by their unique natural defence features, including sequestration of diet-derived compounds, *de novo* biosynthesis, and secretion of toxic chemicals.[43]

1.2.1 Chemical defence in marine invertebrates

Natural selection imposed by extreme living conditions, predators, pathogens, and competitors has led to the evolution of chemical, physical/mechanical, and phenological defences in marine organisms, especially in sessile, or slow-moving invertebrates.[8,44]

Numerous sessile invertebrates, especially within the phyla Porifera and Bryozoa, are unable to escape predators and have had a very long evolutionary history during which they "perfected" their defences. Many sponge species produce spicules (small, needle-like structural components of the skeleton) as a form of physical defence,[45] along with resorting to chemical defences, primarily located in areas that have a higher risk of predation and/or are necessary for reproduction, as postulated by the optimal defence theory. [46-49]

For example, the Micronesian sponge *Oceanapia* sp. allocates the highest concentrations of the feeding-deterrent pyridoacridine alkaloids kuanoniamines C (**18**) and D (**19**) in tissue parts that are most visible to predators.[46,50,51]

Within the phylum Mollusca, while numerous slow-moving species use their calcium carbonate shell for defence purposes,[52] others, especially within the Cephalopoda class, rely on camouflage, autotomy, or their fast-moving capacities to escape predators.[53] Numerous marine gastropods (Class Gastropoda) on the other hand are partially or totally shell-less, on top of being slow-moving, and therefore rely on other mechanisms to increase their chance of survival.[54] Toxic or unpalatable compounds derived from dietary sources or produced *de novo* are prevalent within this class to reduce the risk of predation.[55] The development of

ability to consume chemically defended prey (macroalgae, cyanobacteria, bryozoans, or sponges) is believed to be associated with partial or complete loss of the shell within certain species.[56] Natural products obtained from these prey serve the gastropods in various ways, from the location of sessile prey *via* chemical cues, to the inhibition of potential consumers or viruses, to providing protection against UV radiation.[56]

As such, the chemically defended seaweed *Chlorodesmis fastigiata,* containing mainly the cytotoxic diterpenoid chlorodesmin (**20**)**,** deters feeding by most fish species, but appears to be the exclusive diet of the specialist herbivorous sacoglossans *Elysia* sp. and *Cyerce nigricans*, which are in turn, never attacked by fish.[57] However, (**20**) does not protect *Elysia* sp. from the predatory dorid nudibranch *Gymnodoris* sp. which has previously developed resistance.[57]

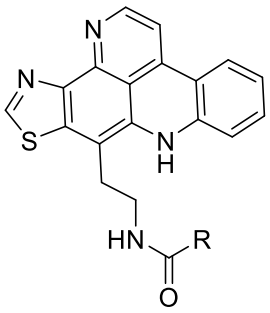

18 R = Et
19 R = Me

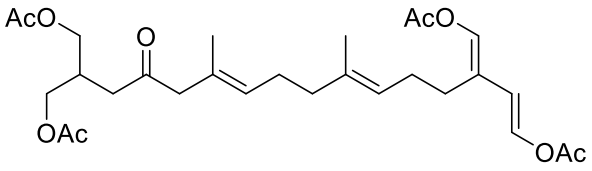

20

1.3 Sponges

Sponges (Phylum: Porifera)[9] are one of the most common and ancient types of marine invertebrates, having arisen around 600 million years ago.[58,59] As sessile organisms, most are filter-feeders, displaying impressive pumping capacities that allow for the sequestration of organic particles and microoorganisms, along with waste removal.[59,60]

Taxonomically speaking, sponges are currently classified in four distinct classes (Figure 1). Calcareous sponges (Class Calcarea) have a calcium carbonate skeleton while glass sponges (Class Hexactinellida) are usually found at great depths, with some species possessing silica spicules arranged in a hexactine pattern. Demosponges (Class Demospongiae) are by far the most common and diverse,[59,60] with some species also possessing silicaceous spicules and/or a spongin (a modified type of collagen) skeleton.[61] Currently, more than 8000 species of sponge have been described and acccepted,[62] with only 1% occurring in freshwater environments.[60]

Kingdom Animalia
- **Phylum** Porifera
  - **Class** Calcarea
    - **Subclass** Calcaronea
    - **Sublass** Calcinea
  - **Class** Demospongiae
    - **Subclass** Heteroscleromorpha
    - **Subclass** Keratosa
      - **Order** Dendroceratida
      - **Order** Dictyoceratida
    - **Subclass** Verongimorpha
  - **Class** Hexactinellida
    - **Sublass** Amphidiscophora
    - **Subclass** Hexasterophora
  - **Class** Homoscleromorpha

Figure 1: Taxonomic classification of sponges according to the World Register of Marine Species (WoRMS).[9] Orders examined in this study are highlighted in blue.

Sponges possess a simple body that has served them well throughout their evolution and has remained essentially unchanged.[58] Despite their relatively simple morphology, sponges display a remarkable complexity of much-needed defence mechanisms. They rely on natural products, crucial for their survival in the extreme environment which they inhabit,[63,64] with their chemical arsenal including mainly alkaloids and terpenoids, along with polyketides, peptides and steroids.[62]

Marine sponges have been one of the most prolific source of MNPs to date, with diverse biological applications, contributing to two of the eight above approved drugs so far.[62] To date, well over 18 000 new compounds have been isolated from the phylum Porifera, with over 200 discovered annually.[62,65-68] Notably, more than half of the isolated compounds show biological activity including cytotoxic, antibacterial, antifungal and antiviral activities.[62]

1.3.1 Sponge-microorganism associations

Sponges house dense and diverse communities of microorganisms, constituting up to 35% of the total sponge biomass.[58] The microorganism diversity extends to more than ten bacterial phyla, including Cyanobacteria, Planctomycetes and Actinobacteria, along with diverse fungi and microalgae.[60,69] Sponges acquire these microorganisms using two pathways; either by selective absorption during feeding from the large pool of bacteria in the surrounding water or by vertical transmission of symbionts through the reproductive stages,[60] allowing sponge-microorganism associations to be maintained from generation to generation.[58]

These symbionts are believed to serve various roles, from nutrition to stabilisation of the sponge skeleton, to secondary metabolite production, providing a strong defence against predators and infectious microorganisms.[60] It has been hypothesised on various occasions that these microorganisms are indeed the original producers of the marine natural products,[70-72] a theory that came to light following a study on metabolite localisation within sponge-microorganism associations by Faulkner *et al*.[70,73,74] This was later corroborated by several sponge compounds showing great similarity with metabolites isolated from terrestrial organisms.[75-77] This is the case for mycalamide A (**21**), isolated from a New Zealand *Mycale* sp., possessing a similar structure to the toxin pederin (**22**), isolated from a terrestrial beetle in Italy.[75]

However, several studies have proved that sponges themselves were the producers of the secondary metabolites.[78-80] So far, only a few studies have identified the actual producers of secondary metabolites of interest;[78-80] such investigations require intense collaboration between chemical ecologists, natural products chemists, biologists and microbiologists.[81]

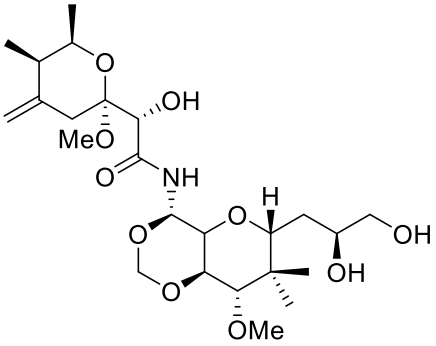

21

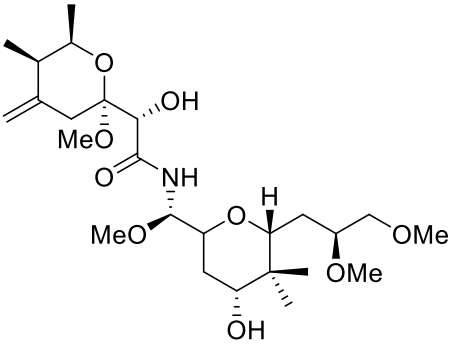

22

Regardless of the actual producer of bioactive secondary metabolites, as resistance of infectious microorganisms towards existing pharmaceuticals increases, marine sponges still provide an attractive alternative to find treatments against bacterial, viral, fungal and parasitic diseases.[82]

1.4 Nudibranchs

Nudibranchs, also referred to as “butterflies of the ocean”,[83,84] are small, usually brightly coloured marine gastropod molluscs from the order Nudibranchia (Phylum: Mollusca, Class: Gastropoda).[9] The name *nudibranch* comes from the Latin *nudus* for "naked," and the Greek *brankhia* for gills, referring to the exposed gills (cerata) on the backs of many species.[85] Nudibranchs are essentially blind and perceive their environment through chemosensory interactions with their two rhinophores[86] (Figure 2). They occur in seas worldwide with the vast majority living on rocky shores in the benthic zone and their size rarely exceeds five cm.[52] With more than 4700 known species, these molluscs display a wide range of colours and shapes.

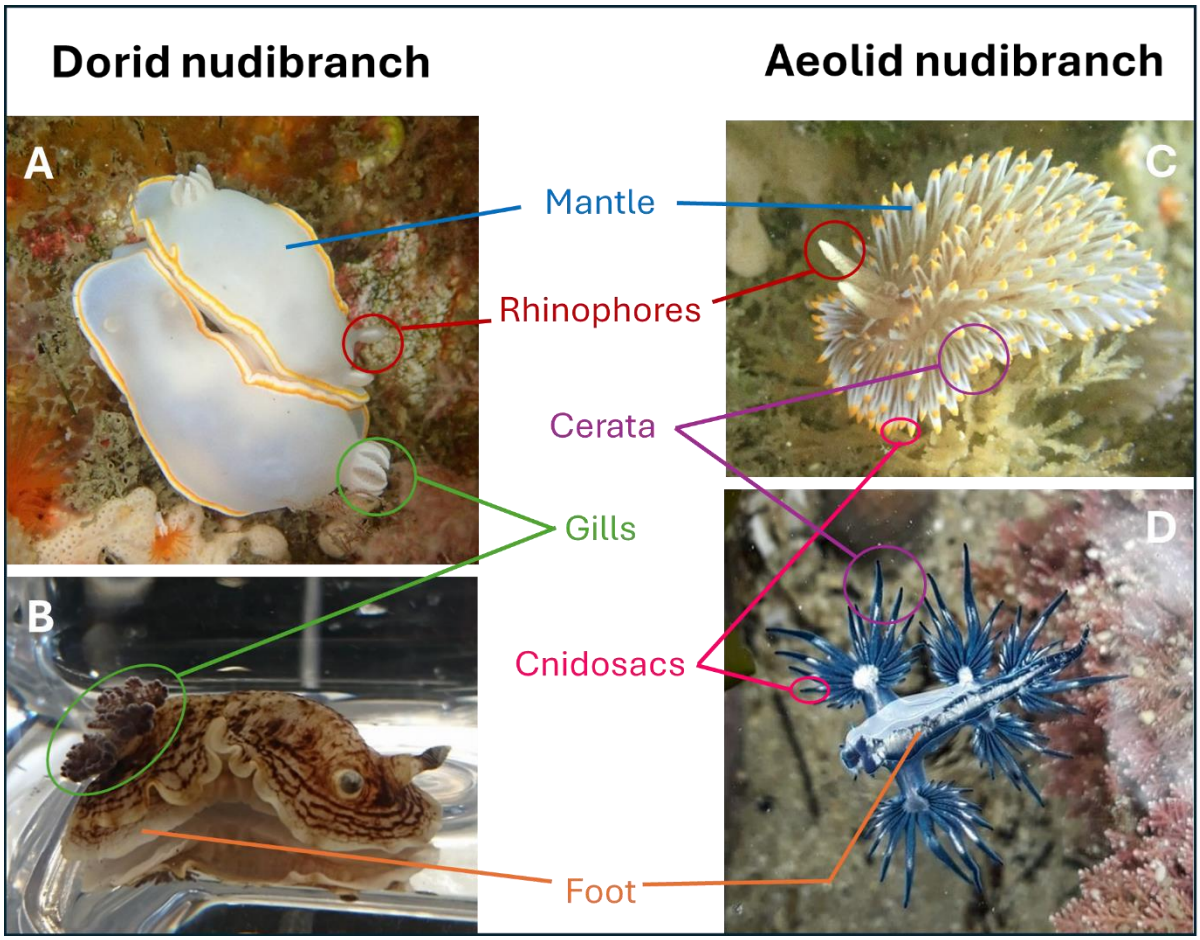

Figure 2: General anatomy of dorid nudibranchs (A- *Goniobranchus aureomarginatus*, 5 cm long courtesy of Warrick Powrie. B- *Aphelodoris luctuosa,* 7 cm long) and aeolid nudibranchs (C- *Antiopella novozealandica*, 1 to 2 cm long, courtesy of Warrick Powrie. D- *Glaucus atlanticus*, 4 cm long, courtesy of Yanika Reiter).

Broadly speaking, nudibranchs can be separated into two groups, the dorids and aeolids, based on their general morphology and digestive glands.[9] Dorid nudibranchs (Suborder Doridina, Figure 3) have an internal, intact digestive gland, a thick mantle that extends over the foot and are distinguished by the exposed, respiratory, plume-like gills circling the anus (Figure 2).[85] In contrast, in aeolid nudibranchs (suborder Cladobranchia, Figure 3), the mantle is extended into long projections, or cerata, that contain a branched digestive gland (Figure 2).[85] The tips of the cerata often hold cnidosacs which usually store stinging cells, or nematocysts, obtained from ingesting cnidarian prey for the nudibranch's own defence.[87] Aeolids lack gills and use their cerata to facilitate gas exchange through the epidermis.[85]

Kingdom Animalia
Phylum Mollusca
Class Gastropoda
Subclass Heterobranchia
Infraclass Euthyneura
Subterclass Acteonimorpha
Subterclass Ringipleura
Superorder Nudipleura
Order Nudibranchia
Suborder Cladobranchia
Suborder Doridina
Order Pleurobranchida
Superorder Ringiculimorpha
Subterclass Tectipleura

Figure 3: Taxonomic classification of nudibranchs according to the World Register of Marine Species (WoRMS).[9] The order examined in this study is highlighted in blue.

1.4.1 Nudibranch defence mechanisms

Despite shedding their shells as larvae, and thereafter remaining shell-less, nudibranchs have few documented predators, most likely as a result of their diverse defence strategies.[85] Common behavioural adaptations include being active at night, autotomy and their use of mimicry and bright colours.[88,89] For example, the predatory bluehead wrasse *Thalassoma bifasciatum* is repelled by yellow, purple and green visual cues,[90] displayed by the nudibranchs *Nembrotha cristata* and *Hypselodoris* (formerly *Risbecia*)[91] *bullockii*.[92,93] In a similar way to

several terrestrial species, such as poison-dart frogs, most nudibranchs rely on aposematism; the association of unpalatability with a warning signal intended for potential predators.[56] This strategy has the advantage of benefiting both the aposematic species and its potential predator. Moreover, Müllerian mimicry, a generalisation of aposematism, has been suggested within certain *Hypselodoris* nudibranchs. [56,94] In contrast, Batesian mimicry is when a species resembles a toxic species, but lacks toxicity, and still therefore benefits from reduced predation,[56] as observed in king snakes mimicking coral snakes.[95]

Some aeolid nudibranchs use an unusual defence mechanism of sequestering nematocysts from their cnidarian prey. These nematocysts are taken up and transported to the tips of the cerata to be incorporated into cnidosacs.[85] If contact with potential prey occurs, these stinging capsules can be fired, delivering their venom. As such, *Glaucus atlanticus* (Figure 2) tear the soft tissues of the tentacles of *Physalia physalis* upon feeding to sequester and concentrate potent nematocysts. To cope with damage from those stinging cells, aeolids appear to use several strategies. These include a maturation process of the stolen nematocysts as they get incorporated into cnidosacs to avoid damage caused by the transportation of charged stinging cells.[87] Furthermore, the presence of a protective cuticle lining in the mouth and in the epithelium has been noted to absorb the damage from a discharged nematocyst. [96,97]

From a natural products perspective, dorids have received more attention than aeolid cladobranchs, probably due to a perceived notion that they use a chemical defence rather than a physical one.[85] Dorid nudibranchs often rely on chemical defence for their survival, and several species can sequester dietary metabolites from specific prey, via selective feeding and accumulation for their own defence.[98] Similarly to numerous gastropod molluscs, nudibranchs have developed resistance strategies to feed upon chemically defended sessile prey (sponges, bryozoans, or cnidarians), an ability believed to be associated with shell-loss.[99]

For all figures in Sections 1.4 and 1.5, arrows are utilised to connect the different prey organisms to predators ingesting the compounds. A colour code relating to sequestration, biotransformation and *de novo* biosynthesis is used (Figure 4). Structures are framed in red when sequestered by the predator, in green when biotransformed for the first time by the predator, in yellow when biotransformed for a second time, and framed in blue when compounds are biosynthesised *de novo*.

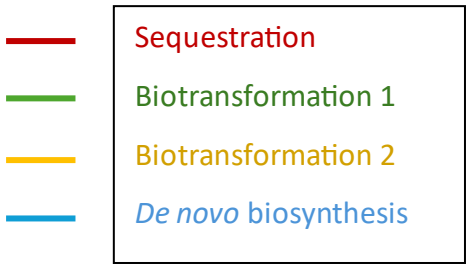

Figure 4: Colour code utilised for sections 1.4 and 1.5.

Some dorids concentrate toxic dietary metabolites in their mantle or in special glands, or mantle dermal formations (MDFs), the most accessible body part to predators.[56,100] This is the case for *Felimare picta* (formerly *Hypselodoris webbi*)[101] which can transfer and accumulate the antifeedant sesquiterpene furodysinin (**23**) from *Dysidea fragilis* in its MDFs, and also spiniferins-1 (**24**) and -2 (**25**) from *Pleraplysilla spinifera* (Figure 5).[102,103]

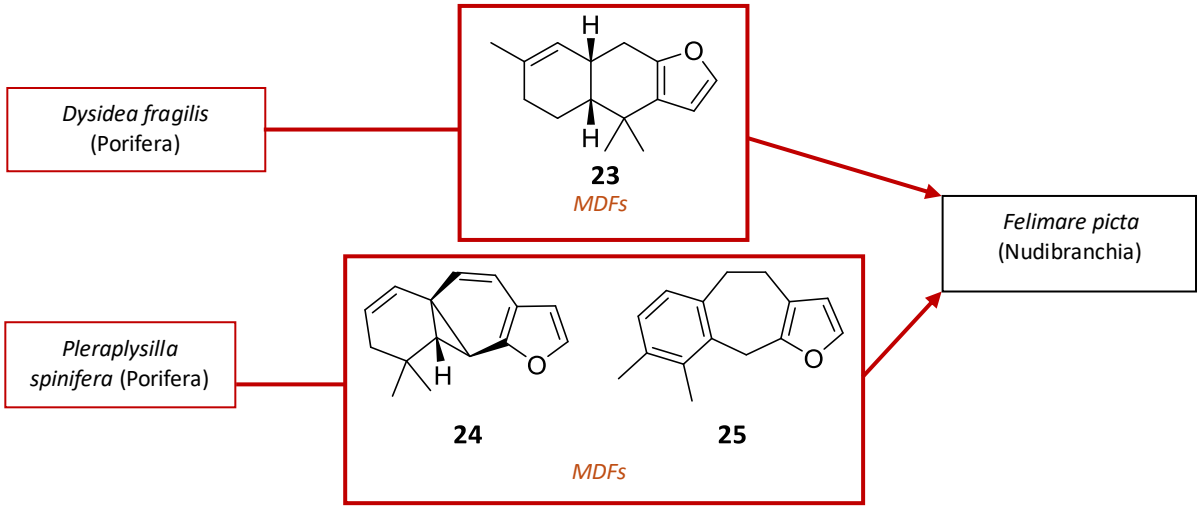

Figure 5: Sequestration of sponge metabolites by *Felimare picta.*

Biotransformation of diet-derived secondary metabolites, often into more toxic forms, is also prevalent, taking place in the digestive glands which contain specialised digestive cells, involved in such biotransformation.[56] Therefore, it has been hypothesised that nudibranchs resort to biotransformation to increase their chemical defence.[56] An example of a two-step biotransformation is displayed by *Felimare* (formerly *Doris*)[104] *orsinii* that also feeds on *Cacospongia mollinor*. The predator-prey relationship has been established, even though both organisms contain different metabolites. The nudibranch *F. orsinii* converts the sponge sesterterpenoid scalaradial (**26**), into deoxoscalarin (**27**) found in the viscera, and then affects a second transformation to produce the sesterterpenoid, 6-keto-deoxoscalarin B (**28**), selectively compartmentalised in the MDFs (Figure 6).[105]

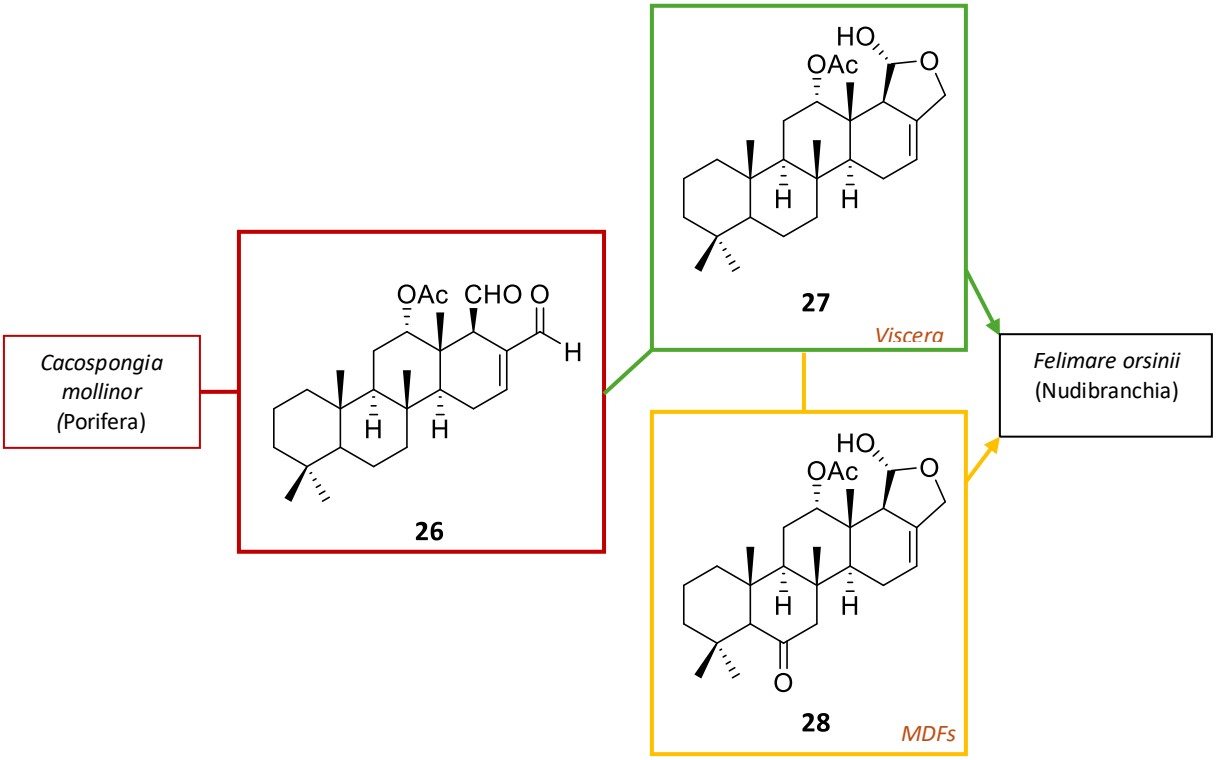

Figure 6: Sequestration and biotransformation of secondary metabolites by *Hypselodoris orsini*.

In contrast, several dorid species are capable of *de novo* biosynthesis, an ability regarded as an evolutionary step beyond the simple accumulation of dietary metabolites, since the organisms become independent of specific food availability.[106,107] In 1985, Cimino *et al.* demonstrated for the first time, through feeding experiments with carbon-14 labelled mevalonic acid, that *Dendrodoris limbata* biosynthesises polygodial (**29**), an antifeedant sesquiterpenoid, *de novo* (Figure 7).[108] Since then, *de novo* biosynthesis has been proven in many more species.[109-112]

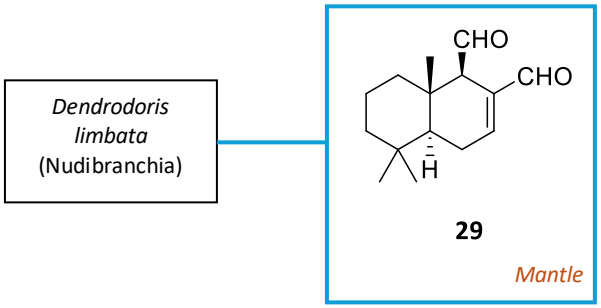

Figure 7: *De novo* biosynthesis of polygodial by *Dendrodoris limbata*.

In terms of defence mechanisms, nudibranchs have also been documented to transfer metabolites to their egg coils. For example, *Jorunna funebris* transfers cytotoxic isoquinolinequinones to its egg masses, believed to prevent predation upon the offspring.[113]

1.5 Sequestration and biotransformation of diet-derived natural products by nudibranchs

Although the role of chemicals in structuring marine ecosystems has received less attention than in terrestrial ecosystems, there has been a surge of research in marine chemical ecology over the past fifteen years.[56] In recent decades, marine molluscs especially have received growing interest,[98] with the study of chemoecological interactions within the order Nudibranchia accounting for a significant number of studies.[56,98] Nudibranchs' invertebrate diet not only allows for subsistence, but may also act as a habitat for themselves and their offspring, to increasing their chemical defence in many cases.[98] This results in specialised behaviour, such as selective feeding, biotransformation, frequent accumulation of metabolites in specialised areas and transfer of metabolites to offspring, especially relevant in the study of chemoecological interactions. With many studies focusing on both the chemistry and ecology of nudibranchs, numerous predator-prey relationships have already been established, featuring unique strategies and a wide range of metabolites.[56,85,98,114] The study of such predator-prey interactions has therefore attracted many naturals products chemists, having the benefit of potentially improving the discovery of diverse MNPs, along with delivering ecological relevance, overall providing a rationale for systematic studies in this area.[98,99,115]

The review below focuses on the chemoecological interactions reported between predator and prey within the order Nudibranchia, from early studies until September 2024. The emphasis is put on the sequestration and biotransformation of diet-derived compounds, and when known, the role, localisation and bioactivities of the metabolites are described. It is arranged by class of compounds sequestered (alkaloids, terpenoids, macrolides, nucleosides and lipids) for each invertebrate prey (sponges, bryozoans and cnidarians).

1.5.1 Sequestration and biotransformation from sponges

Marine sponges are undoubtedly the most common nudibranch prey, and are a prolific source of biologically active secondary metabolites.[62]

Alkaloids

Within sponges, alkaloids are the most prevalent class of secondary metabolites described, with 823 new alkaloids reported between 2009 and 2018 (out of 2762 new metabolites). However, only one nudibranch species, *Jorunna funebris,* has been proven to sequester sponge alkaloids.[62] This nudibranch feeds mainly on *Xestospongia* sp.,[116] from which it sequesters a range of isoquinolinequinones and bistetrahydroisoquinoline alkaloids, including fennebricins A-D (**30-33**) (Figure 8).[117,118] Some of the fennebricins exhibited strong NF-κB inhibitory activity[118] and were cytotoxic against various cells lines,[118] suggesting a link between the cytotoxic activity and their use as chemical defence, both in the mollusc and their prey.

Fennebricin analogues, including jorumycin (**34**), were later reported from the mantle and mucus of an Indian collection of *J. funebris*[113] and jorunnamycins A-C from the mantle, visceral organs and egg ribbons of a Thai collection of *J. funebris*.[116] Jorunnamycin C displayed very potent cytotoxicity (IC_{50} 0.32, 1.5 and 2.8 nM against DU145, HCT116 and QG56 human tumour cell lines, respectively).[113,116] Despite the origin of (**34**) remaining unknown, its isolation from the nudibranch mucus suggests a defensive role, and the isolation of similar metabolites from *Xestospongia* sp. implies a possible predator-prey relationship, although that is yet to be determined.[113,119]

Notably, Zalypsis®, a synthetic derivative of (**34**),[120] showed anti-tumour activity and the Phase II clinical trial for the treatment of Ewing sarcoma was completed in 2021, although no indication of the current status of the drug is listed.[121] This compound exemplifies a promising drug candidate arising from the study of nudibranchs and their prey.

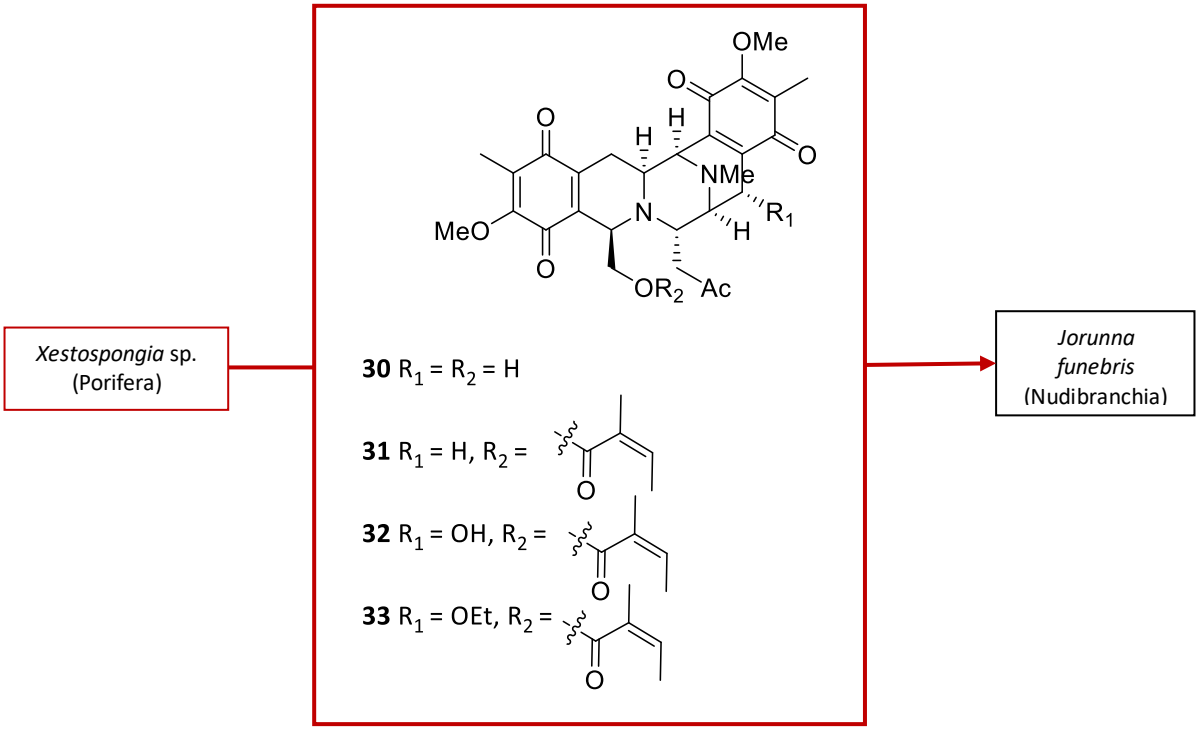

Figure 8: Sequestration of fennebricins by the nudibranch *Jorunna funebris*.

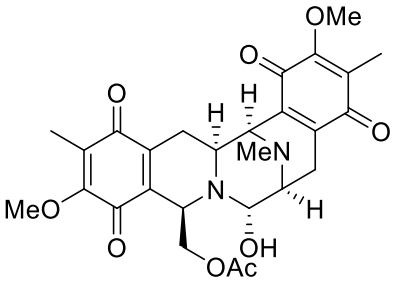

34

Terpenoids

From a secondary metabolite point of view, nudibranchs are especially rich in terpenoids, such as sesquiterpenes, furanosesquiterpenoids and diterpenoids, most often sequestered from their sponge prey.[122] After alkaloids, terpenoids represent the second most prevalent class of compounds reported from sponges, with 693 new terpenoids reported between 2009 and 2018 (out of 2762 new metabolites).[62] Within nudibranchs, terpenoids represent the most prevalent class of compounds sequestered and are often indicative of a predator-prey relationship.[98] Their accumulation in specific nudibranch body parts has been demonstrated several times.[100,114,123,124]

This is the case for the nudibranch *Doriprismatica* (formerly *Doris*)[125] *atromarginata*, that accumulates two deterrent spongian-terpenoids[114,126] spongiatrioltriacetate (**35**) and spongiatriol-diacetate (**36**) in its MDFs, while spongiatriol (**37**),[114] inactive in feeding-deterrence assays, was only found in the mantle and viscera, suggesting localised accumulation as a function of the feeding-deterrent capacity of the metabolites.[100] Along with the three terpenoids (**35-37**), a range of furanoterpene metabolites[114,127-129] and norscalarane[128] were also isolated from several Australian specimens of *Spongia* sp. Further investigations of a separate collection of the nudibranch led to the isolation of scalaranes, including 12-deacetoxy-12-oxodeoxoscalarin (**38**) and 12-deacetyl-12-*epi*-deoxoscalarin (**39**) isolated from both the nudibranch and its *Spongia* sp. prey, supporting their predator-prey relationship.[130]

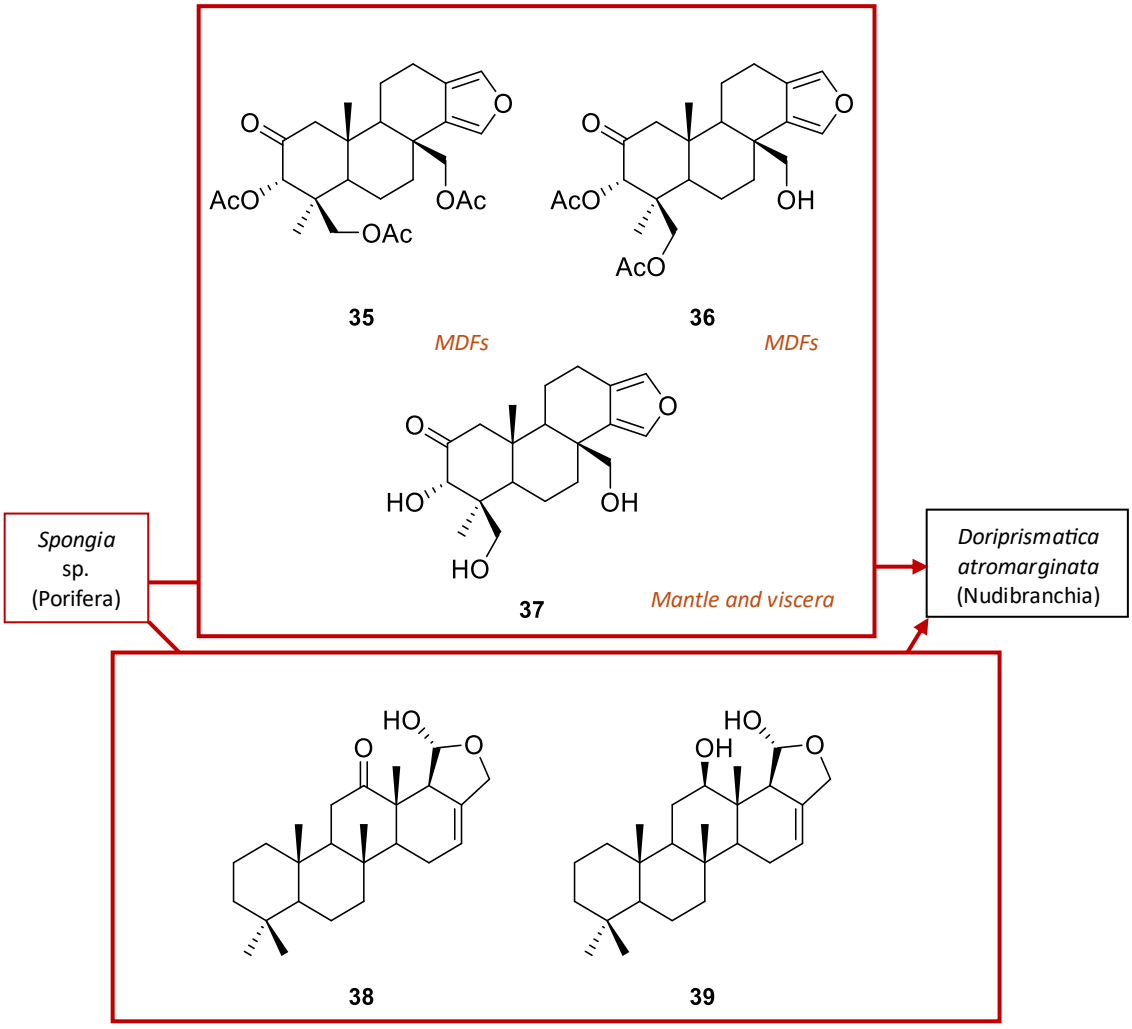

Figure 9: Sequestration of secondary metabolites by *Doriprismatica atromarginata*.

Investigations on the nudibranch *Doriprismatica stellata*, its egg ribbons and the sponge *Spongia* cf. *agaricina* on which they were found, yielded the scaralane-type sesterterpene 12-deacetoxy-4-demethyl-11,24-diacetoxy-3,4-methylenedeoxoscalarin **(40)** (Figure 10).[131] The presence of (**40**) in the sponge supported the predator-prey relationship and its transfer to the eggs is most likely for protective purposes.[98] Compound (**40**) showed antibacterial activity against the Gram-positive bacteria *Arthrobacter crystallopoietes* and *Bacillus megaterium.*[131] The investigations on both *D. stellata* and *D. atromarginata* support the dietary relationship between *Doriprismatica* nudibranchs and scaralane-containing *Spongia* sponges.[98]

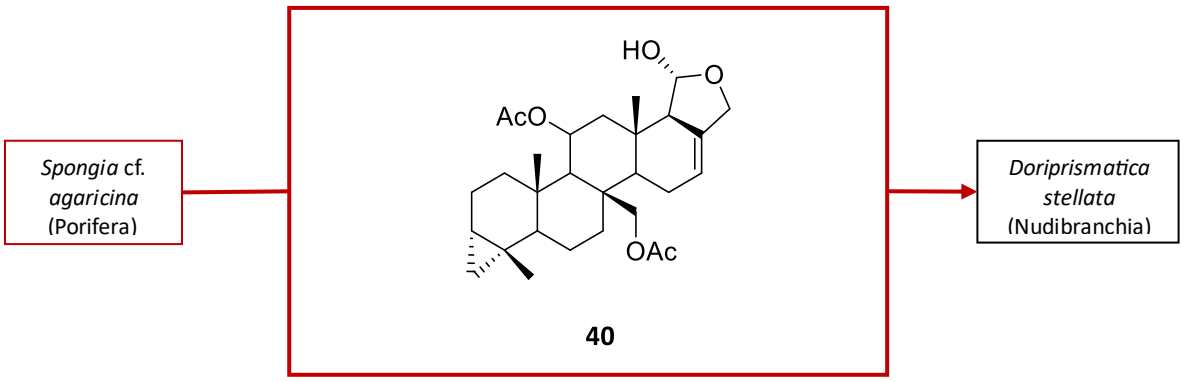

Figure 10: Sequestration of secondary metabolites by *Doriprismatica stellata*.

Also from Australian collections, an extract of the sponge *Acanthodendrilla* sp. yielded two oxygenated sesquiterpenes, caparrapi oxide and arenaran A (**41**),[98] with the latter one, displaying a 6/8 bicyclic ring, also isolated from *Chromodoris strigata* found feeding on the sponge (Figure 11).[132] Arenaran A (**41**) was initially isolated from *Dysidea arenaria* and displayed cytotoxicity against human cancer cell lines (IC_{50} 3.17 and 5.28 µg mL^{-1} for P-388 and HCT-29 cell lines, respectively).

Australian specimens of *Goniobranchus albonares* contain the rearranged diterpene dendrillolide A (**42**), also found from within an encrusting crimson sponge yet to be identified (Figure 11).[133]

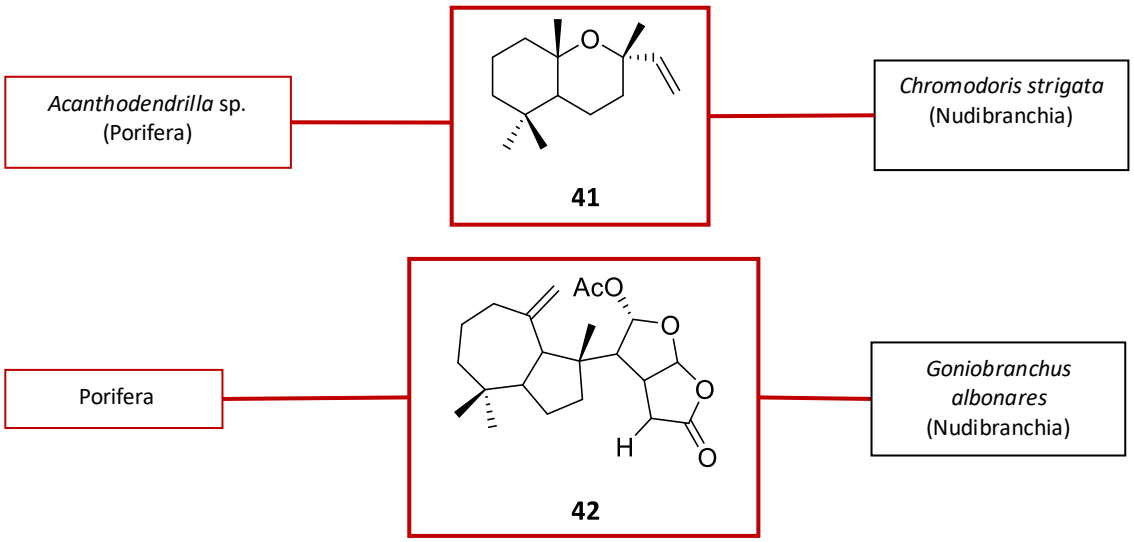

Figure 11: Sequestration of secondary metabolites by *Chromodoris strigata* and *Goniobranchus albonares*.

Another example of accumulation of compounds in specific body areas, along with biotransformation was demonstrated in the nudibranch *Glossodoris pallida*. Laboratory feeding-choice experiments and observation in the wild have shown that the nudibranch feeds on the sponges *Cacospongia mollinor and Hyrtios erecta,* and respectively accumulates scalaradial (**26**) and desacetylscalaradial (**43**) in its MDFs (Figure 12).[123,124] Furthermore, *G. pallida* did not contain any scalarin, a major metabolite of *H. erecta*, and contained relatively more deoxoscalarin (**27**). This suggested that, similarly to *Felimare orsinii* (Figure 6), *Glossodoris pallida* converts compound (**26**), by selective aldehyde reduction, into the less oxygenated deoxyscalarin (**27**) in the digestive gland.[123] Compound (**27**) was also isolated from the egg masses of the nudibranch, suggesting a possible defensive role. The nudibranchs were significantly more susceptible to predation upon removal of their mantle,[123] confirming the accumulation of the feeding-deterrent compounds in the border of the mantle, containing the MDFs.

Glossodoris hikuerensis and *Glossodoris cincta* both contain the sesterterpene heteronemin (**44**) as a major metabolite, also sequestered from *Hyrtios* sponges, which the nudibranchs have been sighted feeding on (Figure 12). Interestingly, (**44**) was also present in their egg masses and was deterrent towards generalist predators.[123]

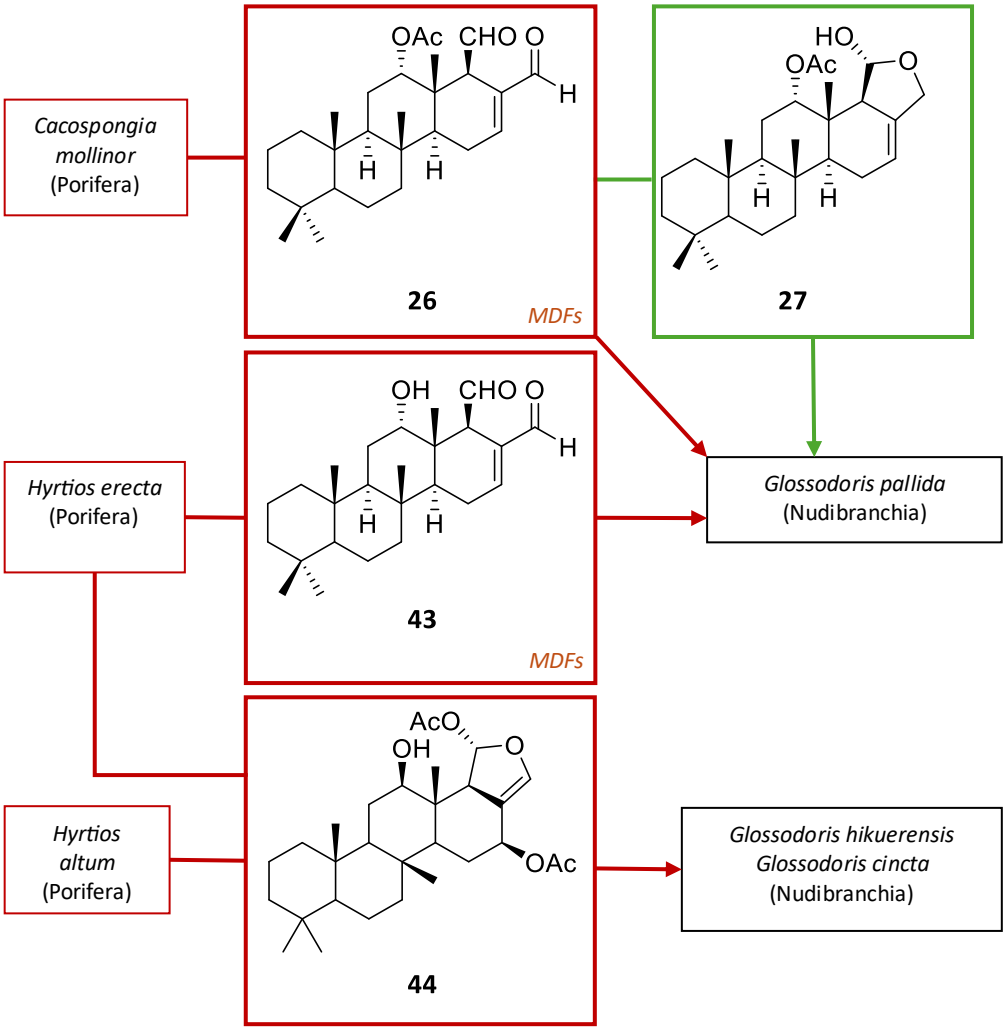

Figure 12: Sequestration and biotransformation of dietary secondary metabolites by *Glossodoris* nudibranchs.

The crude extract from the border of the mantle (including the MDFs) of *Goniobranchus* (formerly *Chromodoris*)[134] *sinensis* contains a mixture of the sponge-derived metabolites aplyroseol-2 (**45**), and its corresponding dialdehyde (**46**),[100] the latter of which could not be isolated because of its easy transformation into the corresponding cyclic hemiacetal (**45**). Compound (**46**) was absent from the viscera of *G. sinensis*, thus suggesting its biotransformation during transfer to the MDFs (Figure 13).[100] Compound (**46**) appears to be three times more concentrated in the MDFs than compound (**45**), suggesting that such transformation may occur to increase the chemical defence of the nudibranch, especially as (**45**) does not show any deterrent activity, while (**46**) induced considerable feeding-deterrence behaviour. Compound (**45**) had previously been isolated from the red-pink encrusting sponge *Aplysilla rosea,* suggesting a dietary origin.[135]

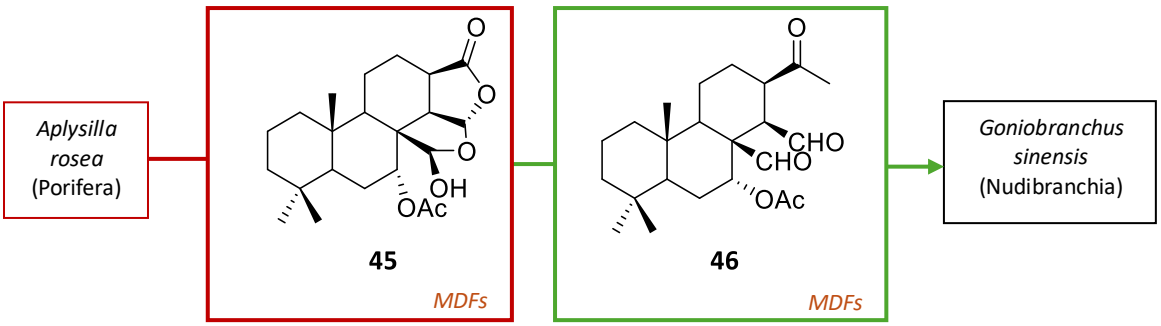

Figure 13: Sequestration and biotransformation of metabolites by *Goniobranchus sinensis*.

The nudibranch *Phyllidia varicosa* sequesters 9-isocyanopupukeanane (**47**), an unusual smelling, tricyclic sesquiterpene isocyanide lethal to fish and crustaceans,[136] and its isomer, 2-isocyanopupukeanane (**48**)[137] from the sponge *Ciocalypta* sp (Figure 14). Furthermore, two anti-feedant 9-thiocyanatopupukeanane sesquiterpene isomers (**49** and **50**) were also isolated as major metabolites from the sponge *Axinyssa aculeata* and from its nudibranch predator *P. varicosa* (Figure 14).[138]

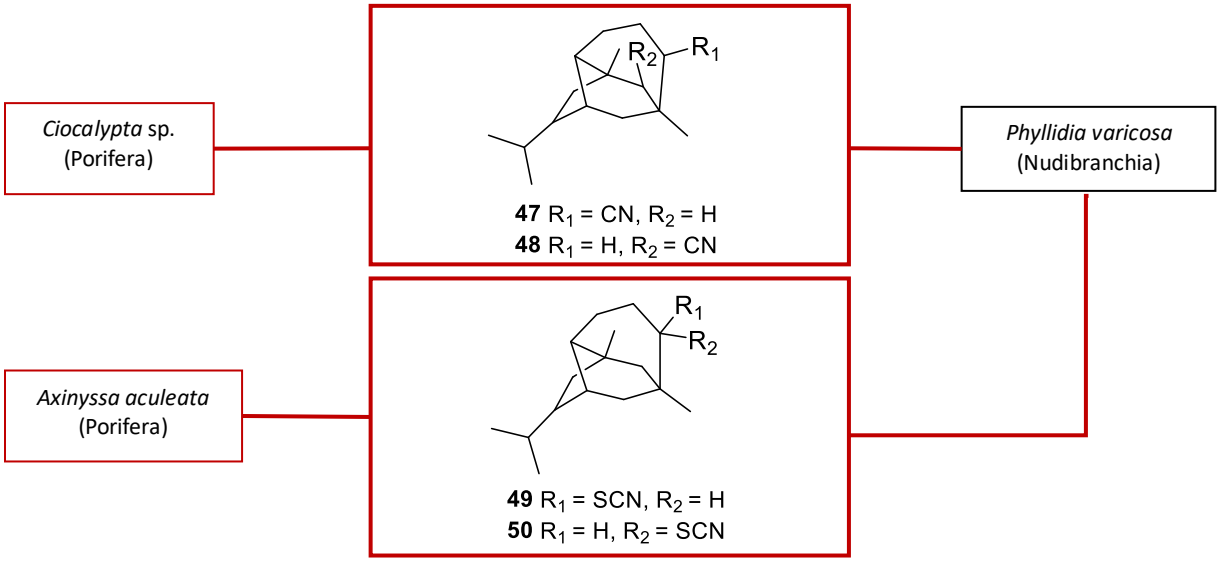

Figure 14: Sequestration of secondary metabolites by *Phyllidia varicosa*.

Several nudibranchs from the *Hypselodoris* and *Felimare* genera are able to selectively prey upon sponges rich in furanosequiterpenoids and accumulate these metabolites in their dorsal glands.[139] This is the case for *Felimare picta* (formerly *Hypselodoris webbi*)[101] reported feeding on three species of sponges, *Chlatria* (formerly *Microciona*)[140] *toxistyla, Pleraplysilla spinifera* and *Dysidea fragilis* (Figure 5 and Figure 15), and rapidly accumulating the sequestered

metabolites in its MDFs.[102,141] The metabolites sequestered include microcionins 1-4 (**51-54**), compound (**23**), along with the highly unstable compounds (**24**) and (**25**) (Figure 5 and Figure 15).[102,141] *Hypselodoris infucata*, *Hypselodoris* (formerly *Rysbecia*)[142] *tryoni* and *Ceratosoma gracillimum*, also sequester compound (**23**), which is found concentrated in the MDFs and shows a strong feeding-deterrent activity at concentrations much lower than those detected in the MDFs.[100] Furthermore, a study of three *Felimare* (formerly *Hypselodoris*)[143] species, *F. cantabrica, F. tricolor and F. villafranca*, from the Cantabrian sea, has shown that all animals possess large amounts of furanosesquiterpenoids, such as longifolin, and nakafuran-9 (**55**), previously reported from sponges and nudibranchs.[103] Compound (**55**) was first isolated from *Dysidea fragilis* and in the sponge predators *Hypselodoris godeffroyana* and *Hypselodoris maridadilus,* along with nakafuran-8 (**56**).[144] Compound (**55**), was also present in *F. picta* and *F. villafranca*, collected in the Mediterranean Sea.[145] Both (**55**) and (**56**) possess antifeedant properties against common reef fishes, *Chaetodon spp.* but no antimicrobial activity. [144]

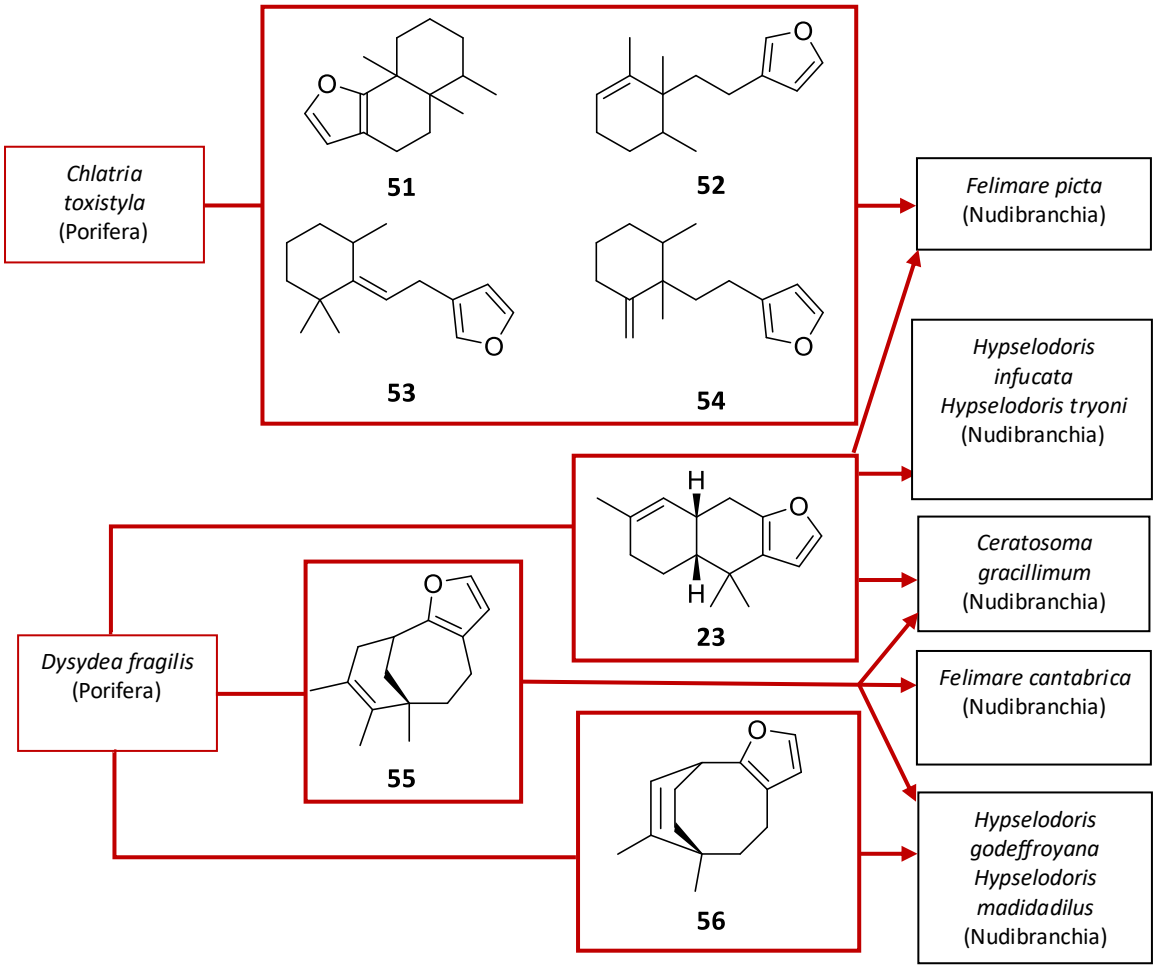

Figure 15: Sequestration of secondary metabolites by *Felimare* and *Hypselodoris* species.

The nudibranch *Felimare* (formerly *Hypselodoris*)[146] *fontandraui*, does not contain MDFs and was investigated to determine whether this animal also lacks chemical defences.[94] *F. fontandraui* diplays a similar colour pattern to other *Felimare* species and could act as a Batesian mimic.[94] However, *F. fontandraui* contains the anti-feedant furanosesquiterpenoid tavacpallescensin (**57**), and its concentration is about four times higher in the mantle rim than in the other external parts, and more than twenty times higher than in the internal organs, causing feeding deterrence against the shrimp *Palaemon elegans*. The presence of compound (**57**) in *Dysidea* sp., on which one individual was found, and in digestive organs, strongly suggests the dietary origin of the compound in the mollusc (Figure 16).[94] Additionally, the study revealed structures in the body wall, just below the border of the mantle whose function was determined as comparable to those of MDFs.[100] It was therefore concluded that *F. fontandraui*, like many other *Felimare* and *Hypselodoris* nudibranchs, is chemically defended and uses structures other than MDFs to store defensive chemicals.[94]

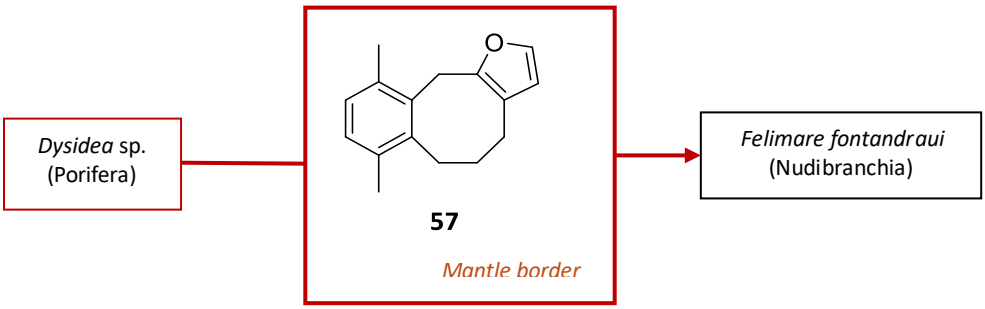

Figure 16: Sequestration of secondary metabolites by *Felimare fontandraui*.

Finally, dendrolasin (**58**) has been isolated from *Chromodoris lochi* and its prey, *Cacospongia* (formerly *Spongia*)[147] *mycofijiensis*, on which the nudibranch was repeatedly observed feeding (Figure 17).[148]

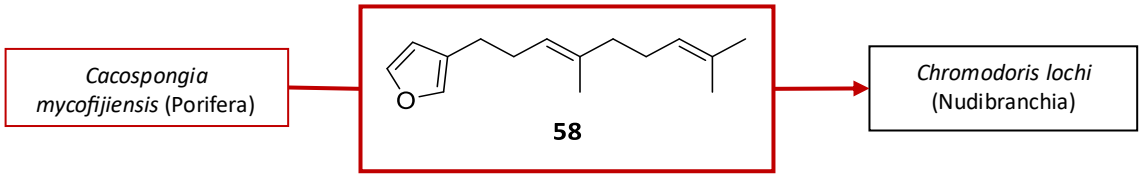

Figure 17: Sequestration of dendrolasin (**58**) by *Chromodoris lochi*.

Terpenoid sequestration in addition to *de novo* biosynthesis

Some nudibranchs, such as *Cadlina luteomarginata*, in addition to sequestering compounds from their diet, can biosynthesise them *de novo*. *C. luteomarginata* is a nudibranch with a fruity odour found along the Pacific coast of America from Alaska to Mexico.[149,150] Luteone (**59**), a twenty-three carbon degraded terpenoid responsible for the pleasant odour of *C. luteomarginata*, was the first compound extracted from its skin in 1981.[150] Further chemical investigations of this nudibranch resulted in the isolation of a wide range of metabolites, such as compounds (**23**) and (**52**), furodysin (**60**) and albicanol (**61**), stored in the external parts of the nudibranch. To date, a total of thirty-eight compounds representing twenty-two different regular carbon skeletons; rearranged, and degraded monoterpenoid,[151-153] sesquiterpenoid,[83,152-154] and diterpenoid,[151,155] have been reported, with several showing anti-feedant properties.[83,153,154] Three of the carbon skeletons were first encountered in *C. luteomarginata*'s metabolites.[156] This great metabolite diversity results from the fact that most of the secondary metabolites are of dietary origin, especially as *C. luteomarginata* consumes at least ten different sponges, including *Axinella* sp., *Aplysilla glacialis*, *Acanthella* sp., and *Dysidea amblia.*[83,153,154]

Interestingly, stable isotope incorporation studies have shown that two sesquiterpenoids, compound (**59**) and albicanyl acetate (**62**) and a diterpene, cadlinaldehyde (**63**), are biosynthesised *de novo* by *C. luteomarginata* and stored in the mantle and MDFs.[156] That report represented the first demonstration of sesterterpenoid biosynthesis by a marine mollusc. Additionally, *C. luteomarginata* is only the second marine mollusc that is known to be capable of both sequestering terpenoids from dietary sources and producing them via *de novo* biosynthesis,[156] the other example being the Mediterranean nudibranch *Dendrodoris grandiflora.*[157] Interestingly, the concentrations of (**59**) and (**63**) are inversely correlated with the availability of similar compounds in the sponge prey. Therefore, *C. luteomarginata* can maintain its chemical defence by sequestering diet-derived secondary metabolites when present and by modulating the production of defensive compounds according to the availability of sponge prey.[56]

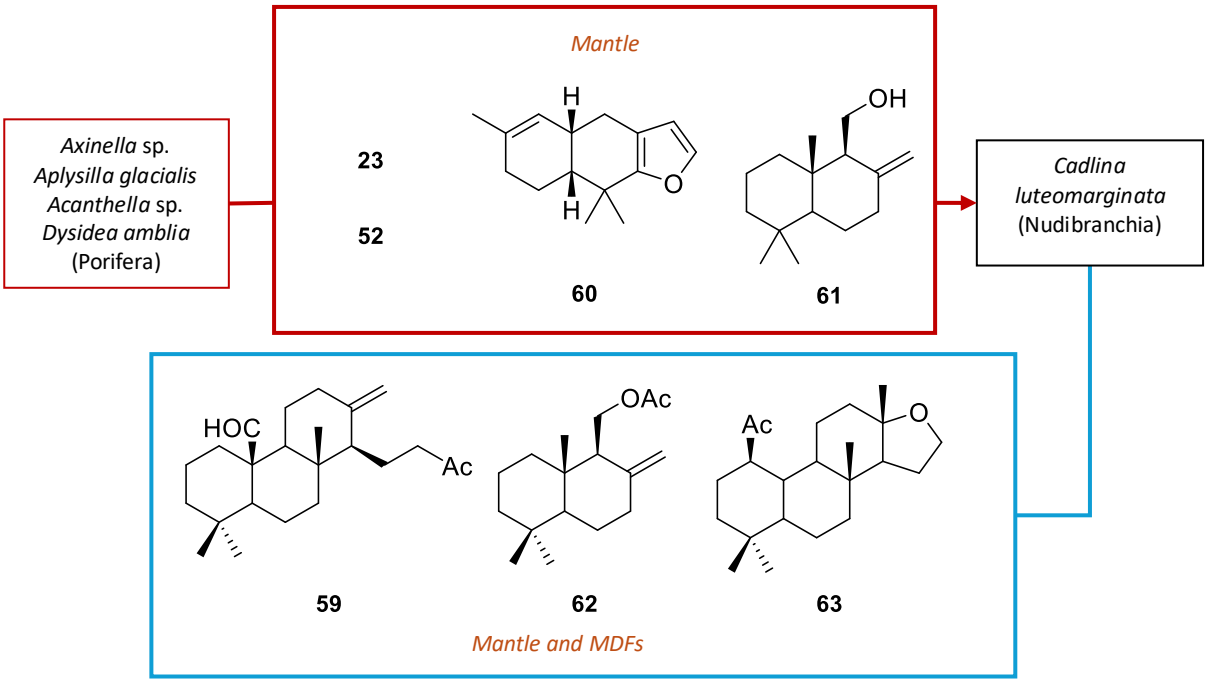

Figure 18: Sequestration and *de novo* biosynthesis of secondary metabolites by *Cadlina luteomarginata*.

Macrolides

Between 2009 and 2018, although the number of bioactive alkaloids and terpenoids reported was largest within the class Porifera, the highest proportion of bioactive compounds was found among macrolides (84.0%),[62] justifying the prevalence of macrolide sequestration within the class Nudibranchia.

As such, the sponge macrolide latrunculin A (**64**), displaying ichtyotoxic[158] and cytotoxic[159] activities, has been identified from several *Chromodoris* nudibranchs, including *C. hamiltoni,*[160] *C. elisabethina,*[161] *C. quadricolor,*[162] *C. annae,*[163] *C. magnifica,*[163] *C. kuiteri,*[163] and *C. lochi.*[148] Macrolide (**64**) was originally identified from the sponges *Negombata* (formerly *Latrunculia*)[164] *magnifica,*[162] *Hyattella* sp.[163] and *Cacospongia mycofijiensis,*[163] on which the nudibranchs were observed feeding (Figure 19).[165] Moreover, typical latrunculid sponge spicules were found in the gut contents of *C. hamiltoni,*[166] suggesting a dietary uptake. Compound (**64**) was the only metabolite present in both the mantle and mantle rim of every species, while the other compounds were only found in the viscera, suggesting localised sequestration for defensive purposes, especially as latrunculin A (**64**) was the most toxic to the brine shrimp *Palaemon serenus.*[163]

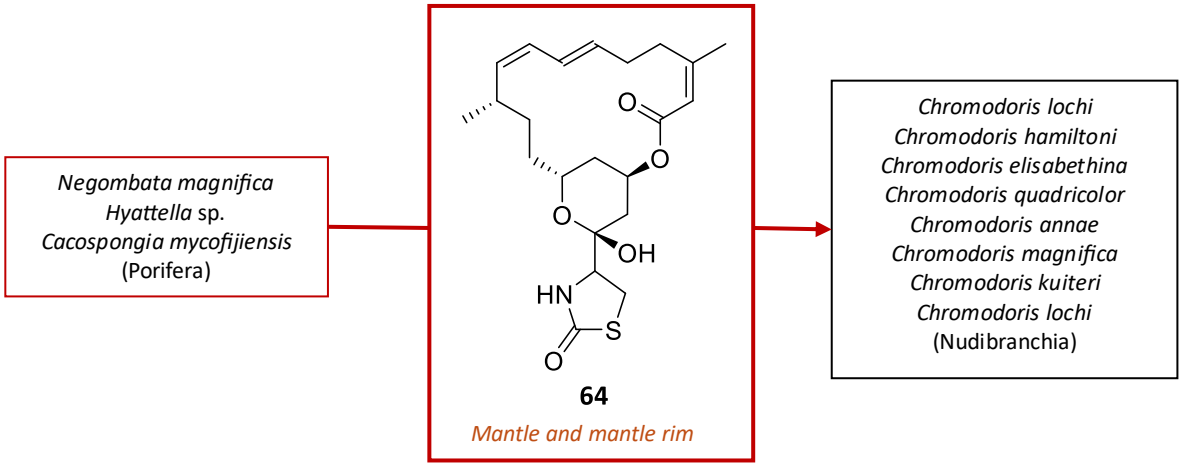

Figure 19: Sequestration of latrunculin by *Chromodoris* nudibranchs.

The large, brilliantly coloured nudibranch *Hexabranchus sanguineus,* or "Spanish dancer", widely studied over the past thirty years, relies on macrolide sequestration and biotransformation for its chemical defence.[167-173] As such, a large variety of trioxazole macrolides has been isolated from the nudibranch, including halichondramides,[167,168,170] kabiramides[167,168] and sanguinamides,[168] as well as the red pigment hurghadin, responsible for the colouration of *H. sangineus*[169] *H. sanguineus* sequesters halichondramide (**65**), dihydrohalichondramide (**66**) and kabiramides B-C (**67-68**) from *Halichondria* sp. on which it exclusively feeds (Figure 20).[167,168,170] Macrolide (**65**), the dominant secondary metabolite from the sponge, is not stored in the nudibranch, suggesting its transformation upon digestion to tetrahydrohalichondramide (**69**),[167] or its selective exclusion.[85] In the case of biotransformation, this process involves two reactions, a double bond hydrogenation and carbonyl reduction, possibly carried out by phase I P450 enzymes.[56] The macrolides, including the modified metabolites, are concentrated in the dorsal mantle, in the digestive gland and in the gonads where the eggs are produced.[167] Several of these macrolides have antifungal activity against *Candida albicans*[168,170] and *Cryptococcus neoformans,*[168] inhibit cell division in fertilised sea urchin eggs[170] and are highly potent inhibitors of fish feeding.[167]

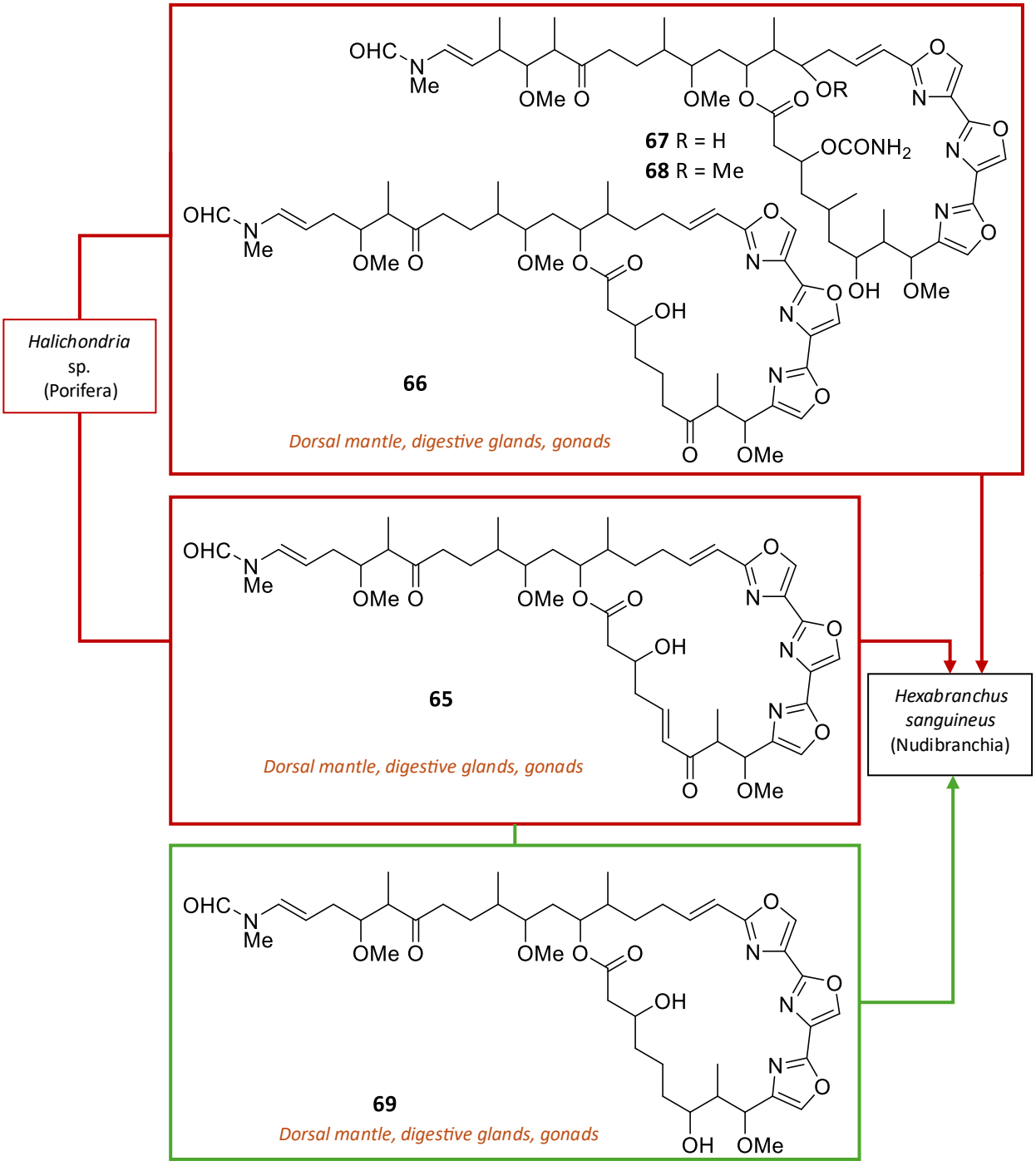

Figure 20: Sequestration and biotransformation of secondary metabolites by *Hexabranchus sangineus*.

Furthermore, chemical investigation of the bright pink eggs of *H. sanguineus* revealed the presence of identical macrolides in the nudibranch and in their egg masses and represented the first confirmatory evidence of the passage of trisoxazole macrolides from sponge to nudibranch to progeny.[167,168,171] Several other macrolides were also isolated from the egg masses, including ulapualides A-E (**70**-**74**),[172,174] and kabiramides A, D and E.[171,174] Notably, the macrolides were found in higher concentration in the egg masses than in the nudibranch itself, suggesting protective functions, although their presence in the mucus of *H. sanguineus* most likely confers protection to the adult as well.[174]

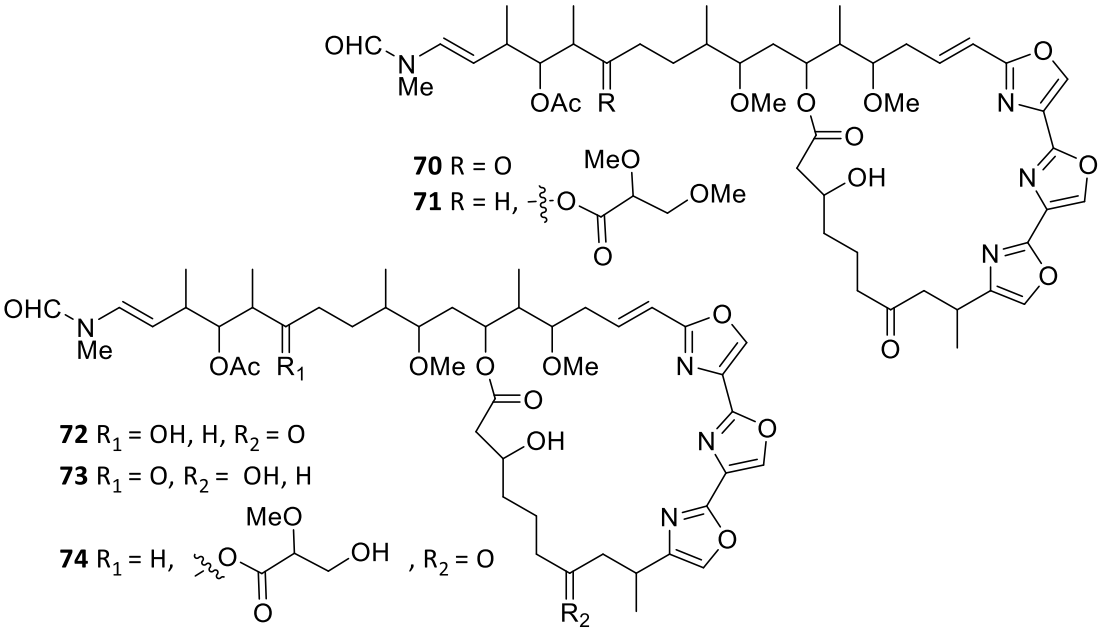

Nucleosides

Nucleoside sequestration may be uncommon in nudibranchs, with only one example documented. The *N*-methylnucleoside doridosine (**75**)**,** a hypotensive compound, was isolated from the nudibranch *Peltodoris* (formerly *Anisodoris*)[175] *nobilis* collected in California, as well as from the sponge *Tedania anhelans* (Figure 21).[176] This nudibranch is also called the speckled sea lemon due to its bright yellow-orange colour and its persistent fruity odour coming from one odoriferous aldehyde.[177]

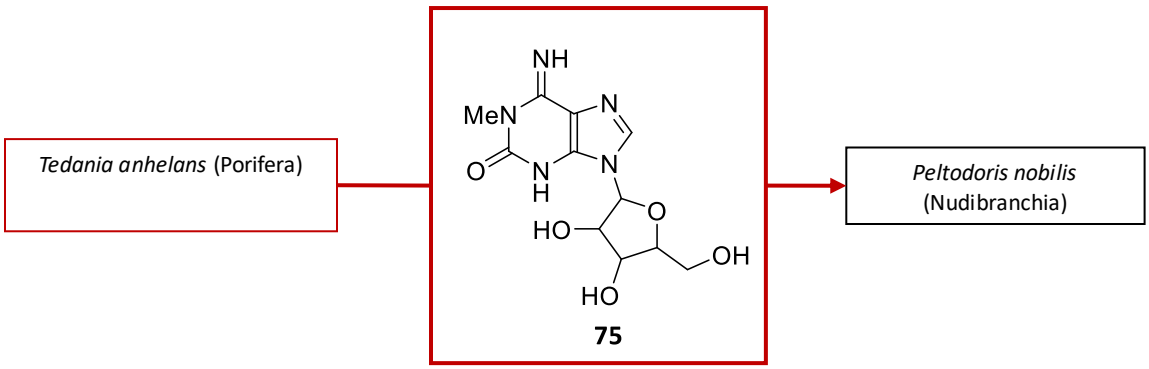

Figure 21: Sequestration of secondary metabolites by *Peltodoris nobilis*.

Lipids

An early study on the nudibranch *Peltodoris atromaculata* reported the polyacetylene alcohols, petroformynes, in the digestive glands of the nudibranch. These are sequestered from the sponge *Petrosia ficiformis,*[178] detected by *P. atromaculata* by means of chemotaxis.[179] In 2014, Ciavatta *et al*. reported the isolation of four fulvinol-polyacetylenes, fulvindione (**76**), fulvinone (**77**), isofulvinol (**78**) and hydroxydehydroisofulvinol (**79**), mainly located in the internal part of the molluscs and sequestered from its sponge prey *Haliclona fulva* (Figure 22).[180] Compound (**79**) was active against SKMEL-28 melanoma cells (IC_{50} 3 µM).

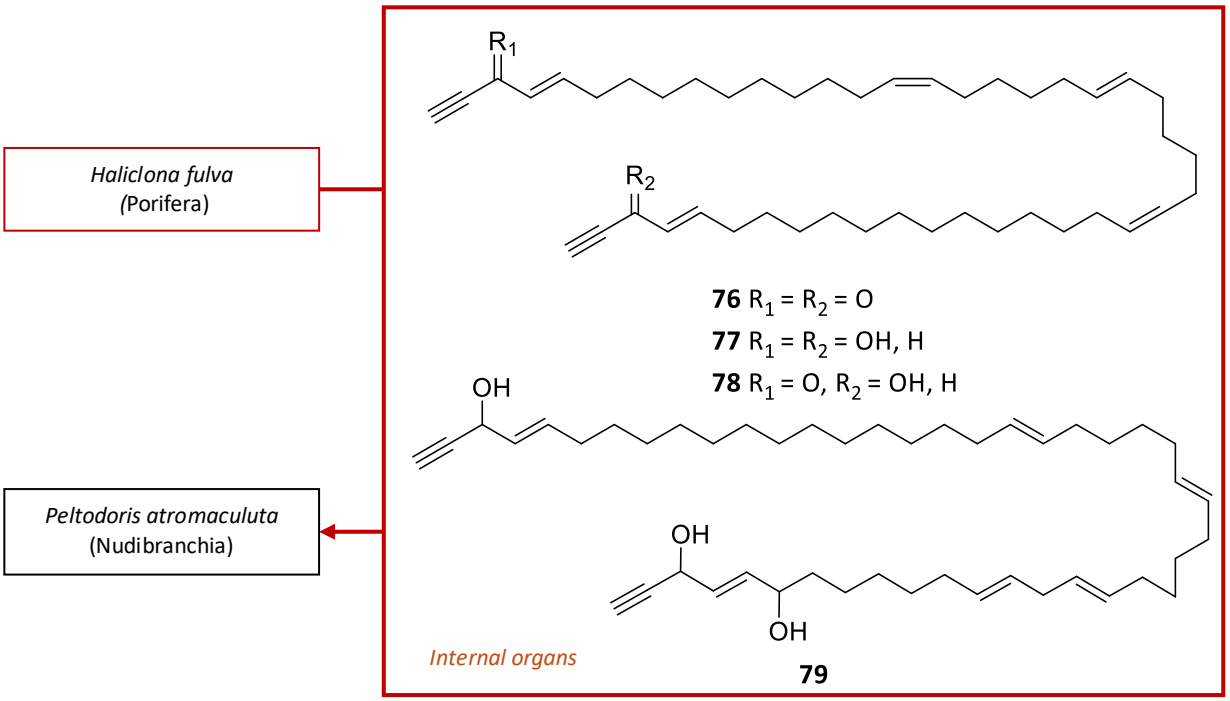

Figure 22: Sequestration of secondary metabolites by *Peltodoris atromaculata*.

1.5.2 Sequestration from bryozoans

Nudibranchs not only sequester metabolites from sponges, but also from bryozoans. These filter-feeding invertebrates are an important source of pharmacologically active metabolites, including primarily alkaloids and polyketides.[181] Since the early 2000s, more than 160 new MNPs have been isolated from the phylum Broyzoa.[65-68,182]

Alkaloids

Alkaloids represent the major class of secondary metabolites within marine bryozoans, with many halogenated compounds, and the main class reported to be sequestered by nudibranchs, especially within the *Tambja* and *Tyrannodoris* genera.

The nembrothid nudibranchs *Tambja abdere* and *T. eliora*, collected from the Gulf of California, both contain the anti-feedant alkaloids tambjamines A-D (**80-83**).[183,184] These are sequestered from their single bryozoan prey *Sessibugula translucens* (Figure 23),[183,184] although some were also isolated from the ascidian *Sigillina* (formerly *Atapozoa*) sp.[185] and cultures of *Streptomyces* sp.[186] Interestingly, *Tyrannodoris* (formerly *Roboastra*) *tigris,* a large carnivorous nudibranch, preys upon *T. abdere and T. eliora* and sequesters the tambjamines (**80-83**) from its nudibranch prey (Figure 23). Compounds (**80-83**) were screened for antimicrobial activity and showed moderate antimicrobial activity against *Escherichia coli, Staphylococcus aureus, Bacillus subtilis* and *Vibrio anguillarum.*[183] Compound (**83**) also displays cytotoxicity to murine melanoma B16 cancer cells (6.7 ug mL^{-1}).[187] *T. abdere* locates its bryozoan prey by detecting, in the water, the presence of compounds (**80**) and (**81**) with a concentration below 10^{-10} M. However, when the concentration exceeds 10^{-8} M, *T. abdere* is deterred.[184] Interestingly, when attacked by *Tyrannodoris tigris, T. abdere* produces a yellow mucus containing large quantities of tambjamines that causes the nudibranch predator to break off its attack, suggesting that the tambjamines are used to repel predators.[183,184] *T. abdere* is therefore able to detect and differentiate between different concentrations of tambjamines.

In contrast, *T. eliora* does not seem to produce a defensive secretion but tries to escape from the attack of *Tyrannodoris tigris* by a vigorous writhing motion. Field observations of

Tyrannodoris tigris suggested that it could easily detect and follow fresh slime trails of *T. abdere and T. eliora,* containing low concentrations of tambjamines, using contact chemoreception.[183] This was corroborated by observing that upon the encounter of a broken trail, *Tyrannodoris tigris* will usually turn around and follow the trail in the reverse direction.[184] *Tyrannodoris tigris* is, so far, the only mollusc reported to follow a trail with mucus containing diet-derived compounds.[56] These observations therefore suggest that the tambjamines in low concentrations are used as both tracking pheromones to determine prey location, respectively *S. translucens* for *T. abdere* and *T. abdere* and *T. eliora* for *Tyrannodoris tigris*, as well as alarm/defensive pheromones in higher concentrations (for example in the mucus) in the case of a predatory attack.[183,184]

Chemical investigation of the nudibranch *Tambja ceutae* led to the isolation of a new member of the tambjamine family, the cytotoxic tambjamine K (**84**).[188] The nudibranch preys on the bryozoan *Viriditentula* (formerly *Bugula*)[189] *dentata*, also containing compound (**84**) in very small amounts, together with compounds (**80**) and (**81**) (Figure 23).[188]

More recently, several new minor tambjamines M-O (**85-87**) have been reported by Berlinck *et al.* from *Viriditentula dentata*, and from its nudibranch predators *Tambja stegosauriformis* and *Tambja brasiliensis* (Figure 23).[190] Notably, similarly to how *Tyrannodoris tigris* preys on two smaller *Tambja* nudibranchs, *Tyrannodoris ernsti* also preys on *T. stegosauriformis* and *T. brasiliensis* and sequesters compounds (**85**-**87**), providing strong evidence of the predator-prey relationship in which tambjamines are caried up the food chain.[98,190] Compounds (**80**), (**82**) and (**83**) were also isolated from all samples and are likely a major constituent of the nudibranch's defences. Interestingly, the authors demonstrated by metabolomics analysis that the tambjamine diversity increased from the bryozoan prey to its nudibranch predators, and attained an even higher diversity on *T. ernsti.*[190]

This is in contrast to results obtained from a previous study within the Prinsep research group conducted on *Tambja* sp. from Australia.[191] The study showed that the nudibranchs contained a lower diversity of tambjamines compared to their *V. dentata* prey, while the eggs contained an even lower diversity of tambjamines, suggesting selective sequestration and transfer to the eggs.[191]

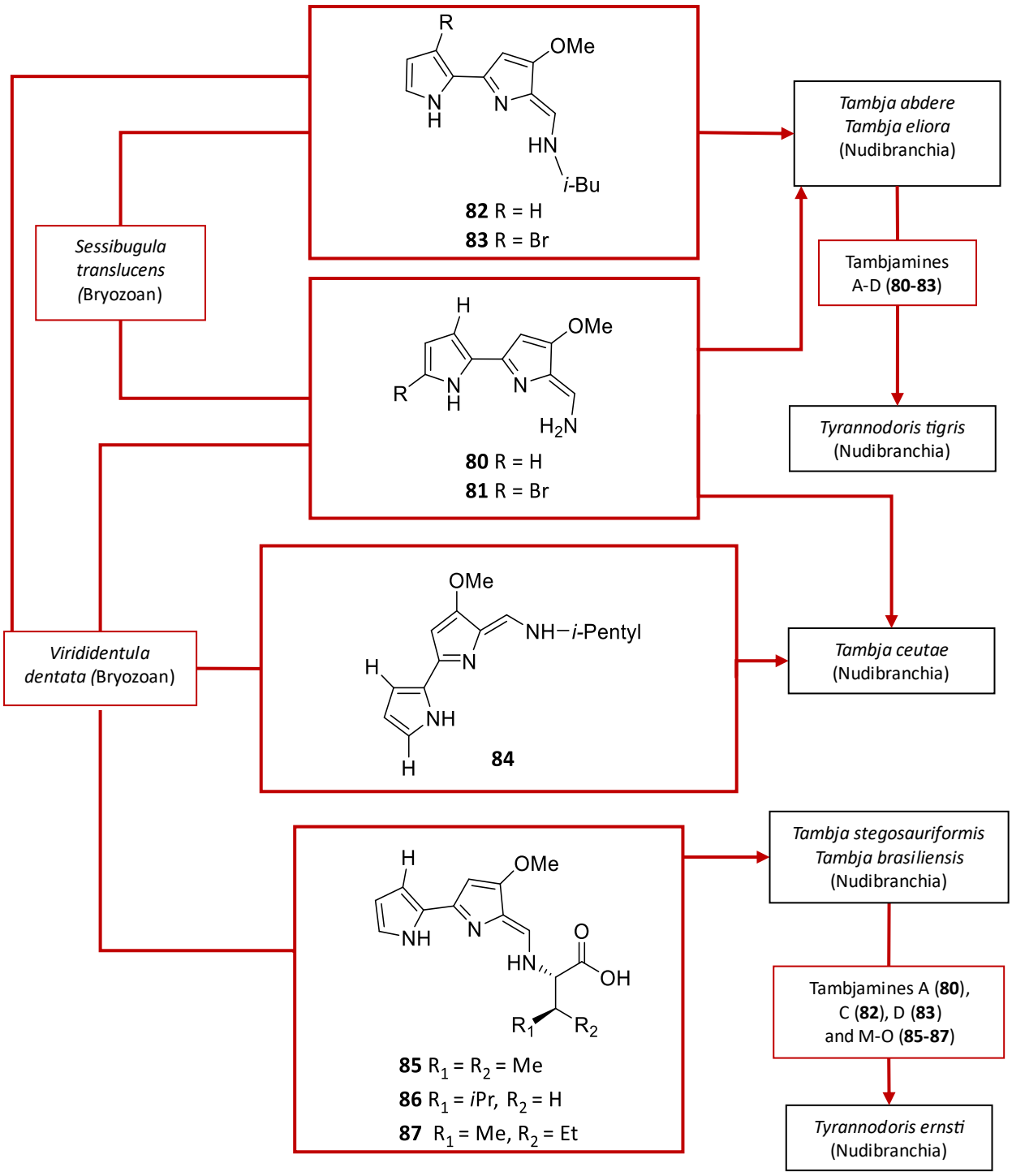

Figure 23: Sequestration of tambjamines by *Tambja* and *Tyrannodoris* nudibranchs.

Tripeptides

Tripeptides are the second class of secondary metabolites reported to be sequestered from bryozoans by nudibranchs, with one example described from the *Antiopella* genus.[85]

The tripeptide janolusimide (**88**) was isolated from the Mediterranean nudibranch *Antiopella* (formerly *Janolus*)[192] *cristatus*,[193] while the *N*-methyl analogue janolusimide B (**89**) was isolated from New Zealand specimens of the bryozoan *Bugulina* (formerly *Bugula*)[194] *flabellata*, a known prey of *A. cristatus* that spreads through biological fouling.[195] Due to the strong similarities between compounds (**88**) and (**89**), a predator-prey relationship between both organisms was suggested.[85] However, compound (**88**) was never detected in the bryozoan, and compound (**89**) was not found in the nudibranchs, therefore it was unclear whether compound (**88**) was sequestered from *B. flabellata* or biotransformed from compound (**89**).[85]

Fortunately, a second investigation into another New Zealand population of *B. flabellata* determined the presence of both compounds (**88**) and (**89**) within the bryozoan (Figure 24).[85,196] Specimens of *Antiopella novozealandica* (formerly *Janolus novozealandicus*)[197] were also investigated and both tripeptides (**88**) and (**89**) were detected by liquid chromatography-mass spectrometry (LC-MS) (Figure 24).[196] Interestingly, the relative abundance of compounds (**88**) and (**89**) was inverted within both predator and prey, with janolusimide (**88**) dominant within *A. novozealandica,* and janolusimide B (**89**) as the major compound in *B. flabellata.*[85] The additional presence of compound (**88**) within an egg mass of *A. novozealandica*, combined with its toxicity to mice (LD 5 mg kg^{-1}, intraperitoneal injection),[193] suggested a defensive role, although additional studies are needed to confirm this.[85]

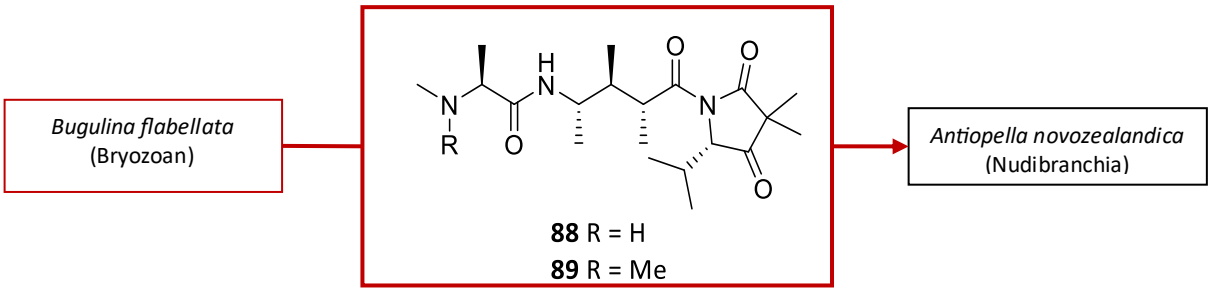

Figure 24: Sequestration of tripeptides (**88**) and (**89**) by the nudibranch *Antiopella novozealandica.*

1.5.3 Sequestration from ascidians and soft corals

Along with sponges and bryozoans, ascidians and soft corals are sought-after nudibranch prey and are prolific producers of MNPs, including primarily alkaloids and peptides.[198] To date, more than 1200 new MNPs have been described from tunicates and sea squirts, including the well-known ecteinascidin 743 (**14**) from *Ecteinascidia turbinata* and plidítepsin (**17**) from *Aplidium albicans,* both mentioned in Section 1.1.3.[199]

Alkaloids

More than 70% of bioactive secondary metabolites isolated from ascidians are alkaloids,[199] and similarly to bryozoans, tambjamines represent the only type of alkaloids sequestered by nudibranchs, reported to date.

As such, more tambjamines, E and F, along with compound (**82**) were isolated from the ascidian *Sigillina* (formerly *Atapozoa*)[200] sp., as well as from its nudibranch predator *Nembrotha* spp.[185,201] Interestingly, the nudibranchs also contained compound (**80**), not found in the ascidians.[201] Overall, concentrations of tambjamines were higher in the nudibranchs, and were the major components of the mucus exuded by *Nembrotha* spp. when irritated.[201] Tambjamines E and F, and several mixtures of tambjamines, were all significant feeding deterrents to carnivorous fishes, suggesting that both the ascidian and its nudibranch predators use the tambjamines as a means of defence against predators.[201] Regarding the origin of the tambjamines, it was suggested that *Sigillina* sp. is capable of biosynthesising the tambjamines, although they could also originate from a microorganism common to both ascidians and bryozoans containing tambjamines.[56,185]

Diterpenes

The cladiellane-based diterpenes, tritoniopsins A-D (**90-93**) were isolated from the South China Sea nudibranch *Tritoniopsis elegans* and its prey, the soft coral *Cladiella krempfi* (Figure 25).[202] Cladiellanes are typical soft coral diterpene metabolites and a number of them possess interesting pharmacological activities.[202] However, only compound (**91**) showed moderate to weak antiproliferative activity against both tumour and normal cell lines.[202] Of note is the relative ratio between compounds (**90**) and (**91**) that was inverted between the prey (**91 > 90**) and the predator (**90 > 91**), suggesting a possible ability to selectively sequester useful metabolites for defensive purposes, or biotransform one to the other.[98]

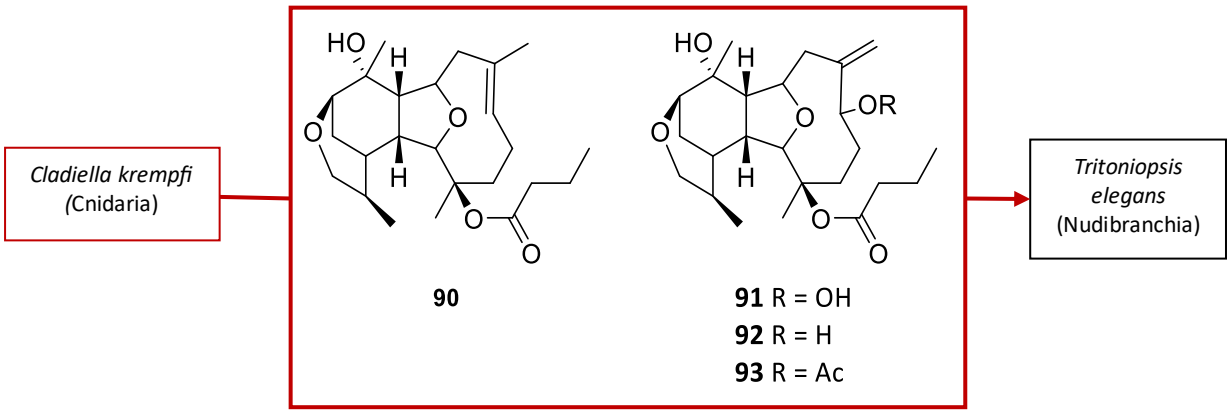

Figure 25: Sequestration of diterpenes by the nudibranch *Tritoniopsis elegans*.

1.6 Research aims

The research described in this thesis relies on chemical ecology-guided investigation to establish novel predator-prey relationships in nudibranchs and identify new bioactive secondary metabolites within New Zealand marine invertebrates. The establishment of predator-prey relationships will be conducted by means of field observations, laboratory-based feeding-choice experiments, morphological analyses and most importantly, chemical analyses of invertebrate prey (sponges and bryozoans), nudibranchs and egg masses. NMR spectroscopy will be utilised to assess the ecological role and origin of the metabolites isolated. Upon collection of nudibranch species not found in the vicinity of any potential prey, chemical investigation will still be carried out on the individuals and their spawned egg mass. The localisation and concentration of metabolites within nudibranchs will also be investigated, by sample dissection and quantitative analysis.

The chemical ecology-guided approach will also be prioritised for discovery of novel bioactive secondary metabolites. As mentioned in the literature,[132] the small size of nudibranchs, especially in Australasia, and weight of crude extract makes the purification and characterisation of metabolites difficult. Therefore, prioritising investigation of the prey, often available in larger quantities, is preferred.[132] The choice of prey will arise from the results of the feeding-choice experiments, acting as a bioassay performed by the nudibranchs, providing guidance towards potentially bioactive prey. Crude extracts of interest will be purified using a range of chromatographic techniques (bench column chromatography, HPLC-UV) and purified compounds will be characterised by 1D/2D NMR spectroscopy and high-resolution electrospray ionisation-mass spectrometry (HR-ESI-MS). Known and new pure compounds isolated will be assessed for cytotoxic activity.

Chapter 2

Chemical analysis of New Zealand marine invertebrates

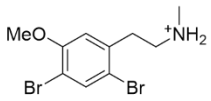

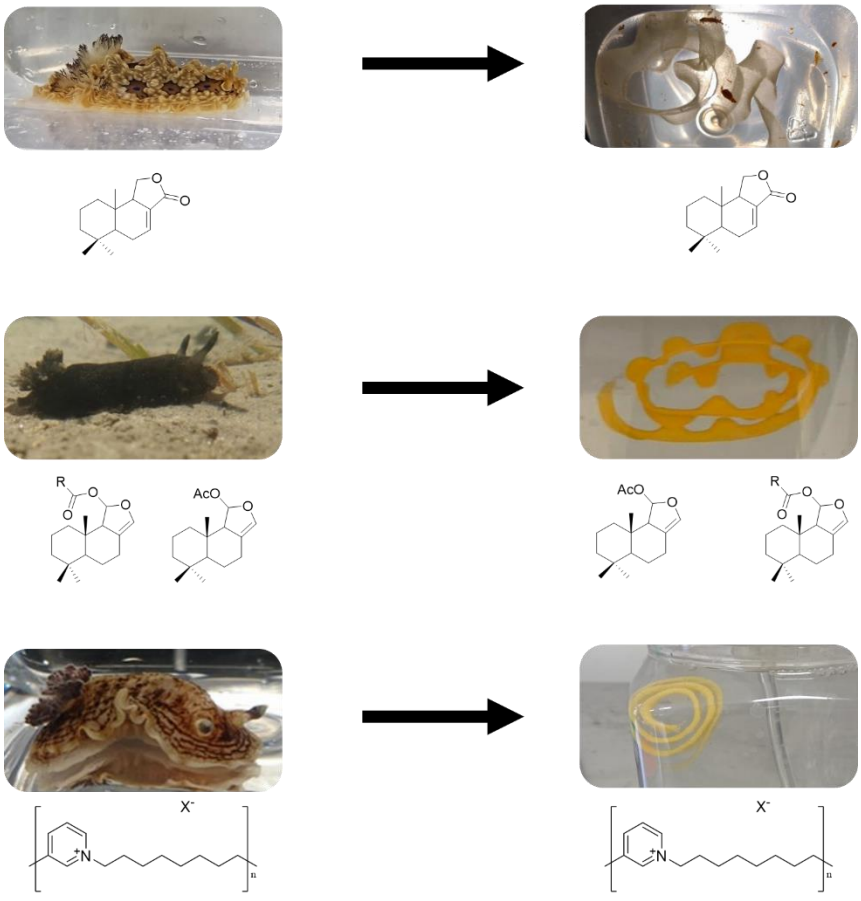

2.1 The New Zealand marine ecosystem

Aotearoa New Zealand is a Pacific archipelago composed of two main islands and no less than 700 offshore islands, most of which are located within close distance to the coast.[203] By covering 4.2 million km^2, the New Zealand Exclusive Economic Zone (EEZ) is one of the largest in the world (Figure 26).[204] Its area spans thirty degrees of latitude and exceeds fifteen times the land area.[204] The EEZ displays a wide range of sea floor reliefs, including the ten kilometres deep Kermadec Trench, part of the Pacific "Ring of Fire". Currently, the half of the EEZ below 2000 metres remains mainly unexplored biologically due to the extreme environment.[204] In 2010, more than 17 000 marine species were documented to inhabit the EEZ waters, including various species of endemic fish, pinnipeds and cetaceans.[204] Numerous species present in different collections remain currently undescribed and the report of new species from New Zealand is common for marine samples.[204] Among the species found within New Zealand waters, the phylum Porifera accounts for more than 1400 species, the phylum Mollusca for more than 3500 and the phylum Bryozoa for over 900 species.[204]

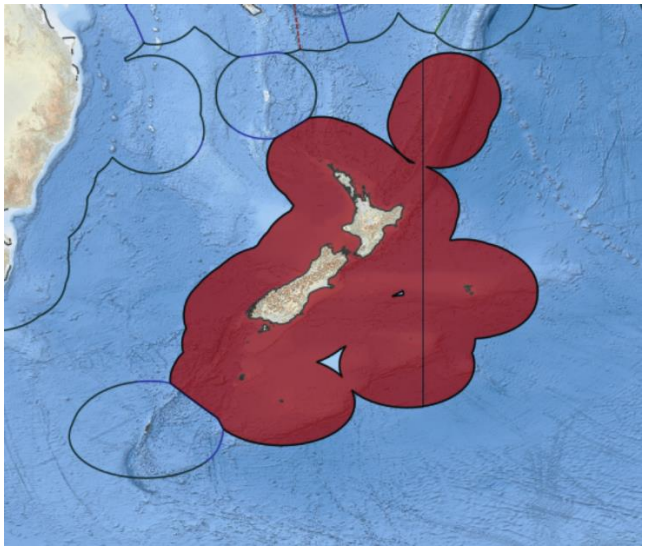

Figure 26: The New Zealand Exclusive Economic Zone.[205] Available under Creative Commons Attribution 4.0 license (CC BY 4.0 License), https://www.marineregions.org/. Latitude 42° 45' 58.1" S (-42.76615°), longitude 71° 43' 45.6" E (71.72934°)

2.2 *Amathia gracei*

Among all the bryozoan species inhabiting New Zealand waters, only eight are found in the freshwater environment, while the remaining species occur in diverse marine environments, from shallow rocky coasts down to great diving depths.[206] Bryozoans are comprised of numerous individuals, or zooids, united in a large colony, and most marine bryozoans display a partially calcified, hard, body wall.[207] Bryozoans rely on feeding zooids to capture small organic particles within the surrounding waters for their nutritional needs. Numerous other types of zooids perform various tasks such as reproduction, nutrient storage, colony strengthening and defence by means of secondary metabolites.[207]

Amathia gracei (Gordon and Spencer Jones, 2013, Figure 27) (Family: Vesiculariidae, Figure 28) is an endemic New Zealand species recently described as a colonial, erect, bushy and densely branching bryozoan.[208] It, along with *A. zealandica*, are the only two endemic species belonging to the *Amathia* genus.[208] Many *Amathia* species display spiral zooid clusters, including *A. gracei* whose zooids are disposed in an anticlockwise spiral on each stolon segment.[208] *A. gracei* was initially described from East Cape in the North Island.[208]

Figure 27: *Amathia gracei* specimen.

Kingdom Animalia
Phylum Bryozoan
Class Gymnolaemata
Order Ctenostomatida
Suborder Vesicularina
Superfamily Vesicularioidea
Family Vesiculariidae
Genus *Amathia*
Species *Amathia gracei*

Figure 28: Taxonomic classification of *Amathia gracei* according to the World Register of Marine Species (WoRMS).[209]

To date, no metabolites have been reported from *Amathia gracei*, although a previous LC-MS study from the Prinsep research group showed that the nudibranch *G. aureomarginatus* contained brominated alkaloids also found within the bryozoan *Amathia gracei* from the same location.[210] This suggested that the nudibranch was preying on the bryozoan and the latter was therefore chemically investigated in this study.

2.2.1 Isolation procedure

A sample of *A. gracei* collected in 2014 from Tauranga harbour had previously been extracted and investigated by reversed phase bench column chromatography by Honours student Cameron Crombie (Figure 29).[211] Numerous brominated metabolites were detected by LC-MS, but no structure could be assigned to any of the compounds. During the current research, four fractions which had not previously been investigated by Cameron Crombie were analysed by LC-MS (Figure 29). Fractions 4 and 7 were of interest because of the presence of brominated compounds (See Chapter 7). Fraction 4 was analysed by HR-ESI-MS and NMR spectroscopy, leading to the isolation of convolutamine L (**94**), previously described from an Australian specimen of *Amathia lamourouxi*.[212]

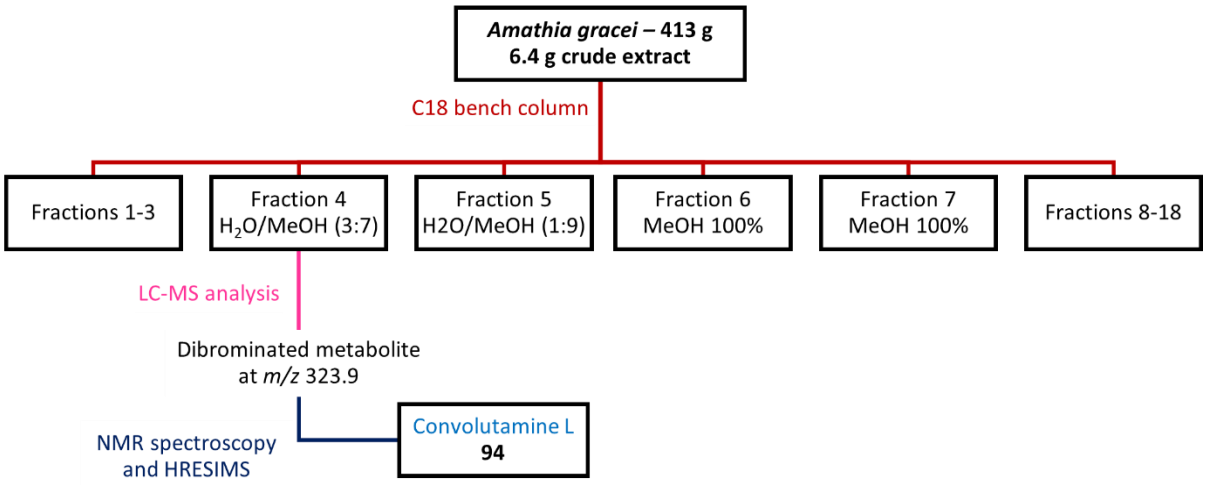

Figure 29: The isolation procedure for convolutamine L (**94**).

2.2.2 Convolutamine L

The HR-ESI-MS analysis (positive ion mode) of convolutamine L (**94**) showed an isotope pattern of ions at *m/z* 321.9721, 323.9704 and 325.9688, in a 1:2:1 ratio, characteristic of the presence of two bromine atoms, and corresponding to a molecular formula of $C_{10}H_{14}Br_2NO$. The ^{1}H NMR spectroscopic data displayed two doublets of doublets at δ_H 3.21 and 3.30, integrating for two protons each and corresponding to two methylene signals, along with two singlets at δ_H 7.02 and 7.70 corresponding to two aromatic protons. The ^{1}H NMR spectrum (Appendix A.1) also displayed one *N*-methyl singlet at δ_H 2.73 and a singlet at δ_H 3.91 integrating for three protons and corresponding to a methoxy group. Likewise, the ^{13}C NMR spectrum displayed signals corresponding to two protonated aromatic carbon signals (δ_C 114.4 and 136.6), two methylene carbon signals (δ_C 32.9 and 48.4), an *N*-methyl resonance (δ_C 33.1) and a methoxy signal (δ_C 56.8). The HMBC correlation H-6/C-7 and the COSY correlation H-7/H-8 allowed for the placement of the methylene chain at position 1 of the aromatic ring (Figure 30). The HMBC correlation H-10/C-8 established the attachment of the nitrogen to the methylene chain and confirmed the position of the *N*-methyl moiety. Finally, the HMBC correlation H-3/C-5 and the shape of the aromatic signal at δ_H 7.02 allowed for its attachment to C-3, or three bonds away from C-5 bearing the methoxy group.

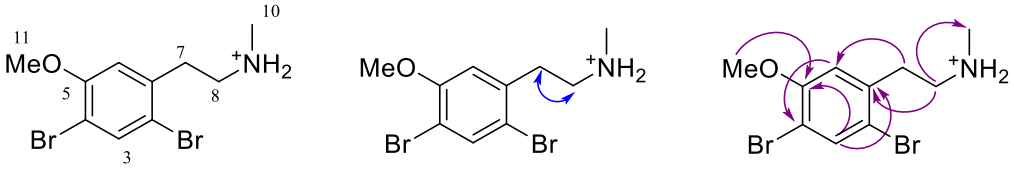

94

Figure 30: Selected COSY (blue) and HMBC (purple) correlations for convolutamine L (**94**).

All spectral data were in agreement with those reported previously for compound (**94**) initially isolated from Australian *A. lamourouxi,* with the slight chemical shift variations (Table 1) attributed to the difference in NMR solvents between the experimental and literature spectra (chloroform-*d versus* DMSO-d_6).[212] Of interest is the difference in peak shape of the *N*-methyl protons between the literature and this work's data because of the coupling with the exchangeable amine protons in DMSO-d_6.

Table 1: ^{1}H and ^{13}C NMR data for convolutamine L **(94)** compared with literature values (DMSO-d_6).[212]

	^{1}H (mult, *J* in Hz)		^{13}C	
Atom	[a] **Experimental**	[b] **Literature**	[a] **Experimental**	[b] **Literature**
1			135.9	136.9
2			114.5	114.1
3	7.70 (s)	7.83 (s)	136.6	135.5
4			[c] 111.7	110.1
5			[c] 155.7	155.1
6	7.02 (s)	7.14 (s)	114.4	115.0
7	3.21 (dd, 6.9, 9.0)	3.01 (dd, 7.0, 8.6)	32.9	31.8
8	3.30 (dd, 6.9, 9.0)	3.15 (m)	48.4	47.4
9-(NH/NH_2)	[d] ND	8.60 (s)		
10	2.73 (s)	2.62 (t, 5.4)	33.1	32.7
11	3.91 (s)	3.87(s)	56.8	56.5

[a] values reported in chloroform-*d*, ^{1}H 600 MHz, ^{13}C 150 MHz, [b] values reported in DMSO-d_6, ^{1}H 500 MHz, ^{13}C 125 MHz (Kleks *et al.* 2020[212]), [c] determined from HMBC, [d] ND Not determined.

2.2.3 Occurrence of brominated alkaloids within the *Amathia* genus

Alkaloids represent the major class of secondary metabolites described from marine bryozoans, with numerous reports of halogenated compounds.[182] The genus *Amathia* particularly has been a rich source of brominated alkaloids.[182,212-226]

The first report of brominated alkaloids from the *Amathia* genus was in 1985 with the description of amathamides A (**95**) and B (**96**) from *A. wilsoni* from the East coast of Tasmania by Blackman *et al.*[226] Both compounds (**95**) and (**96**) are closely related, differing only by the stereochemistry of their double bond. Shortly after, further amathamides, C-F (**97-100**), were reported from various collections of *A. wilsoni* from Tasmania also by Blackman *et al.*[227] No significant variations in the alkaloid content were observed within colonies of the bryozoan from the same location. In contrast, differences were detected between samples collected from different locations.[227] Amathamide G (**101**) was isolated from Tasmanian *A. convoluta*, while *A. pinnata* contained amathamide C (**97**).[228] Finally, amathamide H (**102**) was isolated from Australian *A. wilsoni* and showed modest anti-malarial and anti-trypanosomal activity against the 3D7 and Dd2 strains of *P. falciparum* (IC_{50} 10.2 and 28 µM, respectively), and against *Trypanosoma brucei brucei* growth (IC_{50} 32 µM).[225]

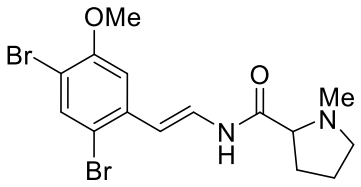

95

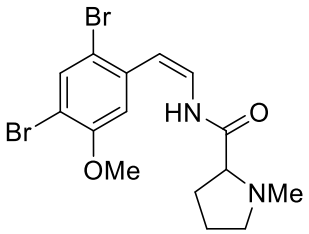

96

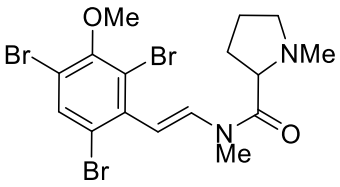

97

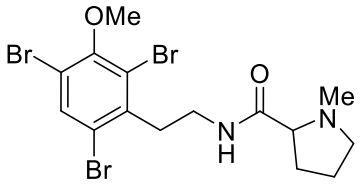

98

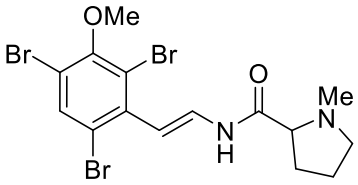

99

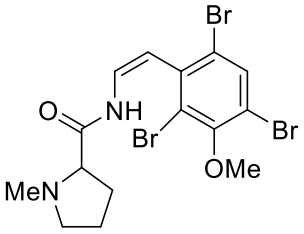

100

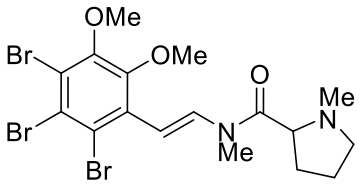

101

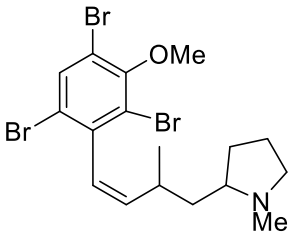

102

Besides compound (**101**), the bryozoan *A. convoluta* has been the source of numerous brominated alkaloids, including convolutamides, convolutindole A, and convolutamines.[213,214,216,221] Convolutamides A-F, isolated from Floridian specimens and displaying unique *γ*-lactam and dibromophenol ring systems, are currently the only members of the convolutamide class known.[213] To note, a mixture of convolutamides A and B exhibited cytotoxicity against L1210 murine leukaemia and KB human epidermoid carcinoma cells (IC_{50} 4.8 and 2.8 μg mL^{-1}, respectively).[213]

β-Phenylethylamine alkaloids are also prevalent within *A. convoluta* from Florida, with an early study reporting the isolation of convolutamines A-E (**103-107**).[214] Further convolutamines, namely F-H (**108-110**), were isolated several years later from Floridian and Tasmanian specimens of *A. convoluta*.[221] Convolutamines I (**111**) and J (**112**) were described by Davis *et al.* in 2011, but this time from *A. tortuosa* from Australia, as part of a programme aiming to identify new antitrypanosomal compounds.[222] Compound (**111**) was the most active against the *T. b. brucei* parasite (IC_{50} value of 1.1 μM).[222] The most recently reported members of the convolutamine class were described in 2020 by Kleks *et al.* from Australian *A. lamourouxi* by means of antiplasmodial activity guided-isolation.[212] Convolutamine K (**113**) displayed moderate activity against the 3D7 strain (IC_{50} value of 1.7 μM) while convolutamine L (**94**) displayed weak activity (IC_{50} value of 11 μM), suggesting that the *N,N*-dimethylpropan-1-ammonium moiety is responsible for the six-fold increase in bioactivity.[212]

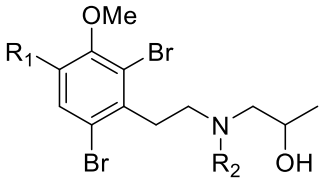

103 R_1 = Br, R_2 = Me
104 R_1 = H, R_2 = Me
105 R_1 = Br, R_2 = H

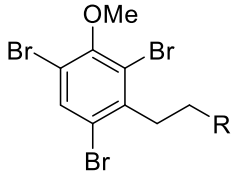

106 R =

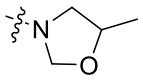

107 R =

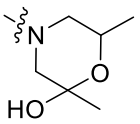

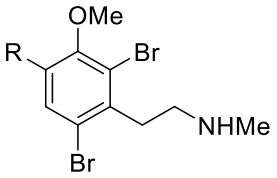

108 R = Br
109 R = H

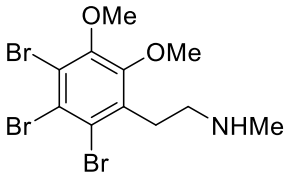

110

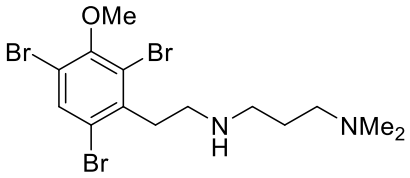

111

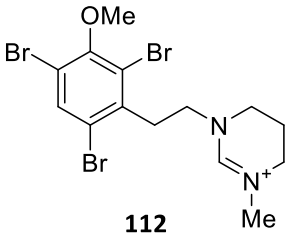

112

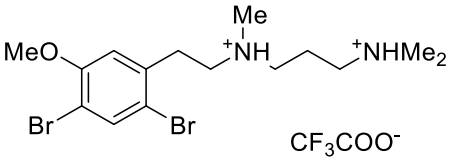

113

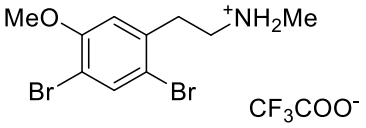

94

The convolutindole class is currently represented by a single member, convolutindole A, obtained from Tasmanian *A. convoluta*, along with compound (**110**) and compound (**101**).[216] The convolutamydine class is closely related to compound (**94**) but differs by the presence of a dibromohydroxyoxindole moiety.[220] Convolutamidyne A, displaying activity in the differentiation of HL-60 cells, was the first member of the class to be described from Floridian *A. convoluta*.[220] Convolutamydines B-E were also reported from *A. convoluta* and convolutamydine B displayed similar activity to convolutamydine A, although to a lesser extent.[215,221]

The first volutamides A-E were described from the temperate Atlantic *A. convoluta* and are biosynthetically related to the amathamides.[218] Recently, further volutamides F-H, were described from the same collection of Australian *A. lamourouxi* that yielded compounds (**94**) and (**113**).[212] Volutamides G and H displayed sub-micromolar antiplasmodial activity against two *P. falciparum* strains (IC_{50} 0.57-0.85 µM).[212]

Sparked by the discovery of volutamides A-E from Atlantic *A. convoluta*, another Atlantic bryozoan, *A. alternata*, was investigated.[219] This resulted in the isolation of four bromotryptamine peptides, alternatamides A-D, among which A-C showed modest antibacterial activity against a variety of strains (MIC values between 4 and 32 μg mL^{-1}).[219]

Another type of brominated alkaloids described from the *Amathia* genus are the dibrominated amathaspiramides, with amathaspiramides A-F (**114-119**) obtained from New Zealand *Amathia wilsoni*.[217] To note, the New Zealand bryozoan extract did not contain any amathamides, which were previously isolated from Australian *A. wilsoni,*[226,227] indicating possible genetic symbiont variability or different environmental conditions for the New Zealand population.[217] Wilsonamines A (**120**) and B (**121**) were also later isolated from Australian *A. wilsoni* and possess a bicyclic hexahydropyrrolo[1,2-*c*]imidazol-1-one ring system so are structurally related to dysibetaine PP from *Dysidea herbacea* mentioned in Chapter 4, Section 4.2.2.[225]

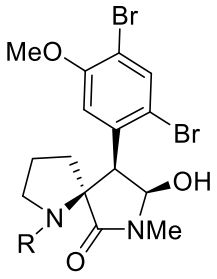

114 R = Me
116 R = H

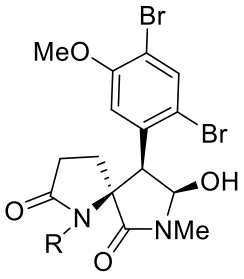

115 R = Me
117 R = H

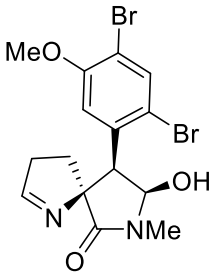

118

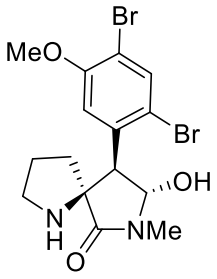

119

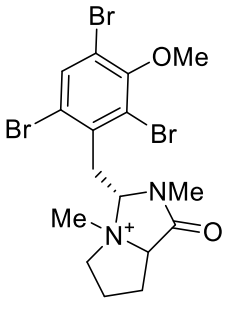

120

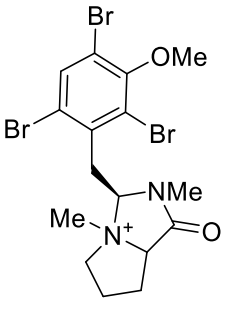

121

Finally, kororamides A and B are tribrominated indole alkaloids isolated from Australian *A. tortuosa.*[223,224] To note, kororamide B also possesses the rare hexahydropyrrolo[1,2-*c*]imidazol-1-one moiety and induced a phenotypic signature on a cell line derived from a Parkinson's disease patient, suggesting that it may affect vesicular trafficking, or the process of transporting molecules using small membrane-bound vesicles, implicated in the disease.[223]

2.2.4 Concluding remarks

Convolutamine L (**94**), initially isolated from Australian *A. lamourouxi*, represents the first metabolite reported from the New Zealand endemic bryozoan *Amathia gracei*. Numerous other minor brominated alkaloids were detected by LC-MS analysis and attempts to isolate these by various chromatographic methods, including ion-exchange columns, silica columns, liquid-liquid partition and reversed phase C18 bench columns were undertaken but proved unsuccessful. These alkaloids were present in minimal quantity, which complicated the purification and characterisation. Attempts to collect a greater quantity of *A. gracei* were undertaken but the bryozoan could not be located at the previous collection site, possibly due to warming sea temperatures or because of the amount of sediments now present after major storm events.

2.3 New Zealand nudibranchs

New Zealand waters house a great diversity of gastropod molluscs, among which are approximately eighty nudibranch species, including twelve endemic species.[206] Up until the early 2000s, there was a lack of studies investigating the chemistry of New Zealand nudibranchs, as mentioned in a 2006 review on the chemistry of Australian and New Zealand molluscs by the Garson research group.[229] The first report of metabolites isolated from New Zealand opisthobranchs was in 2005 when Grkovic *et al*. described several known compounds from four nudibranch species collected in the North Island,[230] among which two, *Ceratosoma amoenum* and *Dendrodoris krusensternii,* were studied over the course of this current research. In 2008, an investigation into two New Zealand species collected off the northern coast of the North Island, namely *Tritonia incerta* and *Aphelodoris luctuosa*, and three previously studied species was reported, and several new compounds were isolated.[231] Some of the metabolites described during these two studies were also isolated during this research and are discussed when relevant.

Despite these two studies,[230,231] very little is known about the ecology and the diet of nudibranch species inhabiting New Zealand waters,[230] and many endemic species remain chemically unstudied. This research aims to provide more insights into the ecology and chemistry of New Zealand nudibranchs by studying previously unexplored endemic species and by reinvestigating species by combining chemical and ecological aspects.

Over the course of this research, six nudibranch species were studied. Three of these, *P. hedgpethi, C. amoenum* and *G. aureomarginatus,* were found in the vicinity of potential prey and their diet was assessed by feeding-choice experiments presented in Chapter 3, followed by chemical investigation described in Chapter 4. The three remaining nudibranchs species *D. krusensternii*, *D. nigra* and *A. luctuosa*, had previously been reported feeding on silicaceous sponges,[206] but in this study, no sponge prey were found in their vicinity, nor were they found on any prey upon collection. Instead, all individuals were either found crawling on sand or sea grass beds, or on rocky substrate lacking any potential prey. Therefore, relevant feeding-choice experiments could not be conducted. Instead, an approach based on cytotoxicity screening, chemical analysis, metabolite distribution studies and morphological analysis was

conducted to offer insights into their chemistry, and the possible origin and role of the metabolites isolated.

2.3.1 Cytotoxicity screening

As part of the approach mentioned above, the crude extracts obtained from whole-body and dissected nudibranch specimens, along with their spawned egg masses, were screened for cytotoxicity against the human cervical cancer cell line HeLa using a MTT assay, prior to being investigated chemically.

The MTT assay is a colorimetric method used to evaluate the metabolic activity of cells. This assay relies on the conversion of the tetrazolium dye MTT (3-(4,5-dimethylthiazol-2-yl)-2,5-diphenyltetrazolium bromide) into insoluble purple formazan crystals, which indicate mitochondrial activity.[232] For most cell lines, including HeLa cells, the mitochondrial activity is related to the number of viable cells. Therefore, this assay has been widely used to assess the *in vitro* cytotoxicity of numerous drugs on cancer cell lines,[232] and on nudibranch extracts and natural products.[163,233,234] Upon dissolution of the formazan crystals with a solubilising solution, the intensity of the purple colour is directly proportional to the number of metabolically active cells, without the need for cell counting.[232] To avoid using a high volume of cell culture grade DMSO, a solubilising solution of sodium dodecyl sulphate and hydrochloric acid (SDS-HCl) was made using a recipe commonly used in the cell culture laboratory where the assay was performed. Details of the assay method can be found in Chapter 7 – Experimental, Section 7.7.6. Prior to the bioassays, the cell viability was assessed with the stain trypan blue whereby dead cells appear blue under a microscope upon the loss of membrane integrity, as opposed to healthy cells which appear white. Only cells above 90% viability were used for the bioassay. Details of the cell viability assessment methodology can be found in Chapter 7 – Experimental, Section 7.7.4.

This screening aimed to provide indirect insights into the metabolite distribution within the nudibranch body and any potential transfer to the egg mass. Upon isolation of metabolites from the crude extracts, the cytotoxicity of the pure compounds was assessed using the same method and compared with the initial cytotoxicity screening to investigate the potential ecological role of the metabolite.

2.4 *Dendrodoris krusensternii*

*Dendrodoris krusensternii (*Figure 31, J. E. Gray., 1850) (Family: Dendrodorididae, Figure 32), formerly known as *Dendrodoris denisoni*,[235] and often referred to as the "gem doris", is one of the largest nudibranchs found in New Zealand, reaching no less than six to seven cm in length on average.[206] It is easily recognisable by its characteristic chocolate brown areas and vivid blue spots found on its mantle, in between pale brown pustules.[206] *D. krusensternii* is prevalent within Indo-Pacific waters, including on the east coast of the North Island of New Zealand, where it is commonly found in the low-tidal zone feeding on silicaceous sponges.[206]

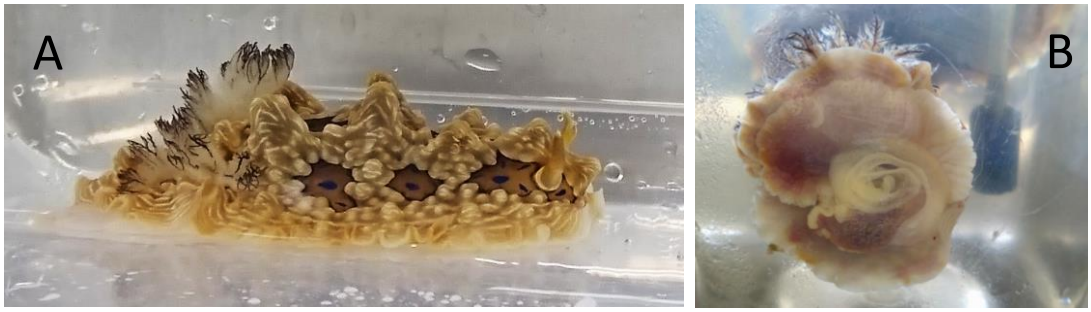

Figure 31: A- *Dendrodoris krusensternii* (7 cm long) crawling in a tank. B- *Dendrodoris krusensternii* spawning in a tank.

Suborder Doridina
Infraorder Doridoidei
Superfamily Phyllidioidea
Family Dendrodorididae
Genus *Dendrodoris*
Species *Dendrodoris krusensternii*

Figure 32: Taxonomic classification of *Dendrodoris krusensternii* according to the World Register of Marine Species (WoRMS).[236]

2.4.1 Cytotoxic activity of crude extracts

A specimen of *D. krusensternii* was collected from Bridge Mount, Otago in 2020 and was extracted whole. Another specimen was collected from Salisbury Wharf in Tauranga (GPS coordinates available Chapter 7 – Experimental, Section 7.2.1) in 2021 and was dissected into mantle and digestive gland, before separate extraction of each body part. One specimen was collected from Dive Crescent, Tauranga (GPS coordinates available Chapter 7 – Experimental, Section 7.2.1) in December 2022 and was kept for a few days in a tank where it spawned an egg mass (Figure 31). Crude extracts of the two nudibranch specimens and the egg mass were screened for cytotoxic activity against HeLa cells following the procedure described in Chapter 7 - Experimental, Section 7.7.6. The nudibranch specimen from Dive Crescent was not screened due to the limited number of wells on the 96-well plates. All the crude extracts displayed minimal cytotoxicity (Table 2). Despite this, the extract of the whole-body specimen was investigated further because the extraction afforded a higher mass of crude extract.

Table 2: IC_{50} values of the crude extracts of *Dendrodoris krusensternii* (whole-body and dissected) and its eggs on HeLa cells using an MTT assay.

Sample	Whole-body	Digestive organs	Mantle	Eggs spawned
IC_{50} (μg mL^{-1})	>100	>100	>100	> 100

2.4.2 Isolation procedure

The crude extract of the whole specimen collected in 2020 from Bridge Mount, Otago was purified by reversed phase bench column chromatography. A fraction displayed similar HR-ESI-MS data to cinnamolide (**122**) previously isolated from New Zealand specimens of *D. krusensternii* by Grkovic *et al*.,[230] and was further purified by normal phase bench column chromatography using a gradient of dichloromethane and methanol to afford compound (**122**) (Figure 33).

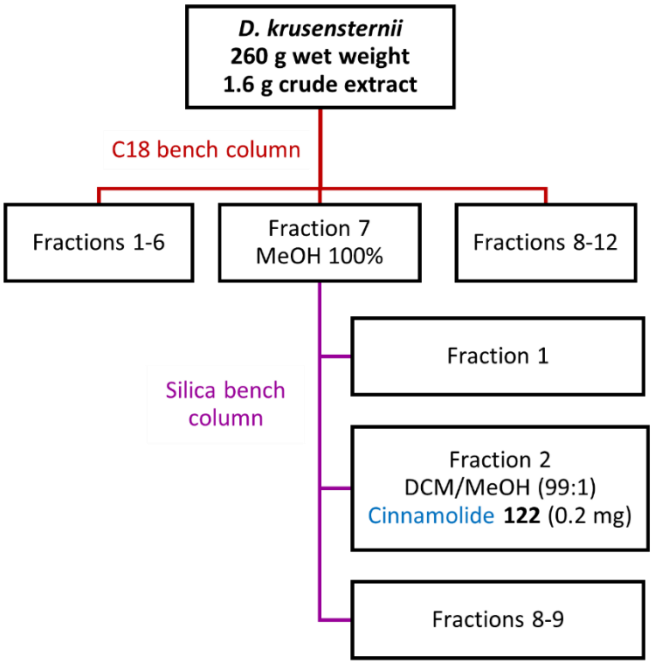

Figure 33 : The isolation procedure for cinnamolide (**122**) from *Dendrodoris krusensternii.*

2.4.3 Cinnamolide

Cinnamolide (**122**) was isolated as a white amorphous solid displaying a $[M + Na]^+$ ion at *m/z* 257.1291 in HR-ESI-MS positive ion mode, corresponding to a molecular formula of $C_{15}H_{22}O_2Na$. The ^1H NMR spectroscopic data (Table 3, Appendix A.2) displayed three methyl singlets at δ_H 0.81, 0.92 and 0.95, each integrating for three protons, along with two oxymethylene protons displayed as two triplets at δ_H 4.04 and 4.38, and one alkenyl proton displayed as a sharp quartet at δ_H 6.88. The carbon spectrum revealed fifteen signals, including one protonated sp^2 signal corresponding to a protonated alkenyl carbon and one quaternary signal at δ_C 170.5 corresponding to a lactone resonance. The ^{13}C NMR spectrum also displayed ten protonated sp^3 signals, including a deshielded resonance at δ_C 67.2 corresponding to a protonated oxymethylene carbon, consistent with the structure of compound (**122**). A series of COSY and HMBC correlations (Figure 34) confirmed the assignment of compound (**122**).

Table 3: ^{1}H and ^{13}C NMR data for cinnamolide (**122**) compared with literature values (chloroform-*d*).[237,238]

	^{1}H (mult, *J* in Hz)	
Atom	[a] **Experimental**	[b] **Literature**
1	1.19 (1H, m) 1.59 (1H, m)	1.10 - 1.70 (6H, m)
2	1.58 (1H, m) 1.48 (1H, m)	
3	1.51 (1H, m) 1.23 (1H, m)	
5	1.39 (1H, m)	1.40 (1H, dd, 5.5, 12)
6	2.11 (1H, m) 2.42 (1H, dq, 20.3, 4.1)	2.12 (1H, dddd, 3.5, 5.0, 12.0, 19.0) 2.42 (1H, dddd, 4.0, 4.0, 5.5, 19.0)
7	6.88 (1H, q, 6.9, 3.4)	6.88 (1H, ddd, 3.5, 3.5, 4.0)
9	2.82 (1H, m)	2.82 (1H, ddddd, 3.5, 4.0, 5.0, 9.5, 9.5)
11	4.04 (1H, t, 9.0) 4.38 (1H, t, 9.0)	[c] ND 4.38 (1H, dd, 9.5, 9.5)
12	0.81 (3H, s)	0.82 (3H, s)
13/14	0.95 (3H, s) 0.92 (3H, s)	0.93 (3H, s) 0.95 (3H, s)

[a] values reported in chloroform-*d*, ^{1}H 600 MHz, [b] values reported in chloroform-*d*, ^{1}H 250 MHz (Hollinshead *et al.* 1983[239]), [c] ND Not determined.

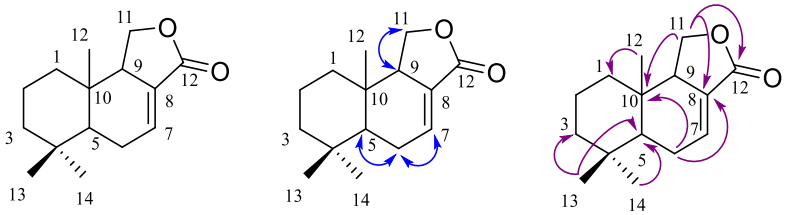

122

Figure 34: Selected COSY (blue) and HMBC (purple) correlations for cinnamolide (**122**).

Many bicyclic drimane sesquiterpenes or drimane-derived sesquiterpenes have been isolated from vascular plants, including compound (**122**) which was first described from the bark of the Madagascan tree *Cinnamosma fragrans*.[237,238] It was subsequently described from *D. krusensternii* from three different collections sites in New Zealand, which represented the first report of compound (**122**) from marine organisms.[230] The occurrence and possible origin of drimane sesquiterpenes is described further in Section 2.5.7 of this chapter. Compound (**122**) was assessed for cytotoxic activity against HeLa cells and displayed minimal activity (IC_{50} 34.2 µM, or 8 µg mL^{-1}), although the activity was much higher than that of the crude extracts of the whole-body, mantle, digestive gland and eggs.

2.4.4 Metabolite distribution

To investigate the possible ecological role of compound (**122**), its distribution within specific parts of the nudibranch's body was examined by LC-MS screening of the crude extracts following the methodology described in Chapter 7 – Experimental, Section 7.1.11. The compound was present in the digestive gland, mantle, whole-body, and egg mass crude extracts (in minimal quantity in the last) (Figure 35). Based on the peak intensities, compound (**122**) appears to be more concentrated in the mantle, which is consistent with a previous study on *D. krusensternii* from New Zealand.[230] Independent of the origin of compound (**122**), its presence in higher concentration in the mantle strongly suggests a defensive role but feeding deterrence studies with locally relevant predators need to be conducted to confirm this.

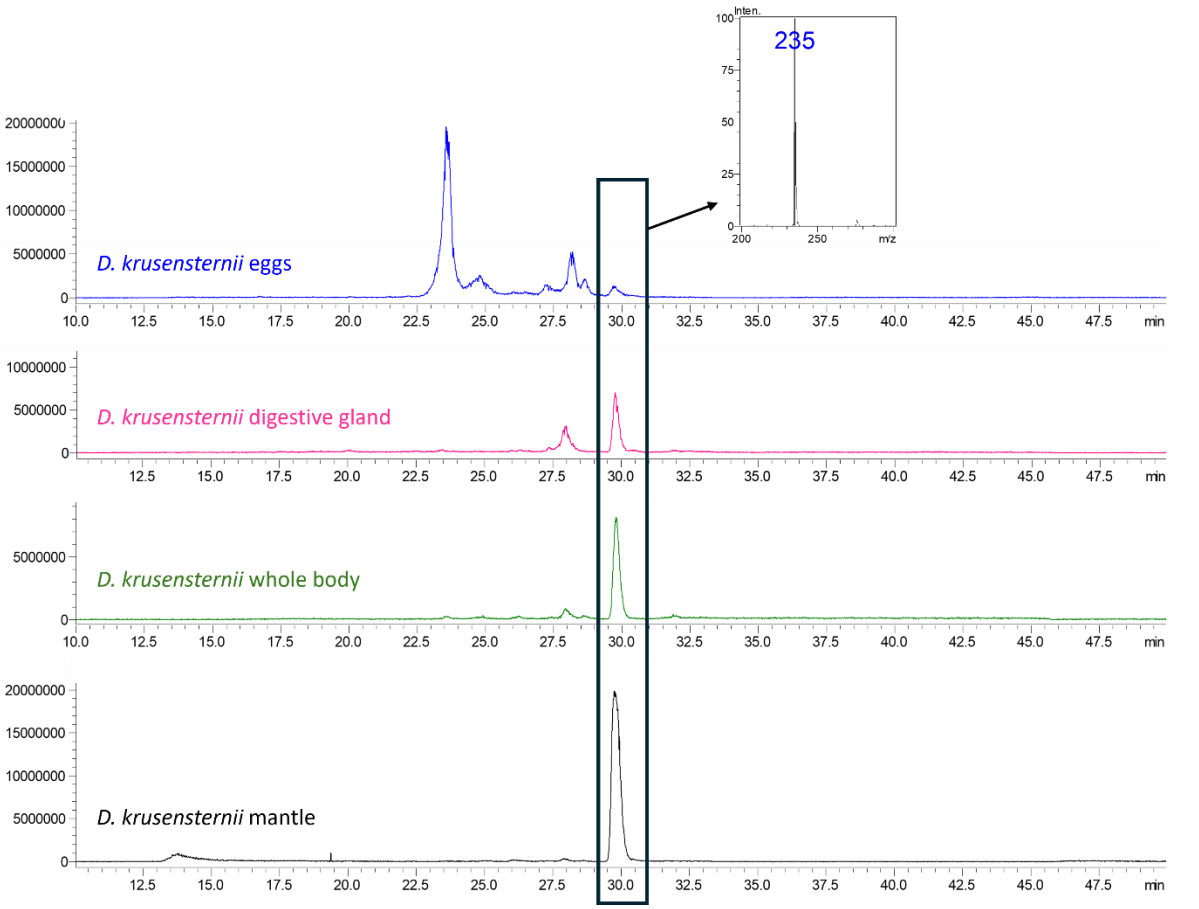

Figure 35: Extracted ion mode (235.2) LC-MS chromatogram (positive ion mode) of the four *Dendrodoris krusensternii* crude extracts showing the presence of cinnamolide (**122**).

In the initial report of compound (**122**) from *D. krusensternii*,[230] it was suggested that the drimane sesquiterpene might be biosynthesised *de novo* because of its presence in individuals from different geographical locations.[230] During this research, similar results were obtained where both whole and dissected specimens, collected from different locations, contained compound (**122**). Surprisingly, cinnamolide (**122**) does not appear in high concentration in the eggs, although this could potentially be explained by the fact that the eggs were spawned when the nudibranch had been in the laboratory setting for a few days and was likely under stress, potentially impacting the viability or quality of the eggs as has been previously reported [240] and the transfer of metabolites.

2.4.5 Investigation of the diet

With the aim to shed more light onto the diet of *D. krusensternii*, a specimen previously collected from Salisbury Wharf was dissected, and the digestive glands were dissolved in nitric acid, and washed, prior to being observed under a stereo microscope to look for the presence of sponge spicules. However, none were observed.

Upon collection of several *D. krusensternii* specimens from the Dive Crescent sponge meadow in December 2022, attempts to establish the nudibranch's diet were conducted by feeding-choice experiments even though the nudibranchs were not found on potential prey at the time of collection. Several sponge species were trialled, however the nudibranchs were extremely unresponsive during the experiments and did not explore the tanks. This species did not survive well in tanks and could only be kept for a couple of days, possibly because of the environmental stressors, such as water temperature and salinity. Based on these results, the focus was shifted to other species to conduct the feeding-choice experiments.

2.4.6 Concluding remarks

The drimane sesquiterpene cinnamolide (**122**) was isolated from a specimen of *D. krusensternii*. Compound (**122**) was present in the digestive organs and in higher concentration in the mantle, which was consistent with a previous study[230] and might suggest a defensive role. Compound (**122**) was also detected in the egg mass, representing the first report of the drimane sesquiterpene from the egg mass of a nudibranch, and is consistent with a potential defensive role. To investigate the ecological role further, collection and extraction of wild spawned eggs is required to determine if compound (**122**) is present and if so, at what concentration.

2.5 *Dendrodoris nigra*

Dendrodoris nigra (Figure 36A, W. Stimpson, 1855) (Family*:* Dendrodorididae, Figure 37) displays a distinctive velvet black to dark grey mantle and black rhinophores with black tips.[206] Adult specimens commonly reach between three to five cm in length and inhabit sheltered shores, at a maximum depth of five metres.[206] *D. nigra* is widespread around the Indo-Pacific region, including along the coast of the North Island of New Zealand, where it feeds on silicaceous sponges.[206] *D. nigra* has been reported feeding on *Halichondria dura* and in Hawaii, on the sponge *Suberites* sp.[241,242]

Figure 36: A- *Dendrodoris nigra* (5 cm long) in a sea grass bed at Pahoia beach. B- Pahoia beach collection site. C- Bright yellow egg masses found alongside *Dendrodoris nigra*. D- Bright yellow egg mass spawned in the laboratory.

Suborder Doridina
Infraorder Doridoidei
Superfamily Phyllidioidea
Family Dendrodorididae
Genus *Dendrodoris*
Species *Dendrodoris nigra*

Figure 37: Taxonomic classification of *Dendrodoris nigra* according to the World Register of Marine Species (WoRMS).[243]

To date, two drimane sesquiterpenes, polygodial (**29**) and olepupuane (**123**), have been isolated from *D. nigra* from Hawaii.[241] Both were antifeedant against the Pacific damsel fish *Dascyllus aruanus,* at comparable concentrations (ED_{50} 15-20 µg mg^{-1} of pellet).[241]

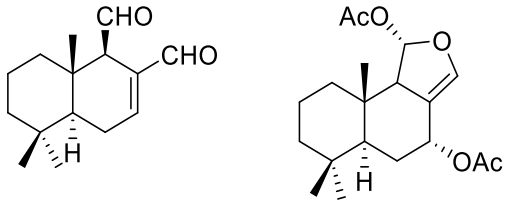

29 **123**

Specimens of *D. nigra* were initially collected at Pahoia beach, Tauranga (GPS coordinates available Chapter 7 – Experimental, Section 7.2.1) in March 2021 in a sea grass bed (Figure 36A and B). The nudibranchs were found in an open shore environment, in the low-tidal zone, at depths between 10 to 40 cm. The specimens were found alongside bright yellow egg masses (Figure 36C), believed to belong to *D. nigra* because of the absence of other nudibranch species at the collection site. Several specimens were collected and kept in a tank for several days and a specimen spawned an egg mass displaying the same colour and shape to the ones found in the wild (Figure 36D), confirming the origin of the wild egg masses. The bright colour of the egg masses was highly noticeable at the collection site, especially at the low depth at which the nudibranchs were collected and could act as a warning signal for potential predators. Surprisingly, no sponges, bryozoans or other potential prey were observed at the collection site, and therefore no relevant feeding-choice experiments could be conducted. Several egg masses and nudibranchs were collected and directly frozen to be investigated chemically.

2.5.1 Cytotoxic activity of crude extracts

Four crude extracts resulting from the separate extraction of a whole-body nudibranch, a dissected specimen (internal organs and mantle) and the spawned egg coil from *D. nigra* (Figure 36D) were screened for cytotoxic activity against HeLa cells. All the crude extracts displayed minimal cytotoxicity (Table 4). Despite this, the crude extract resulting from the extraction of the egg mass was investigated further because of the potential ecological relevance of the bright colouration of the egg mass.

Table 4: IC_{50} values of the crude extracts of *Dendrodoris nigra* (whole-body and dissected) and its eggs on HeLa cells using an MTT assay.

Sample	Whole-body	Digestive organs	Mantle	Eggs spawned
IC_{50} (µg mL^{-1})	>100	>100	>100	> 100

2.5.2 Isolation procedure

An egg mass collected from the wild was extracted and purified by reversed phase bench column chromatography to afford 7-deacetoxy-olepupuane (**124**) and a mixture of drimane esters (**125**) (Figure 38).

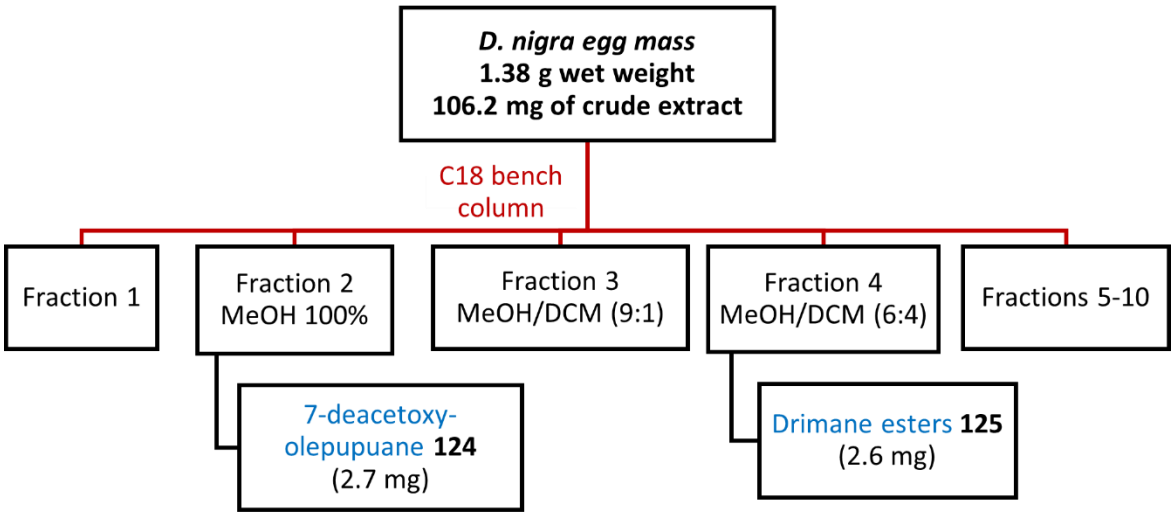

Figure 38: The isolation procedure for 7-deacetoxy-olepupuane **(124)** and drimane esters (**125**) from *Dendrodoris nigra.*

2.5.3 7-Deacetoxy-olepupuane

7-Deacetoxy-olepupuane (**124**) was isolated as a white solid displaying a $[M + Na]^+$ ion at *m/z* 301.1056 in HR-ESI-MS positive ion mode, corresponding to a molecular formula of $C_{17}H_{26}O_3Na$. The ^1H NMR spectrum (Appendix A.3) contained three singlets, each integrating for three protons, at δ_H 0.81, 0.83 and 0.88, representative of three methyl groups, one oxymethine proton doublet at δ_H 6.30, one acetoxy methyl singlet at δ_H 2.07 which integrated

for three protons, along with one deshielded alkenyl proton doublet of doublets at δ_H 6.05. The carbon spectrum contained seventeen signals, including one protonated sp^2 signal at δ_C 134.4 corresponding to the protonated alkenyl signal and one quaternary signal at δ_C 170.1 representing the acetoxy carbonyl group. The ^{13}C NMR spectrum also displayed twelve protonated sp^3 signals, including a deshielded resonance at δ_C 98.3 representative of a dioxygenated oxymethine carbon, consistent with the structure of compound **124**. A series of COSY and HMBC correlations (Figure 39) confirmed the assignment of the drimane sesquiterpene **124** (Table 5).

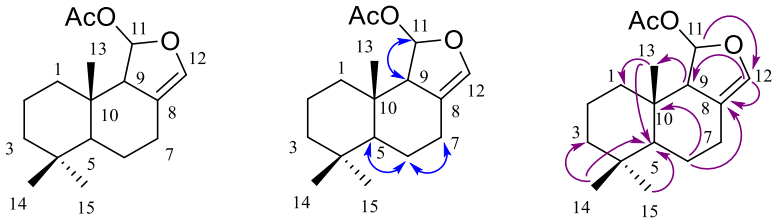

124

Figure 39: Selected COSY (blue) and HMBC (purple) correlations for 7-deacetoxy-olepupuane (**124**).

Table 5: ^{1}H and ^{13}C NMR data for 7-deacetoxy-olepupuane (**124**) compared with literature values (chloroform-*d*).[244]

	^{1}H (mult, *J* in Hz)		^{13}C	
Atom	[a] **Experimental**	[b] **Literature**	[a] **Experimental**	[b] **Literature**
1	1.09 (dddd, 13.1, 13.0, 3.5) 1.63 (bs)	1.08 (dddd, 12.9, 12.9, 3.6, <1 Hz) 1.62 (dddd, 12.9, 3.4, <1 Hz)	39.5	39.3
2	1.55 (ddddd, 14.0, 13.7, 13.6, 3.3, 3.1) 1.45 (ddddd, 12.9, 3.5, 3.4)	1.55 (ddddd, 13.8, 13.6, 12.9, 3.4, 3.4) 1.45 (ddddd, 13.6, 3.8, 3.6)	18.5	18.3
3	1.19 (dddd, 14.2, 13.1, 3.8) 1.42 (14.1, 3.1, 1.8)	1.17 (dddd, 13.8, 13.8, 3.8, <1 Hz) 1.41 (dddd, 13.8, 3.4, <1 Hz)	42.1	42.0
4			33.2	32.9
5	0.98 (dd, 12.5, 2.6)	0.98 (dd, 12.5, 2.6)	53.1	52.9
6	[c] ND 1.69 (dddd, 13.0, 5.9, 2.1, 1.9)	1.25 (ddd, 13.8, 12.7, 12.5m, 3.6) 1.69 (dddd, 12.7, 5.7, 2.6, 1.1)	22.7	22.5
7	2.00 (ddddd, 12.8, 12.2, 6.3, 1.9, 1.5) 2.48 (ddd, 13.8, 5.0, 1.6)	1.98 (ddddd, 13.8, 13.7, 5.7, 1.9, 1.9) 2.46 (ddd, 13.7, 3.6, 1.1)	23.1	23.0
8			114.7	114.3
9	2.28 (bs)	2.25 (bs, 1.8, 1.9, 1.9, <1 Hz)	63.9	63.7
10			37.0	36.8
11	6.30 (d, 2.1)	6.27 (d, 1.8)	98.3	98.1
12	6.05 (dd, 2.1, 2.1)	6.02 (dd, 1.9, 1.9)	134.4	134.2
13	0.81 (s)	0.78 (bs, <1 Hz)	14.1	13.7
14	0.83 (s)	0.80 (bs, <1 Hz, <1 Hz)	21.8	21.5
15	0.88 (s)	0.86 (s)	33.6	33.3
OAc	2.07 (s)	2.05 (s)	21.3 170.1	20.9 169.9

[a] values reported in chloroform-*d*, ^{1}H 600 MHz, ^{13}C 150 MHz, [b] values reported in chloroform-*d*, ^{1}H 400 MHz, ^{13}C 100 MHz (Garson *et al.* 1992[244]), [c] ND Not determined because of overlapping signals.

Compound (**124**) was initially isolated from the temperate marine sponge *Dysidea* sp. from New South Wales, Australia and displayed minimal cytotoxicity against P388 cells *in vitro* (IC_{50} 16.4 µg mL-1).[244] Sesquiterpene (**124**) was later isolated from *Dendrodoris limbata* from Italy and *D. arborescens* from Japan, and both populations are able to biosynthesise it *de novo*.[245] It was suggested that compound (**124**) is a precursor to other drimane sesquiterpenoids upon conversion into the toxic dialdehyde polygodial (**29**) and olepupuane (**123**) for defence purposes.[246] Compound (**124**) differs from compound (**123**), previously isolated from *D. nigra*,[241] by the absence of the acetoxy group at position 7.

2.5.4 Drimane esters

The ^{1}H NMR spectroscopic data of the drimane esters (**125**) (Table 6) displayed identical signals to the ^{1}H NMR spectroscopic data of compound (**124**) (Table 5), except for the absence of the singlet at δ_H 2.07 representative of the acetoxy methyl, and the presence of a broad signal at 5.34 representing alkene protons, along with an intense signal at δ_H 1.26 representing the methylene protons of the alkyl chain. Additionally, a multiplet at δ_H 2.34, representative of the two protons at position 17, was present in the ^{1}H NMR spectrum (Appendix A.4). The short range HMBC correlation H-17/C-16, along with the characteristic chemical shift of the signal confirmed that the two protons were adjacent to the carbonyl group. All spectral data were in agreement with those reported previously for compound (**125**) (Table 6).[247]

LC-MS analysis of the egg crude extract displayed a prominent peak corresponding to a pseudo-molecular ion $[M + H]^+$ at *m/z* 525, consistent with an alkyl chain containing twenty-one carbons and three alkene bonds. This was consistent with the signal at δ_H 5.34 in the ^{1}H NMR spectrum integrating for six alkene protons located on the alkyl chain.

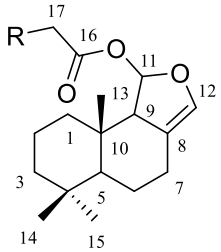

125 R = C19 with three double bonds

Table 6: ^{1}H and ^{13}C NMR data for drimane esters (**125**) compared with literature values (chloroform-*d*).[247]

	^{1}H (mult, *J* in Hz)		^{13}C	
Atom	[a] **Experimental**	[b] **Literature**	[a] **Experimental**	[b] **Literature**
1	[c]	[d]	39.5	39.6
2	[c]	[d]	18.5	18.3
3	[c]	[d]	42.2	42.2
4			33.2	33.2
5	[c]	[d]	53.1	53.1
6	[c]	[d]	22.6	22.7
7	[c]	[d]	23.2	23.3
8			114.6	114.4
9	2.27 (m)	2.30 (m	63.9	64.0
10			37.0	37.0
11	6.31 (1H, d, 2.1)	6.32 (1H, d, 2)	98.2	98.1
12	6.05 (1H, dd, 2.1, 2.1)	6.04 (1H, m, 4)	134.4	134.3
13	0.89 (s)	0.90 (3H)	14.1	14.0
14/15	0.86-0.88 (s)	0.85 (6H, s)	21.7 33.6	21.7 33.6
16			172.9	172.5
17			34.5	34.5
R	5.34 (m) 1.26 (bs)	5.36 (m) 1.25	28.9-29.7	[e] ND

[a] values reported in chloroform-*d*, ^{1}H 600 MHz, ^{13}C 150 MHz, [b] values reported in chloroform-*d* (Cimino *et al.* 1981[247]), [c] identical to compound (**124**), [d] assignment not reported because of the identical carbon resonances with the model compounds heteronemin[248] and perhydrophenanthrenes,[249] [e] ND Not determined.

Drimane esters (**125**) containing a range of fatty acids, were initially isolated from the digestive gland,[247] the hermaphrodite gland and egg masses of *D. limbata*,[241,245] and later on from *Doriopsilla albopunctata* and *Doriopsilla janaina*. It was suggested that compound (**125**) may have a physiological function associated with sexual cycles, and antibacterial protection in the development of the egg mass.[107,245] *D. limbata* and *D. grandiflora* were proven to synthesise the anti-feedant sesquiterpenoid polygodial (**29**) *de novo*, along with compound (**125**).[108,250] Unlike compounds (**29**) and (**123**), the drimane esters (**125**) did not inhibit feeding of the damsel fish *Dascyllus aruanus* at 100 µg mg^{-1}.[241] Compound (**29**) is stored in the mantle while compound (**125**) is found in the digestive glands. The drimane esters (**125**) are believed to be detoxification products of polygodial that could be toxic to *D. limbata* after a long period of time.[108]

2.5.5 Metabolite distribution

To investigate the presence of compounds (**124**) and (**125**) in the nudibranchs and their distribution, the crude extracts used in the cytotoxicity assay (whole-body, digestive gland, mantle and egg mass) were screened by LC-MS in extracted ion mode at *m/z* 279 and 525. The four extracts showed the presence of both compounds (**124**) and (**125**). The concentration of compound (**125**) was relatively consistent in all four extracts, while compound (**124**) was more concentrated in the mantle, followed by the egg mass and digestive glands extracts.

The presence of the drimane esters (**125**) in the digestive glands of *D. nigra* was consistent with its report from the digestive glands of *D. limbata*.[247]

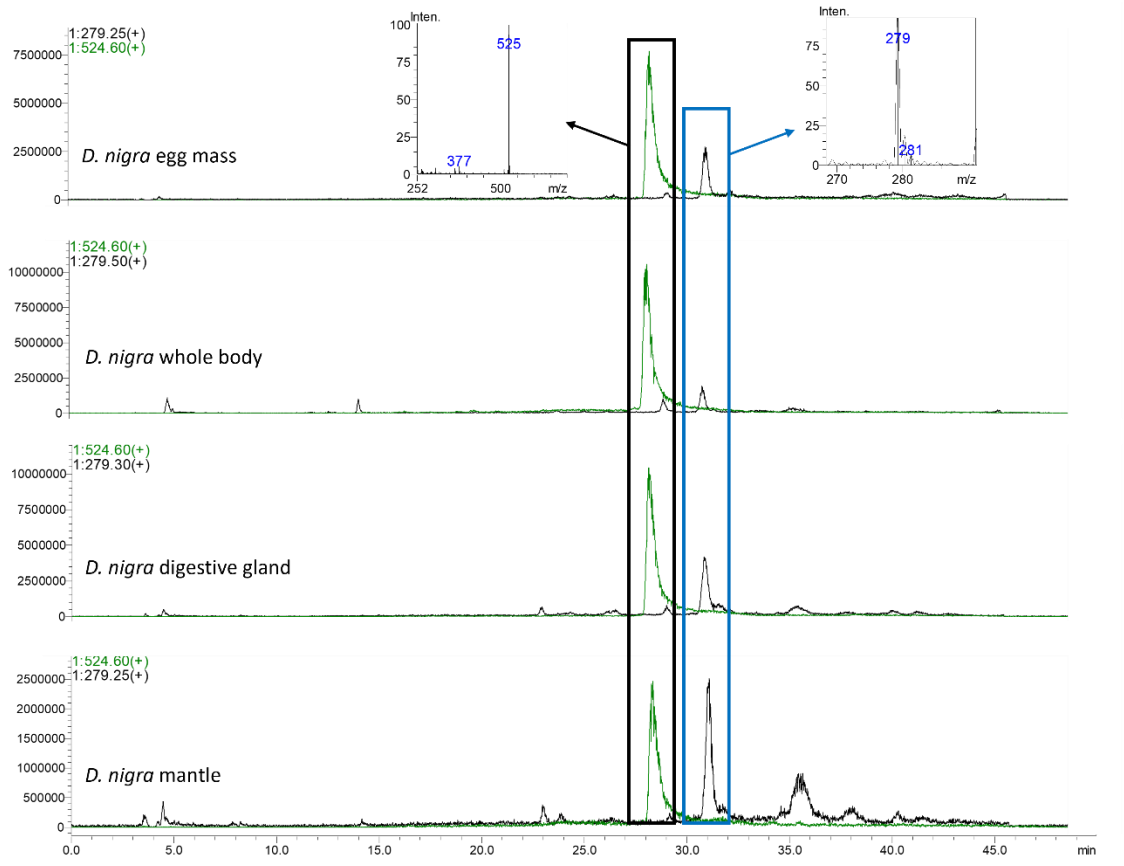

Figure 40: Extracted ion mode (*m/z* 279 and 524) LC-MS chromatogram (positive ion mode) of different *Dendrodoris nigra* crude extracts (whole-body, digestive glands, mantle and eggs) showing the presence of compounds (**124**) (black LC-MS trace) and (**125**) (green LC-MS trace).

2.5.6 Investigation of the diet

The capacity of *Dendrodoris limbata* to biosynthesise *de novo* both compounds (**29**) and (**125**), and of *D. arborescens* to biosynthesise compound (**124**) strongly indicates that *D. nigra* is also able to biosynthesise both compounds.

Despite compounds (**124**) and (**125**) likely originating from *de novo* biosynthesis as opposed to a dietary origin, establishing the diet of *D. nigra* was of interest, especially because compound (**124**) had previously been isolated from *Dysidea* sp.,[244] which is known to inhabit Tauranga waters,[251] although at the time of the initial collection in March 2021, no sponges nor any potential prey were located within the collection site. Interestingly, an estuarine sponge meadow containing primarily three sponge species (*Hymeniacidon* sp., *Halichondria* sp. and *Haliclona* sp.), and potentially *Dysidea* sp., was discovered at Pahoia beach in 2019, but many of the sponges disappeared in 2020 due to severe sedimentation events.[252] The absence of sponge prey during the 2021 observations suggested that the sponge meadow had not recovered from the environmental events.

On a subsequent dive trip in March 2022, efforts were made to investigate the deeper waters surrounding the collection site using SCUBA diving but no sponges of any kind were located. At that time, the population of *D. nigra* at Pahoia beach was abundant, with at least one nudibranch per square metre over a surface of roughly 100 square metres, potentially indicating that the population was prosperous. Two types of filamentous algae were collected from the area, despite it being unlikely that the nudibranchs were feeding on it and were chemically investigated. Neither of the two drimane sesquiterpenoids (**124**) and (**125**) were present in either algal species.

To look for the presence of sponge spicules that could shed more light onto the diet of *D. nigra*, a specimen was dissected, and the digestive glands were observed under a stereo microscope. No sponge spicules were seen. To confirm this, the digestive glands were digested in nitric acid, and washed, before being re-examined under the stereo microscope, although this resulted in the same conclusion. *Dysidea* sponges lack silicaceous sponge spicules and therefore this does not rule out that *D. nigra* is feeding on *Dysidea* sponges, but it does suggest that the nudibranchs are probably not feeding on sponges containing spicules.

On two subsequent collection trips in May and August 2022, attempts were made to collect further specimens of *D. nigra* to prove the *de novo* biosynthesis of both compounds (**124**) and (**125**) but the species could not be located, potentially indicating that the population might not be as prosperous and robust as initially thought. As such, it is likely that *D. nigra* was feeding on the sponge species that used to inhabit the disappeared meadow, and that the nudibranch population died out because of this disappearance and the lack of other potential prey at the collection site.

2.5.7 Occurrence and origin of drimane sesquiterpenes within Dendrodoridídae nudibranchs

Cinnamolide (**122**), 7-deacetoxy-olepupuane (**124**) and the drimane esters (**125**) all display the same drimane sesquiterpene skeleton. This moiety was initially reported in drimenol (**126**), first isolated from the bark of *Drimys winteri* by Appel *et al.*,[253] and has since been reported from a wide range of plants, liverworts, fungi, and marine organisms.[254-260]

Marine sponges, especially of the genus *Dysidea*, have been a prolific source of drimane sesquiterpenes.[256-260] To note, *trans*-dihydroconfertifolin (**127**) was reported from a New Zealand specimen of *Dysidea* sp. and was previously isolated from a Papua New Guinean sponge.[258]

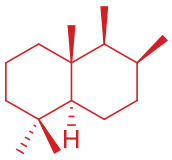

General drimane skeleton

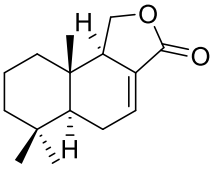

122

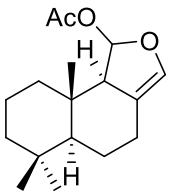

124

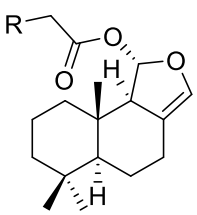

125 R = alkyl (unspecified length)

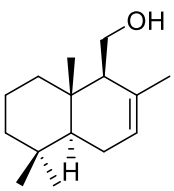

126

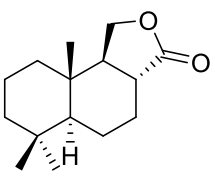

127

Within nudibranchs, the family Dendrodoridae,[261] comprising both *Dendrodoris* and *Doriopsilla* genera, has yielded numerous drimane sesquiterpenoids.[107,247,262-265]

The species *D. albopunctata* and *D. areolata*, both belonging to the *Doriopsilla* genus, contained a range of drimane sesquiterpenes, including the drimane esters (**125**), *ent*-15-acetoxy-pallescensin-A, and isodrimeninol (**128**).[266] *Doriopsilla pelseneeri* from Portugal yielded euryfuran (**129**) and compound (**125**) from the internal gland while *ent*-15-acetoxypallescensin-A was identified from the mantle extract.[267] The antifeedant olepupuane (**123**) was found in *D. albopunctata* and *D. janaina*.[241] The presence of many of these metabolites within sponges suggested a dietary origin in the molluscs,[254] although *de novo* biosynthesis via the acetate/mevalonate pathway of the fatty acid drimane esters (**125**) and *ent*-15-acetoxy-pallescensin-A has been proven in *D. areolata* by means of feeding studies using ^{13}C-labelled glucose.[107]

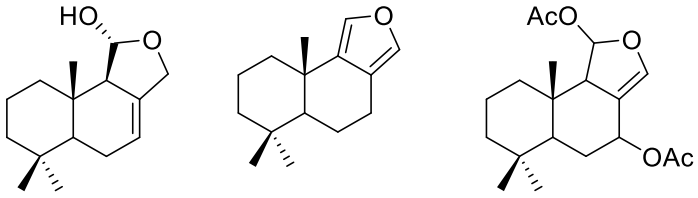

128 **129** **123**

The *Dendrodoris* genus has also yielded a wide range of sesquiterpenoids, including thirteen drimane sesquiterpenes, dendocarbins A-N (**130-143**), along with compound (**128**) and 11-epivaldiviolide (**144**), from Japanese *D. carbunculosa*.[262] *D. carbunculosa* was reported to have a sharp and bitter peppery taste, which was suggested to originate from its main metabolite, compound (**128**) displaying similar sensorial properties.[262] All the drimane sesquiterpenes, isolated from *D. carbunculosa* were tested in a cytotoxicity assay against various strains of murine leukaemia P388 cells. Dendocarbin J (**139**) and compound (**144**) were the most active (IC_{50} 2.5-17 µg mL).[262] Similarly to *D. nigra*, compounds (**29**) and (**123**) were reported from *D. tuberculosa* and *D. krebsii.*[241] As mentioned previously, the origin of compounds (**29**), (**123**) and (**125**) was investigated for three *Dendrodoris* nudibranchs.[108,245,250] *D. grandiflora* and *D. limbata* can biosynthesise polygodial (**29**) and the drimane esters (**125**),[108,250] while *D. arborescens* and *D. limbata* from Japan were proven to biosynthesise 7-deacetoxy-olepupuane (**124**) *de novo*.[245] To note, compound (**124**) was also isolated from a *Dysidea* sponge from Australia.[244]

Investigations of the chemical composition of different populations of *D. krusensternii* from New Zealand and Australia yielded cinnamolide (**122**), initially isolated from the Madagascan tree *Cinnamosma fragrans,*[237,238] as the major metabolite, along with compound (**123**) and the methoxy acetal (**145**).[230] It was suggested that *D. krusensternii* utilises compound (**122**) for defensive purposes.[230]

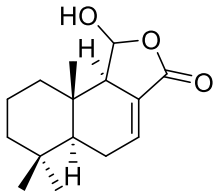

130

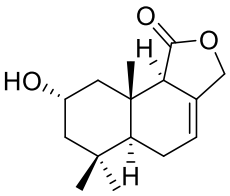

131

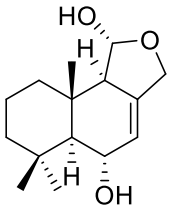

132

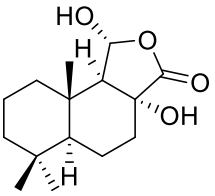

133

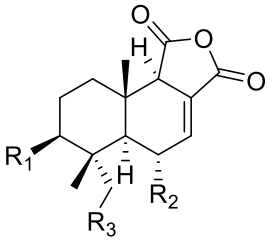

134 R_1 = OH, R_2 = R_3 = H
135 R_1 = R_2 = H, R_3 = OH
136 R_1 = R_3 = H, R_2 = OH
137 R_1 = R_2 = R_3 = H

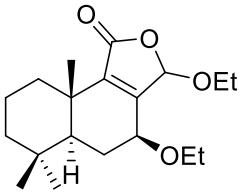

138

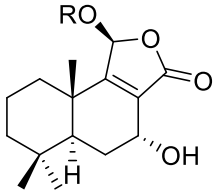

139 R = Et
140 R = H

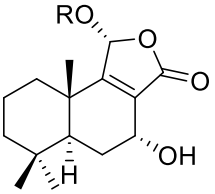

141 R = Et
142 R = H

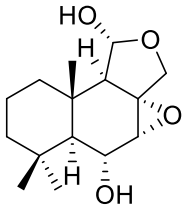

143

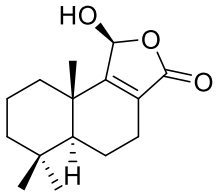

144

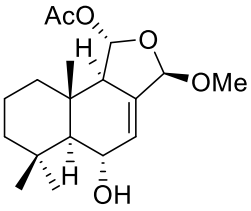

145

2.5.8 Concluding remarks

The two drimane sesquiterpenes (**124**) and **(125**) isolated from *D. nigra* and its egg masses had previously not been reported from this species. Combined with the previous reports of olepupuane (**123**) and polygodial (**29**) from Hawaiian specimens of *D. nigra*, it appears that this species is rich in drimane sesquiterpenes, consistent with other *Dendrodoris* species. The isolation of compound (**124**) from a *Dysidea* sp. sponge is consistent with a dietary origin. However, the absence of *Dysidea* sp. sponges, or any sponge at the collection site, along with the capacity of two other *Dendrodoris* nudibranchs to biosynthesise *de novo* both sesquiterpenoids, points towards a biosynthetic origin. Based on activity, structure and distribution within the nudibranchs, compound (**124**) is believed to be a precursor to other drimane sesquiterpenes involved in the defence mechanism while compound (**125**) might have a physiological function associated with sexual cycles, and antibacterial protection in development of the egg masses.

2.6 *Aphelodoris luctuosa*

Aphelodoris luctuosa (Figure 41, Cheeseman, 1882) (Family*:* Doridiidae, Figure 42) is a dorid nudibranch endemic to New Zealand.[206] It commonly occurs throughout both main islands and display variations in the colouration of the mantle across different geographical locations.[206] In the North Island, individuals display a cream background with brown patterns distributed on the mantle. Adult specimens can reach up to eight cm in length, although between four and six cm is more common.[206] Compared to *D. nigra*, this nudibranch can be found at greater depths, being commonly found between ten to twenty metres deep.[206] *A. luctuosa* is reported to feed on silicaceous sponges[206] and has been observed in areas containing *Latrunculia* sp., but has not been observed to predate on it.[268]

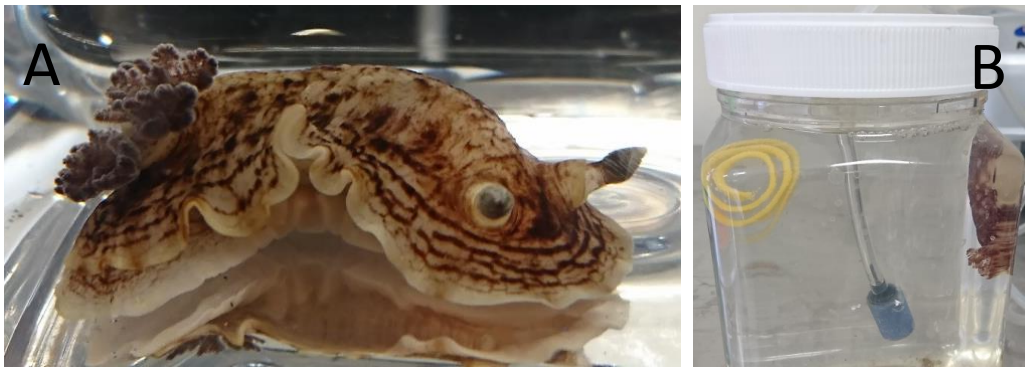

Figure 41: A- *Aphelodoris luctuosa* (7 cm long) crawling in a tank. B- One of the egg masses spawned in a tank by *Aphelodoris luctuosa.*

Suborder Doridina
Infraorder Doridoidei
Superfamily Doridoidea
Family Doridiidae
Genus *Aphelodoris*
Species *Aphelodoris luctuosa*

Figure 42: Taxonomic classification of *Aphelodoris luctuosa* according to the World Register of Marine Species (WoRMS).[269]

2.6.1 Cytotoxic activity of crude extracts

A specimen of *A. luctuosa* was collected from Salisbury Wharf in Tauranga in June 2021, and another individual was collected from Motuputa Island in Tauranga Bay in August 2021. Both specimens were kept in a tank for a few days following their collection and each individual spawned an egg mass (Figure 41). The specimen from Salisbury Wharf and its egg mass were extracted separately following the usual procedure. The specimen from Motuputa Island and its egg mass were put aside and subsequently analysed, as outlined in Section 2.6.2. Another specimen of *A. luctuosa* was collected from Piercy Island, Northland in August 2021 and was dissected into mantle and digestive gland, before separate extraction of each part. The four crude extracts were screened for cytotoxic activity against HeLa cells following the procedure described in Chapter 7 - Experimental, Section 7.7.6. The egg extract was the most active (IC_{50} 8 µg mL^{-1}), followed by the whole-body and digestive gland extracts (IC_{50} 15 µg mL^{-1} each) (Figure 43). The mantle extract displayed minimal activity (IC_{50} > 100 µg mL^{-1}). The difference in activity between the mantle and the digestive gland extracts potentially indicates a different chemical composition or different concentration of compounds. The egg and whole-body extracts were of high interest because of their activity and were investigated first.

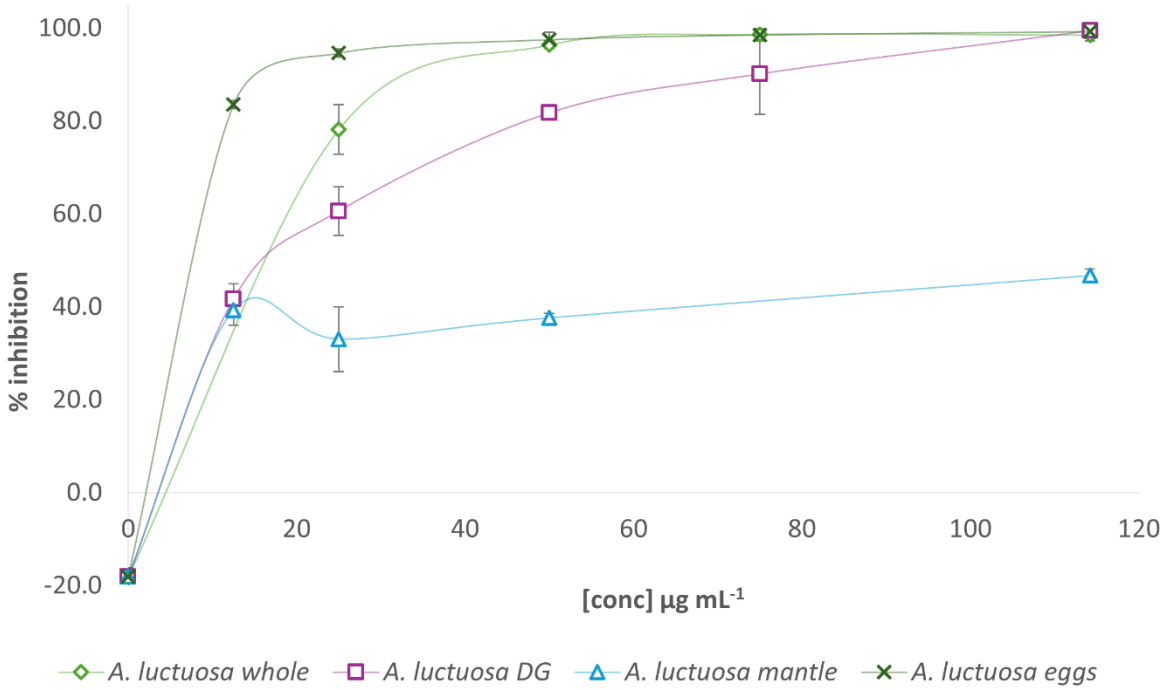

Figure 43: Cytotoxicity of the crude extracts of *Aphelodoris luctuosa* (whole-body, mantle and digestive gland) and its eggs on HeLa cells using an MTT assay.

2.6.2 Isolation procedure

The *A. luctuosa* specimen collected from Motuputa Island and its egg mass were extracted following the usual procedure. Both extracts were purified by reversed phase bench column chromatography to afford a polymeric 3-alkyl pyridinium salt (3-PAPS) (**146**) from early eluting fractions (Figure 44).

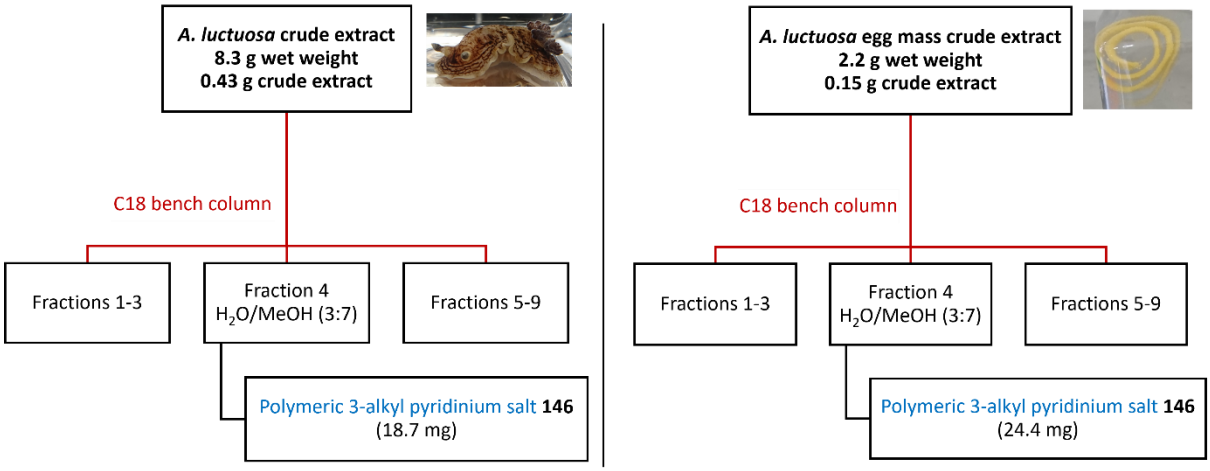

Figure 44: Isolation procedure for 3-PAPS (**146**) from *Aphelodoris luctuosa* and its eggs.

2.6.3 Polymeric 3-alkyl-pyridinium salt

3-PAPS (**146**) was isolated as a yellow-orange product displaying a prominent ion at *m/z* 190.1409 in HR-ESI-MS positive ion mode, initially attributed to a molecular formula of $C_{13}H_{20}N$. The ^{1}H NMR spectrum contained three aromatic signals characteristic of an ABC system [δ_H 7.96 (1H, dd, 6.7, 6.2), 8.38 (1H, d, 7.8), 8.66 (1H, d, 5.1)], along with an aromatic singlet δ_H 8.70 integrating for one proton. The ^{1}H (Appendix A.5) and HSQC NMR spectra also displayed a resonance typical of a methylene envelope at δ_H 1.29 representing eight protons, along with four other methylene signals at δ_H 1.66, 1.98, 2.84 and 4.56, each representative of two protons (Table 7).

The ^{13}C and HSQC NMR spectra revealed the presence of five aromatic carbon signals, including four protonated resonances at δ_C 127.7, 143.4, 144.3 and 145.4, consistent with the presence of a 3-substituted pyridine ring. The ^{13}C and HSQC NMR spectra confirmed the presence of eight methylene signals.

Upon analysis of the fraction containing compound (**146**) by thin layer chromatography (TLC) (with EtOAc/MeOH 1:1), the pyridinium salt did not move from the origin, suggesting a very polar compound. To confirm this, the fraction was purified on Sephadex LH-20 with H_2O/MeOH (1:9) and the compound eluted with the solvent front, suggesting that it was fully excluded from the column, and was therefore larger than 4000-5000 g mol^{-1}.[270] Besides, the compound was soluble in water, which is either a consequence of a high degree of polymerisation[271] or indicated that it is a salt.

The protons represented by the most deshielded methylene signal at δ_H 4.56 showed two HMBC correlations into the aromatic ring (H-7/C-2 and H-7/C-6). Coupled with the characteristic chemical shift of the signal (δ_H 4.56, δ_C 61.8), this indicated that the methylene group was attached to the nitrogen. The protons represented by the methylene signal at δ_H 2.84 showed two HMBC correlations into the aromatic ring (H-14/C-2 and H-14/C-3) which placed the group adjacent to the non-protonated aromatic signal. This allowed for the construction of the polymer, linked head to tail. A series of COSY and HMBC correlations allowed for the construction of the methylene chain and confirmed the substitution of the pyridine moiety (Figure 45). The spectroscopic data did not contain any signal that could be assigned to a terminal methyl or pyridine group, consistent with a cyclic polymeric compound or with a polymer so large that the terminal unit is not observed.

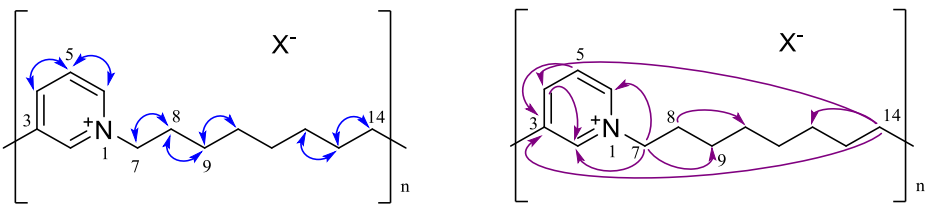

Figure 45: Selected COSY (blue) and HMBC (purple) correlations for compound (**146**).

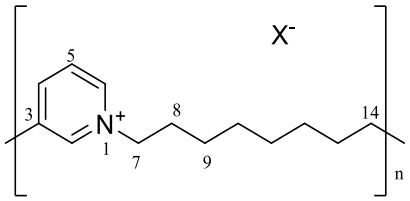

146

Table 7: ^{1}H and ^{13}C NMR data for 3-PAPS (**146**) compared with literature values (methanol-d_4).[272]

	^{1}H (mult, *J* in Hz)		^{13}C	
Atom	[a] **Experimental**	[b] **Literature**	[a] **Experimental**	[b] **Literature**
2	8.70 (1H, s)	8.95 (1H, s)	143.4	145.3
3			144.3	145.7
4	8.38 (1H, d, 7.8)	8.45 (1H, d, 8.0)	145.4	146.6
5	7.96 (1H, dd, 6.2, 6.7)	8.01 (1H, dd, 5,0, 8.0,)	127.7	128.9
6	8.66 (1H, d, 5.1)	8.84 (1H, d, 5.0)	141.6	143.3
7	4.56 (2H, t, 6.2)	4.60 (2H, t, 7.5)	61.8	62.9
8	1.98 (2H, bs)	2.20 (2H, bs)	31.9	32.6
9	1.29 (8H, bs)	1.41 (8H, bs)	25.2	27.3
10			[c] 28.3	[d] 30.2
11			[c] 28.0	[d] 30.2
12			[c] 27.9	[d] 30.0
13	1.66 (2H, bs)	1.73 (2H, bs)	29.6	31.6
14	2.84 (2H, t, 7.1)	2.87 (2H, t, 7.5)	30.6	33.6

[a] values reported in D_2O, ^{1}H 600 MHz, ^{13}C 150 MHz, [b] values reported in methanol-d_4, ^{1}H 400 MHz, ^{13}C 100 MHz (Davies-Coleman *et al.* 1993[244]), [c, d] signals could be interchanged.

Compound (**146**) had previously been isolated from *Callyspongia fibrosa* from Micronesia and displayed identical spectroscopic data.[272] Upon structure elucidation, compound (**146**) was initially thought to be a dimeric structure based on ion-spray spectrometry, due to observation of a peak at *m/z* 379.[272] Fortunately, a large scale synthetic study was carried out by the authors to obtain a higher quantity of material for bioassay, and several cyclic oligomeric derivatives with a different number of subunits were prepared. Comparison of the behaviour of the natural product on TLC with a synthetic dimer showed that the natural product was not a cyclic dimer, and was instead composed of at least eight subunits.[272]

ESI-MS analysis of compound (**146**) resulted in several peaks, including *m/z* 190.1, 379, 284 and 568, which correspond to the cleavage of the subunits in the bond C-3/C-14 (Table 8, Figure 46), consistent with the cleavage reported in the literature.[272] The authors reported that the larger the molecule, the less abundant is the parent ion in ion-spray mass spectrometry and the more abundant is the peak at *m/z* 379, corresponding to two subunits. In our research, the parent ion was not observed, and the peak at *m/z* 379 was of high intensity, confirming a high molecular weight compound.

Table 8: MS/MS Fragmentation of 3-PAPS (**146**) in ESI-MS positive ion mode.

Compound	Peak	Assignment
3-PAPS **146**	190.1	$[\mathbf{1} + H]^+$
	284.7	$[\mathbf{3}^{2+}]/2$
	379.3	$[\mathbf{2}^+]^+$
	568.4	$[\mathbf{3}^{2+}]^+$

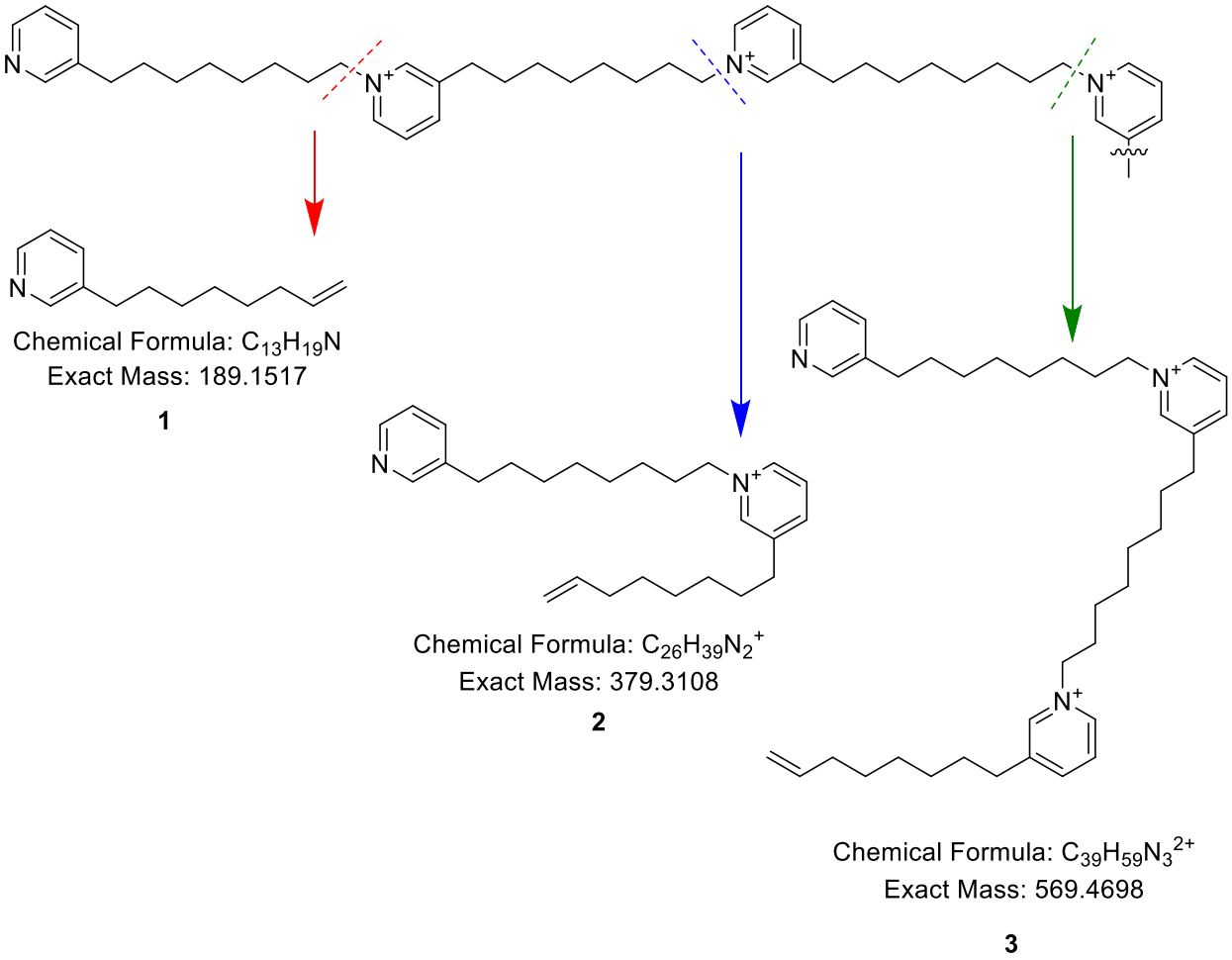

Figure 46: MS/MS fragmentation pattern of compound (**146**) on ESI-MS (positive ion mode).

Compound (**146**) had also previously been isolated from *A. luctuosa* from New Zealand displaying the same subunit, although in that case a terminating unit was observed in an "internal" versus "terminal" ratio of 17:1, suggesting a polymer size of approximately 3200 g mol^{-1}.[231] Additionally, the presence of alternate linking chains, including some with oxygenation, was suggested based on the presence of another deshielded methylene (δ_H 4.62, δ_C 80.2) in NMR spectra of the compound.

In our research, the presence of the deshielded methylene group was also observed in HSQC spectroscopic data (δ_H 4.41, δ_C 79.0), along with other sharp methylene resonances that could potentially belong to alternate linking chains. As mentioned above, the purification and structure elucidation of complex polymers of high molecular weight is extremely difficult and the exact structure of the polymer could not be fully elucidated during this research.

Compound (**146**) was also isolated from the egg mass (Figure 44) and gave identical spectroscopic data (Chapter 7 – Experimental, Section 7.5.4). Metabolite (**146**) was assessed for cytotoxic activity against HeLa cells and displayed minimal activity (IC_{50} 7 µg mL^{-1}), which was similar to the crude extract of the egg mass (IC_{50} 8 µg mL^{-1}). 3-PAPS (**146**) was isolated in high concentration from the eggs (15.4 % dry weight) and the activity observed is attributed to its presence within the egg extract.

2.6.4 Metabolite distribution investigation by qNMR spectroscopy

The distribution of compound (**146**) within the nudibranch body was investigated within five *A. luctuosa* specimens previously collected at Salisbury Wharf in March 2021 and directly frozen upon collection. Undergraduate student Caitlin Berquist carried out the dissection of the five individuals into mantle and digestive gland with stomach, the separate extraction of each part and the TLC analysis of the ten crude extracts obtained. The presence of the compound was detected in each crude extract by TLC.

Quantitative ^{1}H NMR spectroscopy was carried out in D_2O to quantify compound (**146**) in each of the crude extracts. Maleic acid was used as an internal standard because of its solubility in D_2O and the absence of overlap in the resonances of maleic acid and compound (**146**) on ^{1}H NMR spectroscopy. During the sample preparation phase, several ratios of mass of crude extract versus internal standard (Chapter 7 – Experimental, Section 7.6) were trialled to obtain

appropriate signal to noise ratio for both internal calibrant and crude extracts. Upon determination of the appropriate ratio, the samples were prepared accordingly (Chapter 7 – Experimental, Section 7.6).

The five signals at δ_H 4.56, 7.96, 8.38, 8.66, 8.70 were selected for quantitation purposes because of no overlap with other signals. For each sample, the integral values for each resonance were obtained by deconvolution using the Lorentzian function, prior to being averaged and rationalised to obtain the integral value for one proton. The formula displayed in Equation 1 was used to calculate the purity of each crude extract, which is the equivalent of the percentage in mass of compound (**146**) within the amount of crude extract weighed for each sample. This purity value was then converted to obtain the mass concentration of compound (**146**) within each of the crude extracts (mg of compound (**146**) per g of crude extract), which was converted to percentage of dry weight, displayed in Table 9 and Figure 47.[273]

Despite the exact molecular mass of analyte not being known, a value of 190.31 g mol^{-1}, corresponding to the mass of one subunit, was used because the polymeric salt consists of repeating subunits and the integral values are rationalised according to the number of protons. To access the accuracy of this approach, a calculation trial was conducted for one of the samples using the molecular weight of eight subunits (M_A = 1520.48 g mol^{-1}) and using the appropriate number of protons for the whole molecule. The obtained purity value showed a 0.01% difference compared to the value using the molecular weight of one subunit in the calculation. Therefore, it was deemed accurate to use the molecular weight of one subunit for the purity calculations.

Equation 1 : Formula for the purity of the analyte (P_s) calculation.[273]

$$P_S\ [\%] = \frac{n_{IC}.I_A.M_A.m_{IC}.100}{n_A.I_{IC}.M_{IC}.m_S}.P_{IC}$$

n_A = number of protons for the analyte (n_A = 1)
n_{IC} = number of protons for the internal calibrant (n_{IC} = 2)
I_A = integral of the analyte
I_{IC} = integral of the internal calibrant
M_A = molecular weight of the analyte (M_A = 116.07)
M_{IC} = molecular weight of the internal calibrant (M_{IC} = 190.31)
m_S = mass of sample
m_{IC} = mass of internal calibrant
P_{IC} = purity of internal calibrant (P_{IC} =0.995)

On average, the specimens contained a higher concentration of compound (**146**) within the mantle (75.3 versus 61.7 mg g^{-1} in the crude extract). This trend was consistent across all individuals, except specimen 5 (Table 9). The mantle of specimen 1 weighed the most before extraction and was also the one containing the highest concentration of compound (**146**) (the mass of samples and crude extracts is available in Chapter 7 – Experimental, Section 7.6). This trend was consistent in specimens 3 and 5, representing the two smallest mantle samples and containing the two lowest concentrations of compound (**146**), respectively. The smallest samples also yielded the smallest crude extracts, except for specimens 1 and 2. The presence of compound (**146**) in the mantle of each specimen is consistent with a defensive purpose, especially because of the cytotoxic activity of 3-PAPS (**146**) assessed in this research and previously reported.[272]

Table 9: Concentration of compound **(146)** within *Aphelodoris luctuosa* crude extracts.

		Purity					
Specimen	**Body part**	**1st experiment**	**2nd experiment**	**Average**	**Mass of 146 in crude extract (mg)**	**% dry weight**	**Standard deviation**
1	mantle	10.24	9.96	10.10	6.18	10.24	0.14
	internal organs	8.56	8.91	8.74	13.51	8.56	0.18
2	mantle	7.13	6.68	6.91	5.15	7.13	0.23
	internal organs	3.95	3.95	3.95	2.20	3.95	0.00
3	mantle	6.29	6.81	6.55	1.20	6.29	0.26
	internal organs	5.82	5.70	5.76	1.19	5.82	0.06
4	mantle	7.51	7.14	7.30	4.36	7.51	0.19
	internal organs	4.54	4.48	4.51	3.27	4.48	0.03
5	mantle	6.49	6.77	6.63	2.42	6.49	0.14
	internal organs	8.06	7.30	7.68	5.27	8.06	0.38
Average for the five mantle crude extracts (% dry weight)						**7.53**	
Average for the five internal organs crude extracts (% dry weight)						**6.15**	

[a] internal organs refers to digestive gland and stomach

The presence of compound (**146**) in the internal organs of each specimen is consistent with a dietary origin, especially because compound (**146**) was initially isolated from a *Callyspongia* sp. sponge,[272] and 3-alkyl pyridinium salts (3-APSs) are prevalent in a variety of sponges, as discussed in the following section. Specimen 1 yielded the highest mass of the internal organs before extraction, the highest quantity of crude extract and the highest concentration of compound (**146**) but the rest of the specimens did not follow this pattern. As such, specimen 2 yielded the second highest mass of internal organs before extraction, but the second lowest quantity of crude extract and the lowest concentration of compound (**146**) (the mass of samples and crude extracts is available in Chapter 7 – Experimental, Section 7.6)**.** This could be because of the quick transfer of compound (**146**) from the digestive organs to the mantle for defensive purposes, resulting in a lower concentration in the digestive gland and stomach. In the case of the dietary origin of 3-PAPS (**146**), this variation could also result from differences in access to the sponge containing compound (**146**) or could reflect a varied sponge diet.

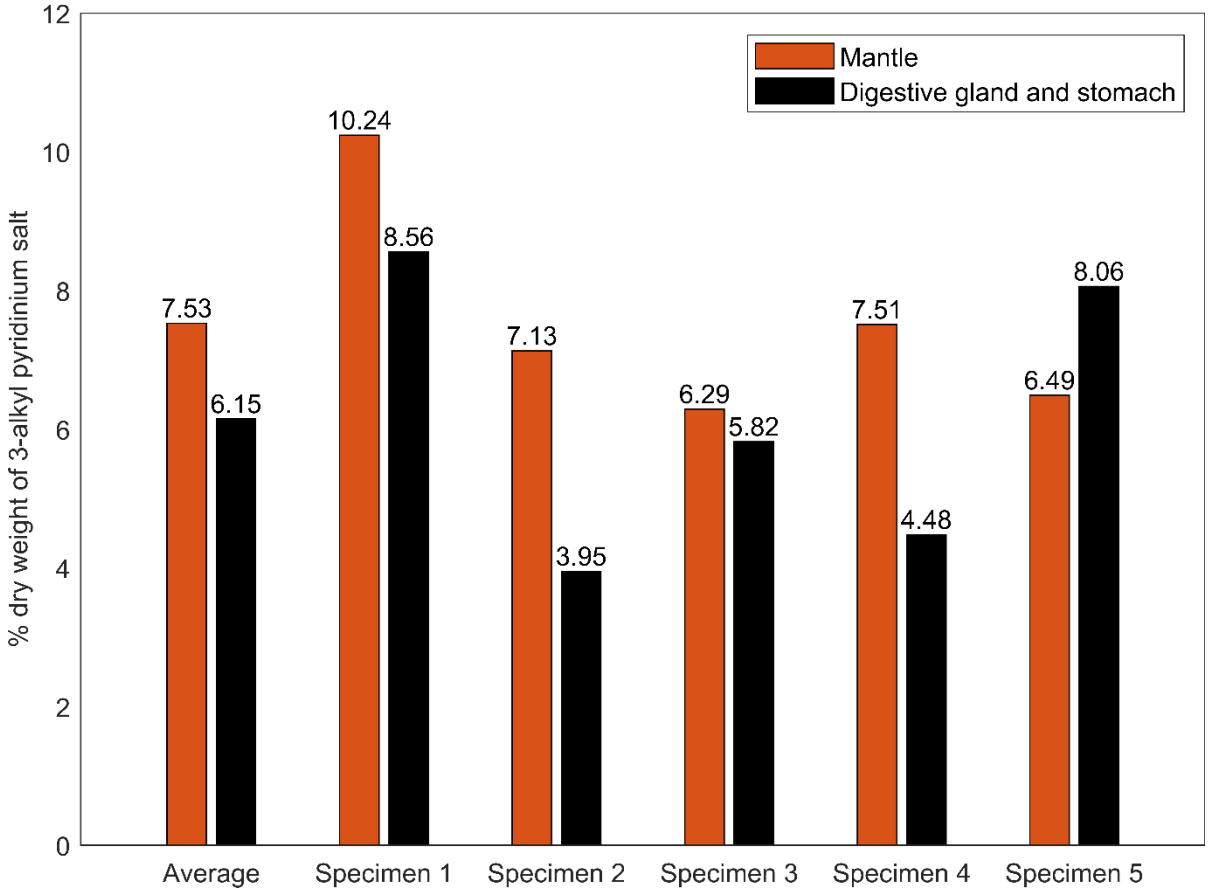

Figure 47: Concentration of compound (**146**) in *Aphelodoris luctuosa* tissues (mantle and digestive organs). Values quantified by ^{1}H NMR spectroscopy and presented as means of duplicate analyses of five nudibranchs.

2.6.5 Occurrence of 3-alkyl pyridinium salt

Marine sponges belonging to the order Haplosclerida have been a prolific source of 3-alkyl pyridine and 3-APSs and these compounds have been suggested to serve as chemical markers of haplosclerid sponges.[271] These compounds were either isolated as monomers displaying varied alkyl chain in terms of length, saturation and branching, as cyclic or linear oligomers, or as mixtures of high molecular weight polymers.[271] Various bioactivities have been reported, including but not limited to antibacterial, antifungal and cytotoxic activities.[274-278]

An early study of the Bahamian sponge *Calyx podatypa* reported the isolation of three *N*-methyl pyridinium salts, xestamines F, G and H (**147-149**)[279] closely related to 3-substituted pyridine xestamines isolated from *Xestospongia* sp.[280] Upon investigation of the antimicrobial properties, the three *N*-methyl pyridinium salts (**147-149**) were 100 times more active than the unsubstituted pyridines against various common strains, although compounds (**147-149**) were much less cytotoxic than xestamines D and E.[279]

A range of cyclic dimeric 3-APSs, cyclostelletamines A-L and dehydrocyclostellettamines D (**150**) and E (**151**) have been isolated from various sponges, such as *Stelleta maxima*,[277] *Xestospongia* sp. and *Pachychalina*. Cyclostelletamines A-F were isolated as muscarinic receptor binding inhibitors,[277] while cyclostelletamine G and dehydrocyclostellettamines D (**150**) and E (**151**) inhibited histone deacetylase K562 human leukaemia cells with minimal activity (IC_{50} between 17 and 80 µM).[276]

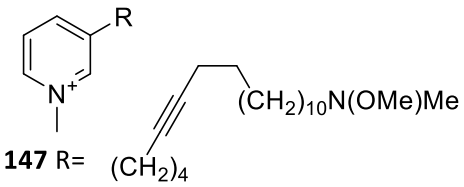

147 R=

148, R= $(CH_2)_{14}N(OMe)Me$

149 R= $(CH_2)_{15}N(OMe)Me$

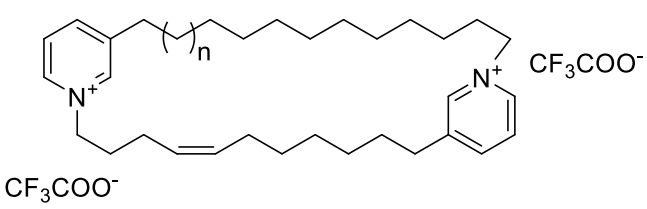

150 n = 1
151 n = 2

The tripyridine linear alkaloids niphatoxins A and B (**152-153**), displaying unsaturation in their alkyl chains, were reported from the Red Sea sponge *Niphates* sp. and displayed cytotoxic activity against the P388 murine lymphoid neoplasm cell line (IC_{50} 0.1 μg mL^{-1}).[281] In 2003, a rare cyclic trimeric 3-AP, viscosamine (**154**), was reported from the Arctic sponge *Haliclona viscosa.*[282] A year later, the acyclic 3-AP, viscosaline (**155**) was also reported from *Haliclona viscosa* from the same location.[283] Compound (**155**) contains a β-alanine moiety within the alkyl chain and could be a precursor of the cyclostelletamines mentioned above.[283] With the refinement of spectroscopic methods, a new monomeric 3-AP, haliclocyclin C (**156**), was isolated from an extract of *H. viscosa.*[275] Several macrocyclic dimeric haliclamines have also been reported from Arctic *H. viscosa*.[284-286] A mixture of cyclohaliclonamines A-E obtained from an Okinawan *Haliclona* sp. was reported to contain the first cyclic tetrameric, pentameric and hexameric 3-APSs containing C_{10} alkyl chains.[287] More recently, two cyclic 3-AP monomers, dehydrohaliclocyclins C (**157**) and F (**158**), along with haliclocyclin C (**156**), were described (using a bioassay and NMR guided-approach) from a New Zealand *Haliclona* sp.[288]

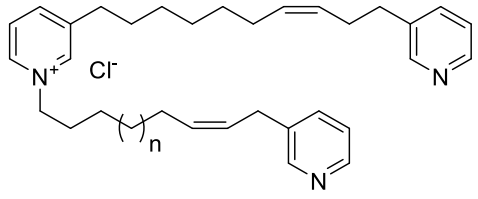

152 n=2
153 n=3

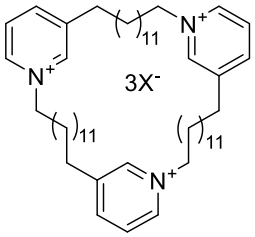

154

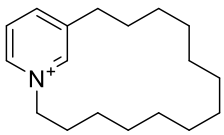

156

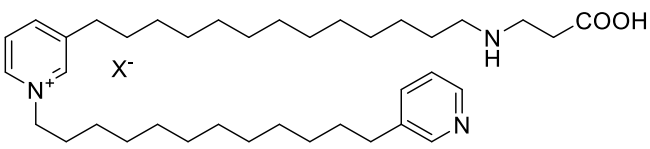

155

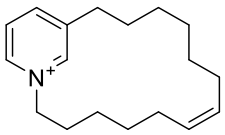

157

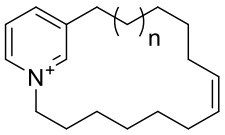

158

As mentioned above, several 3-AP oligomers have been isolated from various Haplosclerida sponges.[272,274,289] Halitoxin (**159**) was the first 3-AP oligomer to be isolated and characterised as a mixture of high molecular weight pyridinium salts from three different *Haliclona* species.[274] The different 3-AP units are connected by saturated alkyl chains containing between eight and eleven carbons.[274] The authors were able to separate the polymer into different molecular weight range fractions, which all displayed the same cytotoxicity against

the KB cancer cell line (ED_{50} 5-7 μg mL^{-1}).[274] Another similar oligomer, amphitoxin (**160**), isolated from the sponge *Amphimedon compressa* and containing a sequence of randomly alternating 3-alkyl and 3-alkenyl pyridinium units in an approximate ratio of 1:1, displayed feeding-deterrence activity against the generalist sponge-feeding wrasse *Thalassoma bifasciatum*.[289] As mentioned earlier, a 1,3-dialkylpyridinium salt oligomer has been reported from the sponge *Callyspongia fibrosa* as an epidermal growth factor (EGF) antagonist, containing the same basic structure as the oligomer described in this research.[272] More 3-PAPSs containing a substantial degree of polymerisation were obtained from a Mediterranean *Haliclona* sp.[290]

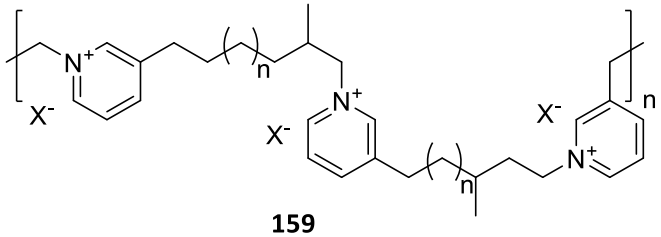

159

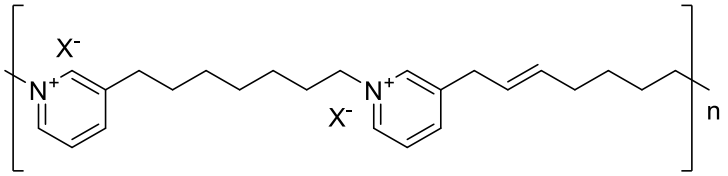

160

The isolation, purification and characterisation of high molecular weight 3-PAPS has been reported as problematic since they often exist as a mixture of different molecular weights (as exhibited for the cyclohaliclonamines) and have a tendency to form aggregates.[271]

2.6.6 Investigation of the diet

As mentioned above, sponges of the order Haplosclerida, including *Haliclona* sp. from New Zealand,[288] contain a variety of 3-AP salts. Several *Haliclona* sp. sponges had previously been recorded at the Salisbury Wharf collection site, including *Haliclona* sp. cf. *fragilis*, *Haliclona tenacior* and *Haliclona* sp.[291] At the time of collection of the species investigated above, no

sponge was observed within the close vicinity of the nudibranchs, nor were the specimens found on any sponge species. Instead, the nudibranchs were found on rocky substrate.

To investigate the source of compound (**146**), a subsequent collection trip was conducted and a sample of *Haliclona* sp. was collected from near the original nudibranch collection site in July 2024 (Figure 48). Undergraduate student Caitlin Berquist carried out the extraction and TLC analysis of the sponge crude extract, followed by fractionation of the extract and NMR analysis. No evidence of pyridinium salts or related compounds was detected in early eluting fractions by TLC, nor by NMR analysis. It was therefore concluded that this sponge is unlikely to constitute the diet of *A. luctuosa* because of the absence of compound (**146**) or related pyridinium salt within it.

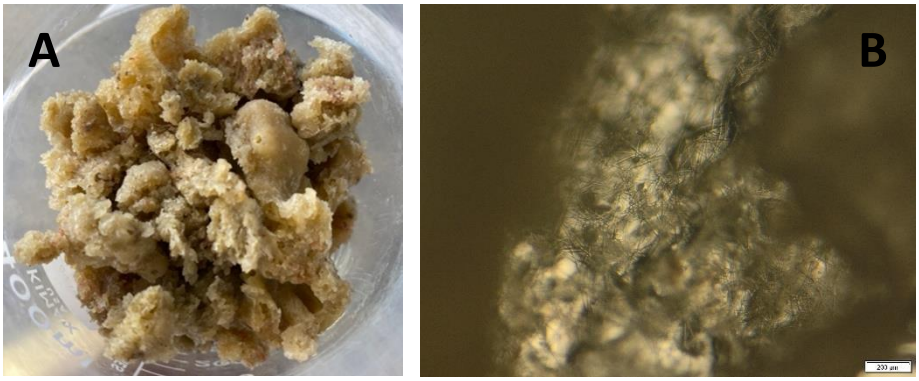

Figure 48: A- *Haliclona* sp. collected at Salisbury Wharf (Courtesy of Caitlin Berquist). B- *Haliclona* sp. displaying oxea spicules observed under a stereo microscope.

To further investigate the diet of *A. luctuosa* and possible source of compound (**146**), morphological analysis of a specimen collected in February 2024 from Karewa Island in the western Bay of Plenty was undertaken. The specimen was dissected into digestive gland and intestines. The intestines were cut open and directly observed under a stereo microscope. Sponge spicules mixed with other material were detected. To better assess the spicule shape, the digestive glands were digested in nitric acid, followed by several washes, prior to being observed under a stereo microscope. The digestive glands contained predominantly oxea, or needle-shaped, sharp spicules containing a mono axis (Figure 49). A microscope slide was then prepared and observed under a compound microscope to assess the size of the spicules. The spicule length ranged from 100 to 150 µm pointed at both ends, which is consistent with the dimensions previously reported for different *Haliclona* species from New Zealand,[291] including

the species inhabiting the waters of the Tauranga harbour (Table 10). Several other spicules were also present and could possibly originate from *Hymeniacidon* species, frequently found nearby *Haliclona* species, although this was not confirmed.

However, oxea spicules are widespread within marine sponges[292] and even though the dimensions of the spicules found within *A. luctuosa* suggest that *Haliclona* sp. could be its main diet, it could also feed on different sponge species with similar spicules in terms of dimensions and shape.

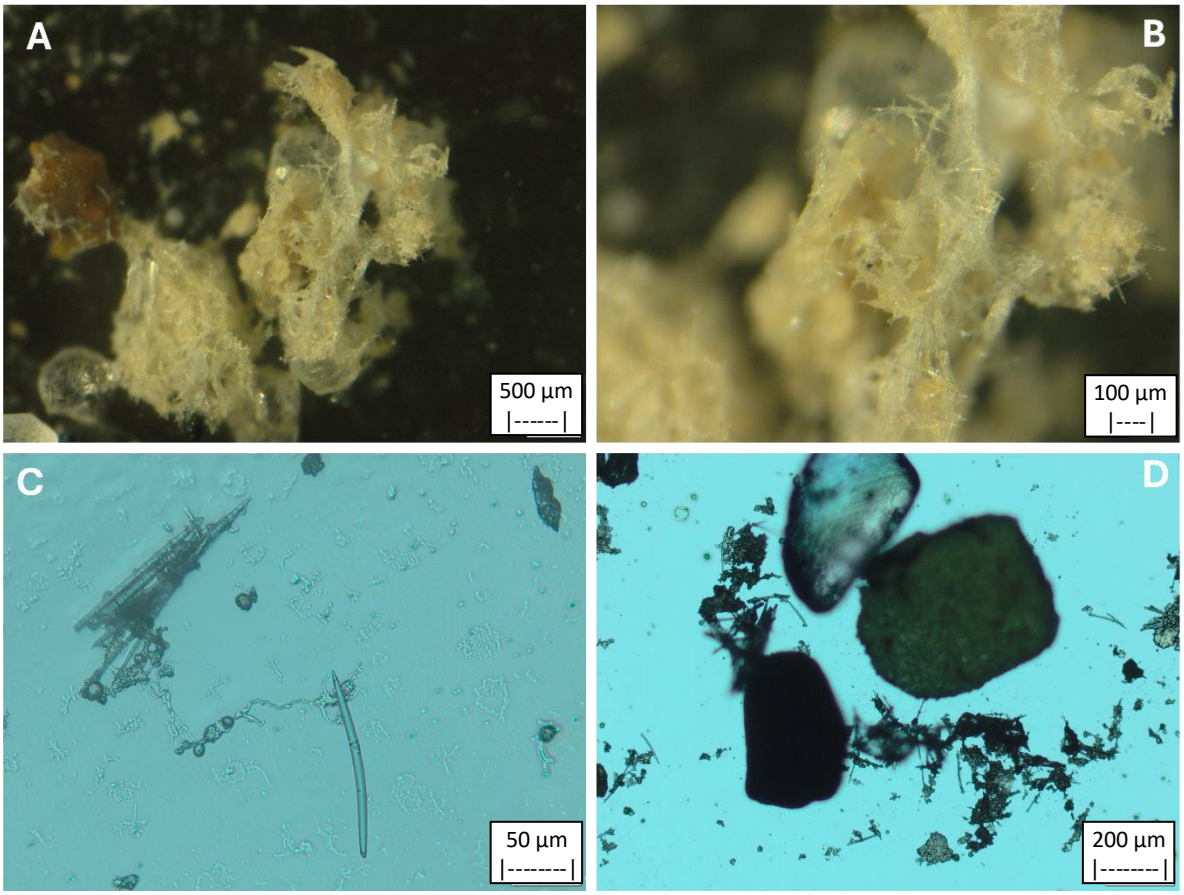

Figure 49: A and B – Digestive glands of *Aphelodoris luctuosa* digested in nitric acid and observed under a stereo microscope. C and D - Digestive glands of *Aphelodoris luctuosa* digested in nitric acid and observed under a compound microscope.

Table 10: Comparison of sponge spicule length between several New Zealand *Haliclona* species[291] and the spicules found in the digestive gland of *Aphelodoris luctuosa.*

Sample	Collection site	Spicule type	Length (µm)
Spicules of *A. luctuosa* present in digestive glands	Karewa Island, Tauranga Bay	Oxea	100-150
Haliclona n. sp.[291]	Salisbury Wharf, Tauranga	Oxea	117-145
Haliclona n.sp. *cf. tenacior*[291]	Salisbury Wharf, Tauranga	Oxea	120-133
Haliclona n.sp. *cf. brondstedi*[291]	Bridge Marina, Tauranga	Oxea	123-148
Haliclona n.sp. *cf. heterofibrosa*[291]	Bridge Marina, Tauranga	Oxea	117-131 152-170
Haliclona fragilis from New Zealand specimens[291]	New Zealand	Oxea	139 (average)[291]
Haliclona heterofibrosa from New Zealand specimens[291]	New Zealand	Oxea	136 (average)[291]

2.6.7 Concluding remarks

Specimens of *A. luctuosa* and an egg mass spawned in captivity were investigated, which resulted in the isolation of a 3-PAPS (**146**) from both extracts. Compound (**146**) displayed the same basic structure as the oligomer described from *Callyspongia fibrosa* from Micronesia, although some units might contain oxygenation or alternative linking chains. Compound (**146**) displayed some cytotoxic activity against HeLa cells and was overall more concentrated in the mantle, consistent with a possible defensive role. This was corroborated by its presence in the egg mass in high concentration. 3-APSs are prevalent in Haplosclerida sponges, especially from the *Haliclona* genus, and compound (**146**) is likely obtained by *A. luctuosa* from its diet. A potential sponge prey, *Haliclona* sp., inhabiting the same collection site as the nudibranchs, was investigated but no 3-APSs were detected, suggesting that the nudibranchs might prey on a different *Haliclona* species. The presence of oxea spicules in the digestive glands of *A. luctuosa* is consistent with the nudibranchs preying on a silicaceous sponge, but determination of which species requires further investigation.

2.7 Summary

In this study, four New Zealand marine invertebrates were investigated. The brominated alkaloid (**94**), previously isolated from *Amathia lamourouxi*, was reported as the first metabolite isolated from the endemic bryozoan *Amathia gracei*. Two *Dendrodoris* nudibranchs, namely *D. krusensternii* and *D. nigra*, were investigated and three drimane sesquiterpenes, (**122**), (**124**) and (**125**), were isolated and characterised. The two drimane sesquiterpenes isolated from *D. nigra* had previously not been described from this species. Finally, the New Zealand endemic nudibranch *A. luctuosa* and its egg mass were investigated. A 3-PAPS (**146**) was isolated from both samples and based on its distribution within the nudibranchs, its presence in the offspring and its cytotoxic activity, it was suggested that the polymer might serve a defensive role.

Over the course of this research, three more nudibranch species were investigated to establish predator-prey relationships. These species were found in the vicinity of potential prey and their preferred diet was assessed by feeding-choice experiments. The results of this work are presented in Chapter 3, followed by chemical investigation described in Chapter 4.

Chapter 3

Investigation of predator-prey relationships by feeding-choice experiments

---

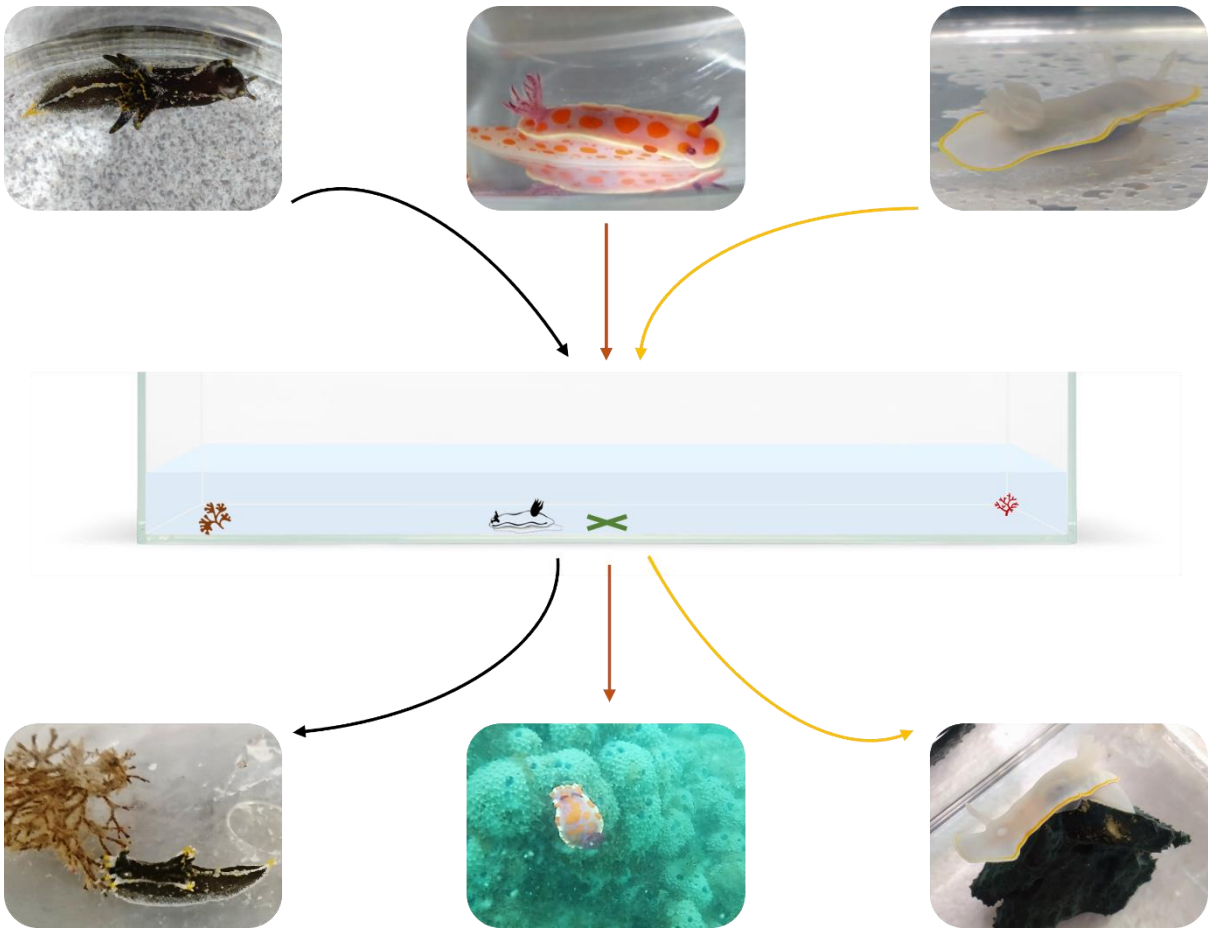

Within the order Nudibranchia, a wide variety of different feeding behaviours are observed. Both specialist feeders, which prey upon a selective choice of organisms, and generalist feeders, which prey upon a broad range of organisms, have previously been identified.[293,294] Feeding-choice and food-detection experiments have been used to investigate these gastropod molluscs to determine their preferential prey and feeding behaviour.[294-298] Such experiments are especially relevant in nudibranchs, reliant on their rhinophores acting as chemosensory receptors to detect olfactory clues in the water.[86] To date, the majority of feeding behaviour studies have focused on aeolid, coral-eating nudibranchs, which are heavily reliant on chemotaxis to detect prey for nematocyst, or stinging cell, sequestration. The detection of prey is also of upmost importance because of larvae settlement and metamorphosis in response to chemical cues from sessile prey organisms.[293,295,299,300]

To date, the diet of dorid nudibranchs has been examined primarily via field studies,[301-306] with only a few feeding-choice experiments conducted under laboratory conditions on spongivorous or bryozoan-eating dorid nudibranchs.[123,297,307] Only the dietary preferences of the spongivorous nudibranchs *Doris* (formerly *Austrodoris*)[308] *kerguelenensis* and *Glossodoris pallida* have been assessed. [123,297] In these studies, the frequency of choices towards a specific sponge species was recorded, either with a flow through or no flow apparatus. In terms of bryozoan-eating dorid nudibranchs, feeding-rate experiments established that the nudibranch *Onchidoris muricata* from the Gulf of Maine prefers feeding on *Electra pilosa* over the invasive species *Membranipora membranacea*.[307]

As mentioned in Chapter 2, only two previous studies focused on the chemistry and ecology of nudibranchs inhabiting New Zealand waters[230,231] and very little is currently known about their diet. During this research, a chemical ecology approach, by means of laboratory-based feeding-choice experiments, was developed. The aim was to offer insight into the dietary preferences of several nudibranch species to establish potential ecological links. For the research reported here, the feeding-choice experiments act as a bioassay carried out by the nudibranchs for guidance towards potential bioactive prey, along with providing initial indications for possible predator-prey relationships. The configuration of the experiments was inspired by previously reported experiments[297,309] and was adapted to suit the aims of this research.

3.1 Establishment of the feeding-choice experiments configuration

3.1.1 Methodology development

Two-channel, flow-through flume-chamber

The initial configuration for the food-choice experiments was inspired from the Atema two channel, flow-through flume chamber used by Munday *et al.* to study the responses of clownfish larvae to olfactory cues (Figure 50).[309] Such a configuration relied on the ability of nudibranchs to locate prey by chemoreception, which has been proven in several cases.[295,299,300] This configuration was trialled on *Dendrodoris krusensternii* and *Dendrodoris wellingtonensis*, along with several prey found in the vicinity, including a *Crella incrustans* sponge, bryozoans, and ascidians. A single nudibranch was placed into the centre of the downstream end of the tank. Two food choices were placed upstream, each of them in one channel to determine the preferred prey, assuming that *D. krusensternii* and *D. wellingtonensis* can locate the prey by chemoreception, and a constant water flow was maintained throughout the channels for all trials. The duration of the experiments was based on previous food-detection experiments carried out on the dorid nudibranch *Doris kerguelensis*.[297] Details of the methodology can be found in Chapter 7 – Experimental, Section 7.7.6. Across the experiments, *D. krusensternii* specimens crawled towards prey in some instances but no prey was eaten. When experiments with *D. wellingtonensis* were conducted, virtually no movement was observed.

Such observations may be because the trialled prey were not appropriate for the studied species. According to Willan *et al.*,[206] both nudibranchs feed on silicaceous sponges, with *D. wellingtonensis* feeding especially on the genera *Halichondria* and *Hymeniacidon*. Upon collection, *D. wellingtonensis* specimens were only found on and in the vicinity of *Crella incrustans*. Also, it might be possible that the flow rate used (0.15 L min^{-1}) was too low for the nudibranchs to properly detect the chemical cues, although from a practical point of view, this could not be changed. Potentially also, the materials used to build the chamber, such as glue, might be incompatible with such experiments, as they may interfere with the nudibranch's food-detection sense. Besides, according to Zimmer-Faust *et al*.,[310] and after correspondence

with Philip Munday, the use of such a two-channel configuration might not be suitable for food-choice experiments in slow-moving animals as it can restrict their mobility, especially after a specimen enters one of the channels. After having considered the possible reasons why no clear results were observed, it was decided to build a rectangular Perspex flow-through chamber to offer greater mobility. The control over the selection of prey and predators was minimal as it was dependent on availability at the time of collection.

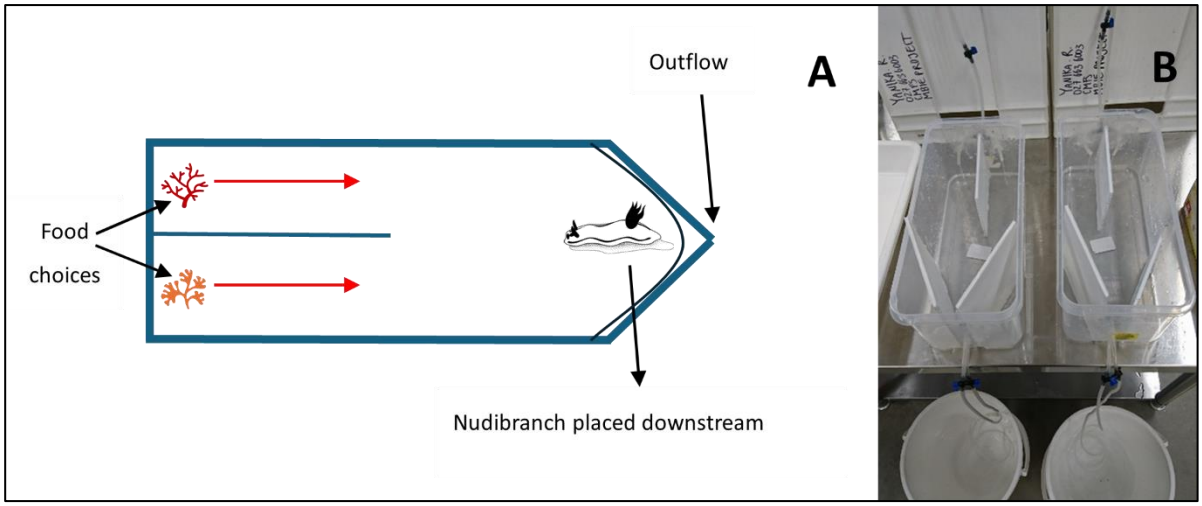

Figure 50 : A- Scheme of the initial Atema flume chamber (30 cm long) used for the feeding-choice experiments, adapted from the configuration used by Munday *et al.*[309] The water inflow is represented with red arrows. B- Initial experimental configuration built for the feeding-choice experiments.

Rectangular, Perspex flow-through chamber

According to advice provided by Philip Munday, a rectangular, Perspex flow-through chamber containing a central drain, was built. For this configuration, the nudibranch was placed in the middle, near the drain, and the prey were placed on opposite ends of the tank. A constant water flow of 0.15 L min^{-1} was maintained. Several inflow configurations were trialled using red and green food-colouring to observe the mixing between the two halves of the tank (Figure 51A). The aim was to allow for minimal mixing between the two solutions, representing the chemical cues being carried by the prey towards the predators.

The dual single inflow resulted in a channelling-type mixing between the two solutions, and the dual Y-type inflow also resulted in unsuitable mixing (Figure 51B and C). The dual 4-inflow configuration provided results closest to those desired, with only the middle area near the drain showing mixing of the solutions (Figure 51D).

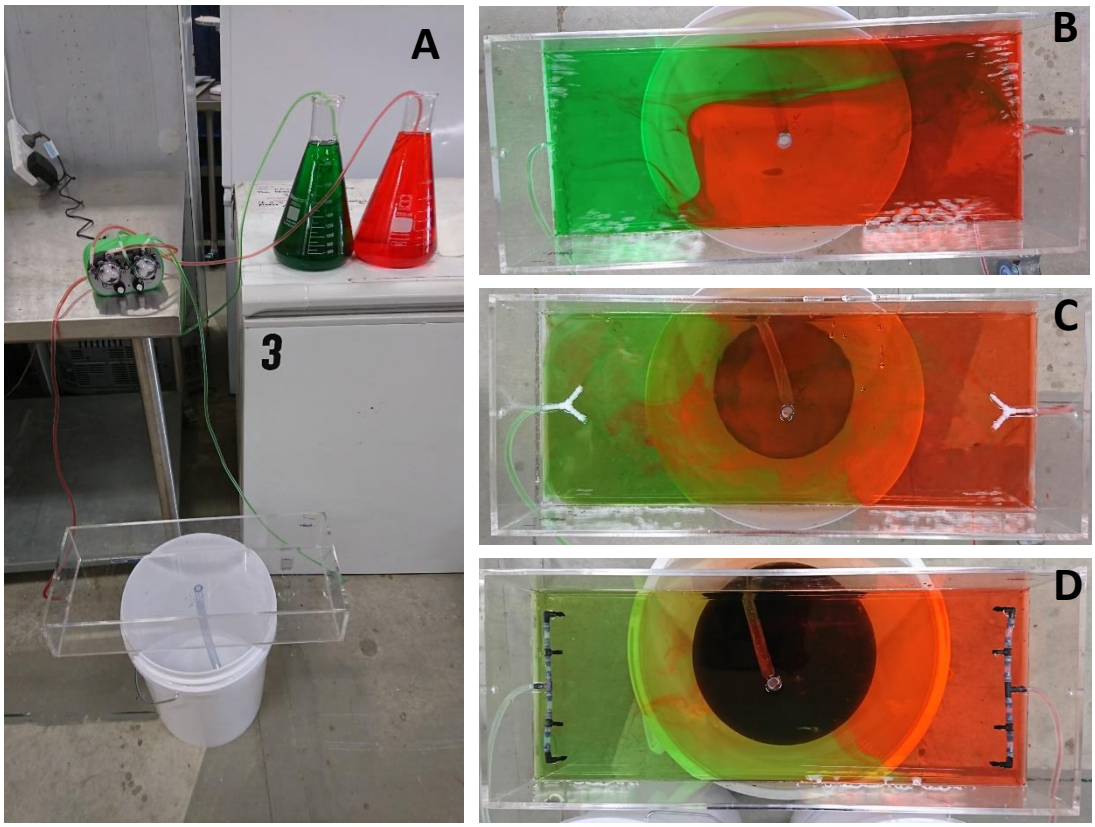

Figure 51: A- General set-up for the colouring trial. Dimensions of the tank: 45 cm x 23 cm x 4.5 cm. B– Dual single inflow. C- Dual Y-type inflow. D– Dual 4-inflow.

The dual 4-inflow configuration was trialled on several nudibranch species, including *Ceratosoma amonenum* and *Goniobranchus aureomarginatus* and two potential sponge prey (*Dysidea teawanui* and *Dictyodendrilla* cf. *dendyi*). Over the trial experiments, only a single *G. aureomarginatus* made a choice and fed on *D.* cf. *dendyi.* The remaining specimens either did not make any choice or did not reach any prey within the time limit. This could be due to the experiments being too short for such slow-moving animals. However, from a practical perspective, it was not possible to conduct longer experiments while maintaining a flow through the chamber as this required vast amounts of sea water. It was therefore decided to change the flow-through configuration to a no-flow system and conduct several longer experiments that would be recorded using a video camera.

3.1.2 Selected configuration

By conducting the feeding-choice experiments using a no-flow configuration, the focus was no longer on the nudibranchs relying on chemotaxis for prey detection. Instead, their dietary preferences were assessed by comparison of the time spent on each prey. This was also more accurate as no previous food-detection experiments were carried out on the nudibranchs studied here to prove that the specimens could detect food by chemotaxis. This configuration was first trialled on *Polycera hedgpethi* specimens and gave statistically significant results (Chapter 3, Section 3.2.2), hence the configuration was chosen for the subsequent experiments.

General procedure

Experiments were carried out using artificial seawater made to match the ocean's salinity in the Bay of Plenty region of New Zealand.[311] The number of experiments conducted on each nudibranch species varied across species and was dependant on the general health of the specimens, but was greater than 26 hours for each specimen tested in the feeding-choice experiments. Prior to each experiment, the nudibranchs were given an acclimation period in the tank used for the experiments without prey. Before the start of the experiment, the nudibranchs were carefully placed back in the centre of the tank and a piece of each test prey was placed at opposite corners of the tank (Figure 52). Each experiment was recorded and a choice for a tested prey was counted when the mouth of the nudibranch was in contact with the prey, as determined by extensive analysis of the recorded videos. Details of the protocol can be found in Chapter 7 – Experimental, Section 7.3.2.

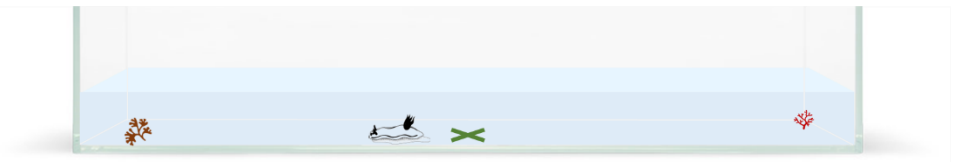

Figure 52: Scheme of the selected feeding-choice configuration (45 cm x 23 cm x 4.5 cm) with the cross representing the starting point of the nudibranch and both prey placed on opposite sides of the tank.

Results analysis and statistical approaches

The no-flow configuration did not favour prey detection as lack of water movement did not allow for the transport of chemical cues. Therefore, to accurately assess dietary preferences, the emphasis was put on the time each specimen spent on each prey choice as an indication of their preferences. By combining the results of multiple, several hours long experiments for each specimen, the results are considered representative because it gives the nudibranchs a chance to graze on their preferred diet for an extended period, while also having the opportunity to explore and change prey if the initially chosen one was not adequate. This approach has not previously been used to access dietary preferences in nudibranchs, with previous reports documenting only the first and subsequent choices of the nudibranchs. The results presented here also include the first and subsequent choices, allowing for comparison between the different approaches.

When only the initial choice the nudibranchs made between the offered prey species was considered, the observed choice frequencies were compared to those expected from a random distribution (*2-tailed binomial* test). When the total number of times a prey was chosen was considered, the observed frequencies were compared to expected frequencies from a random distribution using a *Chi-squared* test. When the total time each specimen spent grazing on each prey was considered, the observed frequencies were compared to expected frequencies from a random distribution also using a *Chi-squared* test.

Species studied

The species studied for their dietary preferences by feeding-choice experiments were the ones found on a potential prey or in its vicinity, as mentioned in Chapter 2, Section 2.3. The specimens studied also had to be collected within appropriate distance from the place where the experiments were conducted to allow for specimens' survival. A few species met these criteria and were therefore studied. This included *Polycera hedgpethi* found on or near two bryozoan species, along with *Ceratosoma amoenum* and *Goniobranchus aureomarginatus*, both found in the same sponge meadow.

3.2 *Polycera hedgpethi*

Polycera hedgpethi (Er. Marcus, 1964, Figure 53) (Family: Polyceridae, Subfamily: Polycerinae, Figure 54) is a dorid nudibranch characterised by the dark pigments on its body and by the gold spots on its tail, rhinophores, tentacles and mantle rim.[206] Although hard to spot around the coasts of New Zealand, this species is found on the coast of many countries, including South Africa and Spain, having spread through biofouling.[206] This explains its abundance in harbours, especially on moorings, from the low intertidal zone to ten metres deep. In New Zealand, it is found on several bryozoan species, including *Bugula neritina, Bugulina flabellata, Bugulina stolonifera* and *Tricellaria occidentalis*.[312] Therefore, because of the numerous prey species *P. hedgpethi* has been found on,[206,312] it represents a relevant species on which to conduct feeding-choice experiments.

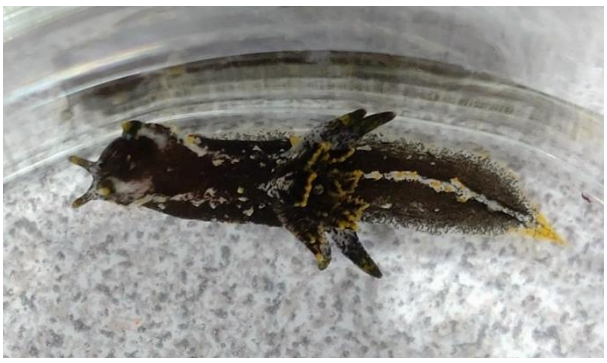

Figure 53: *Polycera hedgpethi* (3 cm long) crawling in a tank.

Suborder Doridina
Infraorder Doridoidei
Superfamily Polyceroidea
Family Polyceridae
Subamily Polycerinae
Genus *Polycera*
Species *Polycera hedgpethi*

Figure 54: Taxonomic classification of *Polycera hedgpethi* according to the World Register of Marine Species (WoRMS).[8]

3.2.1 Collection and field study

A total of six *Polycera hedgpethi* specimens were collected in Tauranga in March 2022, with five individuals collected at Salisbury Wharf, and the remaining individual collected at Tauranga Bridge (GPS coordinates available in Chapter 7 – Experimental, Section 7.2.1). At both locations, the specimens were found on either *Bugula neritina* (Family: Bugulidae) or on an unidentified hydrozoan (Figure 55A). Interestingly, tiny egg cases were present on *B. neritina* specimens (Figure 55B). It is assumed that these belonged to *P. hedgpethi* because their colour, size and shape matched the specimens that the nudibranchs spawned later in the tank (Figures 55C and D). No *Bugulina flabellata, Bugulina stolonifera* or *Tricellaria occidentalis* were observed during collection. Feeding-choice experiments were therefore conducted to assess dietary preferences towards *B. neritina* and the unidentified hydrozoan.

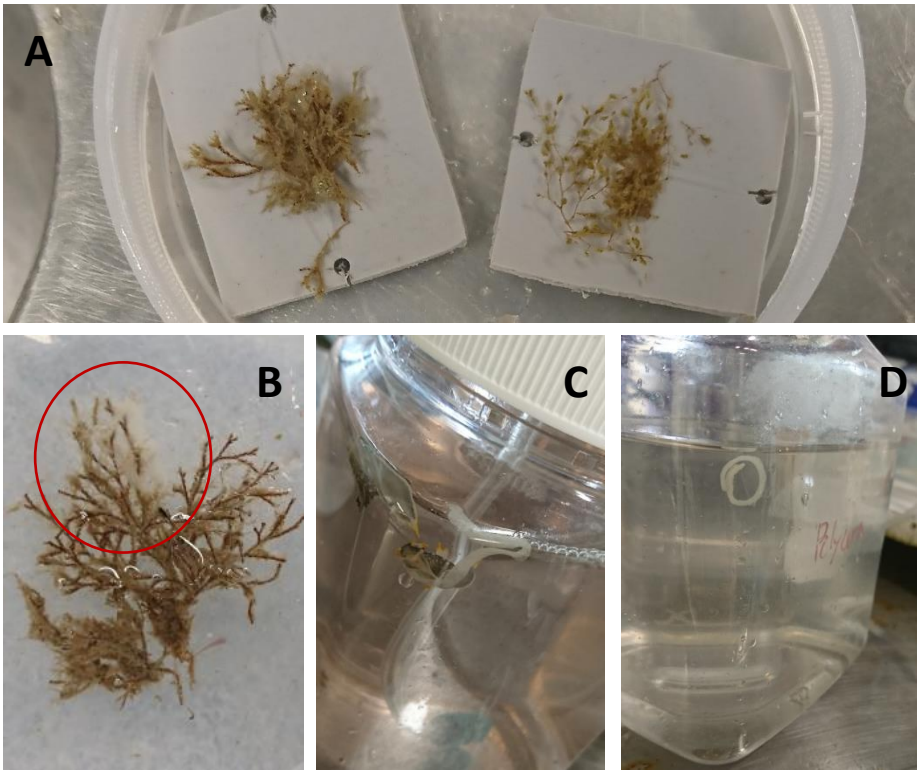

Figure 55: A- *Bugula neritina* (left) and unidentified hydrozoan (right). B- Egg cases found on *Bugula neritina* in the wild (circled in red). C- *Polycera hedgpethi* spawning in a tank. D- Eggs (0.5 cm thick) spawned by *Polycera hedgpethi*.

3.2.2 Feeding-choice experiments

Experiments with *P. hedgpethi* were carried out on five individuals (n = 5) because a specimen from Salisbury Wharf died shortly after collection. Four experiments were conducted, for a total experiment duration of between 26 and 43 hours for each specimen. A total of ten first choices were recorded across the specimens and *B. neritina* was very significantly preferred (*B. neritina:* nine choices, unidentified hydrozoan: one choice; P = 0.0215). The results were similar when the total number of times a potential prey species was chosen were accounted for. A total of seventeen choices were recorded (Table 11) and the nudibranchs also showed a significant preference for *B. neritina* (*B. neritina:* fifteen choices, unidentified hydrozoan: two choices; χ^2 = 9.94). Each nudibranch specimen made at least one choice throughout the duration of the experiments.

Table 11: *Polycera hedgpethi* feeding-choice experiments with two potential prey species. Number of choices considering the first choice and the total number of choices.

Polycera hedgpethi (n = 5)	Number of choices				
	Bugula neritina	*Unidentified hydrozoan*	*Degree of freedom (df)*	χ^2	Significance
[a] First choice	9	1	-	-	P = 0.0215
[b] All choices counted	15	2	1	9.94	P = 0.0016

[a] number of choices considering the first choice (2-tailed binomial test, α = 0.05, P = 0.5), [b] total number of choices (Chi-squared test, α = 0.05).

When the total time each specimen spent grazing on each prey was considered (Table 12), the results were similar, with *B. neritina* being significantly preferred. The difference between the observed and expected frequencies was extremely statistically significant (χ^2 = 97.64 for the cumulative time spent on prey for all the specimens, n = 5). The cumulative total time spent on prey was 56.2 hours and during the remaining hours, the nudibranchs crawled, either at the bottom or on the walls of the tank. Out of the 56.2 hours spent on both prey, a total of 56 hours were spent on *B. neritina* (Table 12) and a total of 0.1 hours on the unidentified hydrozoan. All *P. hedgpethi* specimens spent between 98 to 100% of their time grazing on *B. neritina.* Individual nudibranchs could be recognised by their size and/or shape, and the

behaviour of each individual nudibranch was analysed (Figure 56). The strong preference for *B. neritina* was consistent in every individual ($92.16 < \chi^2 < 100$). Across the whole duration of the experiments, each specimen spent between 7 to 77% of their time on prey. The time spent on each prey for each *P. hedgpethi* specimen per individual is available in Appendix B.1**.**

Table 12: *Polycera hedgpethi* feeding-choice experiments with two potential prey species. Frequency of the total time spent on prey considered.

Polycera hedgpethi specimens (n = 5)	*Bugula neritina*		*Unidentified hydrozoan*		Total			
	Time on prey (h)	Frequency (%)	Time on prey (h)	Frequency (%)	Time on prey (h)	*df*	[a] χ^2	Significance
1	7.8	99	0.1	1	7.9	1	96.04	P < 0.0001
2	15.0	100	0.0	0	15.0	1	100.00	P < 0.0001
3	1.4	98	2.3×10^{-2}	2	1.5	1	92.16	P < 0.0001
4	20.2	100	0.0	0	20.2	1	100.00	P < 0.0001
5	11.6	100	0.0	0	11.6		100.00	P < 0.0001
Cumulative time on prey (h)	**56.0**	**100**	**0.1**	**0**	**56.2**	**1**	**97.64**	**P < 0.0001**

[a] Chi-squared test, α = 0.05.

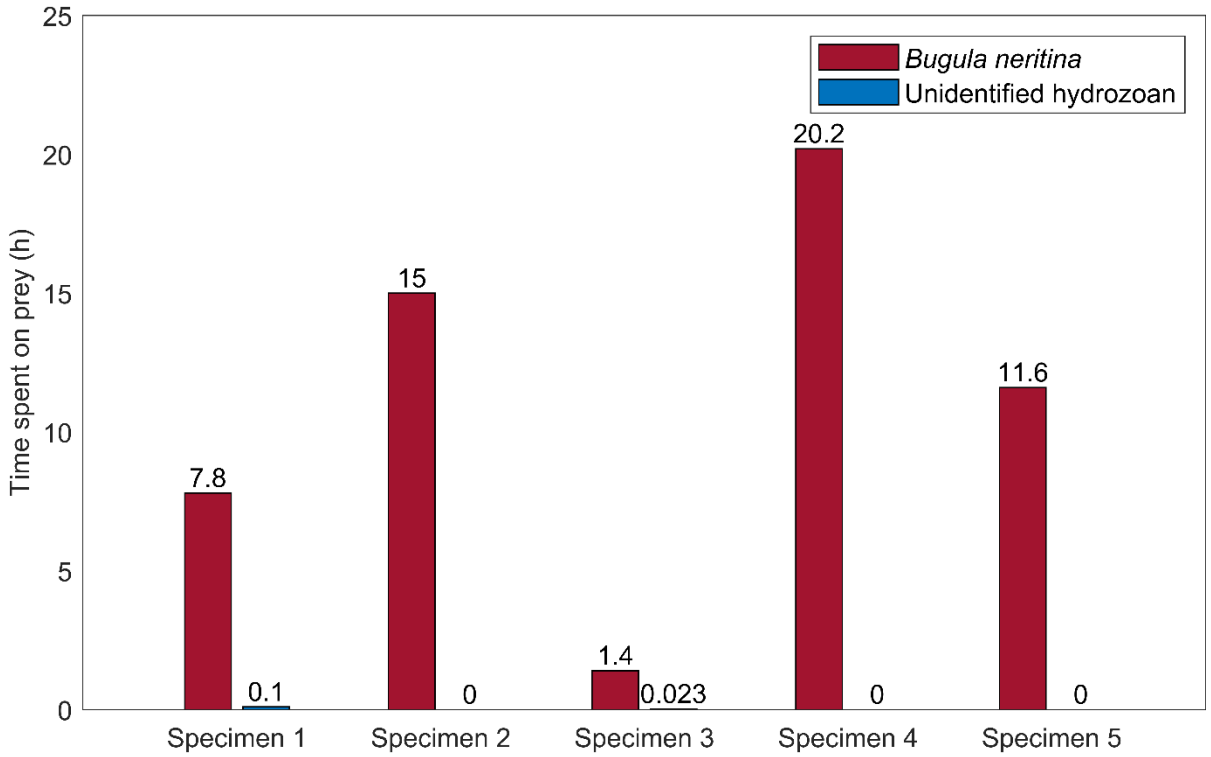

Figure 56: Time spent on prey for each *Polycera hedgpethi* specimen across the feeding-choice experiments (n = 5).

3.2.3 Discussion

The results of the three different data analysis approaches led to the same conclusion: *B. neritina* is significantly preferred over the unidentified hydrozoan (Figure 57). This preference was consistent across every specimen tested. The fact that the results were similar when considering the first choice made and the time spend on prey suggests that *P. hedgpethi* can locate its prey by chemoreception, despite the experiments being conducted without any water flow. These results match observations in the wild, where most specimens were found on *B. neritina*. This preference also explains the presence of the eggs on *B. neritina* as the nudibranchs are potentially sequestering compounds from their prey, hence laying eggs on the bryozoan is likely to offer protection to the offspring. During the feeding-choice experiments, once *B. neritina* was located, several specimens stayed feeding on it for several hours and then continued crawling around the tank, while in many cases, the specimens stayed feeding on *B. neritina* until the end of the experiment (Figure 57). Nudibranchs are grazing organisms and considering the long time the specimens spent on *B. neritina*, one interpretation of the results is that the specimens left the bryozoan when they were satiated.

The nudibranchs were not repulsed upon contact with the unidentified hydrozoan, but they did not show any interest in it. As such, the nudibranchs that chose it, as either a first choice or as a subsequent choice, did not spend more than five minutes at a time on the unidentified hydrozoan. Considering the difference in the time spent on either prey being particularly statistically significant, it indicates that *P. hedgpethi* seems to be a specific predator. However, feeding-choice experiments with more bryozoan species should be conducted to confirm this, especially using species *P. hedgpethi* has previously been reported found on.[312] The chemical analysis of *P. hedgpethi* from a subsequent collection, its eggs and *B. neritina* specimens could potentially establish a chemical link, on top of this ecological link.

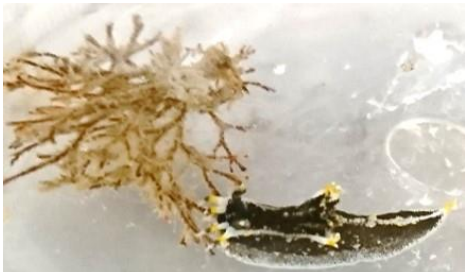

Figure 57: *Polycera hedgpethi* (3 cm long) feeding on *Bugula neritina*.

3.3 *Ceratosoma amoenum*

Ceratosoma amoenum (Cheeseman, 1886, Figure 58) (Family: Chromodorididae, Subfamily: Miamirinae, Figure 59), also known as the "clown nudibranch", can be found in Australasian waters. The large and vivid orange spots covering a predominantly white mantle make it easily recognisable, even though variations in the size and number of spots is prevalent. *C. amoenum* specimens can be found on rocky reefs at a depth of five to fifteen metres. Adult specimens can reach six cm long, although two to three cm is more common. This species is known to feed on sponges,[206] and has been documented to feed on *Dysidea fragilis.*[313]

Figure 58: Two *Ceratosoma amoenum* specimens (each 4 to 5 cm long) crawling in a tank.

Suborder Doridina
Infraorder Doridoidei
Superfamily Chromodoridoidea
Family Chromodorididae
Subamily Miamirinae
Genus Ceratosoma
Species *Ceratosoma amoenum*

Figure 59: Taxonomic classification of *Ceratosoma amoenum* according to the World Register of Marine Species (WoRMS).[8]

3.3.1 Collection and field study

A total of four *C. amoenum* specimens were collected using snorkelling in October 2022 in Dive Crescent, a sponge meadow located three metres deep within Tauranga harbour, New Zealand. The meadow is known to support several species of sponge, among which is the recently reported species *Dysidea teawanui*[251] (Figure 60) (Order: Dictyoceratida, Family: Dysideidae), and an as yet undescribed black sponge, *Dictyodendrilla* cf. *dendyi* (Order: Dendroceratida, Family: Dictyodendrillidae), that has some diagnostic skeletal similarities to *Dictyodendrilla dendyi* (Figure 60) initially reported from northern New Zealand.[314] *C. amoenum* had previously been recorded at this location, and a previous report[251] documented its predation on the distinctive, large, blue sponge *Dysidea teawanui*. For our collection, the specimens were either found on *Dysidea teawanui* or on *D.* cf. *dendyi.* Feeding-choice experiments were then conducted, with *D*. cf. *dendyi* and *Dysidea teawanui* as offered prey, to assess the dietary preferences and possibly establish an ecological link.

Figure 60: A- Underwater photograph of *Dysidea teawanui*[251] (reproduced with permission from the copyright holder), B- *Dictyodendrilla dendyi* (courtesy of the Victoria University of Wellington Marine Natural Products group).

3.3.2 Feeding-choice experiments

Experiments with *C. amoenum* were carried out on four individuals (n = 4), with eleven experiments conducted, for a total experiment duration of 109 hours across all specimens. A total of sixteen first choices were recorded in total and neither sponge was significantly preferred (*D.* cf. *dendyi:* nine choices, *Dysidea teawanui*: seven choices; P = 0.8036). The results were similar when the total number of times a sponge species was chosen were accounted for. A total of nineteen choices were recorded (Table 13) but no nudibranch showed a significant preference for one of the sponges (*D.* cf. *dendyi*: eleven choices, *Dysidea teawanui*: eight choices, $\chi^2 = 0.474$). Each nudibranch specimen made at least three choices throughout the duration of the experiments.

Table 13: *Ceratosoma amoenum* feeding-choice experiments with two sponge species as offered prey. Number of choices considering the first choice and the total number of choices.

Ceratosoma amoenum (n = 4)	Number of choices				
	Dictyodendrilla cf. dendyi	*Dysidea teawanui*	*Degree of freedom (df)*	χ^2	Significance
[a] First choice	9	7	-	-	P = 0.8036
[b] All choices counted	11	8	1	0.47	P = 0.4913

[a] number of choices considering the first choice (2-tailed binomial test, $\alpha = 0.05$, P = 0.5), [b] total number of choices (Chi-squared test, $\alpha = 0.05$).

When the total time each specimen spent grazing on each prey was considered (Table 14), the results indicated that *C. amoenum* significantly prefers *Dysidea teawanui*, with the difference between the observed and expected frequency being statistically significant ($\chi^2 = 10.240$ for the cumulative time spent on prey for all the specimens, n = 4). The total time spent on prey was 91.1 hours and during the remaining hours, the nudibranchs crawled either at the bottom of the tank or on the walls. Out of the 91.1 hours spent on both prey, 31.1 hours were spent on *D. cf. dendyi* (34%) and 60 hours on *Dysidea teawanui* (66%). The behaviour of each individual nudibranch was analysed (Figure 61), and this preference was consistent in every individual ($7.8 < \chi^2 < 92.16$), except one that significantly preferred *D. cf. dendyi* ($\chi^2 = 19.36$). Across the whole duration of the experiment, each specimen spent between 10 to 34% of their time on prey. The time spent on each prey for each *C. amoenum* specimen per individual experiment can be found in Appendix B.2.

Table 14: *Ceratosoma amoenum* feeding-choice experiment with two sponge species as offered prey. Frequency of the total time spent on prey considered.

Ceratosoma amoenum specimens (n = 4)	*Dictyodendrilla cf. dendyi*		*Dysidea teawanui*		Total			
	Time on prey (h)	Frequency (%)	Time on prey (h)	Frequency (%)	Time on prey (h)	*df*	[a] χ^2	Significance
1	26.3	72	10.4	28	36.7	1	19.36	P < 0.0001
2	0.4	2	25.1	98	25.5	1	92.16	P < 0.0001
3	4.1	36	7.3	64	11.4	1	7.84	P = 0.0051
4	0.3	2	17.2	98	17.5	1	92.16	P < 0.0001
Cumulative time on prey (h)	**31.1**	**34**	**60.0**	**66**	**91.1**	**1**	**10.24**	**P = 0.0014**

[a] Chi-squared test, α = 0.05.

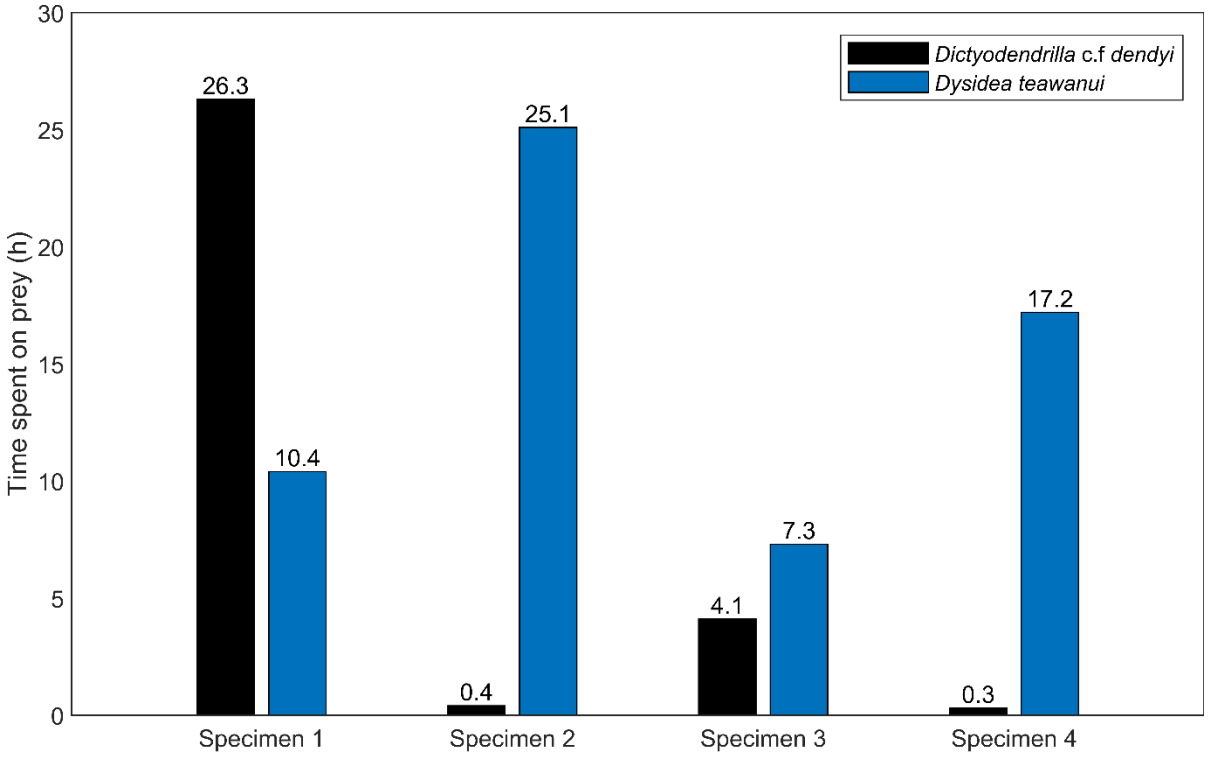

Figure 61: Time spent on prey for each *Ceratosoma amoenum* specimen across the feeding-choice experiments (n = 4).

3.3.3 Discussion

Results obtained when only the first choice a nudibranch made was considered and when all choices were considered provided similar results. Neither sponge was significantly preferred and *C. amoenum* specimens were not repulsed by either sponge before contact with the prey.

This differs from *P. hedgpethi* that showed a significant preference for *B. neritina* when both the first prey choice and all subsequent choices were considered. Therefore, *P. hedgpethi* might be able to more easily locate its prey by chemoreception compared to *C. amoenum*. This difference could also be explained by the fact that *C. amoenum* is a generalist feeder and therefore does not have a strong preference for a specific prey, as opposed to *P. hedgpethi* which tends to behave like a specialist feeder, based on our results.

When the total time each *C. amoenum* specimen spent grazing on either prey was considered, *Dysidea teawanui* was the preferred sponge species, although to a lesser extent than *Polycera* for *B. neritina.* Out of the four *C. amoenum* specimens studied, three had a significant preference for the blue *Dysidea teawanui* sponge. The scars on *Dysidea teawanui*, caused by the nudibranchs' grazing, confirmed that the nudibranchs were feeding on the prey (Figure 62). Once the specimens found *Dysidea teawanui*, they stayed for several hours grazing on it. *C. amoenum* is known to predate on *Dysidea teawanui*[251] and the results reported here match observations in the wild where most of the specimens collected were found on *Dysidea teawanui*. Even though *Dysidea teawanui* appears to be the preferred prey of *C. amoenum*, the idea that it might be a generalist predator cannot be excluded given that *C. amoenum* is widely distributed across Australasian waters and has previously been reported grazing on *Dysidea fragilis*.[313] This generalist predation behaviour could be explained by the fact that *C. amoenum* is not used to eating unpalatable compounds and therefore cannot ingest them in significant quantity, hence why it would feed on several sponges. Although, considering our feeding-choice results and the previous report of the nudibranch on *D. fragilis*, it appears that *C. amoenum* may prefer to feed on the *Dysidea* genus but is not limited to it.

Figure 62: *Dysidea teawanui* fragments (3 to 4 cm long) before (left) and after (right) feeding-choice experiments with *Ceratosoma amoenum.* Published open access under Creative Commons licenses (CC BY-NC-ND and CC BY) by Gris *et al*.[315]

3.4 *Goniobranchus aureomarginatus*

Goniobranchus aureomarginatus (Cheeseman, 1881, Figure 63) (Family: Chromodorididae, Subfamily: Chromodoridinae, Figure 64) is endemic to New Zealand, occurring around both main islands.[206] This species, often referred to as the gold-margined nudibranch, displays a uniformly opaque white mantle and foot, with a brilliant orange-yellow band on the edge of the mantle. Adult specimens usually reach a length of three cm and commonly live on rocky reefs between zero to twenty metres deep.[206] From a taxonomic point of view, many of the species initially belonging to the genus *Chromodoris* have been reclassified as *Goniobranchus* or *Felimare* during the past two decades, including *Goniobranchus aureomarginatus*.[316] Previous studies have shown that nudibranchs from the family Chromodorididae contain secondary spongian terpenoids typically found in sponges such as *Chelonaplysilla*, *Dendrilla*, *Aplysilla* and *Spongionella*.[317] While it is assumed that these nudibranchs feed on these particular sponges, direct observations of such feeding behaviour have not been made.[9,10] Within the *Goniobranchus* genus, several reports documented their spongivorous behaviour[133,206] and similarly to *C. amoenum, G. aureomarginatus* has been documented feeding on *Dysidea fragilis.*[313]

Figure 63: Underwater photograph of two *Goniobranchus aureomarginatus* individuals (each 5 cm long), courtesy of Warrick Powrie).

Suborder Doridina
Infraorder Doridoidei
Superfamily Chromodoridoidea
Family Chromodorididae
Subamily Chromodoridinae
Genus Goniobranchus
Species *Goniobranchus aureomarginatus*

Figure 64: Taxonomic classification of *Goniobranchus aureomarginatus* according to the World Register of Marine Species (WoRMS).[8]

3.4.1 Collection and field study

Goniobranchus aureomarginatus specimens were collected at Dive Crescent, the same sponge meadow inhabited by *C. amoenum,* studied above (GPS coordinates in Chapter 7 – Experimental, Section 7.2.1). Collection took place during two snorkelling trips between October and December 2022. A total of six specimens were collected; three of them were found grazing on *Dictyodendrilla* cf. *dendyi* and three roaming across rock and broken shell substrate. The fact that half of the specimens were found on *D*. cf *dendyi* and that most had black stomachs led to the belief that *D*. cf *dendyi* was their main prey and was preferred to *Dysidea teawanui,* also present in the sponge meadow at the time of collection. Feeding-choice experiments were then conducted to precisely assess the dietary preferences of *G. aureomarginatus* with *D*. cf. *dendyi* and *Dysidea teawanui* as offered prey.

3.4.2 Feeding-choice experiments

Experiments with *G. aureomarginatus* were carried out on the six individuals collected (n = 6), with between eight and eleven experiments conducted, for a total experiment duration of 94 to 124 hours across all specimens. To note, one of the specimens spawned during one of the experiments and analysis of the spawned eggs is reported later (Figure 65A). If the first choice the nudibranchs made between the offered sponge species is considered, a total of thirty-five choices were recorded (Table 15). Similarly to *C. amoenum*, neither sponge was significantly preferred (*D. cf dendyi*: twenty choices, *Dysidea teawanui*: fifteen choices; P = 0.4990). Each nudibranch specimen made at least two first choices of prey throughout the duration of the experiments. The results were similar when the total number of times a sponge species was chosen were accounted for. A total of 62 choices were recorded (Table 15) and no nudibranchs showed significant preference for one of the sponges (*D*. cf *dendyi*: thirty-seven choices, *Dysidea teawanui*: twenty-five choices, $\chi^2 = 2.323$).

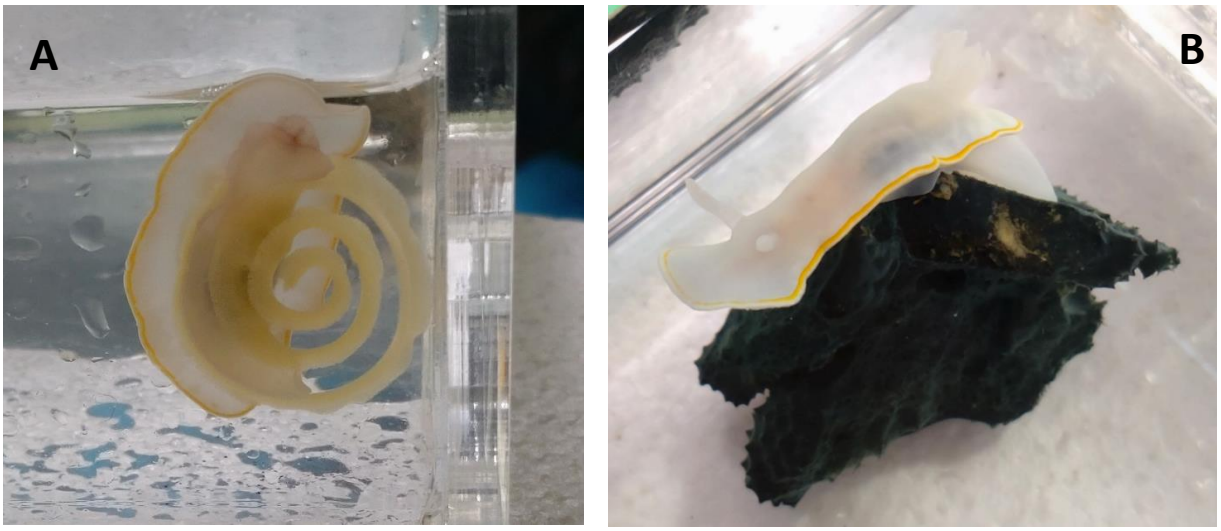

Figure 65: A- *Goniobranchus aureomarginatus* (5 cm long) spawning during an experiment. B- *Goniobranchus aureomarginatus* (5 cm long) crawling on *Dictyodendrilla* cf. *dendyi* during the feeding-choice experiments (published open access under Creative Commons licenses (CC BY-NC-ND and CC BY) by Gris *et al.*[315]

Table 15: *Goniobranchus aureomarginatus* feeding-choice experiments with two sponge species as offered prey. Number of choices considering the first choice and the total number of choices.

Goniobranchus aureomarginatus (n = 6)	Number of choices				
	Dictyodendrilla cf *dendyi*	*Dysidea teawanui*	*Degree of freedom (df)*	χ^2	Significance
[a] First choice	20	15	-	-	P = 0.4990
[b] All choices counted	37	25	1	2.32	P = 0.1275

[a] number of choices considering the first choice (2-tailed binomial test, $\alpha = 0.05$, P = 0.5), [b] total number of choices (Chi-squared test, $\alpha = 0.05$).

When the total time each specimen spent grazing on each prey was considered (Table 16), the results were very different, with *D. cf dendyi* being significantly preferred (Figure 65B). The difference between the observed and expected frequencies was extremely statistically significant ($\chi^2 = 73.96$ for the cumulative time spent on prey for all the specimens, n = 6). The total time spent on prey was 105 hours and during the remaining hours, the nudibranchs crawled, either at the bottom or on the walls of the tank. Out of the 105 hours spent on prey, 97.2 hours were spent on *D. cf dendyi* (93%) (Figure 66) and 7.9 hours on *Dysidea teawanui* (7%). All *G. aureomarginatus* specimens spent between 88 to 99% of their time grazing on *D. cf dendyi*. Individual nudibranchs could be recognised by their size and/or shape, and the

behaviour of each individual nudibranch was analysed (Figure 66). The strong preference for *D. cf dendyi* was consistent in every individual ($57.76 < \chi^2 < 96.04$). Across the whole duration of the experiments, each specimen spent between 7 to 41% of their time on prey. The time spent on each prey for each *G. aureomarginatus* specimen per individual experiment can be found in Appendix B.3.

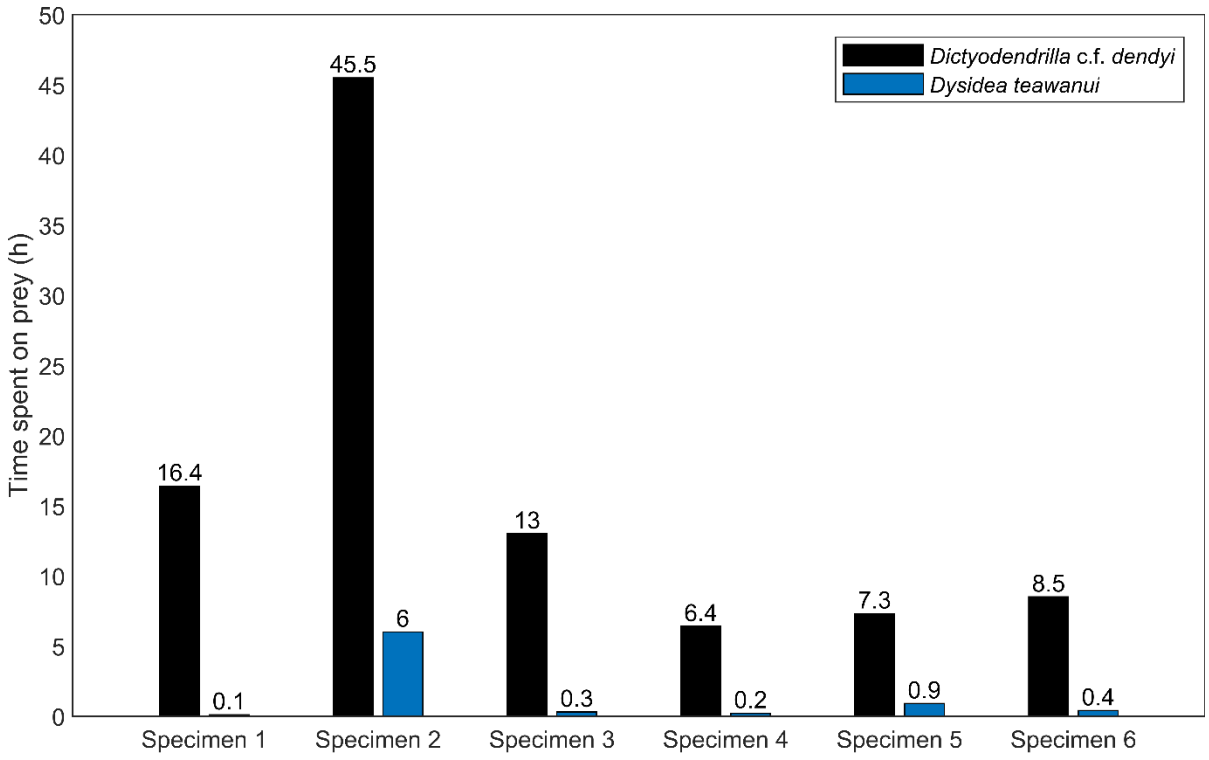

Table 16: *Goniobranchus aureomarginatus* feeding-choice experiment with two sponge species as offered prey. Frequency of the total time spent on prey considered.

Goniobranchus aureomarginatus specimens (n = 6)	*Dictyodendrilla* cf. *dendyi*		*Dysidea teawanui*		Total			
	Time on prey (h)	Frequency (%)	Time on prey (h)	Frequency (%)	Time on prey (h)	*df*	[a] χ^2	Significance
1	16.4	99	0.1	1	16.5	1	96.04	P < 0.0001
2	45.5	88	6.0	12	51.5	1	57.76	P < 0.0001
3	13.0	98	0.3	2	13.3	1	92.16	P < 0.0001
4	6.4	98	0.2	2	6.6	1	92.16	P < 0.0001
5	7.3	89	0.9	11	8.2	1	60.84	P < 0.0001
6	8.5	96	0.4	4	8.9	1	84.64	P < 0.0001
Cumulative time spent on prey (h)	**97.2**	**93**	**7.9**	**7**	**105.0**	**1**	**73.96**	**P < 0.0001**

[a] Chi-squared test, $\alpha = 0.05$.

3.4.3 Discussion

Similarly to *C. amoenum*, the results obtained when only the first choice was considered and when all choices were considered showed that neither sponge was significantly preferred. It also showed that *G. aureomarginatus* was not repulsed by either sponge before contact with the prey. When the total time each nudibranch specimen spent grazing on either sponge was considered, results were significantly different. *G. aureomarginatus* specimens had an extremely clear preference for *D.* cf. *dendyi.* These results match observations in the wild, where half of the specimens collected were found on *D.* cf. *dendyi* and the remaining specimens were found crawling on the seafloor as opposed to on an alternative prey species. During the feeding-choice experiments, once the nudibranchs found *D.* cf. *dendyi*, they either stayed feeding on it for several hours and then continued crawling around the tank or stayed on the sponge until the end of the experiment. Nudibranchs are grazing organisms and considering the long time the specimens spent on *D.* cf. *dendyi*, one interpretation of the results is that the specimens left *D.* cf. *dendyi* when they were satiated. Each time *Dysidea teawanui* was chosen, the nudibranchs specimens crawled through it but very quickly abandoned it, except for one specimen who stayed on *Dysidea teawanui* for a total of 6 hours across all experiments. As these animals are slow-moving, for most of the specimens, the recorded time spent on *Dysidea teawanui* is the time needed to crawl through the sponge. Therefore, *G. aureomarginatus* seems to have no specific interest in grazing on *Dysidea teawanui*. Considering the difference in the time spent on either prey being statistically significant, it indicates that *G. aureomarginatus* seems to be a specific predator. However, feeding-choice experiments with more sponge prey should be conducted to confirm this.

To date, *G. aureomarginatus* has only been reported grazing on *Dysidea fragilis,*[313] which has not been recorded at the collection site. However, the previous study from the Prinsep research group[210] on *A. gracei* (Chapter 2, Section 2.2) showed that *G. aureomarginatus,* was potentially preying on it. However, the bryozoan has not been found at the collection site since 2019. The results presented here suggest that *G. aureomarginatus* had to possibly switch its diet and is now feeding on *D.* cf. *dendyi.* To confirm this, chemical analysis of *G. aureomarginatus* from a subsequent collection, its eggs and *D.* cf. *dendyi* were conducted and the results are presented in Chapter 4.

3.5 Summary

In this research, an experimental configuration to accurately assess dietary preferences of dorid nudibranchs has been developed. Feeding-choice experiments were then conducted on three dorid nudibranch species, including two sponge-eaters and a bryozoan-eater, also possibly feeding on hydrozoans. This resulted in the establishment of three ecological links, with each nudibranch species showing statistically relevant preferences for specific prey. For each species, the results were statistically relevant when the time spend grazing on prey was considered, although *P. hedgpethi's* preference for *B. neritina* was also statistically relevant when the first choice and subsequent choices were examined. Upon investigation of the preferences of *C. amoenum* and *G. aureomarginatus* towards the same two sponges, both nudibranch species displayed different preferences. As such, *C. amoenum* showed a preference for *Dysidea teawanui*, while *G. aureomarginatus* showed a strong preference for *D.* cf. *dendyi*. The results of the experiments matched the observations in the wild, corroborating the ecological links established, the accuracy of the experimental configuration and the approaches taken to analyse the results.

For this research, the feeding-choice experiments acted as a bioassay carried out by the nudibranchs to provide guidance towards potentially bioactive prey and offered insights onto possible predator-prey relationships. Based on these results, nudibranchs of the same species from separate collections, their eggs and their preferential prey were then chemically analysed to investigate the transfer of metabolites to the eggs and the occurrence of secondary metabolites in both prey and predator organisms, which in one instance confirmed the predator-prey relationship and led to the isolation of new metabolites.

Chapter 4

Investigation of predator-prey relationships by chemical analysis

---

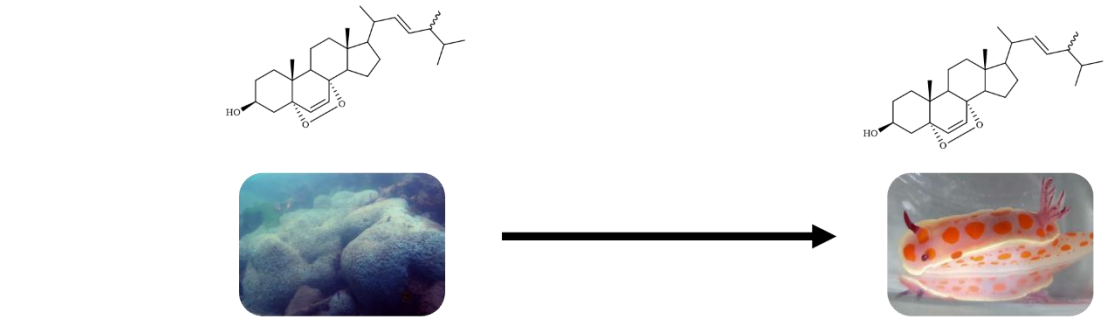

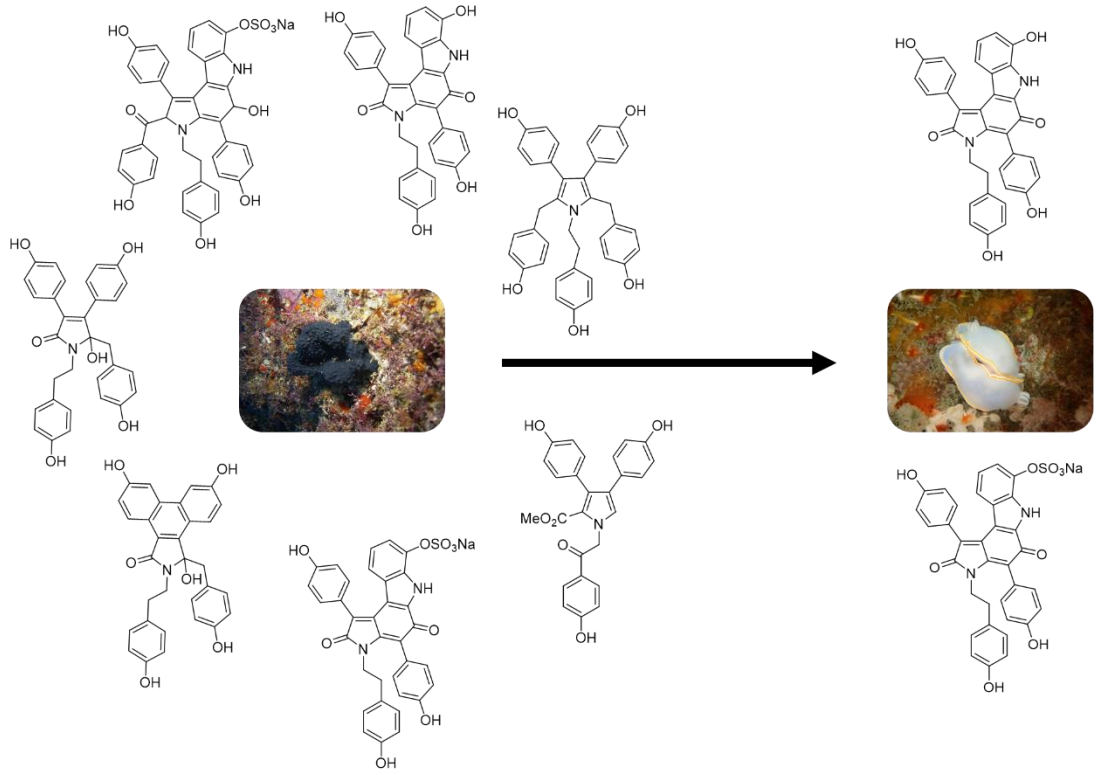

The three nudibranch species, *Polycera hedgpethi*, *Ceratosoma amoenum* and *Goniobranchus aureomarginatus*, previously studied in Chapter 3 for their dietary preferences, along with eggs spawned during captivity, and their preferred prey were analysed to investigate chemical relationships and possible transfer of metabolites to the offspring. The occurrence of secondary metabolites in both predator and preferred prey would establish chemical links and could confirm the predator-prey association.

To conduct the chemical analyses, more specimens of *Ceratosoma amoenum* and *Goniobranchus aureomarginatus,* and their preferred prey, *Dysidea teawanui* and *D*. cf. *dendyi*, respectively, were collected during several dive trips, and subsequently extracted. Fresh *Polycera hedpethi* specimens could not be located after the initial collection and a single *P. hedpethi* specimen which was frozen following feeding-choice experiments, was analysed. The crude extracts were screened for cytotoxicity against a human cervical cancer cell line (HeLa) using a MTT assay, prior to being purified.

The purification of extracts and fractions of interest had been previously guided by LC-MS screening within the Prinsep research group. However, for most of the time during which this research was conducted, no LC-MS instrument was available. Therefore, to purify the extracts of interest, an approach based on TLC and HR-ESI-MS was developed as an alternative guide. To aid in this, the prey extracts were purified first because their extraction afforded a higher concentration of crude extract. The nudibranch and egg extracts were then subsequently purified to investigate the presence of common metabolites. Investigation into the metabolite distribution and morphological analysis is also reported when relevant.

4.1 *Polycera hedgpethi* and *Bugula neritina*

4.1.1 Sample collection and extraction

During the feeding-choice experiments, *P. hedgpethi* showed a strong preference for *B. neritina*. Therefore, a fresh specimen of the bryozoan was collected in May 2022 at Salisbury Wharf, Tauranga for chemical investigation. A single *P. hedgpethi* specimen from New Zealand and four Australian individuals from Melbourne, previously extracted by former student in the group Geoff Tait, were also chemically investigated to study the predator-prey relationship. Two of the egg masses spawned while maintaining the nudibranchs in the laboratory tanks for feeding-choice experiments were also used for chemical analysis.

4.1.2 *Bugula neritina*

Reported metabolites from *Bugula neritina*

Bugula neritina is one of the most common bryozoans[318] and has received considerable attention, which was sparked by an early report describing the potent cytotoxic activity of its crude extract.[319] This prompted the isolation and structural elucidation of the main active component, bryostatin 1 (**161**), which was achieved in 1982 by Pettit *et al*.[320] The 20-membered macrolactone (**161**) has been in numerous clinical trials since the early 2000s and is currently being tested for the treatment of Alzheimer's disease.[321]

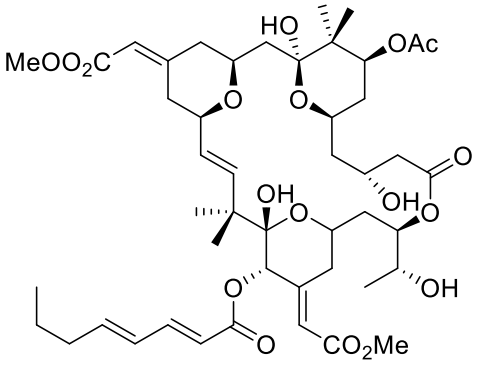

161

Twenty more bryostatins, all displaying a common macrolactone core with three tetrahydropyran rings,[322] have since been described, primarily by Pettit *et al.*[323-333] Reported bioactivities include cognition and memory enhancement along with cytotoxicity.[334]

Aside from bryostatins, compounds belonging to the ceramide class are prevalent in *B. neritina*.[335,336] Ceramides contain an amide-linked, long-chain fatty acid base, and have previously been reported from various marine organisms, including but not limited to starfish,[337] sea anemones,[338,339] and sponges.[340] Ceramide 1 (**162**) and several glycosylated-ceramides, or cerebrosides, such as cerebroside 6 (**163**), were initially reported in 2009 by Tian *et al.* from *B. neritina* inhabiting the South China Sea.[335] In 2014, further ceramides, neritinaceramides A–E (**164-168**), also reported by Tian *et al.,* were described.[336] Aside from bryostatins, ceramides and cerebrosides, a range of alkaloids,[341] fatty aldehydes[342] and sterols[318,343,344] have also been reported from *B. neritina*.

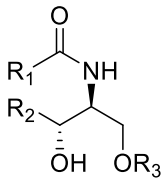

162 $R_1 = (CH_2)_{12}CH_3$, $R_2 = CH{=}CH(CH_2)_{12}CH_3$, $R_3 = H$
163 $R_1 = (CH_2)_{15}CH_3$, $R_2 = CH{=}CH(CH_2)_{12}CH_3$, $R_3 =$ glucose

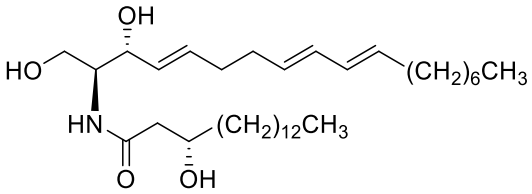

164

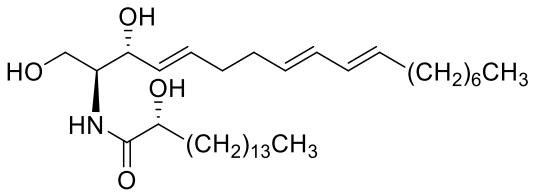

165

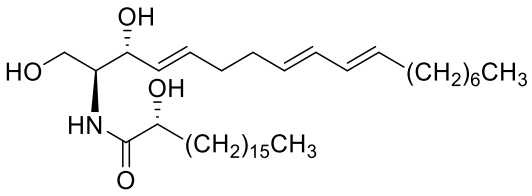

166

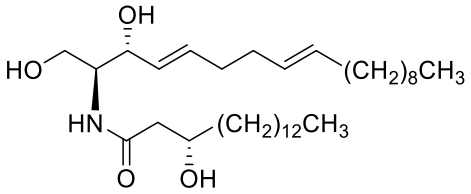

167

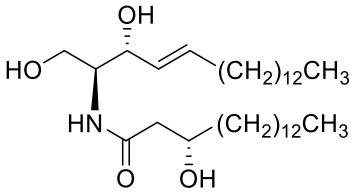

168

Chemical investigation

A crude extract of *B. neritina* was purified by reversed phase bench column chromatography. Each fraction was analysed by TLC and HR-ESI-MS in positive and negative ion mode. None of the fractions displayed noticeable spots on TLC, except for fraction 8 that contained a yellow spot at a high Rf (0.96). No fractions displayed ions corresponding to compounds previously isolated from the *Bugula* genus (Chapter 4 – Section 4.1.2) on HR-ESI-MS (either in positive or negative ion mode), and no other ions of interest were detected. Despite this, as an additional check, five fractions that eluted with mid-range polarity solvents were screened by ^{1}H NMR spectroscopy. Except for fraction 8 that contained cholesterol, no signals corresponding to potential natural products were detected. Therefore, no further purification was carried out.

4.1.3 *Polycera hedgpethi* and its eggs

Cytotoxicity of crude extracts

A single *P. hedgpethi* specimen, and two spawned egg masses were extracted, followed by screening for cytotoxic activity against HeLa cells using the procedure described in Chapter 7 - Experimental, Section 7.7.6. *P. hedgpethi* specimens were judged too small for dissection and therefore, only the whole-body extract was assessed. Chemical investigation of the *B. neritina* specimen was carried out before cytotoxicity screening of the crude extract, although because no natural products were detected, screening the extract afterwards was deemed unnecessary.

The cytotoxicity screening revealed that the egg extract was more cytotoxic (IC_{50} 58 µg mL^{-1}) than the whole-body (IC_{50} >100 µg mL^{-1}), although both extracts displayed minimal activity (Figure 67). Similarly to *H. sanguineus* whose eggs display a greater concentration of certain macrolides than in the nudibranch itself,[171,172,174] it may be possible that *P. hedgpethi* selectively transfers metabolites to its eggs in high concentration. To examine this, both the eggs and nudibranchs were chemically investigated.

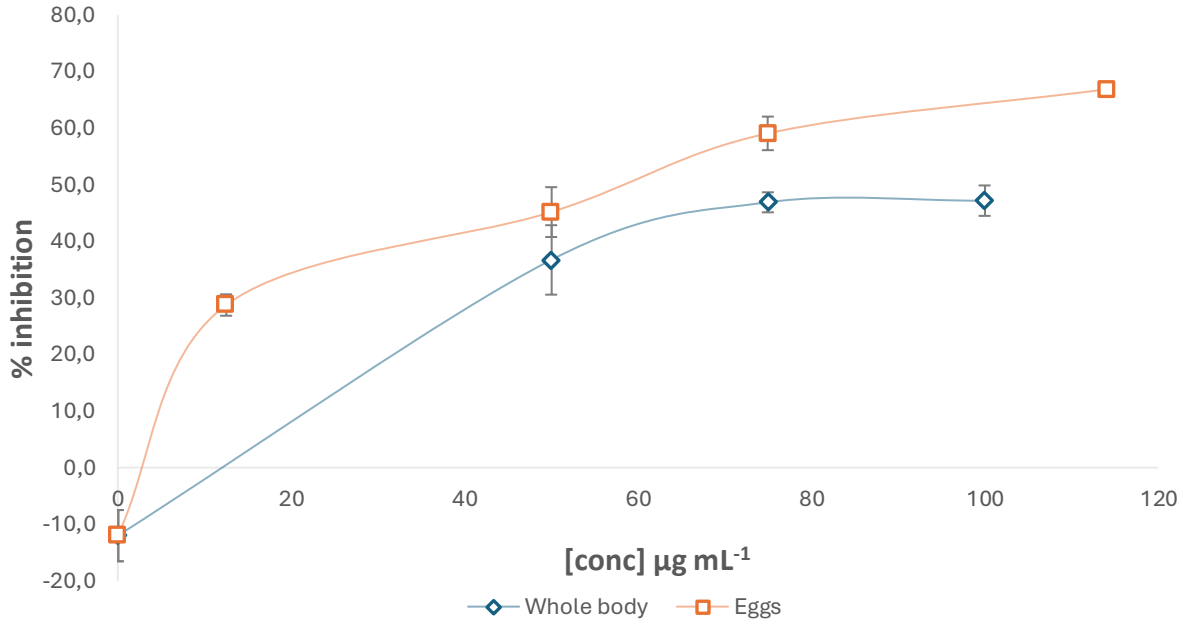

Figure 67: Cytotoxicity of the crude extracts of *Polycera hedgpethi* and its eggs on HeLa cells using an MTT assay.

Reported metabolites from *Polycera* species

Despite currently containing seventy-two species,[345] the genus *Polycera* has received little attention from natural products chemists,[346] with the exception of *P. tricolor*, *P. maderae, P. elegans*, *P. atra*, and *P. hedgpethi.*[177,346-348]

The first report of the chemistry of a Polycerinae nudibranch dates back to 1985 with the description of triophamine (**169**) from *Polycera tricolor*.[177] Compound (**169**) was initially isolated from the dorid nudibranch *Triopha catalinae,*[349] and subsequently isolated from a Chilean specimen of *Thecacera darwinii*.[350] Triophamine (**169**) contains the rare diacylguanidine functionality which is symmetrically bis-acylated by two polyketide acyl residues.[346] The absence of compound (**169**) from the bryozoan prey and its occurrence from specimens inhabiting different collection sites indicated a possible *de novo* biosynthetic origin, which was later proven by *in vivo* feeding experiments with stable isotopes.[351]

The only naturally occurring close analogue of compound (**169**) is limacianine (**170**), isolated from the dorid nudibranch *Limacia clavigera*. In 2019, a study conducted by Carbone *et al.* investigated whether symmetrical diacylguanidines are chemical markers of Polyceridae nudibranchs.[346] Three Polyceridae species, namely *P. maderae*, *P. elegans* and *Thecacera*

pennigera were investigated. Chemical analysis highlighted that *P. maderae* and *T. pennigera* contained compound (**170**), while *P. elegans* contained compound (**169**). These findings agreed with compounds previously reported for other Polyceridae nudibranchs, such as *T. catalinae*, *P. tricolor*, and *L. clavigera,* hence it was suggested that compounds (**169**) and (**170**) are chemical markers of the Polyceridae family.[346]

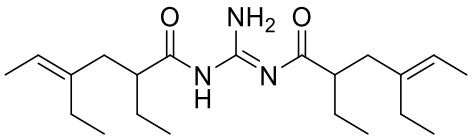

169

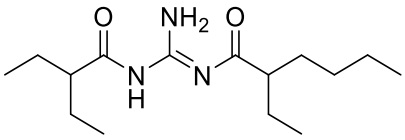

170

The nudibranchs *Polycera atra and P. hedgpethi* from California sequester bryostatins from their bryozoan prey *B. neritina*, and transfer these macrolides to their eggs.[347,348] Of interest is that the bryostatin diversity is thirteen times higher in *P. atra* than in *B. neritina,* and even higher in the egg masses, indicating a defensive role.[347] The difference in bryostatin profiles between *B. neritina* and *P. atra* also indicated that the nudibranch selectively sequesters specific bryostatins.[347]

Chemical investigation

Following the execution of the feeding-choice experiments, several dive trips were conducted to collect additional *P. hedgpethi* specimens, but no further individuals could be located. Therefore, chemical investigation was conducted on a single *Polycera* specimen that was used for the feeding-choice experiments and subsequently frozen. The specimen was extracted, and the crude extract was screened by LC-MS following the methodology described in Chapter 7 – Experimental, Section 7.1.11. Extracted ion mode was utilised to search for the presence of bryostatins, triophamine (**169**) and limaciamine (**170**) but their presence was not detected (Figure 68). The crude extract was also screened by ^{1}H NMR spectroscopy in chloroform-*d* for the presence of the compounds mentioned above, but no characteristic signals were detected. Therefore, no further purification was carried out.

Two of the six egg masses spawned in the laboratory tanks were extracted and screened by LC-MS, but as for New Zealand specimens of *B. neritina* and *P. hedgpethi*, no peaks of any significance were detected in the chromatogram nor ions of interest in the mass spectrum.

To investigate whether Australian specimens may also lack compounds of interest, four *P. hedgpethi* specimens collected near Melbourne, Australia in 2018 were investigated. The combined extract was purified by reversed phase bench column chromatography. Each fraction was analysed by HR-ESI-MS in positive and negative ion mode. None of the fractions displayed ions corresponding to bryostatins or to compounds previously isolated from the *Bugula* genus. Despite this, two fractions that eluted with 100% MeOH were screened by ^{1}H NMR spectroscopy in methanol-d_4. No signals corresponding to potential natural products were detected and no further purification of the extract was carried out.

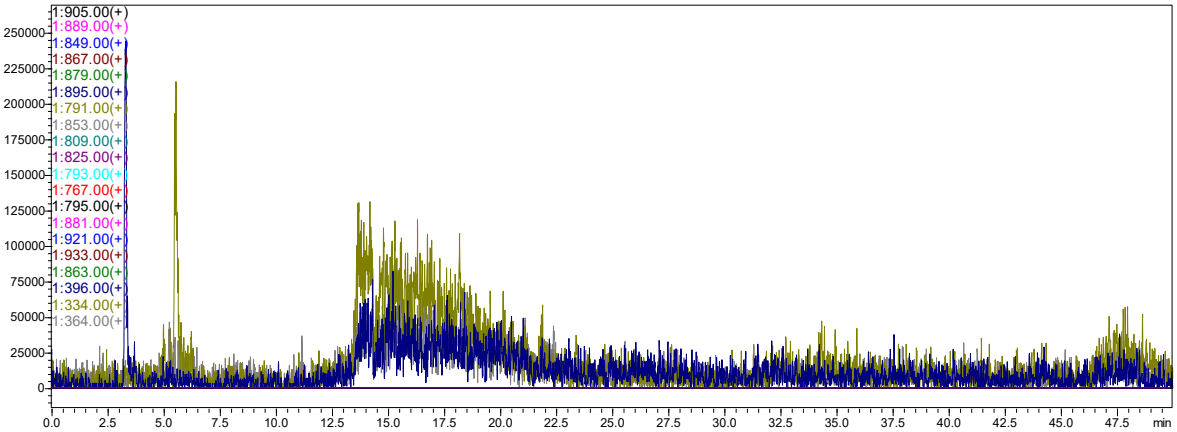

Figure 68: LC-MS chromatogram (extracted ion mode) to screen for the presence of bryostatins and diacylguanidines (**169**) and (**170**).

4.1.4 Concluding remarks

The absence of bryostatins from New Zealand specimens of *B. neritina* or *P. hedgpethi* is consistent with a previous Australasian study conducted within the Prinsep research group.[352] During that study, a Melbourne specimen of *B. neritina* was investigated, and the extracts did not show evidence of bryostatins. Both bryozoan and nudibranch samples from Melbourne were not collected at the same location and therefore, at the time, the basis of a feeding relationship was uncertain.

The feeding-choice experiments conducted during this research proved that *P. hedgpethi* preys on *B. neritina*, but no evidence of a chemical link was found, with no natural products detected in prey, predator and egg extracts. This potentially explains the low cytotoxicity of the extracts observed during the initial screening. With no evidence of the diacylguanidines (**169**) and (**170**) within the studied extracts, the findings reported here disagree with the study conducted by Carbone *et al.* suggesting that symmetrical diacylguanidines are chemical markers of Polyceridae nudibranchs.[346]

The results reported here are also in contrast with two previous Californian studies conducted on *B. neritina*, *P. atra* and *P. hedgpethi*.[347,348] These studies showed that both nudibranchs selectively sequester bryostatins from their bryozoan prey *B. neritina* and transfer certain macrolides to their egg masses for defensive purposes,[347,348] which was not observed in this study. The absence of bryostatins from New Zealand and Australian specimens of *B. neritina* potentially indicates that they do not contain the bacterial symbiont *Candidatus* Endobugula sertula, believed to be the actual producer of the bryostatins.[322]

4.2 *Ceratosoma amoenum* and *Dysidea teawanui*

During the feeding-choice experiments, *C. amoenum* showed a highly significant preference for the large blue *Dysidea teawanui* sponge. Therefore, additional specimens of *Dysidea teawanui* were collected between December 2021 and April 2023 in Dive Crescent to conduct chemical analysis and cytotoxicity screening. Two specimens of *C. amoenum*, collected a year apart from the same location were investigated chemically. Another specimen was used to conduct the cytotoxicity screening. Finally, an egg coil spawned in a tank by a specimen collected in June 2020 was investigated. All samples were extracted following the methodology described in Chapter 7 – Experimental, Section 7.1.4.

4.2.1 Cytotoxicity of crude extracts

The egg extract (IC_{50} > 100 µg mL^{-1}) and *Dysidea teawanui* extract (IC_{50} > 100 µg mL^{-1}) were less cytotoxic than the whole-body nudibranch extract (IC_{50} 82 µg mL^{-1}), although all three extracts displayed minimal activity (Figure 69). As opposed to *P. hedgpethi*, the eggs of *C. amoenum* were less cytotoxic than the whole-body, possibly indicating a lack of bioactive metabolites within the offspring.

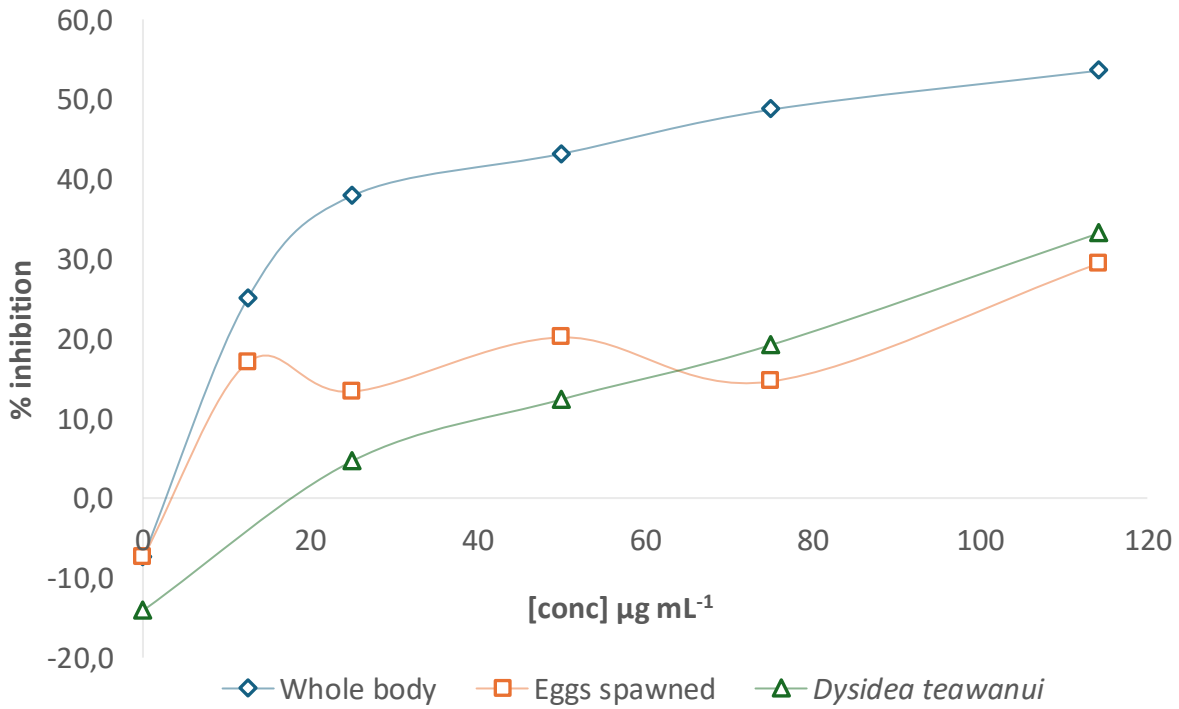

Figure 69: Cytotoxicity of the crude extracts of *Ceratosoma amoenum*, its eggs and *Dysidea teawanui* against HeLa cells using an MTT assay.

4.2.2 *Dysidea teawanui*

Reported metabolites from the genus *Dysidea*

Dysidea is one of the most widespread sponge genera around the world, especially in subtropical and tropical regions.[353] *Dysidea* species have been investigated for over 40 years,[354] resulting in the isolation of a vast number of unique and bioactive metabolites, including, but not limited to, polybrominated phenyl ethers,[355,356] polychlorinated amino acid derivatives,[356] polyhydroxy steroids[357] and terpenoids.[102,358]

Notable metabolites isolated include the unusual dimeric C21 meroterpenoid dysiarenone (**171**) from *Dysidea arenaria.*[358] Compound (**171**) showed potent inhibitory activities against COX-2 expression and PGE_2 production in LPS-stimulated RAW264 macrophages (IC_{50} 6.4 µM).[358] The sesquiterpene-quinone (**172**) and acetylated hydroquinone (**173**) were isolated from a New Zealand specimen of *D.* cf. *cristagalli* as inhibitors of superoxide production (IC_{50} 3 µM and 11 µM, respectively).[359] A neurotoxic α-amino acid derivative, dysibetaine 1 (**174**), was initially isolated from *D. herbacea* from Micronesia, while a subsequent investigation yielded further betaines, such as the dipeptide dysibetaine PP (**175**) mentioned in Chapter 2, and two cyclopropane betaines, (**176**) and (**177**).[360] An investigation into a *D. avara* specimen inhabiting South China Sea waters afforded four sesquiterpene quinones, dysidavarones A–D (**178-181**), displaying the unusual dysidavarane carbon skeleton.[361] The Fijian sponge *D. fragilis* contained dysidazirine (**182**),[362] while a Micronesian specimen contained its optical enantiomer (*4E*)-S-dysidazirine (**183**), along with further azacyclopropenes, including (*4Z*)-dysidazirine (**184**), (*4E*)-S-antazirine (**185**).[363]

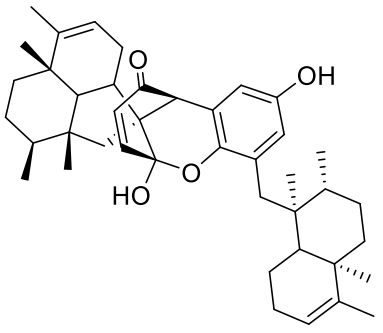

171

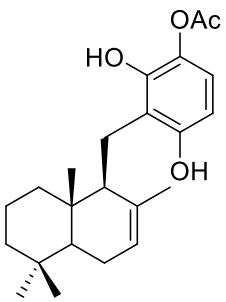

172

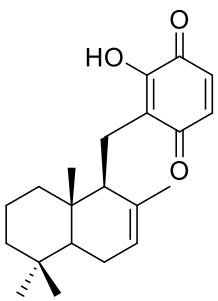

173

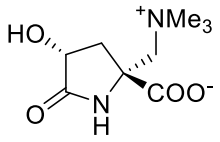

174

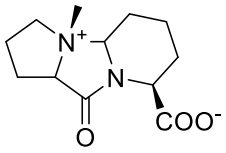

175

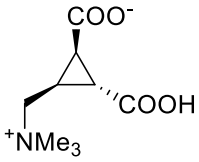

176

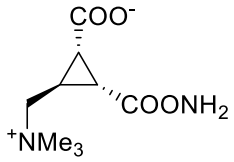

177

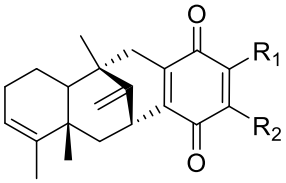

178 R_1 = OEt, R_2 = H
179 R_1 = H, R_2 = OEt

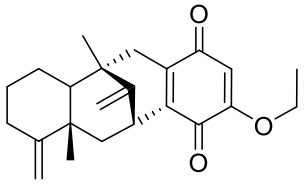

180

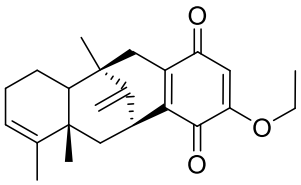

181

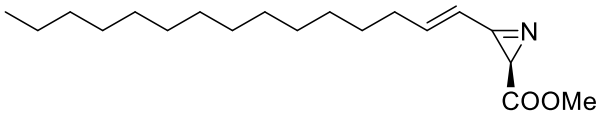

182

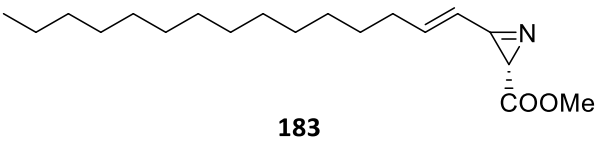

183

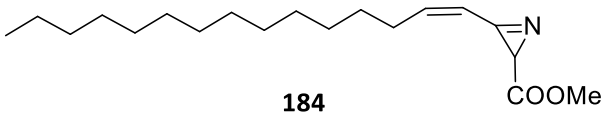

184

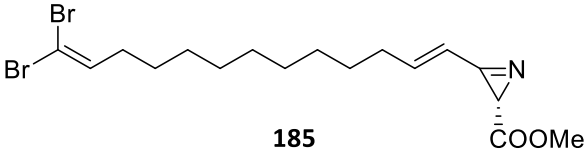

185

Investigation into the cyanobacterial symbionts within *D. herbacea* showed that the sponge contains large quantities of *Oscillatoria spongeliae*[364,365] and that a group of polychlorinated compounds isolated from the whole sponge is limited to the cyanobacterial filaments,[71] almost certainly proving their symbiotic origin.[354]

Isolation procedure

A portion of the frozen *Dysidea teawanui* sponge was extracted and lyophilised. Part of this crude extract was then purified by reversed phase bench column chromatography. The fraction of interest was further purified by normal phase bench column chromatography on silica using a gradient of DCM, EtOAc and MeOH to afford ergosterol peroxide (**186**) (Figure 70).

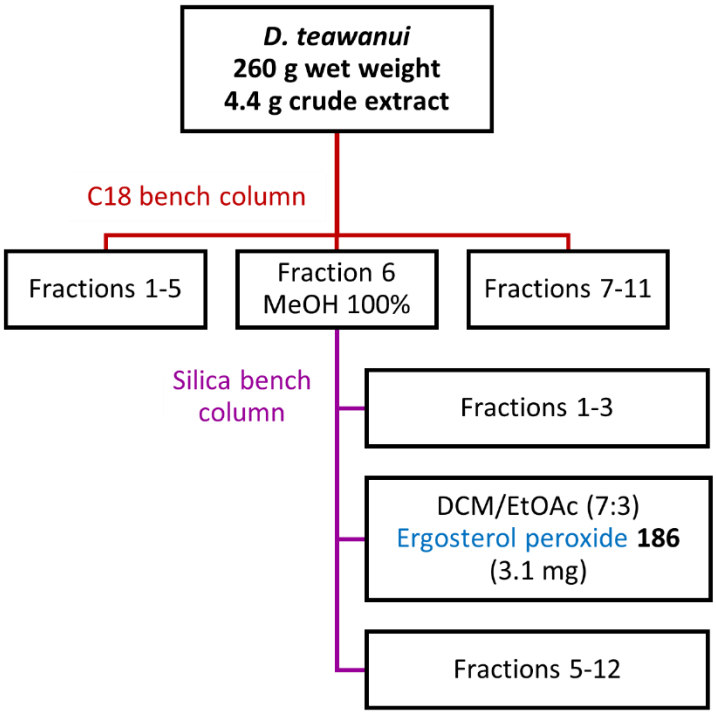

Figure 69: The isolation procedure for ergosterol peroxide (**186**) from *Dysidea teawanui*.

Ergosterol peroxide

Ergosterol peroxide, 5α,8α-epidioxy-24-methylcholesta-6, 22-dien-3β-ol, (**186**) displayed a strong $[M + H]^+$ ion at *m/z* 429 in (+)HR-ESI-MS, corresponding to a molecular formula of $C_{28}H_{45}O_3$. Examination of the ^1H, ^{13}C and HSQC NMR spectra recorded in chloroform-*d* revealed signals characteristic of compound (**186**). For the proton NMR spectrum (Appendix C.1), this included two doublets at δ_H 6.24 and 6.51, accounting for the alkene protons H-6 and H-7, respectively, two doublets of doublets at δ_H 5.13 and 5.19, each accounting for an alkene proton as part of the side chain, along with a multiplet at δ_H 3.97, representative of H-3 adjacent to the hydroxy group. In the ^{13}C NMR spectrum, the presence of four protonated

sp^2 carbon signals at δ_C 130.93, 132.57, 135.54 and 135.56 confirmed the presence of the two alkene groups. The two, strongly deshielded, non-protonated sp^3 carbon signals at δ_C 82.30 and 79.61 revealed the presence of the peroxide moiety. Overall, the spectroscopic data (Table 17) were a close match to previously reported data.[366]

Table 17: ^1H and ^{13}C NMR data for 5α,8α-epidioxy-24-methylcholesta-6,22-dien-3β-ol (**186**) compared with literature values (chloroform-*d*).[366]

	δ_H (mult, *J* in Hz)		δ_C	
Atom	[a] **Experimental**	[b] **Literature**	[a] **Experimental**	[b] **Literature**
1			34.8	34.8
2			30.3	30.3
3	3.97 (m)	3.95 (m)	66.7	66.6
4			37.1	37.1
5			82.3	82.2
6	6.24 (d, 8.3)	6.22 (d, 8.5)	135.6	135.5
7	6.51 (d, 8.3)	6.48 (d, 8,5)	130.9	130.8
8			79.6	79.5
9			51.2	51.3
10			37.1	37.1
11			23.6	23.5
12			39.6	39.6
13			44.7	44.7
14			51.8	51.8
15			20.7	20.8
16			28.9	29.0
17			56.6	56.3
18	0.80 (s)	0.79 (s)	13.0	13.0
19	0.88 (s)	0.86 (s)	18.3	18.3
20			40.0	39.8
21	0.89 (d, 6.2)	0.97 (d, 6.6)	21.1	21.0
22	5.35 (m)	5.17 (dd, 7.5, 15.2)	135.5	135.5
23	5.17 (dd, 7.6, 15.2)	5.11 (dd, 7.8, 15.2)	132.6	132.6
24			43.2	43.2
24(1)	[c] 0.88	0.89 (d, 6.8)	18.2	18.3
25	[c] 0.81	0.79 (d, 7.0)	33.3	33.3
26	[c] 0.87	0.81 (d, 7.2)	20.3	20.2
27			19.8	19.6

[a] values reported in chloroform-*d*, ^1H 600 MHz, ^{13}C 150 MHz, [b] values reported in chloroform-*d*, ^1H 400 MHz, ^{13}C 100 MHz (Gauvin *et al.* 2000)[366], [c] undetermined due to overlapping signals.

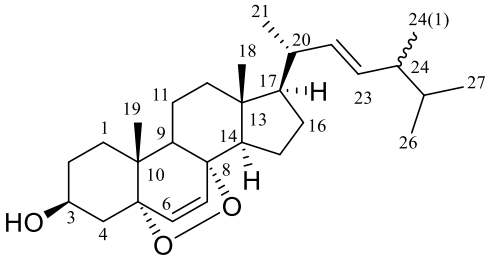

186

Ergosterol peroxide (**186**) was acetylated using pyridine and acetic anhydride to confirm the presence of the hydroxy group. The ^{1}H NMR spectrum of the acetylated ergosterol peroxide was recorded in chloroform-*d* and displayed a multiplet, representative of the proton adjacent to the acetate group (H-3) at δ_H 4.99, indicating a downfield shift of 1.02 ppm. A singlet at δ_H 2.01 also appeared on the spectrum of the acetylated product, proving the acetylation of the hydroxyl group.

Ergosterol peroxide (**186**) has been described from several sponge species including *Luffariella* cf. *variabilis*[366], *Lendenfeldia chondrodes,*[367] and *Monanchora* sp.,[368] and has been reported to inhibit growth of various human cancer cell lines.[368]

Compound (**186**) was accessed for cytotoxic activity against HeLa cells and displayed minimal activity (IC_{50} 74.6 µM, or 32 µg mL^{-1}) (Figure 69).

4.2.3 *Ceratosoma amoenum* and its eggs

Reported metabolites from *Ceratosoma* nudibranchs

Numerous *Ceratosoma* species, especially those displaying a dorsal horn, have previously been investigated and various furanoterpenes were isolated.[231,369,370] This has led to several studies aiming to understand the defence mechanisms of these nudibranchs and the role of their dorsal horn.[100,370]

Spongian-type furanosesquiterpenes, such as dehydrodendrolasin, dehydrolasiosperman, (methylthio)furodysinin and dithiofurodysinin have been isolated from *C. brevicaudatum* collected in South Australia.[369] Thiofurodysinin acetate (**187**), a very uncommon thiosesquiterpene, was also isolated and had also been previously reported from *Dysidea* sp.[371,372] and *Dysidea avara.*[373] Another study on *C. brevicaudatum* showed the presence of five furanosesquiterpenes in the viscera, including furodysinin (**23**), pallescensin-A (**188)** and B (**189**), and dendrolasin (**58**), which were also present in the mantle, along with nakafuran-9 (**55**).[370]

An investigation of New Zealand specimens of *C. amoenum* yielded an interesting ecological observation.[230] Allolaurinterol (**190**), a red algal terpenoid, was found in both the nudibranch *C. amoenum* and the red alga *Hymenena variolosa,* on which the nudibranch was observed at the time of collection.[230] However, based on the physiology of their digestive system, nudibranchs cannot break down algal tissues, meaning that the predator was not feeding on and sequestering metabolites from *H. variolosa*.[230] Compound (**190**) is also present in two local species of *Aplysia* sea hares and the nudibranchs could be feeding on juvenile sea hares, which has previously been observed within the Prinsep research group.[374]

Another investigation into *C. amoenum* specimens from New Zealand described the isolation of furodysinin (**23**)**,** *O*-methyl-furodysinin lactone (**191**) and tetradehydrofurospongin-1 (**192**) from twenty-eight individuals collected off the coast of Northland.[231]

C. gracillimum individuals from the South China Sea also contained furodysinin (**23**) and nakafuran-9 (**55**) in the MDFs of the dorsal horn.[100] Both compounds showed significant feeding deterrent activity at relatively low concentrations (ED_{50} of approximately 1 mg mL^{-1} against palaemonid shrimp).[100] *C. gracillimum*, along with *C. trilobatum* also from the South China Sea, were the focus of a study that aimed to evaluate whether the dorsal horn had a protective role.[370] The main sesquiterpene present in both species was furodysinin (**23**) which was almost exclusively present in the mantle glands concentrated in the dorsal horn, suggesting a defensive role of that dorsal protuberance.[370] This discovery supports the previous hypothesis, suggested by Rudman,[375] that the horn, or the most exposed part, attracts the attention of predators to a distasteful part of the body to reduce damage to the nudibranch.[100] Specimens of *C. trilobatum* from Australia also contained compound (**23**), along with furodysin (**60**) and dendrolasin (**58**) in their viscera, while the mantle also contained compounds (**23**) and (**60**), along with agassizin (**193**) and dehydroherbadysidolide (**194**).[370]

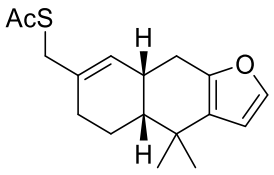

187

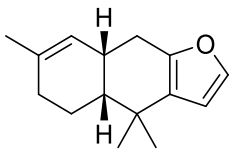

23

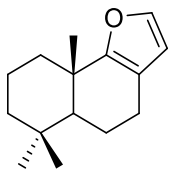

188

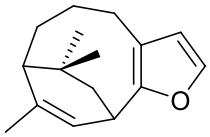

189

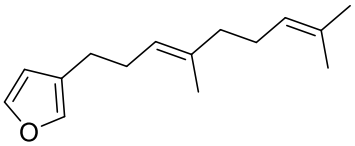

58

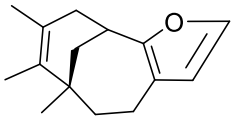

55

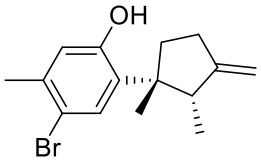

190

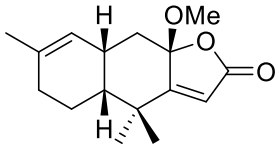

191

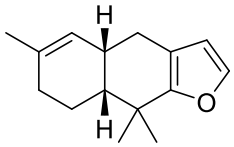

60

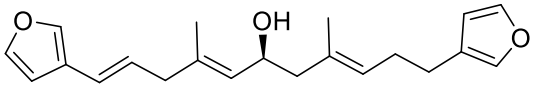

192

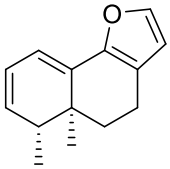

193

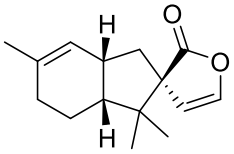

194

Chemical investigation

Two specimens of *C. amoenum* collected in June 2020 and July 2021 at Dive Crescent were investigated. Both specimens were separately extracted, and the crude extracts were purified by reversed phase bench column chromatography. Traces of ergosterol peroxide (**186**) were detected by ^{1}H NMR spectroscopy in several fractions from both extracts. Ergosterol peroxide (**186**) was detected in minimal quantity but the presence of the two doublets at δ_H 6.24 (d, 8.3) and 6.51 (d, 8.3), along with the signals at δ_H 5.13 and 5.19 was characteristic of compound (**186**). Due to the minimal amount of compound (**186**) in the nudibranchs, the metabolite distribution was not studied. Upon analysis of the chloroform soluble fractions obtained from the reversed phase columns by ^{1}H NMR spectroscopy and HR-ESI-MS, no evidence of signals corresponding to compounds (**23**), (**190**), (**191**) and (**192**), previously isolated from New Zealand *C. amoenum* specimens, was detected.

An egg coil that was spawned in June 2020 in a tank, most likely by the specimen studied above, was extracted and purified in a similar manner to the nudibranch specimens. No traces of ergosterol peroxide (**186**) were detected by ^{1}H NMR spectroscopy in chloroform-*d*. The absence of compound (**186**) from the spawned egg mass could explain the lower cytotoxicity of the egg extract compared to the whole-body.

4.2.4 Concluding remarks

Ergosterol peroxide (**186**) has been isolated from *Dysidea teawanui* and represents the first metabolite reported from this newly described species. The presence of compound (**186**), although in minimal quantity, within nudibranch specimens collected a year apart confirms consistent predation upon the large blue sponge. The minimal quantity of compound (**186**) within the *C. amoenum* nudibranchs did not allow for the study of the metabolite distribution across different body parts. Therefore, whether compound (**186**) is sequestered for a specific reason or merely ingested upon predation on the sponge was not determined. Despite this, the chemical investigation of both the nudibranchs and their preferred prey established a chemical link between the two organisms, which confirmed the ecological link uncovered during the feeding-choice experiments. Despite LC-MS screening indicating otherwise, *Dysidea teawanui* may contain other secondary metabolites of interest, although the sponge was not studied further because this study focused on chemical links between predator and prey.

4.3 *Goniobranchus aureomarginatus* and *Dictyodendrilla* cf. *dendyi*

4.3.1 Sample collection and dissection

During several snorkelling trips between December 2021 and October 2022 at Dive Crescent, Tauranga, specimens of *G. aureomarginatus* and *D.* cf. *dendyi* were collected. One nudibranch specimen was dissected into mantle and viscera to conduct the cytotoxicity assay and six more were dissected similarly to conduct chemical analysis on different body parts (Table 18). Another individual was utilised for morphological analysis.

Table 18: Collection and extraction of samples for the investigation of the predator-prey relationship between *Goniobranchus aureomarginatus* and *Dictyodendrilla* cf. *dendyi.*

Nudibranch	Specimens	Collection date	Location	Use
G. aureomarginatus	8	December 2021	Dive Crescent	Chemical analysis
	6	December 2021	Dive Crescent	Dissected, Chemical analysis
	1	October 2022	Dive Crescent	Cytotoxicity assay
	1	October 2022	Dive Crescent	Cytotoxicity assay
	1	January 2023	Dive Crescent	Morphological analysis
***G. aureomarginatus* eggs**	1 coil	Spawned in the laboratory, December 2022		Chemical analysis and cytotoxicity assay
Sponge				
D.* cf. *dendyi	-	December 2021	Dive Crescent	Chemical analysis
	-	March, October and December 2022	Dive Crescent	Chemical analysis

4.3.2 Cytotoxicity of crude extracts

Five crude extracts resulting from the separate extraction of the whole-body of a nudibranch, a dissected specimen (viscera and mantle), a spawned egg coil and the preferred prey of *G. aureomarginatus* were screened for cytotoxic activity against HeLa cells following the procedure described in Chapter 7 - Experimental, Section 7.7.6. The entire body and mantle extracts were the most active, while the egg coil, viscera and *D.* cf. *dendyi* extracts displayed minimal activity (Table 19). By comparison with the high cytotoxicity of the whole nudibranch extract, the low cytotoxicity of the egg extract (Figure 71) indicated a potential lack of bioactive metabolites present. The eggs were spawned during the feeding-choice experiments, and it might be possible that keeping the nudibranchs in a situation of prolonged stress could impact the quality of the eggs and the transfer of metabolites.

The *D.* cf. *dendyi* extract displayed a constant low inhibition percentage as the concentration tested increased (Figure 71). The difference between the cytotoxic activity of *D.* cf. *dendyi* and the whole nudibranch extract was surprising. Indeed, the nudibranchs displayed a strong preference for the *D.* cf. *dendyi* sponge during the feeding-choice experiments, hence according to these results, it is likely that both organisms contain identical metabolites. Chemical investigation of both extracts was carried out to investigate any relationship.

Table 19: IC_{50} values of the crude extracts of *Goniobranchus aureomarginatus* (whole-body and dissected) and its eggs, and *Dictyodendrilla* cf. *dendyi* on HeLa cells using an MTT assay.

Sample	**Whole-body**	**Viscera**	**Mantle**	**Eggs spawned**	***D.* cf. *dendyi***
IC_{50} (µg mL^{-1})	15	>100	13	> 100	> 100

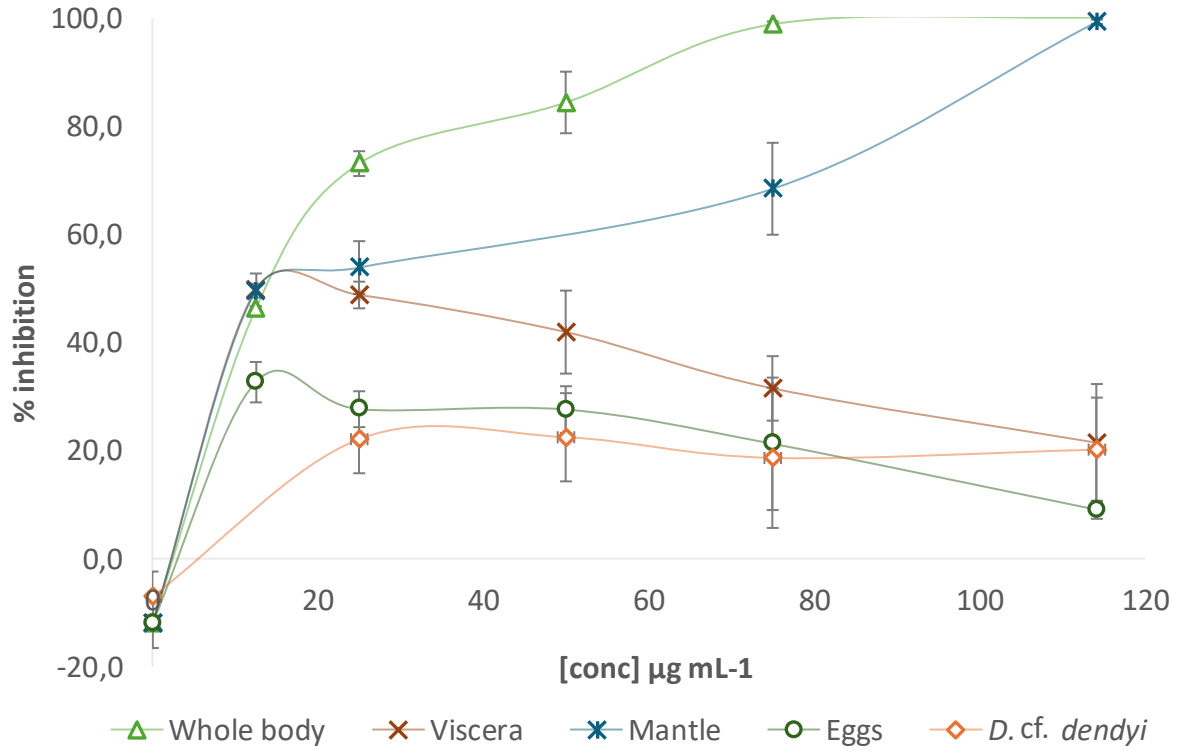

Figure 71: Cytotoxicity of the crude extracts of *Goniobranchus aureomarginatus* (whole-body and dissected) and its eggs, and *Dictyodendrilla* cf. *dendyi* on HeLa cells using an MTT assay.

4.3.3 *Dictyodendrilla* cf *dendyi*

Reported metabolites from the genus *Dictyodendrilla*

To date, primarily Australian, New Zealand and Japanese specimens of *Dictyodendrilla* sponges have been investigated for their metabolites, resulting in the isolation of a number of terpenes and highly substituted aryl-pyrrole alkaloids.[376-382] The first report of natural products from the genus *Dictyodendrilla* dates back to 1987 with the isolation of the furanosequiterpenoid pallescensone (**195**) from a New Zealand specimen of *Dictyodendrilla cavernosa.*[376] In the following three years, two more publications from the same research group reported dictyodendrillolide (**196**) from an Australian *Dictyodendrilla* sp. specimen and two diterpenes, spongian-16-one (**197**) and spongia-15,16-dione (**198**) from a subsequent collection of a New Zealand *D. cavernosa* specimen.[377,383]

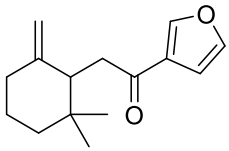

195

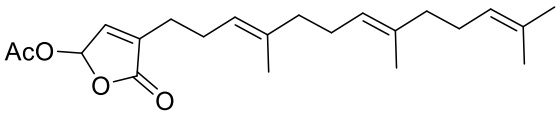

196

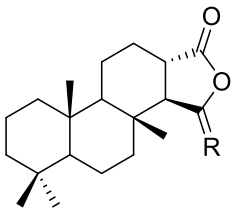

197 R= H, H
198 R = O

In 1993, following a search for inhibitors of aldose reductase, Sato *et al*. reported the first dictyodendrin natural products, with the description of pyrrolo[2,3-c]carbazole spirolactone 1a (**199**), its chromatographically separable protonated form 1b (**200**), along with the planar congener 2a (**201**).[379] The structure of compound (**199**) was confirmed by X-ray crystallographic analysis of the acetate analogue 1d (**202**), prepared from the corresponding free phenol 1c (**203**) obtained by hydrolysis of compound (**199**). Compounds (**199-201**) were isolated from a dark green Japanese *Dictyodendrilla* sp. specimen and all inhibited aldose reductase (IC_{50} values approximately 100 nM). In 1995, three new oxygenated sesquiterpenes, dictyodendrillins A-C (**204-206**)**,** along with the known sesquiterpene dendrolasin (**58**), were reported from a South Australian *Dictyodendrilla* sp..[380] In 2002, further dictyodendrins A-E (**207-211**), along with compound (**199**) and (**201**) (the latter as the sodium salt), were isolated from a Japanese specimen of *D. verongiformis* by means of bioassay guided fractionation in a search for telomerase inhibitors.[382] Compounds (**199**), (**207-211**) and the sodium salt of (**201**) showed 100% inhibition of telomerase activity at a concentration of 50 μg mL^{-1} and were reported to be the first telomerase-inhibitory marine natural products.[382] The authors suggested that, by the presence of the tyramine moiety and phenol groups, dictyodendrins are biogenetically related to lamellarins,[384] lukianols,[385] polycitones,[386,387] storniamide A,[388] and prunolides,[389] isolated from either tunicates or sponges. Upon hydrolysis of compounds (**199**) and (**207-211**), the corresponding phenol was obtained, which was later isolated as dictyodendrin F (**212**) from a *Ianthella* sp. specimen by Capon *et al*.[390]

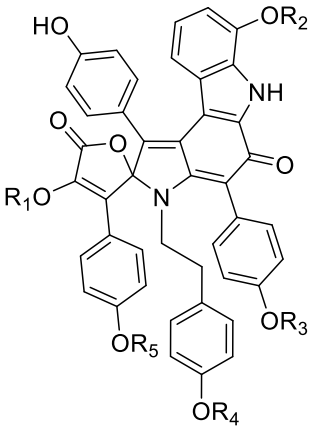

199 $R_1 = R_3 = R_4 = R_5 = H$, $R_2 = SO_3Na$
200 $R_1 = R_3 = R_4 = R_5 = H$, $R_2 = SO_3H$
202 $R_1 = R_2 = R_3 = R_4 = R_5 = Ac$
203 $R_1 = R_2 = R_3 = R_4 = R_5 = H$

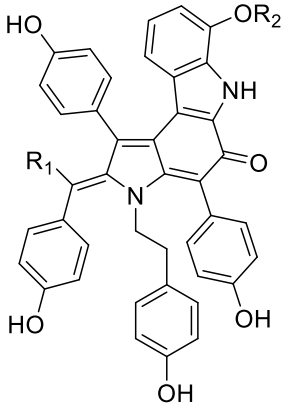

201 $R_1 = CO_2Me$, $R_2 = SO_3H$
211 $R_1 = H$, $R_2 = SO_3Na$

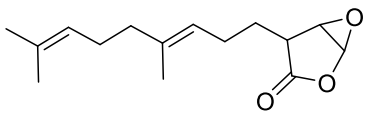

204

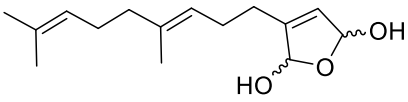

205

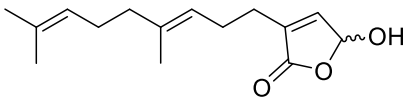

206

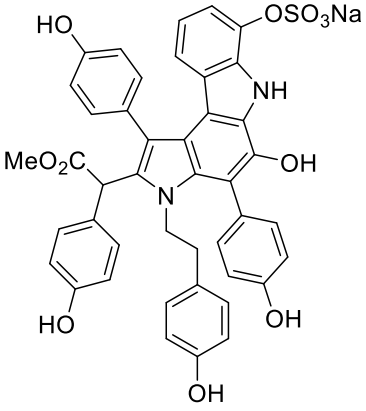

207

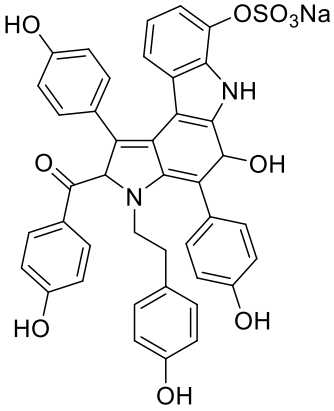

208

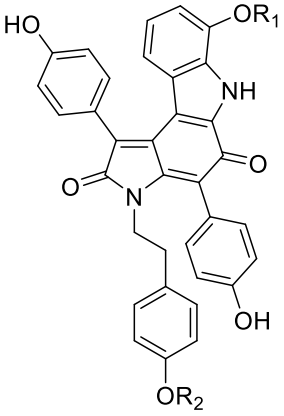

209 $R_1 = SO_3Na$, $R_2 = H$
210 $R_1 = R_2 = SO_3Na$
212 $R_1 = R_2 = H$

Upon investigation of a New Zealand specimen of *D. dendyi*, doctoral student John Ryan reported the isolation of dictyodendrins C (**209**), D (**210**), F (**212**), and seven lamellarins (**213-219**).[391]

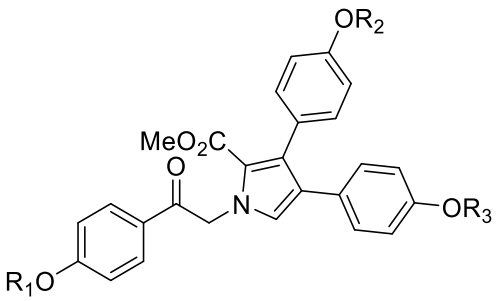

213 $R_1 = R_2 = R_3 = H$
214 $R_1 = H$, $R_2 = R_3 = SO_3Na$
215 $R_1 = Me$, $R_2 = H$, $R_3 = SO_3Na$
216 $R_1 = Me$, $R_2 = R_3 = SO_3Na$

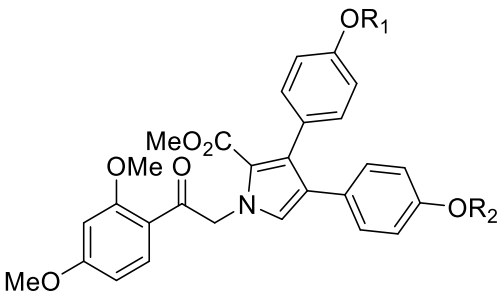

217 $R_1 = R_2 = H$
218 $R_1 = H$, $R_2 = SO_3Na$
219 $R_1 = Me$, $R_2 = SO_3Na$

In 2005, a Japanese *Dictyodendrilla* sp. specimen yielded the antibacterial and antifungal bis-indole alkaloid dendridine A (**220**), along with the previously reported makaluvamine O (**221**) and aureol (**222**).[381] Two rearranged diterpenes, omriolides A (**223**) and B (**224**) were reported from a southern Kenyan sponge *Dictyodendrilla* aff. *retiara*.[378]

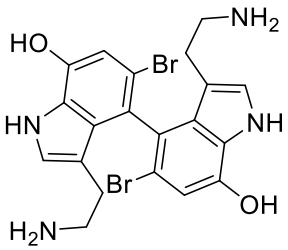

220

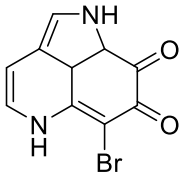

221

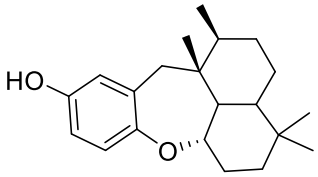

222

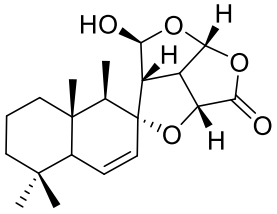

223

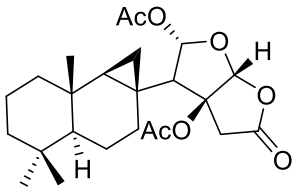

224

Isolation procedure for the initial extraction

The crude extract of a sample of *D.* cf. *dendyi* collected in December 2021 (Table 18) was purified by reversed phase bench column chromatography. TLC analysis of the fractions indicated the presence of a wide array of brightly coloured compounds, especially within the early eluting fractions, from H_2O/MeOH (1:1) to MeOH 100% (fractions 3 to 8 in Figure 72). These fractions were further purified using a combination of reversed phase bench column chromatography and size exclusion chromatography. This resulted in the isolation and characterisation of the known compounds dictyodendrins C (**209**) and D (**210**) (Figure 73).

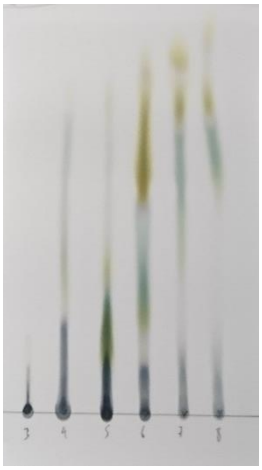

Figure 71: Thin layer chromatography (EtOAc/MeOH 5:1) of early eluting *Dictyodendrilla* cf. *dendyi* fractions after initial C18 reversed phase purification.

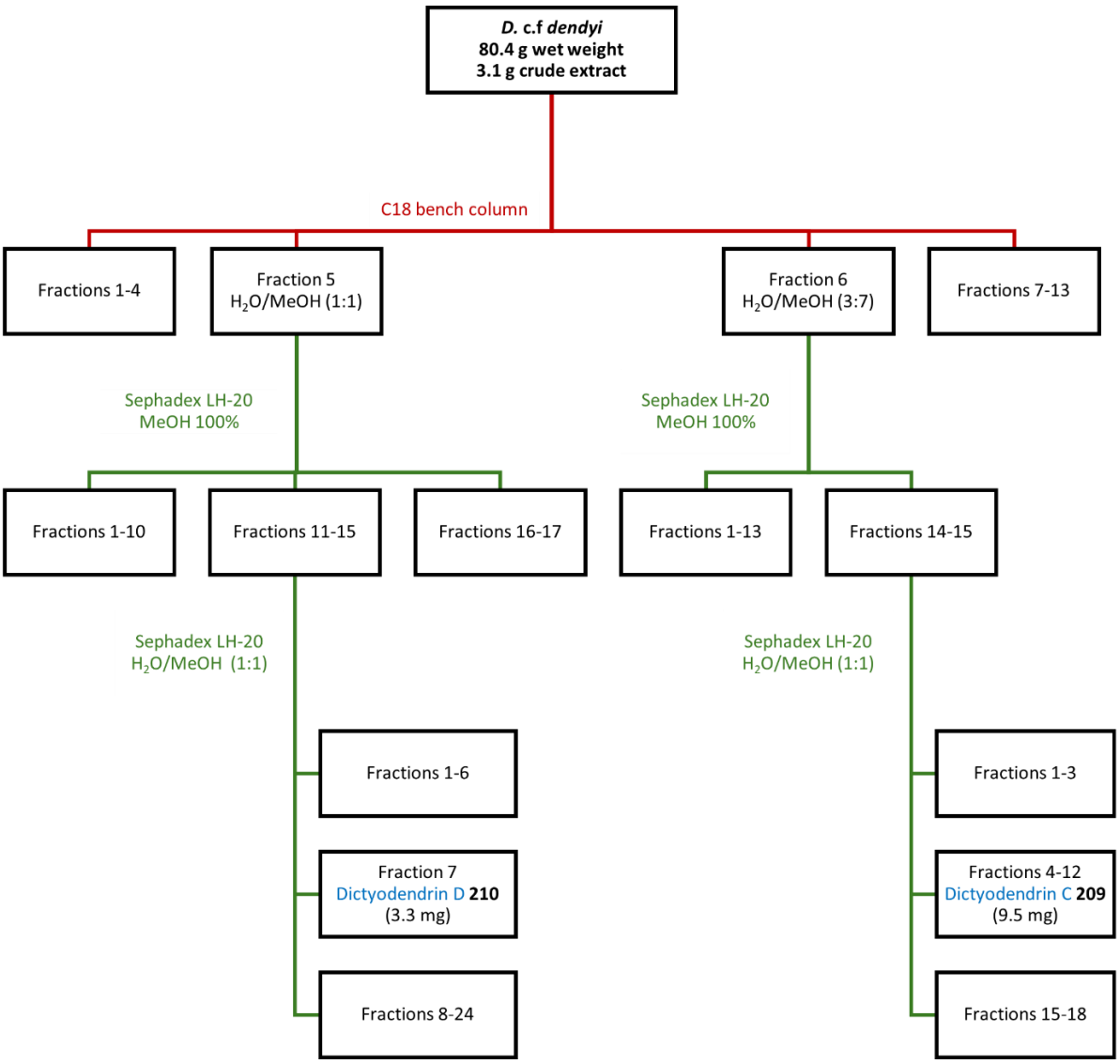

Figure 73: The isolation procedure for dictyodendrins C (**209**) and D (**210**) from *Dictyodendrilla* cf. *dendyi.*

Dictyodendrin C

HR-ESI-MS analysis (negative ion mode) yielded a $[M - Na]^-$ ion at *m/z* 635.1803, corresponding to a molecular formula of $C_{34}H_{23}N_2O_9S$. Examination of the ^1H NMR spectrum (Figure 74, Appendix C.2) and HSQC spectroscopic data revealed the presence of ten signals, including two methylene signals (δ_H 2.41, 3.44) accounting for four methylene protons and eight aromatic signals (δ_H 6.15, 6.57, 6.66, 6.73, 6.91, 6.93, 7.22, 7.25, 7.32), accounting for a total of fifteen aromatic protons. Three of the aromatic signals integrated for one proton each and displayed an AMX pattern [δ_H 6.15 (1H, d, 8.3), δ_H 6.73 (1H, dd, 8.0, 8.0) and δ_H 7.22 (1H, d, 7.7)], typical of a trisubstituted aromatic ring.

The ^{13}C and HSQC NMR data showed the presence of twenty-eight carbon signals, comprising one carbonyl signal (δ_C 180.7), sixteen quaternary sp^2 carbon resonances (δ_C 114.0, 119.4, 123.8, 124.1, 126.7, 130.0, 130.4, 133.4, 133.7, 135.4, 140.7, 150.4, 156.9, 159.2, 160.3, 173.3), nine protonated sp^2 carbon signals (δ_C 116.0, 116.1, 116.4, 118.2, 121.9, 122.4, 130.9, 133.5, 133.9), and two methylene carbon resonances (δ_C 34.9, 44.2).

A series of COSY and HMBC correlations (Figure 75) allowed for the identification of the known tyramine-based pyrrolocarbazole alkaloid, dictyodendrin C (**209**). Interpretation of COSY correlations led to three pairs of mutually coupled signals each representing two protons, ascribable to 1,4-disubstituted aromatic rings: ring F - δ_H 6.57 coupled with δ_H 6.66, ring G - δ_H 6.91 coupled with δ_H 7.32 and ring E - δ_H 6.93 coupled with δ_H 7.25. The protonated carbon chemical shifts values between 116.0 - 116.4 ppm and between 130.9-133.9 ppm, along with the quaternary carbon chemical shifts between 156.9 - 160.3 ppm, were characteristic of *para*-substituted phenols.

Additionally, the COSY spectrum showed that the methylene signals at δ_H 2.41 and 3.44 were mutually coupled. HMBC correlations from the proton resonance at δ_H 2.41 to the carbon signals at C-26/30 at δ_C 130.9, bearing the protons resonating at δ_H 6.66, allowed for the construction of a tyramine unit containing ring F. The signal at δ_H 3.44 showed HMBC correlations to the carbon signals for C-2 and C-16, positioning the tyramine unit on N-1, consistent with the chemical shift of H-23 (δ_H 3.44). The COSY spectrum also showed that the three remaining aromatic signals (a doublet at δ_H 6.15, a doublet of doublets at δ_H 6.73 and a doublet at δ_H 7.22), integrating for one proton each, were coupled. The downfield shift of the

doublet at δ_H 7.22 compared to the other two resonances allowed for its positioning on C-9, *ortho*- to the sulphate group. The HMBC correlations H-7/C-11 and H-7/C-5 allowed for the doublet at δ_H 6.15 to be attached to C-7. The doublet of doublets at δ_H 6.73 represented H-8 because of the HMBC correlations from it to C-6 and C-10, consistent with the proton resonating as a doublet of doublets. The HMBC correlations between H-31,34/C-3 indicated the attachment of ring G at position 3. The HMBC correlations between H-18,22/C-15 showed the attachment of ring E at position 15.

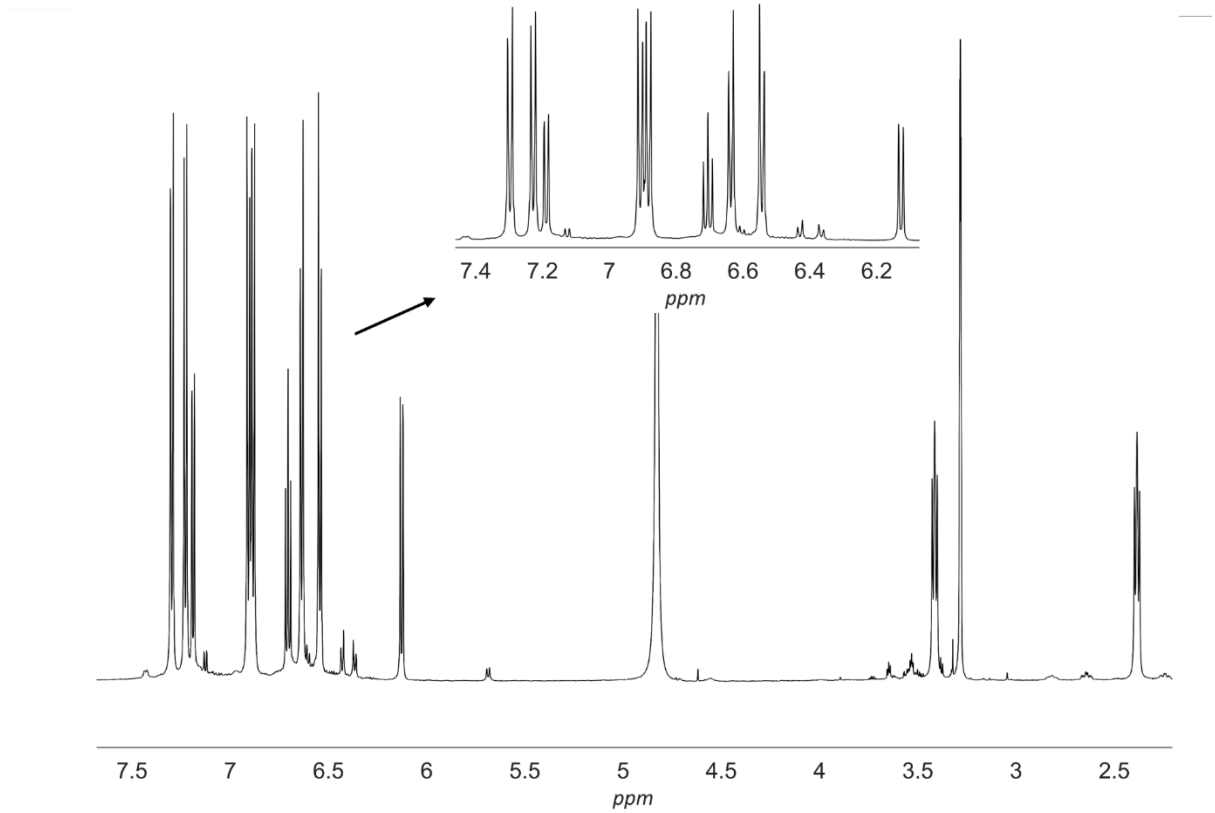

Figure 74: ^{1}H NMR spectrum (methanol-d_4, 600 MHz) of dictyodendrin C (**209**).

The presence of the carbazole moiety was deduced by the HMBC correlations H-7/C-5, H-7/C-11, H-8/C-10 and H-8/C-6 and H-8/C-10. The rest of the assignments of the carbazole moiety signals were deduced by comparison with the NMR data of dictyodendrin A (**207**), due to the proton-deficient character of such a moiety, which meant that they were no protonated carbons close enough to the carbons of this moiety to give HMBC correlations.[382]

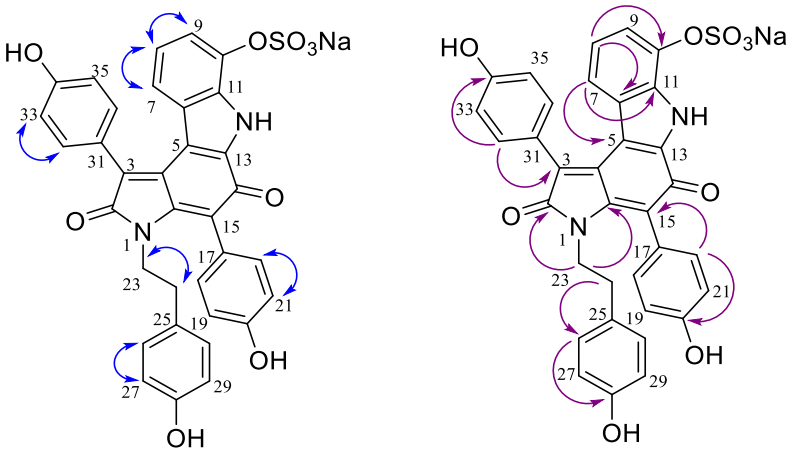

Figure 75: COSY (blue) and selected HMBC (purple) correlations for dictyodendrin C (**209**).

Table 20: ^{1}H and ^{13}C NMR assignments determined for dictyodendrin C (**209**) compared with literature values (methanol-d_4).[382]

	δ_H (mult, *J* in Hz)		δ_C		COSY	HMBC
Atom	[a] **Experimental**	[b] **Literature**	[a] **Experimental**	[b] **Literature**	[a] **Experimental**	
2			173.3	173.2		
3			130.4	130.4		
4			135.3	135.2		
5			114.0	114.0		
6			126.7	126.8		
7	6.15 (1H, d, 8.3)	6.13 (1H, d, 8.1)	121.8	121.8		C-5, C-9, C-11
8	6.73 (1H, dd, 8.0, 8.0)	6.70 (1H, dd, 8.1, 8.1)	122.4	122.3	H-7	C-6, C-10
9	7.22 (1H, d, 7.7)	7.19 (1H, d, 8.1)	118.2	118.2	H-9	C-8, C-10, C-11
10			140.7	140.6		
11			133.4	133.4		
13			133.7	[c] ND		
14			180.7	180.7		
15			119.4	[d] 129.4		
16			150.4	150.3		
17			124.1	124.0		
18/22	7.25 (2H, d, 8.5)	7.22 (2H, d, 8.6)	[e] 133.8	133.4	H-19/21	C-15, C-20
19/21	6.93 (2H, d, 8.5)	6.90 (2H, d, 8.6)	[f] 116.1	116.0		C-17, C-20
20			159.2	159.3		
23	3.41 (2H, t, 7.8)	3.40 (2H, t, 8.1)	44.2	46.1	H-24	C-2, C-16, C-24, C-30
24	2.38 (2H, t, 8.0)	2.73 (2H, t, 8.1)	34.9	34.9		C-23, C-26/30
25			130.0	130.0		
26/30	6.66 (2H, d, 8.4)	6.63 (2H, d, 8.4)	130.9	130.9	H-27-29	C-28
27/29	6.57 (2H, d, 8.4)	6.55 (2H, d, 8.4)	[f] 116.0	116.0		C-26/30, C-28
28			156.9	157.0		
31			123.7	123.6		
32/36	7.32 (2H, d, 8.5)	7.30 (2H, d, 8.6)	[e] 133.5	133.4	H-33/35	C-3, C-34
33/35	6.91(2H, d, 8.5)	6.88 (2H, d, 8.6)	116.4	116.4		C-31, C-34
34			160.3	160.3		

[a] values reported in methanol-d_4, ^{1}H 600 MHz, ^{13}C 150 MHz, [b] values reported in methanol-d_4, ^{1}H 600 MHz, ^{13}C 150 MHz according to Warabi *et al.*[382], [c] not determined, [d] the value reported appears downfield compared to the carbon at position 15, reported at 119.3 ppm, for the closely related dictyodendrin D (**210**),[382] possibly due to a typographical error, [e] assignment may be interchanged, [f] assignment may be interchanged.

All spectral data were in agreement with those reported previously for compound (**209**) (Table 20), confirming the molecular formula obtained by HR-ESI-MS.[382]

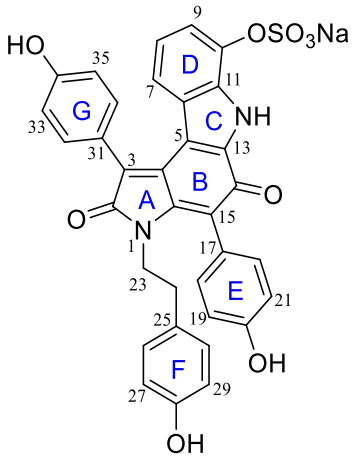

209

Dictyodendrin D

Dictyodendrin D (**210**) was isolated as a brown amorphous solid displaying a $[M - Na]^-$ ion at *m/z* 737.2428 in HR-ESI-MS (negative ion mode), corresponding to a molecular formula of $C_{34}H_{22}N_2O_{12}S_2Na$. The NMR spectroscopic data (Appendix C.3) were almost superimposable on those of dictyodendrin C (**209**), except for a 0.56 ppm downfield shift for H-27,29 and a 3.2 ppm upfield shift for C-28. Both shifts suggested the presence of a sodium sulphate group, confirmed by the 102-unit mass difference between compounds (**209**) and (**210**), corresponding to the deprotonation of a hydroxy group and the addition of a SO_3Na group. Therefore, dictyodendrin D differs only by sulphation of a 4-phenol moiety from compound (**209**). All spectral data were in agreement with those reported previously for dictyodendrin D (**210**) (Table 21).[382]

Table 21: ^{1}H and ^{13}C NMR assignments determined for dictyodendrin D (**210**) compared with literature values (methanol-d_4).[382]

	δ_H (mult, *J* in Hz)		δ_C	
Atom	[a] **Experimental**	[b] **Literature**	[a] **Experimental**	[b] **Literature**
2			173.2	173.2
3			130.4	130.5
4			135.2	135.0
5			114.0	114.0
6			126.7	126.8
7	6.18 (1H, d, 8.2)	6.15 (1H, d, 8.1)	121.9	121.9
8	6.74 (1H, dd, 8.1, 7.9)	6.72 (1H, dd, 8.1, 8.1)	122.4	122.4
9	7.22 (1H, d, 7.8)	7.20 (1H, d, 8.1)	118.2	118.2
10			140.8	140.7
11			133.4	133.5
13			133.7	133.7
14			180.8	180.6
15			119.4	119.3
16			150.1	150.2
17			124.0	124.0
18/22	7.28 (2H, d, 8.6)	7.24 (2H, d, 8.6)	133.8	133.8
19/21	6.95 (2H, d, 8.6)	6.92 (2H, d, 8.6)	116.2	116.3
20			159.3	158.8
23	3.47 (2H, t, 8.2)	3.44 (2H, t, 8.1)	43.9	44.0
24	2.51 (2H, t, 8.2)	2.48 (2H, t, 8.1)	35.2	35.1
25			135.8	135.8
26/30	6.78 (2H, d, 8.6)	6.76 (2H, d, 8.6)	130.5	130.5
27/29	7.11 (2H, d, 8.6)	7.04 (2H, d, 8.6)	122.4	122.3
28			152.5	152.8
31			123.7	123.7
32/36	7.37 (2H, d, 8.8)	7.34 (2H, d, 8.6)	133.5	133.5
33/35	6.92 (2H, d, 8.8)	6.90 (2H, d, 8.6)	116.4	116.5
34			160.4	160.6

[a] values reported in methanol-d_4, ^{1}H 600 MHz, ^{13}C 150 MHz; [b] values reported in methanol-d_4, ^{1}H 600 MHz, ^{13}C 150 MHz according to Warabi *et al.*[382]

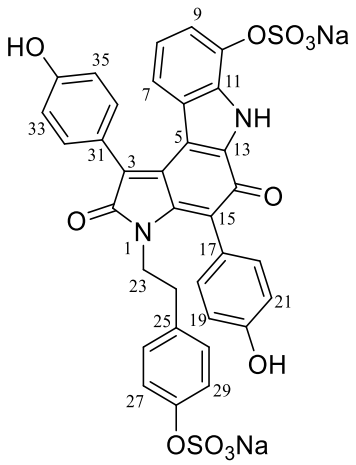

210

Isolation procedure for the large-scale extraction

To afford the isolation of minor compounds detected during the isolation of compounds (**209**) and (**210**), a larger extraction of *D.* cf. *dendyi* was carried out. The lyophilised crude extract obtained was separated into three equal parts, and each was purified by reversed phase C18 bench column chromatography. Each fraction from each C18 reversed phase column was analysed on TLC (Figure 76) and based on the elution solvent and TLC profile, fractions were combined (separation tree available in Appendices C.4 and C.5).

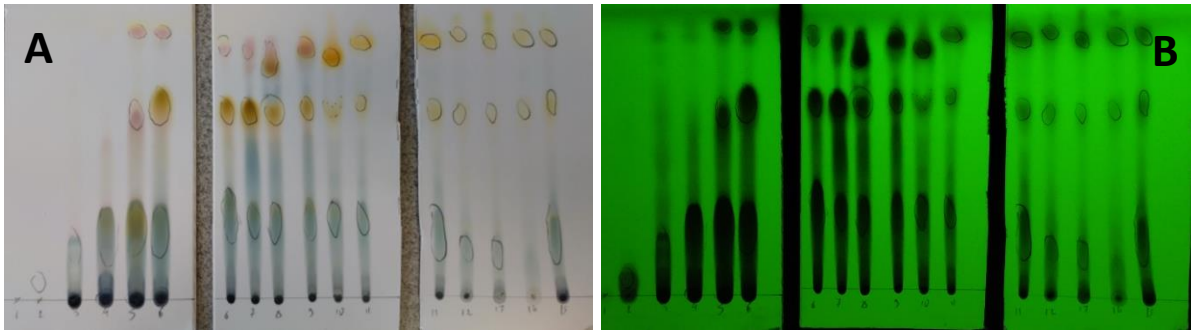

Figure 75: An example of the TLC plates obtained for the *Dictyodendrilla* cf. *dendyi* fractions after initial C18 purification. A- visible light. B- under UV light at 254 nm.

Fractions of interest were further purified using a combination of C18 reversed phase bench column chromatography and size exclusion chromatography (separation trees available in Appendices C.6 and C.7). ^{1}H NMR spectroscopy and HR-ESI-MS analysis were used to guide the isolation of compounds. This resulted in the isolation and characterisation of the known compounds dictyodendrins B (**208**) and F (**212**), dactylpyrrole A (**225**), denigrins E (**226**) and G (**227**), lamellarin O1 (**228**) and pyrrolo[2,3-c]carbazole spirolactone 1a (**199**).

Dictyodendrin F

Dictyodendrin F (**212**) was isolated as a brown amorphous solid displaying a pseudo-molecular ion $[M - H]^-$ at *m/z* 555.1556 in HR-ESI-MS (negative ion mode), corresponding to a molecular formula of $C_{34}H_{23}N_2O_6$. The NMR spectroscopic data (Appendix C.8) were almost superimposable on those of dictyodendrin C, with the most visible changes represented by a 0.64 ppm upfield shift for H-9 and a 5.3 ppm downfield shift for C-10. Both shifts suggested the removal of a sodium sulphate group, confirmed by the loss of 102 mass units between compounds (**209**) and (**212**). Therefore, dictyodendrin F (**212**) was confirmed as the non-sulphated version of compound (**209**). All spectral data were in agreement with those reported previously for compound (**212**) (Table 22).[391]

Table 22: ^1H and ^{13}C NMR assignments determined for dictyodendrin F (**212**) compared with literature values (methanol-d_4).[391]

	δ_H (mult, *J* in Hz)		δ_C	
Atom	[a] **Experimental**	[b] **Literature**	[a] **Experimental**	[b] **Literature**
2			173.4	173.2
3			130.1	129.8
4			135.2	135.4
5			114.1	113.9
6			126.4	126.2
7	5.83 (1H, dd, 7.5, 1.6)	5.81 (1H, dd, 6.9, 2.2)	116.5	116.3
8	6.58 (1H, m)	6.56 (1H, m)	122.4	123.1
9	6.58 (1H, m)	6.56 (1H, m)	110.0	109.9
10			146.0	146.0
11			130.7	130.7
13			133.7	133.1
14			180.9	180.8
15			119.4	119.1
16			150.1	150.3
17			124.2	124.0
18/22	7.24 (2H, d, 8.5)	7.21 (2H, d, 8.1)	133.8	133.7
19/21	6.93 (2H, d, 8.6)	6.91 (2H, d, 8.5)	116.1	116.0
20			159.2	159.2
23	3.43 (2H, t, 7.6)	3.38 (2H, t, 7.9)	44.1	44.0
24	2.41 (2H, t, 7.9)	2.37 (2H, t, 7.9)	34.9	34.8
25			135.8	129.9
26/30	6.66 (2H, d, 8.6)	6.63 (2H, d, 8.5)	130.9	130.7
27/29	6.57 (2H, m)	6.56 (2H, m)	116.0	115.9
28			156.9	156.9
31			123.7	123.7
32/36	7.31 (2H, d, 8.7)	7.29 (2H, d, 8.4)	133.5	133.4
33/35	6.90 (2H, d, 8.7)	6.88 (2H, d, 8.2)	116.3	116.2
34			160.1	160.1

[a] values reported in methanol-d_4, ^1H 600 MHz, ^{13}C 150 MHz, [b] values reported in methanol-d_4, ^1H 600 MHz, ^{13}C 150 MHz according to J. Ryan 2007.[391]

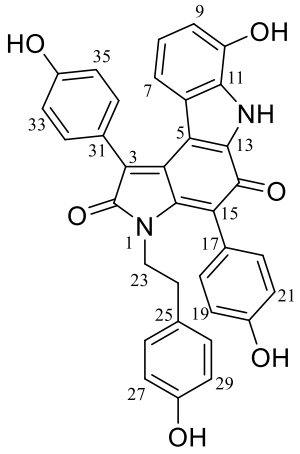

212

Dictyodendrin B

Dictyodendrin B (**208**) was isolated as a yellow amorphous solid displaying a pseudo-molecular ion $[M - H]^-$ at *m/z* 741.1316 in HR-ESI-MS (negative ion mode), corresponding to a molecular formula of $C_{41}H_{29}N_2O_{10}S$. The molecular formula of compound (**208**) was larger than that of compound (**209**) by a C_7H_5O unit, consistent with the addition in part of a phenol ring. This was corroborated by the presence of two additional doublets at δ_H 6.56 and 7.34 in the ^{1}H NMR spectrum, demonstrating the *para*-substitution of ring H. Dictyodendrin B (**208**) was isolated in minimal quantity (0.2 mg) and only the ^{1}H NMR spectrum could be acquired. Despite this, the strong agreement of the proton NMR values and the HR-ESI-MS data with the literature values for compound (**208**) (Table 23) confirmed its isolation.[382]

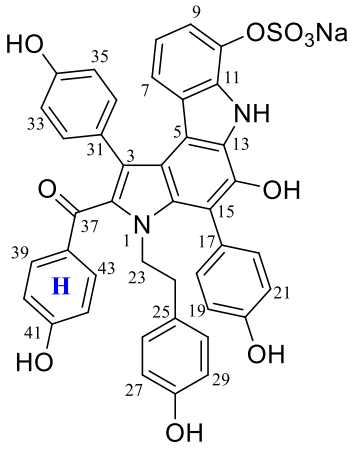

208

Table 23: ^{1}H NMR assignments determined for dictyodendrin B (**208**) compared with literature values (methanol-d_4).[382]

	δ_H (mult, *J* in Hz)	
Atom	[a] **Experimental**	[b] **Literature**
7	6.01 (1H, d, 8.1)	5.99 (1H, d, 8.3)
8	[c] 6.57 (1H, m)	6.55 (1H, dd, 7.9,
9	7.18 (2H, d, 8.0)	7.16 (1H, d, 7.9)
18/22	7.45 (2H, d, 8.4)	7.43 (2H, d, 8.6)
19/21	7.02 (2H, d, 8.2)	7.00 (2H, d, 8.8)
23	3.97 (2H, t, 7.8)	3.94 (2H, t, 7.4)
24	2.48 (2H, t, 7.1)	2.46 (2H, t, 7.4)
26/30	6.42 (2H, d, 8.8)	6.39 (2H, d, 8.8)
27/29	6.48 (2H, d, 8.1)	6.45 (2H, d, 8.8)
32/36	7.06 (2H, d, 8.6)	7.04 (2H, d, 8.6)
33/35	6.65 (2H, d, 8.5)	6.63 (2H, d, 8.6)
39/43	7.34 (2H, d, 8.5)	7.32 (2H, d, 8.8)
40/42	[c] 6.56 (2H, d, 7.8)	6.53 (2H, d, 8.8)

[a] values reported in methanol-d_4, ^{1}H 600 MHz, ^{13}C 150 MHz, [b] values reported in methanol-d_4, ^{1}H 600 MHz, ^{13}C 150 MHz according to Warabi *et al.*,[382] [c] overlapping signals.

Dactylpyrrole A

Dactylpyrrole A (**225**) was isolated as a yellow amorphous solid and its molecular formula was deduced to be $C_{31}H_{24}NO_6$ from a pseudo-molecular ion $[M - H]^-$ at *m/z* 506.1216 in HR-ESI-MS (negative ion mode). The ^{1}H NMR spectrum (Appendix C.9) displayed two ABX aromatic systems [system 1 - δ_H 7.33 (dd, 8.8, 2.4), δ_H 8.01 (d, 2.4) and δ_H 8.50 (d, 8.8); [system 2 - δ_H 7.11 (dd, 8.8, 2.4), δ_H 7.91 (d, 2.4) and δ_H 8.83 (d, 8.8)], along with four aromatic doublets integrating for two protons each (δ_H 6.21, 6.25, 6.78, 7.22), representing two *para*-disubstituted aromatic rings. Each doublet displayed peak shape characteristic of magnetic inequivalence for a *para*-disubstituted benzene, confirming the assignment. Compound (**225**) was isolated in minimal quantity (0.2 mg) and only the ^{1}H NMR spectrum could be acquired. Despite this, the strong agreement of the proton NMR values and the HR-ESI-MS data with the literature values for dactylpyrrole A (**225**) (Table 24) confirmed its isolation.

Table 24: ^{1}H NMR assignment determined for dactylpyrrole A (**225**) compared with literature values (methanol-d_4).[2]

	δ_H (mult, *J* in Hz)	
Atom	[a] **Experimental**	[b] **Literature**
6	[c] 3.62 (m) 3.85 (ddd, 13.8, 12.2, 5.4)	[c] 3.62 (m) 3.85 (ddd, 13.6, 11.9, 5.2)
7	2.92 (dt, 12.3, 5.1) 3.08 (td, 12.3, 5.1)	2.93 (ddd, 12.7, 12.5, 5.3) 3.08 (ddd, 12.4, 12.3, 5.1)
9/13	7.22 (d, 8.4)	7.22 (d, 8.4)
10/12	6.78 (d, 8.4)	6.78 (d, 8.4)
14	3.50 (d, 14.1) [c] 3.62 (m)	3.51 (d, 14.1) [c] 3.62 (m)
16/19	6.25 (d, 8.7)	6.25 (d, 8.7)
17/20	6.21 (d, 8.7)	6.21 (d, 8.7)
22	8.50 (d, 8.8)	8.50 (d, 8.8)
23	7.33 (dd, 8.8, 2.4)	7.34 (dd, 8.8, 2.4)
25	8.01 (d, 2.4)	8.02 (d, 2.4)
29	7.91 (d, 2.4)	7.92 (d, 2.4)
31	7.11 (dd, 8.8, 2.4)	7.12 (dd, 8.8, 2.4)
32	8.83 (d, 8.8)	8.84 (d, 8.8)

[a] values reported in methanol-d_4, 600 MHz, [b] values reported in methanol-d_4, 600 MHz (Kang *et al.* 2020),[392] [c] overlapping signals.

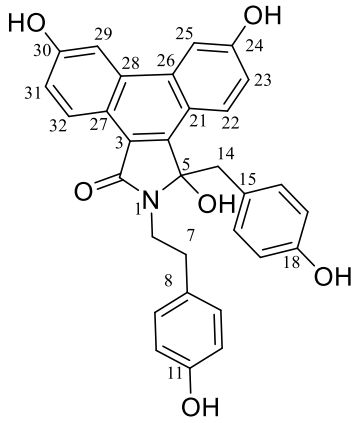

225

Denigrin E

Denigrin E (**226**) was isolated as a magenta amorphous solid displaying a pseudo-molecular ion $[M + H]^+$ at *m/z* 582.1633 in HR-ESI-MS positive ion mode, corresponding to a molecular formula of $C_{38}H_{34}NO_5$. The ^{1}H and HSQC NMR spectra displayed only a limited number of signals, including two triplets typical of a tyramine unit at δ_H 2.43 and 3.57. Integration of the aromatic doublet at δ_H 6.66 revealed that it represented four protons, suggesting a

symmetrical molecule. The ^{1}H NMR spectrum looked identical to that of denigrin E (**226**) acquired in methanol-d_4. The assignment of compound (**226**) by Kang *et al.* was reported in pyridine-d_5 because of the overlap between the aromatic signals in the ^{1}H NMR spectrum that the authors initially recorded in methanol-d_4.[392] In this research, several compounds closely related to compound (**226**) were characterised in methanol-d_4 (Chapter 5), therefore the ^{1}H and ^{13}C NMR assignments (Table 25) and spectra (Appendices C.10 and C.11) of compound (**226**) in methanol-d_4 are reported here.

Table 25: ^{1}H and ^{13}C NMR assignments for denigrin E (**226**) in methanol-d_4.

Atom	δ_H (mult, *J* in Hz) [a]	δ_C [a]
2/5		128.3
3/4		123.3
6	3.57 (2H, t, 7.4)	47.3
7	2.43 (2H, t, 7.6)	37.7
8		131.0
9/13	6.66 (2H, d, 8.6)	130.9
10/12	6.63 (2H, d, 8.7)	116.1
11		157.0
14/33	3.80 (4H, s)	30.7
15/34		132.9
16/20-35/39	6.92 (4H, d, 8.5)	129.9
17/19-36/38	6.70 (4H, d, 8.5)	116.3
18/37		156.7
21/27		129.7
22/26-28/32	6.91 (4H, d, 8.4)	132.5
23/25-29/31	6.61 (4H, d, 8.5)	115.6
24/30		156.1

[a] values reported in methanol-d_4, ^{1}H 600 MHz, ^{13}C 150 MHz.

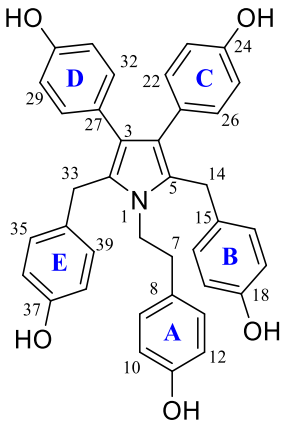

226

Denigrin G

Denigrin G (**227**) was isolated as an orange amorphous solid, and its molecular formula was deduced to be $C_{31}H_{26}NO_6$ from a pseudo-molecular ion $[M - H]^-$ at *m/z* 508.1843 in HR-ESI-MS (negative ion mode). The ^1H NMR spectrum contained eight aromatic doublets integrating for two protons each, representing four *para*-disubstituted benzene groups. Each doublet displayed peak shape characteristic of magnetic inequivalence for a *para*-disubstituted benzene. The ^{13}C NMR spectrum contained a quaternary carbon signal at δ_C 94.7, consistent with an oxygen and nitrogen-substituted carbon, which in compound (**227**) is attached to a hydroxy group and to the nitrogen of the pyrrole core. All spectral data were in agreement with those reported previously for compound (**227**) (Table 26).[392]

Table 26: ^1H and ^{13}C NMR assignments determined for denigrin G (**227**) compared with literature values (methanol-d_4).[392]

	δ_H (mult, *J* in Hz)		δ_C	
Atom	[a] **Experimental**	[b] **Literature**	[a] **Experimental**	[b] **Literature**
2			171.7	171.6
3			132.3	132.2
4			151.6	151.5
5			94.7	94.7
6	3.52 (td, 12.9, 5.3) 3.71 (td, 12.8, 5.1)	3.52 (dt, 12.9, 5.3) 3.71 (td, 12.8, 5.0)	43.6	43.6
7	2.91 (td, 12.8, 5.3) 2.98 (m)	2.89 (td, 12.5, 5.3) 2.98 (m)	35.6	35.6
8			131.6	131.6
9/13	7.15 (d, 8.4)	7.15 (d, 8.1)	130.8	130.8
10/12	6.75 (d, 8.4)	6.75 (d, 8.1)	116.3	116.3
11			157.0	157.0
14	2.98 (d, 14.3) 3.21 (d, 14.1)	2.98 (d, 14.0) 3.21 (d, 14.0)	41.6	41.6
15			126.9	126.8
16/20	6.57 (d, 8.6)	6.57 (d, 8.3)	131.8	131.8
17/19	6.53 (d, 8.6)	6.53 (d, 8.3)	115.5	115.5
18			157.3	157.3
21			125.0	124.9
22/26	7.42 (d, 8.8)	7.43 (d, 8.5)	132.6	132.6
23/25	6.71 (d, 8.8)	6.71 (d, 8.5)	116.0	116.0
24			159.6	159.7
27			124.3	124.2
28/32	6.87 (d, 8.6)	6.87 (d, 8.2)	131.8	131.8
29/31	6.68 (d, 8.8)	6.68 (d, 8.2)	116.2	116.2
30			158.5	158.5

[a] values reported in methanol-d_4, 600 MHz, [b] values reported in methanol-d_4, 600 MHz (Kang *et al.* 2020).[392]

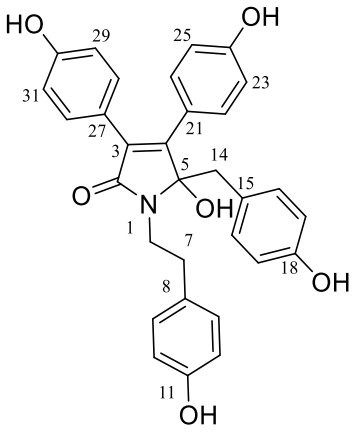

227

Lamellarin O1

Lamellarin O1 (**228**) displayed a strong pseudo-molecular ion $[M - H]^-$ at *m/z* 442.0991 HR-ESI-MS (negative ion mode), corresponding to a molecular formula of $C_{26}H_{21}NO_6$. The ^1H NMR spectrum in methanol-d_4 (Appendix C.12) included six aromatic doublets integrating for 2 protons each, representing three *para*-disubstituted benzene groups. Each doublet displayed peak shape characteristic of magnetic inequivalence for a *para*-disubstituted benzene. The ^{13}C NMR spectrum also indicated the presence of symmetry within the molecule with twenty distinct resonances. The ^1H and ^{13}C NMR spectra also revealed the presence of aromatic methine (δ_H 7.08, δ_C 128.7), deshielded methylene (δ_H 5.81, δ_C 56.7) and methoxy (δ_H 3.43, δ_C 50.9 groups). Analysis of the COSY and HMBC spectra led to assembly of the structure of compound (**228**) and all spectral data were in agreement with those previously reported (Table 27).[392]

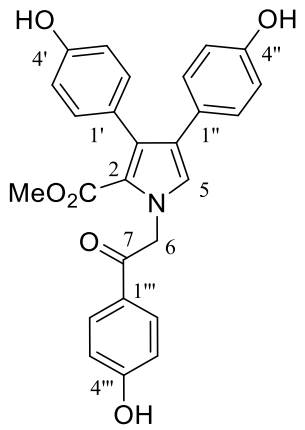

228

Table 27: ^{1}H and ^{13}C NMR assignments determined for lamellarin O1 (**228**) compared with literature values (methanol-d_4).[393]

	δ_H (mult, *J* in Hz)		δ_C	
Atom	[a] **Experimental**	[b] **Literature**	[a] **Experimental**	[b] **Literature**
2			120.8	121.0
3			132.4	132.8
4			126.0	126.1
5	7.08 (s)	7.07 (s)	128.6	128.7
6	5.81 (s)	5.81 (s)	56.7	56.8
7			194.8	194.8
1'			128.6	128.8
2'/6'	7.00 (d, 8.3)	7.00 (d, 8.6)	132.9	133.1
3'/5'	6.71 (d, 8.4)	6.70 (d, 8.6)	115.3	115.5
4'			157.2	157.3
1''			127.5	127.7
2''/6''	6.910 (d, 8.5)	6.91 (d, 8.8)	130.4	130.6
3''/5''	6.58 (d, 8.5)	6.58 (d, 8.8)	115.8	116.0
4''			156.6	156.8
1'''			127.5	127.0
2'''/6'''	7.98 (d, 8.8)	7.95 (d, 8.5)	131.7	132.0
3'''/5'''	6.907 (d, 8.7)	6.85 (d, 8.5)	116.5	117.4
4'''			163.9	167.1
2-CO_2CH_3			164.3	164.0
2-CO_2CH_3	3.43 (s)	3.42 (s)	50.9	51.1

[a] values reported in methanol-d_4, 600 MHz, [b] values reported in methanol-d_4, 600 MHz (Zhang *et al.* 2012).[393]

Pyrrolo[2,3-c]carbazole spirolactone 1a

Pyrrolo[2,3-c]carbazole spirolactone 1a (**199**) was isolated as a pink amorphous solid and its molecular formula was deduced to be $C_{43}H_{29}N_2O_{12}S$ from a pseudo-molecular ion $[M - Na]^-$ at *m/z* 797.1284 in HR-ESI-MS (negative ion mode). The ^{1}H NMR spectrum displayed two methylene signals at δ_H 2.35 and 2.99, ABC aromatic signals [δ_H 5.70 (d, 8.3), δ_H 6.60 (dd, 8.3, 8.3) and δ_H 7.15 (d, 7.5)], along with other broad, unresolved aromatic signals.

Compound (**199**) was isolated as part of a mixture (1.1 mg), and the minimal quantity did not allow for further purification. Despite this, the strong agreement of the experimental data (characteristic proton NMR signals, product colour, and HR-ESI-MS data) with those previously reported for compound (**199**), confirmed its presence in the *D.* cf. *dendyi* extract.[379]

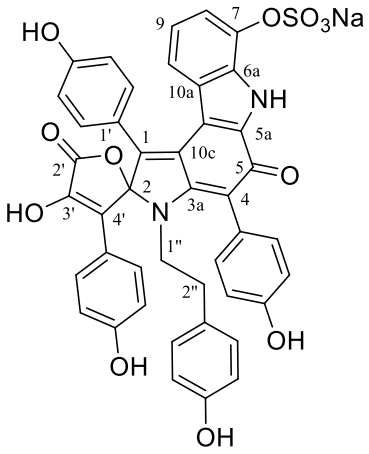

199

4.3.4 Discussion

Chemical analysis of the sponge yielded nine known polyaromatic aryl pyrroles, namely dictyodendrins B (**208**), C (**209**), D (**210**) and F (**212**), as well as denigrins E (**226**) and G (**227**), dactylpyrrole A (**225**), lamellarin O1 (**228**) and pyrrolo[2,3-c]carbazole spirolactone 1a (**199**). Polyaromatic pyrrole alkaloids are prevalent within the Demospongiae class and their occurence in marine organisms is discussed in further detail in Chapter 5, Section 5.2.5. The cytotoxic activity of the pure compounds (**209**), (**210**), (**212**), (**225**), (**226**) and (**228**) is presented in Chapter 5, Section 5.3.1.

As stated in the section above, dictyodendrins B (**208**), C (**209**) and D (**210**) have been described from *D. verongiformis*, a Japanese marine sponge.[382] Compounds (**209**) and (**210**) are structurally very similar, only differing by the presence of either one or two sodium sulphate groups. Further dictyodendrins A (**207**) and E (**211**) were reported from the same sponge.[382] Dictyodendrin F (**212**) was reported as a natural product from a southern Australian marine sponge, *Ianthella* sp.,[390] and then subsequently from a *Dactylia* sp. marine sponge.[392] Lamellarin O1 (**228**), initially described from a New Zealand specimen of *D. dendyi*, along with lamellarin O and O2 have also been reported from an Australian *Ianthella* sp. marine sponge.[393] Lamellarin alkaloids feature a 3,4-diarylpyrrole system and have been reported from diverse marine organisms, although primarily from ascidians[394-397] and sponges.[398,399] Some of the lamellarin alkaloids, such as lamellarins I, K and L are cytotoxic to various tumour

cell lines (IC_{50} 0.25 μg mL^{-1} against P388 and A549 cancer cell lines).[396,400] Denigrins E (**226**), G (**227**) and dactylpyrrole A (**225**), along with further denigrins and dactylpyrroles B-C have been reported from a *Dactylia* sponge.[392]

4.3.5 *Goniobranchus aureomarginatus*

Reported metabolites from *Goniobranchus* species

Despite *Goniobranchus* nudibranchs inhabiting most tropical regions, most of the specimens investigated so far were collected in Australia and numerous metabolites have been described by the Garson research group.[317,401-405] These specimens are predominantly known to feed on sponges that contain rearranged and oxygenated diterpenes with various skeletons. To note, numerous species formerly classified as *Chromodoris* have recently been reclassified as *Goniobranchus*[134,316,406-411] and are therefore included here.

The first report on the chemistry of *Goniobranchus* nudibranchs dates to 1988 with the description of the rearranged cytotoxic and antimicrobial diterpene chromodorolide A (**229**) from *Goniobranchus* (formerly *Chromodoris*)[408] *cavae*.[412] In 2012, the structural elucidation of four oxygenated diterpenes from a single dissected specimen of *Goniobranchus* (formerly *Chromodoris*)[407] *albopunctatus* was described.[413] Three of the diterpenes, namely 20-acetoxyspongian-16-one (**230**), 20-oxyspongian-16-one propionate (**231**) and 12α,20-dioxyspongian-16-one dipropionate (**232**), were isolated from the mantle tissue, while 12α-acetoxyspongian-16-one (**233**) was located in the digestive tissues. The rearranged diterpenes dendrillolide A (**42**) and 12-acetoxy dendrillolide A (**234**) were reported from Australian specimens of *Goniobranchus albonares*, with compound (**42**) also found within an encrusting crimson sponge yet to be identified.[133] An investigation into the skin extract of four *Goniobranchus* (formerly *Chromodoris*) species also reported dendrillolide A (**42**) from *Goniobranchus* (formerly *Chromodoris*)[410] *gleniei*, along with 12-desacetoxyshahamin C, and shahamin K.[414] The same study reported three acetoxspongians, namely 12β,15α,16α-triactetoxypongian (**235**), 6α,15α,16α-triacetoxyspongian (**236**) and 6α,12α,15α,16 α-tetracetoxysponagan (**237**) from the skin extract of *Goniobranchus* (formerly *Chromodoris*)[409] *geminus*.[414] Shahamin F was described from *Goniobranchus* (formerly *Chromodoris*)[411] *annulata.*[414]

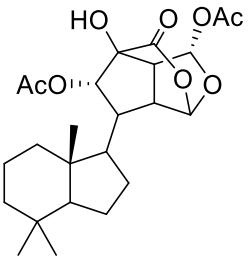

229

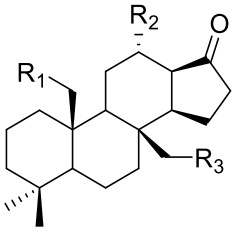

230 R_1 = OAc, R_2 = R_3 = H
231 R_1 = OCOEt, R_2 = R_3 = H
232 R_1 = R_2 = OCOEt, R_3 = H
233 R_1 = R_3 = H, R_2 = OAc

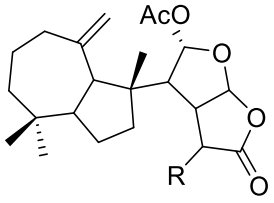

42 R=H
234 R=OAc

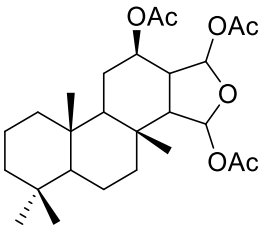

235

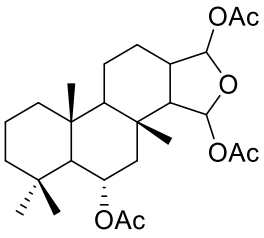

236

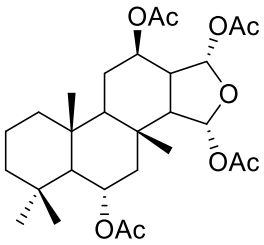

237

Australian specimens of *G. splendidus*, possessing conspicuous red spots on a white body and a yellow rim, have been widely studied over the past decade for their chemical composition and unpalatability.[401,404,415,416] Five norditerpenes, gracilins M-Q (**238-242**) and aplytandiene-3 (**243**) were initially reported from two South East Queensland specimens of *G. splendidus*, along with several known diterpenes including gracilins A (**244**), B, C and G, aplysulfurin 10, spongian-16-one (**197**) and 7α -acetoxyspongian-16-one.[417] A separate collection of four specimens of *G. splendidus* from Sydney yielded a different chemical composition, with rearranged norditerpenes displaying tetrahydroaplysulphurin, tyrinnal or gracilin skeletons, such as splendidalactone-1 (**245**) and 2 (**246**), and tyrinnal B (**247**), along with previously reported oxygenated terpenes.[404] An Eastern Australian collection of a single specimen of *G. splendidus* yielded once again a different chemical composition, including various terpenes, among which some were previously reported from molluscs and/or their dietary sponges.[403] The gut extract of a single *G. splendidus* specimen from North Queensland afforded the cytotoxic epoxygoniolide-1 (**248**) (IC_{50} 10.18 µM, against human colorectal SW620 cancer cell line), along with gonioline (**249**).[415] Their isolation from the gut extract suggested a dietary origin.[415] Spongionellin-2 was isolated from a single specimen of *G. splendidus* from Queensland.[401] *G. splendidus* individuals collected from five different sites along the

southeast coast of Australia were tested for their unpalatability against the rock-pool shrimp *Palaemon serenus* and all extracts were unpalatable, although the extent varied between geographical locations.[416]

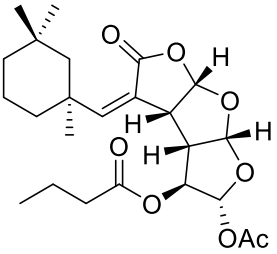

238

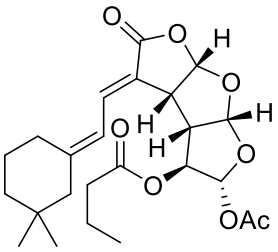

239

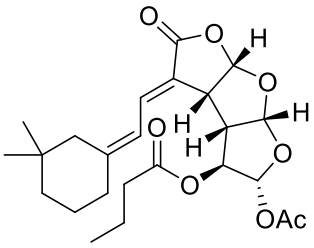

240

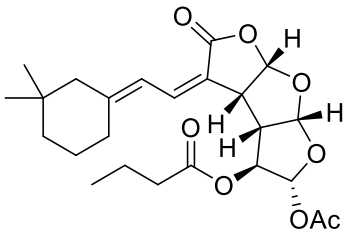

241

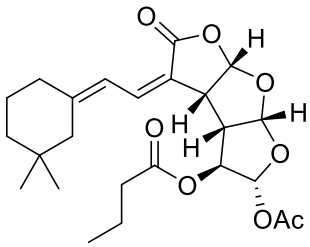

242

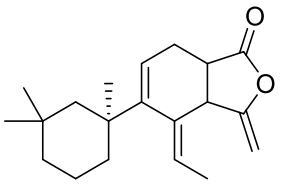

243

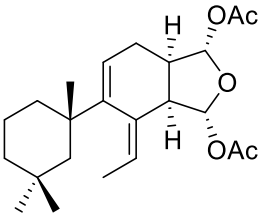

244

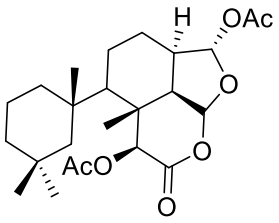

245

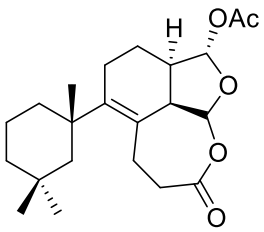

246

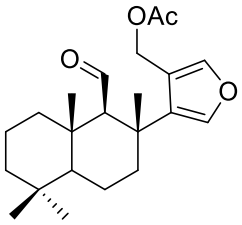

247

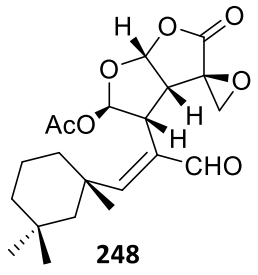

248

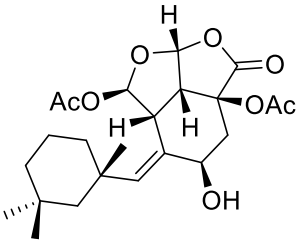

249

Daphnelactone (**250**), along with gracilin A (**244**) were described from the mantle of *G. daphne*, while aplysulfurin was isolated from the gut tissues.[417] Two Australian specimens of *G. verrieri* contained verrielactone (**251**) as the major compound, while a single specimen of a species related to *G. splendidus* yielded tetrahydroaplysulphurin-4 (**252**), along with

previously reported terpenes.[404] Investigation of an Australian collection of five individuals of *G. collingwoodi* yielded the oxygenated terpenes 12-acetoxypolyrhaphin C and 7α-acetoxyisoagatholactone, along with previously reported metabolites.[401]

As previously stated, the crude extract from the border of the mantle of *Goniobranchus* (formerly *Chromodoris*)[134] *sinensis* contains a mixture of the sponge-derived metabolites aplyroseol-2 (**45**), and its corresponding dialdehyde (**46**), of possible dietary origin.[100]

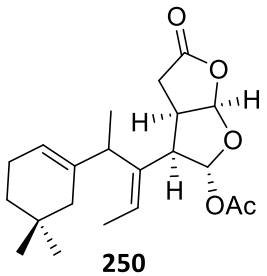

250

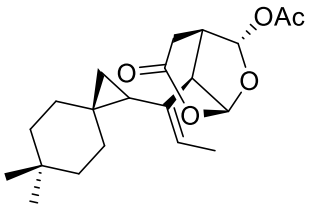

251

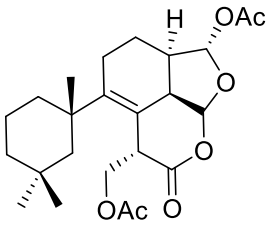

252

Spongian diterpenes have primarily been isolated from sponges of the order Dictyoceratida and Dendroceratida, including compounds (**197**) and (**198**) from *Dictyodendrilla cavernosa*, but also from nudibranch predators. As such, spongian-16-one (**197**) has previously been isolated from a Japanese specimen of *Goniobranchus* (formerly *Chromodoris*)[406] *obsoletus*.[418] A wide range of spongian-16-one diterpenes were reported from the mantle tissue of a single Australian specimen of *G. collingwoodi*, while the known metabolites spongian-16-one (**197**), 12α-acetoxyspongian-16-one, luffarin-X, and acetylelatol were isolated from the digestive tissues, supporting the selective sequestration in specific body parts, possibly serving ecological roles.[402] Extracts of the mantle and viscera of a collection of *Goniobranchus aureopurpureus* from New South Wales and *Goniobranchus* sp. from Queensland afforded eleven previously unreported diterpenoids possessing a tetracyclic spongian-16-one scaffold, with most of them isolated from the mantle tissues.[419]

A rearranged spongian diterpene, chromolactol (**253**), was obtained from the mantle extract of *G. coi* collected from Queensland.[420] An investigation of two *G. coi* individuals from a separate collection in Queensland resulted in the isolation of two perhydroazulene-containing metabolites, the diterpene epoxide (**254**) and keto-functionalised norditerpene

(**255**).[421] Finally, eight individuals of *G. geometricus* collected in Queensland were extracted and a total of nineteen rearranged terpenes were isolated, including secoshahamin (**256**), initially isolated from a Japanese marine sponge, and (—)-shahamin L, along with (—)-15-desacetoxy-12-acetoxydendrillolide A. The establishment of the relative configuration of compound (**256**) was conducted using a combination of spectroscopic, modelling, and computational approaches.[422]

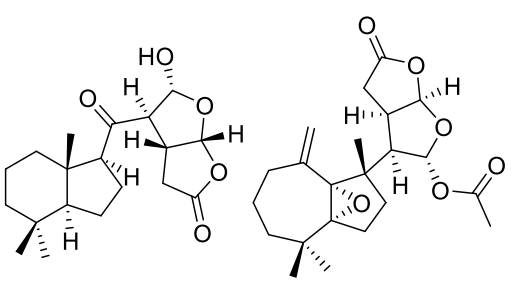

253

254

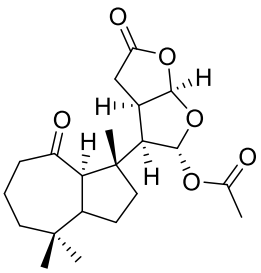

255

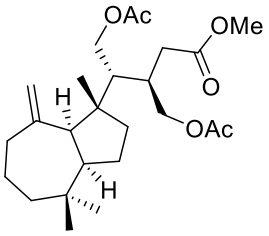

256

Isolation procedure

With spectral and spectrometric information of the main *D.* cf. *dendyi* metabolites in hand, the purification of the nudibranch extract was carried out to investigate the presence of common metabolites. Fifteen whole *G. aureomarginatus* specimens collected in December 2021 at Dive Crescent were extracted. The resulting crude extract was purified in a similar way to the *D.* cf. *dendyi* extract, by reversed phase C18 bench column chromatography. Thin layer chromatography (TLC) revealed several brightly coloured compounds, especially within the early eluting fractions, from H_2O/MeOH (1:1) until MeOH 100% (fractions 3 to 6 in Figure 77A). TLC of fraction 5 from *G. aureomarginatus* versus three of the early eluting *D.* cf. *dendyi* fractions indicated that they may contain identical metabolites (Figure 77B). Fraction 5 from the nudibranch extract was further purified in a similar way to the *D.* cf. *dendyi* extract, using Sephadex LH-20. This resulted in the isolation of the known compounds dictyodendrins C (**209**) and F (**212**) (Figure 78). Fraction 6 displayed a strong UV visible spot at a high Rf value (0.78) and was further purified with reversed phase C18 chromatography to afford a mixture of the known terpenes gracilin A (**244**) and 6α,15α,16α-triacetoxyspongian (**236**).

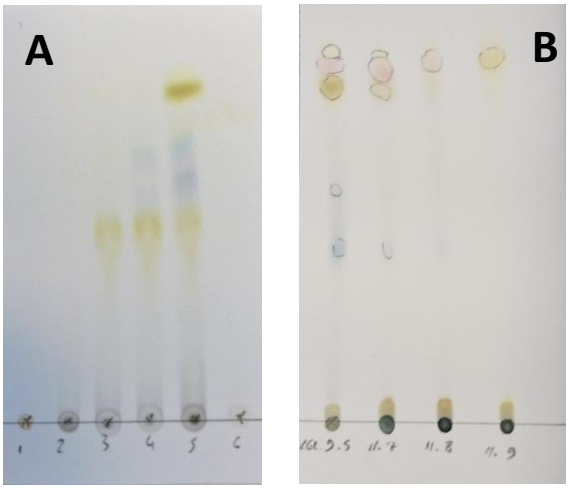

Figure 76: A- TLC plate (EtOAc/MeOH 5:1) of early eluting *Goniobranchus aureomarginatus* fractions after initial C18 purification. B- TLC plate (EtOAc 100%) of one *Goniobranchus aureomarginatus* fraction (left) and three *Dictyodendrilla* cf. *dendyi* fractions after initial C18 purification.

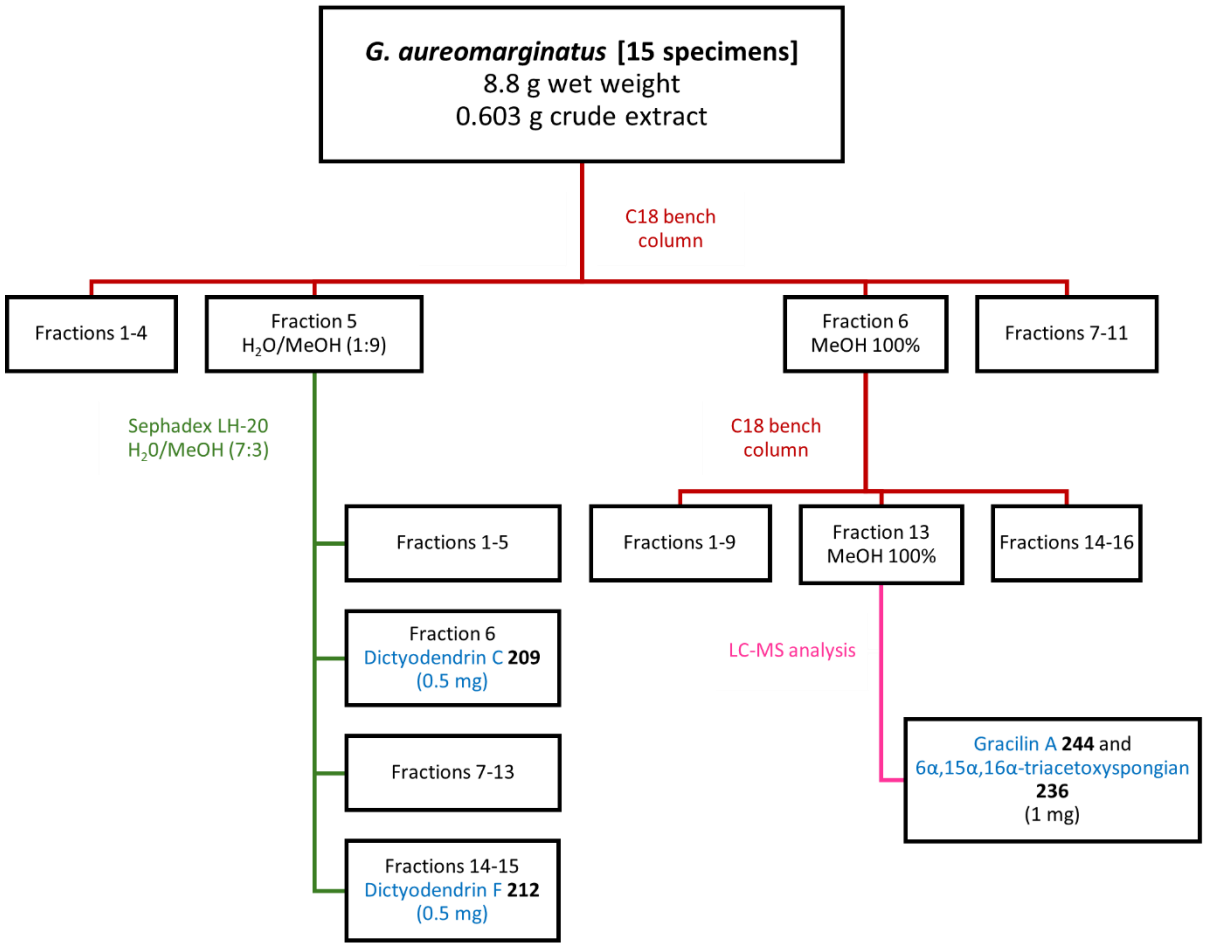

Figure 78: The isolation procedure for dictyodendrins C (**209**), F (**212**), gracilin A (**244**) and 6α,15 α,16α -triacetoxyspongian (**236**) from *Goniobranchus aureomarginatus*.

Dictyodendrins C and F

Dictyodendrins C (**209**) and F (**212**) were both isolated from the whole nudibranch extract, although in minimal quantity (0.5 mg each) and only the ^{1}H NMR spectra could be acquired. Each metabolite displayed identical *m/z* ions in HR-ESI-MS (positive and negative ion modes) compared to compounds **209** and F **212** isolated from *D.* cf. *dendyi*. The strong agreement of the proton NMR values and the HR-ESI-MS data with those previously reported for compounds **209** and **212**, both in the literature and in *D.* cf. *dendyi* (Table 28 and Table 29) confirmed their presence.[382] The isolation of compounds **209** and **212** from both *D.* cf. *dendyi* and *G. aureomarginatus* further establishes the relationship between the two organisms and confirms the predation of *D.* cf. *dendyi* by *G. aureomarginatus*. Dictyodendrins belong to a rare class of marine alkaloids and to date had only been reported from three marine sponge species[382,390,391] and never from molluscs.

Table 28: ^{1}H NMR assignments determined for dictyodendrin C (**209**) compared with literature values (methanol-d_4) and to compound (**209**) isolated from *Dictyodendrilla* c.f. *dendyi*.[2]

	δ_H (mult, *J* in Hz)		
Atom	[a] ***G. aureomarginatus***	[a] ***D.* cf. *dendyi***	[b] **Literature**
7	6.13 (1H, d, 8,3)	6.15 (1H, d, 8.3)	6.13 (1H, d, 8.1)
8	6.70 (1H, dd, 8.1, 8.0)	6.73 (1H, dd, 8.0, 8.0)	6.70 (1H, dd, 8.1, 8.1)
9	7.19 (1H, d, 7.8)	7.22 (1H, d, 7.7)	7.19 (1H, d, 8.1)
18/22	7.23 (2H, d, 8.6)	7.25 (2H, d, 8.5)	7.22 (2H, d, 8.6)
19/21	6.91 (2H, d, 8.6)	6.93 (2H, d, 8.5)	6.90 (2H, d, 8.6)
23	[c]	3.41 (2H, t, 7.8)	3.40 (2H, t, 8.1)
24	2.41 (2H, t, 7.9)	2.38 (2H, t, 8.0)	2.73 (2H, t, 8.1)
26/30	6.64 (2H, d, 8.5)	6.66 (2H, d, 8.4)	6.63 (2H, d, 8.4)
27/29	6.55 (2H, d, 8.5)	6.57 (2H, d, 8.4)	6.55 (2H, d, 8.4)
32/36	7.30 (2H, d, 8.6)	7.32 (2H, d, 8.5)	7.30 (2H, d, 8.6)
33/35	6.88 (2H, d, 8.7)	6.91(2H, d, 8.5)	6.88 (2H, d, 8.6)

[a] values reported in methanol-d_4, ^{1}H 600 MHz, [b] values reported in methanol-d_4, ^{1}H 600 MHz (Warabi *et. al*),[382] [c] undetermined due to overlapping signals.

Table 29: ^{1}H NMR assignments determined for dictyodendrin F (**212**) compared with literature values (methanol-d_4) and to compound (**212**) isolated from *Dictyodendrilla* c.f. *dendyi*.[2]

	δ_H (mult, *J* in Hz)		
Atom	[a] ***G. aureomarginatus***	[a] ***D.* cf. *dendyi***	[b] **Literature**
7	5.83 (1H, dd, 7.7, 1.5)	5.83 (1H, dd, 7.5, 1.6)	5.81 (1H, dd, 6.9, 2.2)
8	6.58 (1H, m)	6.58 (1H, m)	6.56 (1H, m)
9	6.58 (1H, m)	6.58 (1H, m)	6.56 (1H, m)
18/22	7.26 (2H, d, 8.3)	7.24 (2H, d, 8.5)	7.21 (2H, d, 8.1)
19/21	6.94 (2H, d, 8.3)	6.93 (2H, d, 8.6)	6.91 (2H, d, 8.5)
23	[c]	3.43 (2H, t, 7.6)	3.38 (2H, t, 7.9)
24	2.42 (2H, t, 7.9)	2.41 (2H, t, 7.9)	2.37 (2H, t, 7.9)
26/30	6.67 (2H, d, 9.0)	6.66 (2H, d, 8.6)	6.63 (2H, d, 8.5)
27/29	6.57 (2H, m)	6.57 (2H, m)	6.56 (2H, m)
32/36	7.32 (2H, d, 9.0)	7.31 (2H, d, 8.7)	7.29 (2H, d, 8.4)
33/35	6.90 (2H, d, 8.3)	6.90 (2H, d, 8.7)	6.88 (2H, d, 8.2)

[a] values reported in methanol-d_4, ^{1}H 600 MHz, [b] values reported in methanol-d_4, ^{1}H 600 MHz, according to J. Ryan 2007,[391] [c] overlapping signals.

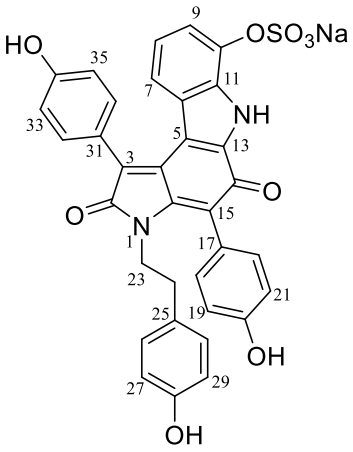

209

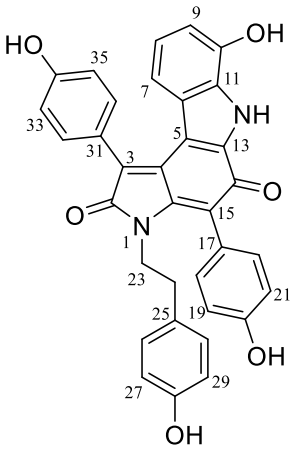

212

Gracilin A and 6α,15α,16α-triacetoxyspongian

Based on TLC analysis, several fractions of interest from the initial C18 reversed phase bench column on the extract of *G. aureomarginatus* were selected and analysed by LC-MS in positive ion mode following the methodology described in Chapter 7 – Experimental, Section 7.1.11. The chromatogram of fraction 13, that eluted with 100% MeOH from the bench column, displayed two strong peaks at 34.9 and 35.5 minutes (Figure 79). The mass spectrum of each

peak contained a sodiated $[M + Na]^+$ parent ion (at *m/z* 487 for 6α,15α,16α-triacetoxyspongian (**236**) and at *m/z* 413 for gracilin A (**244**), respectively) (Table 30). Along with the parent ions, several fragments representative of the loss of acetic acid groups were observed, indicative of the initial presence of acetoxy groups. These included the fragments at *m/z* 345 and 285 for compound (**236**) and at *m/z* 331 and 271 for compound (**244**) (Table 30).

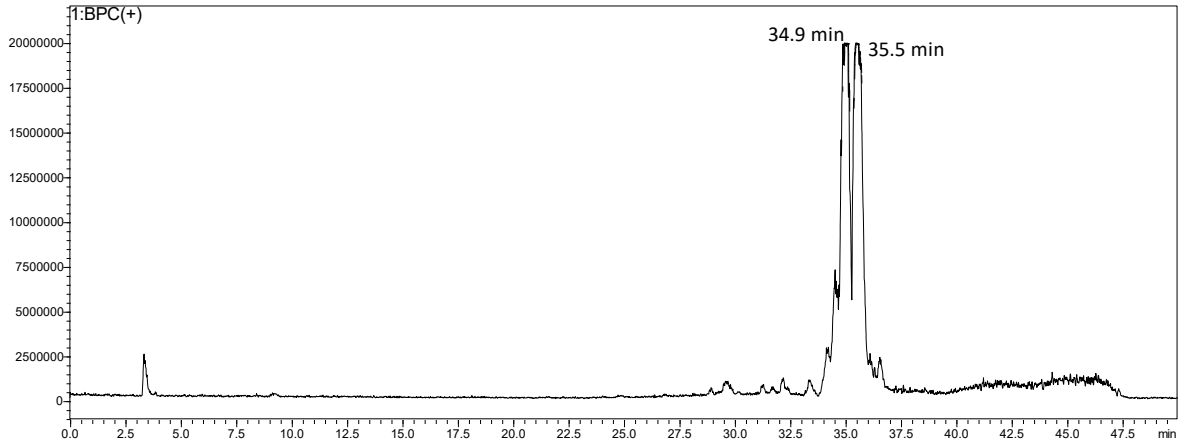

Figure 79: LC-MS chromatogram of fraction 13 (positive ion mode).

Table 30: The MS^2 fragments of gracilin A (**244**) and 6α,15α,16α-triacetoxyspongian (**236**) (positive ion mode).

Compound	Retention time (min)	Parent ion $[M + Na]^+$	M (g mol^{-1})	Mass loss (g mol^{-1})	Attributable fragment loss	Fragment ion (*m/z*)
6α,15α,16α-Triacetoxyspongian	34.9	487	464	120	2 x AcOH	345
				162	2 x AcOH + CH_2CO	302
				180	3 x AcOH	285
Gracilin A	35.5	413	390	60	AcOH	331
				102	AcOH + CH_2CO	288
				120	2 x AcOH	271

Due to the minimal quantity of the impure mixture (1 mg), it was not purified further. Instead, characterisation of the mixture by ^1H NMR spectroscopy (Appendix C.13) in methanol-d_4 was conducted. Integration of the aromatic signals corresponding to each compound revealed a 3:5 ratio of (**236**:**244**). Characteristic signals for compound (**244**) included a broad quartet for an olefinic proton at δ_H 5.42 (q, J=6.9), a doublet of doublets for another olefinic proton at δ_H 5.94 (dd, 7.3, 3.9), two doublets accounting for two acetoxy methine protons at δ_H 5.86 (d,

J=1.5) and 6.00 (d, J=1.3), along with two acetoxymethyl signals at δ_H 2.03 and 2.05, integrating for three protons each. Characteristic signals for compound (**236**) included three signals representing three acetoxymethine protons at δ_H 5.36 (m), 6.12 (s) and 6.15 (d, 7.2), along with three acetoxymethyl signals at δ_H 2.04, 2.06 and 2.07, integrating for three protons each. The agreement of characteristic proton NMR chemical shifts (Table 31) and mass spectrometry fragments with literature data for gracilin A (**244**) and 6α,15α,16α-triacetoxyspongian (**236**) confirmed their presence, despite the experimental spectrum being recorded in methanol-*d*$_4$, as opposed to chloroform-*d* in the literature.[414,423]

Table 31: ^{1}H NMR assignments (methanol-*d*$_4$) of characteristic signals determined for gracilin A (**244**) and 6α,15α,16α-triacetoxyspongian (**236**) compared with literature values (chloroform-*d*).[423,414]

	δ_H (mult, *J* in Hz)			
	Compound **244**		Compound **236**	
Atom	[a] **Experimental**	[b] **Literature**	[a] **Experimental**	[c] **Literature**
2	1.43 ([d])	[e] 1.46 (m)	-	-
6	1.64 (d, 7.0)	[e] 1.59 (d, 6.9)	5.36 (m[f])	5.23 (dt, 11.1, 3.6)
7	5.42 (q, 6.9)	5.34 (q, 6.9)	2.16 (m[g])	2.14 (dd, 12.3, 3.5)
11	5.94 (dd, 7.3, 3.9)	5.85 (dd, 6.9, 4.0)	-	-
12a	2.30 (ddd, 14.7, 7.4, 2.2)	2.25 (ddd, 14.8, 6.9, 1.8)	-	-
12b	1.77 (ddd, 14.8, 6.6, 3.9)	1.76 (ddd, 14.8, 6.5, 4.0)	-	-
13	2.84 (m)	2.75 (dddd, 9.0, 6.5, 1.8, 1.6)	2.63 (m[h])	2.58 (q, 7.4)
15	6.00 (d, 1.3)	5.99 (d, 1.5)	6.12 (s)	6.08 (s)
16	5.86 (d, 1.5)	5.86 (d, 1.6)	6.15 (d, 7.2)	6.10 (d, 7.5)
17	0.89 (s)	0.84 (s)	[f] ND	1.2 (s)
18	1.04 (s)	0.97 (s)	[f] ND	1.08 (s)
19	1.31 (s)	1.22 (s)	0.96 (s)	0.96 (s)
20	-	-	0.85 (s)	0.89 (s)
CH_3CO	2.03 (s) 2.05 (s)	2.03 (s) 2.05 (s)	2.07 (3H, s) 2.06 (3H, s) 2.04 (3H, s)	2.10 (3H, s) 2.05 (3H, s) 2.04 (3H, s)

[a] values reported in methanol-*d*$_4$, 600 MHz, [b] values reported in chloroform-*d*, 500 MHz (Mayol *et al*. 1985),[423] [c] values reported in chloroform-*d*, 400 MHz (De Silva *et al.* 1991),[414] [d, f-g] unresolved signals, [e] overlapping signals, [f] ND not determined.

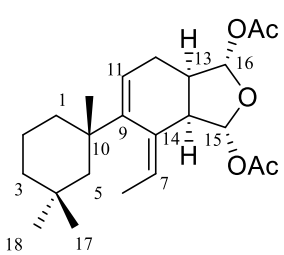

244

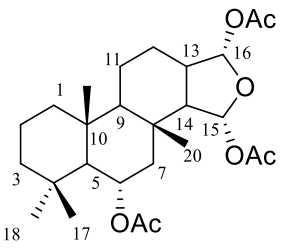

236

Gracilin A (**244**) was initially isolated from *Spongionella gracilis*,[423] and later on described from Australian specimens of *G. splendidus*, as well as from the mantle and mantle rim of *G. daphne*.[417] Gracilin A (**244**) previously showed some cytotoxicity (IC_{50} < 0.30 µg.mL^{-1}) against HeLa S3 cells and was reported as a potent inhibitor of phospholipase A_2 (PLA2) with a 69% inactivation efficiency.[424] The diterpenoid (**236**) was initially reported from the skin extract of *Goniobranchus* (formerly *Chromodoris*)[409] *geminus* from Sri Lankan waters.[414]

Gracilin A (**244**) and 6α,15α,16α-triacetoxyspongian (**236**) were not isolated from *D.* cf. *dendyi*, nor from *Dysidea teawanui*. However, the reported presence of compound (**244**) in *S. gracilis* indicates a possible dietary origin, despite no records of *Spongionella* species within our collection site.

Metabolite distribution

To investigate the possible ecological role of the four metabolites (**209**), (**212**), (**236**) and (**244**) isolated from fifteen whole nudibranchs, the distribution of compounds within specific parts of the nudibranch's body was investigated by dissecting several specimens into mantle and viscera. For dictyodendrins C (**209**) and F (**212**), the purpose was specifically to determine if both metabolites are being sequestered for possible defence purposes or simply ingested while feeding and detected due to their higher concentration compared to other metabolites. For the two oxygenated terpenoids (**244**) and (**236**), the metabolite distribution investigation aimed to determine if they could be of dietary origin by being specifically located in the viscera, and/or if they could have a possible defensive role by being present in the mantle.

Six *G. aureomarginatus* specimens collected at Dive Cresent were dissected into mantle and viscera (Figure 80).

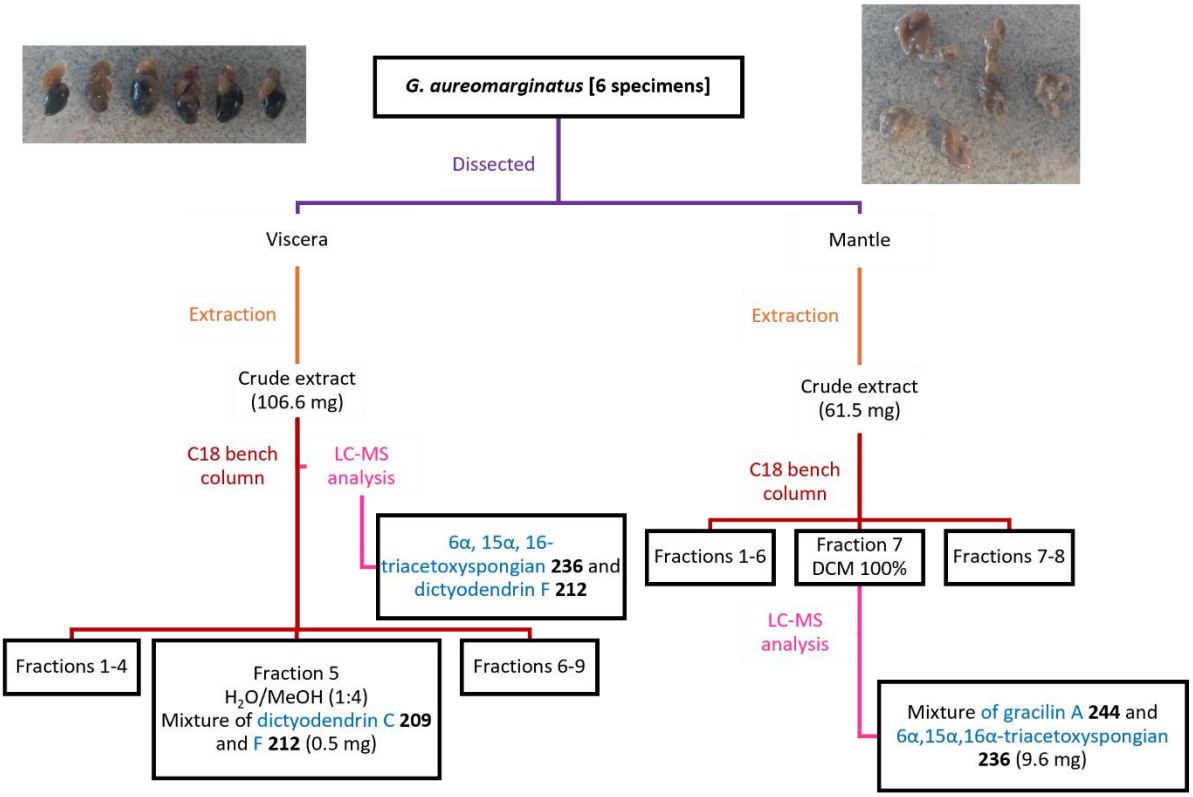

Figure 79: Isolation procedure for the study of metabolite distribution within *Goniobranchus aureomarginatus*.

The crude extract of the viscera was analysed by LC-MS in positive ion mode following the methodology described in Chapter 7 – Experimental, Section 7.1.11. Analysis of the chromatogram and mass spectrum in extracted ion mode revealed the presence of dictyodendrin F (**212**) and 6α,15α,16α-triacetoxyspongian (**236**) (Figure 81), but neither gracilin A (**244**) nor dictyodendrin C (**209**) were detected.

To note, compound (**209**) had not previously been detected from the LC-MS analysis of the whole-body extract and is believed to undergo acid hydrolysis because of the formic acid (FA) present in both mobile phases (0.1%). Therefore, the sulphate groups would be hydrolysed, leading to the phenol analogue (**212**) and to an increase in intensity of the corresponding peak. It is also believed that compound (**210**) undergoes the same hydrolysis upon analysis. Knowing this, the viscera extract was purified and analysed further utilising LC-MS and HR-ESI-MS that did not involve any formic acid.

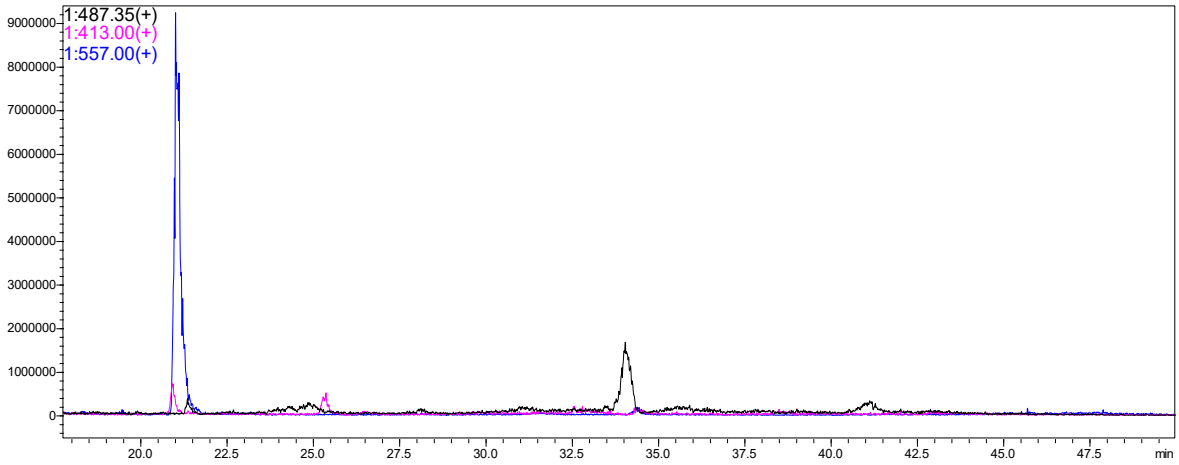

Figure 81: LC-MS chromatogram of the viscera crude extract displaying dictyodendrin F (**212**, blue trace) and 6α,15α,16α-triacetoxyspongian (**236**, black trace).

The viscera extract was then purified separately by C18 reversed phase chromatography. Each fraction of the column was analysed by HR-ESI-MS. Fraction 5 (Figure 80) displayed sodiated ions corresponding to dictyodendrins C (**209**) and F (**212**). The fraction was analysed by ^{1}H NMR spectroscopy in methanol-d_4 and the presence of both compounds was confirmed (Figure 82).

The crude extract of the mantle was purified separately by C18 reversed phase chromatography. Each fraction was analysed by HR-ESI-MS and no fractions displayed ions corresponding to dictyodendrins C (**209**) or F (**212**), establishing their selective presence in the viscera. Fraction 7 (Figure 80) was analysed by LC-MS in positive ion mode, using the same method as for the whole nudibranch extract. The mass spectra and retention times of two peaks at 34.9 and 35.5 minutes matched those of gracilin A (**244**) and 6α,15α,16α-triacetoxyspongian (**236**).

Investigation of the metabolite distribution within *G. aureomarginatus* showed that dictyodendrins C (**209**) and F (**212**) are selectively present in the viscera, consistent with their dietary origin from *D.* cf. *dendyi*, upon which it was shown to preferentially prey. Their absence from the mantle extract indicates that compounds (**209**) and (**212**) likely do not serve a defensive role for the nudibranch. Instead, it appears that the nudibranchs are ingesting the compounds upon feeding but are not sequestering them.

6α,15α,16α-Triacetoxyspongian (**236**) was present in both the mantle and viscera extracts, indicating a potential dietary origin and a defensive role. Compound (**136**) was previously reported from the skin extract of *G. geminus* but no bioactivity was reported.[414]

Gracilin A (**244**) was selectively present in the mantle, indicating that it might serve a defensive role. This is consistent with previous reports of its cytotoxic activity against HeLa S3 cells and as a phospholipase A_2 inhibitor.[424]

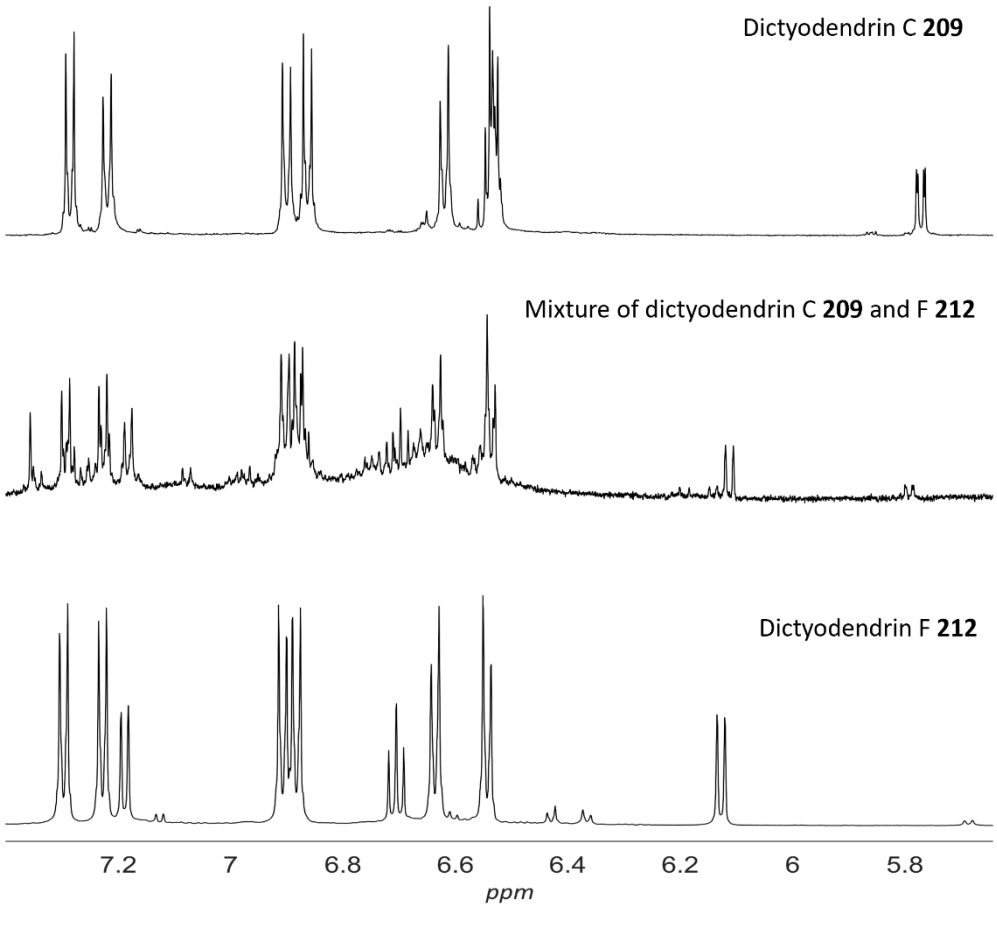

Figure 81: Representation of the aromatic section of the ^{1}H NMR spectrum of a fraction of the viscera extract containing dictyodendrins C (**209**) and F (**212**)

Chemical composition across different locations

To investigate whether the chemical composition of *G. aureomarginatus* would be similar across different geographical locations in New Zealand, a single specimen, collected in December 2020 at Monarch Wharf, Otago, New Zealand was extracted whole. Another specimen collected at the same location and date was dissected between mantle and viscera, and each body part was separately extracted. The extracts were assessed for cytotoxicity using the same method as for the *G. aureomarginatus* extracts from Tauranga and the values were compared across the two locations. Overall, the extracts from Otago specimens were much less cytotoxic than the ones from Tauranga (Table 32).

Among the six nudibranchs extracts, that is the whole-body, mantle and viscera extracts from Tauranga and the whole-body, mantle and viscera extracts from Otago respectively, both mantles were the most cytotoxic when comparing the extracts within each location (Table 32). However, the mantle extract from the Tauranga specimen had a lower IC_{50} value than the Otago extract (IC_{50} 13 versus 75 µg mL^{-1}). This could indicate that, similarly to Tauranga individuals, the Otago specimens may contain cytotoxic terpenoids in the mantle, although potentially at lower concentrations or different compositions. Both viscera extracts displayed minimal activity, which may indicate that specimens at both locations feed on a similar diet and that the compounds ingested are not cytotoxic or are rapidly diverted to the mantle.

Based on the low cytotoxic activity of both mantle and viscera extracts from the Otago specimen, it is not surprising that the whole-body extract also displayed minimal activity.

Table 32: IC_{50} values of the crude extracts of *Goniobranchus aureomarginatus* (whole-body and dissected) from Tauranga and Otago collections.

	***G. aureomarginatus* extracts**					
	Tauranga collection			Otago collection		
	Whole-body	Viscera	Mantle	Whole-body	Viscera	Mantle
IC_{50} (µg mL^{-1})	15	>100	13	>100	100	75

To investigate the chemical composition of the Otago and Tauranga specimens, the three crude extracts obtained from the Otago specimens were analysed by LC-MS following the methodology described in Chapter 7 – Experimental, Section 7.1.11. Retention times and mass spectra were compared with previously analysed fractions containing the known aryl pyrrole alkaloids and terpenoids.

Traces of 6α,15α,16α-triacetoxyspongian (**236**) were detected in extracted ion mode in the whole-body, viscera and mantle crude extracts, although in minimal quantity. No trace of dictyodendrin F (**212**), gracilin A (**244**) or any other aryl pyrrole alkaloid previously isolated was present. No *Dictyodendrilla* sponges were observed within the collection area of *G. aureomarginatus* in Otago. Therefore, the absence of arylpyrrole alkaloids from the Otago individuals indicate that they probably consume different prey or other organisms. The presence of gracilin A (**244**) in the Tauranga individuals is likely responsible for the high cytotoxicity of the mantle extract, while its absence from the Otago individuals may explain the low activity observed for these extracts.

Morphological analysis

To investigate whether the two terpenoids (**236**) and (**244**) could originate from different sponge prey, morphological analysis was conducted to search for sponge spicules originating from different species. A single specimen collected in January 2023 from the same sponge meadow as the specimen studied above, was dissected to separate the mantle, digestive glands and intestines. The intestines were cut open under a dissection microscope and carefully observed. No sponge spicules were detected in the intestines. The digestive glands, harder to observe directly under the dissection microscope, were digested in nitric acid prior to observation. Similarly to the intestines, no sponge spicules were detected in the digestive glands. These findings were consistent with *G. aureomarginatus* preying on *D.* cf. *dendyi* as *Dictyodendrilla* sponges lack free silica spicules.[425] Although, microscopic examination did not provide information regarding the possible origin of the two terpenoids (**236**) and (**244**), it appears that the nudibranchs either do not feed on sponges other than *D.* cf. *dendyi*, or feed on other sponges that also lack spicules.

4.3.6 *Goniobranchus aureomarginatus* eggs

The crude extract of the egg coil spawned by *G. aureomarginatus* from Tauranga during the feeding experiments was analysed by LC-MS following the methodology described in Chapter 7 – Experimental, Section 7.1.11. Surprisingly, none of the compounds previously isolated from *D.* cf. *dendyi* or *G. aureomarginatus* were detected in the extract using extracted ion mode. This could be explained by the fact that the eggs were spawned when the nudibranch had been in the laboratory setting for a few days and was likely under stress because of possible differences in water temperature and salinity compared to their natural environment. Another stressor for the nudibranchs is the handling required for the feeding-choice experiments, resulting in what the specimens likely perceive as an attack from a predator. Environmental stressors, such as temperature increase and salinity, have previously been linked to a decrease in egg viability for gastropod molluscs.[240] Whether this could potentially impact the transfer of metabolites is yet to be determined and would require comparison of chemical composition of laboratory versus wild spawned eggs.

Additionally, several dorid nudibranchs, such as *H. sanguineus*[167] and *T. abdere*,[184] release a mucus with distasteful metabolites upon attack by a predator or in a stressful situation, and it could be the case for *G. aureomarginatus.* Upon being kept in a prolonged situation of stress, *G. aureomarginatus* could have exhausted its reserve of metabolites and therefore could not transfer any upon spawning.

4.3.7 Concluding remarks

The *D.* cf. *dendyi* extract yielded a range of aryl pyrrole alkaloids, namely dictyodendrins B (**208**), C (**209**), D (**210**) and F (**212**), denigrins E (**226**) and G (**227**), dactylpyrrole A (**225**), lamellarin O1 (**228**) and pyrrolo[2,3-c]carbazole spirolactone 1a (**199**). These have mainly been reported from several sponge species,[382,390,392,393] with compounds (**209**), (**210**) and (**212**) reported from a New Zealand specimen of *D. dendyi.*[391]

Two of these alkaloids, dictyodendrins C (**209**) and F (**212**) were also present in the nudibranch predator *G. aureomarginatus*, which confirmed the predator-prey relationship. A chemical link was therefore established, on top of the ecological link revealed during the feeding-choice experiments and the field observations. Two terpenoids, gracilin A (**244**) and 6α,15α,16α-triacetoxyspongian (**236**), were also detected and isolated as a mixture in the nudibranch extract.

Investigation into the metabolite distribution within the nudibranchs was carried out to explore the potential role of these metabolites for the nudibranch. The study showed the selective presence of the two alkaloids (**209**) and (**212**) in the viscera, while 6α,15α,16α-triacetoxyspongian (**236**) was present in both viscera and mantle extracts. Gracilin A (**244**) was however selectively present in the mantle.

The selective presence of compounds (**209**) and (**212**) in the viscera indicated that the nudibranchs are preying on the sponge but not necessarily sequestering the compounds for a defensive purpose. Indeed, if sequestration were happening, the compounds would likely have been in the mantle as well, which is not the case. This is corroborated by the fact that the two alkaloids isolated from the nudibranchs are the ones present in the highest concentration in the sponge, hence why they are likely ingested in higher concentration than the other alkaloids. It is quite likely that the nudibranchs ingest other aryl pyrrole alkaloids from the sponge, but these are probably at too low a concentration to allow their detection within the nudibranchs.

A previous study from the Prinsep research group showed that *G. aureomarginatus* contained brominated alkaloids also found within the bryozoan *Amathia gracei* that used to inhabit the Dive Crescent sponge meadow,[210] hence the study of *A. gracei* in Chapter 2, Section 2.2. Since 2019, the bryozoan has not been found at that collection site, possibly due to warming sea temperatures or because of the amount of sediments now present. It is therefore possible that *G. aureomarginatus* had to switch its diet and is now feeding on *D.* cf. *dendyi* for nutrition purposes as opposed to sequestering compounds for its defence.

The presence of 6α,15α,16α-triacetoxyspongian (**236**) in both the mantle and viscera indicated its potential dietary origin, despite being absent from the two sponges investigated, along with a potential defensive role, despite no bioactivity previously reported for compound (**236**). The selective presence of gracilin A (**244**) in the mantle highlights that it is likely to serve a defensive role.

The study of the chemical composition of *G. aureomarginatus* specimens from Otago showed that 6α,15α,16α-triacetoxyspongian (**236**) was the only metabolite in common with the Tauranga specimens, indicating that the population probably preys on different sponges.

To investigate whether the two terpenoids (**236**) and (**244**) could originate from a different sponge prey, morphological analysis was conducted to search for sponge spicules. No spicules were detected in a Tauranga individual, which was consistent with it primarily preying on *D.* cf. *dendyi* as this sponge lacks spicules. Therefore, the origin of compounds (**236**) and (**244**) remains unknown, despite the presence of 6α,15α,16α-triacetoxyspongian (**236**) in the viscera indicating a dietary origin, and the selective presence of gracilin A (**244**) in the mantle pointing towards a possible *de novo* biosynthetic origin or highly efficient transfer to the mantle.

4.4 Summary

The three nudibranch species, namely *P. hedgpethi*, *C. amoenum* and *G. aureomarginatus,* previously studied for their dietary preferences by means of feeding-choices experiments, were investigated chemically. Through cytotoxicity screening, an overview on the bioactivity of the crude extracts was obtained, which was later linked to the metabolites isolated. To purify the extracts of interest, an approach based on TLC and HR-ESI-MS and LC-MS analysis was developed to guide the purification.

The chemical investigation of *P. hedgpethi* and *B. neritina* did not yield any secondary metabolites and in this case, the chemistry failed to provide a link. Despite this, the results of the feeding-choice experiments showed an ecological link between the two organisms.

The presence of ergosterol peroxide (**186**) within both *Dysidea teawanui* and *C. amoenum* established a chemical link between the two organisms, which confirmed the ecological link uncovered during the feeding-choice experiments. However, compound (**186**) is a common metabolite isolated from many sponges, so could also be obtained from other prey of *C. amoenum*.

The extract of the black sponge *D.* cf. *dendyi* yielded a range of aryl pyrrole alkaloids and two of them, dictyodendrins C (**209**) and F (**212**) were also isolated from *G. aureomarginatus*, which confirmed the predator-prey relationship. Moreover, prior to this study, dictyodendrins had never been reported from molluscs. Two terpenoids, (**236**) and (**244**), were also isolated as a mixture from the nudibranchs. The metabolite distribution within the nudibranchs showed that compounds (**209**) and (**212**) were only present in the viscera, likely ruling out a defensive role, while compound (**236**) was present in both the viscera and mantle. On the other hand, compound (**244**) was only located in the mantle, indicating a possible defensive role. Upon investigation of *G. aureomarginatus* from the South Island of New Zealand, compound (**236**) was detected, while the other compounds were not.

Overall, this study provided insight into the chemistry of three dorid nudibranchs species and established chemical links for two “predator-preferred prey” associations established during the feeding-choice experiments. Moreover, this research uncovered a wide range of known aryl pyrrole alkaloids from the *D.* cf. *dendyi* sponge that are of high interest for their unique structures and bioactivities. Further minor compounds were also detected within the extract and their structure elucidation is presented in the following chapter.

Chapter 5

New denigrin alkaloids from further analysis of the marine sponge *Dictyodendrilla* cf. *dendyi*

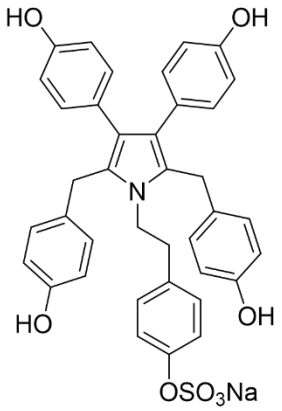

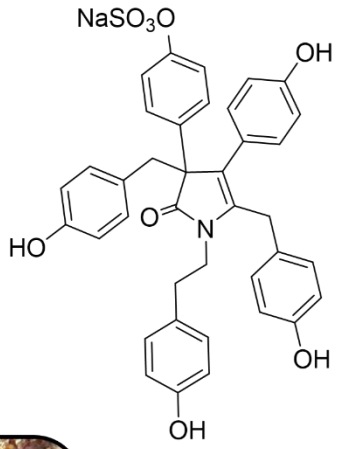

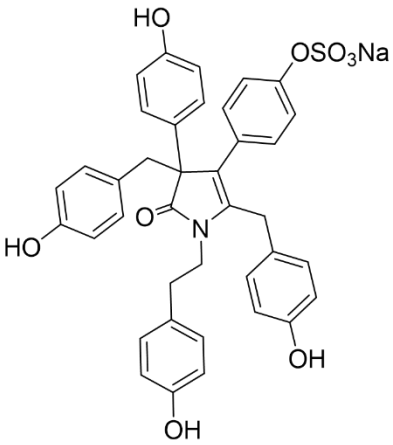

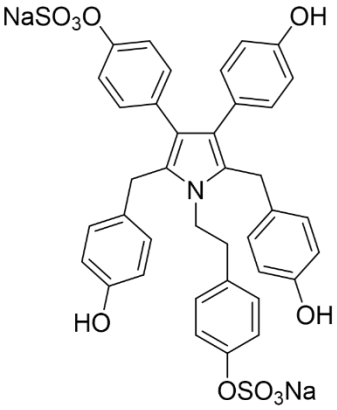

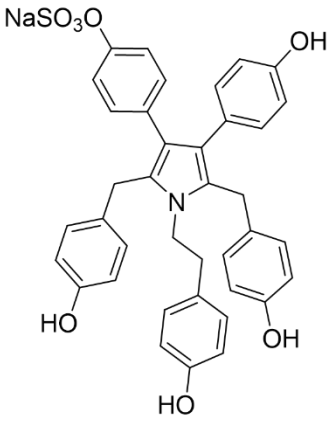

During this research, the New Zealand marine sponge *Dictyodendrilla* cf. *dendyi* was established as the preferred prey of the nudibranch *G. aureomarginatus* by feeding-choice experiments described in Chapter 3. The chemical analysis of both organisms was reported in Chapter 4. As such, the investigation of the *D.* c.f. *dendyi* sponge yielded a total of nine known aryl pyrrole alkaloids, namely dictyodendrins B (**208**), C (**209**), D (**210**) and F (**212**), denigrins E (**226**) and G (**227**), dactylpyrrole A (**225**), lamellarin O1 (**228**) and pyrrolo[2,3-c]carbazole spirolactone 1a (**199**), while two of these compounds, dictyodendrins C (**209**) and F (**212**), were isolated from the nudibranch extract, confirming the predator-prey relationship.

Following this study, the crude extract resulting from the large-scale extraction of *D.* c.f. *dendyi* was further investigated, with a focus on the minor compounds. This resulted in the isolation and structure elucidation of five new denigrin alkaloids, described in this Chapter. The cytotoxic activity of these five compounds, along with six of the known polyaromatic pyrroles, was then assessed towards the human cervical cancer cell line HeLa using an MTT assay and the results are presented in Section 5.3.1.

5.1 Occurrence and bioactivities of denigrin alkaloids

The denigrins are a rare class of highly substituted pyrrole and pyrrolidone alkaloids, to date only described from marine sponges.[392,426] The first three denigrins A–C (**257-259**) (Figure 83) were isolated in 2014 by Kumar *et al.* with the aim of identifying new antitubercular agents from the Indian marine sponge *Dendrilla nigra*.[426] Denigrin C (**259**) exhibited moderate activity against *Mycobacterium tuberculosis* (MIC 4 μg mL^{-1}).[426] The total synthesis of denigrins A (**257**) and B (**258**) was achieved in three and five steps, respectively, from maleic anhydride by Karak *et al.* in 2018.[427]

In 2020, further denigrins D–G (**260**)**,** (**226**)**,** (**261**) and (**227**), respectively (Figure 83) were isolated from a collection of *Dactylia* sp. nov. from the Maldives, as a means to establish potential new inhibitors of the oncogenic PAX3-FOXO1 fusion gene (Figure 83).[392] The structure elucidation of compound (**260**) required the use of $^{1}H–^{15}N$ HMBC and LR-HSQMBC NMR experiments on account of the proton-deficient nature of the denigrins.

In 2022, the total synthesis of compound (**226**) from *para*-anisaldehyde and its oxidative conversion into denigrin D (**260**), through a unique rearrangement, was reported by Chen *et al.*[428] The authors confirmed the structures of both natural products and reported obtaining denigrin D (**260**) in 61% yield when denigrin E (**226**) was reacted with *t*-BuOOH at 80 °C in the presence of $Mo(CO)_6$.

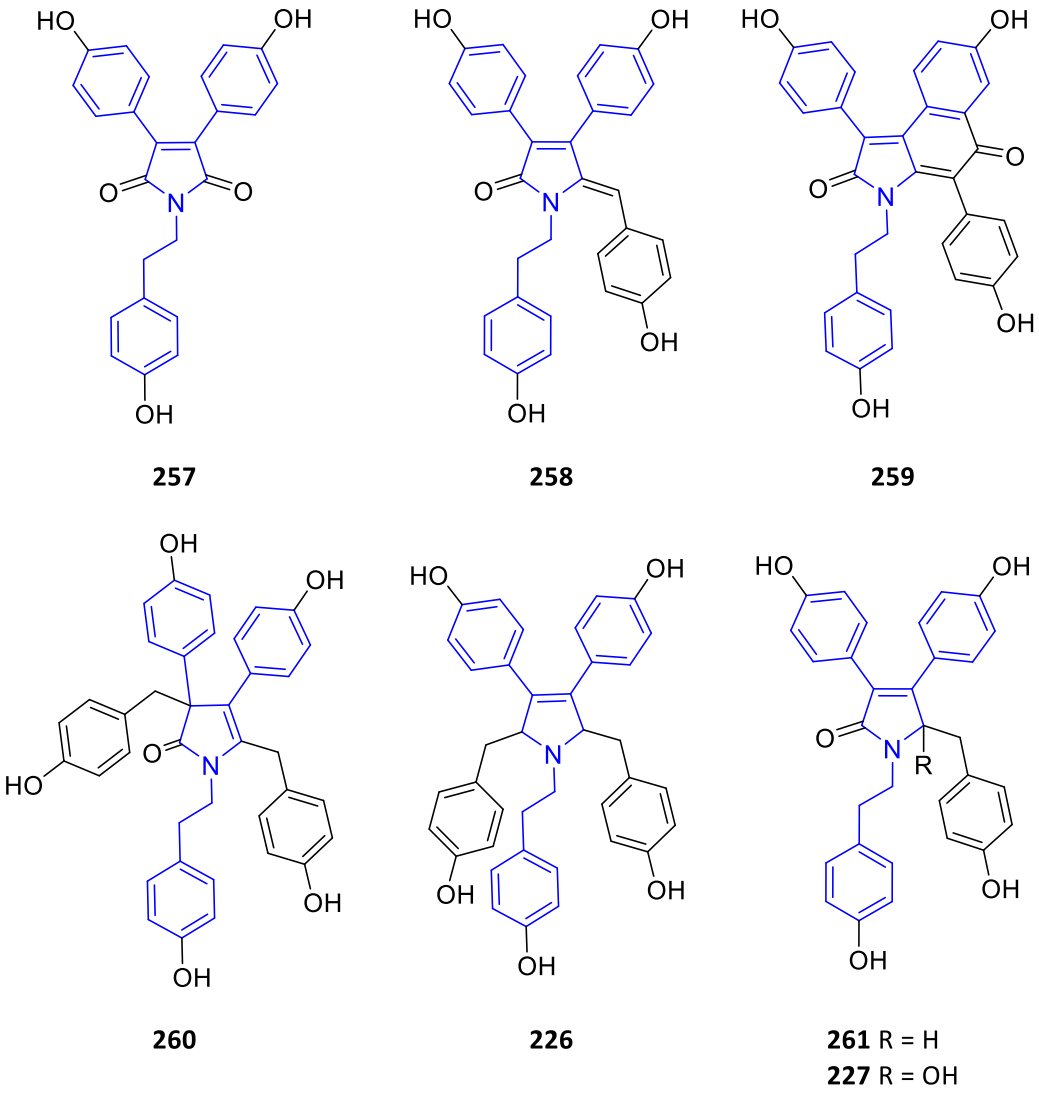

Figure 83 : Structures assigned to the previously reported denigrins with the general structure of denigrin type compounds displayed in blue.

5.2 Further denigrin alkaloids from *Dictyodendrilla* cf. *dendyi*

5.2.1 Isolation procedure for denigrins H-K

Following the investigation of the *D.* c.f. *dendyi* sponge (order: Dendroceratida, family: Dictyodendrillidae) described in Chapter 4, the crude extract resulting from a larger extraction of sponge was further investigated. As described in Chapter 4, Section 4.3.3, this extract was initially separated into three equal parts, and each was purified by reversed phase C18 chromatography. From these columns, several later eluting fractions were combined based on their TLC profile and elution solvent, as displayed in Appendix D.1. These fractions, along with some previously obtained from the initial purification procedure were further purified using a combination of C18 reversed phase bench column chromatography, followed by repeated size exclusion chromatography, as shown in Appendix D.2. The purification procedure afforded a mixture of two new polyaromatic alkaloids, denigrins H (**262**) and I (**263**), along with the new alkaloids denigrin J (**264**) and K (**265**), all sulphated derivatives of either denigrin D (**260**) or E (**226**) (Figure 83).

Separation of the mixture of denigrins H and I

Denigrin H (**262**) and I (**263**) were initially isolated as a mixture displaying a strong $[M - Na]^-$ ion at *m/z* 678.1058 on HR-ESI-MS. From the mass spectrum, it was suggested that only one compound was present, although the ^1H and ^{13}C NMR spectra in methanol-d_4 displayed too many signals to match the mass of the compound. From the integration of aromatic signals in the ^1H NMR spectrum, it was suggested that the mixture contained a 1:1 ratio of two closely related compounds, both with the same molar mass. A method was developed on LC-MS using a C18 column to separate the two peaks corresponding to the two compounds (Chapter 7 – Experimental, Section 7.5.6). With the parameters for the resolution of both peaks in hand, the mixture was purified by HPLC to obtain the new sulphated alkaloids denigrin H (**262**) and I (**263**) (Figure 84).

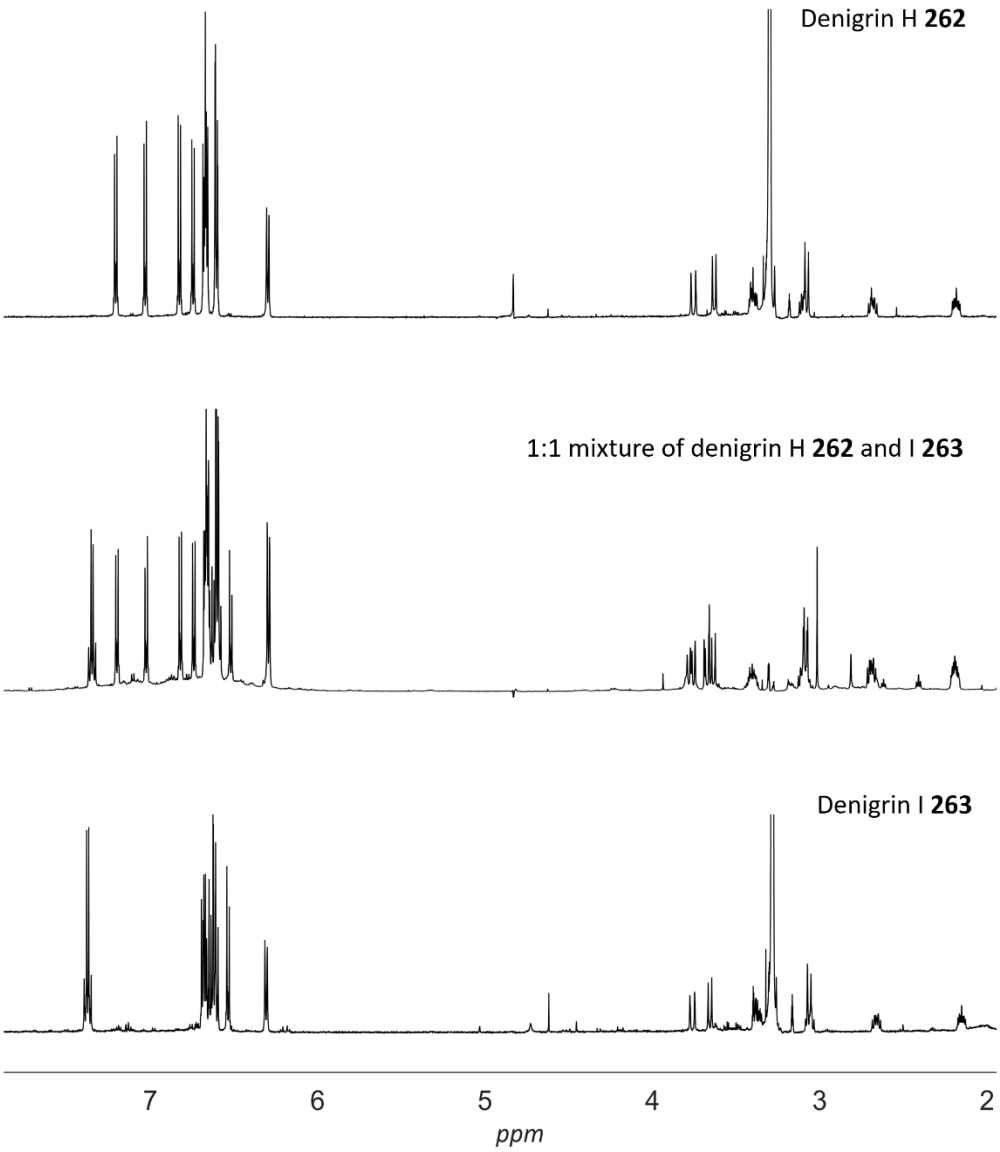

Figure 84: A- ^{1}H NMR spectrum of denigrin H (**262**). B- ^{1}H NMR spectrum of the mixture of denigrins H (**262**) and I (**263**). C- ^{1}H NMR spectrum of denigrin I (**263**).

5.2.2 Denigrin H

Denigrin H (**262**) was isolated as a light yellow, amorphous solid exhibiting UV absorption maxima at 226 and 279 nm. The IR spectrum showed strong absorptions for the hydroxy (3369 cm^{-1}) and carbonyl (1663 cm^{-1}) groups. HR-ESI-MS yielded the $[M - Na]^-$ ion at *m/z* 678.1803 (Appendix D.3), corresponding to a molecular formula of $C_{38}H_{32}NO_9S$. The ^1H NMR and HSQC spectroscopic data of compound (**262**) (Figure 85 and Table 33) displayed eight methylene proton signals (δ_H 2.19, 2.70, 3.09, 3.11, 3.28, 3.41, 3.64, 3.77) representing four methylene groups and ten doublets (δ_H 6.34, 6.64, 6.65, 6.705, 6.712, 6.72, 6.79, 6.87, 7.07, 7.25) accounting for a total of 20 aromatic protons, indicating five *para*-substituted aromatic rings, with each doublet displaying a peak shape characteristic of magnetic inequivalence for *para*-disubstituted benzene.

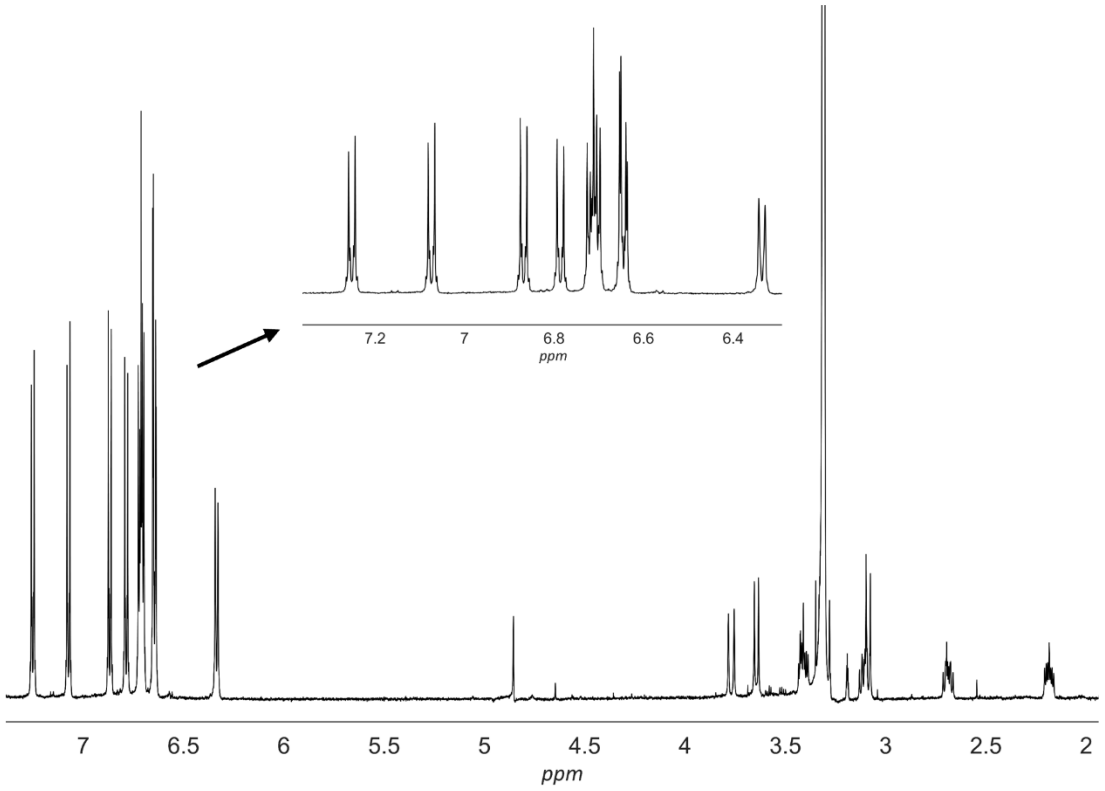

Figure 85: ^1H NMR spectrum (methanol-d_4) of denigrin H (**262**).

The ^{1}H NMR spectrum (Appendix D.4) of compound (**262**) was analogous to that of denigrin D (**260**) recorded in methanol-d_4,[392] except for two aromatic doublets shifted downfield to 6.79 and 7.07, instead of within the 6.56–6.71 ppm region, with the COSY spectrum indicating that the protons represented by these doublets were mutually coupled. By comparison with the ^{1}H NMR data of dictyodendrin D (**210**)[382] (a closely related alkaloid), these chemical shifts are characteristic of the presence of a sulphate group in the *para*-position of an aromatic ring, consistent with the 102 mass unit difference between denigrin H (**262**) and denigrin D (**260**).[392]

The ^{13}C and HSQC NMR spectroscopic data (Figure 86, Table 33 and Appendices D.5, D.6 and D.8) showed the presence of twenty-eight carbon signals, comprising one carbonyl signal (δ_C 183.6), twelve quaternary sp^2 carbon resonances (δ_C 124.8, 128.2, 128.4, 130.8, 131.7, 132.0, 140.1, 152.8, 157.1, 157.3, 157.6, 158.1), one quaternary sp^3 carbon signal (δ_C 62.3), ten protonated sp^2 carbon signals (δ_C 115.8, 116.2, 116.8, 116.9, 122.1, 129.0, 130.0, 130.1, 130.9, 132.5), and four methylene carbon resonances (δ_C 31.0, 34.9, 38.5, 44.4).

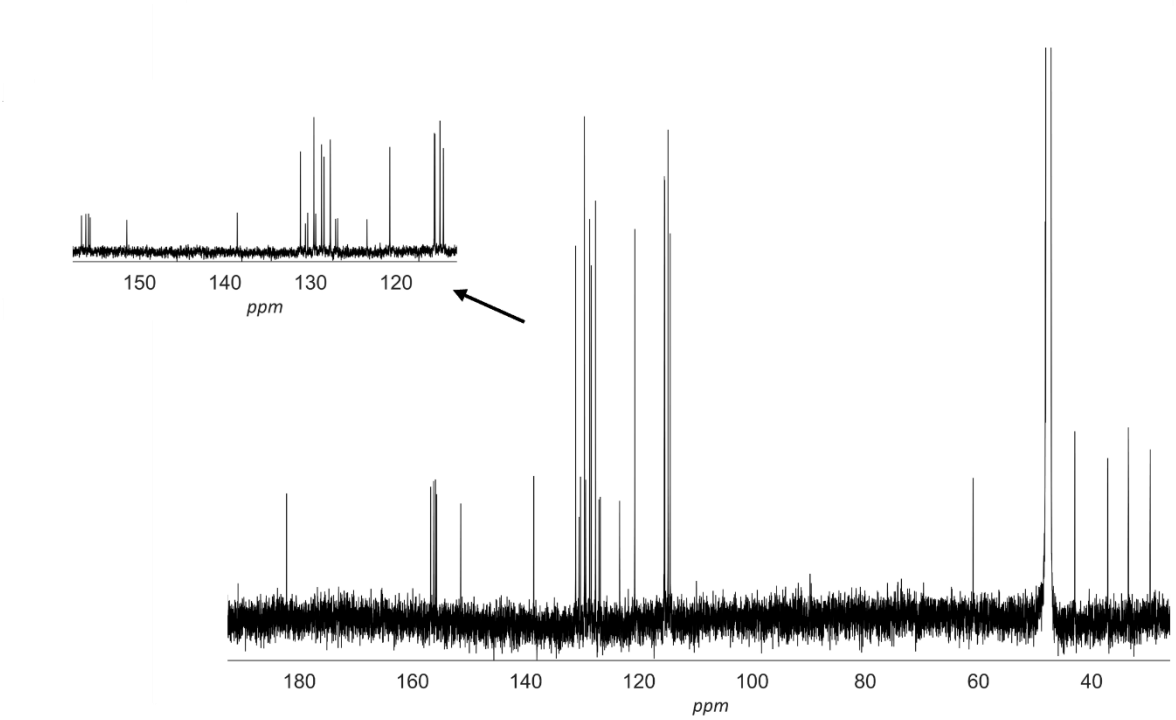

Figure 86: ^{13}C NMR spectrum (methanol-d_4) of denigrin H (**262**).

In a similar way to denigrin D, the assignments of the four *para*-phenol groups and a *para*-substituted phenyl group were established by combined analysis of characteristic ^{13}C chemical shifts, HMBC correlations and COSY couplings (Figure 87, Figure 88 and Figure 89, Appendices D.7 and D.9). The HMBC correlations H-35,39/C-33, H-35,39/C-37, and H-33/C-2, C-3 and C-4, along with the COSY correlation H-35,39/H36,38 established the presence of ring E, part of a *para*-hydroxybenzyl unit, at C-3 (Figure 87). The HMBC correlations H-28,32/C-3 and H-28,32/C-30, along with the COSY correlation H-28,32/H-29,31 established that ring D, a *para*-hydroxyphenyl group, was also attached at C-3 (Figure 87). The COSY correlations H-6/H-7 and H-9,13/H-10,12, along with the HMBC correlations H-9,13/C-7, H-9,13/C-11 and H-6/C-2 confirmed ring A as part of a tyramine moiety attached to N-1 (Figure 87).

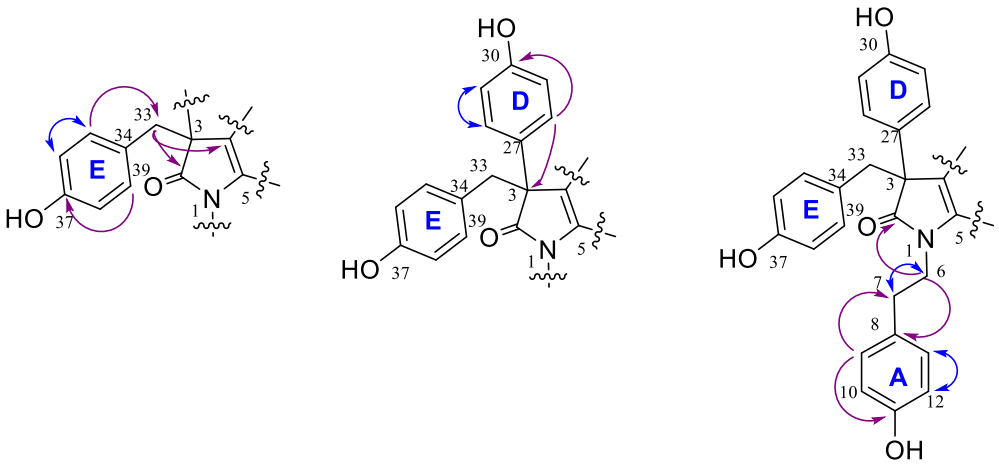

Figure 87: COSY (blue) and HMBC (purple) correlations for the construction of rings A, D and E of denigrin H (**262**).

The HMBC correlations H-16,20/C-14, H-16,20-C-18 and H-14/C-5 and the COSY correlation H-16,20/H-17,19 established ring B as part of the second *para*-hydroxybenzyl unit, attached at C-5 (Figure 88).

Finally, the HSQC data determined that the aromatic doublet at δ_H 7.07 represented the proton attached to the carbon at δ_C 122.2, consistent with a carbon *ortho*- to a sulphate group,[382] and the HMBC correlation H-22,26/C-24 established that the carbon at δ_C 152.9 bore a sulphate group (Figure 88).[382] Additional HMBC correlation H-22,26/C-4 and COSY correlation H-22,26/H-23,25 confirmed the attachment of ring C at C-4 and thus that compound (**262**) was the 24-sulphate of denigrin D (**260**).

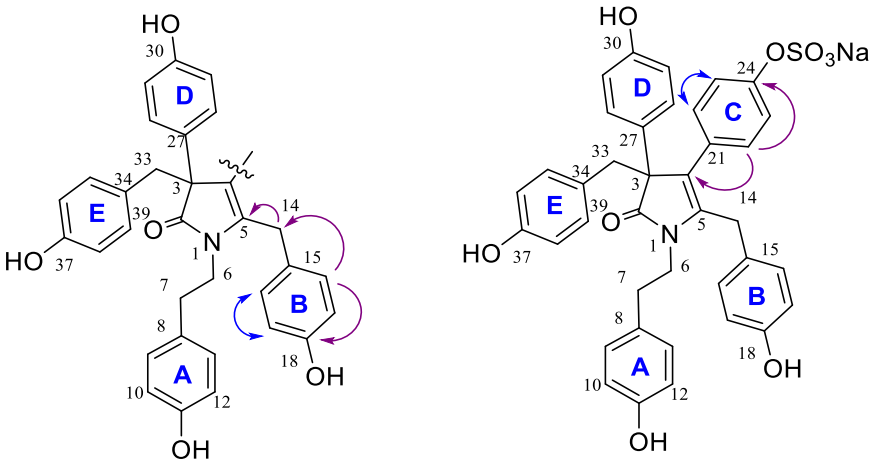

Figure 88: COSY (blue) and HMBC (purple) correlations for the construction of rings B and C of denigrin H (**262**).

Overall, the COSY and HMBC key correlations were analogous to those of denigrin D[392] and confirmed a tyramine unit, two *para*-hydroxybenzyl units, and two *para*-hydroxyphenyl units attached to a pyrrolidone core (Figure 89). The complete assignment of denigrin H (**262**) is presented in Table 33. Measurement of the optical rotation of compound (**262**) at the sodium D line, (589 nm) resulted in a value of 0°, suggesting that it is present as a racemic mixture, consistent with the results reported for denigrin D (**260**).[392]

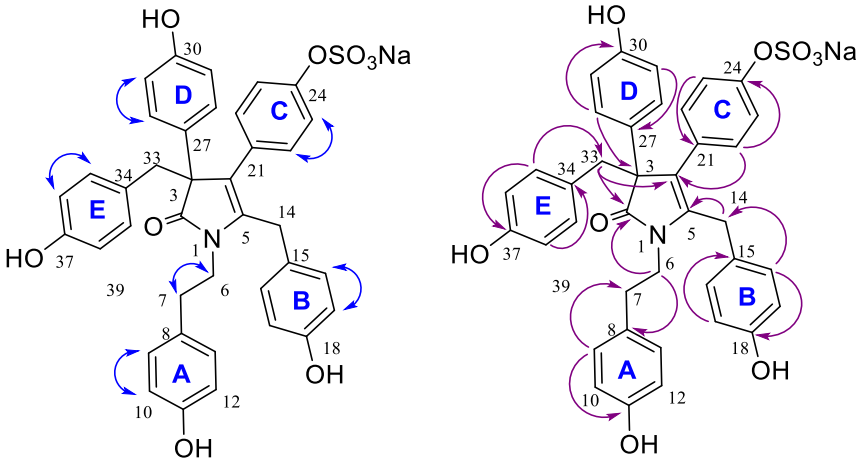

Figure 89: COSY (blue) and selected HMBC (purple) correlations for denigrin H (**262**).

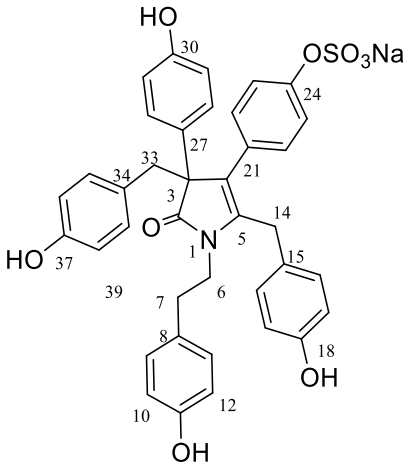

262

Table 33: ^{1}H and ^{13}C NMR assignments determined for denigrin H (**262**).

No.	[a] δ_C	[b] δ_H, (mult, *J* in Hz)	HMBC (^{1}H to ^{13}C)	COSY
2	183.6			
3	62.3			
4	124.8			
5	139.9			
6	44.4	3.41 (1H, m)		H-6, H-7
		[c] 3.11 (1H, m)	C-2	H-7
7	34.9	2.70 (1H, m)	C-6, C-9/13	H-7
		2.19 (1H, m)	C-8, C-9/13	
8	130.8			
9/13	130.9	[d] 6.712 (2H, d, 8.5)	C-7, C-11	H-9/13
10/12	116.2	6.65 (2H, d, 8.5)	C-8	
11	157.1			
14	31.0	3.77 (1H, d, 17.0)	C-5, C-15, C-16/20	H-14
		[e] 3.28 (1H, m)	C-4, C-5, C-15, C-16/20	
15	128.2			
16/20	130.1	6.34 (2H, d, 8.4)	C-14, C-18	
17/19	116.9	[d] 6.705 (2H, d, 8.6)	C-15	H-16/20
18	157.3			
21	131.7			
22/26	130.0	6.79 (2H, d, 8.9)	C-4, C-24	
23/25	122.1	7.07 (2H, d, 8.9)	C-24, C-21	H-22/26
24	152.8			
27	132.0			
28/32	129.0	7.25 (2H, d, 8.8)	C-3, C-30	H-29/31
29/31	116.8	6.87 (2H, d, 8.8)	C-27	
30	158.1			
33	38.5	3.64 (1H, d, 12.9)	C-3, C-4, C-34, C-35/39	H-33
		[c] 3.09 (1H, d (12.7)	C-2, C-3, C-34, C-35/39	
34	128.4			
35/39	132.5	6.72 (2H, d, 8.7)	C-33, C-37	H-36/38
36/38	115.8	6.64 (2H, d, 8.6)	C-34	
37	157.6			

[a] recorded at 150 MHz in methanol-d_4, [b] recorded at 600 MHz in methanol-d_4,
[c] signal overlap, [d] values given to 3 decimal places to separate signals,
[e] signal partially obscured.

5.2.3 Denigrin I

Denigrin I (**263**) was obtained as light yellow, amorphous solid exhibiting UV absorption maxima at 225 and 278 nm. The IR spectrum showed similar strong absorptions to those of compound (**262**) for the hydroxy (3369 cm^{-1}) and carbonyl (1663 cm^{-1}) groups. HR-ESI-MS returned the $[M - Na]^-$ ion at *m/z* 678.1807 (Appendix D.10), corresponding to a molecular formula of $C_{38}H_{32}NO_9S$ and confirming that compound (**263**) had an identical molecular formula to compound (**262**).

The ^{13}C NMR and HSQC spectroscopic data (Table 34 and Appendices D.12 and D.14) indicated the presence of twenty-eight signals, including one carbonyl signal (δ_C 182.9), twelve quaternary sp^2 carbon resonances (δ_C 124.9, 126.1, 128.40, 128.41, 130.8, 137.9, 138.7, 153.5, 157.1, 157.2, 157.58, 157.63), one quaternary sp^3 carbon signal (δ_C 62.4), ten protonated sp^2 carbon resonances (δ_C 115.7, 116.0, 116.2, 116.8, 122.8, 128.8, 130.1, 130.3, 131.0, 132.6), and four methylene carbon signals (δ_C 31.1, 34.9, 38.6, 44.3). The ^{13}C NMR spectrum was almost superimposable on that of compound (**262**), with the two signals at δc 122.8 and 153.5 indicating that compound (**263**) also contained a sulphate group.

As for compound (**262**), the ^1H NMR and HSQC spectroscopic data of compound (**263**) (Figure 90, Table 34 and Appendix D.11) displayed eight methylene proton signals (δ_H 2.18, 2.69, 3.08, 3.09, 3.29, 3.41, 3.68, 3.79) representing the four methylene groups and ten aromatic doublets, comprising a total of 20 protons, indicating five *para*-substituted benzene groups (δ_H 6.34, 6.56, 6.63, 6.65, 6.66, 6.68, 6.706, 6.714, 7.39, 7.42), with each doublet displaying a peak shape characteristic of magnetic inequivalence for *para*-disubstituted benzene. The COSY and HMBC key correlations (Appendix D.15) were analogous to those of compound (**262**) and confirmed a tyramine unit, two *para*-hydroxybenzyl units, one *para*-hydroxyphenyl unit, and an additional *para*-substituted phenyl unit attached to a pyrrolidone core identically to compound (**262**).

The COSY spectrum (Appendix D.13) indicated that the two most downfield signals, characteristic of a sulphated aromatic ring, were mutually correlated, and the HMBC correlations of H-28,32/C-3 and H-28,32/C-30 revealed attachment of the sulphated ring D at C-3, indicating that compound (**263**) is the 30-sulphate of denigrin D (**260**).

The complete assignment of compound (**263**) is presented in Table 34. Measurement of the optical rotation of denigrin I (**263**) also resulted in a value of 0°, suggesting that like denigrin H (**262**), compound (**263**) is present as a racemic mixture (consistent with the results reported for denigrin D (**260**)).[392]

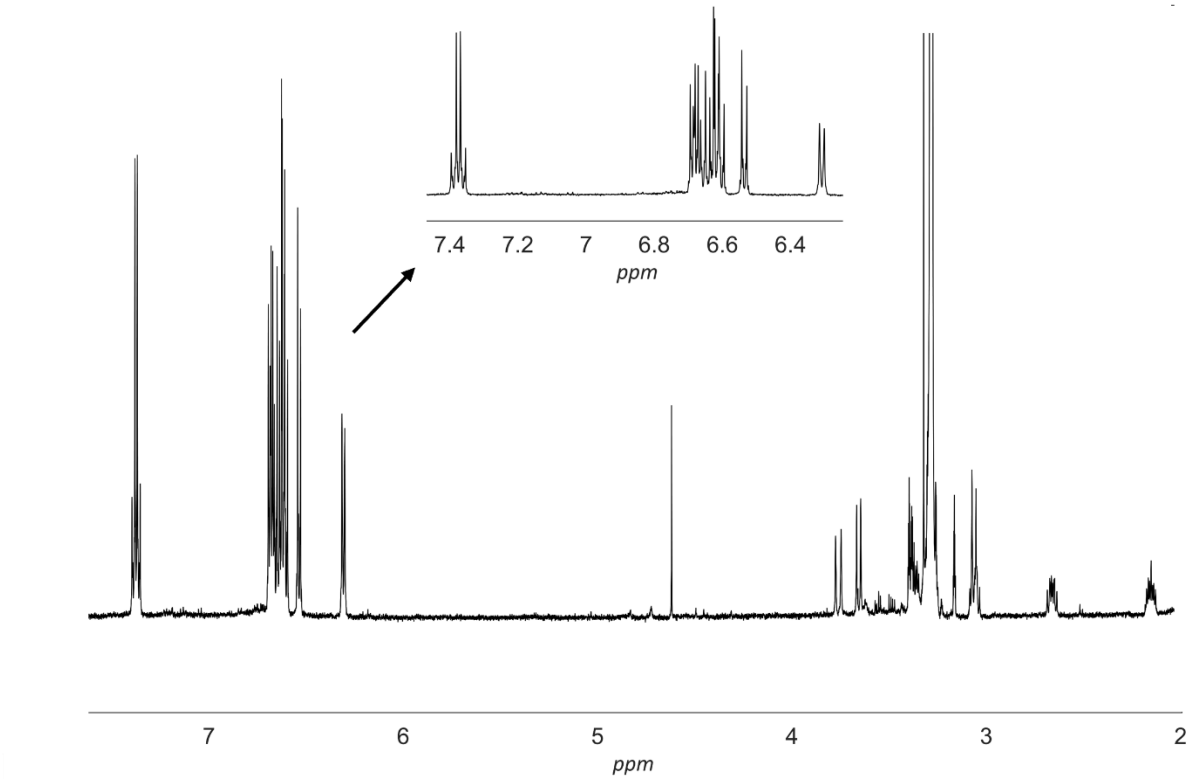

Figure 90: ^{1}H NMR spectrum (methanol-d_4) of denigrin I (**263**).

Table 34: ^{1}H and ^{13}C NMR assignments determined for denigrin I (**263**).

No.	[a] δ_C	[b] δ_H, (mult, *J* in Hz)	HMBC (^{1}H to ^{13}C)	COSY
2	182.9			
3	62.4			
4	124.9			
5	138.7			
6	44.3	3.41 (1H, m) [c] 3.08 (1H, m)	 C-2	H-6, H-7 H-7
7	34.9	2.69 (1H, m) 2.18 (1H, ddd)	C-9/13 C-6, C-9/13	H-7
8	130.6			
9/13	131.0	[d] 6.706 (2H, d, 8.4)	C-7, C-11	H-9/13
10/12	116.2	6.65 (2H, d, 8.6)	C-8	
11	157.1			
14	31.1	3.79 (1H, d, 16.9) [e] 3.29 (1H, m)	C-5, C-15, C-16/20 C-4, C-5, C-15, C-16/20	H-14
15	[f, g] 128.40			
16/20	130.1	6.34 (2H, d, 8.3)	C-14, C-18	
17/19	116. 8	6.714 [d] (2H, d, 8.4)	C-15	H-16/20
18	157.2			
21	126.1			
22/26	130.3	6.66 (2H, d, 8.9)	C-4, C-24	H-22/26
23/25	116.0	6.56 (2H, d, (8.7)	C-21, C-24	
24	[g] 157.63			
27	137.9			
28/32	128.8	7.42 (2H, d, 9.1)	C-3, C-30	H-29/31
29/31	122.8	7.39 (2H, d, 9.0)	C-27, C-30	
30	153.5			
33	38.6	3.68 (1H, d, 12.9) [c] 3.09 (1H, d, 12.7)	C-3, C-4, C-34, C-35/39 C-2, C-3, C-35/39, C-34	H-33
34	[f, g] 128.41			
35/39	132.6	6.68 (2H, d, 8.6)	C-33	H-36/38
36/38	115.7	6.63 (2H, d, 8.7)	C-34, C-37	
37	[g] 157.58			

[a] recorded at 150 MHz in methanol-d_4, [b] recorded at 600 MHz in methanol-d_4, [c] signal overlap [d] values given to 3 decimal places to separate signals, [e] signal partially obscured, [f] assignment interchangeable, [g] values given to 2 decimal places to separate signals.

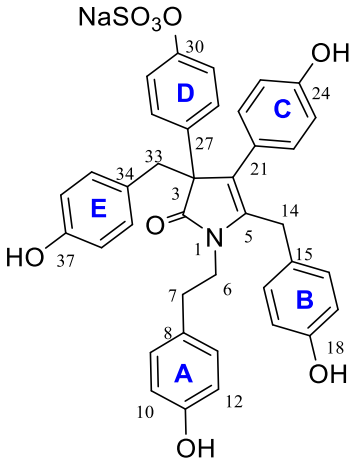

263

5.2.4 Denigrin J

Denigrin J (**264**) was isolated as a dark green, amorphous solid exhibiting UV absorption maxima at 224 (λ_{max}) and 273 nm. The IR spectrum showed strong absorptions for the hydroxy (3246 cm^{-1}) group with the absence of a carbonyl absorption. HR-ESI-MS yielded the $[M - Na]^-$ ion at *m/z* 662.1857 (Appendix D.16), corresponding to a molecular formula of $C_{38}H_{32}NO_8S$.

The combined ^{13}C and HSQC NMR data (Table 35) indicated the presence of seventeen carbon signals, including eight quaternary sp^2 carbon resonances (δ_C 123.4, 128.3 129.7, 132.8, 136.6, 152.6, 156.1, 156.7), six protonated sp^2 carbon signals (δ_C 115.6, 116.3, 122.5, 130.0, 130.6, 132.5) and three methylene carbon signals (δ_C 30.7, 37.7, 47.1). The ^{13}C NMR spectroscopic data (Appendix D.18) were almost superimposable on those of denigrin E (**226**) recorded in methanol-*d*$_4$ (Chapter 4, Table 25), indicating that the two compounds were closely related, with the key differences being one protonated sp^2 signal shifted downfield to δc 122.5 instead of 116, and one quaternary sp^2 carbon signal at δc 152.6, instead of δc 157.0, indicative of a sulphur-bearing carbon. As for compound (**262**), these δ_C shifts were characteristic of the presence of a sulphate group in the *para*-position of an aromatic ring, consistent with the 102 mass unit difference between compound (**262**) and denigrin E (**226**).

The ^1H (Figure 91, Appendix D.17) and HSQC (Appendix D.20) NMR spectra of compound (**262**) showed three signals for methylene protons (δ_H 2.45, 3.59, 3.85) and six aromatic doublets (δ_H 6.61, 6.69, 6.78, 6.92, 6.93, 7.13), with each doublet displaying a peak shape characteristic of magnetic inequivalence for a *para*-disubstituted benzene. The integration of the aromatic protons, allowing that the doublets at δ_H 6.92 and 6.93 were integrated together, revealed a ratio of 2:2:1:4:1, indicating the symmetry of the molecule. The chemical shifts of the doublets at δ_H 7.13 and 6.78 were a close match with the aromatic protons on the sulphated aromatic ring of dictyodendrin D.[382]

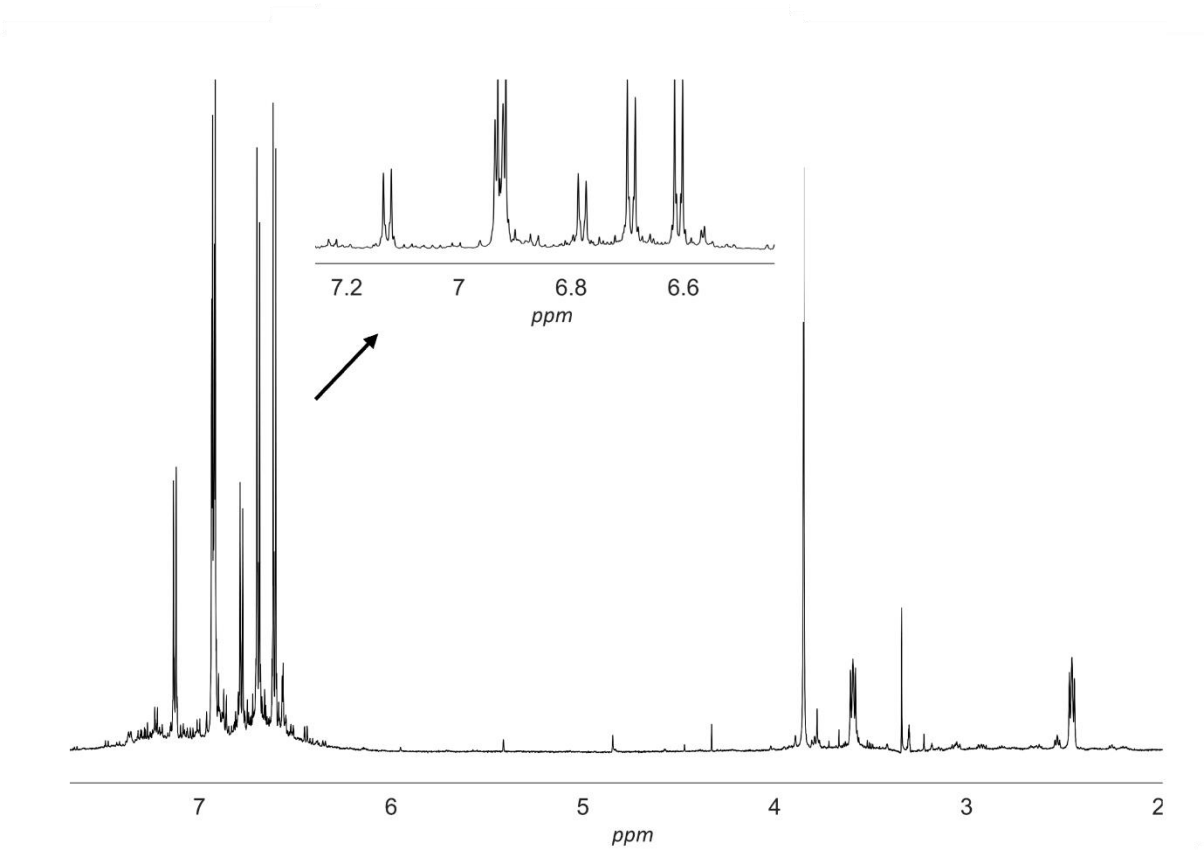

Figure 91: ^{1}H NMR spectrum (methanol-d_4) of denigrin J (**264**).

The COSY and key HMBC correlations (Figure 92, Table 35, Appendices D.19 and D.21) were analogous to those of denigrin E (**226**)[392] and confirmed a tyramine unit, two *para*-hydroxybenzyl units, and two *para*-hydroxyphenyl units attached to a pyrrole core. The HMBC correlation H-22,26/C-4 (H-28,32/C-3) established the *para*-hydroxyphenyl groups at C-3 and C-4, while the HMBC correlations of H-16,20/C-14 (H35,39/C-33) and H-14-C-5 (H-33/C-2) revealed that the *para*-hydroxybenzyl groups were substituted at C-2 and C-5. The COSY correlation H-6/H-7 and the HMBC correlations of H-7/C-9,13 and H-9,13/C-11 indicated the presence of the sulphate group in the *para*-position of the tyramine unit, consistent with the symmetry of the molecule and indicating that compound (**262**) is the 11-sulphate of compound (**226**). The complete assignment of compound (**262**) is presented in Table 35.

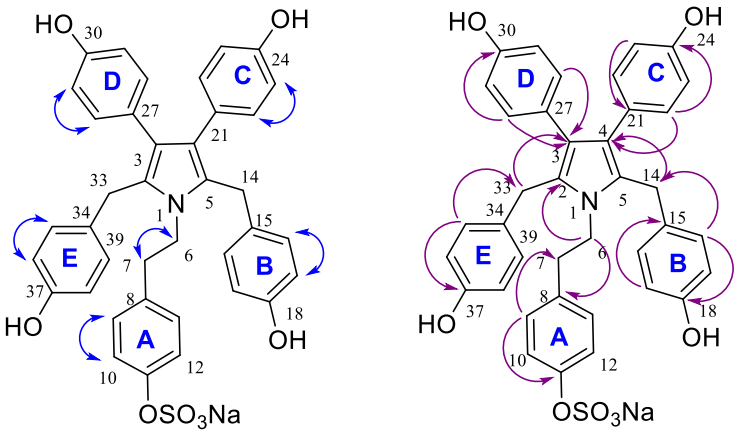

Figure 92: COSY (blue) and selected HMBC (purple) correlations for denigrin J (**264**).

Table 35: ^{1}H and ^{13}C NMR assignments determined for denigrin J (**264**).

No.	[a] δ_C	[b] δ_H, (mult, *J* in Hz)	HMBC (^{1}H to ^{13}C)	COSY
2/5	128.3			
3/4	123.4			
6	47.1	3.59 (2H, m)	C-7, C-2/5	H-7
7	37.7	2.45 (2H, m)	C-6, C-9/13, C-8	
8	136.6			
9/13	130.6	6.78 (2H, d, 8.5)	C-7, C-11	
10/12	122.5	7.13 (2H, d 8.4)	C-8, C-11	H-9/13
11	152.6			
14/33	30.7	3.85 (4H, s)	C-3/4, C-2/5, C-16/20–35/39, C-15/34	
15/34	132.8			
16/20–35/39	130.0	6.93 (4H, d, 8.6)	C-14/33, C-18/37	H16/20-35/39
17/19–36/38	116.3	6.69 (4H, d, 8.5)	C-15/34, C-18/37	
18/37	156.7			
21/27	129.7			
22/26–28/32	132.5	6.92 (4H, d, 8.6)	C-3/5, C-24/30	H23/25-29/31
23/25–29/31	115.6	6.61 (4H, d, 8.7)	C-21/27, C-24/30	
24/30	156.1			

[a] recorded at 150 MHz in methanol-d_4, [b] recorded at 600 MHz in methanol-d_4.

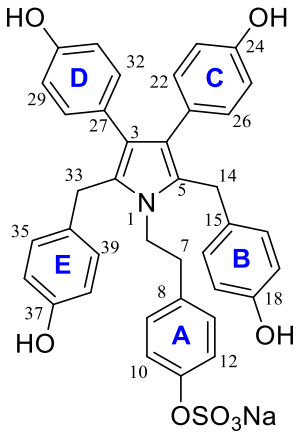

264

5.2.5 Denigrin K

Denigrin K (**265**) was purified as a light green, amorphous solid with identical UV absorption maxima to compound (**264**) and an IR absorption for an hydroxy (3365 cm^{-1}) group. HR-ESI-MS returned the $[M - Na]^-$ ion at *m/z* 662.1855 (Appendix D.22), corresponding to a molecular formula of $C_{38}H_{32}NO_8S$ and indicating that compound (**265**) had an identical molecular formula to compound (**264**).

The ^{13}C NMR spectroscopic data (Table 36 and Appendix D.24) showed the presence of twenty-eight signals, suggesting a breach in the symmetry of the molecule. The combined ^{13}C NMR and HSQC data confirmed the presence of fourteen quaternary sp^2 carbon signals (δ_C 122.9, 123.4, 128.68, 128.73, 129.4, 130.94, 132.7, 132.8, 135.2, 151.6, 156.2, 156.68, 156.70, 157.0), ten protonated sp^2 carbon resonances (δ_C 115.7, 116.1, 116.30, 116.32, 121.9, 129.87, 129.92, 130.92, 132.0, 132.5), and four methylene carbon signals (δ_C 30.57, 30.63, 37.6, 47.3), in addition to two signals at δc 121.9 and 151.6 characteristic of the presence of a sulphate group.

The ^1H (Figure 93, Appendix D.23) and HSQC (Appendix D.26) NMR spectra of compound (**265**) contained three signals for methylene protons (δ_H 2.45, 3.58, 3.80) and ten aromatic doublets (δ_H 6.62, 6.63, 6.66, 6.70, 6.70, 6.89, 6.91, 6.92, 7.06, 7.12) accounting for 20 protons, indicating that each of the aromatic rings was *para*-substituted, with each doublet displaying a peak shape characteristic of such magnetic inequivalence. The key COSY and HMBC correlations (Appendices D.25 and D.27) were analogous to those of compound (**264**) and

confirmed the same tyramine unit, two *para*-hydroxybenzyl units, one *para*-hydroxyphenyl unit, and an additional *para*-substituted phenyl unit linked identically to the pyrrole core. The HMBC correlations of H-28,32/C-3 and H-28,32/C-30 revealed the presence of the sulphate group in the *para*-position of the D ring, consistent with the absence of symmetry and indicating that compound (**265**) is the 30-sulphate of denigrin E (**226**). The complete assignment of compound (**265**) is presented in Table 36.

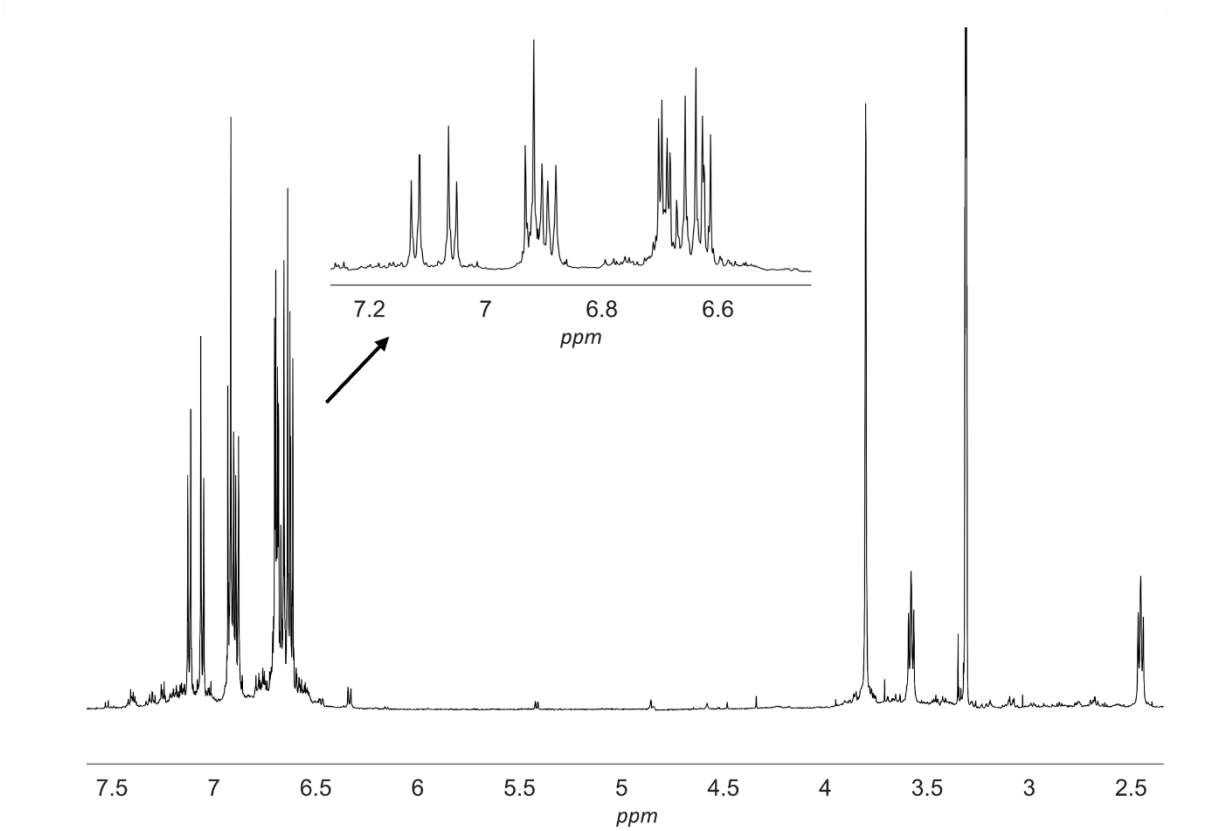

Figure 93: ^{1}H NMR spectrum (methanol-d_4) of denigrin K (**265**).

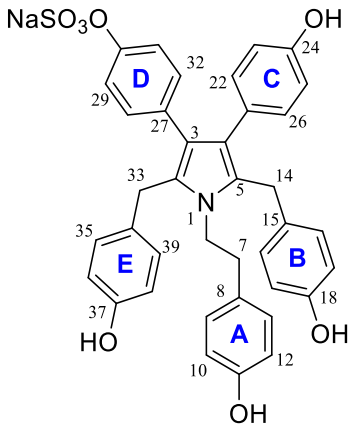

265

Table 36: ^{1}H and ^{13}C NMR assignments determined for denigrin K (**265**).

No.	[a] δ_C	[b] δ_H (mult, *J* in Hz)	HMBC (^{1}H to ^{13}C)	COSY
2	[c, d] 128.73			
3	122.9			
4	123.4			
5	[c, d] 128.68			
6	47.3	3.58 (2H, m)	C-2, C-7, C-5	H-7
7	37.6	2.45 (2H, m)	C-6, C-9/13	
8	[c] 130.94			
9/13	[c] 130.92	6.66 (2H, d, 9.0)	C-7, C-11	
10/12	116.1	6.63 (2H, d, 8.3)	C-8, C-11	
11	157.0			
14/33	30.57 30.63	3.80 (4H, s)	C-2, C-3, C-4, C-5, C-15, C-16/20, C-35/39, C-34	
15	[e] 132.7			
16/20	[c, f] 129.92	[g] 6.89 (2H, d, 8.3)	C-14/33, C-18	H17/19
17/19	[c, h] 116.32	[i] 6.70 (2H, d, 9.0)	C-15, C-18	
18	[c, j] 156.68			
21	129.4			
22/26	132.5	6.92 (2H, d 9.0)	C-4, C-24	H-23/25
23/25	115.7	6.62 (2H, d, 8.3)	C-21, C-24	
24	156.2			
27	135.2			
28/32	132.0	7.06 (2H, d, 8.6)	C-3, C-30	
29/31	121.9	7.12 (2H, d, 8.3)	C-27, C-30	H-28/32
30	151.6			
34	[e] 132.8			
35/39	[c, f] 129.87	[g] 6.91 (2H, d, 8.3)	C-14/33, C-37	H-36/38
36/38	[c, h] 116.30	[i] 6.69 (2H, d, 8.3)	C-14/33, C-34, C-37	
37	[c, j] 156.70			

[a]recorded at 150 MHz in in methanol-d_4, [b] recorded at 600 MHz in in methanol-d_4, [c] values given to 2 decimal places to resolve signals, [d-j] assignment may be interchanged.

5.2.6 Isolation procedure for denigrin L

During the isolation procedure of denigrins J-K (**264-265**), it was observed that these sulphated compounds yield a pink spot on TLC (Rf between 0.42 and 0.46) with MeOH/EtOAc (5:1) as the elution solvent. These spots were the same colour as that corresponding to denigrin E (**226**), whose spot was observed at a higher Rf value (0.875) with the same elution solvent.

Upon reinvestigation of the TLC of a fraction obtained from the initial extraction of *D.* cf. *dendyi,* a pink spot at a low Rf (0.05) was observed upon elution with the same solvent as above (Figure 95), potentially indicating the presence of a more polar compound related to denigrins E (**226**), J (**264**) and K (**265**). Therefore, the fractions of interest were further purified on Sephadex LH-20. This resulted in the isolation and characterisation of denigrin L (**266**) (Figure 94).

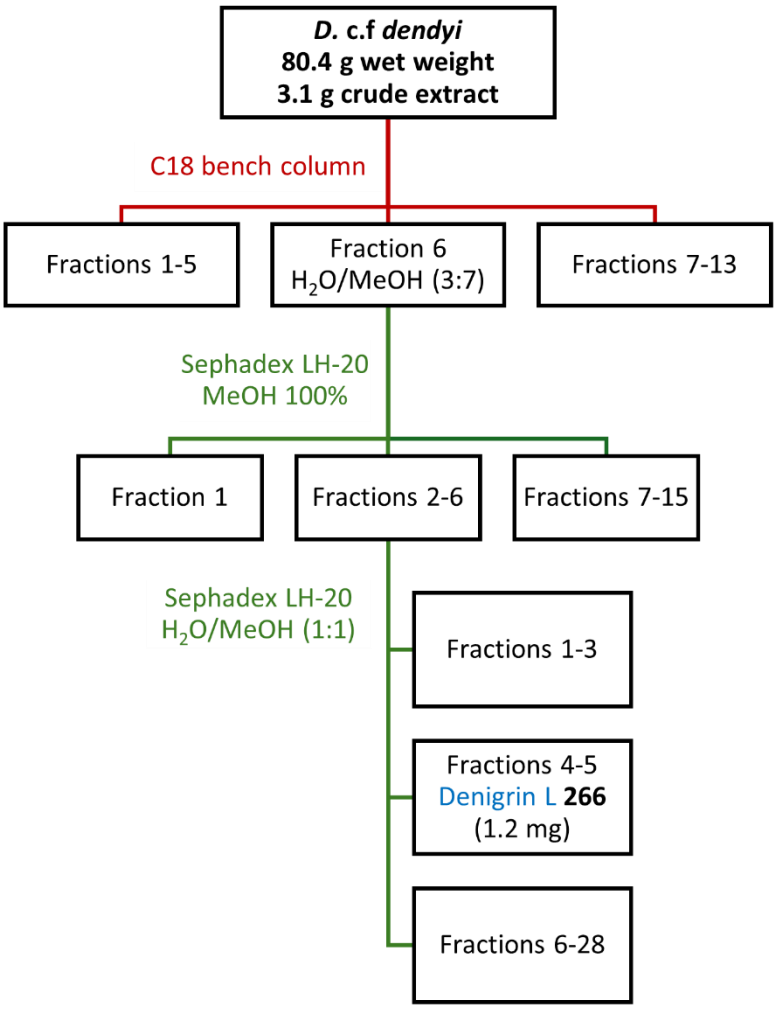

Figure 94: Isolation procedure for denigrin L (**266**).

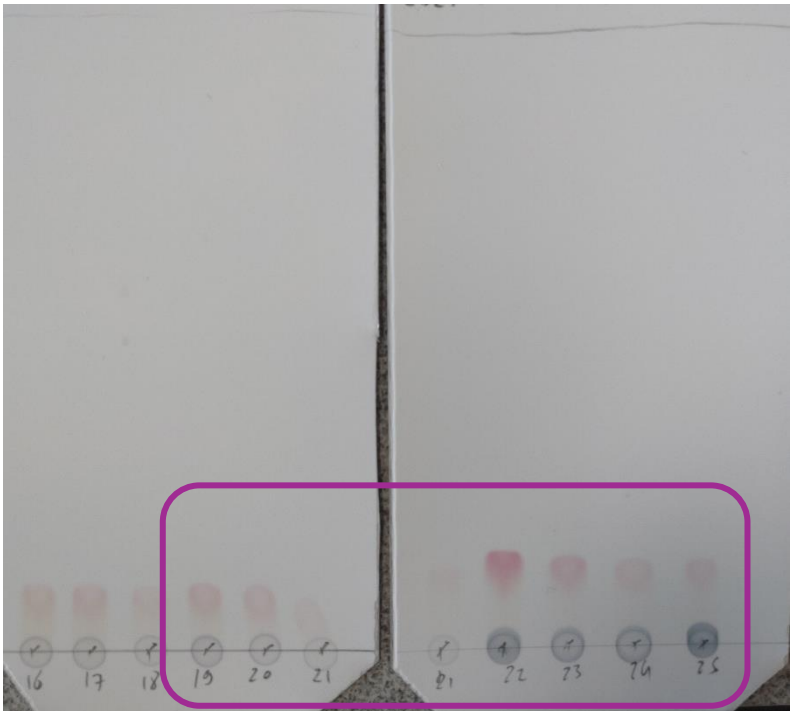

Figure 94: TLC (EtOAc/MeOH 5:1) of several fractions containing denigrin L (**266**) as a pink spot in fractions 19 to 25. Solvent front displayed as the pencil lines.

5.2.7 Denigrin L

Denigrin L (**266**) was obtained as an amorphous solid exhibiting similar UV absorption maxima and IR absorptions to those of compounds (**264**) and (**265**). HR-ESI-MS returned the $[M - Na]^-$ ion at *m/z* 764.1225 (Appendix D.28), corresponding to a molecular formula of $C_{38}H_{31}NO_{11}S_2Na$.

The ^{13}C NMR spectrum (Appendix D.30) contained twenty-seven signals indicating a non-symmetrical compound. The combined ^{13}C and HSQC NMR data confirmed the presence of fourteen quaternary sp^2 carbon resonances (δ_C 123.0, 123.5, 128.6, 128.7, 129.3, 132.6, 132.7, 135.1, 136.5, 151.7, 152.5, 156.3, 156.78, 156.83), ten protonated sp^2 carbon signals (δ_C 115.8, 116.37, 116.41, 121.9, 122.5, 129.96, 130.00, 130.4, 132.0, 132.6), and three methylene carbon resonances (δ_C 30.7, 37.6, 47.2). The two protonated sp^2 signals at δc 122.5 and 121.9 and the two quaternary sp^2 carbon signals at δ_C 152.5 and 151.7 indicated the presence of two sulphate groups, consistent with a mass difference of 102 between compound (**264**) and compound (**266**).

The ^{1}H (Figure 96, Appendix D.29) and HSQC (Appendix D. 32) NMR spectra of compound (**266**) contained four signals for methylene protons (δ_H 2.45, 3.61, 3.87, 3.94) and eight aromatic doublets (δ_H 6.63, 6.708, 6.710, 6.80, 6.95, 7.09, 7.14, 7.14), confirming the lack of symmetry of the compound, despite the doublet at 6.95 integrating for six protons, with each doublet displaying a peak shape characteristic of magnetic inequivalence for a *para*-substituted benzene. The COSY and HMBC key correlations (Appendices D.31 and D.33) were analogous to those of compound (**264**) and compound (**265**) and confirmed the same tyramine unit, two *para*-hydroxybenzyl units, one *para*-hydroxyphenyl unit, and an additional *para*-substituted phenyl unit linked identically to the pyrrole core. The HMBC correlations of H-28,32/C-3 and H-28,32/C-30 revealed the presence of one sulphate group in the *para*-position of the D ring and the H-7/C-9,3 and H-9,13/C-11 correlations placed the second group in the *para*-position of the A ring; therefore, denigrin L (**266**) is the 11- and 30-disulphated analogue of denigrin E (**226**). The complete assignment of compound (**266**) is presented in Table 37.

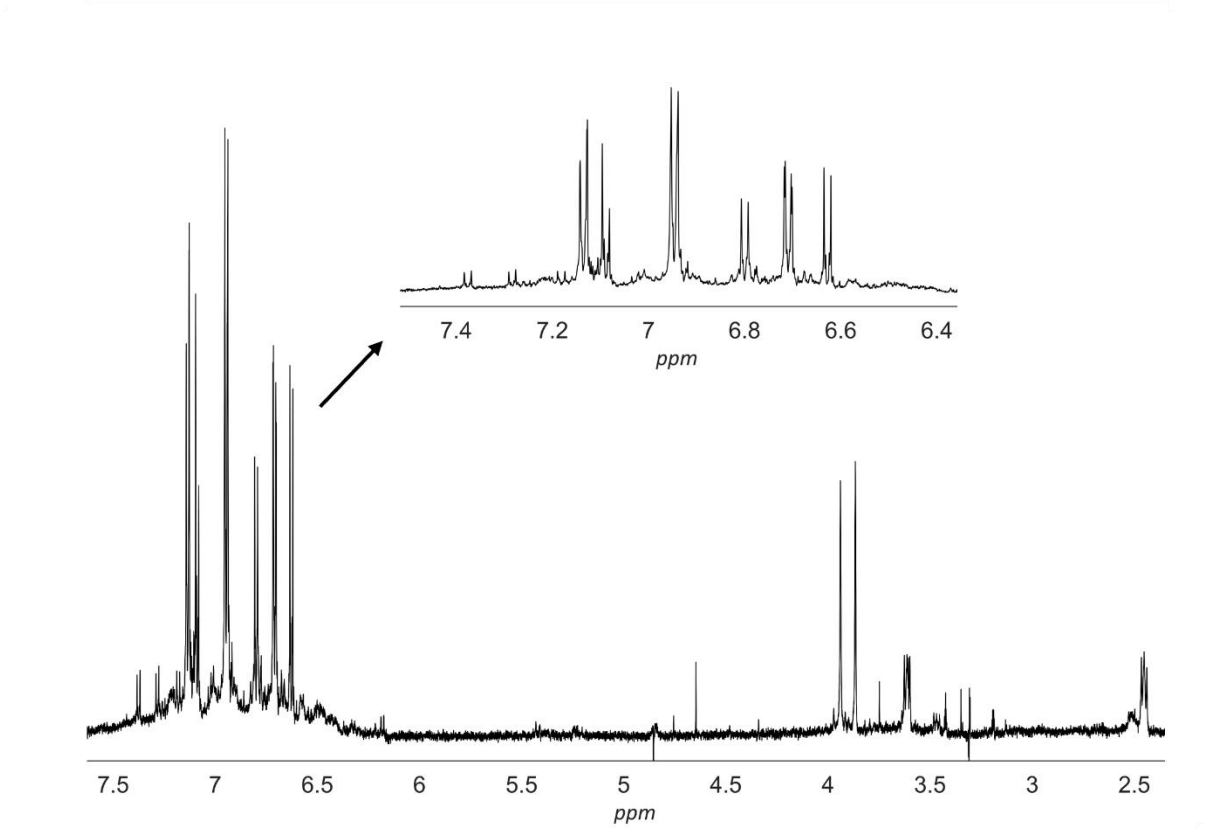

Figure 96: ^{1}H NMR spectrum (methanol-d_4) of denigrin L (**266**).

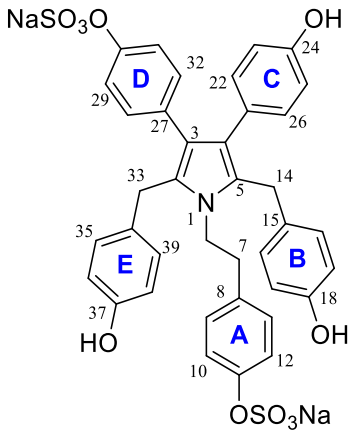

266

Table 37: ^{1}H and ^{13}C NMR assignments determined for denigrin L (**266**).

No.	[a] δ_C	[b] δ_H (mult, *J* in Hz)	HMBC (^{1}H to ^{13}C)	COSY
2	[c] 128.6			
3	123.0			
4	123.5			
5	[c] 128.7			
6	47.2	3.61 (2H, m)	C-2, C-5	H-7
7	37.6	2.45 (2H, m)	C-9/13, C-8	
8	136.5			
9/13	130.4	6.80 (2H, d, 8.6)	C-7, C-11	
10/12	122.5	[d] 7.14 (2H, d, 8.6)	C-7, C-8	H-9/13
11	152.5			
14	30.7	3.94 (2H, s)	C-2, C-3, C-15	
15	[e, f] 132.7			
16/20	[g, h] 130.00	[i] 6.95 (2H, d, 8.6)	C-18	C-17-19
17/19	[g, j] 116.41	[k, l] 6.710 (2H, d, 8.6)	C-15, C-18	
18	[g, m] 156.83			
21	129.3			
22/26	[e] 132.6	[h] 6.95 (2H, d, 8.6)	C-4, C-24	C-23/25
23/25	115.8	6.63 (2H, d, 8.7)	C-21, C-24	
24	156.3			
27	[f] 135.1			
28/32	132.0	7.09 (2H, d, 8.8)	C-3, C-30	
29/31	121.9	[d] 7.14 (2H, d, 8.6)	C-30	H-28/32
30	151.7			
33	30.7	3.87 (2H, s)	C-4, C-5, C-34	
34	[e, f] 132.6			
35/39	[g, h] 129.96	[i] 6.95 (2H, d, 8.6)	C-37	C-36/38
36/38	[g, j] 116.37	[k, l] 6.708 (2H, d, 8.6)	C-34, C37	
37	[g, m] 156.78			

[a] recorded at 150 MHz in methanol-d_4, [b] recorded at 600 MHz in in methanol-d_4, [c-e, h-j, l-m] assignment may be interchanged, [f] assigned based on denigrin J (**264**) and K (**265**), [g] values given to 2 decimal places to separate signals, [k] values given to 3 decimal places to separate signals.

5.2.8 Oxidative rearrangement of denigrin E derivatives

Pyrrole cores are known to undergo rapid oxidation in the presence of air, leading to a wide array of possible rearrangements.[429,430] In this research, it was observed that denigrin K (**265**) underwent a rearrangement within a few days of being dissolved in methanol-d_4 and stored in an NMR tube, likely due to exposure to air and possibly to light. The mixture obtained contained in part, *para*-hydroxybenzaldehyde (**267**), formed by oxidation of the hydroxybenzyl groups in positions 14 and 33, with HR-ESI-MS and ^{1}H NMR spectroscopic data analogous to those reported in the literature in methanol-d_4 (Figure 97).[431] The oxidative conversion of denigrin E (**226**) into denigrin D (**260**) was first reported in 2022 by Chen *et al.*[428] The authors examined several oxidants and reported obtaining compound (**260**) in 61% yield when compound (**226**) was reacted with *t*-BuOOH at 80 °C in the presence of $Mo(CO)_6$. Interestingly, when denigrin E permethyl ether was treated with MoOPH, denigrin D permethyl ether was obtained in 14% yield, along with variable quantities of *para*-anisaldehyde. In this research, traces of the $[M + Na]^+$ ion at 724 in positive ion mode and the $[M - Na]^-$ ion at 678 in negative ion mode were detected in the decomposition mixture by HR-ESI-MS, possibly corresponding to the formation of compound (**262**) and/or compound (**263**)**.** However, neither of the two products could accurately be detected in the mixture by ^{1}H NMR spectroscopy, possibly due to low yield of such rearrangements from simple exposure to air.

Since compounds (**264**) and (**266**) both contain a pyrrole core and possess structures closely related to compound (**265**), both could potentially undergo similar oxidative rearrangement. Therefore, while purifying the *D.* c.f. *dendyi* extract, fractions that contained denigrins J-K (**264-265**) were stored under nitrogen and kept in solution for a minimal amount of time.

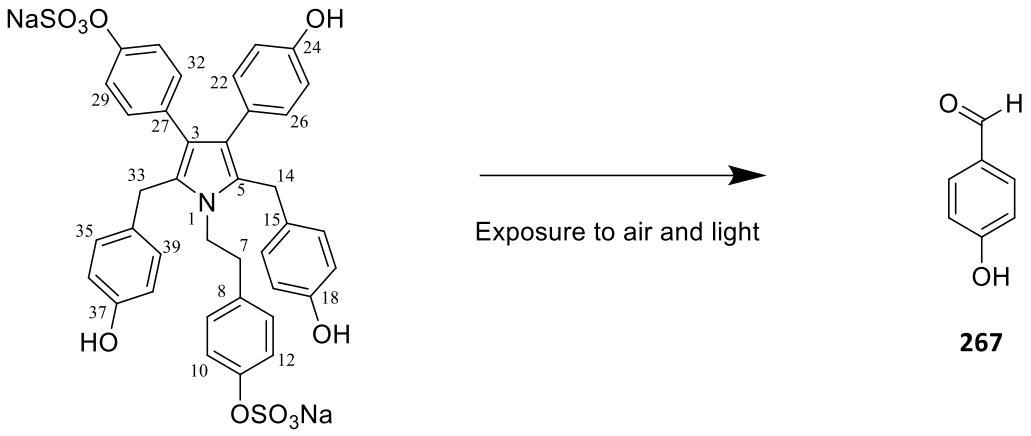

265 **267**

Figure 97: Oxidative conversion of compound (**265**) to compound (**267**).

5.2.9 Occurrence, bioactivities and biogenesis of polyaromatic pyrrole and pyrrolidone alkaloids

The denigrins,[392,426] including the new sulphated derivatives isolated during this research, along with the previously mentioned dictyodendrins,[382] dactylpyrroles[392] and lamellarins[393] belong to a large class of polyaromatic pyrrole and pyrrolidone alkaloids, which also include the lukianols,[385] rigidins,[432-434] polycitrins,[386] storniamides,[388] ningalins,[435] purpurone,[436] polycitones,[386,387] and ianthellidones,[393] isolated from tunicates and sponges. These different classes of compounds, displaying a wide range of bioactivities, differ by the substitution pattern and the arrangement of the rings attached to the pyrrole core.

Among these classes, the rigidins display one of the simplest structures featuring a pyrrolopyrimidine moiety. The first rigidin alkaloid, rigidin A (**268**), was isolated in 1990 from the Okinawan tunicate *Eudistoma* cf. *rigida* as a potent calmodulin antagonist (IC_{50} 50 µM).[433] In 2003, further rigidins, B-D (**269-271**) were described from another Okinawan tunicate, *Cystodytes* sp.[432] In a preliminary study, compounds (**269-271**) displayed cytotoxicity against murine leukaemia L1210 cells.[432] A few months later, another rigidin analogue, rigidin E (**272**), was reported from the Papua New Guinean tunicate *Eudistoma* sp.[434] Rigidins A (**268**) and E (**272**) were tested for cytotoxicity against HCT 116 human colon carcinoma and A431 human epidermoid carcinoma cell lines, although only minimal growth inhibition was observed.[434]

The ningalin family is currently represented by four members, ningalins A-D (**273-276**), isolated in 1997 from a *Didemnum* sp. from Western Australia.[435] As opposed to rigidins suggested to be derived from tyrosine by amino acid condensation reactions, it is believed that compounds (**273-276**) are derived from the condensation of 3,4-dihydroxyphenylalanine (DOPA) amino acid, respectively from two, three, four and five units.[435] Purpurone (**277**), isolated from the marine sponge *Iotrochota* sp. from Palau, is closely related to ningalin D (**276**), differing only by the absence of one hydroxy group on the ring part of the tyramine unit.[436] Compound (**277**) inhibited ATP-citrate lyase activity with an IC_{50} of 7 µM.[436]

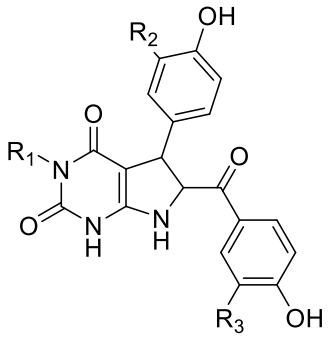

268 $R_1 = R_2 = R_3 = H$
269 $R_1 = R_2 = H$, $R_3 = OMe$
270 $R_1 = R_3 = H$, $R_2 = OMe$
271 $R_1 = H$, $R_2 = R_3 = OMe$
272 $R_1 = Me$, $R_2 = R_3 = H$

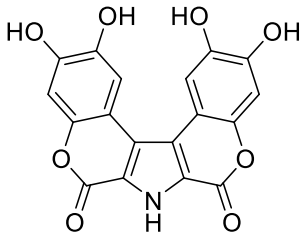

273

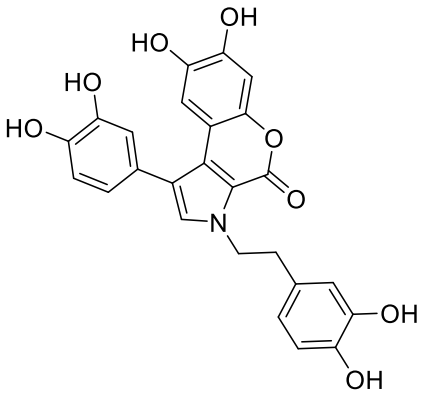

274

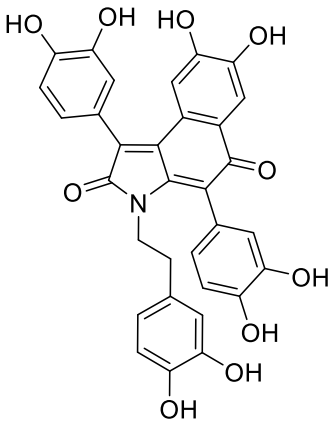

275

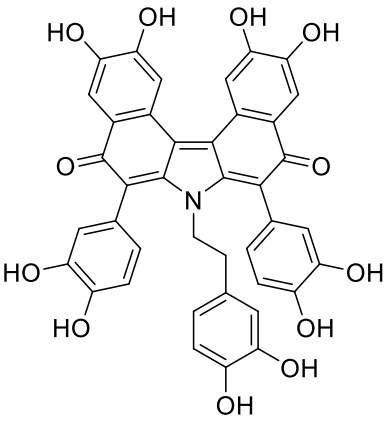

276

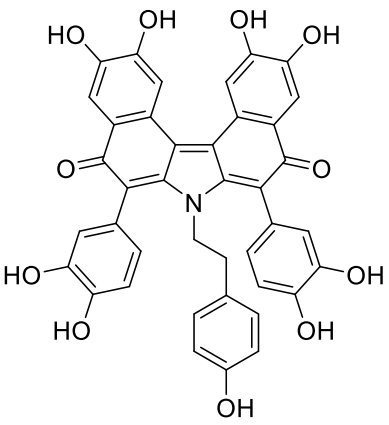

277

Polycitrins A (**278**) and B (**279**), isolated in 1994 by Rudi *et al.* from the South African ascidian *Polycitor* sp. are currently the only members of the polycitrin family, closely related to the lamellarin and ningalin class, all sharing a common 3,4-diaryl pyrrole core.[386] Polycitone A (**280**) was also isolated and this pentamethyl, semi-synthetic analogue inhibited the growth of SV40 transformed fibroblast cells at a concentration of 10 mg mL^{-1}.[386] In 2000, another member of the polycitone class, polycitone B (**281**), was reported by the same group from an extract of *Polycitor africanus* from Madagascar.[387] Compound (**281**) differed from compound (**280**) by the absence of a tyramine unit attached to the core nitrogen atom.[387] The crude extract of *P. africanus* strongly inhibited retroviral reverse transcriptase and cellular DNA polymerases and the activity was traced to compound (**280**), also isolated from the extract.[387]

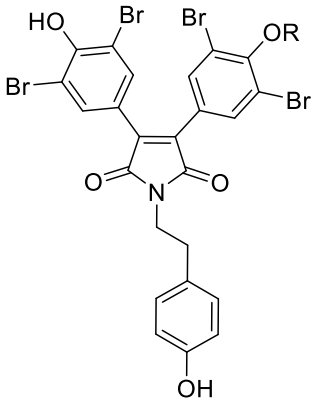

278 R = H
279 R = Me

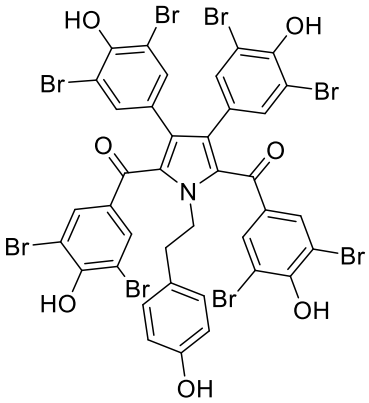

280

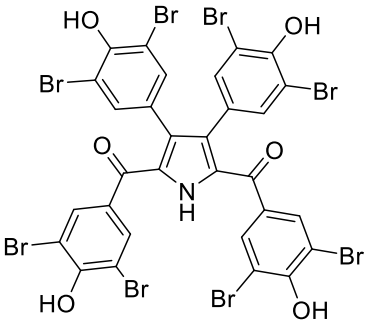

281

Currently, the lukianol class is represented by two compounds, lukianol A (**282**) and its iodo derivative lukianol B (**283**), both isolated from an encrusting ascidian from Palmyra atoll.[385] Both compounds (**282**) and (**283**) contain an *N*-alkylpyrrolecarboxylic acid moiety, relatively rare in the marine environment.[385]

Another class of polyaromatic pyrrole alkaloids of interest is the storniamide family, only reported from the marine sponge *Cliona* sp, and currently represented by storniamides A-D (**284-287**) isolated in 1993 from an Argentinian collection of the sponge.[388] Compounds (**284-287**) contain an uncommon amide moiety attached to the pyrrole core and are closely related to the lukianols, policytones and policytrins.[388] In terms of biogenesis, it was suggested that compounds (**284-287**) are of peptide origin, derived from five tyrosine units followed by hydroxylation of the aromatic rings, giving rise to the different compounds.[388] All four compounds showed antibiotic activity against three Gram-positive bacteria*,* namely *S. aureus*, *B. subtilis* and *M. luteus,* at 50 µg/disk but failed to show activity against Gram-negative bacteria or *Candida albicans.*[388]

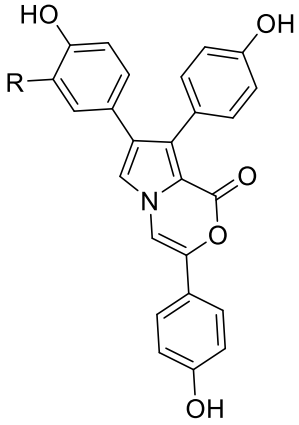

282 R = H
283 R = I

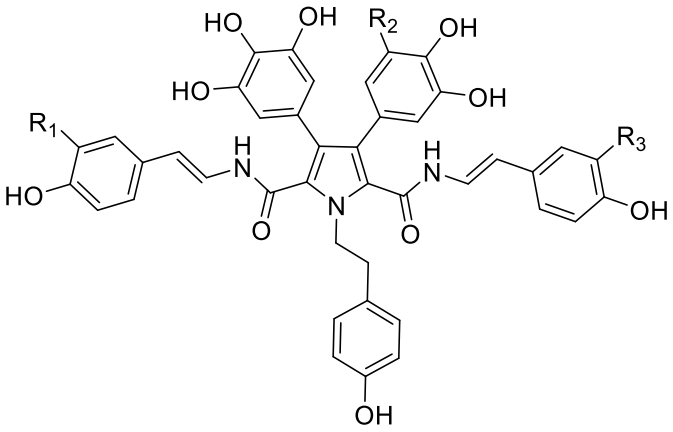

284 $R_1 = R_3 = H$, $R_2 = OH$
285 $R_1 = H$, $R_2 = R_3 = OH$
286 $R_1 = R_3 = OH$, $R_2 = H$
287 $R_1 = R_2 = R_3 = OH$

In 2010, a series of pyrrole alkaloids, primarily sulphated, baculiferins A-O (**288-302**), along with purpurone (**277**) and ningalin A (**273**), were reported from the Chinese marine sponge *Iotrochota baculifera*.[437] Baculiferins K (**298**) and M–N (**300-301**) were found to be potent inhibitors of the HIV-1 IIIB virus in MAGI cells (IC_{50} < 0.4 μg mL^{-1}).[437] A possible biosynthetic pathway for the formation of the baculiferins derived from L-DOPA was presented.[437] Compounds (**288-295**) were proposed to originate from five aromatic amino acid residues, while the asymmetric skeleton of compounds (**296-298**) was suggested to arise from the condensation of three DOPA residues with tyramine, followed by similar reactions leading to the formation of compounds (**288-295**). For baculiferin (**299-301**), the acetic acid residue is believed to originate from glycine instead of tyramine.[437]

Finally, alkaloids belonging to the ianthellidone class were initially reported in 2012 from a southern Australian marine sponge, *Ianthella* sp. as part of a search for protease β-secretase (BACE) inhibitiors.[393] This class of compounds includes several furanones, along with the pyrrolidones ianthellidones A-F **303-308**. Ianthellidone F **308** displayed modest protease β-secretase (BACE) inhibitory activity and both the pyrrolidone and furanone ianthellidones showed low to no cytotoxicity when measured in a range of assays against several human mammalian, bacterial and fungal cell lines.[393]

Dictyodendrins F-J (**212**), (**309-312**), respectively, were isolated from the same sponge and three of them exhibited significant BACE inhibitory activity (IC_{50} 1–2 mM), and were established as the dominant BACE inhibitory metabolites within the sponge extract.[390]

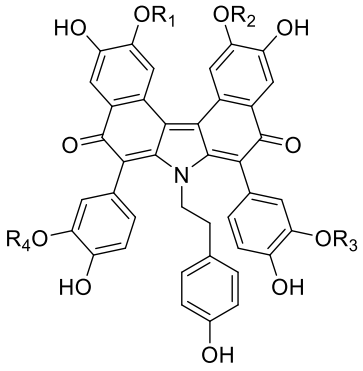

288 $R_1 = R_3 = R_4 = H$, $R_2 = SO_3H$
289 $R_1 = R_2 = R_4 = H$, $R_3 = SO_3H$
290 $R_1 = R_2 = H$, $R_3 = R_4 = SO_3H$
291 $R_1 = R_2 = SO_3H$, $R_3 = R_4 = H$
292 $R_1 = R_4 = H$, $R_2 = R_3 = SO_3H$
293 $R_1 = R_3 = H$, $R_2 = R_4 = SO_3H$
294 $R_1 = H$, $R_2 = R_3 = R_4 = SO_3H$
295 $R_1 = R_2 = R_3 = SO_3H$, $R_4 = H$

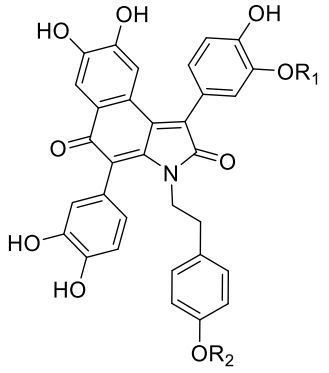

296 $R_1 = SO_3H$, $R_2 = H$
297 $R_1 = H$, $R_2 = SO_3H$
298 $R_1 = R_2 = H$

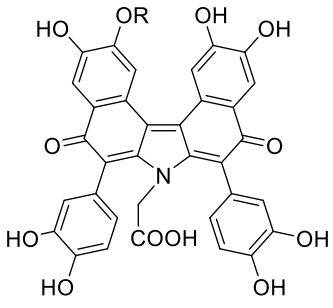

299 R = H
300 R = SO_3H

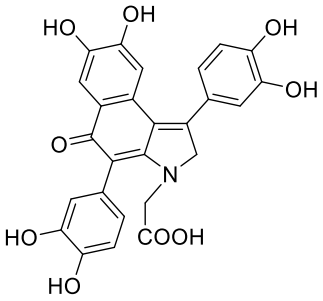

301

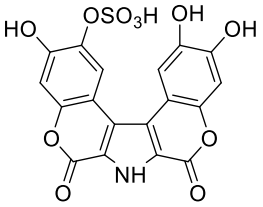

302

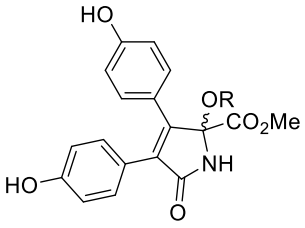

303 R = H
304 R = Et

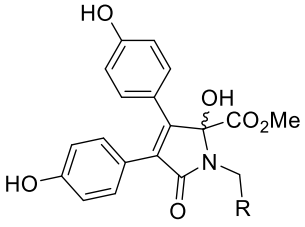

305 R = OMe
306 R = OEt
307 R = CO_2Et

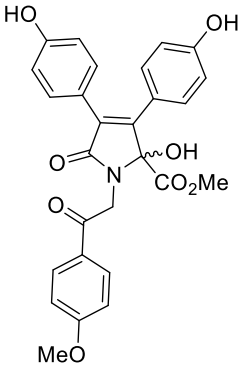

308

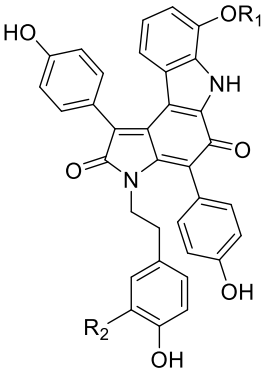

212 $R_1 = R_2 = H$
309 $R_1 = Me$, $R_2 = H$
310 $R_1 = H$, $R_2 = Br$
311 $R_1 = H$, $R_2 = I$

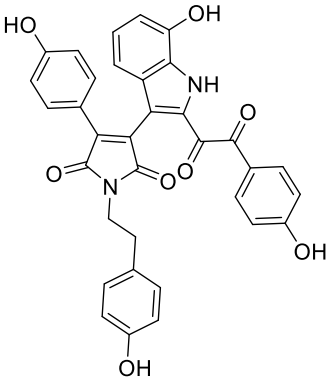

312

5.3 Cytotoxic activity

Denigrins H-L (**262-266**), along with six of the known polyaromatic pyrroles also described from *D.* cf. *dendyi* in Chapter 4, namely dictyodendrins C (**209**), D (**210**), and F (**212**), denigrin E (**226**), dactylpyrrole A (**225**), and lamellarin O1 (**228**), were assessed for cytotoxic activity towards the human cervical cancer cell line HeLa using an MTT assay. Details of the assay method development and the selected method can be found in Chapter 7 – Experimental, Section 7.7.5. Dictyodendrin B (**208**) and denigrin G (**227**) were not available in sufficient quantity to be tested, while pyrrolo[2,3-c]carbazole spirolactone 1a (**199**) was impure.

5.3.1 Cytotoxic activity of eleven polyaromatic alkaloids

The tested compounds mentioned above showed minimal activity (Table 38, Figure 98 and Figure 99). Dictyodendrin F (**212**) was the most active of these compounds (IC_{50} 57 µM) but the activity was still only at a level considered inactive by widely accepted standards.[66] Compound (**212**) has previously been shown to exhibit minimal activity against the P-glycoprotein (P-gp)-overexpressing multi-drug resistant variant SW620 Ad300 (IC_{50} > 30 µM), and weak cytotoxicity against the colorectal cancer cell line SW620 (IC_{50} 8.5 µM), showing increased selectivity for the SW620 cell line.[390] Lamellarin O1 (**228**) was also previously shown to exhibit minimal cytotoxic activity against both SW620 and SW620 Ad300 cells lines (IC_{50} > 30 µM).[393] It is possible that these compounds could display increased selectivity to other cell lines but the minimal amount of compounds isolated did not allow for further testing. Besides, with dictyodendrins A-E (**207-211**) all displaying at least one sulphate moiety and exhibiting 100% inhibition of telomerase activity at a concentration of 50 µg mL^{-1}, it would be of interest to measure the anti-telomerase activity of the new sulphated denigrins (**262-266**).

Table 38: IC_{50} values for denigrins H-L (**262-266**), dictyodendrins C (**209**), D (**210**), and F (**212**), denigrin E (**226**), dactylpyrrole A (**225**) and lamellarin O1 (**228**) against HeLa cells.

Compound	**IC_{50} (µM)**
Denigrin H **262**	> 100
Denigrin I **263**	78
Denigrin J **264**	> 100
Denigrin K **265**	> 100
Denigrin L **266**	> 100
Denigrin E **226**	> 100
Dictyodendrin C **209**	> 100
Dictyodendrin D **210**	60
Dictyodendrin F **212**	57
Dactypyrrole A **225**	> 100
Lamellarin O1 **228**	> 100

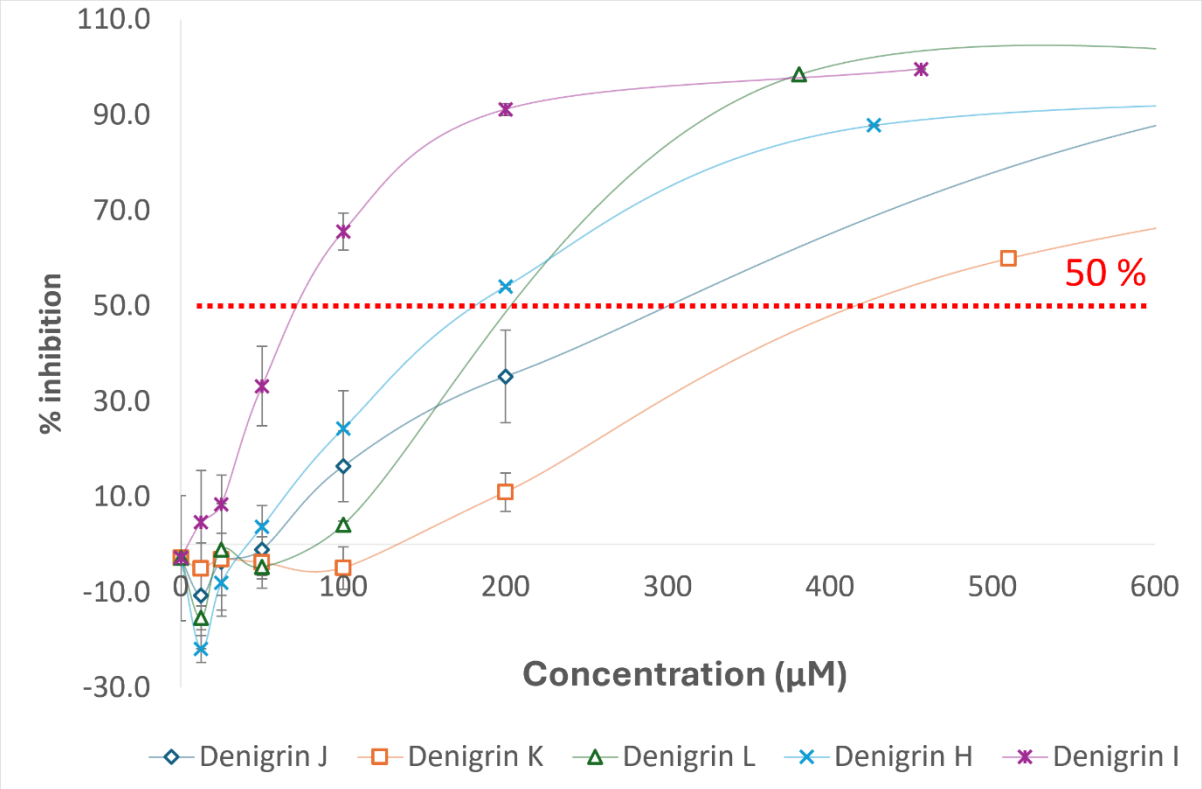

Figure 98: Toxicity of denigrins H-L (**262-666**) to HeLa cells with the lower end of the concentrations tested displayed.

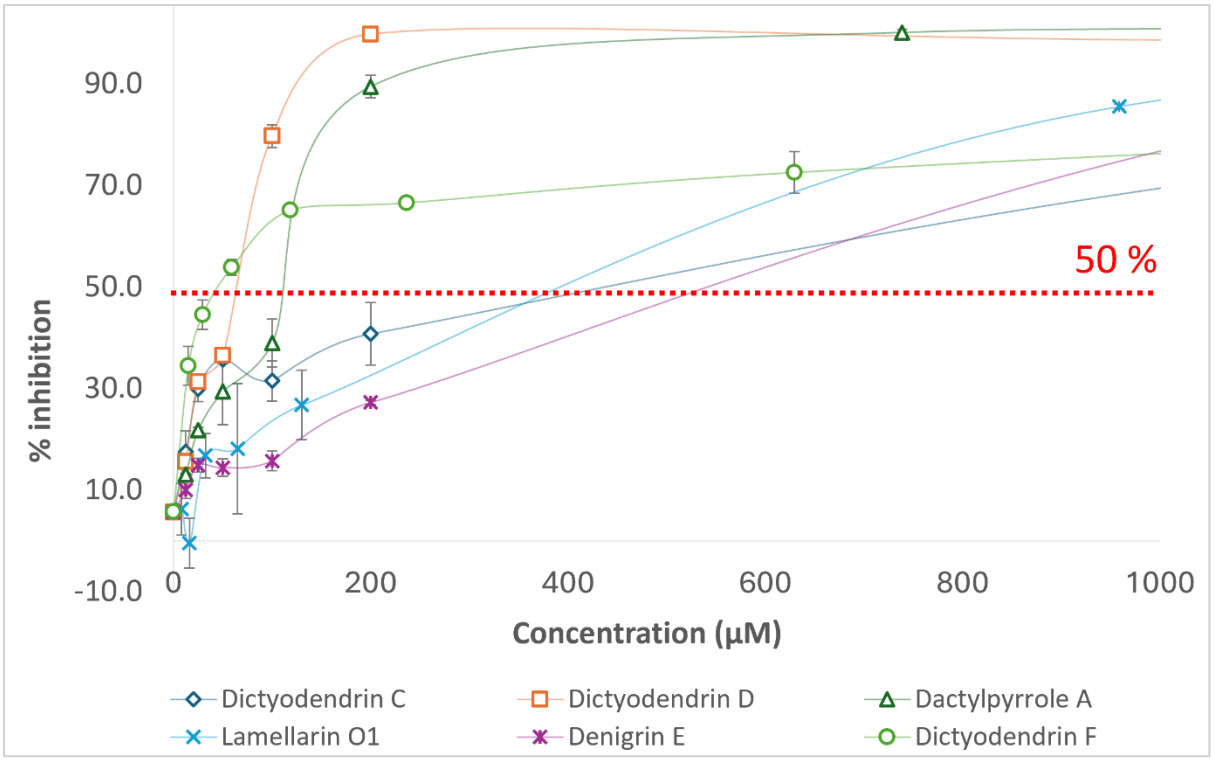

Figure 99: Toxicity of dictyodendrins C (**209**), D (**210**), F (**212**), denigrin E (**226**), dactylpyrrole A (**225**) and lamellarin O1 (**228**) to HeLa cells with the lower end of the concentrations tested displayed.

5.4 Concluding remarks

During this study, the *D.* c.f. *dendyi* crude extract was further investigated to isolate minor compounds using an HR-ESI-MS guided isolation. The investigation resulted in the isolation and structural elucidation of denigrins H–L (**262-266**), five new sulphated derivatives of either denigrin D or E. Compounds (**262-266**) represent the first sulphated derivatives of the denigrin class. Their structures were elucidated by interpretation of 1- and 2D NMR spectroscopic data, and HR-ESI-MS spectrometric data, as well as comparison with literature data. The denigrins are a rare class of highly substituted pyrrole and pyrrolidone alkaloids that, so far, have been only described from two marine sponges.[392,426]

The cytotoxicity of compounds (**262-266**) towards the human cervical cancer cell line HeLa, along with that of six of the known polyaromatic pyrroles previously isolated from the *D.* c.f. *dendyi* crude extract, was assessed using an MTT assay and minimal activity was observed.

Chapter 6

Conclusion and Future Recommendations

This research provided insights into the ecology and chemistry of primarily unstudied New Zealand marine invertebrates, by means of chemical ecology-guided searching for new bioactive secondary metabolites. As such, predator-prey relationships in nudibranchs were established for three species (*Polycera hedgpethi*, *Ceratosoma amoenum* and *Goniobranchus aureomarginatus*) by means of field studies and laboratory-based feeding-choice experiments. Two of these predator-prey relationships (*C. amoenum* - *Dysidea teawanui* and *G. aureomarginatus* - *Dictyodendrilla* cf. *dendyi*) were confirmed by chemical investigation through the isolation of shared metabolites, namely ergosterol peroxide (**186**) for the *C. amoenum* - *Dysidea teawanui* relationship, and dictyodendrins C (**209**) and F (**212**) for the *G. aureomarginatus* - *D.* cf. *dendyi* relationship, highlighting the relevance of such an approach. Several other nudibranch species, *Dendrodoris krusensternii, Dendrodoris nigra* and *Aphelodoris luctuosa*, were also chemically investigated. Due to a lack of potential prey observations, it was not possible to run feeding-choice experiments. These species yielded a range of secondary metabolites, previously reported from other marine invertebrates: cinnamolide (**122**) from *D. krusensternii*, 7-deacetoxy-olepupuane (**124**) and the drimane esters (**125**) from *D. nigra*, and a 3-PAPS (**146**) present in high concentration within *A. luctuosa* and its eggs. Other less common or endemic nudibranch species may be worthy of ecological and chemical investigations. However, the lack of predictability of nudibranch populations in terms of seasonality, prey availability and varying environmental conditions, poses challenges for such studies.

The study of the predator-prey relationship in *Goniobranchus aureomarginatus* nudibranchs led to the chemical investigation of a Dictyodendrillid marine sponge, *Dictyodendrilla* cf. *dendyi*, revealing the presence of numerous polyaromatic pyrrole and pyrrolidone alkaloids. Purification of a sponge extract by means of TLC, NMR spectroscopy and HR-ESI-MS guided isolation resulted in the characterisation of nine known alkaloids, dictyodendrins B-D (**208**-**210**) and F (**212**), denigrins E (**226**) and G (**227**), dactylpyrrole A (**225**), lamellarin O1 (**228**) and

pyrrolo[2,3-c]carbazole spirolactone 1a (**199**), along with five new sulphated alkaloids, denigrins H-L (**262-265**). During the purification of the sponge extract, minor compounds were detected and the use of a metabolomic approach via molecular networking would be of high interest to offer a comprehensive visualisation of the secondary metabolites present within the sponge.

The new and known arylpyrrole alkaloids isolated in this research were assessed in a single general cytotoxic assay due to the minimal amounts obtained, although more bioassays should be conducted in future studies, despite results indicating that the compounds were not particularly active. Previously reported sulphated dictyodendrins were inhibitors of telomerase activity, while the non-sulphated phenol analogue was inactive, therefore a telomerase inhibition assay would be relevant for the new sulphated denigrins characterised in this research. Such an assay had not been conducted at the University of Waikato previously and attempts to develop the assay were conducted as part of this research, but failed to succeed in a timely manner, highlighting the need for future study. Total synthesis of these alkaloids is of high interest to afford larger quantities of pure compounds, to allow several pharmaceutically relevant bioassays to be performed.

The metabolites isolated in this study were not assessed in ecologically relevant bioassays, which would be of interest in future studies. Feeding-deterrence assays with relevant predators would be pertinent, especially for metabolites isolated from the mantle of nudibranch species and from the eggs, such as the 3-PAPSs. Such a study would provide additional insights into the ecology of nudibranchs, including defence mechanisms.

Nudibranch diets are understudied, with little information available in the literature, especially for New Zealand endemic species. Selection of organisms for feeding-choice experiments is therefore challenging and can be misleading. To assess the diet of various species, the study of their radula, or mouth parts, could provide further information about their dietary preferences, perhaps with different radula shapes allowing, or restricting, the nudibranchs to prey on specific types of organisms. Preliminary work has been conducted on the radula of *Goniobranchus aureomarginatus* and scanning-electron microscope (SEM) images were obtained (Figure 100). Future studies are needed to dissect more radulae from various species, especially species for which the diet is known, allowing comparison of the shape and dimensions of the teeth across species feeding on various marine invertebrates.

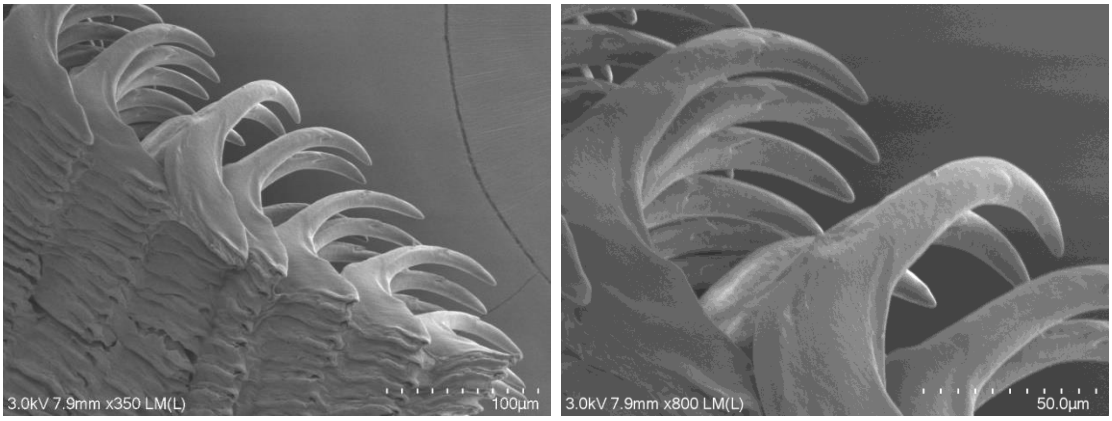

Figure 99: Scanning electron microscope (SEM) images of the radula of *Goniobranchus aureomarginatus.*

Chapter 7

Experimental

7.1 General experimental procedures

7.1.1 Solvents

Solvents used for general purposes (methanol, ethanol, dichloromethane and ethyl acetate) were purchased as drum grade and distilled in the laboratory. Water used for chemical analyses was Millipore Milli-Q grade (18.2 MΩ cm^{-1}). Water used for morphological analyses was double distilled grade. Petroleum spirit was supplied as analytical reagent grade by BDH Laboratory supplies (England). Solvents used for HPLC and LC-MS analysis (methanol and acetonitrile) were supplied as gradient-grade for liquid chromatography (LiChrosolv®) by Supelco. Formic acid for analysis (98-100 %, ACS) was supplied by Scharlau. Deuterated solvents used for NMR experiments were either supplied in bottles (Chloroform-d, 99.8 atom % D, Sigma Aldrich) or ampoules (D_2O, methanol-d_4, chloroform-*d*, 99.9 atom % D each, Sigma Aldrich, 0.5 - 1 mL). Nitric acid (65 %) used for morphological analyses was supplied as analysis grade by Merck (EMSURE®).

7.1.2 Nudibranch dissection

Nudibranch samples were thawed prior to being dissected. The specimen was positioned so that a careful incision on the mantle could be performed using scissors without piercing the internal organs. The skin was then carefully removed by pulling from both sides of the incision using tweezers. When necessary, the digestive glands and stomach were separated from the other internal organs. Each body part of interest was placed in a labelled vial and kept at -20 °C in a chest freezer until extraction. The remaining parts were discarded following the procedure for biological waste.

7.1.3 Morphological analysis

The digestive glands of the sample of interest were placed in a test tube and pierced, prior to adding concentrated nitric acid (5 mL) to dissolve the tissues. The contents of the test tube were mixed using a vortex mixer then left to soak for 30 minutes. The supernatant was removed using a Pasteur pipette before adding double distilled water (5 mL). This was followed by sonication for 30 seconds and removal of the supernatant using a Pasteur pipette. Two more washes with double distilled water (2 x 5 mL) were conducted, followed by two similar washes with ethanol. After removal of the ethanol supernatant during the last wash, ethanol (5 to 10 drops) was then added back to the tube and the contents were carefully poured onto a microscope slide. The slide was allowed to air dry for 24 hours before observation under an Olympus SZX12 stereo microscope and an Olympus BX551 compound microscope, both equipped with a camera.

7.1.4 Extraction

The sample was thawed and soaked overnight in a mixture of MeOH/DCM (3:1), then blended using a tissue homogeniser (Ultra Turrax), or a commercial blender for large scale extractions, and filtered under vacuum. The extraction steps were repeated several times with a 1-hour soaking time until the filtrate was colourless. The filtrates were combined, and the solvent was removed under reduced pressure. The extract was then transferred to a capped vial using the minimum amount of DCM and MeOH, before being dried under a flow of nitrogen. For several samples, the crude extract was then lyophilised to obtain a dry powder.

7.1.5 Thin layer chromatography

Thin layer chromatography (TLC) used aluminum sheets (20 x 20 cm) coated with silica gel 60 F_{254} supplied by Merck. Each sheet was equally divided into eight smaller plates (5 x 10 cm). The crude extracts or fractions were dissolved in a minimal amount of MeOH before being spotted onto the TLC plate using a glass capillary. The plate was eluted using a mixture of EtOAc/MeOH (5:1) unless specified otherwise, before being visualised under a UV lamp at 254 nm.

7.1.6 Reversed phase C18 bench column chromatography

The reversed phase purifications were carried out with C18 YMC-gel ODS-A (YMC). Lyophilised crude extracts were ground into a fine powder using a mortar and pestle and loaded as a solid. Non lyophilised extracts were dissolved in a minimum volume of DCM or MeOH and loaded onto the column. The sample vial was then rinsed with a minimal amount of MeOH which was also loaded onto the column. Columns were run with a steep, stepwise gradient from 100% H_2O, to 100% MeOH, to 100% DCM. Elution was achieved under nitrogen gas pressure (approximately 20 psi). Fractions were collected manually as follows: 40 mL fractions for a 20 g column and 100 mL fractions for a 50 g column, unless obvious banding was observed.

7.1.7 Size exclusion chromatography

Size exclusion chromatography was performed using Sephadex LH-20, (either with a 30 g or a 150 g column). The column was packed in 100% MeOH. The sample was dissolved in a minimal amount of MeOH before being loaded on to the column head. Elution was achieved with either a mixture of H_2O and MeOH or with 100% MeOH. In the case of elution with a mixture of H_2O and MeOH, the column was packed the day before in the elution solvent to allow for equilibration.

7.1.8 Normal phase bench column chromatography

Normal phase flash column chromatography was conducted on silica (Davisil, 60 Å, 35-70 μ). The sample was dissolved in a minimum volume of DCM which was also loaded onto the column head. The sample vial was then rinsed with a minimal amount of MeOH and loaded onto the column. Elution was achieved with a steep stepwise gradient of either 100% DCM to 100% MeOH, or 100% DCM, to 100% EtOAc, to 100% MeOH.

7.1.9 Sample preparation for high performance liquid chromatography and liquid chromatography mass spectrometry analysis

Samples for LC-MS and HPLC analysis were prepared by adding MeOH (0.5 mL) to the sample vial, before transferring the supernatant to a glass syringe equipped with a Luer lock syringe filter (0.22 µm, PTFE) and filtering it into a LC-MS vial. The syringe filter was then rinsed with MeOH (2 X 0.25 mL) to obtain the LC-MS sample (1 mL total).

7.1.10 High performance liquid chromatography

High performance liquid chromatography (HPLC) was conducted using a Shimadzu system equipped with a SCL-40 system controller, a LC-40D XS solvent delivery module, a SIL-40C XS auto sampler, a CTO-40C column oven and an SPD-M40 UV−vis detector, operating under LabSolutions software. A Phenomenex Luna C18 column (5 µ, 100 Å, 150 × 4.6 mm, kept at 40 °C) was used for HPLC purification with a gradient elution of H_2O/MeOH (both containing 0.1 % formic acid) over 34 minutes at 1 mL min^{-1}.

7.1.11 Liquid chromatography mass spectrometry screening

LC-MS was performed using a Shimadzu system equipped with a SCL-40 system controller, a LC-40D XS solvent delivery module, a SIL-40C XS auto sampler, a CTO-40C column oven, a SPD-M40 UV−vis detector and a LCMS-8045 triple quadrupole detector, operating under LabSolutions software. The UV-vis detector scanned between 190 to 800 nm in 8 nm intervals. The mass spectrometer was equipped with a heated ESI probe with a capillary voltage of 4 kV in positive mode and -3 kV in negative mode, and a nebulising gas flow of 2.9 L min^{-1}. The mass spectrometer was operated in alternating positive and negative ion mode with an event time of 0.2 s using a Q3 scan experiment. The ions were scanned between 200 and 1000 *m/z*, unless otherwise specified. A Phenomenex Luna C18 column (5 µ, 100 Å, 150 × 4.6 mm, kept at 40 °C) with a gradient elution of H_2O/ACN (both containing 0.1 % formic acid) over 50 minutes at 0.3 mL min^{-1} was used, unless otherwise specified (Figure 101).

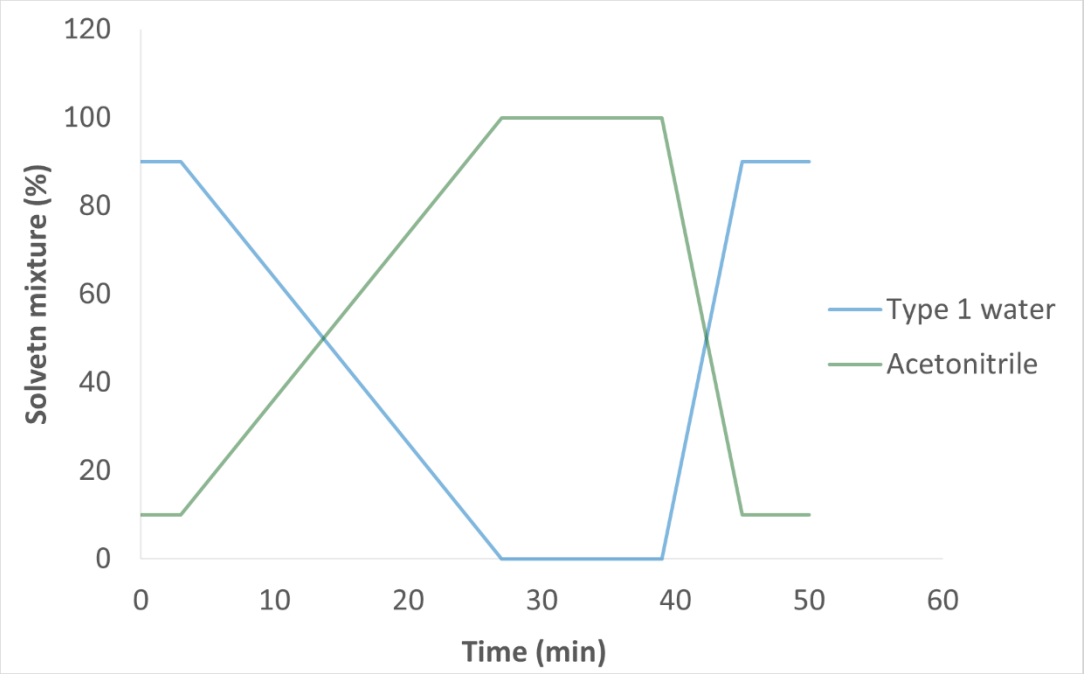

Figure 100: Gradient of both organic and aqueous mobile phases for standard LC-MS analysis.

7.1.12 High resolution mass spectrometry

HR-ESI-MS mass spectra were recorded using a Bruker Daltonics MicrOTOF electrospray ionisation mass spectrometer. Sodium formate solution was used for calibration. Samples were dissolved in a few drops of distilled MeOH, and one drop of each sample was added to an Eppendorf tube pre-filled with 1.5 mL of MeOH. Samples were vortexed for 30 seconds before use to ensure separation of undissolved solids. Spectra were recorded with a Capillary Exit voltage of 90 to 150 V in positive ion mode and -90 to -150 V in negative ion mode.

7.1.13 Nuclear magnetic resonance spectroscopy

NMR experiments were performed on a JEOL ECZR spectrometer (600 MHz for ^{1}H and 150 MHz for ^{13}C) and are referenced to deuterium oxide (^{1}H: 4.79 ppm), methanol-d_4 (^{1}H: 3.31 ppm, ^{13}C: 49.0 ppm) or chloroform-*d* (^{1}H: 7.26 ppm, ^{13}C: 77.2 ppm). Delta NMR Data Processing Software (v6.2.0) was used for spectroscopic analyses.

7.1.14 Infrared spectroscopy

Infrared spectra were recorded with a Jasco FT/IR-6X spectrometer using an ATR unit. Samples were dissolved in a minimal amount of MeOH before being transferred on the diamond ATR crystal.

7.1.15 Ultraviolet spectroscopy

Ultraviolet spectra were measured with an Agilent Cary 300 UV-Vis spectrophotometer. Samples were dissolved in MeOH before being transferred to a quartz cuvette.

7.1.16 Optical rotation

Optical rotation was recorded on an Optical Activity AA-5 polarimeter at the sodium D line (589 nm). Samples were dissolved in either MeOH or chloroform before being transferred to the measuring cell (5 cm x 0.5 cm)

7.2 Sample collection, identification, maintenance and extraction

All samples were collected by hand using free diving on SCUBA diving between 2018 and July 2024. The collection of samples from Tauranga was carried out under the MPI Fisheries Special Permit (698-3) - Project M1: Biodiscovery and diversity collection. The samples from Otago were collected under the University of Otago Special Permit (823-3). Voucher specimens are kept at the University of Waikato in Hamilton and are listed in Table 40.

Nudibranch samples were identified from the e-guide on New Zealand marine biota "Super sea slugs, a guide to the sea slugs of New Zealand" developed by the National Institute of Water and Atmospheric Research (NIWA) marine taxonomy group (Willan *et al.* 2020).[206] Sponge samples were identified by Christopher Battershill and bryozoan samples by Dennis Gordon.

Invertebrate samples used for chemical analysis and egg coils collected in the wild were directly frozen on ice and then kept at -20 °C in a chest freezer. Nudibranch and prey samples used for feeding-choice experiments were kept alive in ambient seawater in 1 L plastic tanks. The seawater was oxygenated at the Aquatic Research Centre at the University of Waikato, Hamilton. Nudibranch species were kept separately, with individual specimens of each species either kept separately or in pairs, for one to two days prior to experiments and deprived of food. If spawning occurred, the egg mass was directly removed from the tank and frozen at -20 °C in a chest freezer.

7.2.1 Collection sites

During the course of this research, samples were collected from several locations in New Zealand and Australia, as displayed in the table below (Table 39). Voucher specimens were kept for most of the samples collected (Table 40).

Table 39: GPS coordinates for the sample collection sites for this research.

Collection site	Depth (m)	Environment	GPS coordinates
Dive Crescent, Tauranga, Bay of Plenty, New	3 - 8	Rocky reef	37° 40' 44.7" S 176° 10' 15.8"
Salisbury Wharf, Tauranga, Bay of Plenty,	3 - 7	Sand bed with pilings	37° 38' 25.5" S 176° 10' 51.9"
Motuputa Island, Tauranga, Bay of Plenty,	10 - 15	Cliff, rocky reef	37° 37' 09.*8" S* 176° 26' 52.9"
Tauranga Bridge, Tauranga, Bay of Plenty,	5 - 10	Rocky reef	37° 41' 16.7" S 176° 10' 21.4"
Pahoia Beach, Bay of Plenty, New Zealand	>1	Sea grass bed	37° 37' 37.1" S 176° 00' 27.0"
Bridge Mount, Otago, New Zealand	Unknown	Unknown	Unknown
Sandringham, Melbourne, Australia	Unknown	Unknown	37° 56' 50.1" S 144° 59' 43.9"
Altona, Melbourne, Australia	Unknown	Unknown	37° 52' 12.3" S 144° 50' 45.6"
Weller's Rock, Otqgo, New Zealand	Unknown	Unknown	Unknown

Table 40: Table of the voucher specimens kept for this research

Species	Quantity	Code	Collection date	Collection site
Dendrodoris krusensternii	1 specimen	*D. krusen* 4	30/06/2021	Salisbury Wharf
Dendrodoris krusensternii	1 specimen	*D. krusen* 16	10/12/2022	Dive Crescent
Dendrodoris nigra	1 specimen	*D. nig* 7	11/03/2022	Pahoia Beach
Aphelodoris luctuosa	1 specimen	*A. luct* 13	13/12/2021	Salisbury Wharf
Ceratosoma amoenum	1 specimen	*C. amoe* 9	22/07/2021	Dive Crescent
Goniobranchus aureomarginatus	1 specimen	24 WR 1-1	01/03/2024	Weller's Rock
Goniobranchus aureomarginatus	1 specimen	*G. aureo* 29	10/12/2022	Dive Crescent
Dysidea teawanui	50 g	*D. teawanui*	31/03/2022	Dive Crescent
Dictyodendrilla. c.f dendyi	50 g	*D.* cf. *dendyi*	10/12/2022	Dive Crescent
***Haliclona* sp.**	20 g	*Haliclona*	11/07/2024	Salisbury Wharf

7.3 Feeding choice experiments

7.3.1 Methodology development

Two-channel, flow-through flume-chamber

Feeding-choice experiment trials using the two-channel, flow-through flume chambers were conducted under laboratory conditions at the Coastal marine field station in Tauranga. Two flume chambers were built from plastic containers (40 cm x 15 cm x 15 cm). A constant water flow (0.15 L min^{-1}) of filtered ocean water was maintained throughout the chambers for all trials using a water pump. Specimens of *Dendrodoris krusensternii* and *Dendrodoris wellingtonensis* were used for the trials and were collected at Salisbury Wharf, Tauranga. The specimens were kept in 1L tanks without food for 48 hours before the trials. Seven experiments between 20 to 70 minutes each were carried out and pictures were taken every five minutes to record the position of the nudibranchs during the experiments.

Rectangular, Perspex flow-through chamber

Feeding-choice experiment trials using the rectangular, Perspex flow-through chamber were conducted under laboratory conditions at the Coastal marine field station in Tauranga. A rectangular Perspex flow-through chamber (45 cm x 23 cm x 4.5 cm) containing a central drain was built. The total flow rate was set to 0.15 L min^{-1}. Solutions of red and green food colouring dyes were used to prepare the coloured solutions, and each solution was pumped to a different side of the tank using a two-channel water pump. Different inflow configurations were trialled, including a Y-type inflow and 4-inflow configurations, of which the latter provided results closest to those desired.

Several nudibranch species, including *Ceratosoma amoenum* and *Goniobranchus aureomarginatus*, and two possible sponge prey (*Dysidea teawanui* and *Dictyodendrilla* cf. *dendyi*) were collected in December 2021 from Dive Crescent and trialled using the 4-inflow configuration. The nudibranchs were kept without food for twenty-four hours prior to the experiments. Several nudibranch specimens of the same species were placed within the same tank. The nudibranchs were given an initial 5-minute acclimation period without any prey

present. The prey were then introduced (one on each side near the water inflow) and the behaviour of the specimens was analysed over a one-hour period.

7.3.2 Selected no-flow configuration - general protocol

Feeding-choice experiments using the no-flow configuration were conducted under laboratory conditions at the Aquatic research centre at Waikato University. Experiments were conducted in a room kept at 20 °C (close to ambient sea temperature at the time). The number of experiments conducted on each nudibranch species varied across species and specimens based on general health of the specimens used for the experiments. Artificial seawater was prepared using Crystal Sea®Marinemix to a salinity between 35 to 36 ppt. The tanks used were either a Perspex tank (45 cm x 23 cm x 4.5 cm) or plastic containers (35 cm x 20 cm x 10 cm) and across the experiments, the same individuals were placed in the same tank. The depth of water was set a few cm lower on the Perspex tank to allow comparable volumes of water across the tanks and was such that the organisms were completely submerged in all instances.

Prior to each experiment, the nudibranchs were given an acclimation period of five to ten minutes and placed at the centre of the tank. Nudibranchs were then carefully placed back in the centre of the tank and a piece of each prey tested was placed at opposite corners of the tank. For the Perspex tank, prey pieces were placed a few cm away from the corners to allow comparable distance between the prey across the tanks. For each prey tested, the main specimen was kept under oxygenated seawater in a separate container. Portions of prey of similar size (two to three cm in diameter) were used. Prey pieces used for the feeding-choice experiments were taken from the main specimen and exposed to the air for the shortest amount of time possible while being transferred to the tanks for the experiments. No signs of deterioration in their condition were observed during the experiments. Water was oxygenated during the experiments which were carried out in natural light during the day and artificial light (provided by a LED Batten fixed above the tanks) during the night.

Each experiment was recorded using the timelapse mode of a GoPro Hero 8 camera. A choice for a tested prey was counted when the mouth of the nudibranch was in contact with the prey, as determined by extensive analysis of the recorded videos. After each experiment, the tanks were emptied and rinsed thoroughly with tap water, before being filled again with artificial

seawater. Fresh pieces of prey were used at the beginning of each experiment and the placement of prey was alternated between experiments. No specimens died during the experiments.

7.3.3 *Polycera hedgpethi*

Experiments with *P. hedgpethi* were conducted on five individuals (n = 5), with four experiments run, for a total experiment duration of 26 to 43 hours for each individual. All five *P. hedgpethi* individuals were placed in the Perspex tank (45 cm x 23 cm x 4.5 cm) for each of the experiments. Two prey species, the bryozoan *Bugula neritina* and an unidentified hydrozoan were tested.

7.3.4 *Ceratosoma amoenum*

Experiments with *C. amoenum* were conducted on four individuals (n = 4) and lasted for a total of 109 hours, representing eleven experiments. The four *C. amoenum* individuals were placed in the same plastic tank for the feeding-choice experiments (35 cm x 20 cm x 10 cm). Two potential prey sponge species, *Dysidea teawanui* and *D.* cf. *dendyi* were tested.

7.3.5 *Goniobranchus aureomarginatus*

Experiments with *G. aureomarginatus* were carried out on six individuals (n = 6), with between eight and eleven experiments conducted, for a total experiment duration of 94 to 124 hours for each individual. Either one or two *G. aureomarginatus* individuals were placed per tank and each individual remained in the same tank for each experiment. Two potential prey sponge species, *Dysidea teawanui* and *D.* cf. *dendyi* were tested.

7.4 Sample extraction for predator-prey investigation

7.4.1 *Polycera hedgpethi* and *Bugula neritina*

To investigate the predator-prey relationship between *Polycera hedgpethi* and *Bugula neritina*, samples were collected and extracted as shown in Table 41.

Table 41: Collection and extraction of samples for the investigation of a predator-prey relationship between *Polycera hedgpethi* and *Bugula neritina.*

Sample	Specimens	Collection date	Location	Use	Wet weight (g)	Crude extract (g)
P. hedgpethi	4	December 2017 and January 2018	Melbourne, Australia	Chemical analysis	NA	0.075
	1	March 2022	Salisbury Wharf, Tauranga, NZ	Cytotoxicity assay and chemical analysis	0.20	0.009
P. hedgpethi eggs	2 coils	Spawned (laboratory), March 2022		Chemical analysis and cytotoxicity	0.09	0.009
B. neritina	-	May 2022	Salisbury Wharf, Tauranga, NZ	Chemical analysis	3.79	0.097

7.4.2 *Ceratosoma amoenum* and *Dysidea teawanui*

To investigate the predator-prey relationship between *Ceratosoma amoenum* and *Dysidea teawanui*, samples were collected and extracted as shown in Table 42.

Table 42: Collection and extraction of samples for the investigation of a predator-prey relationship between *Ceratosoma amoenum* and *Dysidea teawanui.*

Sample	Specimens	Collection date	Location	Use	Wet weight (g)	Crude extract (g)
C. amoenum	1	June 2020	Dive Crescent, NZ	Chemical analysis	2.59	0.190
	1	July 2021	Dive Crescent, NZ	Chemical analysis	2.98	0.175
	1	July 2021	Dive Crescent, NZ	Cytotoxicity assay	2.16	0.144
C. amoenum eggs	1 coil	Spawned (laboratory), June 2020		Chemical analysis	0.29	0.037
	1 coil	Spawned (laboratory), December 2020		Cytotoxicity assay	0.62	0.038
Dysidea teawanui	-	December 2021	Dive Crescent, NZ	Chemical analysis	260.00	9.250
	-	April 2023	Dive Crescent, NZ	Cytotoxicity assay	120.44	2.795

7.4.3 *Goniobranchus aureomarginatus* and *D.* cf. *dendyi*

To investigate the predator-prey relationship between *Goniobranchus aureomarginatus* and *D.* cf. *dendyi*, samples were collected and extracted as shown in Table 18 and Table 43.

Table 43: Collection and extraction of samples for the investigation of a predator-prey relationship between *Goniobranchus aureomarginatus* and *Dictyodendrilla* cf. *dendyi.*

Sample	Specimens	Collection date	Location	Use	Wet weight (g)	Crude extract (g)
G. aureomarginatus	8	December 2021	Dive Crescent	Chemical analysis	8.8 g	0.603
	6	December 2021	Dive Crescent	Chemical analysis	Viscera: 1.3	0.106
					Mantle: 0.7	0.062
	1	October 2022	Dive Crescent	Cytotoxicity assay	Viscera: 0.3	0.039
					Mantle: 0.1	0.011
	1	October 2022	Dive Crescent	Cytotoxicity assay	0.4	0.047
	1	January 2023	Dive Crescent	Morphological analysis		
Eggs	1 coil	Spawned (laboratory), December 2022		Chemical analysis and cytotoxicity	0.5	0.020
D.* cf. *dendyi	-	December 2021	Dive Crescent	Chemical analysis	80.4	3.149 (lyophilised)
	-	March, October and December	Dive Crescent	Chemical analysis	417.8	13.269 (lyophilised)

7.5 Isolation of secondary metabolites

7.5.1 Isolation of two brominated alkaloids from *Amathia gracei*

A sample of *A. gracei* was collected by hand using SCUBA-diving from Tauranga harbour in 2014 by Christopher Battershill. The sample was exhaustively extracted using the general extraction methodology described above in Section 7.1.4 and the resulting crude extract (6.40 g) was purified by reversed phase bench column chromatography using the methodology described in Section 7.1.6. Fraction 4 (476.3 mg), that eluted with H_2O/MeOH (3:7) was analysed by LC-MS using the methodology described in Section 7.1.11, except for the use of an event time of 1 s, a scanning range between 200 and 800 *m/z* and a gradient elution of H_2O/ACN (both containing 0.1 % FA) over 70 minutes (Figure 102). The LC-MS chromatogram showed the presence of a dibrominated compound at *m/z* 324. A portion (5 mg) of the fraction was analysed by HR-ESI-MS and NMR in chloroform-*d* to identify convolutamine L (**94**).

Convolutamine L (**94**): dark yellow amorphous solid; ^{1}H and ^{13}C NMR, Table 1, page 46; HR-ESI-MS *m/z* 323.9704 $[M + H]^+$ (calculated for $C_{10}H_{14}Br_2NO$, 323.9417). All spectroscopic data were in agreement with those reported.[212]

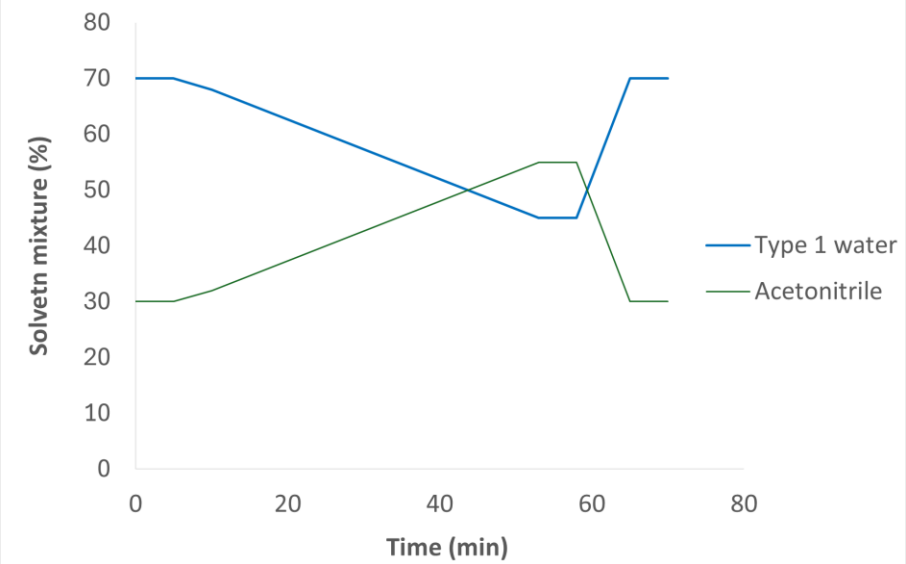

Figure 101: Gradient of both aqueous (Type 1 water) and organic (acetonitrile) mobile phases used for the analysis of the fraction of *Amathia gracei.*

7.5.2 Isolation of cinnamolide from *Dendrodoris krusensternii*

A specimen of *D. krusensternii* was collected by hand by Warrick Powrie using SCUBA-diving from Bridge Mount, Otago in 2020. The specimen (45.7 g) was extracted using the general extraction methodology described above in Section 7.1.4. The resulting crude extract (1.58 g) was purified by reversed phase bench column chromatography (20 g) using the methodology described in Section 7.1.6. The fraction that eluted with 100 % MeOH (21.5 mg) was further purified on normal phase chromatography (6.7 g) with a gradient of DCM and MeOH to afford cinnamolide (**122**) (0.2 mg) from the fraction eluting with DCM/MeOH (99:1).

Cinnamolide (**122**): white amorphous solid (0.2 mg); ^{1}H and ^{13}C NMR, Table 3, page 57; ESI(+)MS *m/z* 257 $[M + Na]^+$, 491 $[2M + Na]^+$; HR-ESI-MS *m/z* 257.1291 $[M + Na]^+$ (calculated for $C_{15}H_{22}O_2Na$, 257.1517). All spectroscopic data were in agreement with those reported.[239]

7.5.3 Isolation of two drimane sesquiterpenes from *Dendrodoris nigra*

A yellow egg mass belonging to *Dendrorodis nigra* was collected by hand by Lauren Gris in March 2021 from Pahoia beach. The specimen (1.38 g) was extracted using the general extraction methodology described in Section 7.1.4. The resulting crude extract (106.2 mg) was purified by reversed phase bench column chromatography (20 g) using the methodology described in Section 7.1.6. The fraction that eluted with 100 % MeOH afforded 7-deacetoxy-olepupuane (**124**) (2.7 mg), while the fraction that eluted with MeOH/DCM (4:6) afforded drimane esters (**125**) (2.6 mg).

7-Deacetoxy-olepupuane (**124**): white amorphous solid (2.7 mg); ^{1}H and ^{13}C NMR, Table 5, page 64; ESI(+)MS *m/z* 301 $[M + Na]^+$, 579 $[2M + Na]^+$; HR-ESI-MS *m/z* 301.1056 $[M + Na]^+$ (calculated for $C_{17}H_{26}O_3Na$, 301.1780). All spectroscopic data were in agreement with those reported.[244]

Drimane esters (**125**): off-white amorphous solid (2.6 mg); ^{1}H and ^{13}C NMR, Table 6, page 66; ESI(+)MS *m/z* 525 $[M + Na]^+$. All spectroscopic data were in agreement with those reported.[247]

7.5.4 Isolation of polymeric 3-alkyl pyridinium salt from *Aphelodoris luctuosa*

A specimen of *A. luctuosa* was collected by hand using SCUBA-diving from Motuputa Island, Bay of Plenty in August 2021 by Lauren Gris. The specimen (8.3 g) was extracted using the general extraction methodology described in Section 7.1.4. The resulting crude extract (430 mg) was purified by reversed phase bench column chromatography (20 g) using the methodology described in Section 7.1.6. The fraction that eluted with H_2O/MeOH 3:7 afforded 3-PAPS (**146**) (18.7 mg).

The egg mass (2.2 g) spawned in June 2021 by the *A. luctuosa* specimen mentioned above was extracted using the general extraction methodology described in Section 7.1.4. The resulting crude extract (146 mg) was purified on reversed phase C18 bench column chromatography (20 g) following the methodology described in Section 7.1.6. The fraction that eluted with H_2O/MeOH 3:7 also afforded compound (**146**) (24.4 mg).

Polymeric 3-alkyl pyridinium salt (**146**): yellow orange product (18.7 mg); ^{1}H and ^{13}C NMR, Table 7, page 77; ESI(+)MS *m/z* 190 $[M + H]^+$, 284 $[3M^{2+}/2]^+$, 379 $[2M^+]^+$, 568 $[3M^{2+}]^+$; HR-ESI-MS *m/z* 190.1409 $[M + H]^+$ (calculated for $C_{13}H_{20}N$, 190.1596). All spectroscopic data were in agreement with those reported.[231,288]

7.5.5 Isolation of 5α,8α-epidioxy-24-methylcholesta-6-diene-3β-ol from *Dysidea teawanui*

A specimen of *Dysidea teawanui* was collected by Lauren Gris from Dive Crescent using SCUBA-diving in January 2022. The specimen (260 g) was extracted using the general extraction methodology described in Section 7.1.4. The resulting crude extract was then lyophilised to afford 9.25 g of dry powder, which was divided into two parts. One part (4.4 g) was purified by reversed phase bench column chromatography (20 g) using the methodology described in Section 7.1.6. The fraction that eluted with 100% MeOH (72.3 mg) was further purified on normal phase chromatography using a gradient of 100% DCM, to 100% EtOAc, to 100% MeOH. The fraction that eluted with DCM/EtOAc (7:3) afforded ergosterol peroxide, 5α,8α-epidioxy-24-methylcholesta-6, 22-dien-3β-ol (**186**) (3.1 mg).

Two specimens of *C. amoenum* were collected in June 2020 and July 2021 by Lauren Gris at Dive Crescent, Tauranga by SCUBA-diving. Both specimens were separately extracted, and the two crude extracts obtained (190 mg and 175 mg, Table 41) were purified on reversed phase C18 bench column chromatography following the methodology described in Section 7.1.6. Traces of ergosterol peroxide (**186**) were detected by ^{1}H NMR spectroscopy in chloroform-*d* in several fractions from both extracts eluting with MeOH/DCM (9:1) to MeOH/DCM (1:1).

Ergosterol peroxide, 5α,8α-epidioxy-24-methylcholesta-6-diene-3β-ol (**186**)**:** $[\alpha]^{20}_{D}$ -30.4° ($CHCl_3$); ^{1}H and ^{13}C NMR, Table 17, page 126; ESI(+)MS *m/z* 429 $[M+H]^+$; HR-ESI-MS *m/z* 429.4499 $[M + H]^+$ (calculated for $C_{28}H_{45}O_3$, 429.3369). All spectroscopic data were in agreement with those reported.[366]

7.5.6 Isolation of metabolites from *Dictyodendrilla* cf. *dendyi*

Initial extraction of *D.* cf. *dendyi*

A specimen of *D.* cf. *dendyi* was collected by hand by SCUBA-diving in December 2021 at Dive Crescent, Tauranga (GPS coordinate in Table 39). The specimen (80 g) was extracted using the general extraction methodology described in Section 7.1.4. The resulting crude extract was then lyophilised to afford 3.1 g of dry powder, which was purified by reversed phase bench column chromatography (50 g) using the methodology described in Section 7.1.6.

The fraction that eluted with H_2O/MeOH (1:1) (211.9 mg) was further purified on Sephadex LH-20 (150 g) with 100% MeOH. Fractions 11 to 15 were combined based on TLC and ESI-MS analyses, prior to being further purified on Sephadex LH-20 with H_2O/MeOH (1:1) to afford the known compound dictyodendrin D (**210**) (3.3 mg) in fractions 7 and 8.

The fraction that eluted with H_2O/MeOH (3:7) (77.2 mg) from the C18 bench column was further purified on Sephadex LH-20 (150 g) with 100% MeOH. Based on TLC and ESI-MS analyses, fractions 14 and 15 were combined, and fractions 2 to 6 were also combined separately. Fractions 14 and 15 (14.3 mg) were further purified on Sephadex LH-20 with H_2O/MeOH (1:1) to afford the known compound dictyodendrin C (**209**) (9.5 mg) in fractions 4 to 12. Fractions 2-6 (11.6 mg) were also further purified on Sephadex LH-20 (30 g) with H_2O/MeOH (1:1) to afford the new compound denigrin L (**266**) (1.2 mg).

Dictyodendrin C (**209**)**:** brown-yellow, amorphous solid; ^{1}H and ^{13}C NMR, Table 20, page 140; ESI(+)MS *m/z* 681 $[M + Na]^+$, ESI(-)MS *m/z* 635 $[M - Na]^-$; HR-ESI-MS *m/z* 635.1803 $[M - Na]^-$ (calculated for $C_{34}H_{23}N_2O_9S$, 635.1124). All spectroscopic data were in agreement with those reported.[382]

Dictyodendrin D (**210**)**:** brown-yellow, amorphous solid; ^{1}H and ^{13}C NMR, Table 21, page 142; ESI(+)MS *m/z* 783 $[M+Na]^+$, ESI(-)MS *m/z* 737 $[M - Na]^-$, 357 $[M/2-Na]^-$; HR-ESI-MS *m/z* 737.0445 $[M - Na]^-$ (calculated for $C_{34}H_{22}N_2O_{12}S_2Na$, 737.0512). All spectroscopic data were in agreement with those reported.[382]

Denigrin L (**266**): light blue amorphous solid; UV (MeOH) λ_{max} (log ε) 223 nm (4.35), 277 (4.00) nm; IR (MeOH) ν_{max} 3367, 1579, 1508, 1414, 1355, 1236, 1169 cm^{-1}; ^{1}H and ^{13}C NMR, Table 37, page 196; ESI(+)MS *m/z* 810 $[M + Na]^+$; ESI(-)MS *m/z* 370 $[M/2 - Na]^-$; 764 $[M - Na]^-$; HR-ESI-MS *m/z* 764.1225 $[M - Na]^-$ calculated for $C_{38}H_{31}NO_{11}S_2Na$, 764.1242).

Large scale extraction of *D.* cf. *dendyi*

Other specimens of *D.* cf. *dendyi* were collected by hand by Lauren Gris using SCUBA-diving in March, June and October 2022 at Dive Crescent, Tauranga and kept frozen until extraction. The specimens (418 g) were extracted using the general extraction methodology described in Section 7.1.4. The resulting crude extract was then lyophilised to afford 13.3 g of dry powder, which was divided into three equal parts. Each part was purified separately by reversed phase bench column chromatography (50 g) using the methodology described in Section 7.1.6. Fractions that eluted with similar solvent ratios and that displayed similar TLC profiles were then recombined, leading to seven different fractions (F1-F7), as displayed in Appendices C.4, C.5 and D.1, and were processed as follows:

Fraction 1 (537 mg) was further purified by reversed phase bench column chromatography (20 g) using the methodology described in Section 7.1.6. The fraction eluting with H_2O/MeOH (4:6) (57.3 mg) was further purified on Sephadex LH-20 with H_2O/MeOH (1:1). Fraction 10 from this column afforded the new compound denigrin J (**264**) (2.1 mg), while fractions 18 and 19 were recombined (3 mg) based on TLC and ESI-MS analyses and were further purified on Sephadex LH-20 with H_2O/MeOH (7:3). Fraction 10 from the second LH-20 column afforded dictyodendrin B (**208**) (0.2 mg) while fractions 13 and 14 afforded the known compound

denigrin G (**227**) (1.5 mg). From the initial C18 bench column chromatography on fraction 1, the fraction eluting with H_2O/MeOH (3:7) (25.4 mg) was further purified on Sephadex LH-20 with H_2O/MeOH (1:1). Based on TLC and ESI-MS analyses, fraction 11 from this column was recombined with two other fractions from other columns as displayed in Appendix C.6 and the mixture (7.8 mg) was further purified on Sephadex LH-20 with H_2O/MeOH (3:7). Fractions 19 and 20 from the second LH-20 column were recombined to afford the known compound dactylpyrrole A (**225**) (1.5 mg). Finally, from the initial C18 bench column chromatography on fraction 1, the fraction eluting with H_2O/MeOH (1:1) (60.8 mg) was further purified on Sephadex LH-20 (150 g) with H_2O/MeOH (1:1). Fractions 9 and 10 from this column were combined (33.9 mg) based on TLC analyses and were further purified on Sephadex LH-20 with H_2O/MeOH (1:1) to afford the impure pyrrolo[2,3-c]carbazole spirolactone 1a (**199**) (0.7 mg).

Fraction 2 from the initial C18 column (233 mg) was further purified by reversed phase bench column chromatography (20 g) using the methodology described in Section 7.1.6. Three fractions eluting from H_2O/MeOH (1:1) and H_2O/MeOH (3:7) (105.9 mg) were combined based on TLC and ESI-MS analyses and were further purified on Sephadex LH-20 with H_2O/MeOH (1:1) to afford the new compound denigrin K (**265**) in fraction 2 (1.4 mg).

Fraction 3 from the initial C18 column (179 mg) was further purified by reversed phase bench column chromatography (20 g) using the methodology described in Section 7.1.6. The fraction eluting with H_2O/MeOH (3:7) (74.1 mg) was further purified on Sephadex LH-20 (150 g) with MeOH 100% and fraction 7 from this column (3.2 mg) was then further purified on Sephadex LH-20 (30 g) with H_2O/MeOH (3:7) to afford the known compound lamellarin O1 (**228**) (1.7 mg) in fraction 5.

Fraction 4 from the initial C18 column (278 mg) was further purified by reversed phase bench column chromatography (20 g) using the methodology described in Section 7.1.6. The fraction eluting with H_2O/MeOH (1:9) (42.7 mg) was further purified on Sephadex LH-20 (30 g) with MeOH 100% and fraction 12 from this column afforded the known compound denigrin E (**226**) (4.3 mg).

Fraction 5 from the initial C18 column (264 mg) was further purified by reversed phase bench column chromatography (20 g) using the methodology described in Section 7.1.6. The fraction eluting with H_2O/MeOH (1:9) (18.8 mg) was further purified on Sephadex LH-20 (30 g) with

MeOH 100%. Fractions 4 to 6 from this column were combined based on TLC and ESI-MS analyses to afford the known compound dictyodendrin F (**212**) (1.6 mg).

Several early eluting fractions from the initial C18 bench columns on fraction 1 to 7 (23 mg) and from several Sephadex LH-20 purifications displayed similar TLC and ESI-MS profiles and were combined (23 mg) before being further purified on Sephadex LH-20 (30 g) with H_2O/MeOH (3:7). Based on TLC, NMR spectroscopy and ESI-MS analyses, fractions 26 to 30 contained the same 1:1 mixture of denigrin H (**262**) and denigrin I (**263**) (3.4 mg) and the fractions were combined. The purification of the mixture was conducted by HPLC using a Phenomenex Luna C18 column (5 µ, 100 Å, 150 × 4.6 mm, kept at 40 °C) with a gradient elution of H_2O/MeOH (60:40 – 47:53, v/v, containing 0.1 % FA) over 34 minutes at 1 mL min^{-1} using a PDA detector at 220 nm (Figure 103) to obtain denigrin H (**262**) (1.2 mg) and I (**263**) (0.8 mg).

As a general note, fractions containing denigrin J (**264**), K (**265**) or L (**266**) were stored dry in vials conditioned under nitrogen gas due to these compounds being prone to oxidative rearrangement. For NMR analysis, the compounds were dissolved in methanol-d_4, placed into NMR tubes conditioned under nitrogen gas and kept in solution for a minimal amount of time.

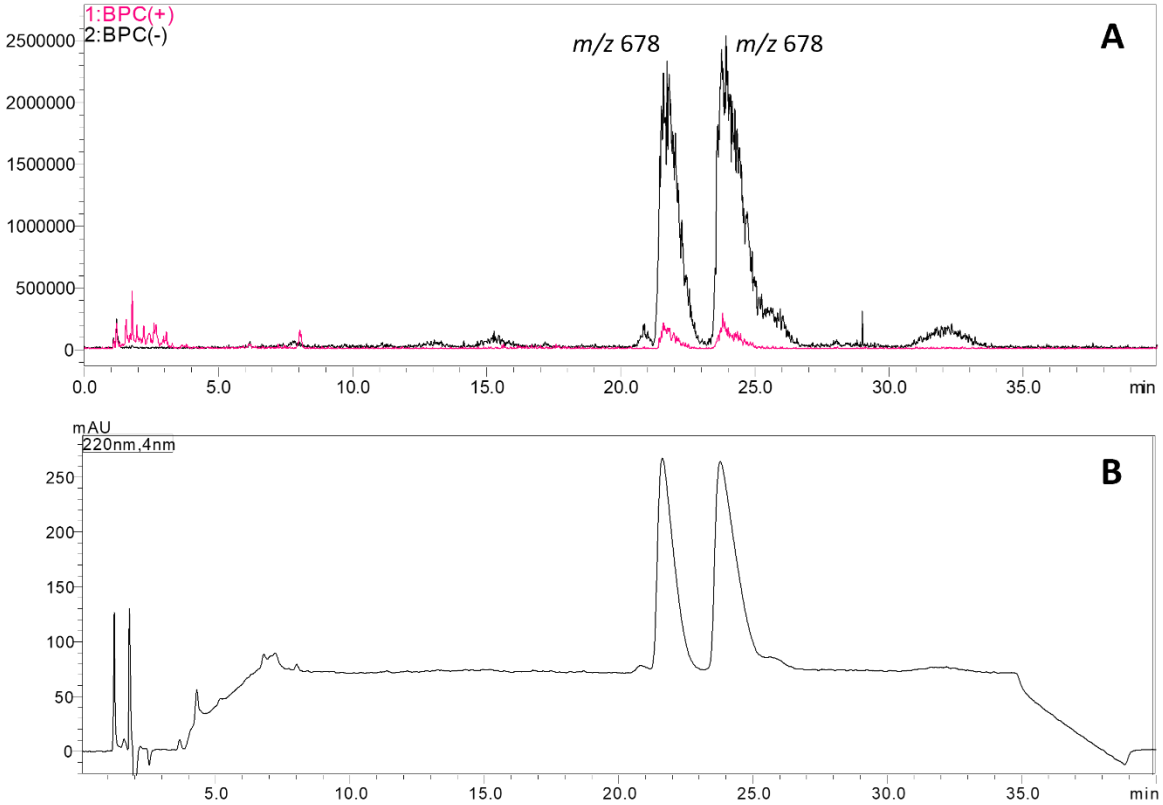

Figure 102: A- LC-MS chromatogram showing the resolution of both peaks corresponding to denigrin H (**262**) (right) and I (**263**) (left). B- PDA chromatogram at 220 nm for the separation of denigrin H (**262**) (right) and I (**263**).

The separation trees for the isolation of the compounds below are displayed in Appendices C.6, C.7 and D.2.

Dictyodendrin F (**212**)**:** greenish brown, amorphous solid; ^{1}H and ^{13}C NMR, Table 22, page 144; ESI(+)MS *m/z* 579 $[M + Na]^+$, 1135 $[2M + Na]^+$, ESI(-)MS *m/z* 555 $[M - H]^-$, 1111 $[2M - H]^-$; HR-ESI-MS *m/z* 555.1525 $[M - Na]^-$ (calculated for $C_{34}H_{23}N_2O_6$, 555.1556). All spectroscopic data were in agreement with those reported.[390]

Dictyodendrin B (**208**)**:** yellow, amorphous solid; ^{1}H NMR, Table 23, page 146; ESI(+)MS *m/z* 787 $[M + Na]^+$, ESI(-)MS *m/z* 370 $[M/2 - H]^-$; 741 $[M - Na]^-$; HR-ESI-MS *m/z* 741.1316 $[M - H]^-$ (calculated for $C_{41}H_{29}N_2O_{10}S$, 741.1553). All spectroscopic data were in agreement with those reported.[390]

Dactylpyrrole A (**225**)**:** yellow, amorphous solid; ^{1}H NMR, Table 24, page 147; ESI(+)MS *m/z* 530 $[M + Na]^+$, 1037 $[2M + Na]^+$, ESI(-)MS *m/z* 506 $[M - H]^-$, 1013 $[2M - H]^-]^-$; HR-ESI-MS *m/z* 506.1216 $[M - H]^-$ (calculated for $C_{31}H_{24}NO_6$, 506.1604). All spectroscopic data were in agreement with those reported.[392]

Denigrin E (**226**): magenta, amorphous solid; ^{1}H and ^{13}C NMR, Table 25, page 148; ESI(+)MS *m/z* 584 $[M + H]^+$, 606 $[M + Na]^+$, 1189 $[2M + Na]^+$; ESI(-)MS *m/z* 582 $[M - H]^-$, 1165 $[2M - H]^-$; HR-ESI-MS *m/z* 582.1633 $[M - H]^+$ (calculated for $C_{38}H_{34}NO_5$, 582.2280). All spectroscopic data were in agreement with those reported.[392]

Denigrin G (**227**): orange, amorphous solid; ^{1}H and ^{13}C NMR, Table 26, page 149; ESI(+)MS *m/z* 532 $[M + Na]^+$, 1041 $[2M + Na]^+$; ESI(-)MS *m/z* 508 $[M - H]^-$, 1041 $[2M - H]^-$; HR-ESI-MS *m/z* 508.1843 $[M - H]^-$ (calculated for $C_{31}H_{26}NO_6$, 508.1760). All spectroscopic data were in agreement with those reported.[392]

Lamellarin O1 (**228**)**:** ^{1}H and ^{13}C NMR, Table 27, page 151; ESI(+)MS *m/z* 466 $[M + Na]^+$, 909 $[2M + Na]^+$, ESI(-)MS *m/z* 442 $[M - H]^-$, 885 $[2M - H]^-$; HR-ESI-MS *m/z* 442.0991 $[M - H]^-$ (calculated for $C_{26}H_{21}NO_6$, 443.1369). All spectroscopic data were in agreement with those reported.[393]

Pyrrolo[2,3-c]carbazole spirolactone 1a (**199**)**:** ESI(+)MS *m/z* 843 $[M + Na]^+$, ESI(-)MS *m/z* 376 $[(M – Na)/2]^-$, 797.1284 $[M - Na]^-$; HR-ESI-MS *m/z* 797.1284 $[M - Na]^-$ (calculated for $C_{43}H_{29}N_2O_{12}S$, 797.1441). All spectroscopic data were in agreement with those reported.[379]

Denigrin H (**262**): light yellow amorphous solid; $[\alpha]^{20}_D$ 0° (MeOH); UV (MeOH) λ_{max} (log ε) 226 nm (4.42), 279 (4.09) nm; IR (MeOH) ν_{max} 3369, 1663, 1590, 1515, 1442, 1351, 1238, 1175 cm^{-1}; ^{1}H and ^{13}C NMR, Table 33, page 183; ESI(+)MS *m/z* 724 $[M + Na]^+$; ESI(-)MS *m/z* 678 $[M - Na]^-$, 700 $[M - H]^-$, 1379 $[2M - Na]^-$; HR-ESI-MS *m/z* 678.1803 $[M - Na]^-$ (calculated for $C_{38}H_{32}NO_9S$, 678.1803).

Denigrin I (**263**) : light yellow amorphous solid; $[\alpha]^{20}_D$ 0° (MeOH); UV (MeOH) λ_{max} (log ε) 225 nm (4.38), 278 (4.00) nm; IR (MeOH) ν_{max} 3369, 1665, 1593, 1514, 1440, 1353, 1240, 1173 cm^{-1}; ^{1}H and ^{13}C NMR, Table 34, page 186; ESI(+)MS *m/z* 724 $[M + Na]^+$; ESI(-)MS *m/z* 678 $[M - Na]^-$, 700 $[M - H]^-$; HR-ESI-MS *m/z* 678.1807 $[M - Na]^-$ (calculated for $C_{38}H_{32}NO_9S$, 678.1803).

Denigrin J (**264**): dark green amorphous solid; UV (MeOH) λ_{max} (log ε) 224 nm (4.53), 276 (4.10) nm; IR (MeOH) ν_{max} 3246, 1594, 1510, 1436, 1360, 1230, 1169 cm^{-1}; ^{1}H and ^{13}C NMR, Table 35, page 189; ESI(+)MS *m/z* 708 $[M + Na]^+$; ESI(-)MS *m/z* 662 $[M - Na]^-$; HR-ESI-MS *m/z* 662.1857 $[M - Na]^-$ (calculated for $C_{38}H_{32}NO_8S$, 662.1849).

Denigrin K (**265**): light green amorphous solid; UV (MeOH) λ_{max} (log ε) 224 nm (4.40), 277 (4.05) nm; IR (MeOH) ν_{max} 3365, 1594, 1513, 1431, 1356, 1238, 1171 cm^{-1}; ^{1}H and ^{13}C NMR, Table 36, page 192; ESI(+)MS *m/z* 708 $[M + Na]^+$; ESI(-)MS *m/z* 662 $[M - Na]^-$; HR-ESI-MS *m/z* 662.1855 $[M - Na]^-$ (calculated for $C_{38}H_{32}NO_8S$, 662.1849).

Processing of NMR spectra

The baselines of the ^{13}C NMR spectra of denigrins I (**263**), J (**264**) and K (**265**) were corrected with a polynomial correction and the zero-fill value was increased from 1 to 30 to resolve close signals. The baseline of the ^{13}C NMR spectrum of denigrin H (**262**) was corrected with a piecewise linear correction. The line broadening on the ^{13}C NMR spectrum for denigrin K (**265**) was reduced from 2 to 1 Hz to enable resolution of the overlapping signals at 130.9 ppm and that on the ^{13}C NMR spectrum for denigrin I (**263**) was also reduced from 1.4 to 0.4 Hz to enable resolution of the signals at 128.40 and 128.41 ppm.

7.5.7 Isolation of metabolites from *Goniobranchus aureomarginatus*

Whole-body specimens

Fifteen specimens of *G. aureomarginatus* were collected by Lauren Gris from Dive Cresent, Tauranga by hand using SCUBA-diving in December 2021. The specimens (8.8 g) were extracted using the general extraction methodology described in Section 7.1.4. The resulting crude extract (602.8 mg) was purified by bench column chromatography on reversed phase C18 (20 g) following the methodology described in Section 7.1.6. The fraction that eluted with H_2O/MeOH (1:9) (7.1 mg) was further purified on Sephadex LH-20 with H_2O/MeOH (7:3). Fraction 6 afforded dictyodendrin C (**209**) (0.5 mg) while fractions 14 and 15 were combined to afford dictyodendrin F (**212**) (0.5 mg).

The fraction eluting with MeOH 100% (46.4 mg) from the C18 bench column was further purified by bench column chromatography on reversed phase C18 (20 g) following the methodology described in Section 7.1.6. The fraction eluting with MeOH 100% afforded a mixture (1 mg) of gracilin A (**244**) and 6α,15α,16α-triacetoxyspongian (**236**).

Dictyodendrin C (**209**)**:** brown-yellow, amorphous solid; ^{1}H NMR, Table 28, page 159; ESI(-)MS *m/z* 635 $[M - Na]^-$. All spectroscopic data were in agreement with those reported from *D*. cf. *dendyi* (Section 7.5.6) and from the literature.[382]

Dictyodendrin F (**212**)**:** greenish brown, amorphous solid; ^{1}H NMR, Table 29, page 160; ESI(+)MS *m/z* 579 $[M + Na]^+$, ESI(-)MS *m/z* 555 $[M - H]^-$. All spectroscopic data were in agreement with those reported from *D.* cf. *dendyi* (Section 7.5.6) and from the literature.[390]

Gracilin A (**244**)**:** ^{1}H NMR, Table 31, page 162; ESI(+)MS *m/z* 413 $[M + Na]^+$, 331 $[M - AcOH]^+$, 288 $[M – AcOH – CH_2CO]^+$, 271 $[M – 2AcOH]^+$. All spectroscopic data were in agreement with those reported.[423]

6α,15α,16α-Triacetoxyspongian (**236**)**:** ^{1}H NMR, Table 31, page 162; ESI(+)MS *m/z* 487 $[M + Na]^+$, 345 $[M – 2AcOH]^+$, 302 $[M – 2AcOH - CH_2CO]^+$, 285 $[M – 3AcOH]^+$. All spectroscopic data were in agreement with those reported.[414]

Dissected specimens

SIx specimens of *G. aureomarginatus* were collected by Lauren Gris from Dive Cresent, Tauranga by hand using SCUBA-diving in December 2021. The specimens were dissected into mantles (0.73 g) and digestive glands with stomachs (1.26 g) following the methodology described in Section 7.1.2. The digestive glands with stomachs were extracted using the general extraction methodology described in Section 7.1.4. The resulting crude extract (106.2) mg was analysed by LC-MS using the general screening methodology described in Section 7.1.11, and showed the presence of 6α,15α,16α-triacetoxyspongian (**236**) and dictyodendrin F (**212**).

The extract was then purified by reversed phase C18 bench column chromatography on reversed phase C18 (20 g) following the methodology described in Section 7.1.6. The fraction that eluted with H_2O/MeOH (2:8) afforded a mixture of dictyodendrins C (**209**) and F (**212**) (0.5 mg).

The mantles were extracted using the general extraction methodology described in Section 7.1.4. The resulting crude extract (61.5 mg) was then purified by reversed phase C18 bench column chromatography on (20 g) following the methodology described in Section 7.1.6. The fraction (9.6 mg) eluting with DCM 100% was analysed by LC-MS using the general screening methodology described in Section 7.1.11, which indicated the presence of gracilin A (**244**) and 6α,15α,16α-triacetoxyspongian (**236**).

Gracilin A (**244**)**:** ESI(+)MS *m/z* 413 $[M + Na]^+$, 331 $[M - AcOH]^+$, 288 $[M – AcOH – CH_2CO]^+$, 271 $[M – 2AcOH]^+$. All spectrometric data were in agreement with those reported.[423]

6α,15α,16α-Triacetoxyspongian (**236**)**:** ESI(+)MS *m/z* 487 $[M + Na]^+$, 345 $[M – 2AcOH]^+$, 302 $[M – 2AcOH - CH_2CO]^+$, 285 $[M – 3AcOH]^+$. All spectrometric data were in agreement with those reported.[414]

7.6 Quantitative NMR spectroscopy

Five specimens of *A. luctuosa* were collected by Lauren Gris by hand using SCUBA-diving in March 2021 from Salisbury Wharf, Tauranga. Each specimen was dissected between mantle and digestive glands with stomach using the methodology described in Section 7.1.2. Each part was then extracted using the methodology described in Section 7.1.4 to afford ten crude extracts, which were then lyophilised (Table 44).

Table 44: Masses of *Aphelodoris luctuosa* samples and resulting crude extracts.

Specimen	Body part	Mass of sample (g)	Mass of crude extract (mg)
1	mantle	1.2423	60.4
	digestive glands with stomach	0.1371	157.8
2	mantle	1.1962	72.2
	digestive glands with stomach	0.6067	55.7
3	mantle	0.1193	19.0
	digestive glands with stomach	0.1105	20.5
4	mantle	0.4100	58.1
	digestive glands with stomach	0.5375	72.9
5	mantle	0.2578	37.3
	digestive glands with stomach	0.5695	65.4

The internal standard for the quantitative NMR experiments, maleic acid, was kept in a desiccator. Sample preparation was conducted using a four-digit high precision balance. The appropriate amount of maleic acid was measured into a vial, followed by addition of the appropriate amount of crude extract to the same vial. 1 ampoule of D_2O (0.75 mL) was then added to the vial and the mixture was transferred to an NMR tube.

To determine the appropriate ratio of crude extract *versus* internal standard, the crude extract of the digestive gland with stomach of specimen 1 was used. The first trial sample was prepared using 6.1 mg of maleic acid and 5.5 mg of crude extract but ^{1}H NMR spectroscopic analysis indicated that intensity of signals corresponding to the crude extract was too low compared to the intensity of the peak corresponding to the maleic acid. A second trial sample of maleic acid (2.6 mg) and crude extract (19.9 mg) gave better results but the intensity of the signals corresponding to the crude extract were still too low compared to those of the internal

standard. A third trial sample of maleic acid (1.1 mg) and crude extract (22.8 mg) gave appropriate results. These proportions were selected to prepare the remaining samples.

An inversion recovery experiment was run on one of the samples to obtain the t1 and 90° pulse values. The values were obtained as follows: t1 = 8.767612 s and 90° pulse = 9.38635 µs. The relaxation delay was obtained by multiplying the t1 value by 5 to allow for complete relaxation of the nuclei between pulses (relaxation delay = 43.83806 s). Each sample was run in duplicate with 16 scans recorded per experiment.

The NMR spectra were processed using the Lorentzian function and the integral values were added accordingly for each signal of interest. The formula displayed in Chapter 2, Section 2.6.4 was used to calculate the purity of each crude extract which was then converted to obtain the mass concentration of the pyridinium salt within each of the crude extracts (mg of compound (**146**) per g of crude extract), as displayed in Table 45.

Table 45: Sample preparation and concentration of compound (**146**) within *Aphelodoris luctuosa* samples.

		Mass (mg)		
			Sample preparation for NMR experiments	
Specimen	**Body part**	**Crude extract**	**Internal standard**	**Crude extract**
1	mantle	60.4	1.2	21.7
	internal organs	157.8	1.4	24.4
2	mantle	72.2	1.1	20.8
	internal organs	55.7	1.0	20.6
3	mantle	19.0	0.9	14.5
	internal organs	20.5	1.1	15.8
4	mantle	58.1	1.0	23.2
	internal organs	72.9	1.2	22.4
5	mantle	37.3	1.3	23.6
	internal organs	65.4	0.9	21.8

[a] internal organs refers to digestive gland and stomach

7.7 Cell culture and bioassay

The human cervical cancer cell line, HeLa, was used for the bioassays conducted during the course of this study and was purchased from the American Tissue Culture Collection (ATCC) (Number CCL-2). As a general note, a Sanyo™ incubator kept at 37°C with 5% CO_2 was used for cell culture and bioassays.

7.7.1 Reviving HeLa cervical cancer cells

A cryovial containing previously frozen HeLa human cervical cancer cells at passage 16 was taken from an -80°C freezer and placed in a Styrofoam box filled with ice. The cells were rapidly thawed by immersing the cryovial in a 37°C water bath for two minutes until only a small piece of ice remained. The cryovial was then transferred to a sterile tissue culture hood, where pre-warmed (37°C) complete growth media (2 mL) was carefully added and gently mixed using a pipette. The entire solution was transferred to a labelled T-25 flask and incubated. The following day, the cells were examined under a microscope to confirm their revival and adherence to the flask.

7.7.2 Culturing of cells

The cell culture experiments were carried out in a physical containment level two (PC2 facility). The cells were grown in Minimum Essential Medium (MEM, Gibco) supplemented with 100X units of penicillin/streptomycin (Gibco) and 10 % foetal bovine serum (FBS, Gibco). Culturing was carried out using T-25 and T-75 treated flasks (Biofil) in a standard humidified incubator (Sanyo™). The cells used for the experiments presented in this research were no more than ten passages from the original passage number. The media was replaced on alternate days.

7.7.3 Subculturing of cells

Subculturing of cells was performed approximately every 4 days when they reached near confluency (85 – 90 %) to keep cells growing under exponential phase. The old media was removed prior to addition of PBS (2 mL) (Gibco) to wash the cells. The PBS was then discarded, followed by addition of 0.25% prewarmed (37 °C) trypsin (5 mL) (Gibco). The flask was incubated for approximately 5 minutes or until detachment of cells. Prewarmed complete growth media (5 mL) was added to the cell solution to stop the reaction, followed by transfer to a 15 mL centrifuge tube and centrifugation in a Heraeus Megafuge 1.0 (5 minutes, at 200 rcf, at room temperature). The supernatant was removed prior to resuspending the cell pellet in an appropriate amount of prewarmed (37 °C) media. The solution was split and transferred accordingly to either T-25 or T-75 flasks. The cells were then replaced back in the incubator.

7.7.4 Cell counting and cell viability

Cells used for cell counting and viability assessment were taken after centrifugation when the cell pellet was resuspended in prewarmed media. Before sampling cells, the solution was mixed multiple times with a Pasteur pipette. Cell solution (50 µL) was pipetted out and transferred to a microcentrifuge tube, along with trypan blue (50 µL) for staining. The solution was then thoroughly mixed with a Pasteur pipette. The haemocytometer was cleaned with 70% ethanol, air dried and covered with a cover slip. The cell and trypan blue solution (10 µL) was then transferred to each chamber of the haemocytometer. Using the counting grid, cells were counted in each chamber within the four corner squares. The number was averaged by eight to obtain the estimated number of cells per square and the cell concentration obtained using the equation below (Equation 2). To obtain the total number of cells in the solution, the concentration calculated from Equation 2 was multiplied by the total volume of cell solution.

Equation 2 : Formula to calculate the concentration of cells using a haemocytometer.

$$Cell\ concentration\ (cells\ per\ mL) = Average\ cell\ number \times 2 \times 10^4$$

2 = dilution factor
10^4 = factor recommended by the manufacturer to account for the volume counted compared to the volume added

Trypan blue was used to assess the viability of the cells. In each of the squares counted mentioned above, the number of stained and unstained cells was recorded and the percentage viability calculated using the equation below (Equation 3). Only cells above 90% viability were used for the bioassay.

Equation 3 : Calculation of the percentage of cell viability using trypan blue.

$$\%\ cell\ viability = \left(\frac{Unstained\ cells}{Total\ cells}\right) \text{x } 100$$

7.7.5 Cytotoxic activity of eleven arylpyrrole alkaloids

MTT assay - method development

Based on the amount of compound isolated, the methodology development utilised the compound isolated in the highest quantity: dictyodendrin C (**209**). The methodology for the MTT assay was based on the protocol described for the cytotoxicity testing of dictyodendrins F-J (**212**), (**309**-**312**), respectively,[390] but the protocol was slightly adapted to suit the needs of this research. As such, after seeding, the cells were incubated for 24 hours instead of 18 hours to suit the timing of experimental work.

Five dilutions of dictyodendrin C (**209**) were prepared at concentrations between 125 and 2000 µM in 5% aqueous DMSO from a stock solution made at 1.444 x 10^4 µM (Table 46). After addition of 20 µL of each dilution in duplicate (or 5% aq DMSO for the solvent control) in 180 µL of adjusted media, the cells were incubated for 24 hours instead of 68 hours. The solution of MTT was freshly prepared to a concentration of 5 mg mL^{-1} in PBS and filter sterilised (0.45 µm). 10 µL of the solution was then added to each well. The solubilising solution was made up by dissolving SDS (10g) in sterile type 1 water (23 mL), followed by the addition of 1M HCl (1 mL) and glacial acetic acid to adjust pH to 4.7, and an aliquot (100 µL) was added to each well. Use of such solubilising solution required another hour of incubation time to fully dissolve the crystals, before the absorbance was measured on a plate reader at 570 nm, with a background absorbance reading at 655 nm.

Table 46: Calculations of dilutions for dictyodendrin C (**209**).

	Volume (µL)			
Concentration of dilution (µM)	Total dilution	Stock solution	5% aq DMSO	Concentration in well (20µl in 180µl media)
2000.0	1000.0	138.5	861.5	200.0
1000.0	1000.0	69.3	930.7	100.0
500.0	1000.0	34.6	965.4	50.0
250.0	1000.0	17.3	982.7	25.0
125.0	1000.0	8.7	991.3	12.5

Upon subtracting the background values from the readings at 570 nm, the absorbance values ranged from 0.01 to 0.04, which was not sufficient for data analysis. This may be because the cells were seeded at a concentration too low to accurately measure the metabolic activity. The seeding was conducted at a density of 2 000 cells per well, according to the protocol, although the cell line used here was different.[390] Comparison with another protocol which used HeLa cells for conducting a MTT assay,[438] indicated that the cells should be seeded at a higher concentration for the next trial.

The cell concentration was increased to 30 000 cells per well and the experiment repeated following the same methodology as described above, except that samples and controls were run in triplicate on each plate. Two different positive controls were also added. As such, dilutions of DMSO were prepared to obtain a final concentration in the wells of 1%, 5% and 10%. A sample of pure Peach ice solution was also diluted by a factor 10, 100 and 1000 in PBS to obtain three separate diluted samples. A higher concentration of dictyodendrin C (1444 µM in the well) was also tested to allow for the potential low cytotoxicity of compound (**209**) (Table 46).

Upon analysing the results, the absorbance readings subtracted from the background readings for compound (**209**) now ranged from 0.78 to 1.6 which was acceptable, confirming the need to use increased cell concentrations. The DMSO controls showed 98% inhibition for the 5% dilutions and 100% inhibition for the 10% dilutions. The Peach ice controls also succeeded by showing 97% inhibition for the 100-fold dilution and 100% for the 10-fold dilution. Relatively low % inhibition was obtained for the concentrations of compound (**209**) tested, therefore another higher concentration well (3609 µM in the well) was added on the plate for the next experiment.

With these parameters in hand, the protocol was repeated for dictyodendrin C (**209**) and was also carried out for the ten remaining samples. On account of the minimal amount of compounds isolated, the compounds to be tested were added in duplicate on each plate and two identical plates were run.

Selected protocol

Near confluent cells in log-phase were harvested and seeded evenly in 96-well cell culture plates (Biofil) at a density of 1.5×10^5 cells per mL, each well containing 200 µL of cell culture medium. Empty wells were filled with 200 µL of PBS. The plates were then incubated for 24 hours to allow for cell adhesion. The media was aspirated, and the cells were washed with PBS (200 µL) before adding adjusted media (150 or 180 µL) to cell wells. Compounds were dissolved in 5% aqueous DMSO (v/v) to prepare stock solutions (Table 47).

Table 47: Preparation of the stock solutions for each of the compounds tested in the MTT assay.

	Mass (g)	Molecular weight (g mol^{-1})	n (mol)	n (µmol)	Volume of DMSO added (mL)	Concentration stock solution (µM)
Dictyodendrin C	0.0095	658	1.44×10^{-5}	14.44	1.0	14437.69
Dictyodendrin D	0.0033	760	4.34×10^{-6}	4.34	0.4	10855.26
Dictyodendrin F	0.0014	556	2.52×10^{-6}	2.52	0.4	6294.96
Denigrin E	0.0043	583	7.38×10^{-6}	7.38	0.5	14751.29
Dactypyrrole A	0.0015	507	2.96×10^{-6}	2.96	0.4	7396.45
Lamellarin O1	0.0017	443	3.84×10^{-6}	3.84	0.4	9593.68
Denigrin H	0.0012	701	1.71×10^{-6}	1.71	0.4	4279.60
Denigrin I	0.0008	701	1.14×10^{-6}	1.14	0.25	4564.91
Denigrin J	0.0021	685	3.07×10^{-6}	3.07	0.40	7664.23
Denigrin K	0.0014	685	2.04×10^{-6}	2.04	0.40	5109.49
Denigrin L	0.0012	787	1.52×10^{-6}	1.52	0.40	3811.94

Five dilutions within the range of 125–2000 µM were then prepared from the stock solutions for each compound tested (Table 48). Two other concentrations were also tested by adding either 20 µL or 50 µL of each stock solution to the wells (Table 48).

Table 48: Dilution preparations for each pure compound tested in the MTT assay.

		Volume (µL)			Final concentration in well (µM)	
	Concentration of dilutions (µM)	**Total dilution**	**Stock solution**	**5% aq DMSO**	**20 µL of the stock solution, or dilution, in 180 µL media**	**50 µL of stock solution in 150 µL media**
Dictyodendrin D					1085.5	2713.8
	2000.0	100.0	18.4	81.6	200.0	
	1000.0	100.0	9.2	90.8	100.0	
	500.0	100.0	4.6	95.4	50.0	
	250.0	100.0	2.3	97.7	25.0	
	125.0	100.0	1.2	98.8	12.5	
Dictyodendrin F					629.5	1573.7
	2366.9	100.0	37.6	62.4	236.7	
	1183.5	100.0	18.8	81.2	118.3	
	591.7	100.0	9.4	90.6	59.2	
	295.9	100.0	4.7	95.3	29.6	
	151.1	100.0	2.4	97.7	15.1	
Denigrin E					1475.1	3687.8
	2000.0	100.0	13.6	86.4	200.0	
	1000.0	100.0	6.8	93.2	100.0	
	500.0	100.0	3.4	96.6	50.0	
	250.0	100.0	1.7	98.3	25.0	
	125.0	100.0	0.8	99.2	12.5	
Dactypyrrole A					739.6	1849.1
	2000.0	100.0	27.0	73.0	200.0	
	1000.0	100.0	13.5	86.5	100.0	
	500.0	100.0	6.8	93.2	50.0	
	250.0	100.0	3.4	96.6	25.0	
	125.0	100.0	1.7	98.3	12.5	
Lamellarin O1					959.4	2398.4
	1300.7	100.0	13.6	86.4	130.1	
	650.4	100.0	6.8	93.2	65.0	
	325.2	100.0	3.4	96.6	32.5	
	162.6	100.0	1.7	98.3	16.3	
	81.3	100.0	0.8	99.2	8.1	
Denigrin H					428.0	1069.9
	2000.0	100.0	46.7	53.3	200.0	
	1000.0	100.0	23.4	76.6	100.0	
	500.0	100.0	11.7	88.3	50.0	
	250.0	100.0	5.8	94.2	25.0	
	125.0	100.0	2.9	97.1	12.5	
Denigrin I					456.5	
	2000.0	100.0	43.8	56.2	200.0	
	1000.0	100.0	21.9	78.1	100.0	
	500.0	100.0	11.0	89.0	50.0	
	250.0	100.0	5.5	94.5	25.0	
	125.0	100.0	2.7	97.3	12.5	
Denigrin J					766.4	1916.1
	2000.0	100.0	26.1	73.9	200.0	
	1000.0	100.0	13.0	87.0	100.0	
	500.0	100.0	6.5	93.5	50.0	
	250.0	100.0	3.3	96.7	25.0	
	125.0	100.0	1.6	98.4	12.5	
Denigrin K					510.9	1277.4
	2000.0	100.0	39.1	60.9	200.0	
	1000.0	100.0	19.6	80.4	100.0	
	500.0	100.0	9.8	90.2	50.0	
	250.0	100.0	4.9	95.1	25.0	
	125.0	100.0	2.4	97.6	12.5	

		Volume (µL)			Final concentration in well (µM)	
	Concentration of dilutions (µM)	**Total dilution**	**Stock solution**	**5% aq DMSO**	**20 µL of the stock solution, or dilution, in 180 µL media**	**50 µL of stock solution in 150 µL media**
Denigrin L					381.2	953.0
	2000.0	100.0	52.5	47.5	200.0	
	1000.0	100.0	26.2	73.8	100.0	
	500.0	100.0	13.1	86.9	50.0	
	250.0	100.0	6.6	93.4	25.0	
	125.0	100.0	3.3	96.7	12.5	

Aliquots (20 or 50 µL) of each dilution, or of 5% aqueous DMSO for control wells, were added in duplicate. After 68 hours of incubation, the plates were centrifuged (80 rcf, for five minutes, at room temperature) before replacing the media with fresh media (200 µL) and 5 mg mL^{-1} MTT reagent (10 µL) (Sigma, USA). Following MTT addition, the plates were incubated for an additional 4 hours. The plates were centrifuged for 5 minutes more, and the MTT media was replaced with prewarmed solubilising solution (100 µL). Formazan crystals were dissolved by shaking on an Alphatech Torrey Pines orbital mixer for 5 minutes and the plates were further incubated for 30 minutes. Once homogenised, the samples were measured on a plate reader (Bio-Rad 680) at 570 nm, with a background absorbance reading at 655 nm, as outlined above.

Results analysis

To analyse the results, for each well, the readings from the background measurements at 655 nm were subtracted from the readings at 570 nm to obtain the optical density (OD) of the corrected samples. With the samples, controls and blanks run in duplicate on each 96-well plate, the absorbance values were then averaged accordingly. The average blank reading for the wells containing only media was subtracted from the other readings. Finally, the percentage cell inhibition for each of the averaged values was calculated using the equation below.[232]

Equation 4 : Formula for the calculation of the percentage of inhibition for the MTT assay.

$$\%\,\text{inhibition} = 100 - \left[\left(\frac{\text{OD corrected sample}}{\text{OD corrected solvent control}}\right)\text{x}100\right]$$

OD corrected samples = optical reading substracted from background measurement
OD corrected solvent control = optical reading of the solvent control (media and cells) substracted from background measurement.

The percentage inhibition obtained on both plates for each concentration and for each sample was averaged. The standard errors of the mean (SEM) from two replicates were calculated as the error bar of data. The IC_{50} value was obtained graphically with Microsoft Office Excel as the concentration of the compound required for 50% inhibition of the cancer cells.

7.7.6 Cytotoxicity screening of the crude extracts

The protocol for the cytotoxicity screening of crude extracts was closely related to the assay conducted on the arylpyrrole alkaloids, with the main change being the change of diluent from 5% aqueous DMSO to 100% MeOH to allow for greater solubility of the extracts and some of the pure compounds isolated.

Near confluent cells in log-phase (passage 24) were harvested and seeded evenly in 96-well cell culture plates (Biofil) at a density of 1.5×10^5 cells per mL, each well containing 200 µL of cell culture medium. Empty wells were filled with PBS (200 µL). The plates were then incubated for 24 hours to allow for cell adhesion. The media was aspirated, and the cells were washed with PBS (200 µL) before adding adjusted media (190 µL) to cell wells.

To prepare the stock solutions, each crude extract (4 mg) was dissolved in MeOH (1.75 mL) to obtain a concentration of 2286 µg mL^{-1}. The stock solution for the crude extract of *Polycera hedgpethi* was prepared by dissolving the crude extract (2 mg) in MeOH (1 mL) to obtain a concentration of 2000 µg mL^{-1}. The stock solution for cinnamolide (**122**) was prepared by dissolving compound (**122**) (0.2 mg) in MeOH (100 µL) to obtain a concentration of 2000 µg mL^{-1}. Five dilutions were then prepared from the stock solutions, as displayed in Table 49.

Table 49: Dilution preparations for each crude extract and pure compound tested in the MTT assay.

		Volume (µL)			
	Concentration of dilutions (µg mL^{-1})	**Total dilution**	**Stock solution**	**MeOH**	**Final concentration in well (µM) (10 µL of the stock solution in 190 µL media)**
General crude extracts					114.3
	1500	1000	656.3	343.8	75.0
	1000	1000	437.5	562.5	50.0
	500	1000	218.8	781.3	25.0
	250	1000	109.4	890.6	12.5
Polycera hedgpethi					114.3
	1500	25	16.4	8.6	75.0
	1000	25	10.9	14.1	50.0
	500	25	5.5	19.5	25.0
	250	25	2.7	22.3	12.5
Cinnamolide					100.0
	1500	25	16.4	8.6	75.0
	1000	25	10.9	14.1	50.0
	500	25	5.5	19.5	25.0
	250	25	2.7	22.3	12.5

Aliquots of each dilution and stock solutions, or of 100% MeOH for solvent controls, or of 5% aqueous DMSO for positive control wells (10 µL), were added in duplicate. The rest of the procedure was identical to the one used for the cytotoxicity assessment of the eleven arylpyrrole alkaloids described in Section 7.7.5, Subsection - Selected protocol.

The experiment was replicated for most of the samples using cells at passage 26 at 20 days interval to assess the reproducibility of the experiments. The results of the two replicates were then averaged to obtain the final results.

Appendices

Appendix A. ^{1}H NMR spectra relevant to Chapter 2 **250**

A.1. ^{1}H NMR spectrum (chloroform-d, 600 MHz) of convolutamine L (94) 250

A.2. ^{1}H NMR spectrum (chloroform-d, 600 MHz) of cinnamolide (122) 251

A.3. ^{1}H NMR spectrum (chloroform-d, 600 MHz) of 7-deacetoxy-olepupuane (124) 252

A.4. ^{1}H NMR spectrum (chloroform-d, 600 MHz) of drimane esters (125) 253

A.5. ^{1}H NMR spectrum (D_2O, 600 MHz) of 3-PAPS (146) 254

Appendix B. Complementary data for the feeding-choice experiments described in Chapter 3 **255**

B.1. *Polycera hedgpethi* – time spent on each prey (h) per specimen per individual experiment 255

B.2. *Ceratosoma amoenum* – time spent on each prey (h) per specimen per individual experiment 256

B.3. *Goniobranchus aureomarginatus* – time spent on each prey (h) per specimen per individual experiment 257

Appendix C. NMR spectra and separation trees relevant to Chapter 4 **258**

C.1. ^{1}H NMR spectrum (chloroform-*d*, 600 MHz) of ergosterol peroxide (186) 258

C.2. ^{1}H NMR spectrum (methanol-d_4, 600 MHz) of dictyodendrin C (209) 259

C.3. ^{1}H NMR spectrum (methanol-d_4, 600 MHz) of dictyodendrin D (210) 260

C.4. Fraction combinations (F1-F3) for the large scale *D*. cf. *dendyi* extract 261

C.5. Fraction combinations (F4-F5) for the large scale *D*. cf. *dendyi* extract 262

C.6. Isolation procedure for spirolactone 1a (199), dictyodendrin B (208), denigrin G (227) and dactylpyrrole A (225) 263

C.7. Isolation procedure for dictyodendrin F (212), denigrin E (226) and lamellarin O1 (228) 264

C.8. ^{1}H NMR spectrum (methanol-d_4, 600 MHz) of dictyodendrin F (212) 265

C.9. ^{1}H NMR spectrum (methanol-d_4, 600 MHz) of dactypyrrole A (225) 266

C.10. ^{1}H NMR spectrum (methanol-d_4, 600 MHz) of denigrin E (226) 267

C.11. ^{13}C NMR spectrum (methanol-d_4, 150 MHz) of denigrin E (226) 268

C.12. ^{1}H NMR spectrum (methanol-d_4, 600 MHz) of lamellarin O1 (228) 269

C.13. ^{1}H NMR spectrum (methanol-d_4, 600 MHz) of the mixture of gracilin A (244) and 6α,15α,16α- triacetoxyspongian (236) 270

Appendix D. Separation trees, NMR and HR-ESI-MS spectra relevant to Chapter 5 **271**

D.1. Fraction combinations (F6-F7) for the large scale *D.* cf. *dendyi* extract 271

D.2. Isolation procedure for denigrins H-K (262-265) _____272
D.3. HR-ESI-MS spectrum of denigrin H (262) in negative ion mode_____273
D.4. ^{1}H NMR spectrum (methanol-d_4, 600 MHz) of denigrin H (262)_____274
D.5. ^{13}C NMR spectrum (methanol-d_4, 150 MHz) of denigrin H (262) _____275
D.6. ^{13}C NMR spectrum expansion 1 (methanol-d_4, 150 MHz) of denigrin H (262) _____276
D.7. COSY spectrum (methanol-d_4) of denigrin H (262) _____277
D.8. gHSQC spectrum (methanol-d_4) of denigrin H (262) _____278
D.9. gHMBC spectrum (methanol-d_4) of denigrin H (262) _____279
D.10. HR-ESI-MS spectrum of denigrin I (263) in negative ion mode _____280
D.11. ^{1}H NMR spectrum (methanol-d_4, 600 MHz) of denigrin I (263) _____281
D.12. ^{13}C NMR spectrum (methanol-d_4, 150 MHz) of denigrin I (263)_____282
D.13. COSY spectrum (methanol-d_4) of denigrin I (263) _____283
D.14. gHSQC spectrum (methanol-d_4) of denigrin I (263) _____284
D.15. gHMBC spectrum (methanol-d_4) of denigrin I (263)_____285
D.16. HR-ESI-MS spectrum of denigrin J (264) in negative ion mode _____286
D.17. ^{1}H NMR spectrum (methanol-d_4, 600 MHz) of denigrin J (264) _____287
D.18. ^{13}C NMR spectrum (methanol-d_4, 150 MHz) of denigrin J (264)_____288
D.19. COSY spectrum (methanol-d_4) of denigrin J (264) _____289
D.20. gHSQC spectrum (methanol-d_4) of denigrin J (264) _____290
D.21. gHMBC spectrum (methanol-d_4) of denigrin J (264)_____291
D.22. HR-ESI-MS spectrum of denigrin K (265) in negative ion mode _____292
D.23. ^{1}H NMR spectrum (methanol-d_4, 600 MHz) of denigrin K (265)_____293
D.24. ^{13}C NMR spectrum (methanol-d_4, 150 MHz) of denigrin K (265) _____294
D.25. COSY spectrum (methanol-d_4) of denigrin K (265) _____295
D.26. gHSQC spectrum (methanol-d_4) of denigrin K (265)_____296
D.27. gHMBC spectrum (methanol-d_4) of denigrin K (265) _____297
D.28. HR-ESI-MS spectrum of denigrin L (266) in negative ion mode _____298
D.29. ^{1}H NMR spectrum (methanol-d_4, 600 MHz) of denigrin L (266)_____299
D.30. ^{13}C NMR spectrum (methanol-d_4, 150 MHz) of denigrin L (266) _____300
D.31. COSY spectrum (methanol-d_4) of denigrin L (266) _____301
D.32. gHSQC spectrum (methanol-d_4) of denigrin L (266) _____302
D.33. gHMBC spectrum (methanol-d_4) of denigrin L (266) _____303

Appendix A. ^{1}H NMR spectra relevant to Chapter 2

A.1. ^{1}H NMR spectrum (chloroform-*d,* 600 MHz) of convolutamine L (**94**)

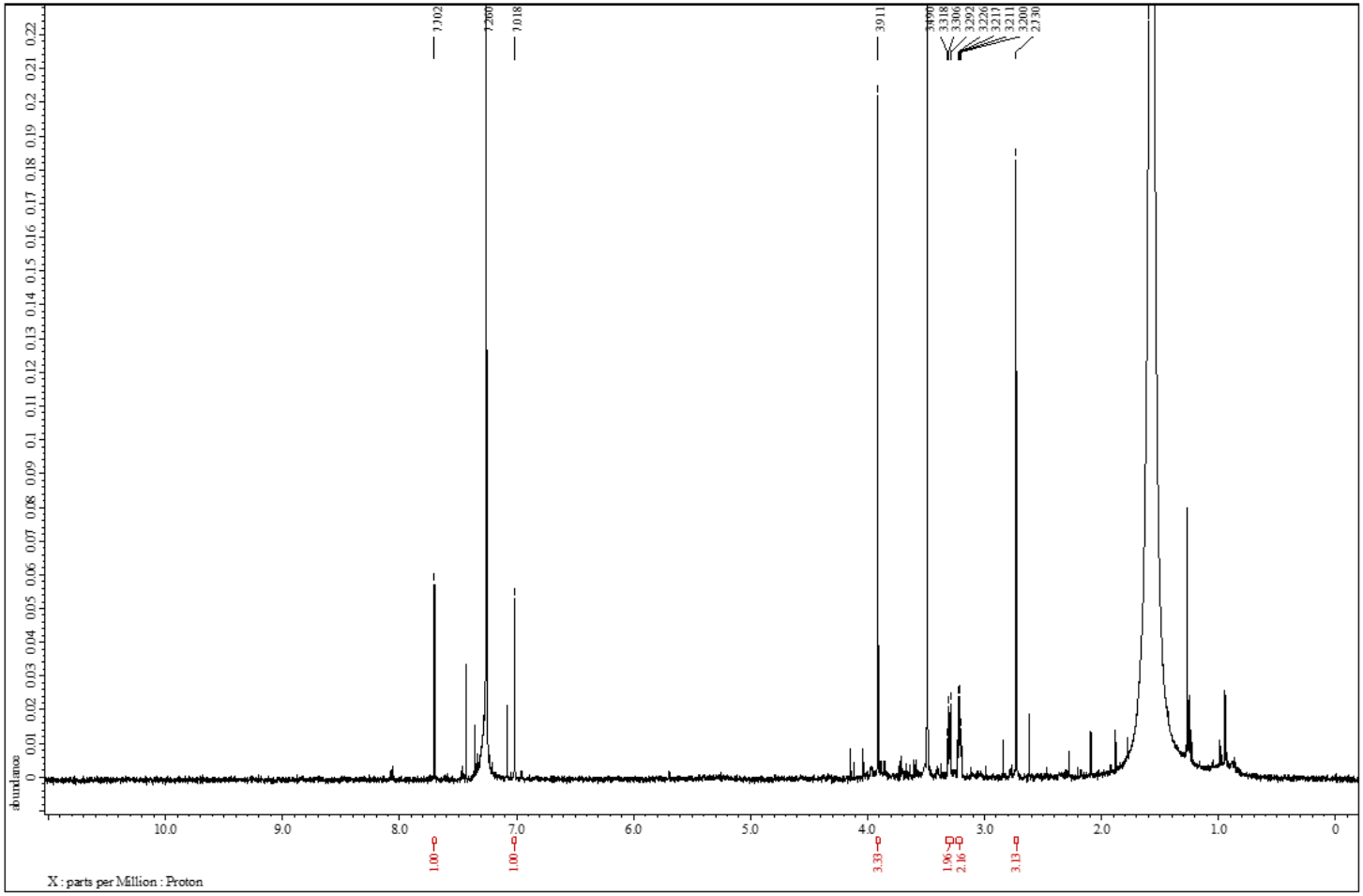

A.2. ^{1}H NMR spectrum (chloroform-*d,* 600 MHz) of cinnamolide (**122**)

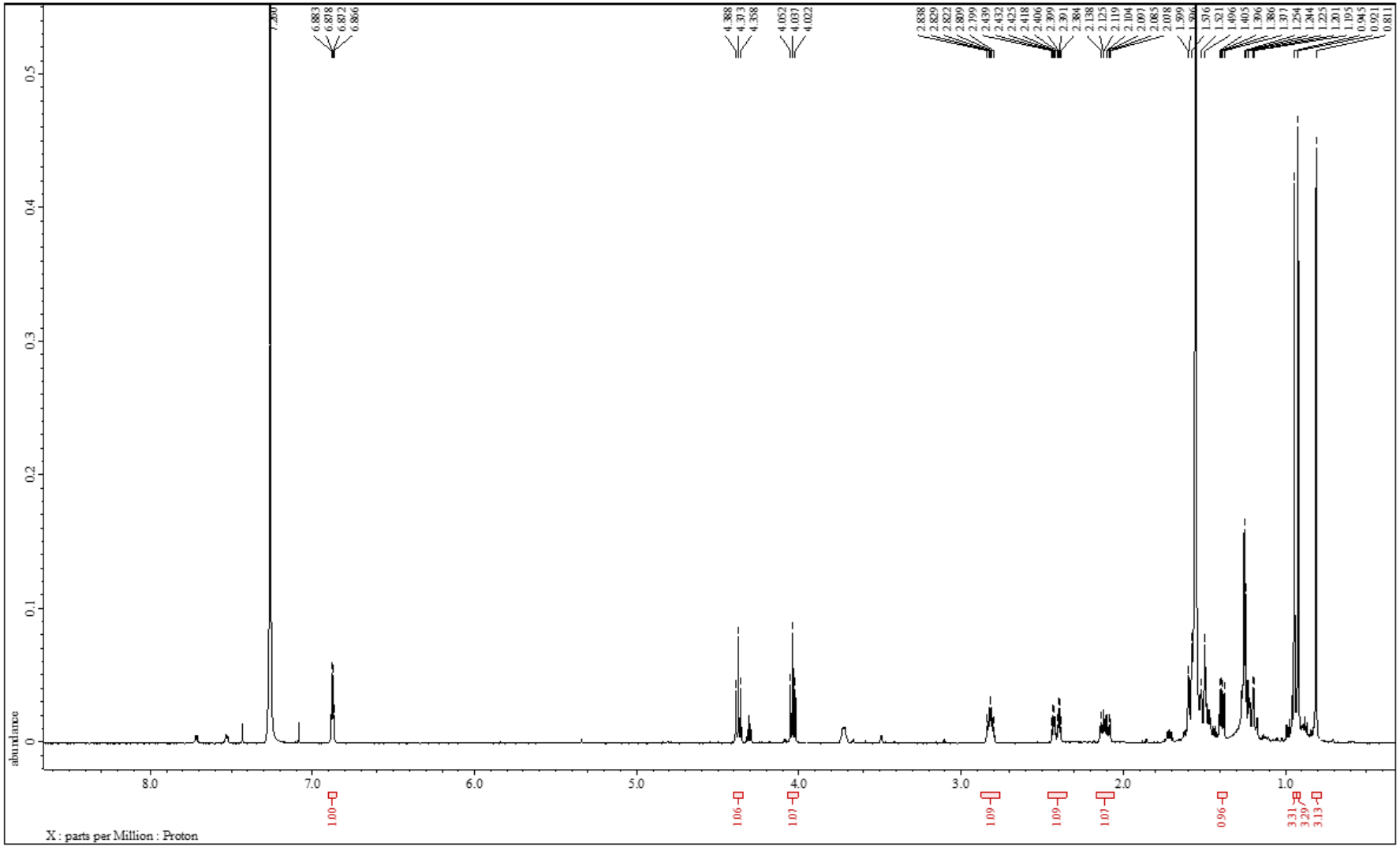

A.3. ^{1}H NMR spectrum (chloroform-*d,* 600 MHz) of 7-deacetoxy-olepupuane (**124**)

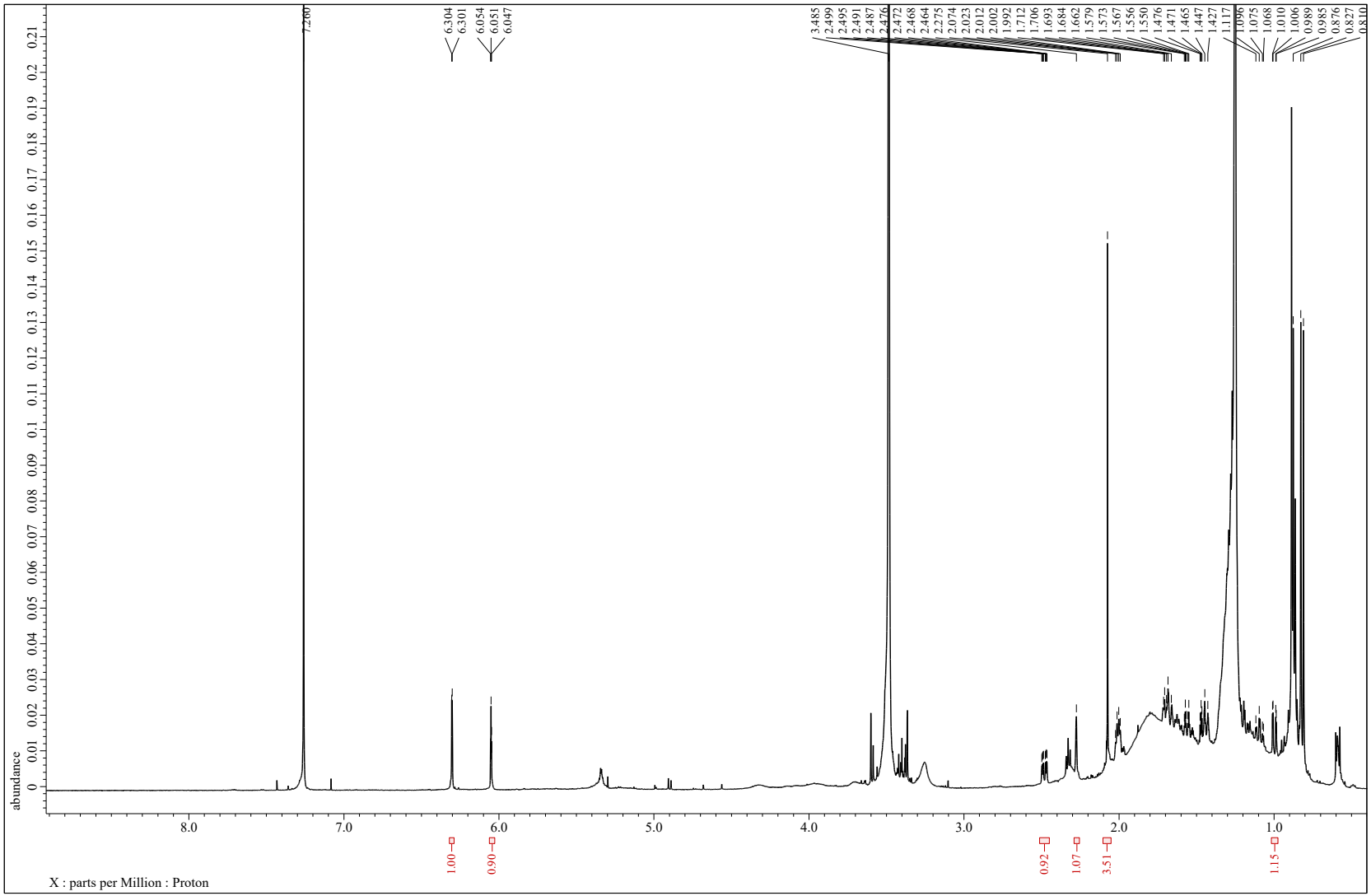

A.4. ^{1}H NMR spectrum (chloroform-*d,* 600 MHz) of drimane esters (**125**)

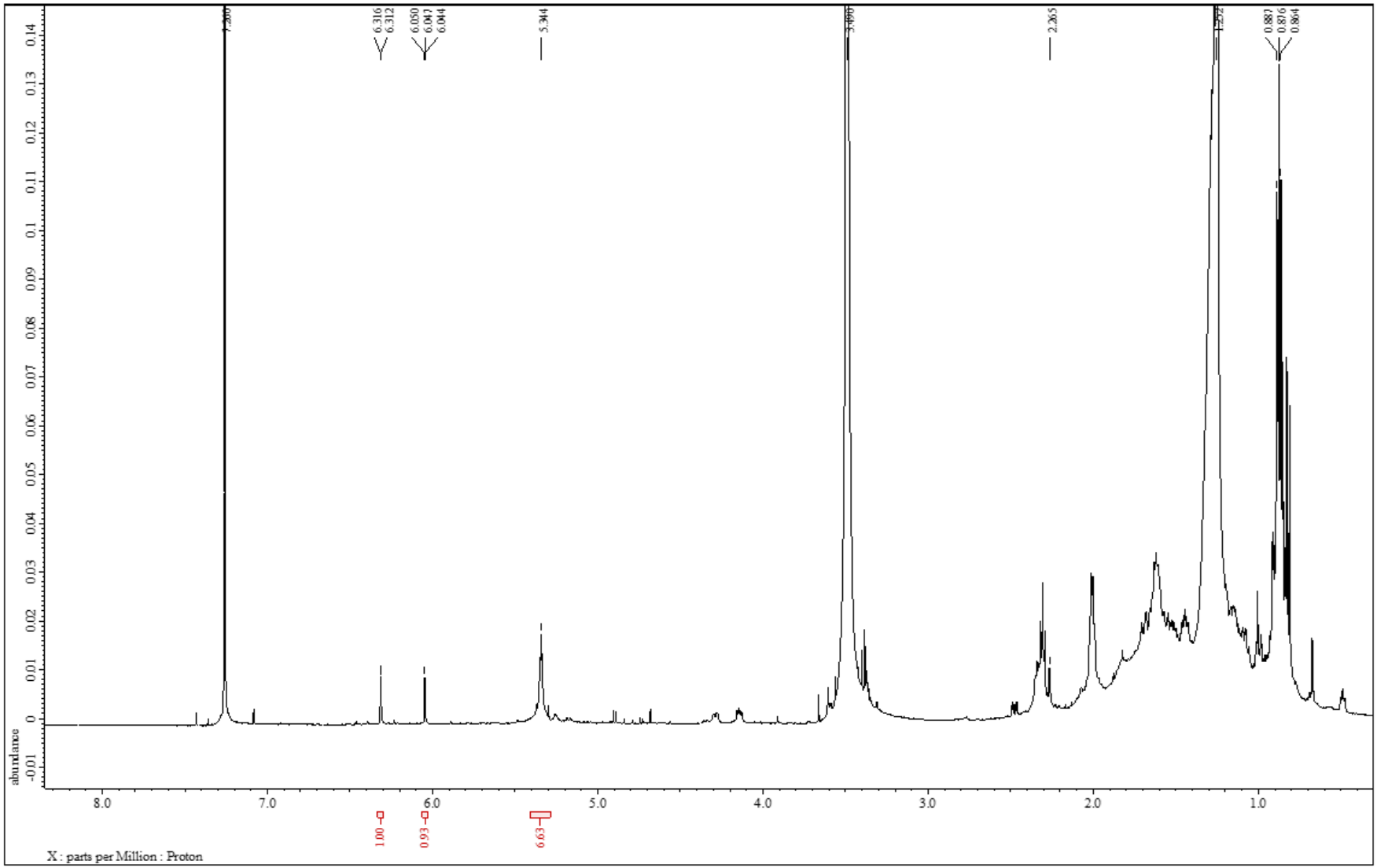

A.5. ^{1}H NMR spectrum (D_2O, 600 MHz) of 3-PAPS (**146**)

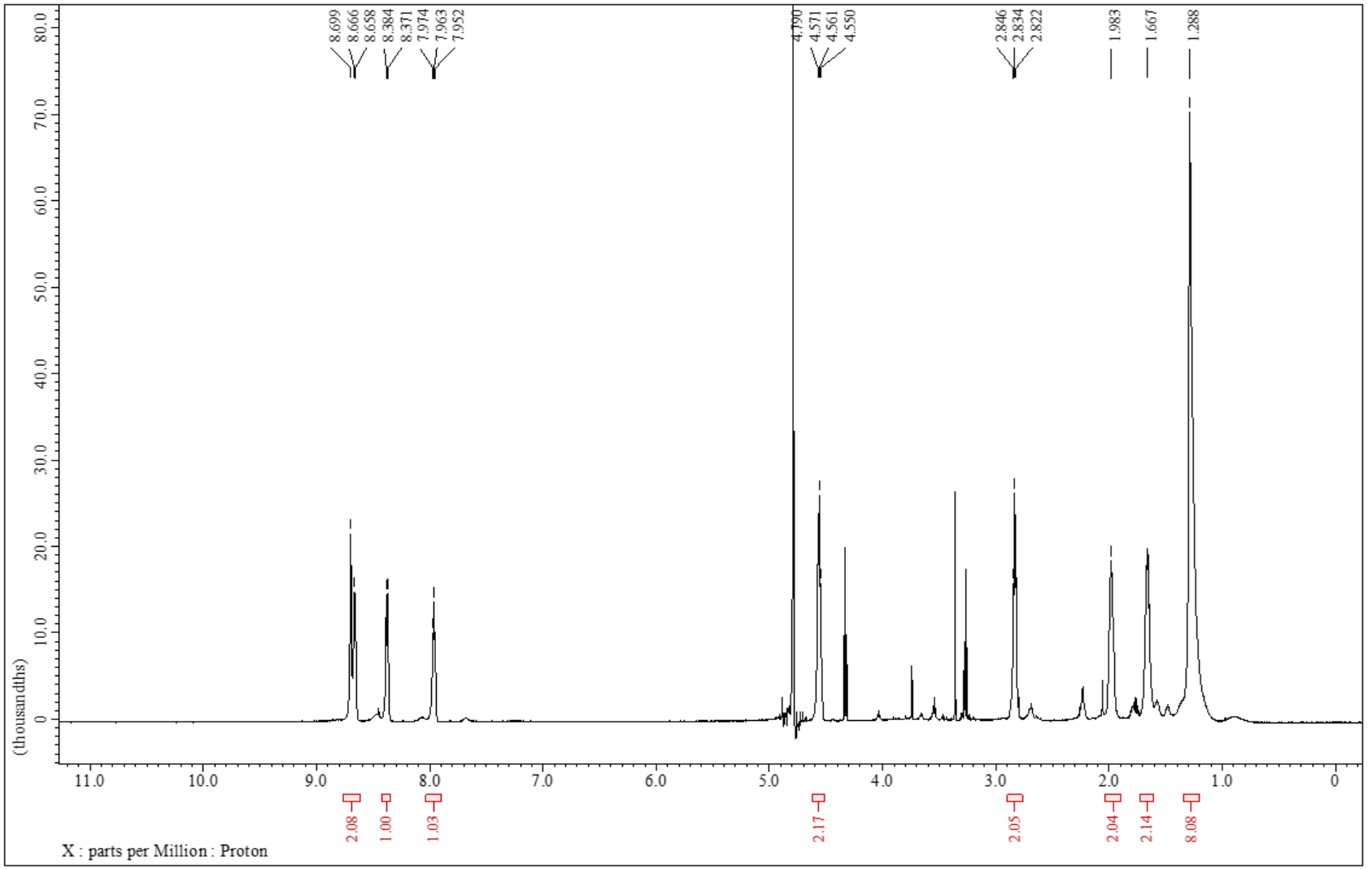

Appendix B. Complementary data for the feeding-choice experiments described in Chapter 3

B.1. *Polycera hedgpethi* – time spent on each prey (h) per specimen per individual experiment

		Specimens				
Experiment	**Prey**	**1**	**2**	**3**	**4**	**5**
1	*B. neritina*	0.00	0.00	0.76		6.75
	Unidentified hydrozoan	0.09	0.00	0.02		0.00
2	*B. neritina*	5.77	0.00	0.68	5.07	4.83
	Unidentified hydrozoan	0.00	0.00	0.00	0.00	0.00
3	*B. neritina*	2.03	15.00	0.00	10.17	0.00
	Unidentified hydrozoan	0.00	0.00	0.00	0.00	0.00
4	*B. neritina*	0.00		0.00	5.00	
	Unidentified hydrozoan	0.00		0.00	0.00	
Cumulative time spent on prey (h)	***B. neritina***	**7.80**	**15.00**	**1.44**	**20.23**	**11.58**
	Unidentified hydrozoan	**0.09**	**0.00**	**0.02**	**0.00**	**0.00**

B.2. *Ceratosoma amoenum* – time spent on each prey (h) per specimen per individual experiment

		Specimens			
Experiment	**Prey**	**1**	**2**	**3**	**4**
1	*Dysidea teawanui*	0.0	0.0	7.3	6.0
	D. cf. *dendyi*	0.0	0.0	0.0	0.2
2	*Dysidea teawanui*	0.0	0.2	0.0	0.0
	D. cf. *dendyi*	0.0	0.0	2.9	0.0
3	*Dysidea teawanui*	0.0	0.0	0.0	0.0
	D. cf. *dendyi*	0.0	0.0	0.0	0.0
4	*Dysidea teawanui*	0.0	9.5	0.0	0.0
	D. cf. *dendyi*	0.0	0.3	0.0	0.0
5	*Dysidea teawanui*	0.0	0.0	0.0	0.0
	D. cf. *dendyi*	0.0	0.0	0.0	0.0
6	*Dysidea teawanui*	10.5	15.3	0.0	11.2
	D. cf. *dendyi*	0.0	0.0	0.0	0.0
7	*Dysidea teawanui*	0.0	0.0	0.0	0.0
	D. cf. *dendyi*	0.0	0.0	1.3	0.0
8	*Dysidea teawanui*	0.0	0.2	0.0	0.0
	D. cf. *dendyi*	0.0	0.0	0.0	0.0
9	*Dysidea teawanui*	0.0	0.0	0.0	0.0
	D. cf. *dendyi*	0.0	0.0	0.0	0.0
10	*Dysidea teawanui*	0.0	0.0	0.0	0.0
	D. cf. *dendyi*	2.3	0.0	0.0	0.0
11	*Dysidea teawanui*	0.0	0.0	0.0	0.0
	D. cf. *dendyi*	24.0	0.0	0.0	0.1
Cumulative time spent on prey (h)	***Dysidea teawanui***	**10.4**	**25.1**	**7.3**	**17.2**
	D.* cf. *dendyi	**26.3**	**0.4**	**4.1**	**0.3**

B.3. *Goniobranchus aureomarginatus* – time spent on each prey (h) per specimen per individual experiment

		Specimens					
Experiments	**Prey**	**1**	**2**	**3**	**4**	**5**	**6**
1	*Dysidea teawanui*	0.0	0.0	0.0	0.2	0.4	0.0
	D. cf. *dendyi*	11.9	0.0	0.0	0.0	1.2	0.0
2	*Dysidea teawanui*	0.0	0.5	0.0	0.0	0.0	0.1
	D. cf. *dendyi*	0.4	0.9	0.4	0.0	0.0	0.0
3	*Dysidea teawanui*	0.0	0.3	0.1	0.0	0.2	0.3
	D. cf. *dendyi*	2.6	1.0	0.1	0.0	0.1	0.0
4	*Dysidea teawanui*	0.0	0.0	0.0	0.0	0.2	0.0
	D. cf. *dendyi*	0.1	9.1	0.0	0.0	0.0	0.0
5	*Dysidea teawanui*	0.0	0.0	0.1	0.0	0.0	0.0
	D. cf. *dendyi*	0.0	0.0	0.0	0.0	0.5	5.2
6	*Dysidea teawanui*	0.0	0.0	0.0	0.0	0.0	0.0
	D. cf. *dendyi*	0.0	5.9	12.5	0.0	0.0	0.0
7	*Dysidea teawanui*	0.0	0.0	0.0	0.0	0.0	0.0
	D. cf. *dendyi*	0.0	9.8	0.0	6.4	5.5	0.9
8	*Dysidea teawanui*	0.0	0.0	0.0	0.0	0.0	0.0
	D. cf. *dendyi*	0.9	0.0	0.0	0.0	0.0	2.4
9	*Dysidea teawanui*	0.0	5.2				
	D. cf. *dendyi*	0.0	0.0				
10	*Dysidea teawanui*	0.0	0.0				
	D. cf. *dendyi*	0.4	4.9				
11	*Dysidea teawanui*	0.0	0.0				
	D. cf. *dendyi*	0.0	13.9				
Cumulative time spent on prey (h)	***Dysidea teawanui***	**0.1**	**6.0**	**0.3**	**0.2**	**0.9**	**0.4**
	D.* cf. *dendyi	**16.4**	**45.5**	**13.0**	**6.4**	**7.3**	**8.5**

Appendix C. NMR spectra and separation trees relevant to Chapter 4

C.1. ^{1}H NMR spectrum (chloroform-*d*, 600 MHz) of ergosterol peroxide (**186**)

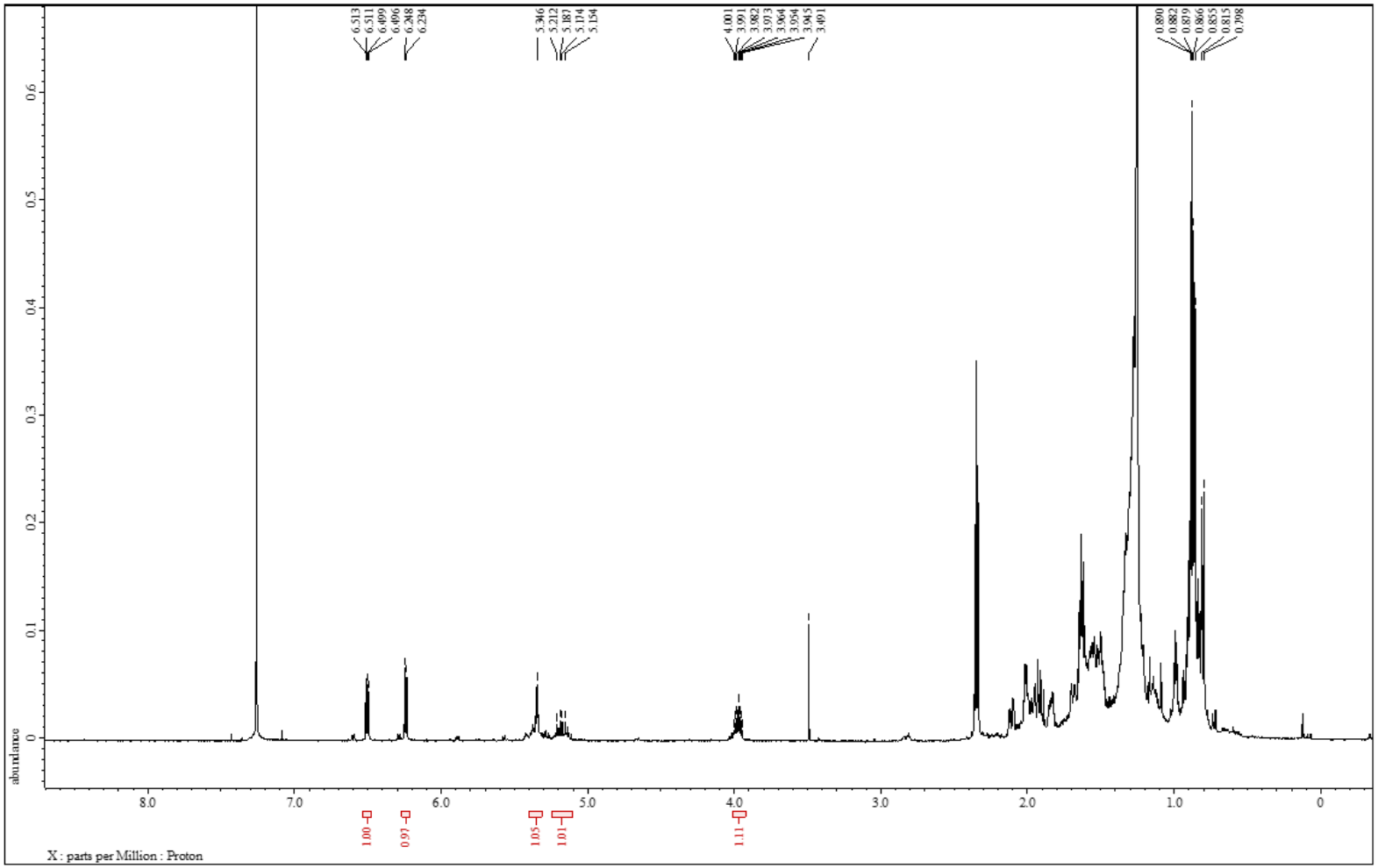

C.2. ^{1}H NMR spectrum (methanol-d_4, 600 MHz) of dictyodendrin C (**209**)

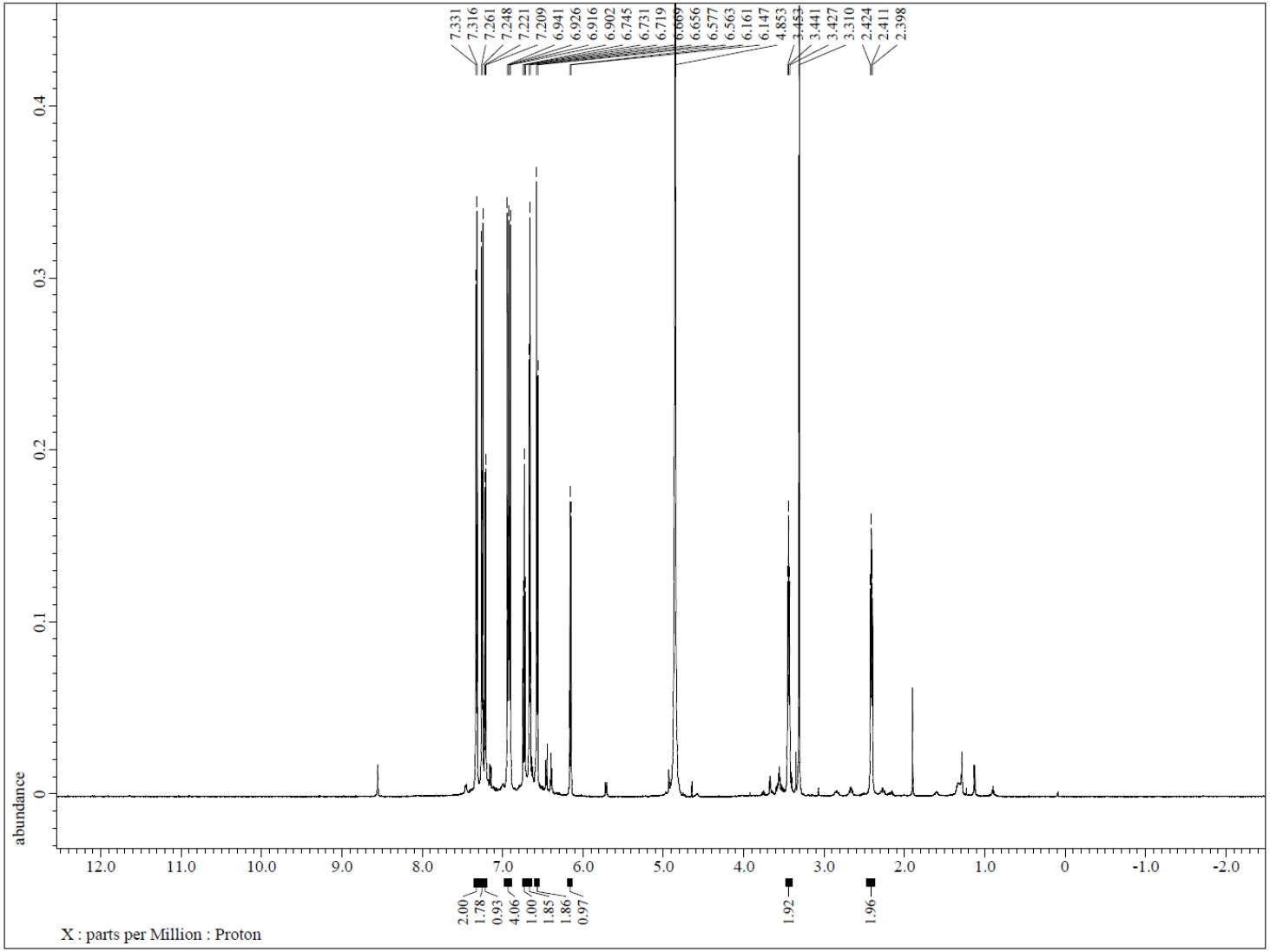

C.3. ^{1}H NMR spectrum (methanol-d_4, 600 MHz) of dictyodendrin D (**210**)

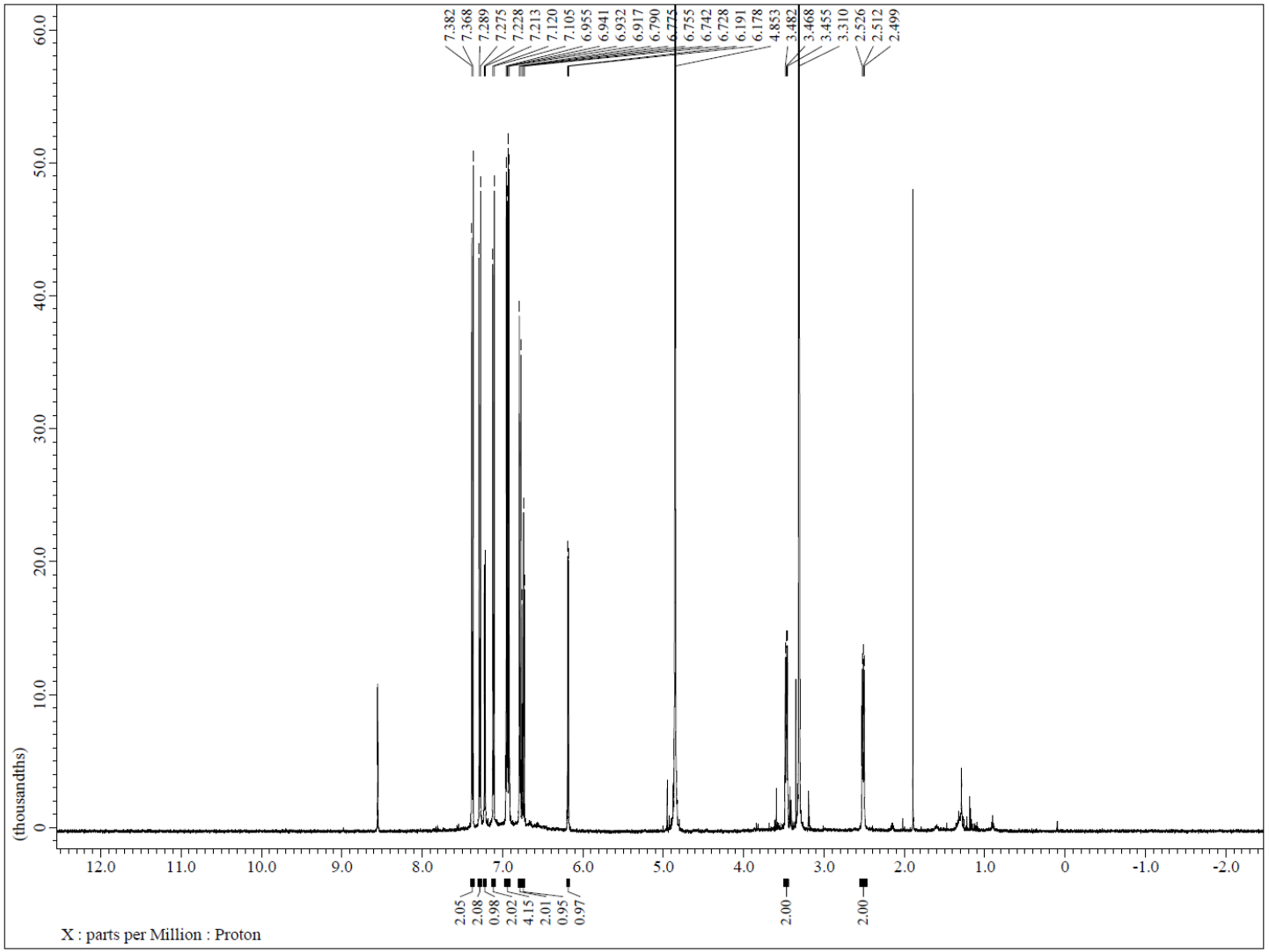

C.4. Fraction combinations (F1-F3) for the large scale *D*. cf. *dendyi* extract

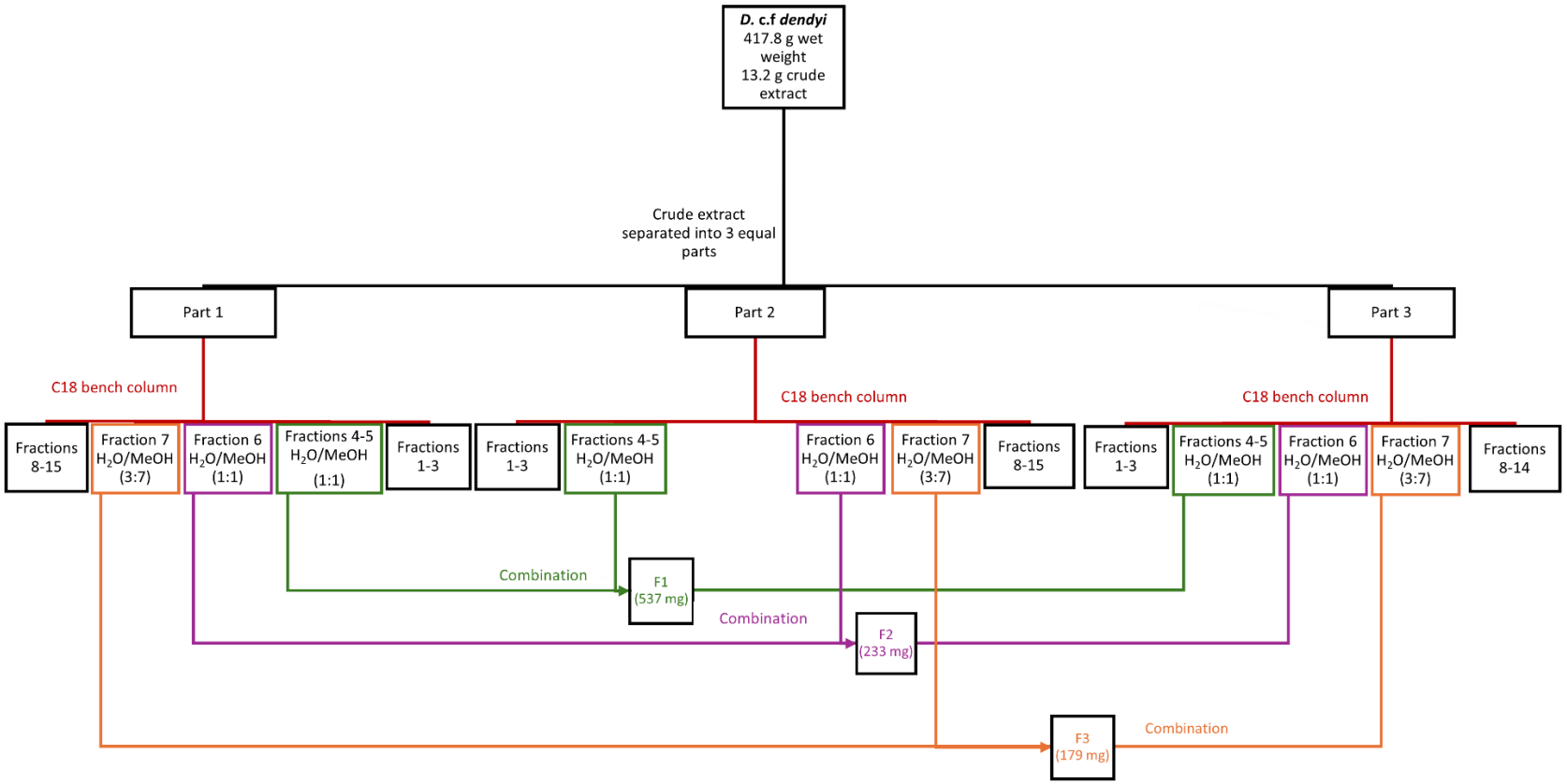

C.5. Fraction combinations (F4-F5) for the large scale *D*. cf. *dendyi* extract

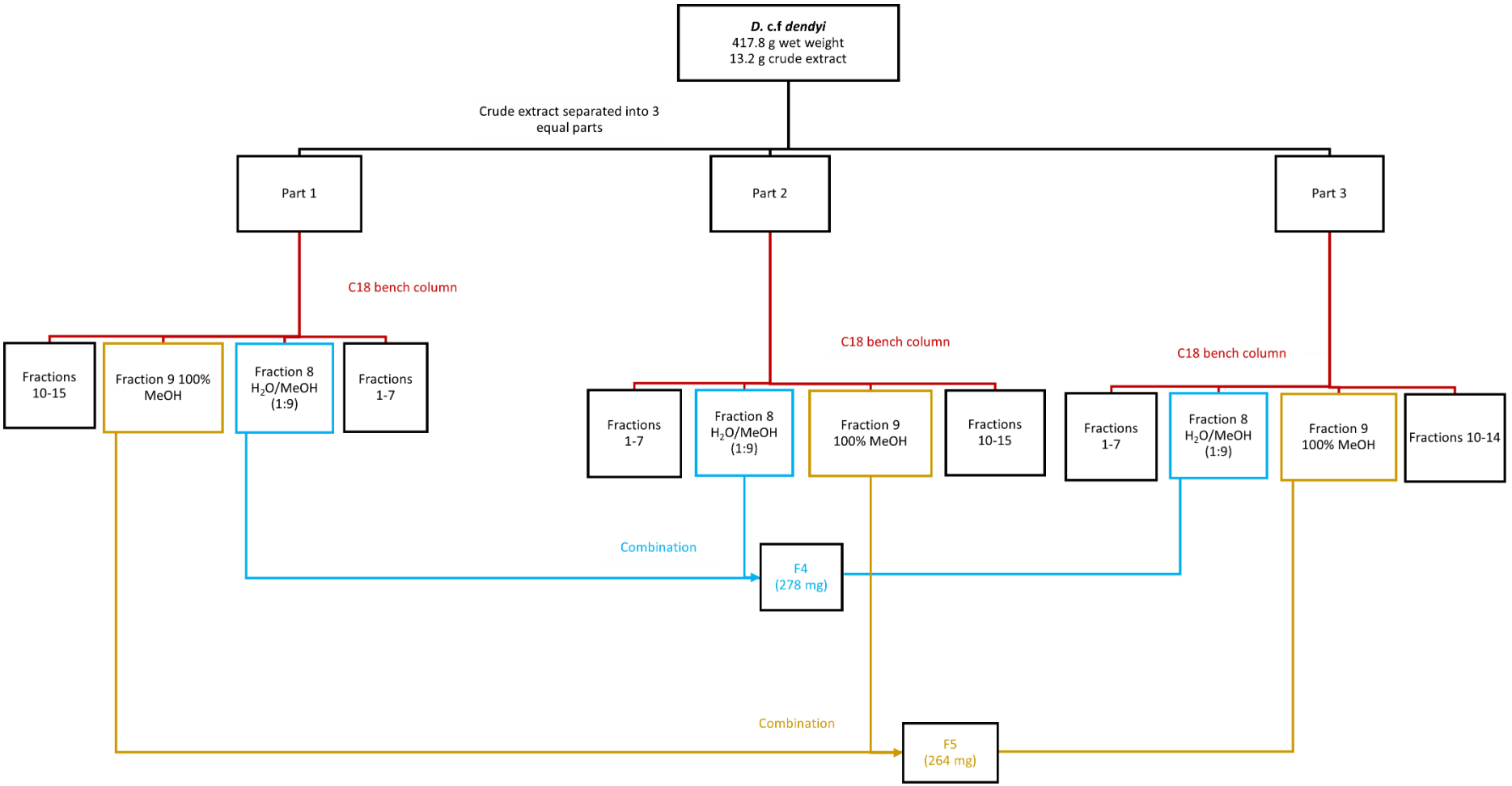

C.6. Isolation procedure for spirolactone 1a (**199**), dictyodendrin B (**208**), denigrin G (**227**) and dactylpyrrole A (**225**)

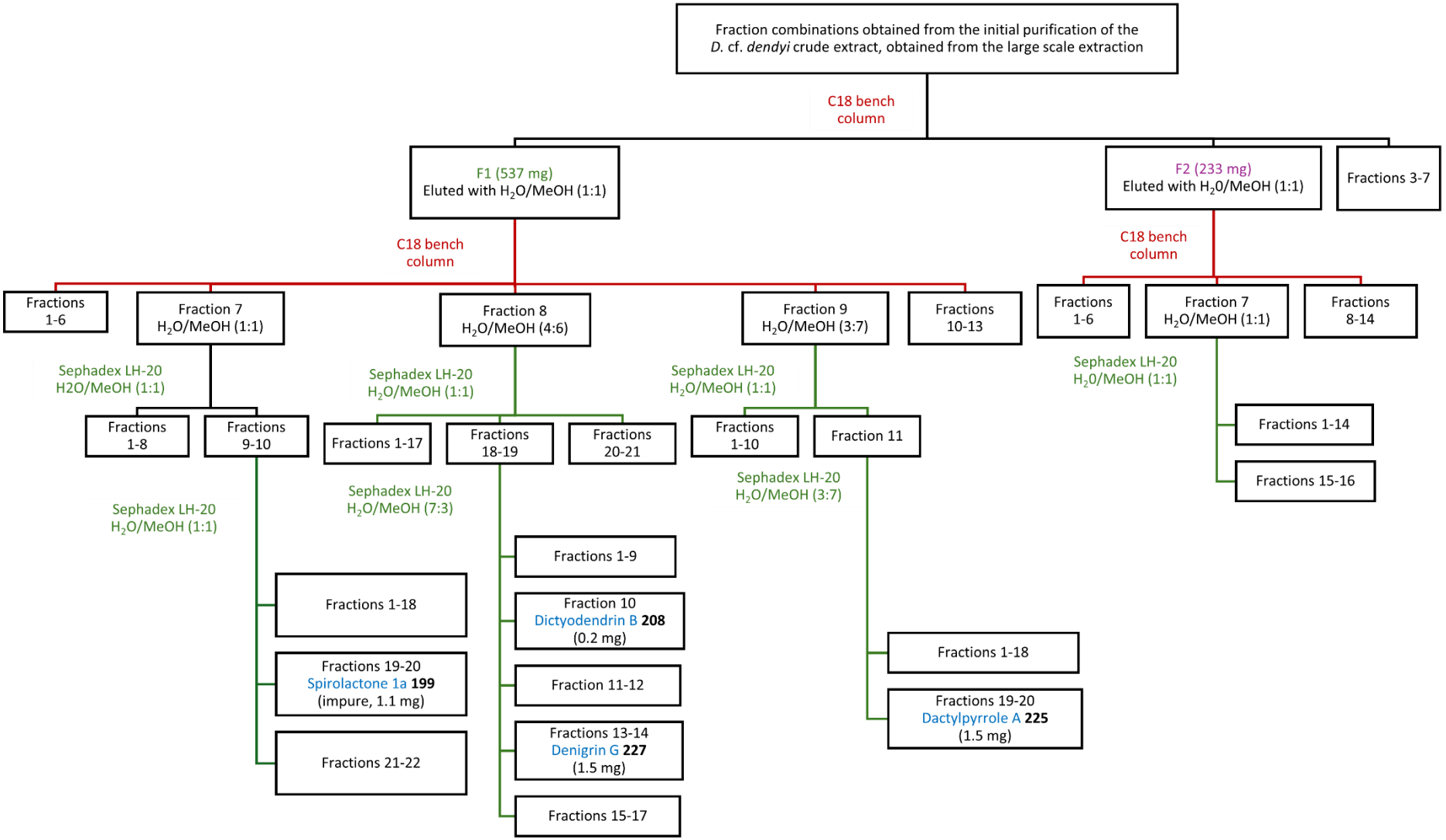

C.7. Isolation procedure for dictyodendrin F (**212**), denigrin E (**226**) and lamellarin O1 (**228**)

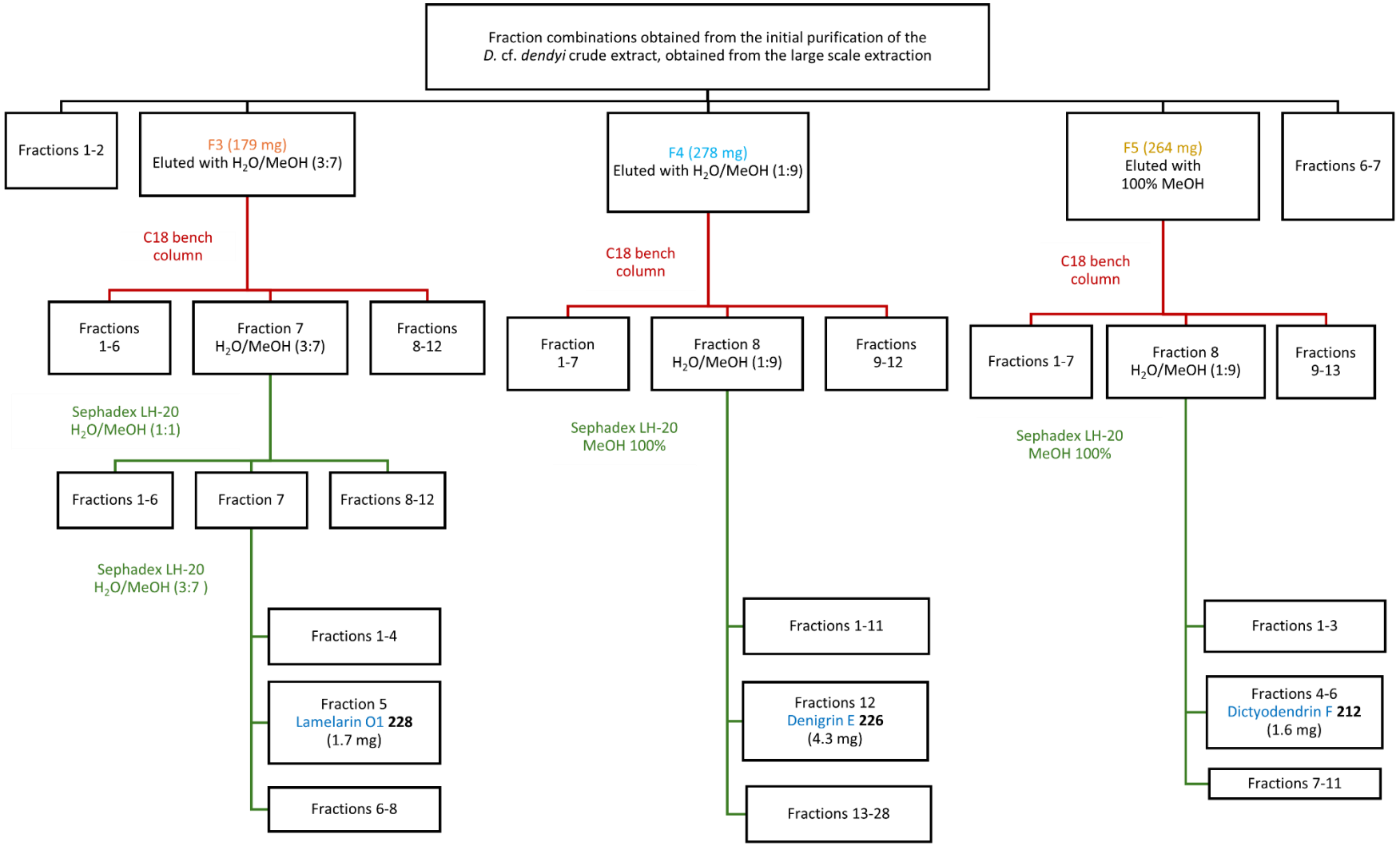

C.8. ^{1}H NMR spectrum (methanol-d_4, 600 MHz) of dictyodendrin F (**212**)

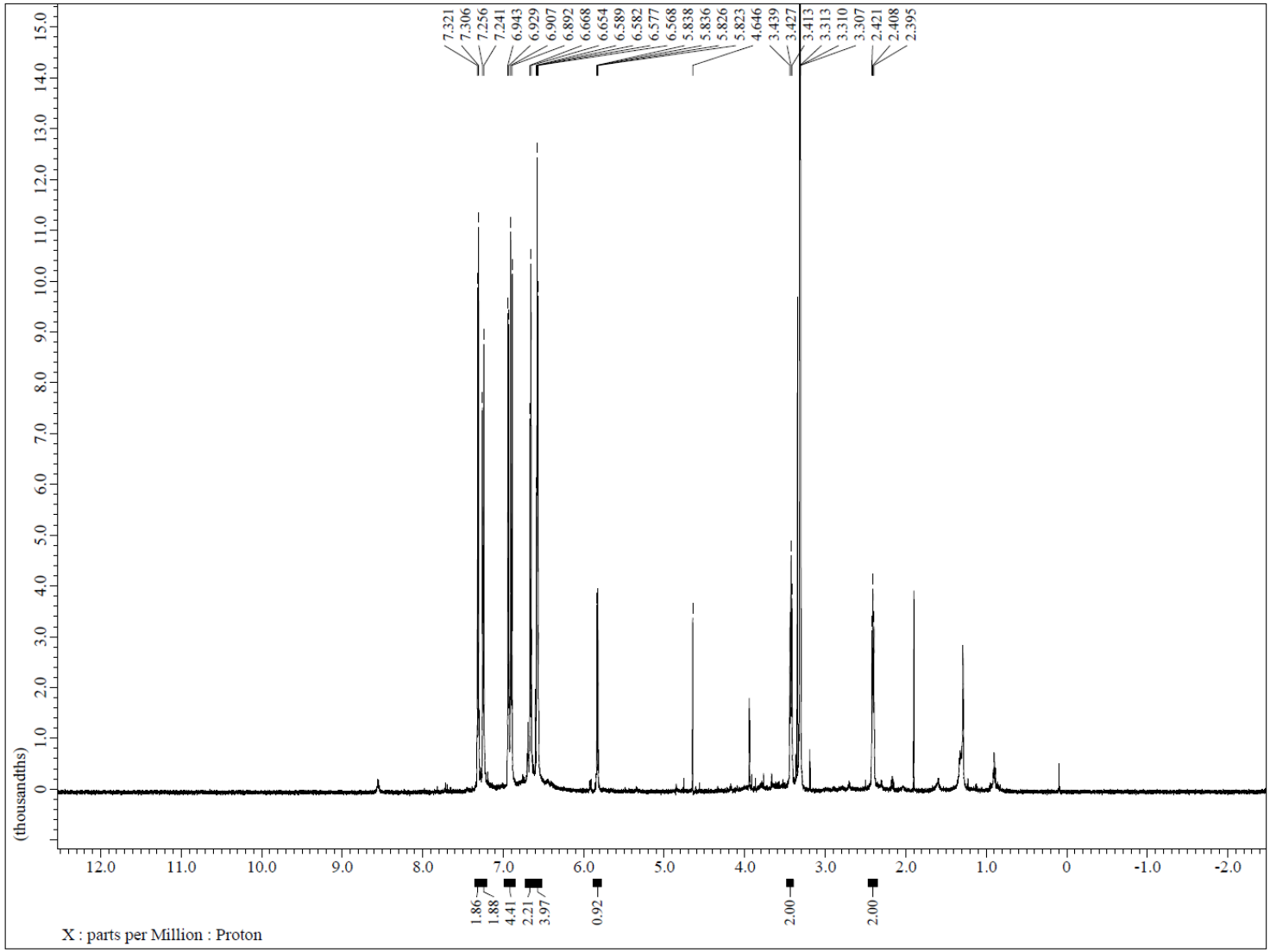

C.9. ^{1}H NMR spectrum (methanol-d_4, 600 MHz) of dactypyrrole A (**225**)

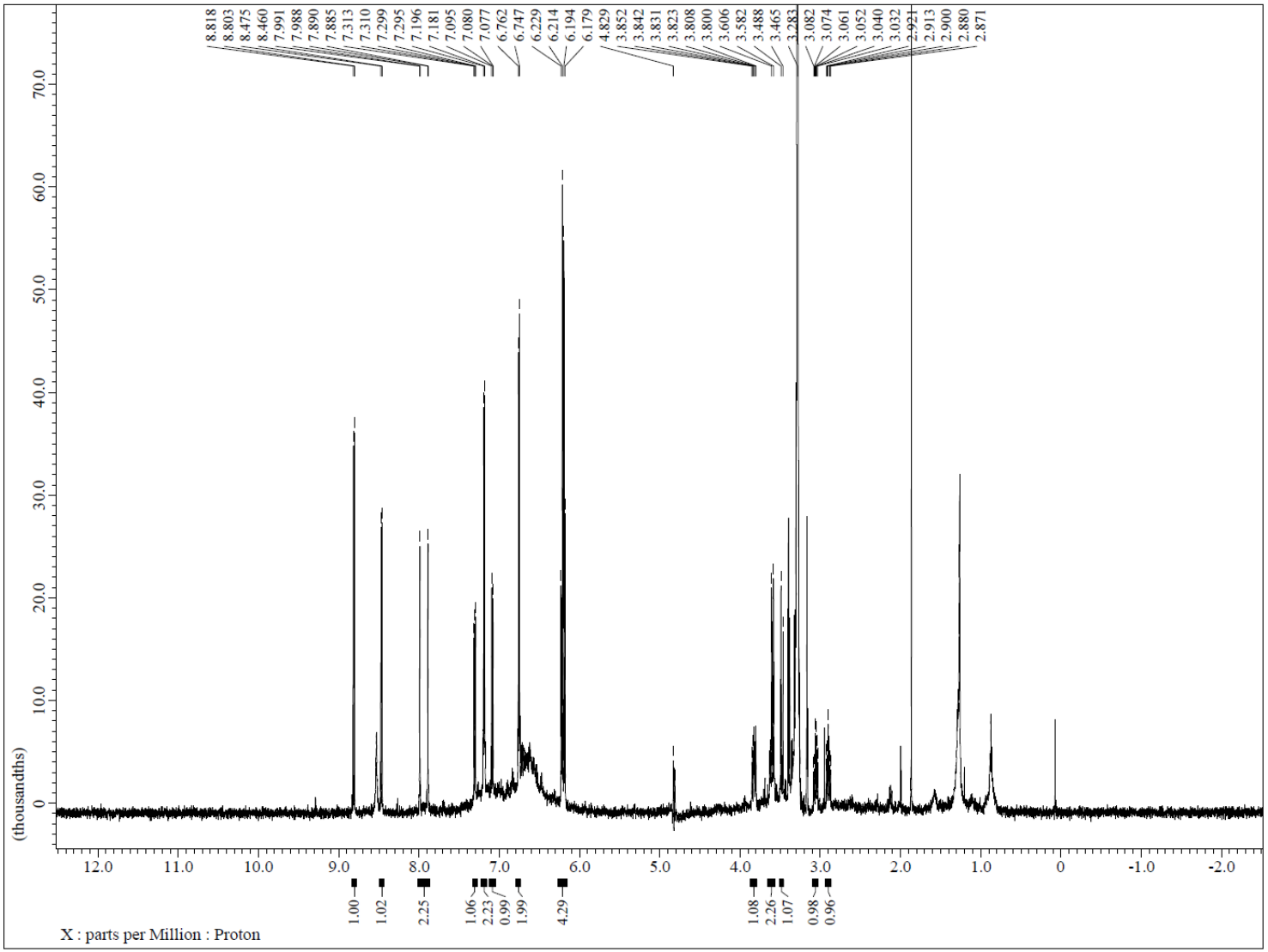

C.10. ^{1}H NMR spectrum (methanol-d_4, 600 MHz) of denigrin E (**226**)

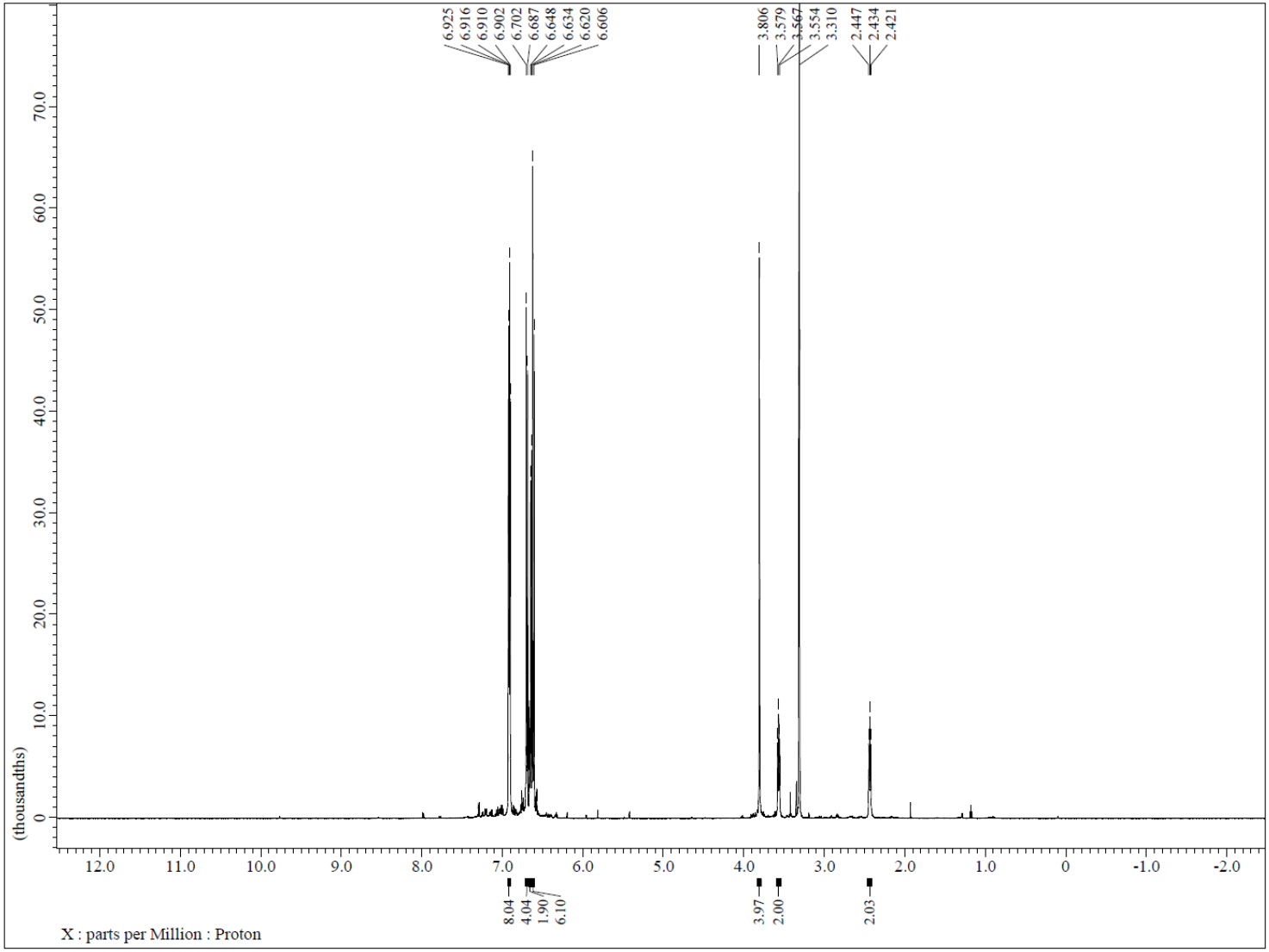

C.11. ^{13}C NMR spectrum (methanol-d_4, 150 MHz) of denigrin E (**226**)

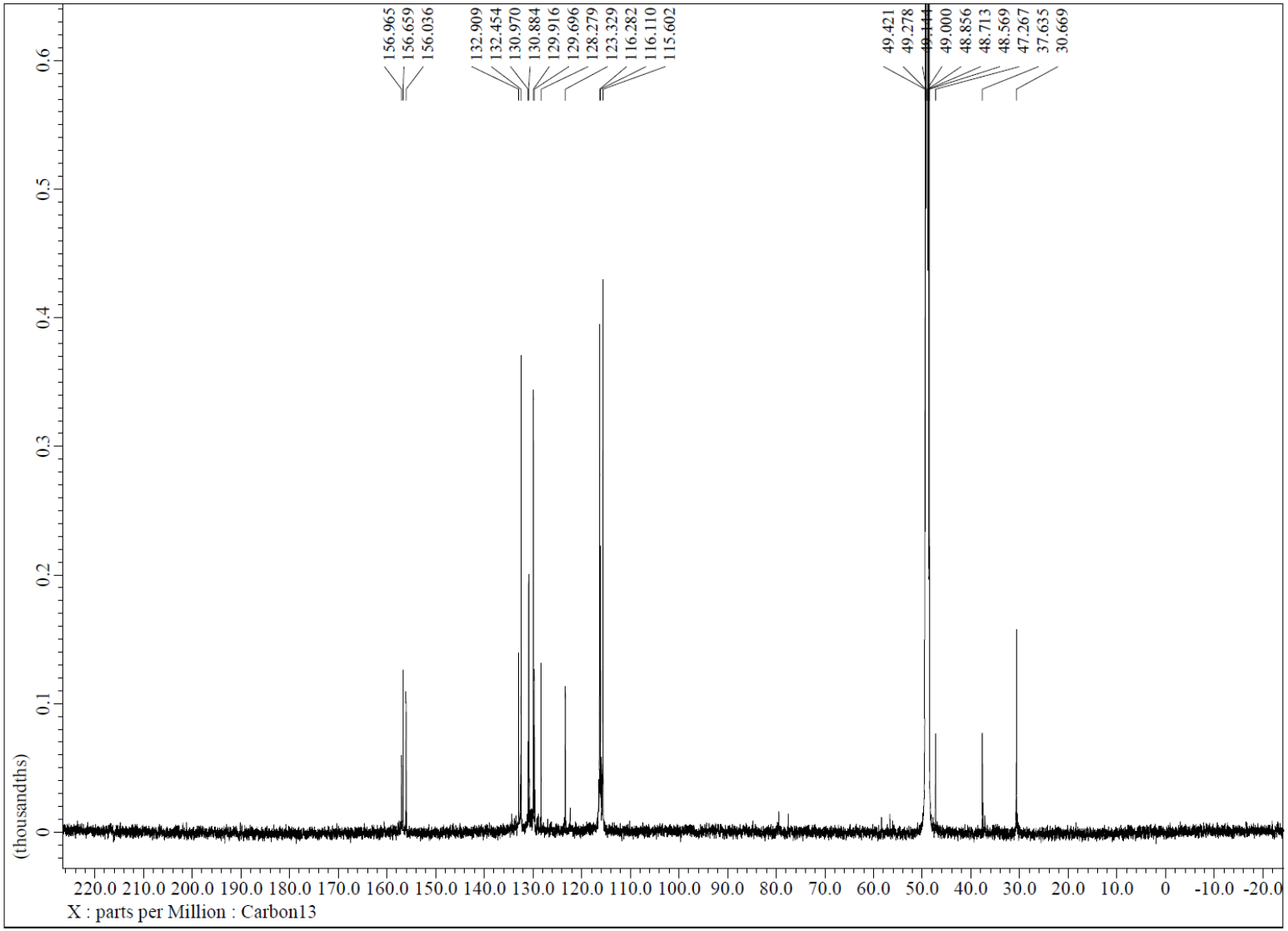

C.12. ^{1}H NMR spectrum (methanol-d_4, 600 MHz) of lamellarin O1 (**228**)

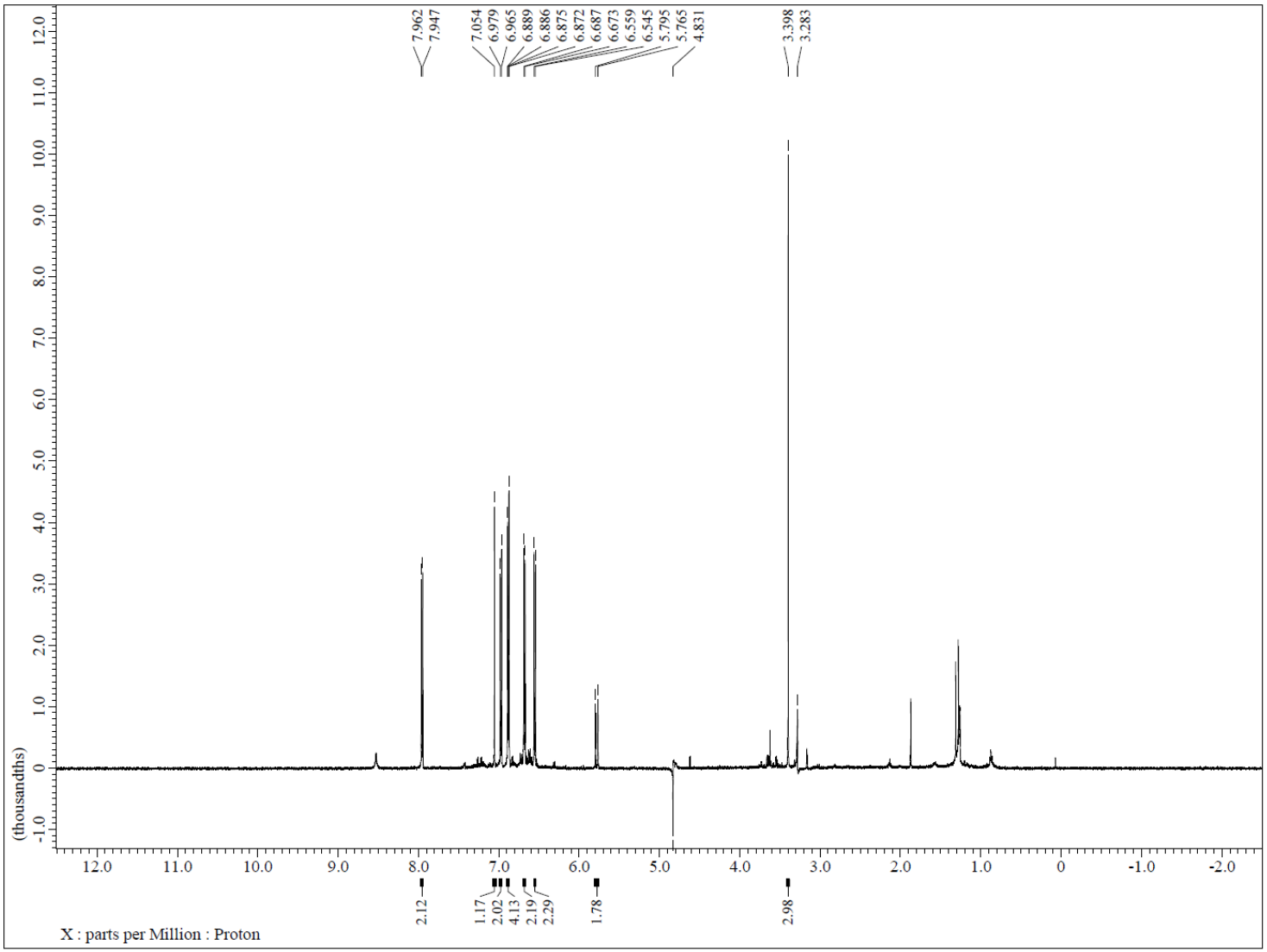

C.13. ^{1}H NMR spectrum (methanol-d_4, 600 MHz) of the mixture of gracilin A (**244**) and 6α,15α,16α-triacetoxyspongian (**236**)

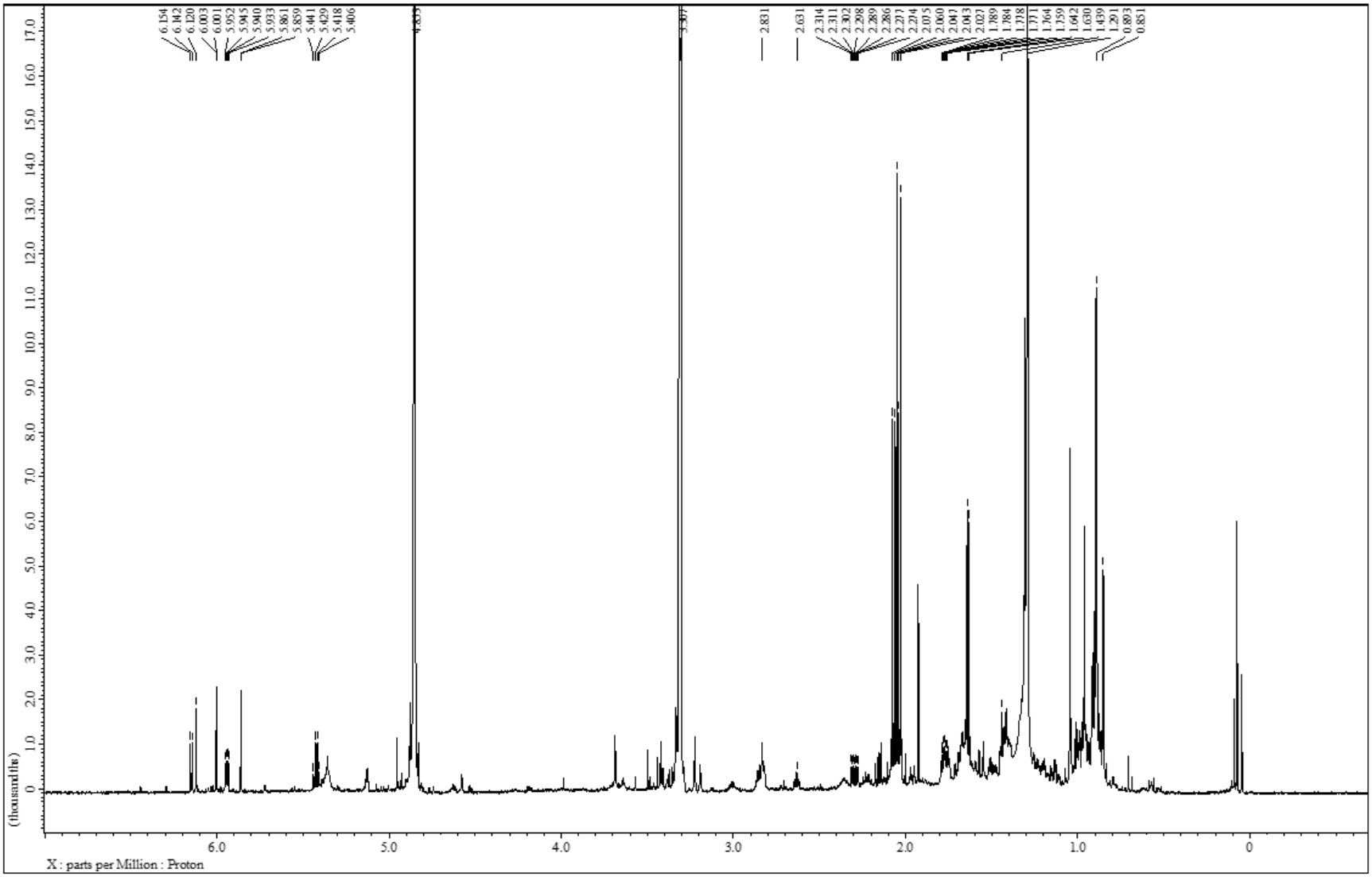

Appendix D. Separation trees, NMR and HR-ESI-MS spectra relevant to Chapter 5

D.1. Fraction combinations (F6-F7) for the large scale *D.* cf. *dendyi* extract

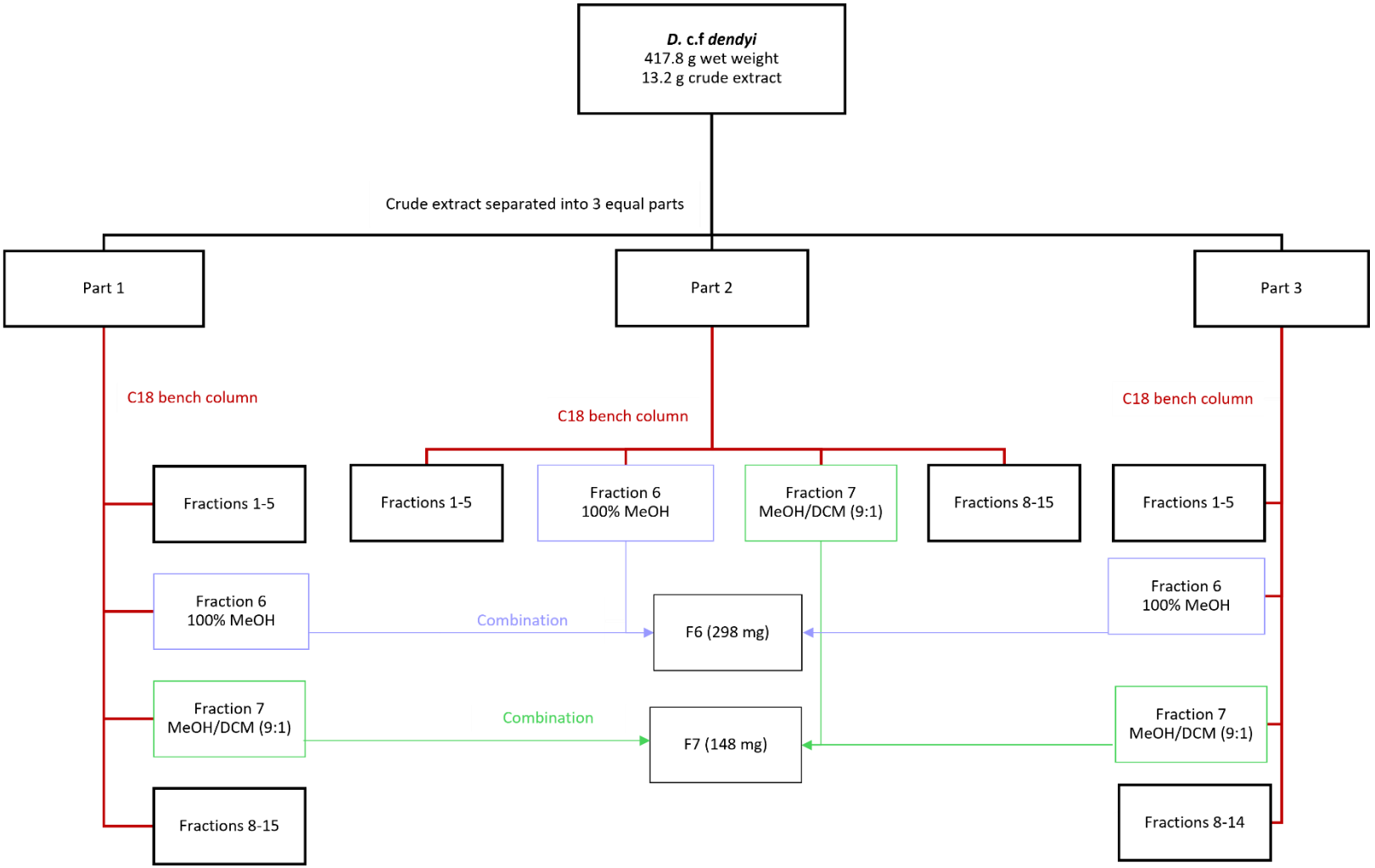

D.2. Isolation procedure for denigrins H-K (**262-265**)

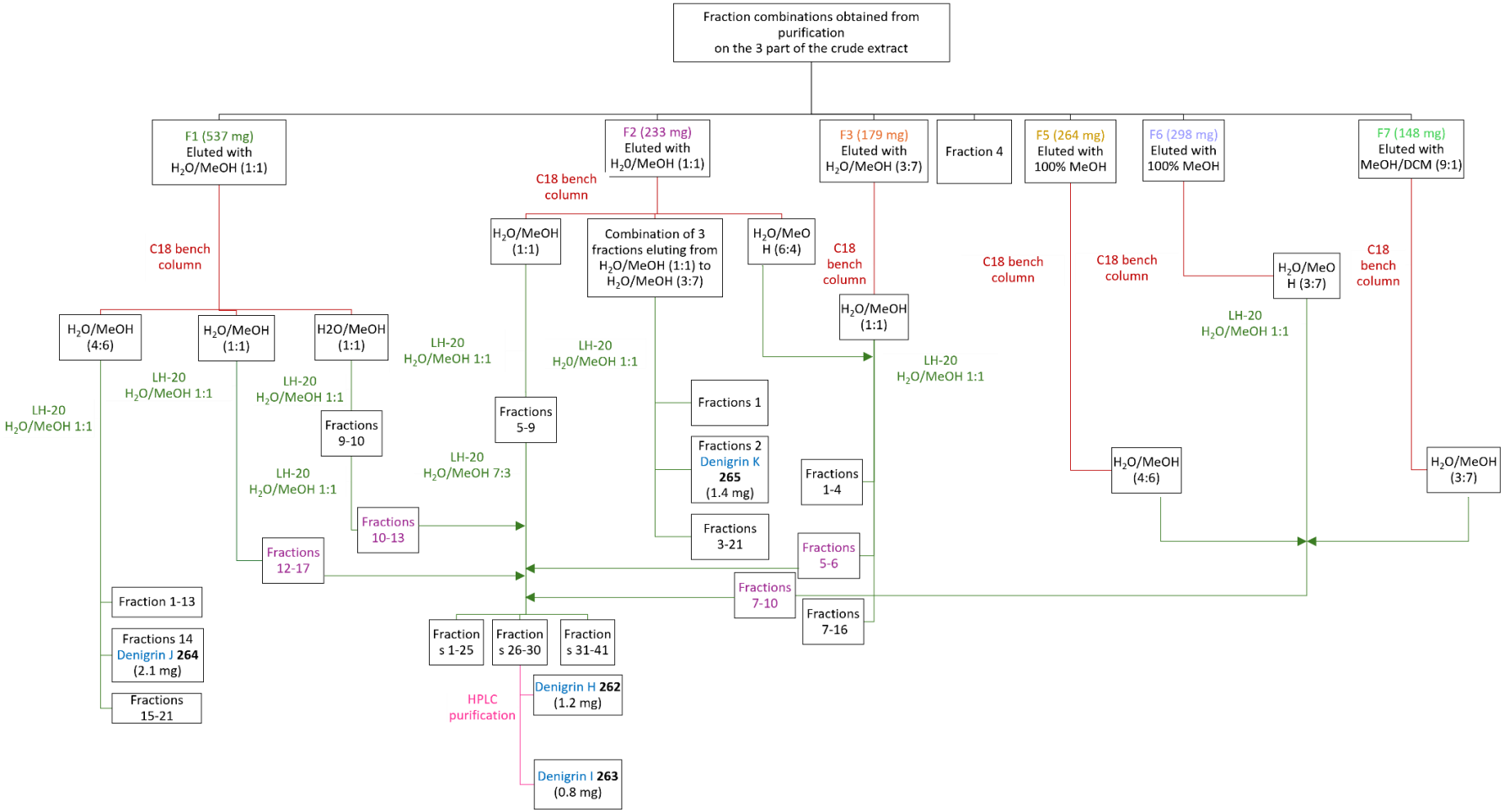

D.3. HR-ESI-MS spectrum of denigrin H (**262**) in negative ion mode

Acquisition Parameter

Source Type	ESI	Ion Polarity	Negative	Set Corrector Fill	46 V
n/a	n/a	Set Capillary Exit	-150.0 V	Set Pulsar Pull	800 V
Scan Begin	50 m/z	Set Hexapole RF	80.0 V	Set Pulsar Push	800 V
Scan End	1500 m/z	Set Skimmer 1	-50.0 V	Set Reflector	1700 V
		Set Hexapole 1	-25.0 V	Set Flight Tube	8600 V
				Set Detector TOF	2250 V

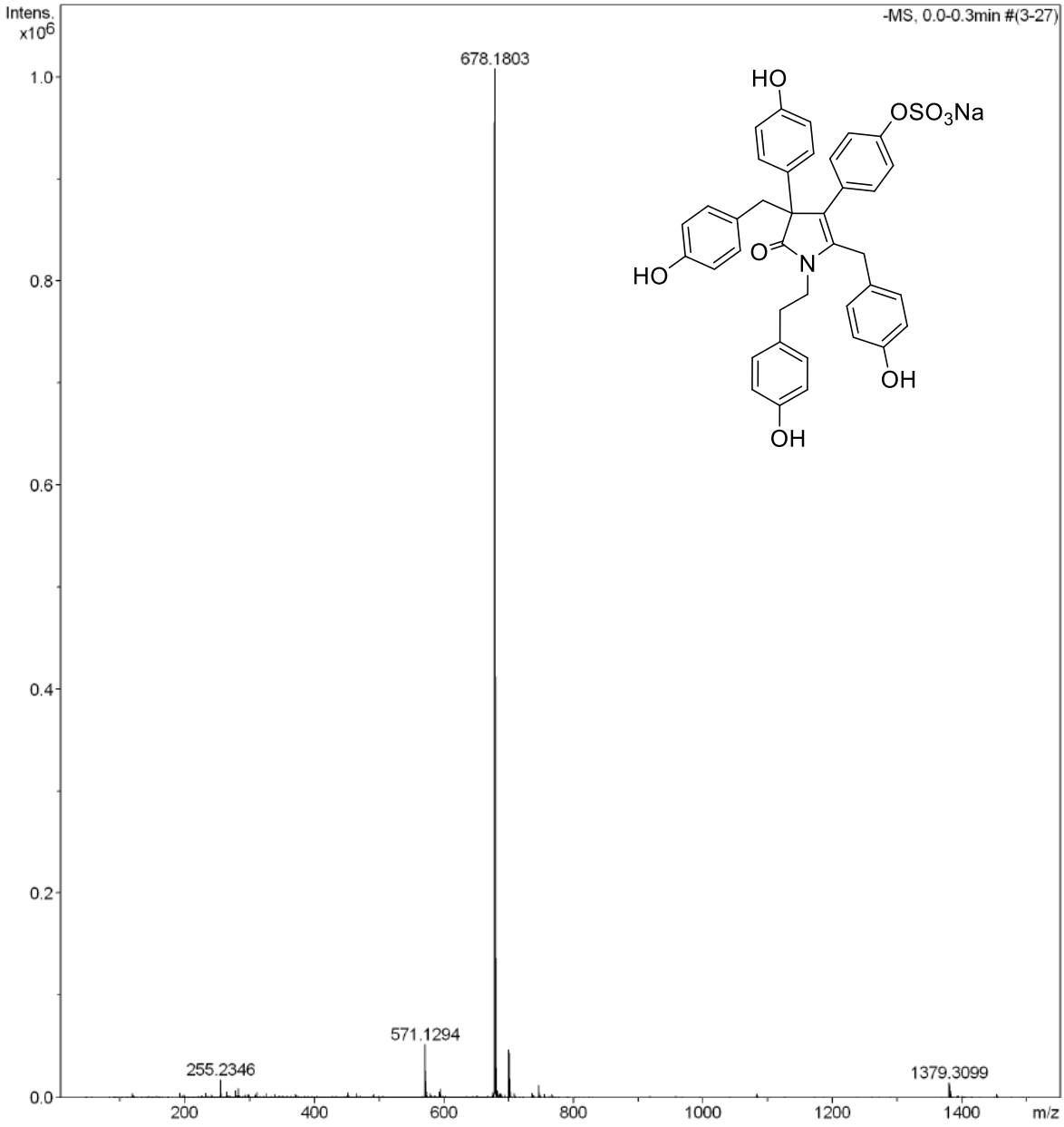

D.4. ^{1}H NMR spectrum (methanol-d_4, 600 MHz) of denigrin H (**262**)

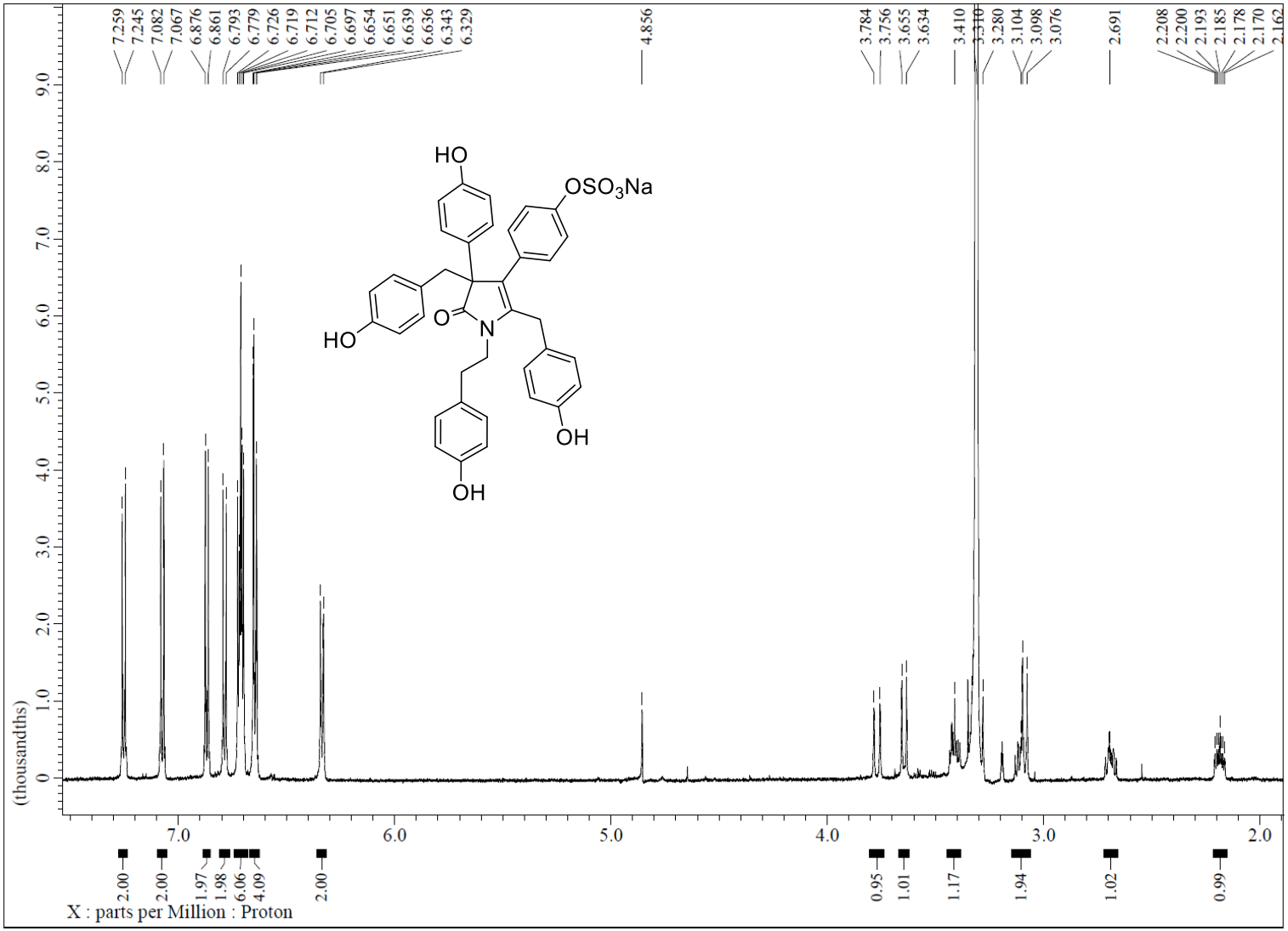

D.5. ^{13}C NMR spectrum (methanol-d_4, 150 MHz) of denigrin H (**262**)

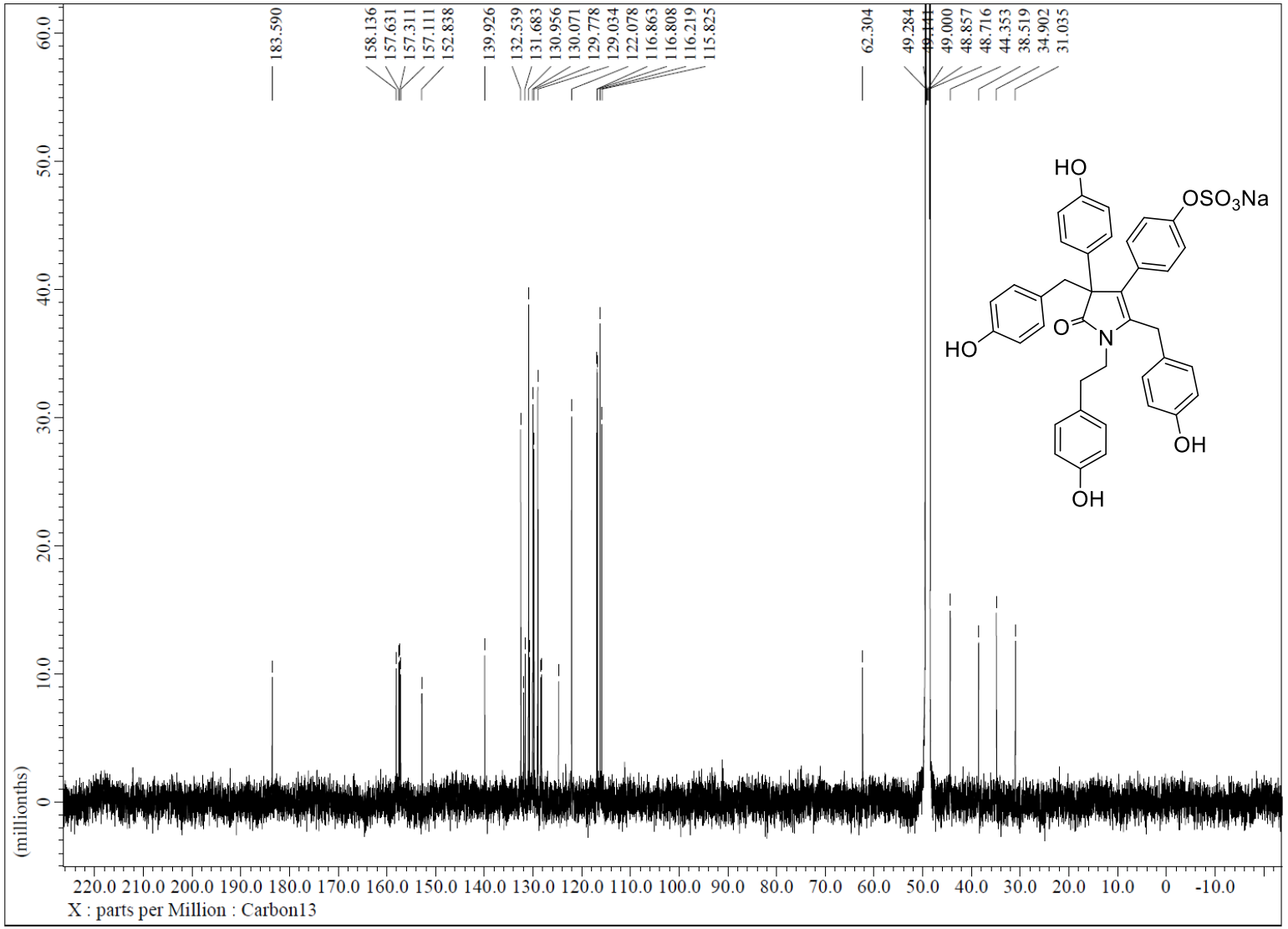

D.6. ^{13}C NMR spectrum expansion 1 (methanol-d_4, 150 MHz) of denigrin H (**262**)

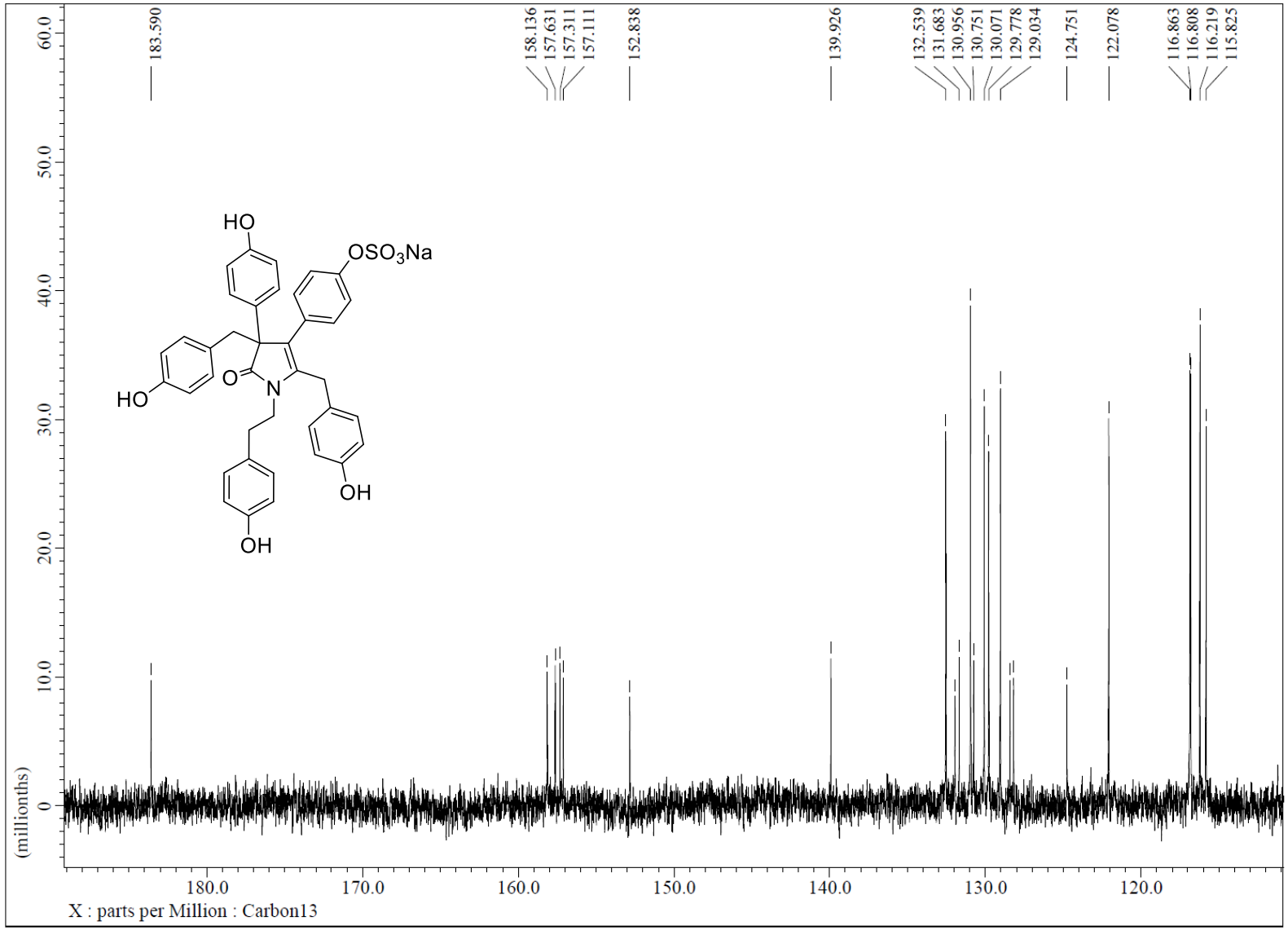

D.7. COSY spectrum (methanol-d_4) of denigrin H (**262**)

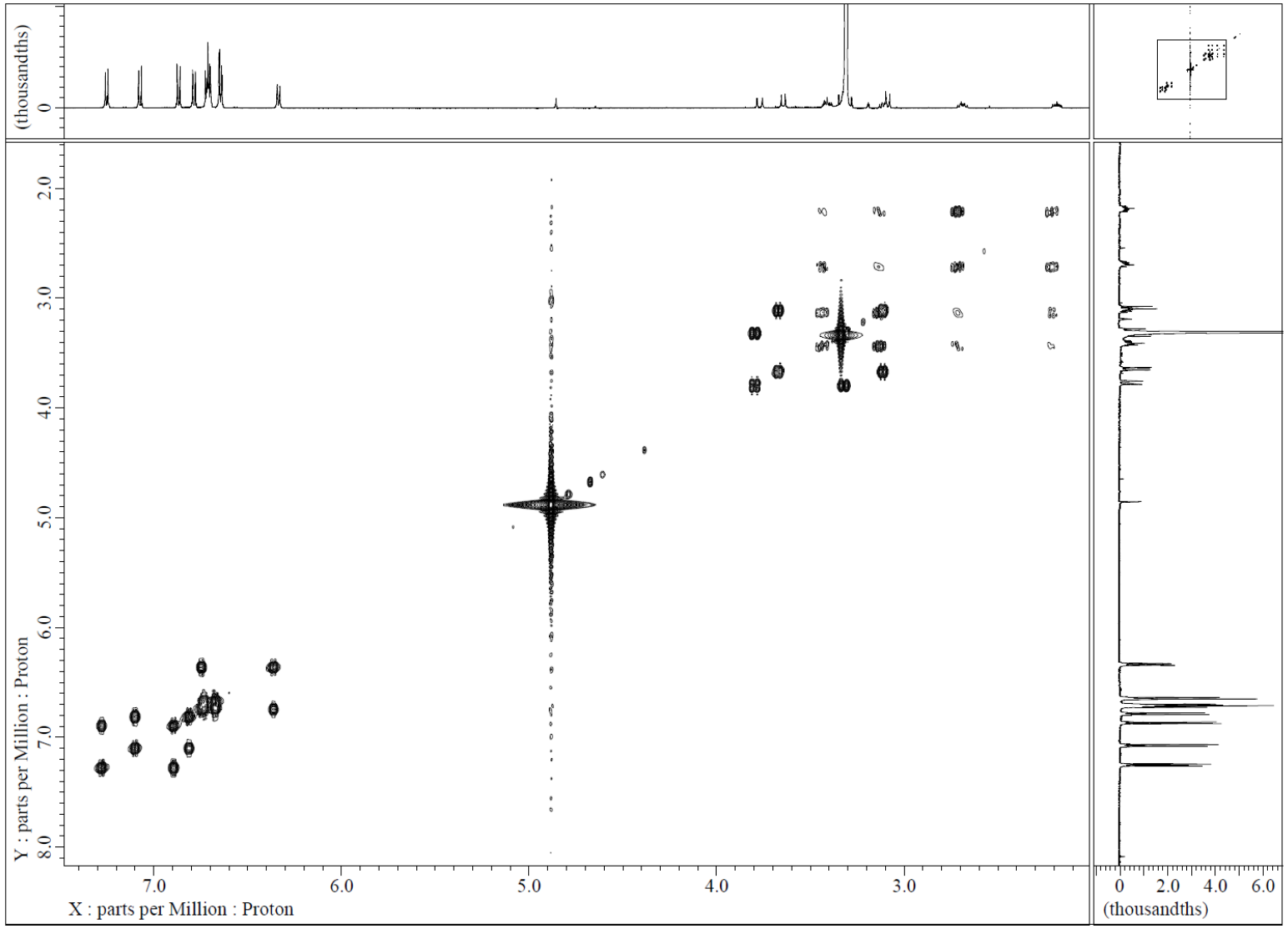

D.8. gHSQC spectrum (methanol-d_4) of denigrin H (**262**)

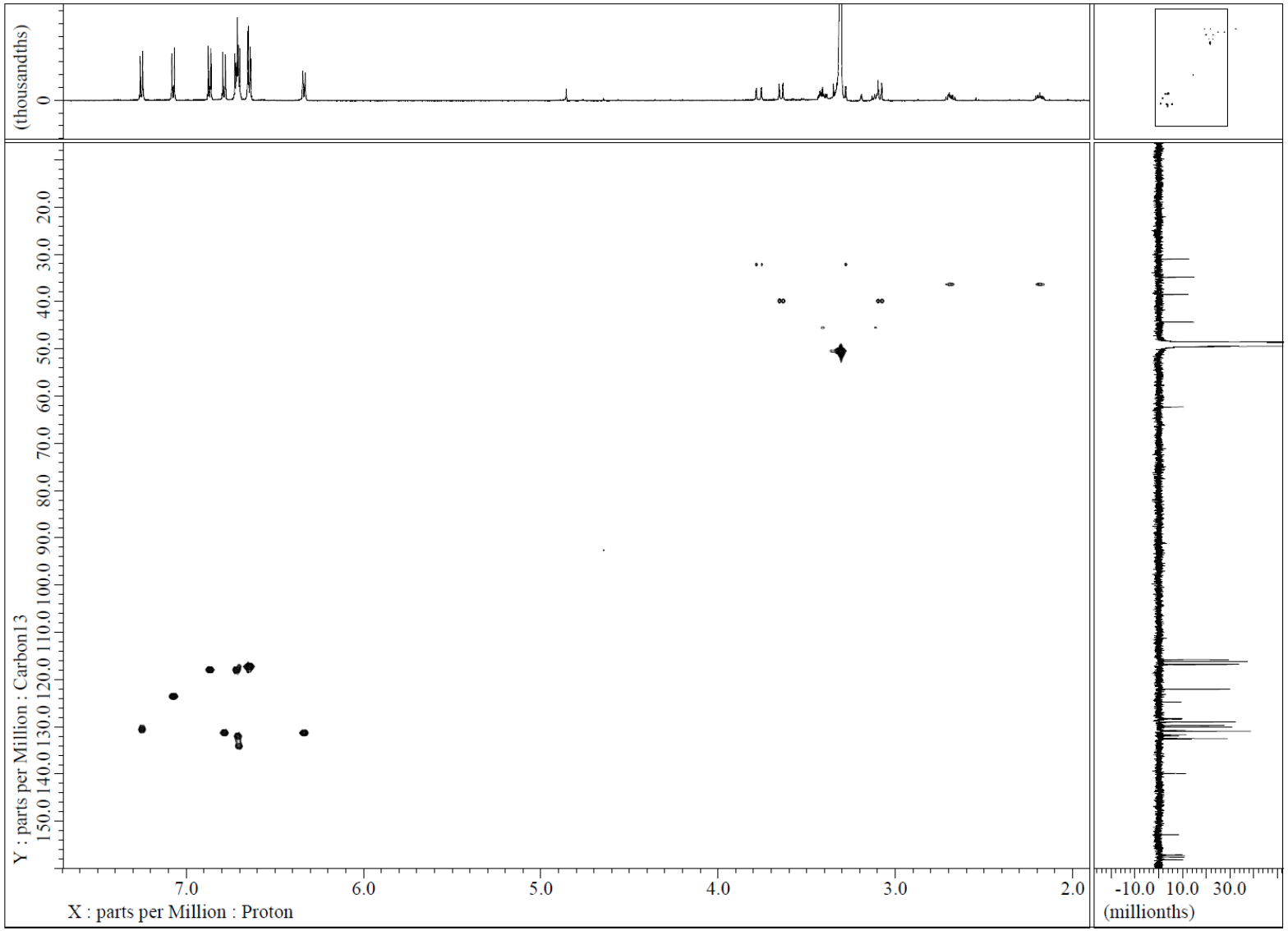

D.9. gHMBC spectrum (methanol-d_4) of denigrin H (**262**)

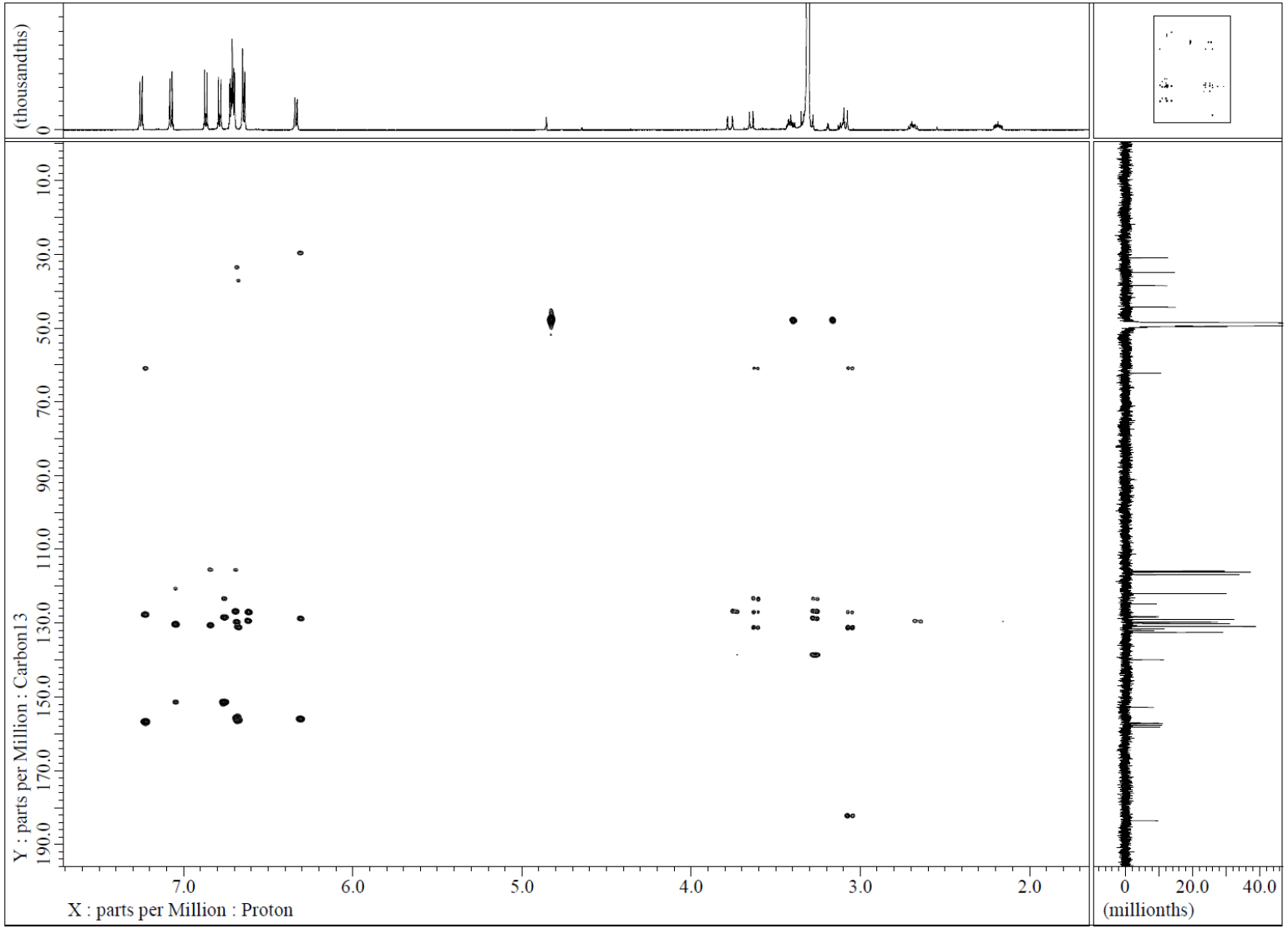

D.10. HR-ESI-MS spectrum of denigrin I (**263**) in negative ion mode

Acquisition Parameter

Source Type	ESI	Ion Polarity	Negative	Set Corrector Fill	46 V
n/a	n/a	Set Capillary Exit	-150.0 V	Set Pulsar Pull	800 V
Scan Begin	50 m/z	Set Hexapole RF	80.0 V	Set Pulsar Push	800 V
Scan End	1500 m/z	Set Skimmer 1	-50.0 V	Set Reflector	1700 V
		Set Hexapole 1	-25.0 V	Set Flight Tube	8600 V
				Set Detector TOF	2250 V

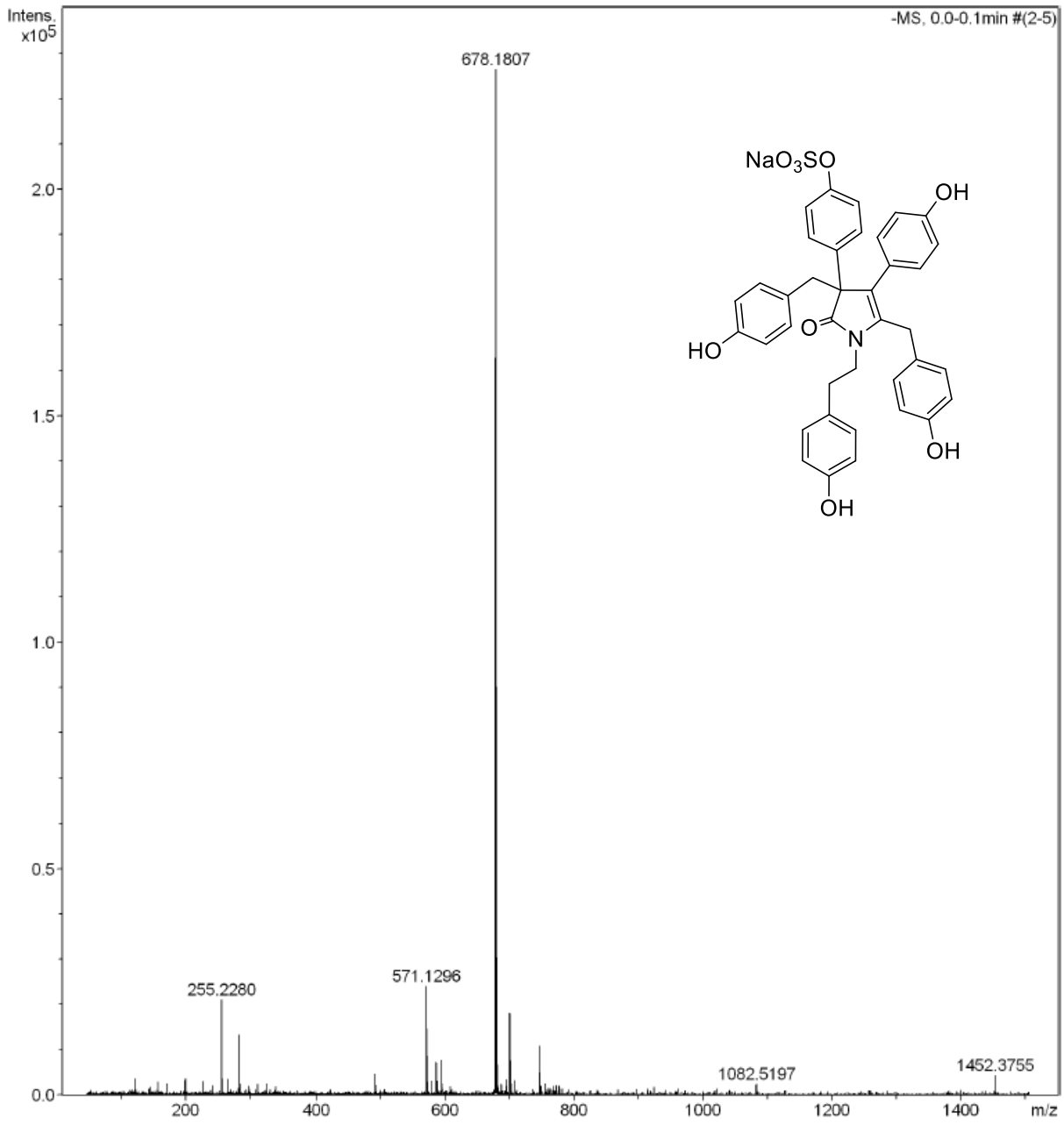

D.11. ^{1}H NMR spectrum (methanol-d_4, 600 MHz) of denigrin I (**263**)

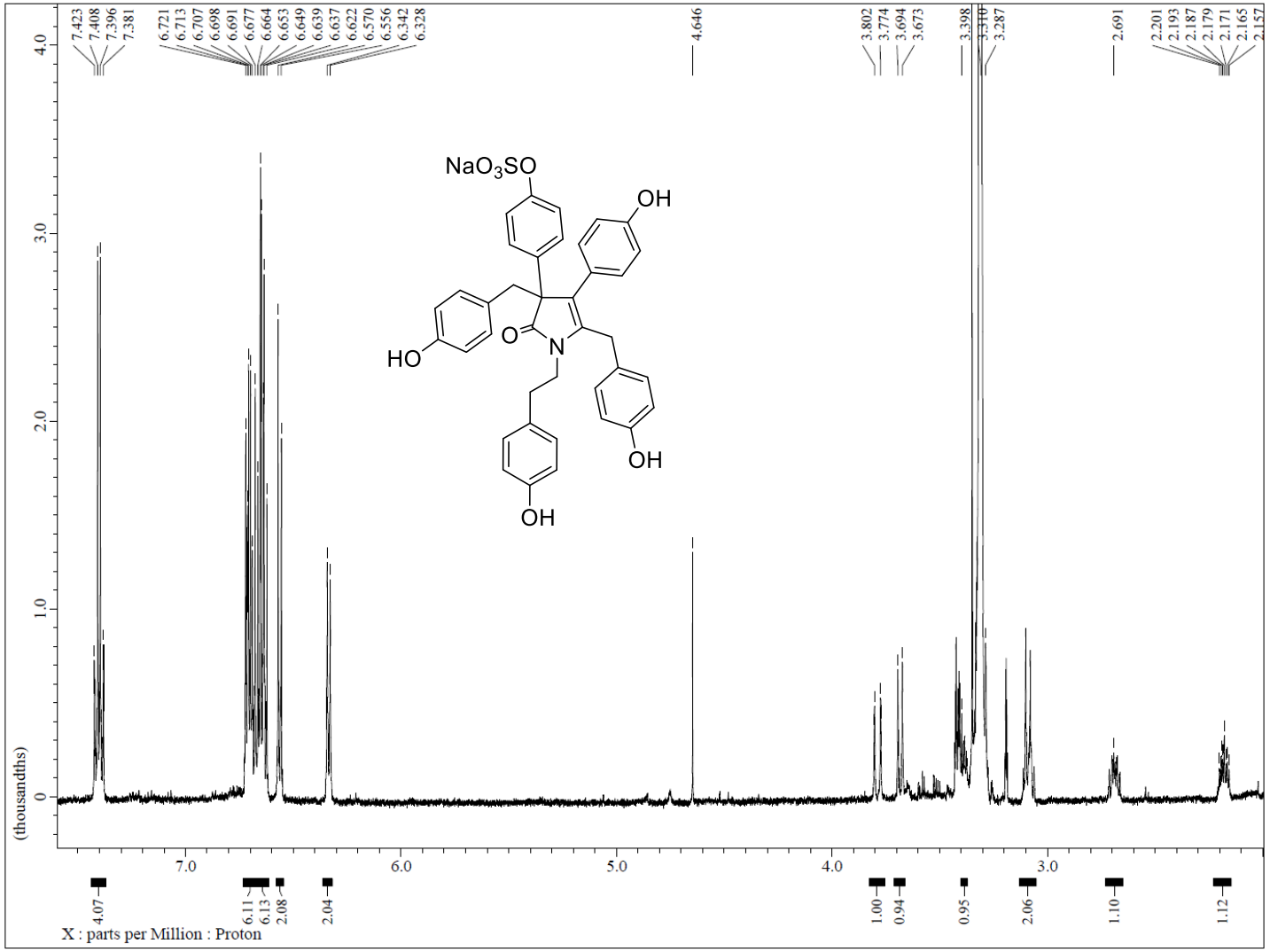

D.12. ^{13}C NMR spectrum (methanol-d_4, 150 MHz) of denigrin I (**263**)

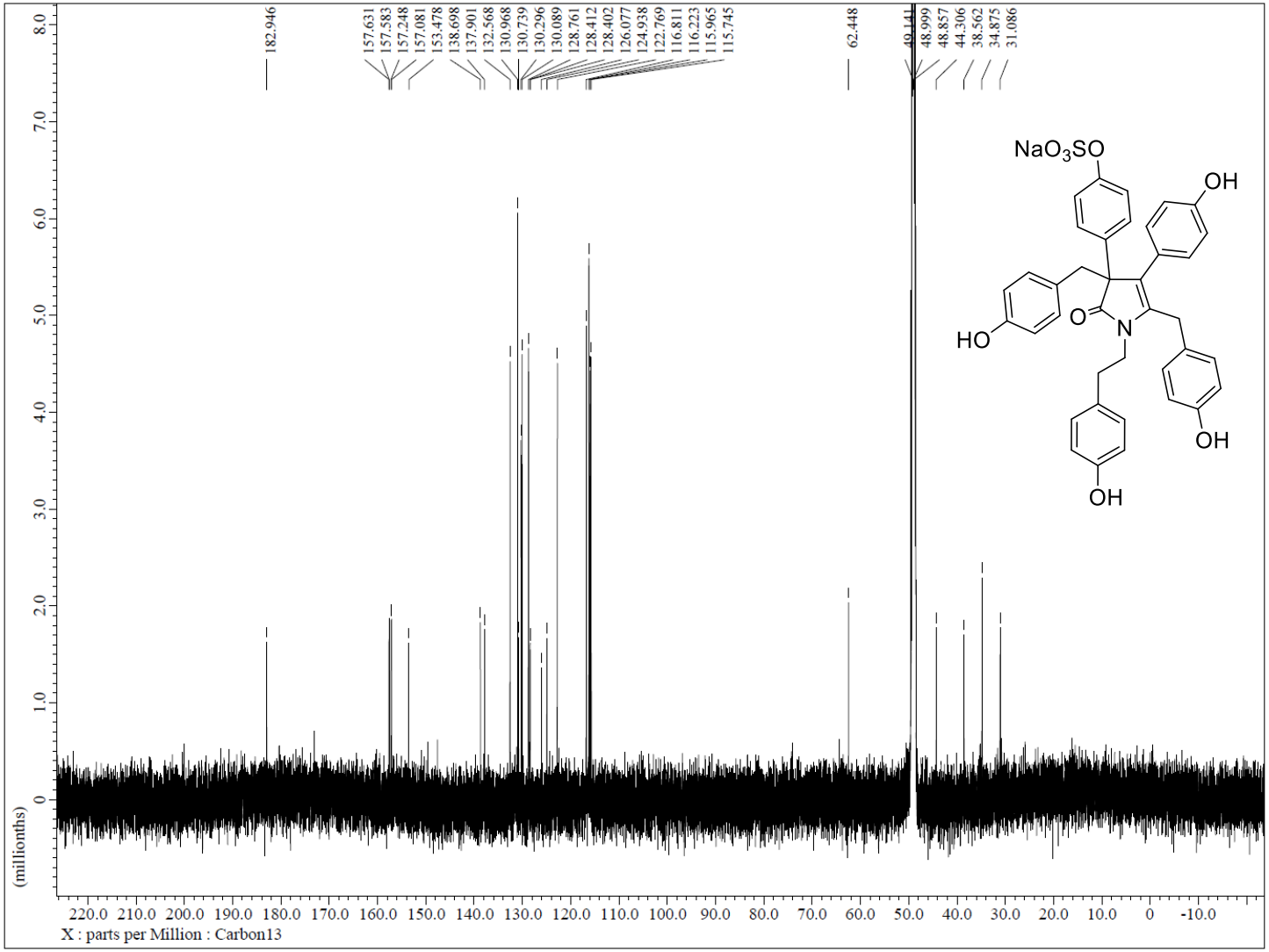

D.13. COSY spectrum (methanol-d_4) of denigrin I (**263**)

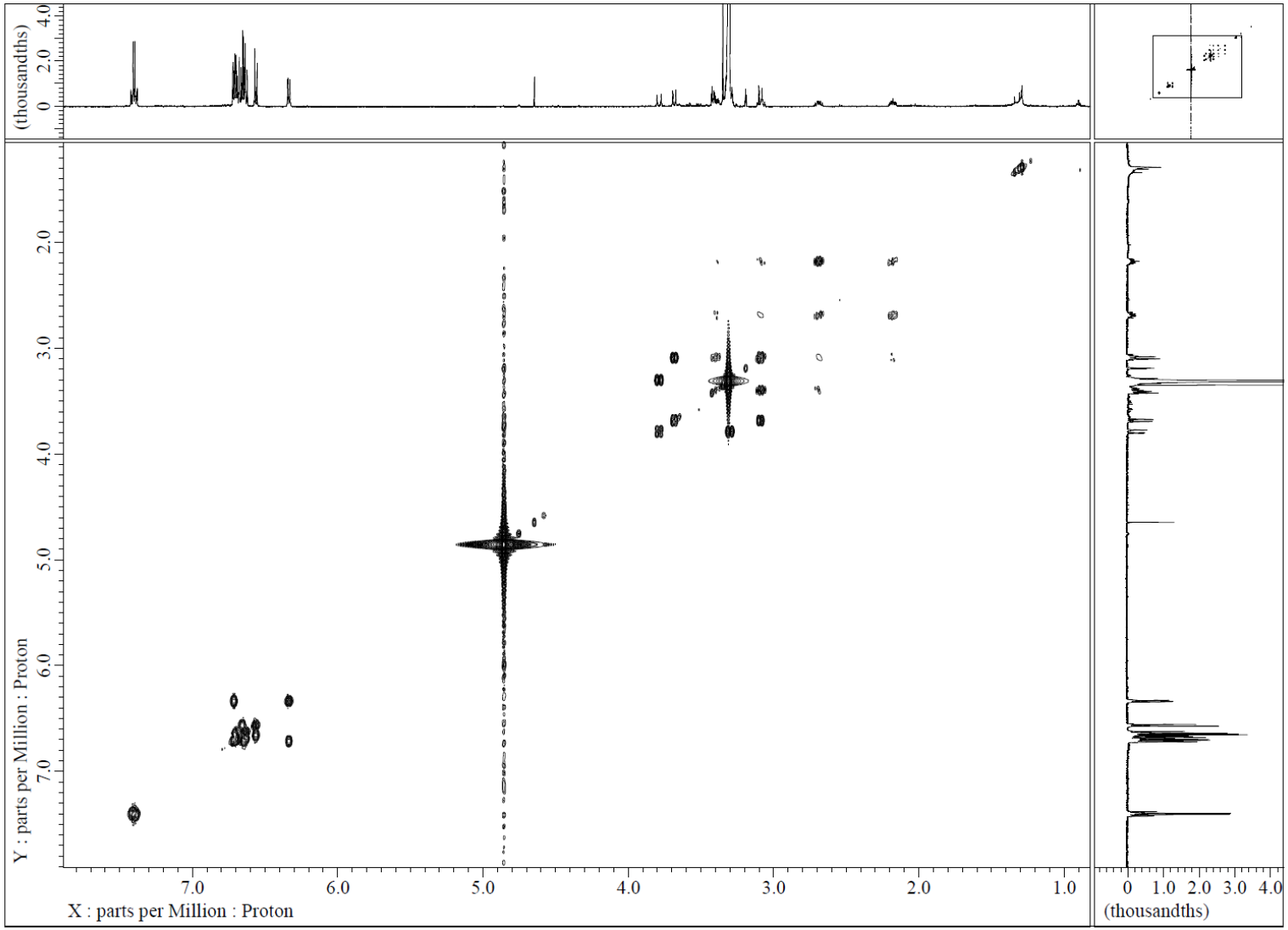

D.14. gHSQC spectrum (methanol-d_4) of denigrin I (**263**)

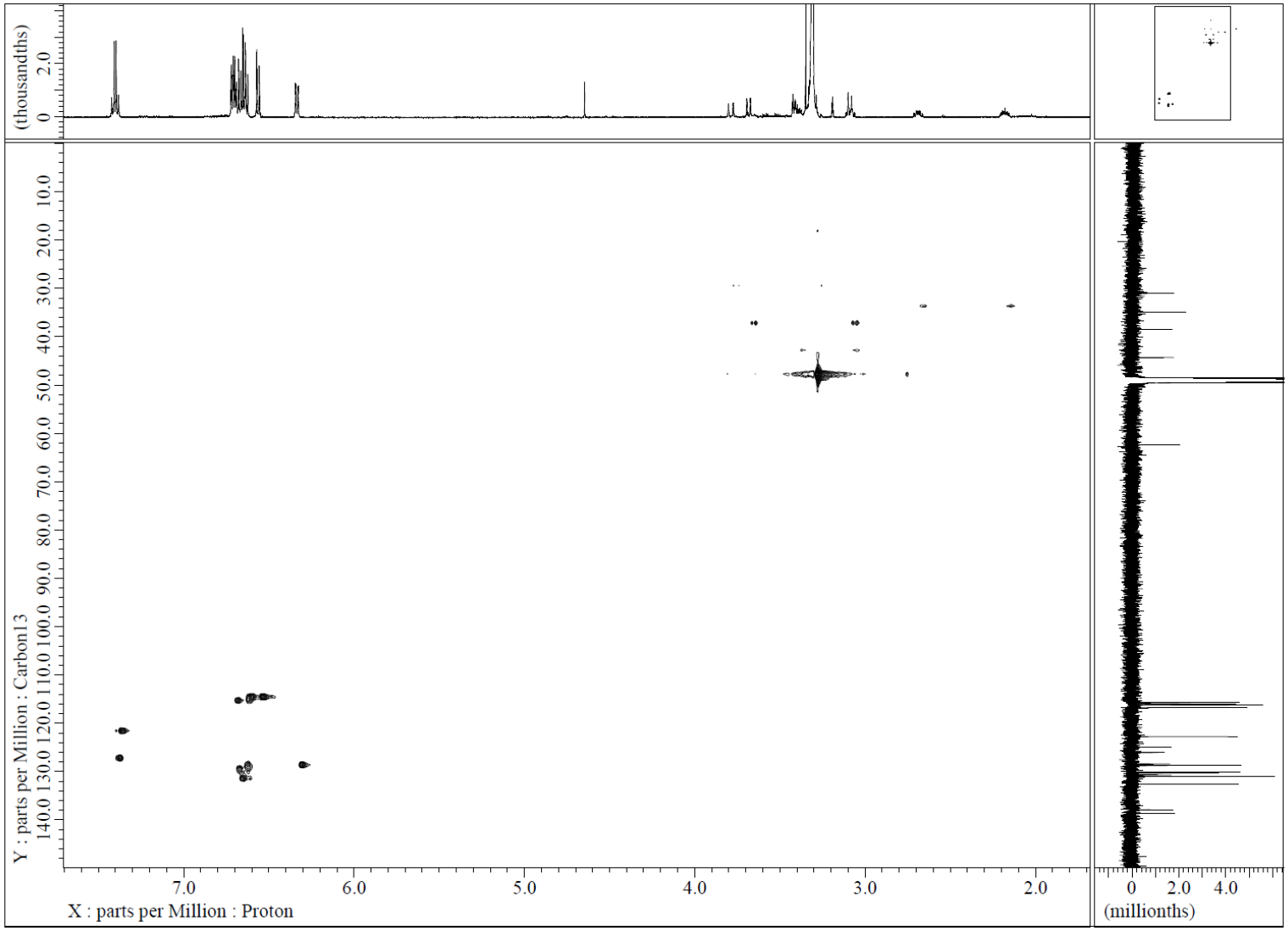

D.15. gHMBC spectrum (methanol-d_4) of denigrin I (**263**)

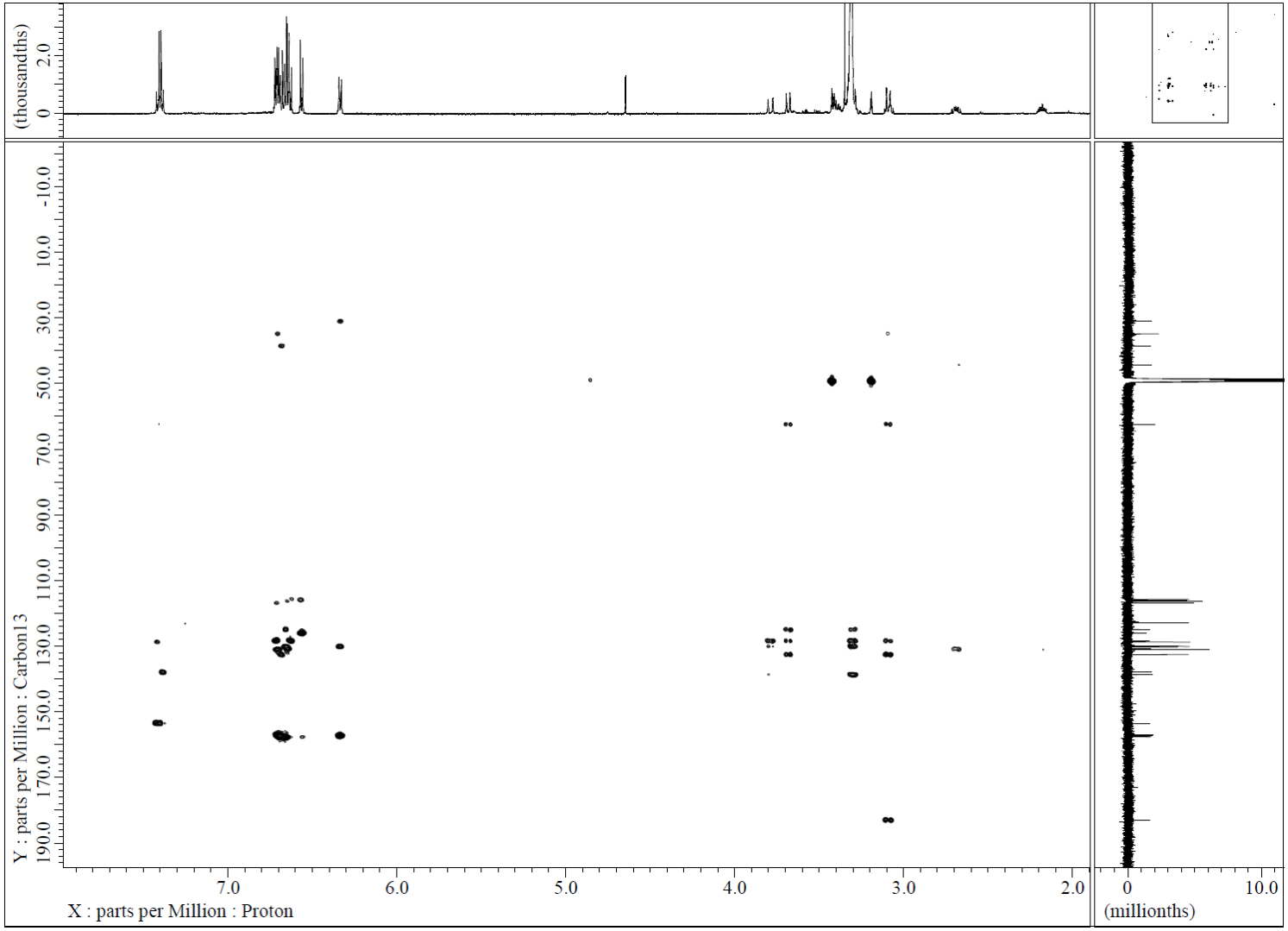

D.16. HR-ESI-MS spectrum of denigrin J (**264**) in negative ion mode

Acquisition Parameter

Source Type	ESI	Ion Polarity	Negative	Set Corrector Fill	46 V
n/a	n/a	Set Capillary Exit	-150.0 V	Set Pulsar Pull	800 V
Scan Begin	50 m/z	Set Hexapole RF	80.0 V	Set Pulsar Push	800 V
Scan End	1500 m/z	Set Skimmer 1	-50.0 V	Set Reflector	1700 V
		Set Hexapole 1	-25.0 V	Set Flight Tube	8600 V
				Set Detector TOF	2250 V

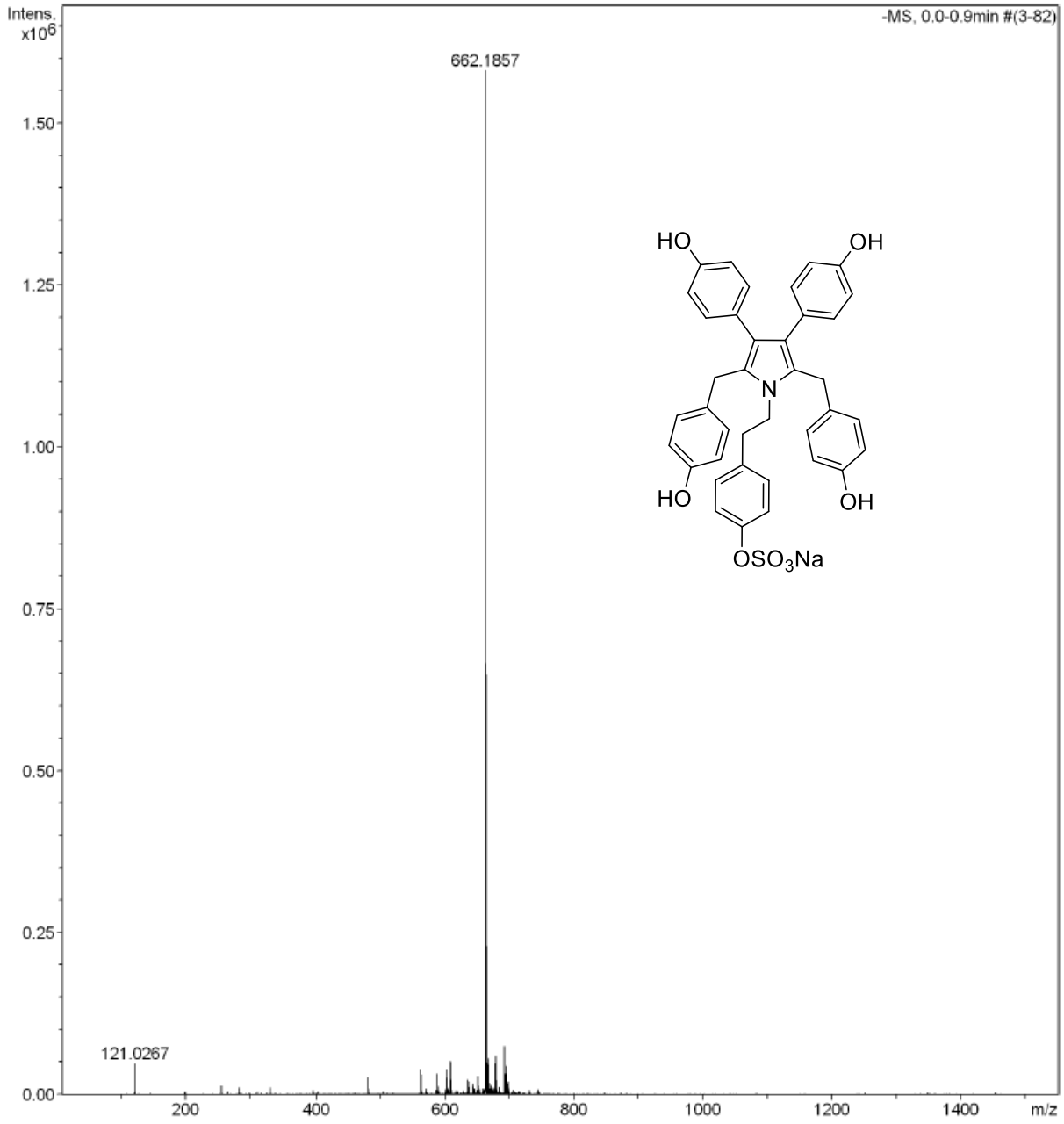

D.17. ^{1}H NMR spectrum (methanol-d_4, 600 MHz) of denigrin J (**264**)

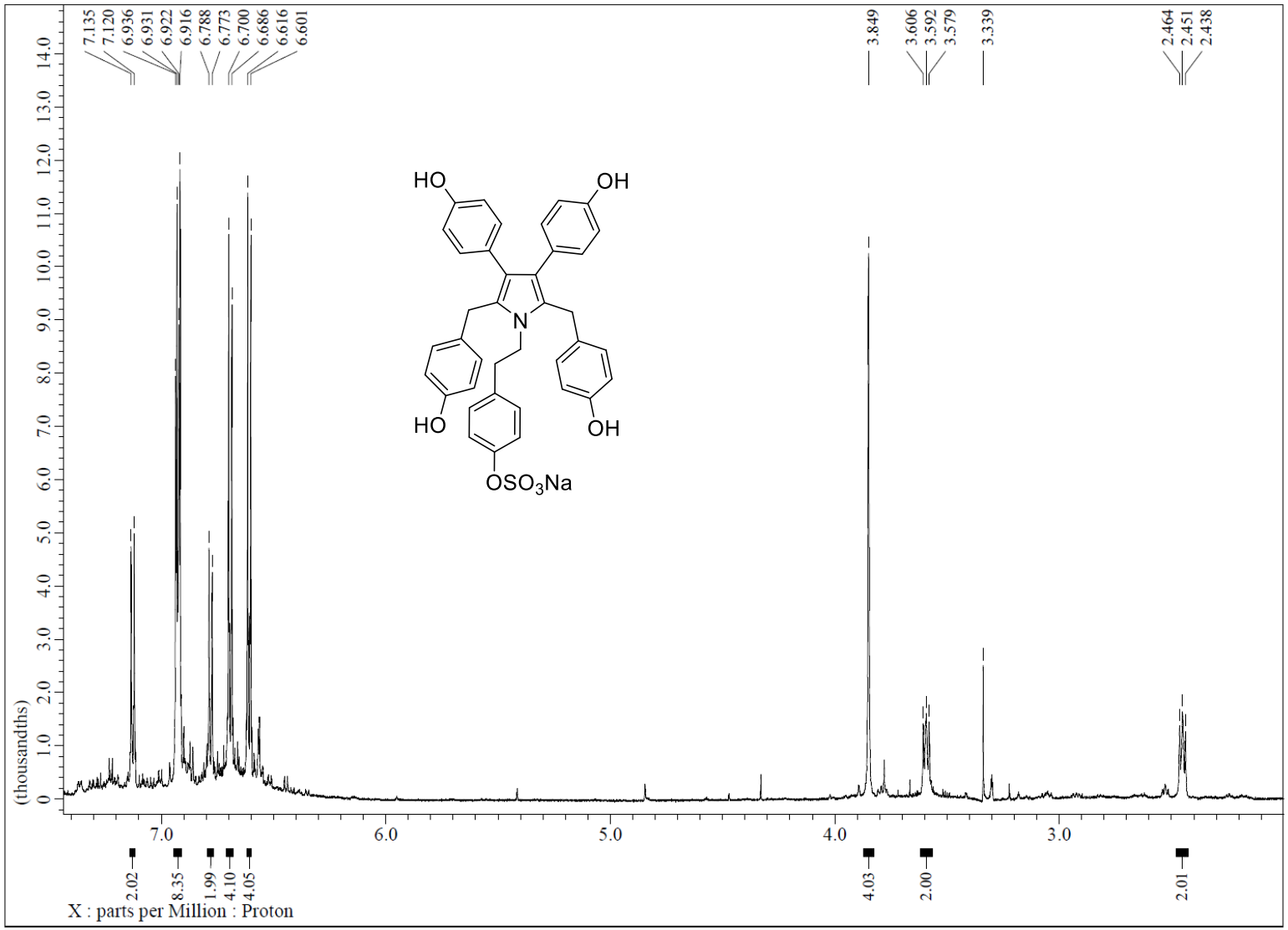

D.18. ^{13}C NMR spectrum (methanol-d_4, 150 MHz) of denigrin J (**264**)

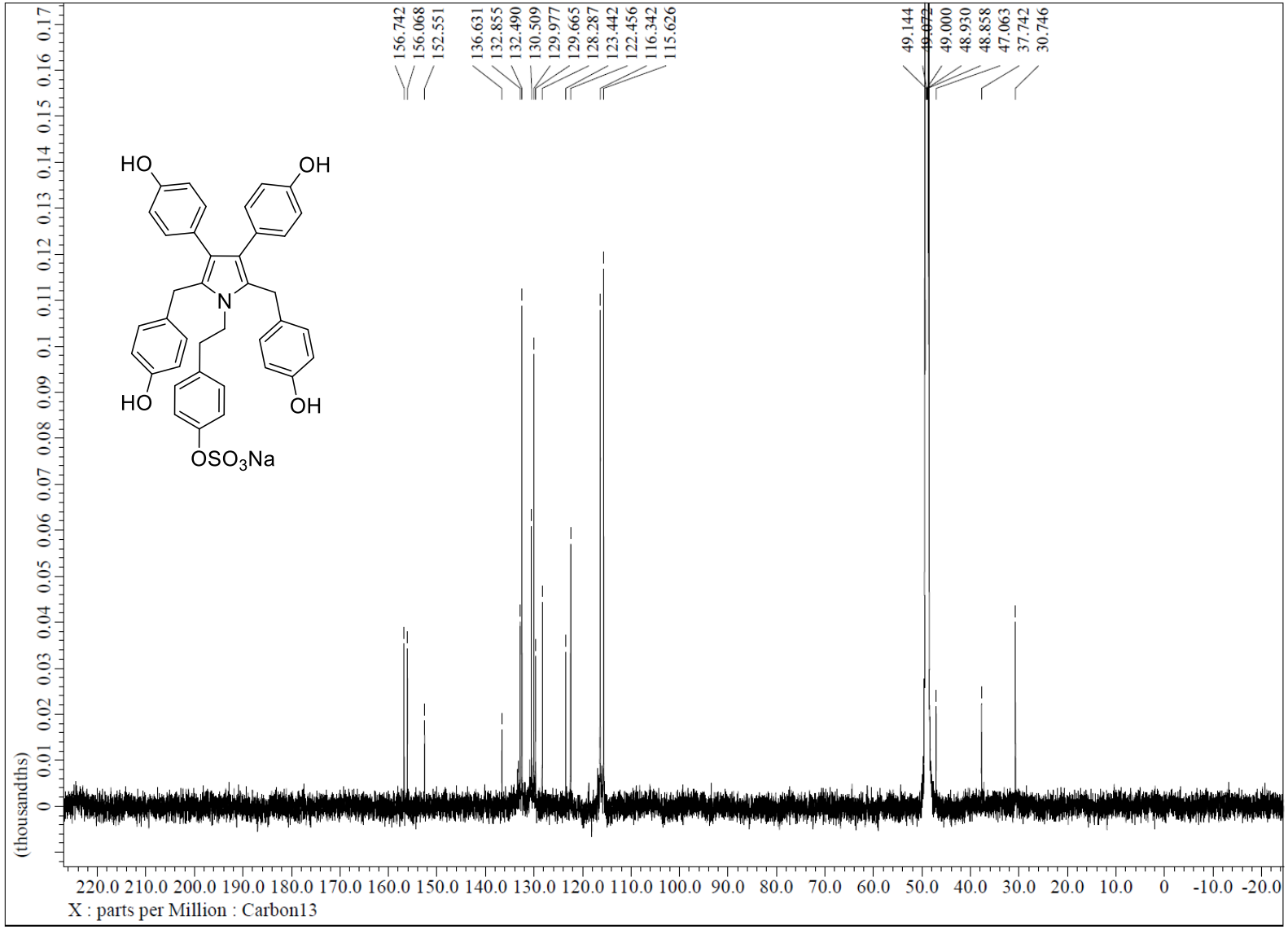

D.19. COSY spectrum (methanol-d_4) of denigrin J (**264**)

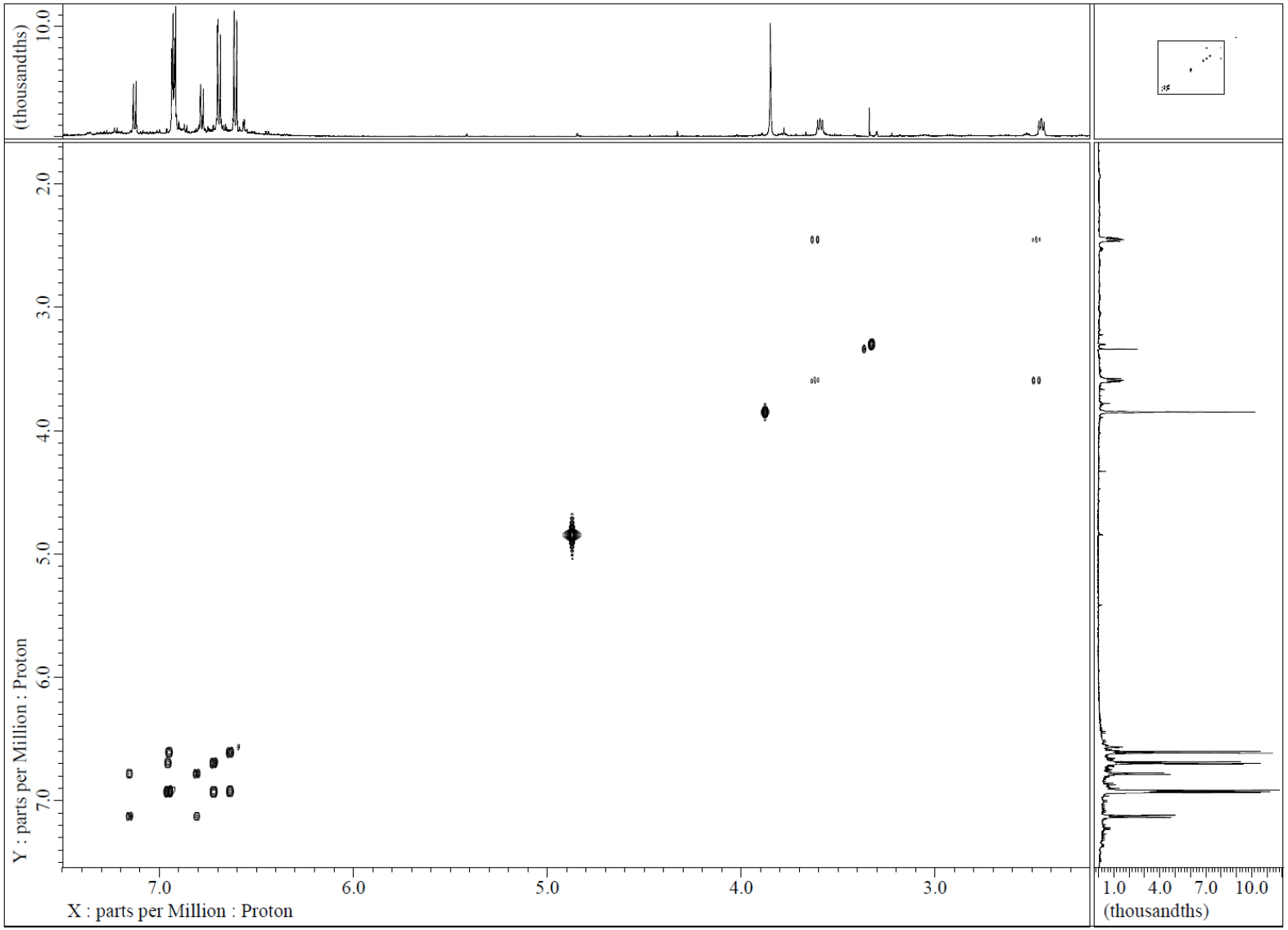

D.20. gHSQC spectrum (methanol-d_4) of denigrin J (**264**)

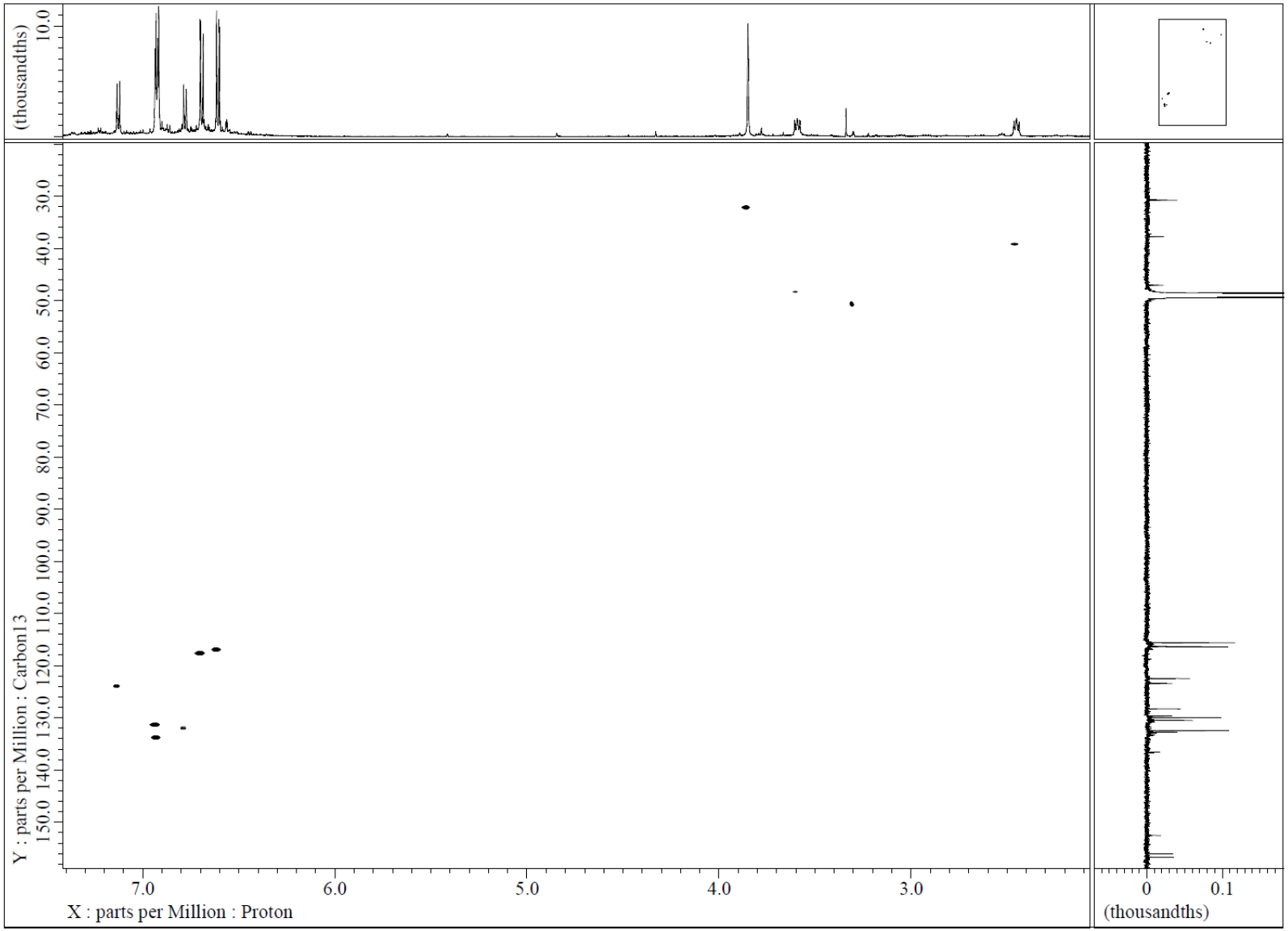

D.21. gHMBC spectrum (methanol-d_4) of denigrin J (**264**)

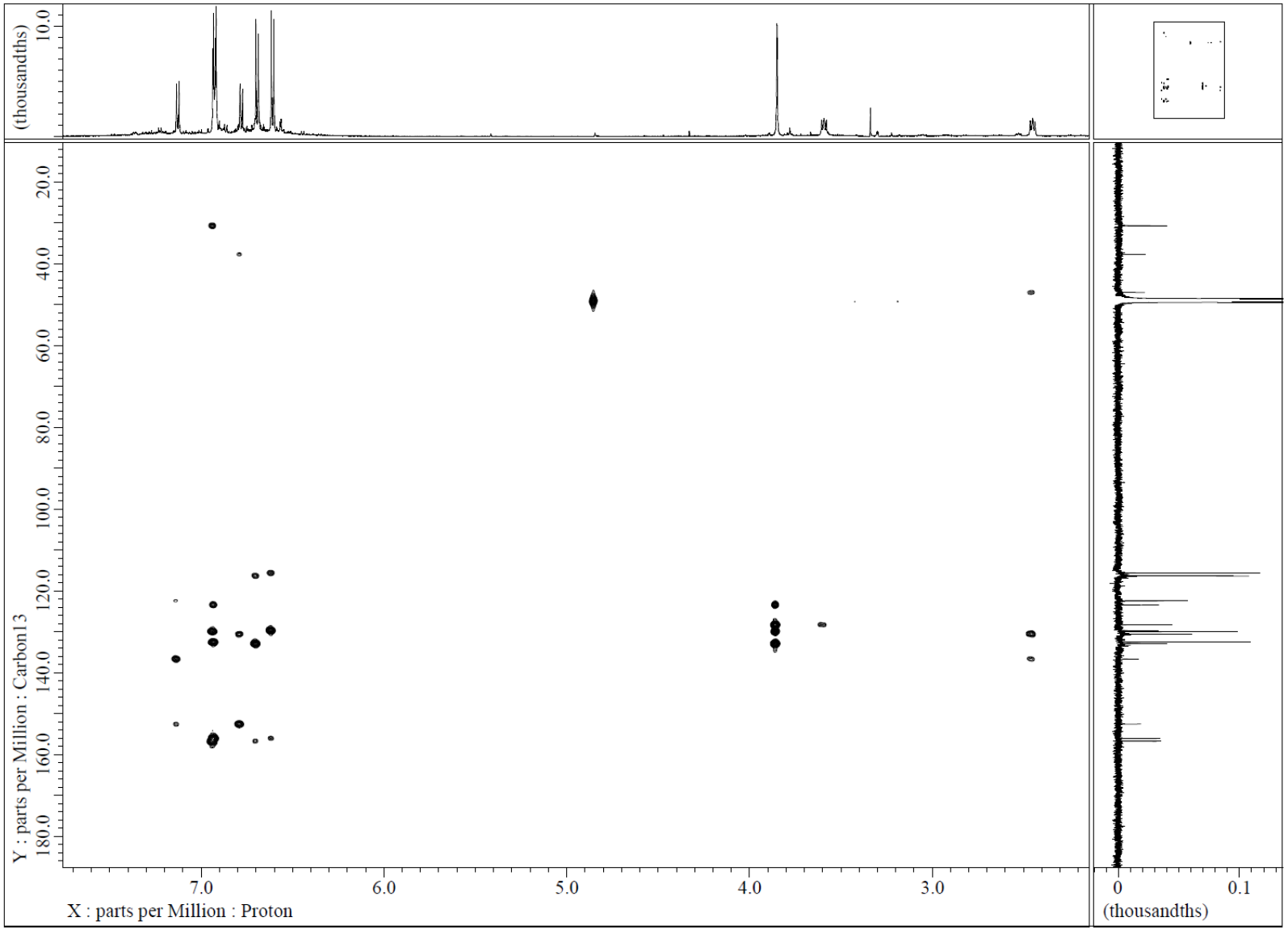

D.22. HR-ESI-MS spectrum of denigrin K (**265**) in negative ion mode

Acquisition Parameter

Source Type	ESI	Ion Polarity	Negative	Set Corrector Fill	46 V
n/a	n/a	Set Capillary Exit	-150.0 V	Set Pulsar Pull	800 V
Scan Begin	50 m/z	Set Hexapole RF	80.0 V	Set Pulsar Push	800 V
Scan End	1500 m/z	Set Skimmer 1	-50.0 V	Set Reflector	1700 V
		Set Hexapole 1	-25.0 V	Set Flight Tube	8600 V
				Set Detector TOF	2250 V

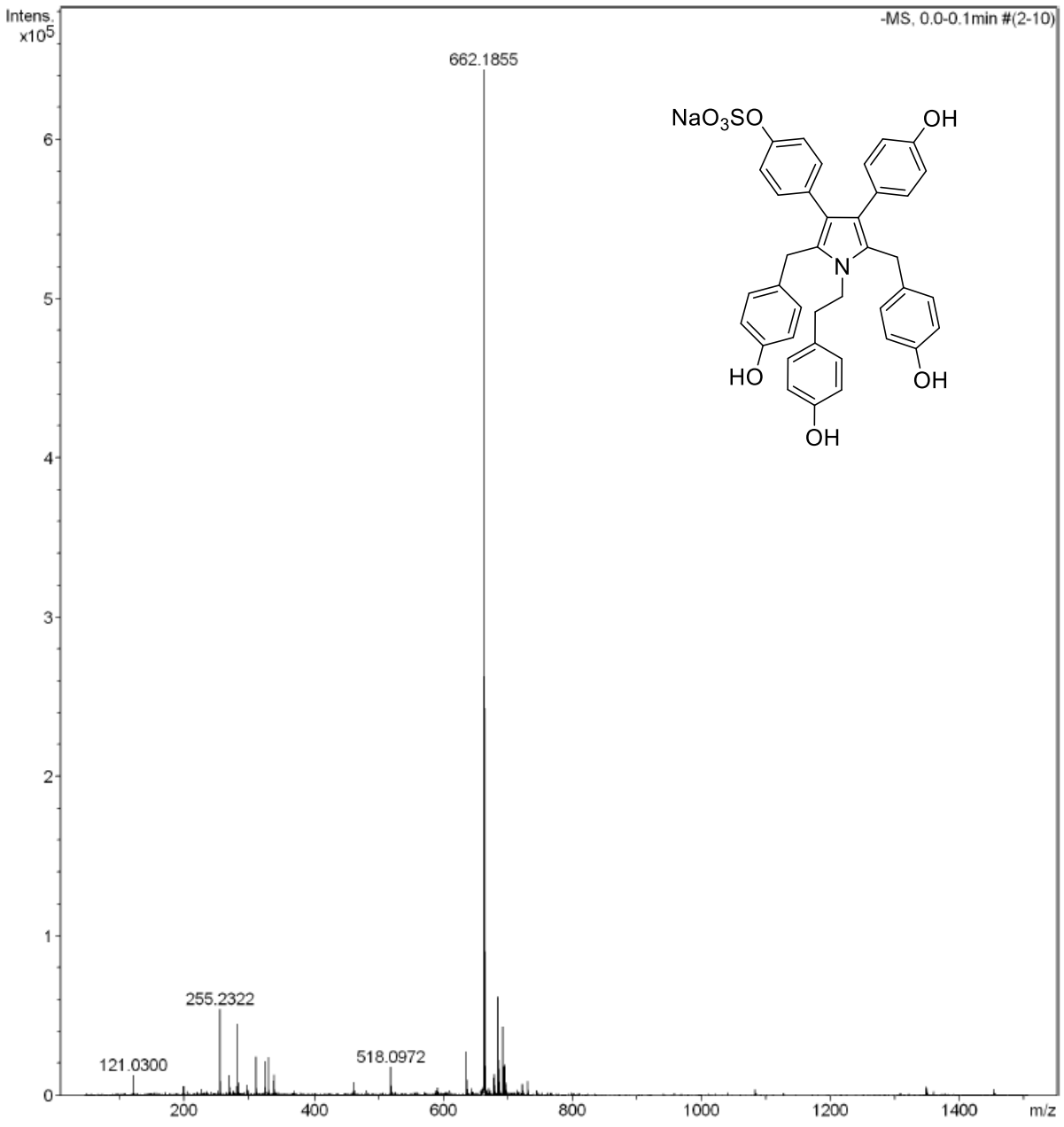

D.23. ^{1}H NMR spectrum (methanol-d_4, 600 MHz) of denigrin K (**265**)

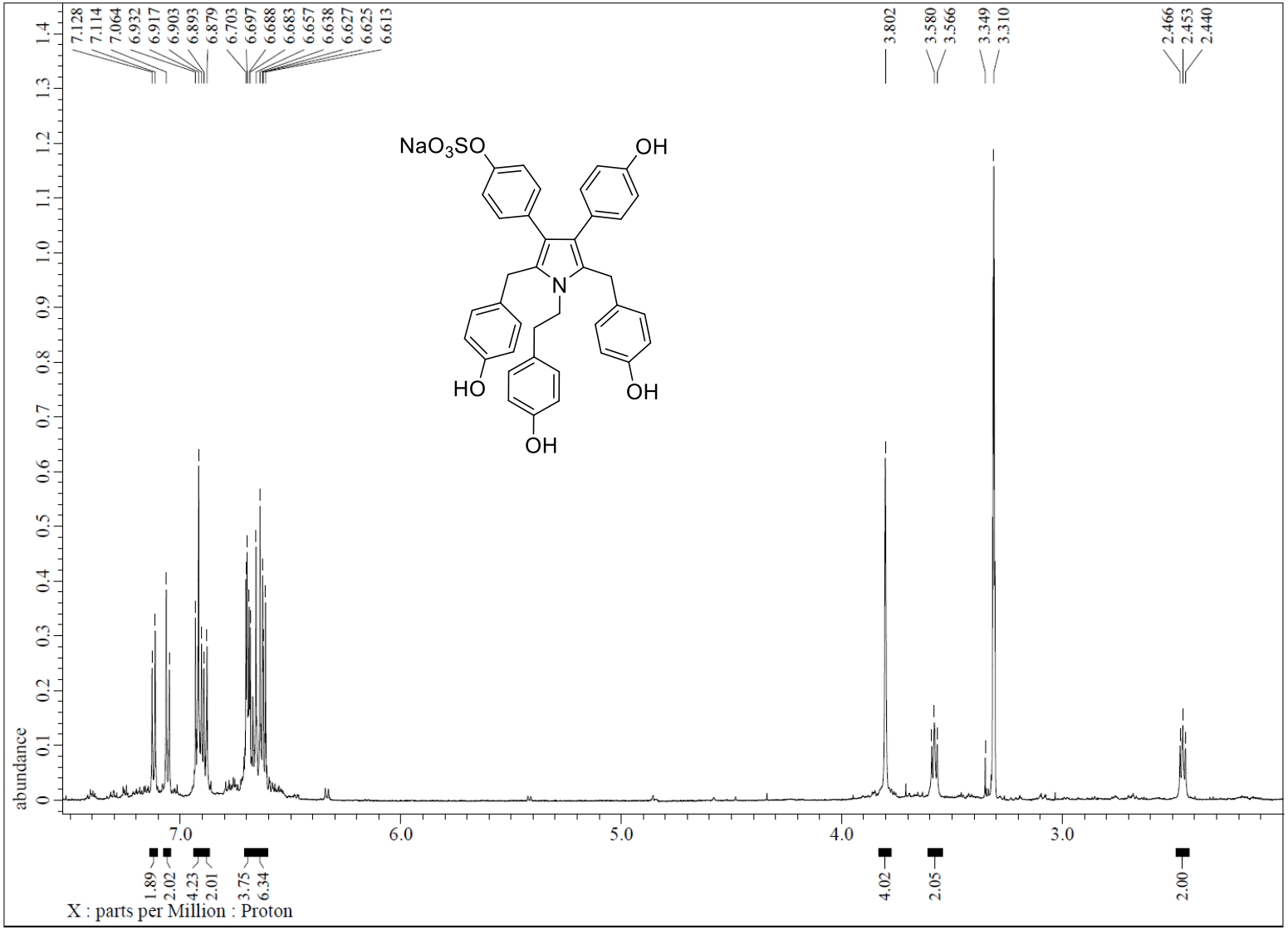

D.24. ^{13}C NMR spectrum (methanol-d_4, 150 MHz) of denigrin K (**265**)

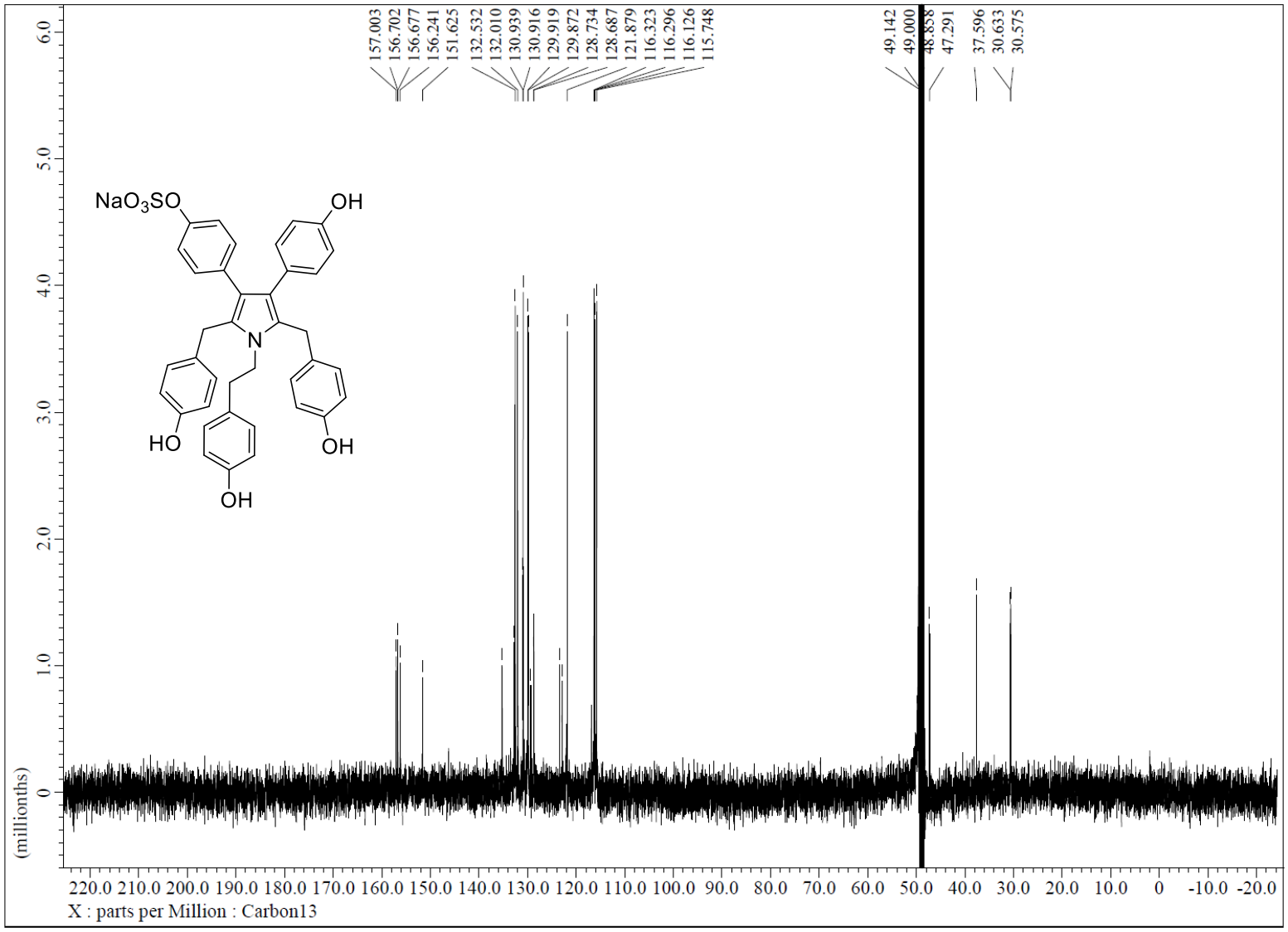

D.25. COSY spectrum (methanol-d_4) of denigrin K (**265**)

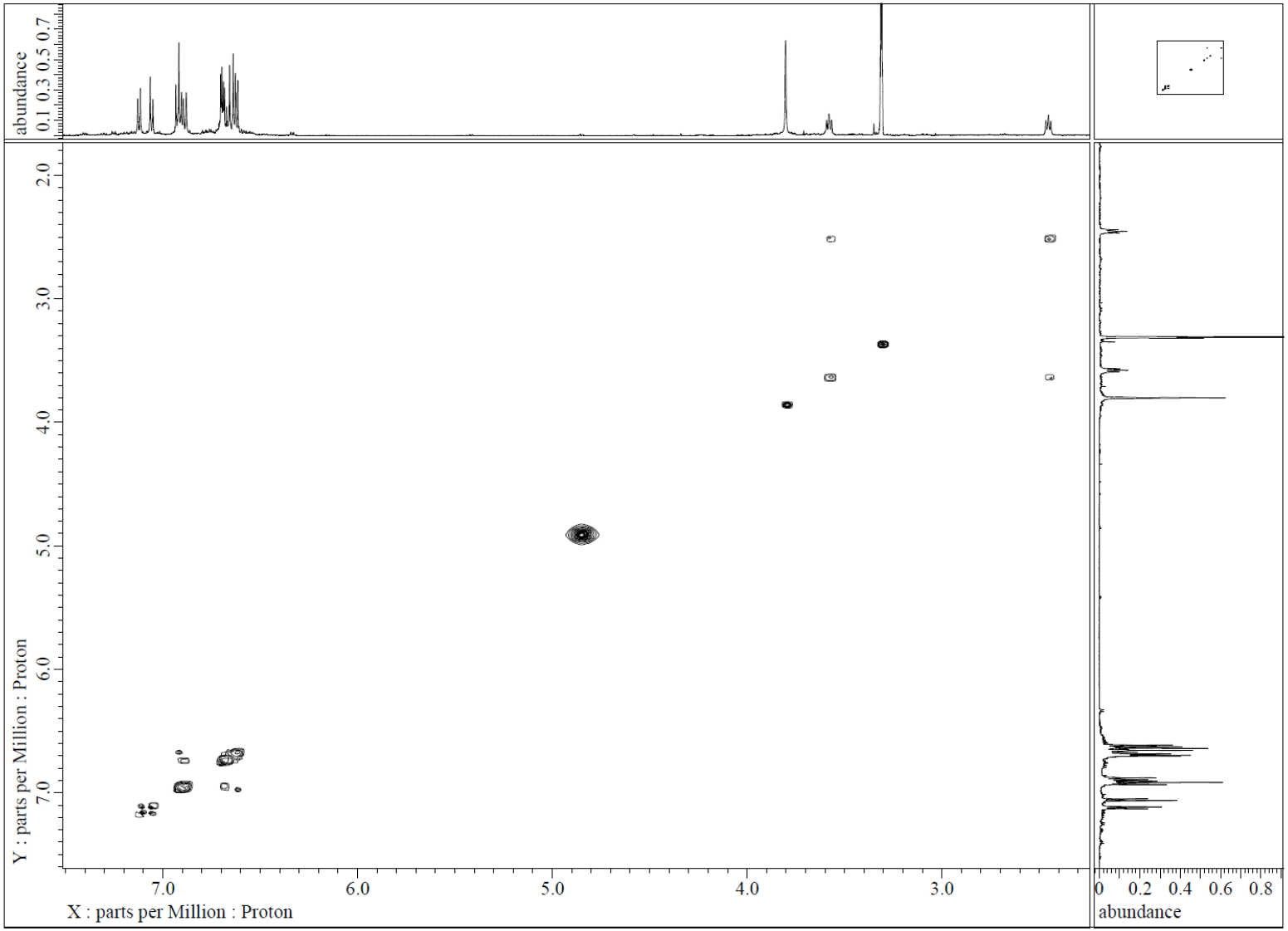

D.26. gHSQC spectrum (methanol-d_4) of denigrin K (**265**)

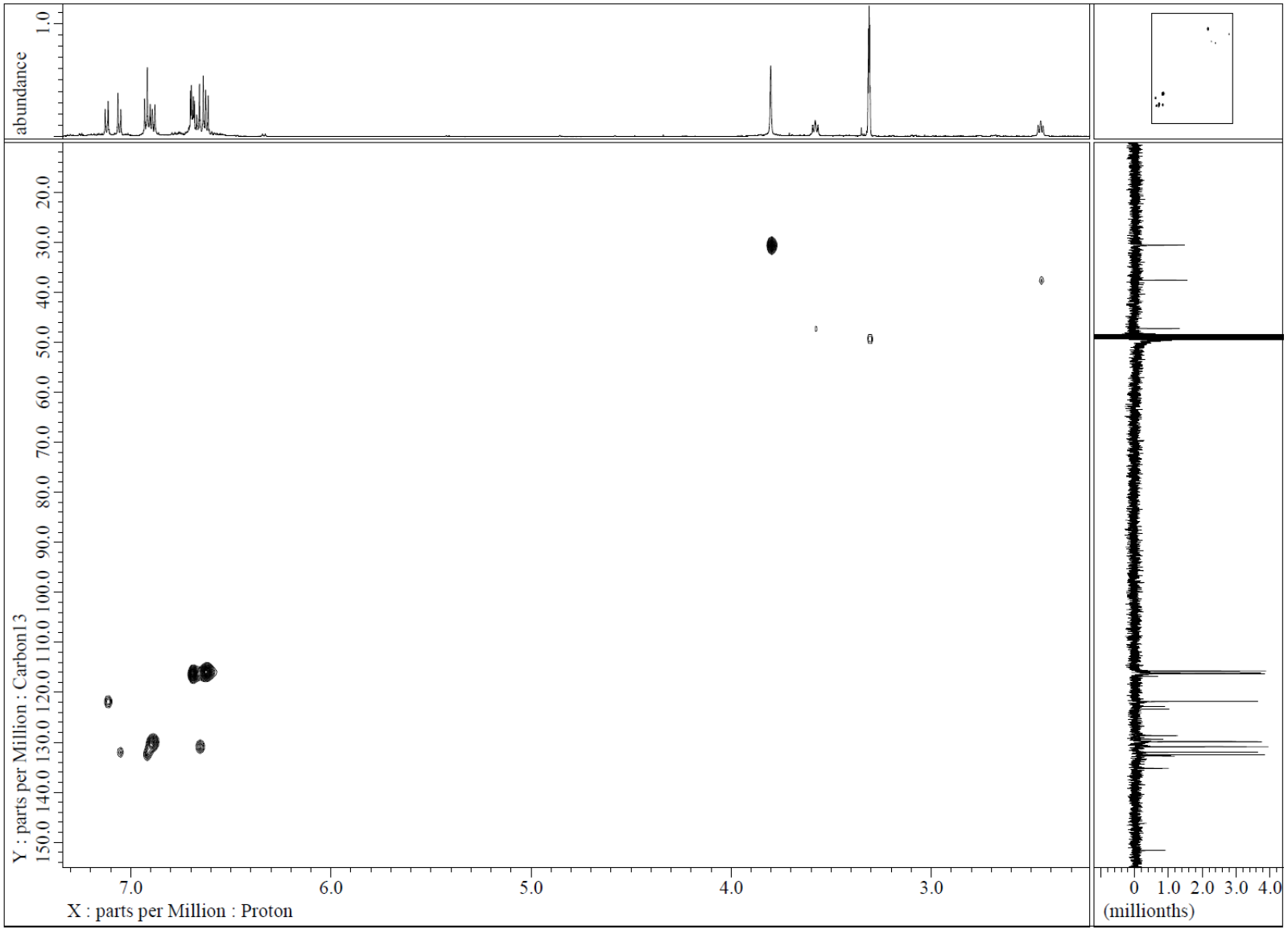

D.27. gHMBC spectrum (methanol-d_4) of denigrin K (**265**)

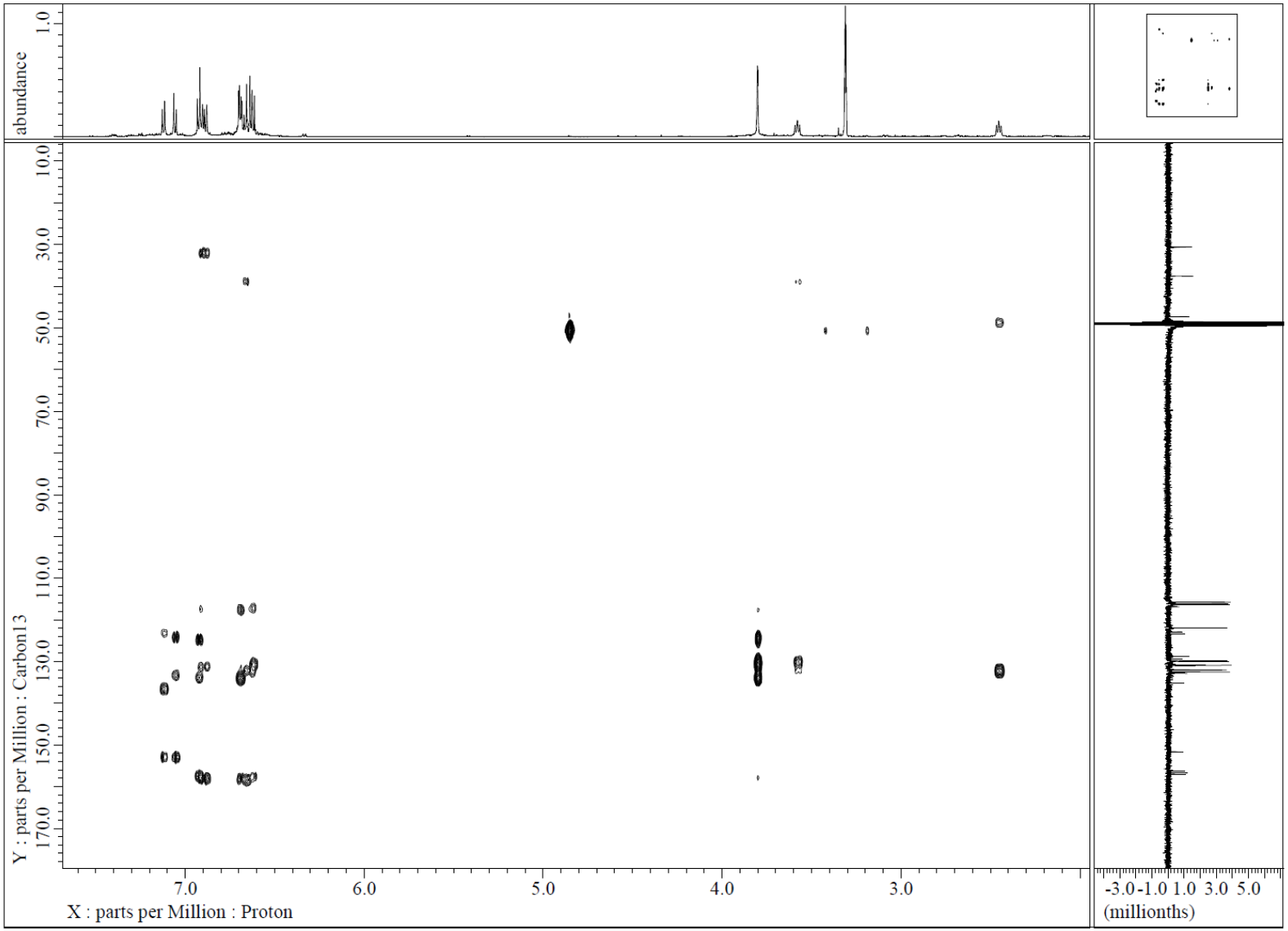

D.28. HR-ESI-MS spectrum of denigrin L (**266**) in negative ion mode

Acquisition Parameter

Source Type	ESI	Ion Polarity	Negative	Set Corrector Fill	46 V
n/a	n/a	Set Capillary Exit	-150.0 V	Set Pulsar Pull	800 V
Scan Begin	50 m/z	Set Hexapole RF	80.0 V	Set Pulsar Push	800 V
Scan End	1500 m/z	Set Skimmer 1	-50.0 V	Set Reflector	1700 V
		Set Hexapole 1	-25.0 V	Set Flight Tube	8600 V
				Set Detector TOF	2250 V

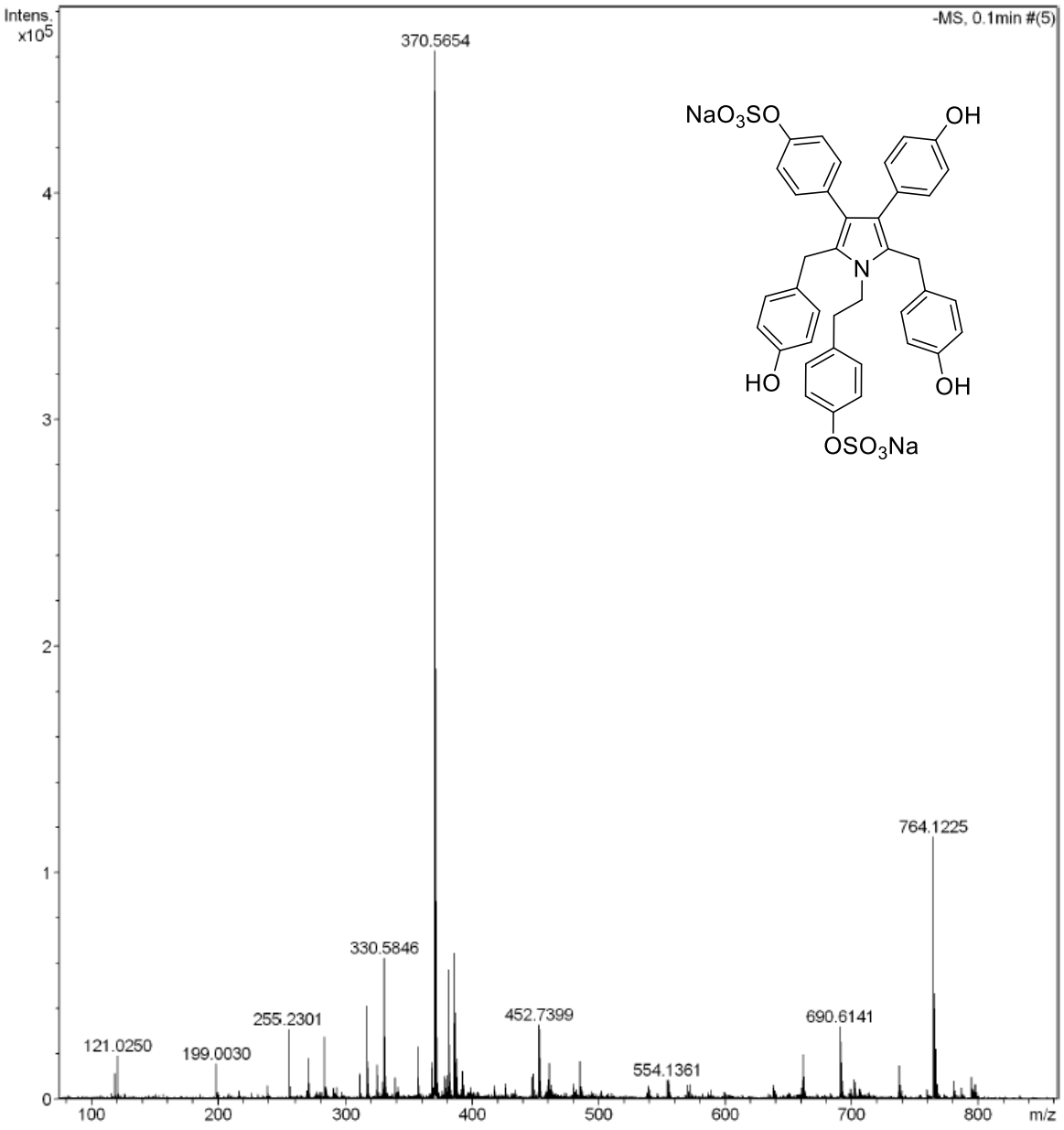

D.29. ^{1}H NMR spectrum (methanol-d_4, 600 MHz) of denigrin L (**266**)

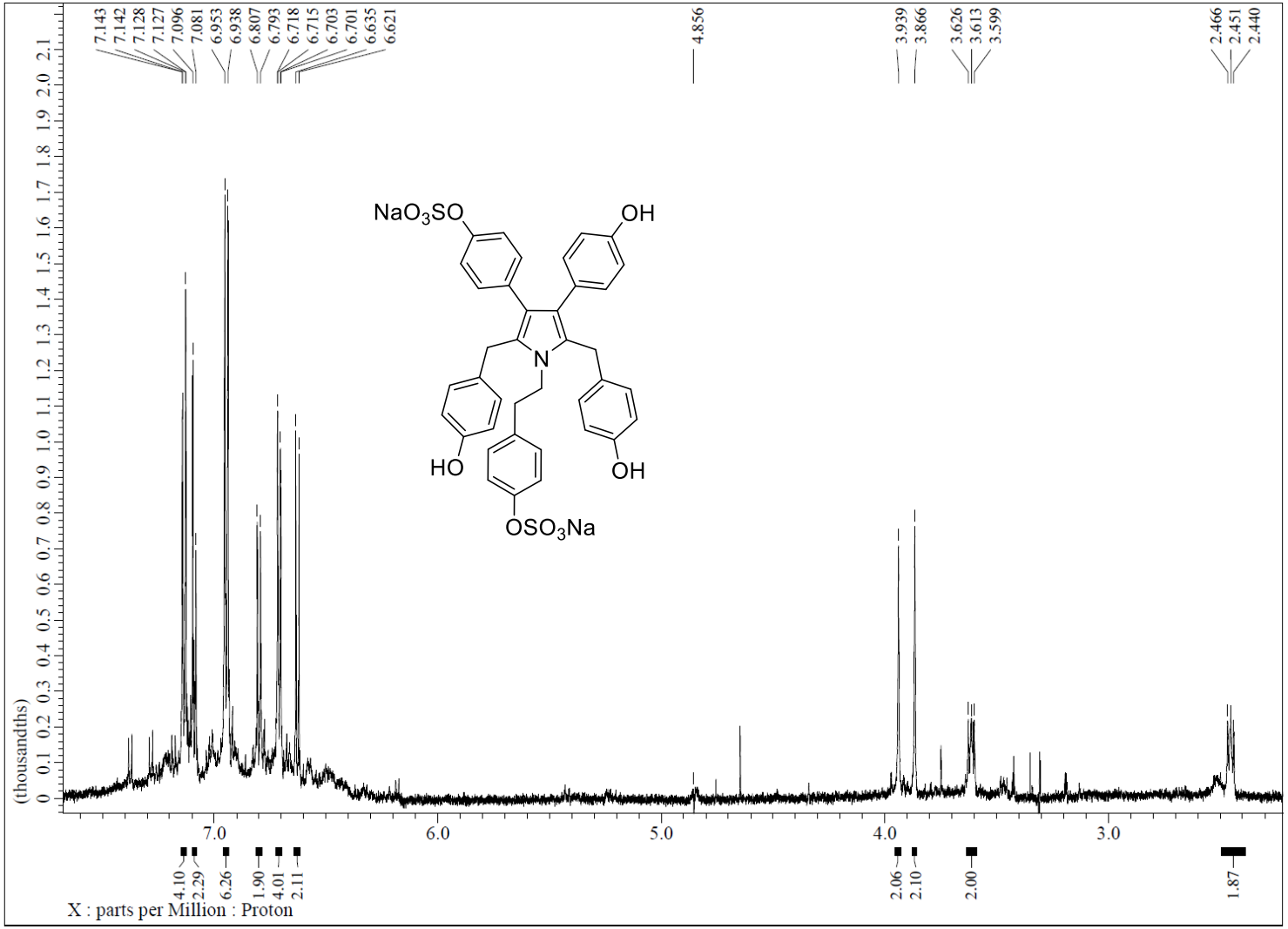

D.30. ^{13}C NMR spectrum (methanol-d_4, 150 MHz) of denigrin L (**266**)

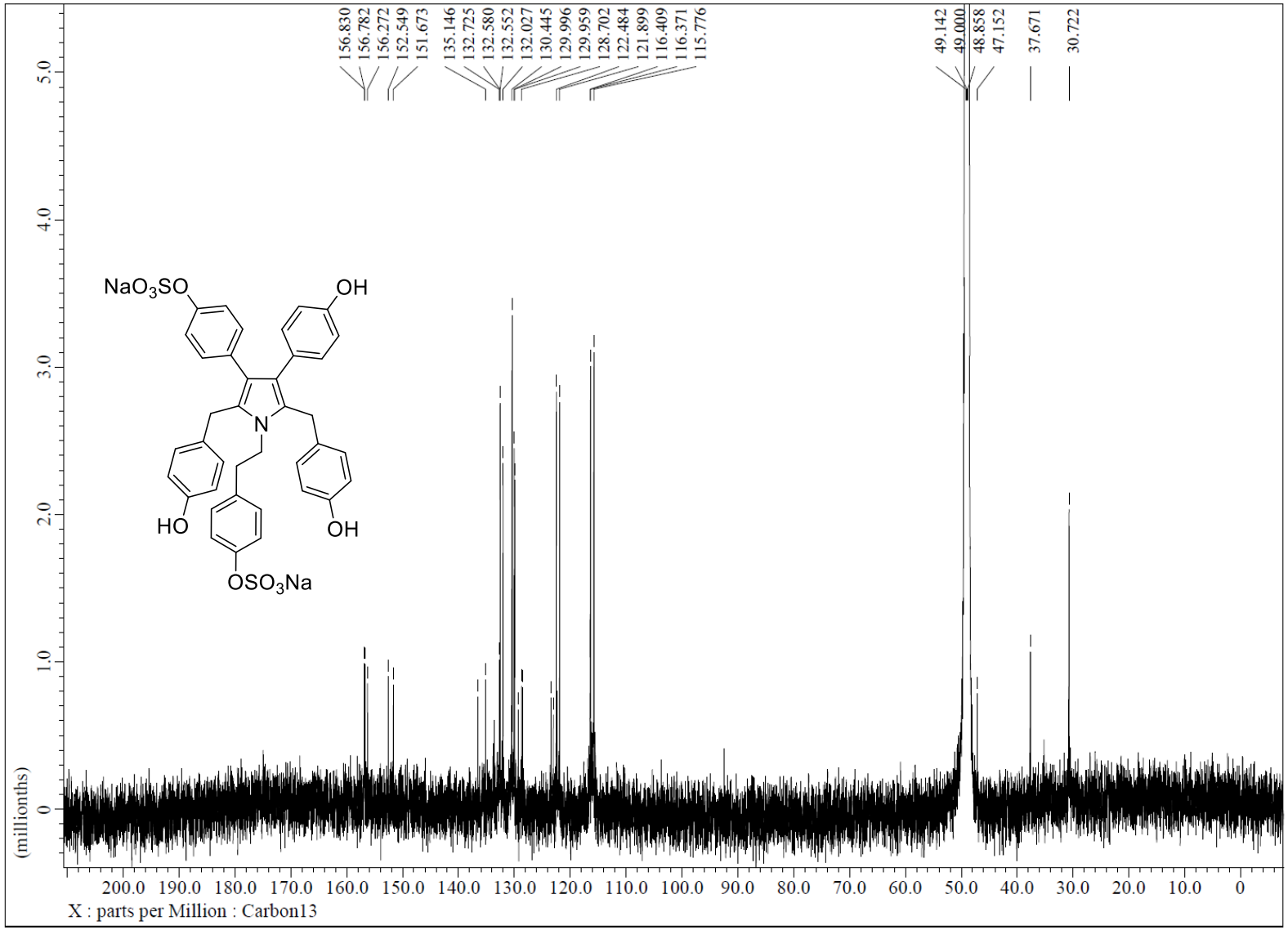

D.31. COSY spectrum (methanol-d_4) of denigrin L (**266**)

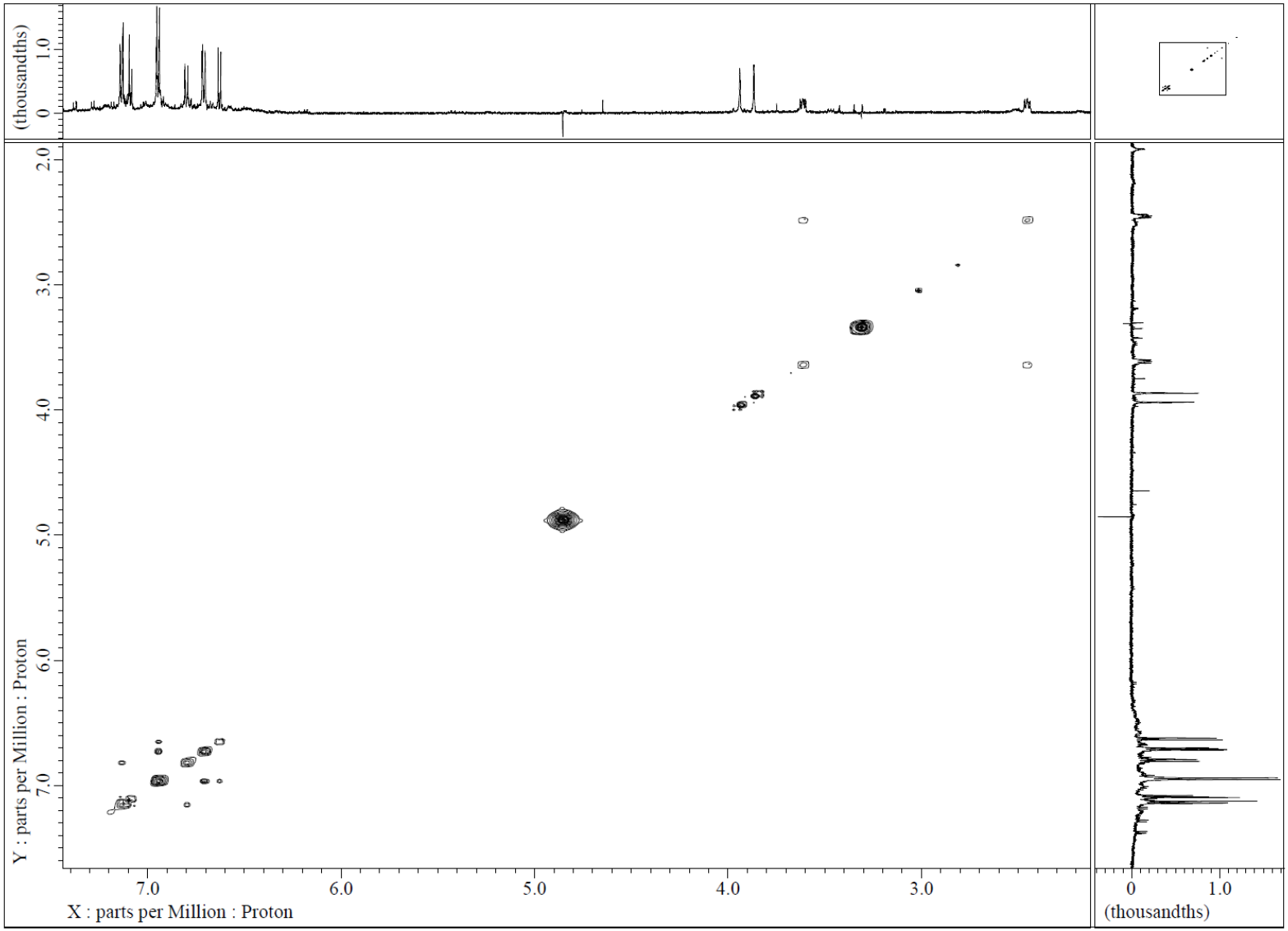

D.32. gHSQC spectrum (methanol-d_4) of denigrin L (**266**)

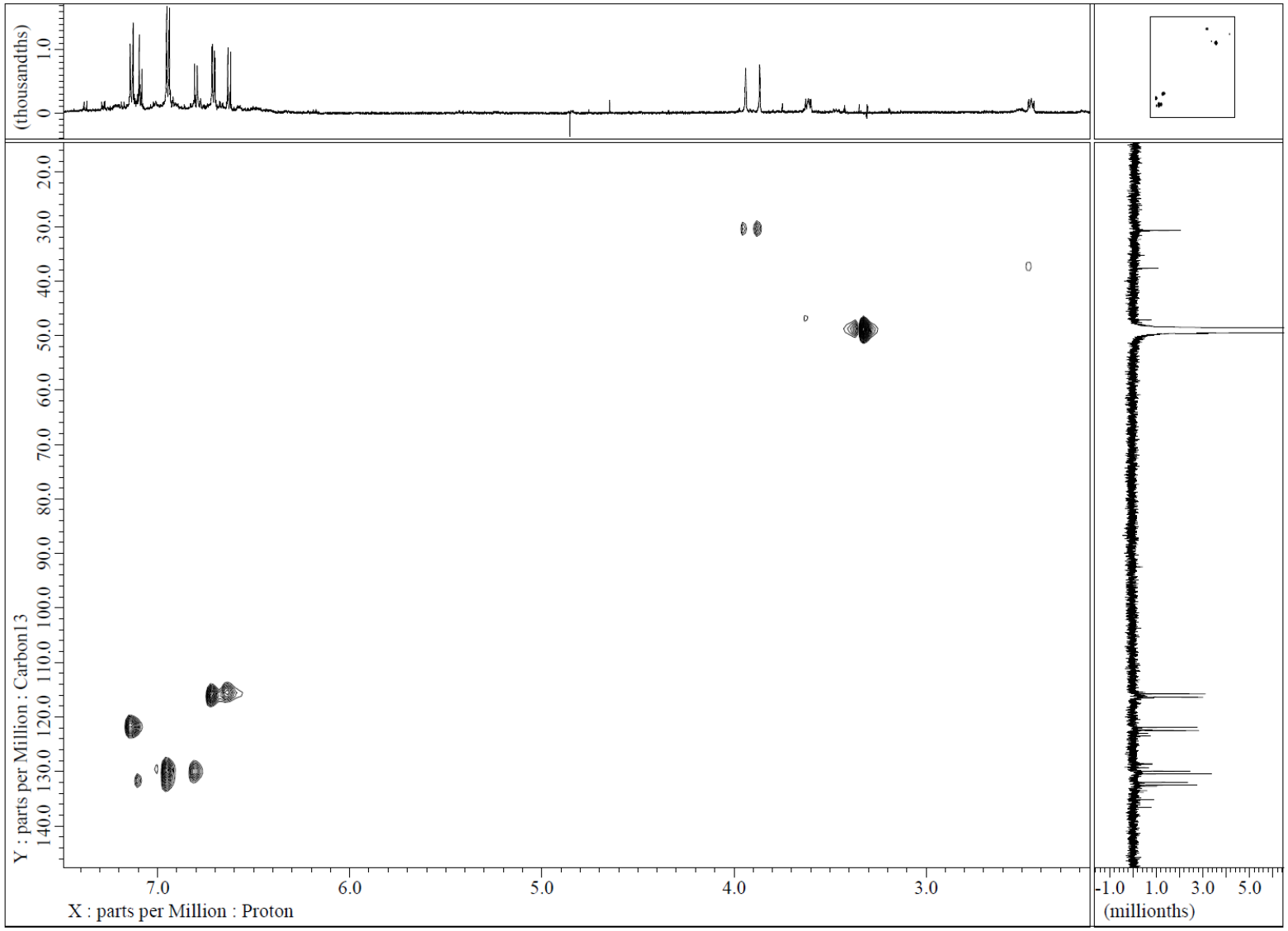

D.33. gHMBC spectrum (methanol-d_4) of denigrin L (**266**)

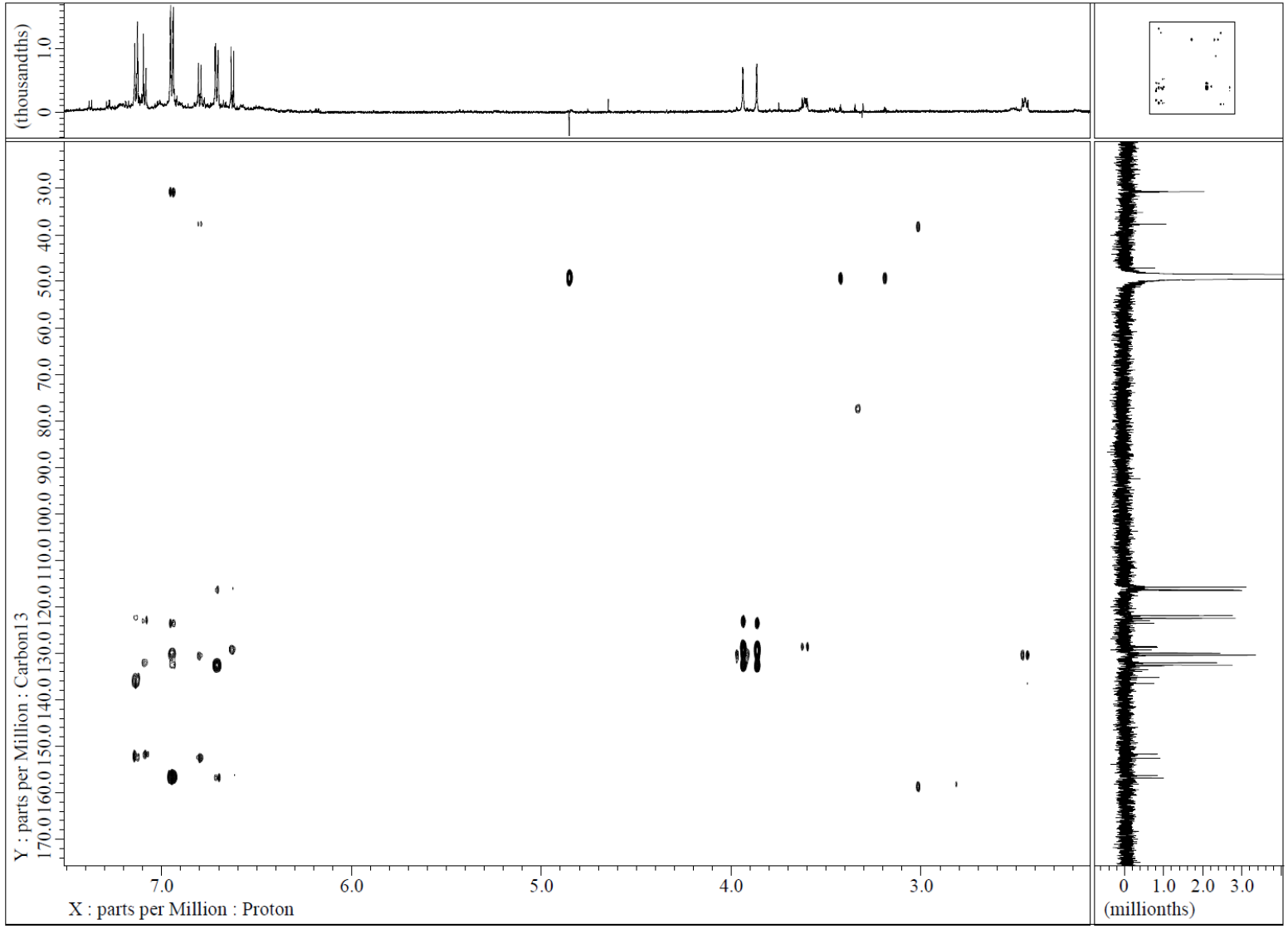

References

1. G. M. Cragg and D. J. Newman, *Biochim. Biophys. Acta - Gen. Subj.*, 2013, **1830**, 3670-3695.
2. D. A. Dias, S. Urban and U. Roessner, *Metabolites*, 2012, **2**, 303-336.
3. R. R. N. Alves, T. P. R. Oliveira, I. L. Rosa and A. B. Cunningham, in *Animals in Traditional Folk Medicine: Implications for Conservation*, eds. R. R. N. Alves and I. L. Rosa, Springer Berlin Heidelberg, Berlin, Heidelberg, 2013, pp. 263-287.
4. E. Voultsiadou, *J. Ethnopharmacol.*, 2010, **130**, 237-247.
5. A. D. Kinghorn, L. Pan, J. N. Fletcher and H. Chai, *J. Nat. Prod.*, 2011, **74**, 1539-1555.
6. D. J. Newman, G. M. Cragg and K. M. Snader, *Nat. Prod. Rep.*, 2000, **17**, 215-234.
7. M. S. Butler, *J. Nat. Prod.*, 2004, **67**, 2141-2153.
8. U. Lindequist, *Biomol. Ther. (Seoul)*, 2016, **24**, 561-571.
9. World Register of Marine Species, **https://www.marinespecies.org/**, accessed on 6 October, 2024.
10. P. Snelgrove, *Planta Med.*, 2016, **82**, 790-799.
11. A. Putz and P. Proksch, in *Annual Plant Reviews Volume 39: Functions and Biotechnology of Plant Secondary Metabolites*, 2010, pp. 162-213.
12. World Register of Marine Species, *Cryptotethya crypta* (de Laubenfels, 1949), **https://www.marinespecies.org/aphia.php?p=taxdetails&id=1341805**, accessed on 19 December, 2024.
13. W. Bergmann and R. J. Feeney, *J. Org. Chem.*, 1951, **16**, 981-987.
14. W. Bergmann and M. F. Stempien Jr., *J. Org. Chem.*, 1957, **22**, 1575-1577.
15. W. Bergmann and D. C. Burke, *J. Org. Chem.*, 1956, **21**, 226-228.
16. T. F. Molinski, D. S. Dalisay, S. L. Lievens and J. P. Saludes, *Nat. Rev. Drug Discov.*, 2009, **8**, 69-85.
17. W.-Y. Lu, H.-J. Li, Q.-Y. Li and Y.-C. Wu, *Biorg. Med. Chem.*, 2021, **35**, 116058.
18. W. Bergmann, D. H. Gould and E. M. Low, *J. Org. Chem.*, 1945, **10**, 570-579.
19. W. Bergmann and E. M. Low, *J. Org. Chem.*, 1947, **12**, 67-75.
20. W. Bergmann, H. P. Schedl and E. M. Low, *J. Org. Chem.*, 1945, **10**, 580-586.
21. D. J. Faulkner, *Nat. Prod. Rep.*, 2001, **18**, 1R-49R.
22. T. L. Simmons, E. Andrianasolo, K. McPhail, P. Flatt and W. H. Gerwick, *Mol. Cancer Ther.*, 2005, **4**, 333-342.
23. E. Schantz, V. Ghazarossian, H. Schnoes, F. Strong, J. Springer, J. O. Pezzanite and J. Clardy, *J. Am. Chem. Soc.*, 1975, **97**, 1238-1239.
24. J. Bordner, W. E. Thiessen, H. A. Bates and H. Rapoport, *J. Am. Chem. Soc.*, 1975, **97**, 6008-6012.
25. A. Yokoo, *Bull. Chem. Soc. Jpn.*, 1950, **71**.
26. Y. Kato and P. Scheuer, *Pure Appl. Chem.*, 1975, **41**, 1-14.
27. M. O. Ishitsuka, T. Kusumi and H. Kakisawa, *J. Org. Chem.*, 1988, **53**, 5010-5013.
28. C. Tringali, G. Oriente, M. Piattelli, C. Geraci, G. Nicolosi and E. Breitmaier, *Can. J. Chem.*, 1988, **66**, 2799-2802.
29. M. A. Ghareeb, M. A. Tammam, A. El-Demerdash and A. G. Atanasov, *Curr. Res. Biotechnol.*, 2020, **2**, 88-102.

30. K. L. Rinehart, T. G. Holt, N. L. Fregeau, J. G. Stroh, P. A. Keifer, F. Sun, L. H. Li and D. G. Martin, *J. Org. Chem.*, 1990, **55**, 4512-4515.
31. O. Aseyev, J. M. Ribeiro and F. Cardoso, *Expert Opin. Pharmacother.*, 2016, **17**, 589-600.
32. Y. Hirata and D. Uemura, *Pure and Applied Chemistry*, 1986, **58**, 701-710.
33. G. R. Pettit, C. L. Herald, M. R. Boyd, J. E. Leet, C. Dufresne, D. L. Doubek, J. M. Schmidt, R. L. Cerny, J. N. A. Hooper and K. C. Rutzler, *J. Med. Chem.*, 1991, **34**, 3339-3340.
34. S. J. Hickford, J. W. Blunt and M. H. Munro, *Biorg. Med. Chem.*, 2009, **17**, 2199-2203.
35. N. C. Richardson, Y. L. Kasamon, H. Chen, R. A. de Claro, J. Ye, G. M. Blumenthal, A. T. Farrell and R. Pazdur, *The Oncologist*, 2019, **24**, e180-e187.
36. M. Wijewickrama, A. Greene and I. Cock, *Pharmacogn Rev.*, 2023, **17**.
37. M. Barreca, V. Spanò, A. Montalbano, M. Cueto, A. R. Díaz Marrero, I. Deniz, A. Erdoğan, L. Lukić Bilela, C. Moulin, E. Taffin-de-Givenchy, F. Spriano, G. Perale, M. Mehiri, A. Rotter, O. P. Thomas, P. Barraja, S. P. Gaudêncio and F. Bertoni, *Mar. Drugs*, 2020, **18**, 619.
38. S. Alonso-Álvarez, E. Pardal, D. Sánchez-Nieto, M. Navarro, M. D. Caballero, M. V. Mateos and A. Martín, *Drug Des. Devel. Ther.*, 2017, 253-264.
39. European Medicines Agency, **https://www.ema.europa.eu/en/aplidin**, accessed on 6 October, 2024.
40. F. Pereira, *Expert Opin. Drug Discov.*, 2019, **14**, 717-722.
41. P. Landete, O.-A. Caliman-Sturdza, J. A. Lopez-Martin, L. Preotescu, M.-C. Luca, A. Kotanidou, P. Villares, S.-P. Iglesias, P. Guisado-Vasco and E.-M. Saiz-Lou, *Clin. Infect. Dis.*, 2024, ciae227.
42. M. C. Leal, J. Puga, J. Serodio, N. C. Gomes and R. Calado, *PLoS One*, 2012, **7**, e30580.
43. R. Calado, R. Mamede, S. Cruz and M. C. Leal, *Mar. Drugs*, 2022, **20**, 389.
44. M. Carbone, M. L. Ciavatta, E. Manzo, X.-L. Li, E. Mollo, I. W. Mudianta, Y.-W. Guo and M. Gavagnin, *Mar. Drugs*, 2019, **17**, 603.
45. V. J. Paul, *Chemical defenses of benthic marine invertebrates*, Cornell University Press, 1992.
46. D. F. Rhoades and R. G. Cates, in *Biochemical interaction between plants and insects*, Springer, 1976, pp. 168-213.
47. B. Haefner, *Drug Discov. Today*, 2003, **8**, 536-544.
48. D. J. Faulkner, *Antonie Van Leeuwenhoek*, 2000, **77**, 135-145.
49. C. Thoms, P. J. Schupp, M. Custódio, G. Lôbo-Hajdu, E. Hajdu and G. Muricy, *Porifera research: biodiversity, Innovation and sustainability*, 2007, **28**, 627-637.
50. C. Eder, P. Schupp, P. Proksch, V. Wray, K. Steube, C. E. Müller, W. Frobenius, M. Herderich and R. W. van Soest, *J. Nat. Prod.*, 1998, **61**, 301-305.
51. P. Schupp, C. Eder, V. Paul and P. Proksch, *Mar. Biol.*, 1999, **135**, 573-580.
52. J.-M. Kornprobst, *Encyclopedia of Marine Natural Products*, 2014.
53. B. Salvador, M. Cabanellas-Reboredo, M. E. Garci, Á. F. González and J. Hernández-Urcera, *Ecol. Evol.*, 2024, **14**, e11107.
54. K. Fisch, C. Hertzer, N. Böhringer, Z. Wuisan, D. Schillo, R. Bara, F. Kaligis, H. Wägele, G. König and T. Schäberle, *Mar. Drugs*, 2017, **15**, 384.
55. A. E. Winters, A. M. White, A. S. Dewi, I. W. Mudianta, N. G. Wilson, L. C. Forster, M. J. Garson and K. L. Cheney, *J. Chem. Ecol.*, 2018, **44**, 384-396.
56. L. Bornancin, I. Bonnard, S. C. Mills and B. Banaigs, *Nat. Prod. Rep.*, 2017, **34**, 644-676.
57. M. E. Hay, J. R. Pawlik, J. E. Duffy and W. Fenical, *Oecologia*, 1989, **81**, 418-427.

58. U. Hentschel, J. Piel, S. M. Degnan and M. W. Taylor, *Nat. Rev. Microbiol.*, 2012, **10**, 641-654.
59. C.-W. Li, J.-Y. Chen and T.-E. Hua, *Science*, 1998, **279**, 879-882.
60. T. R. A. Thomas, D. P. Kavlekar and P. A. LokaBharathi, *Mar. Drugs*, 2010, **8**, 1417-1468.
61. M. Kelly, Splendid Sponges, a guide to the sponges of New Zealand., https://niwa.co.nz/coasts-and-oceans/marine-identification-guides-and-fact-sheets,
62. L.-L. Hong, Y.-F. Ding, W. Zhang and H.-W. Lin, *Mar. Life Sci. Technol.*, 2022, **4**, 356-372.
63. C. Calcabrini, E. Catanzaro, A. Bishayee, E. Turrini and C. Fimognari, *Mar. Drugs*, 2017, **15**, 310.
64. N. L. Thakur and W. E. G. Müller, *Curr. Sci.*, 2004, **86**, 1506-1512.
65. A. R. Carroll, B. R. Copp, R. A. Davis, R. A. Keyzers and M. R. Prinsep, *Nat Prod Rep*, 2020, **37**, 175-223.
66. A. R. Carroll, B. R. Copp, R. A. Davis, R. A. Keyzers and M. R. Prinsep, *Nat. Prod. Rep.*, 2023, **40**, 275-325.
67. A. R. Carroll, B. R. Copp, R. A. Davis, R. A. Keyzers and M. R. Prinsep, *Nat. Prod. Rep.*, 2022, **39**, 1122-1171.
68. A. R. Carroll, B. R. Copp, R. A. Davis, R. A. Keyzers and M. R. Prinsep, *Nat. Prod. Rep.*, 2021, **38**, 362-413.
69. J. Liang, J. She, J. Fu, J. Wang, Y. Ye, B. Yang, Y. Liu, X. Zhou and H. Tao, *Mar. Drugs*, 2023, **21**, 236.
70. C. A. Bewley, N. Holland and D. J. Faulkner, *Experientia*, 1996, **52**, 716-722.
71. M. Unson and D. Faulkner, *Experientia*, 1993, **49**, 349-353.
72. J. Piel, *Nat. Prod. Rep.*, 2009, **26**, 338-362.
73. E. W. Schmidt, C. A. Bewley and D. J. Faulkner, *J. Org. Chem.*, 1998, **63**, 1254-1258.
74. E. W. Schmidt, A. Y. Obraztsova, S. K. Davidson, D. J. Faulkner and M. G. Haygood, *Mar. Biol.*, 2000, **136**, 969-977.
75. N. B. Perry, J. W. Blunt, M. H. Munro and L. K. Pannell, *J. Am. Chem. Soc.*, 1988, **110**, 4850-4851.
76. U. Hentschel, M. Schmid, M. Wagner, L. Fieseler, C. Gernert and J. Hacker, *FEMS Microbiol. Ecol.*, 2001, **35**, 305-312.
77. D. J. Newman and R. T. Hill, *J. Ind. Microbiol. Biotech.*, 2006, **33**, 539-544.
78. S. Rohde, S. Nietzer and P. J. Schupp, *PLoS One*, 2015, **10**, e0132236.
79. C. Salomon, T. Deerinck, M. Ellisman and D. Faulkner, *Mar. Biol.*, 2001, **139**, 313-319.
80. J. E. Thompson, K. D. Barrow and D. J. Faulkner, *Acta Zoologica*, 1983, **64**, 199-210.
81. N. B. Lopanik, *Funct. Ecol.*, 2014, **28**, 328-340.
82. M. D. Unson, N. D. Holland and D. J. Faulkner, *Mar. Biol.*, 1994, **119**, 1-11.
83. J. E. Thompson, R. P. Walker, S. J. Wratten and D. J. Faulkner, *Tetrahedron*, 1982, **38**, 1865-1873.
84. R. C. ANDERSON, *International Zoo Yearbook*, 1995, **34**, 65-70.
85. L. J. Dean and M. R. Prinsep, *Nat. Prod. Rep.*, 2017, **34**, 1359-1390.
86. B. F. Murphy and M. G. Hadfield, *Comp. Biochem. Physiol., Part A: Physiol.*, 1997, **118**, 727-735.
87. D. Obermann, U. Bickmeyer and H. Wägele, *Toxicon*, 2012, **60**, 1108-1116.
88. J. A. Miller and M. Byrne, *Invertebr. Biol.*, 2000, **119**, 167-176.
89. J. M. Newcomb, L. E. Kirouac, A. A. Naimie, K. A. Bixby, C. Lee, S. Malanga, M. Raubach and W. H. Watson, *Biol. Bull.*, 2014, **227**, 263-273.

90. A. M. Miller and J. R. Pawlik, *Anim. Behav.*, 2013, **85**, 339-347.
91. World Register of Marine Species, *Risbecia bullockii* (Collingwood, 1881), https://www.marinespecies.org/aphia.php?p=taxdetails&id=599825, accessed on 11 October, 2024.
92. M. Pola, J. L. Cervera and T. M. Gosliner, *Scientia Marina*, 2008, **72**, 145-183.
93. H. E. Epstein, J. M. Hallas, R. F. Johnson, A. Lopez and T. M. Gosliner, *Zool. J. Linn. Soc.*, 2018, **186**, 116-189.
94. M. Haber, S. Cerfeda, M. Carbone, G. Calado, H. Gaspar, R. Neves, V. Maharajan, G. Cimino, M. Gavagnin, M. T. Ghiselin and E. Mollo, *Biol. Bull.*, 2010, **218**, 181-188.
95. D. W. Pfennig, W. R. Harcombe and K. S. Pfennig, *Nature*, 2001, **410**, 323-323.
96. P. G. Greenwood, *Toxicon*, 2009, **54**, 1065-1070.
97. P. T. Ottuso, *Cutis*, 2009, **83**, 237-239.
98. Z. H. Chen, Y. W. Guo and X. W. Li, *Nat. Prod. Rep.*, 2023, **40**, 509-556.
99. D. J. Faulkner and M. T. Ghiselin, *Mar. Ecol. Prog. Ser.*, 1983, **13**, 295-301.
100. M. Carbone, M. Gavagnin, M. Haber, Y.-W. Guo, A. Fontana, E. Manzo, G. Genta-Jouve, M. Tsoukatou, W. B. Rudman, G. Cimino, M. T. Ghiselin and E. Mollo, *PLoS One*, 2013, **8**, e62075.
101. World Register of Marine Species, *Hypselodoris webbi* (A. d'Orbigny, 1839), https://www.marinespecies.org/aphia.php?p=taxdetails&id=156137, accessed on 11 October, 2024.
102. A. Fontana, F. Giménez, A. Marin, E. Mollo and G. Cimino, *Experientia*, 1994, **50**, 510-516.
103. A. Fontana, C. Avila, E. Martinez, J. Ortea, E. Trivellone and G. Cimino, *J. Chem. Ecol.*, 1993, **19**, 339-356.
104. World Register of Marine Species, *Doris orsinii (*Vérany, 1846), https://www.marinespecies.org/aphia.php?p=taxdetails&id=564002, accessed on 11 October, 2024.
105. G. Cimino, A. Fontana, F. Giménez, A. Marin, E. Mollo, E. Trivellone and E. Zubía, *Experientia*, 1993, **49**, 582-586.
106. G. Cimino and M. T. Ghiselin, *Chemoecology*, 1999, **9**, 187-207.
107. A. Fontana, A. Tramice, A. Cutignano, G. D'Ippolito, M. Gavagnin and G. Cimino, *J. Org. Chem.*, 2003, **68**, 2405-2409.
108. G. Cimino, S. De Rosa, S. De Stefano, G. Sodano and G. Villani, *Science*, 1983, **219**, 1237-1238.
109. E. I. Graziani, R. J. Andersen, P. J. Krug and D. John Faulkner, *Tetrahedron*, 1996, **52**, 6869-6878.
110. J. Kubanek and R. J. Andersen, *J. Nat. Prod.*, 1999, **62**, 777-779.
111. T. Barsby, R. G. Linington and R. J. Andersen, *Chemoecology*, 2002, **12**, 199-202.
112. E. I. Graziani and R. J. Andersen, *J. Am. Chem. Soc.*, 1996, **118**, 4701-4702.
113. A. Fontana, P. Cavaliere, S. Wahidulla, C. G. Naik and G. Cimino, *Tetrahedron*, 2000, **56**, 7305-7308.
114. R. Kazlauskas, P. Murphy, R. Wells, K. Noack, W. Oberhansli and P. Schonholzer, *Aust. J. Chem.*, 1979, **32**, 867-880.
115. G. Cimino and M. Ghiselin, *Chemoecology*, 1999, **9**, 187-207.
116. K. Charupant, K. Suwanborirux, S. Amnuoypol, E. Saito, A. Kubo and N. Saito, *Chem. Pharm. Bull. (Tokyo)*, 2007, **55**, 81-86.

117. W.-F. He, Y. Li, M.-T. Feng, M. Gavagnin, E. Mollo, S.-C. Mao and Y.-W. Guo, *Fitoterapia*, 2014, **96**, 109-114.
118. R.-Y. Huang, W.-T. Chen, T. Kurtán, A. Mándi, J. Ding, J. Li, X.-W. Li and Y.-W. Guo, *Future Med. Chem.*, 2016, **8**, 17-27.
119. A. Fontana, M. L. Ciavatta, L. DeSouza, E. Mollo, C. G. Naik, P. Parameswaran, S. Wahidullah and G. Cimino, *J. Indian Inst. Sci.*, 2001, **81**, 403-415.
120. B. Petek and R. Jones, *Molecules*, 2014, **19**, 12328-12335.
121. Study of Zalypsis® (PM00104) in Patients With Unresectable Locally Advanced and/or Metastatic Ewing Family of Tumors (EFT) Progressing After at Least One Prior Line of Chemotherapy. NCT01222767, https://clinicaltrials.gov/study/NCT01222767?intr=zalypsis&rank=1, accessed on 22 January, 2025.
122. C. Avila, *Mar. Drugs*, 2020, **18**, 162.
123. S. D. Rogers and V. J. Paul, *Mar. Ecol. Prog. Ser.*, 1991, **77**, 221-232.
124. C. Avila and V. J. Paul, *Mar. Ecol. Prog. Ser.*, 1997, **150**, 171-180.
125. World Register of Marine Species, *Doris atromarginata* (Cuvier, 1804), https://www.marinespecies.org/aphia.php?p=taxdetails&id=558471, accessed on 11 October, 2024.
126. A. Fontana, E. Mollo, D. Ricciardi, I. Fakhr and G. Cimino, *J. Nat. Prod.*, 1997, **60**, 444-448.
127. E. D. De Silva, P. J. Scheuer, *Heterocycles*, 1982, **17**, 167-170.
128. K. W. L. Yong, I. W. Mudianta, K. L. Cheney, E. Mollo, J. T. Blanchfield and M. J. Garson, *J. Nat. Prod.*, 2015, **78**, 421-430.
129. M. J. Somerville, E. Mollo, G. Cimino, W. Rungprom and M. J. Garson, *J. Nat. Prod.*, 2006, **69**, 1086-1088.
130. A. Fontana, P. Cavaliere, N. Ungur, L. D'Souza, P. S. Parameswaram and G. Cimino, *J. Nat. Prod.*, 1999, **62**, 1367-1370.
131. C. Hertzer, S. Kehraus, N. Böhringer, F. Kaligis, R. Bara, D. Erpenbeck, G. Wörheide, T. F. Schäberle, H. Wägele and G. M. König, *Beilstein J. Org. Chem.*, 2020, **16**, 1596-1605.
132. P. T. Narbutas, J. K. Clegg, G. K. Pierens, K. L. Cheney, A. M. Ganderton and M. J. Garson, *Aust. J. Chem.*, 2020, **73**, 948-955.
133. I. W. Mudianta, A. M. White and M. J. Garson, *Nat. Prod. Commun.*, 2015, **10**, 865-868.
134. World Register of Marine Species, *Chromodoris sinensis* (Rudman, 1985), https://www.marinespecies.org/aphia.php?p=taxdetails&id=559731, accessed on 4, November 2024.
135. P. Karuso and W. C. Taylor, *Aust. J. Chem.*, 1986, **39**, 1629-1641.
136. B. J. Burreson, P. J. Scheuer, J. Finer and J. Clardy, *J. Am. Chem. Soc.*, 1975, **97**, 4763-4764.
137. M. R. Hagadone, B. J. Burreson, P. J. Scheuer, J. S. Finer and J. Clardy, *Helv. Chim. Acta*, 1979, **62**, 2484-2494.
138. Yasman, R. A. Edrada, V. Wray and P. Proksch, *J. Nat. Prod.*, 2003, **66**, 1512-1514.
139. A. Fontana, E. Trivellone, E. Mollo, G. Cimino, C. Avila, E. Martinez and J. Ortea, *J. Nat. Prod.*, 1994, **57**, 510-513.
140. World Register of Marine Species, *Microciona toxistyla* Sarà, 1959, https://www.marinespecies.org/aphia.php?p=taxdetails&id=133087, accessed on 11 October, 2024.
141. G. Guella, I. Mancini, A. Guerriero and F. Pietra, *Helv. Chim. Acta*, 1985, **68**, 1276-1282.

142. World Register of Marine Species, *Risbecia tryoni* (Garrett, 1873), https://www.marinespecies.org/aphia.php?p=taxdetails&id=558642, accessed on 11 October, 2024.
143. World Register of Marine Species, *Hypselodoris* W. Stimpson, 1855, https://www.marinespecies.org/aphia.php?p=taxdetails&id=137784, accessed on 11 October, 2024.
144. G. Schulte, P. J. Scheuer and O. J. McConnell, *Helv. Chim. Acta*, 1980, **63**, 2159-2167.
145. C. Avila, G. Cimino, A. Fontana, M. Gavagnin, J. Ortea and E. Trivellone, *J. Chem. Ecol.*, 1991, **17**, 625-636.
146. World Register of Marine Species, *Hypselodoris fontandraui* (Pruvot-Fol, 1951), https://www.marinespecies.org/aphia.php?p=taxdetails&id=139149,
147. World Register of Marine Species, *Spongia mycofijiensis* (Kakou, Crews & Bakus, 1987), https://www.marinespecies.org/aphia.php?p=taxdetails&id=193681, accessed on 11 October, 2024.
148. Y. Kakou, P. Crews and G. J. Bakus, *J. Nat. Prod.*, 1987, **50**, 482-484.
149. K. Gustafson, R. J. Andersen, H. Cun-Heng and J. Clardy, *Tetrahedron Lett.*, 1985, **26**, 2521-2524.
150. J. Hellou, R. Andersen, S. Rafii, E. Arnold and J. Clardy, *Tetrahedron Lett.*, 1981, **22**, 4173-4176.
151. M. Tischler, R. J. Andersen, M. I. Choudhary and J. Clardy, *J. Org. Chem.*, 1991, **56**, 42-47.
152. D. L. Burgoyne, E. J. Dumdei and R. J. Andersen, *Tetrahedron*, 1993, **49**, 4503-4510.
153. E. J. Dumdei, J. Kubanek, J. E. Coleman, J. Pika, R. J. Andersen, J. R. Steiner and J. Clardy, *Can. J. Chem.*, 1997, **75**, 773-789.
154. J. Hellou, R. J. Andersen and J. E. Thompson, *Tetrahedron*, 1982, **38**, 1875-1879.
155. M. Tischler and R. J. Andersen, *Tetrahedron Lett.*, 1989, **30**, 5717-5720.
156. J. Kubanek, E. I. Graziani and R. J. Andersen, *J. Org. Chem.*, 1997, **62**, 7239-7246.
157. G. Cimino, S. De Rosa, S. De Stefano, R. Morrone and G. Sodano, *Tetrahedron*, 1985, **41**, 1093-1100.
158. R. K. Okuda, D. Klein, R. B. Kinnel, M. Li and P. J. Scheuer, *Pure Appl. Chem.*, 1982, **54**, 1907-1914.
159. C. Hayot, O. Debeir, P. Van Ham, M. Van Damme, R. Kiss and C. Decaestecker, *Toxicol Appl Pharmacol*, 2006, **211**, 30-40.
160. J. Pika and D. J. Faulkner, *Tetrahedron*, 1995, **51**, 8189-8198.
161. R. K. Okuda and P. J. Scheuer, *Experientia*, 1985, **41**, 1355-1356.
162. K. A. Alvi, B. M. Peters, H. M. Lisa and C. Phillip, *Tetrahedron*, 1993, **49**, 329-336.
163. K. L. Cheney, A. White, I. W. Mudianta, A. E. Winters, M. Quezada, R. J. Capon, E. Mollo and M. J. Garson, *PLoS One*, 2016, **11**, e0145134.
164. World Register of Marine Species, *Latrunculia magnifica* (Keller, 1889), https://www.marinespecies.org/aphia.php?p=taxdetails&id=192127, accessed on 11 October, 2024.
165. W. Rudman and P. Bergquist, *Molluscan Res.*, 2007, **27**, 60–88-60–88.
166. K. McPhail and M. T. Davies-Coleman, *Tetrahedron*, 1997, **53**, 4655-4660.
167. J. R. Pawlik, M. R. Kernan, T. F. Molinski, M. K. Harper and D. J. Faulkner, *J. Exp. Mar. Biol. Ecol.*, 1988, **119**, 99-109.
168. D. S. Dalisay, E. W. Rogers, A. S. Edison and T. F. Molinski, *J. Nat. Prod.*, 2009, **72**, 732-738.

169. Y. Guo, M. Gavagnin, E. Mollo, E. Trivellone, G. Cimino and I. Fakhr, *Tetrahedron Lett.*, 1998, **39**, 2635-2638.
170. M. R. Kernan, T. F. Molinski and D. J. Faulkner, *J. Org. Chem.*, 1988, **53**, 5014-5020.
171. S. Matsunaga, N. Fusetani, K. Hashimoto, K. Koseki, M. Noma, H. Noguchi and U. Sankawa, *J. Org. Chem.*, 1989, **54**, 1360-1363.
172. S. M. Parrish, W. Yoshida, B. Yang and P. G. Williams, *J. Nat. Prod.*, 2017, **80**, 726-730.
173. W. Zhang, M. Gavagnin, Y.-W. Guo, E. Mollo, M. T. Ghiselin and G. Cimino, *Tetrahedron*, 2007, **63**, 4725-4729.
174. J. A. Roesener and P. J. Scheuer, *J. Am. Chem. Soc.*, 1986, **108**, 846-847.
175. World Register of Marine Species, *Anisodoris nobilis* (MacFarland, 1905), https://www.marinespecies.org/aphia.php?p=taxdetails&id=581820, accessed on 11 October, 2024.
176. F. Fuhrman, G. Fuhrman, Y. Kim, L. Pavelka and H. Mosher, *Science*, 1980, **207**, 193-195.
177. K. Gustafson and R. J. Andersen, *Tetrahedron*, 1985, **41**, 1101-1108.
178. D. Castiello, G. Cimino, S. De Rosa, S. De Stefano and G. Sodano, *Tetrahedron Lett.*, 1980, **21**, 5047-5050.
179. D. Castiello, G. Cimino, S. De Rosa, S. De Stefano, G. Izzo and G. Sodano, 1979.
180. M. L. Ciavatta, G. Nuzzo, K. Takada, V. Mathieu, R. Kiss, G. Villani and M. Gavagnin, *J. Nat. Prod.*, 2014, **77**, 1678-1684.
181. B. Figuerola and C. Avila, *Mar. Drugs*, 2019, **17**, 477.
182. X. R. Tian, H. F. Tang, X. L. Tian, J. J. Hu, L. L. Huang and K. R. Gustafson, *Future Med. Chem.*, 2018, **10**, 1497-1514.
183. B. Carté and D. J. Faulkner, *J. Org. Chem.*, 1983, **48**, 2314-2318.
184. B. Carté and D. J. Faulkner, *J. Chem. Ecol.*, 1986, **12**, 795-804.
185. N. Lindquist and W. Fenical, *Experientia*, 1991, **47**, 504-506.
186. S. Nakajima, K. Kojiri and H. Suda, *J. Antibiot.*, 1993, **46**, 1894-1896.
187. A. C. Granato, J. H. H. L. D. Oliveira, M. H. R. Seleghim, R. G. S. Berlinck, M. L. Macedo, A. G. Ferreira, R. M. D. Rocha, E. Hajdu, S. Peixinho, C. O. Pessoa, M. O. Moraes and B. C. Cavalcanti, *Quim. Nova*, 2005, **28**, 192-198.
188. M. Carbone, C. Irace, F. Costagliola, F. Castelluccio, G. Villani, G. Calado, V. Padula, G. Cimino, J. Lucas Cervera, R. Santamaria and M. Gavagnin, *Bioorg. Med. Chem. Lett.*, 2010, **20**, 2668-2670.
189. World Register of Marine Species, *Bugula dentata* (Lamouroux, 1816), https://www.marinespecies.org/aphia.php?p=taxdetails&id=234109, accessed on 11 October, 2024.
190. M. Takaki, V. F. Freire, K. J. Nicacio, A. F. Bertonha, N. Nagashima, R. Sarpong, V. Padula, A. G. Ferreira and R. G. S. Berlinck, *J. Nat. Prod.*, 2021, **84**, 790-796.
191. M. R. Prinsep, unpublished work.
192. World Register of Marine Species, *Janolus cristatus* (Delle Chiaje, 1841), https://www.marinespecies.org/aphia.php?p=taxdetails&id=140855, accessed on 22 January, 2024.
193. G. Sodano and A. Spinella, *Tetrahedron Lett.*, 1986, **27**, 2505-2508.
194. World Register of Marine Species, *Bugula flabellata* (Thompson in Gray, 1848), https://www.marinespecies.org/aphia.php?p=taxdetails&id=111152, accessed on 22 January, 2024.

195. J. Wang, M. R. Prinsep, D. P. Gordon, M. J. Page and B. R. Copp, *J. Nat. Prod.*, 2015, **78**, 530-533.
196. L. J. Dean, M. R. Prinsep and R. Fairweather, *Chemical Theft: The Sequestration of Natural Products by New Zealand Nudibranchs from their Bryozoan Prey*, NZIC-16, The New Zealand Institute of Chemistry Conference, Queenstown - New Zealand, August, 2016. 21-24, http://www.nzic16.org/.
197. World Register of Marine Species, *Janolus novozealandicus* (Eliot, 1907), https://www.marinespecies.org/aphia.php?p=taxdetails&id=599238, accessed on 22 January, 2024.
198. C. Ramesh, B. R. Tulasi, M. Raju, N. Thakur and L. Dufossé, *Mar. Drugs*, 2021, **19**, 308.
199. X. Dou and B. Dong, *Mar. Drugs*, 2019, **17**, 670.
200. World Register of Marine Species, *Atapozoa* (Brewin, 1946), https://www.marinespecies.org/aphia.php?p=taxdetails&id=248226,
201. V. J. Paul, N. Lindquist and W. Fenical, *Mar. Ecol. Prog. Ser.*, 1990, 109-118.
202. M. L. Ciavatta, E. Manzo, E. Mollo, C. A. Mattia, C. Tedesco, C. Irace, Y.-W. Guo, X.-B. Li, G. Cimino and M. Gavagnin, *J. Nat. Prod.*, 2011, **74**, 1902-1907.
203. V. E. Neall and S. A. Trewick, *Philosophical Transactions of the Royal Society B: Biological Sciences*, 2008, **363**, 3293-3308.
204. D. P. Gordon, J. Beaumont, A. MacDiarmid, D. A. Robertson and S. T. Ahyong, *PLoS One*, 2010, **5**, e10905.
205. Flanders Marine Institute, https://www.marineregions.org/, accessed on 28 November, 2024.
206. R. C. Willan and N. Davey, Super sea slugs, a guide to the sea slugs of New Zealand, https://niwa.co.nz/oceans/marine-identification-guides-and-fact-sheets/super-sea-slugs,
207. D. P. Gordon and S. Mills, Bountiful bryozoans, a guide to the bryozoans of New Zealand, https://niwa.co.nz/oceans/identification-guides/bountiful-bryozoans,
208. D. P. Gordon and M. Spencer-Jones, *Zootaxa*, 2013, **3647**, 75–95.
209. World Register of Marine Species, *Amathia gracei* (Gordon & Spencer Jones, 2013), https://www.marinespecies.org/aphia.php?p=taxdetails&id=730616, accessed on 21, November 2024.
210. M. R. Prinsep, unpublished work.
211. C. Crombie, unpublished work.
212. G. Kleks, D. C. Holland, E. K. Kennedy, V. M. Avery and A. R. Carroll, *J. Nat. Prod.*, 2020, **83**, 3435-3444.
213. H.-P. Zhang, H. Shigemori, M. Ishibashi, T. Kosaka, G. R. Pettit, Y. Kamano and J. Kobayashi, *Tetrahedron*, 1994, **50**, 10201-10206.
214. H.-P. Zhang, Y. Kamano, H. Kizu, H. Itokawa, G. R. Pettit and C. L. Herald, *Chem. Lett.*, 1994, 2271-2274.
215. H.-P. Zhang, Y. Kamano, Y. Ichihara, H. Kizu, K. Komiyama, H. Itokawa and G. R. Pettit, *Tetrahedron*, 1995, **51**, 5523-5528.
216. C. K. Narkowicz, A. J. Blackman, E. Lacey, J. H. Gill and K. Heiland, *J. Nat. Prod.*, 2002, **65**, 938-941.
217. B. D. Morris and M. R. Prinsep, *J. Nat. Prod.*, 1999, **62**, 688-693.
218. A. M. Montanari, W. Fenical, N. Lindquist, A. Y. Lee and J. Clardy, *Tetrahedron*, 1996, **52**, 5371-5380.
219. N.-K. Lee, W. Fenical and N. Lindquist, *J. Nat. Prod.*, 1997, **60**, 697-699.

220. Y. Kamano, H.-P. Zhang, Y. Ichihara, H. Kizu, K. Komiyama and G. R. Pettit, *Tetrahedron Lett.*, 1995, **36**, 2783-2784.
221. Y. Kamano, A. Kotake, H. Hashima, I. Hayakawa, H. Hiraide, H.-P. Zhang, H. Kizu, K. Komiyama, M. Hayashi and G. R. Pettit, *Collect. Czechoslov. Chem. Commun.*, 1999, **64**, 1147-1153.
222. R. A. Davis, M. Sykes, V. M. Avery, D. Camp and R. J. Quinn, *Biorg. Med. Chem.*, 2011, **19**, 6615-6619.
223. Y. Dashti, M.-L. Vial, S. A. Wood, G. D. Mellick, C. Roullier and R. J. Quinn, *Tetrahedron*, 2015, **71**, 7879-7884.
224. A. R. Carroll, S. J. Wild, S. Duffy and V. M. Avery, *Tetrahedron Lett.*, 2012, **53**, 2873-2875.
225. A. R. Carroll, S. Duffy, M. Sykes and V. M. Avery, *Org. Biomol. Chem.*, 2011, **9**, 604-609.
226. A. J. Blackman and D. J. Matthews, *Heterocycles*, 1985, **23**, 2829.
227. A. Blackman and R. Green, *Aust. J. Chem.*, 1987, **40**, 1655-1662.
228. A. Blackman, T. Eldershaw and S. Garland, *Aust. J. Chem.*, 1993, **46**, 401-405.
229. M. Garson, in *Molluscs: From Chemo-ecological Study to Biotechnological Application*, eds. G. Cimino and M. Gavagnin, Springer Berlin Heidelberg, Berlin, Heidelberg, 2006, pp. 159-174.
230. T. Grkovic, D. Appleton and B. Copp, *CiNZ*, 2005, **4**, 12-15.
231. J. M. Wojnar, PhD thesis, Victoria University of Wellington, **2008**.
232. J. van Meerloo, G. J. L. Kaspers and J. Cloos, in *Cancer Cell Culture: Methods and Protocols*, ed. I. A. Cree, Humana Press, Totowa, NJ, 2011, pp. 237-245.
233. B. C. Cavalcanti, H. V. N. Júnior, M. H. R. Seleghim, R. G. S. Berlinck, G. M. A. Cunha, M. O. Moraes and C. Pessoa, *Chemico-Biological Interactions*, 2008, **174**, 155-162.
234. V. Ruiz-Torres, C. Rodríguez-Pérez, M. Herranz-López, B. Martín-García, A.-M. Gómez-Caravaca, D. Arráez-Román, A. Segura-Carretero, E. Barrajón-Catalán and V. Micol, *Biomolecules*, 2019, **9**, 771.
235. World Register of Marine Species, *Dendrodoris denisoni* (Angas, 1864), https://www.marinespecies.org/aphia.php?p=taxdetails&id=537017, accessed on 25 November, 2024.
236. World Register of Marine Species, *Dendrodoris krusensternii* (J. E. Gray, 1850), https://www.marinespecies.org/aphia.php?p=taxdetails&id=550448, accessed on 25 November, 2024.
237. L. Canonica, A. Corbella, P. Gariboldi, G. Jommi, J. Křepinský, G. Ferrari and C. Casagrande, *Tetrahedron*, 1969, **25**, 3895-3902.
238. L. Canonica, A. Corbella, G. Jommi, J. Křepinský, G. Ferrari and C. Casagrande, *Tetrahedron Lett.*, 1967, **8**, 2137-2141.
239. D. M. Hollinshead, S. C. Howell, S. V. Ley, M. Mahon, N. M. Ratcliffe and P. A. Worthington, *J. Chem. Soc., Perkin Trans. 1*, 1983, DOI: 10.1039/P19830001579, 1579-1589.
240. R. Przeslawski, *Molluscan Res.*, 2004, **24**, 43-63.
241. R. K. Okuda, P. J. Scheuer, J. E. Hochlowski, R. P. Walker and D. J. Faulkner, *J. Org. Chem.*, 1983, **48**, 1866-1869.
242. G. McDonald and J. Nybakken, *The Veliger*, 1999, **42**, 62-66.
243. World Register of Marine Species, *Dendrodoris nigra* (W. Stimpson, 1855), https://www.marinespecies.org/aphia.php?p=taxdetails&id=139519, accessed on 26 November, 2024.

244. M. J. Garson, A. F. Dexter, L. K. Lambert and V. Liokas, *J. Nat. Prod.*, 1992, **55**, 364-367.
245. A. Fontana, M. L. Ciavatta, T. Miyamoto, A. Spinella and G. Cimino, *Tetrahedron*, 1999, **55**, 5937-5946.
246. H. Gaspar, A. Cutignano, T. Ferreira, G. A. Calado, G. Cimino and A. Fontana, *J. Nat. Prod.*, 2008, **71**, 2053-2056.
247. G. Cimino, S. De Rosa, S. De Stefano and G. Sodano, *Tetrahedron Lett.*, 1981, **22**, 1271-1272.
248. R. Kazlauskas, P. Murphy, R. Quinn and R. Wells, *Tetrahedron Lett.*, 1976, **17**, 2631-2634.
249. F. W. Wehrli, T. Wirthlin, *Interpretation of carbon-13 NMR spectra.*, Heyden, London, 1976.
250. G. Cimino, S. De Rosa, S. De Stefano and G. Sodano, *Pure Appl. Chem.*, 1986, **58**, 375-386.
251. S. P. McCormack, M. Kelly and C. N. Battershill, *Zootaxa*, 2020, **4780**, 523–542.
252. E. Russell, L. Gris, M. R. Prinsep, M. Kelly and C. N. Battershill, *A newly discovered estuarine sponge habitat from New Zealand: a rare and vulnerable assemblage.*, 11th World Sponge Conference, Leiden, The Netherlands, October, 2022.
253. H. Appel, C. Brooks and K. Overton, *J. Chem. Soc. (Resumed)*, 1959, 3322-3332.
254. F. Dumas, M. Kousara, L. Chen, L. Wei and F. Le Bideau, in *Stud. Nat. Prod. Chem.*, ed. R. Atta ur, Elsevier, 2017, vol. 52, pp. 269-302.
255. G. N. Belofsky, P. R. Jensen, M. K. Renner and W. Fenical, *Tetrahedron*, 1998, **54**, 1715-1724.
256. A. Montagnac, M.-T. Martin, C. Debitus and M. Pais, *J. Nat. Prod.*, 1996, **59**, 866-868.
257. M. Butler and R. Capon, *Aust. J. Chem.*, 1993, **46**, 1255-1267.
258. M. Stewart, P. M. Fell, J. W. Blunt and M. H. Munro, *Aust. J. Chem.*, 1997, **50**, 341-348.
259. J. Thompson, R. Walker and D. Faulkner, *Mar. Biol.*, 1985, **88**, 11-21.
260. C. Hellio, M. Tsoukatou, J.-P. Marechal, N. Aldred, C. Beaupoil, A. S. Clare, C. Vagias and V. Roussis, *Mar. Biotechnol.*, 2005, **7**, 297-305.
261. World Register of Marine Species, Dendrodorididae, O'Donoghue, 1924 (1864), https://www.marinespecies.org/aphia.php?p=taxdetails&id=23026, accessed on 28 November, 2024.
262. Y. Sakio, Y. J. Hirano, M. Hayashi, K. Komiyama and M. Ishibashi, *J. Nat. Prod.*, 2001, **64**, 726-731.
263. A. Fontana, G. Villani and G. Cimino, *Tetrahedron Lett.*, 2000, **41**, 2429-2433.
264. C. Avila, G. Cimino, A. Crispino and A. Spinella, *Experientia*, 1991, **47**, 306-310.
265. A. Spinella, L. A. Alvarez, C. Avila and G. Cimino, *Tetrahedron Lett.*, 1994, **35**, 8665-8668.
266. M. Gavagnin, E. Mollo, G. Calado, S. Fahey, M. Ghiselin, J. Ortea and G. Cimino, *Chemoecology*, 2001, **11**, 131-136.
267. H. Gaspar, M. Gavagnin, G. Calado, F. Castelluccio, E. Mollo and G. Cimino, *Tetrahedron*, 2005, **61**, 11032-11037.
268. A. R. Duckworth and C. N. Battershill, *N. Z. J. Mar. Freshw. Res.*, 2001, **35**, 935-949.
269. World Register of Marine Species, *Aphelodoris luctuosa* (Cheeseman, 1882), https://www.marinespecies.org/aphia.php?p=taxdetails&id=599222, accessed on 29, November 2024.
270. K. Křenek, P. Marhol, Ž. Peikerová, V. Křen and D. Biedermann, *Food Res. Int.*, 2014, **65**, 115-120.

271. T. Turk, K. Sepčić, I. Mancini and G. Guella, *Stud. Nat. Prod. Chem.*, 2008, **35**, 355-397.
272. M. T. Davies-Coleman, D. J. Faulkner, G. M. Dubowchik, G. P. Roth, C. Polson and C. Fairchild, *J. Org. Chem.*, 1993, **58**, 5925-5930.
273. G.F. Pauli, *J. Med. Chem*, http://pubs.acs.org/doi/full/10.1021/jm500734a, 2014.
274. F. J. Schmitz, K. H. Hollenbeak and D. C. Campbell, *J. Org. Chem.*, 1978, **43**, 3916-3922.
275. G. Schmidt, C. Timm and M. Köck, *Z. Naturforsch. B*, 2011, **66**, 745-748.
276. N. Oku, K. Nagai, N. Shindoh, Y. Terada, R. W. Van Soest, S. Matsunaga and N. Fusetani, *Bioorg. Med. Chem. Lett.*, 2004, **14**, 2617-2620.
277. N. Fusetani, N. Asai, S. Matsunaga, K. Honda and K. Yasumuro, *Tetrahedron Lett.*, 1994, **35**, 3967-3970.
278. J. H. H. L. de Oliveira, A. Grube, M. Köck, R. G. S. Berlinck, M. L. Macedo, A. G. Ferreira and E. Hajdu, *J. Nat. Prod.*, 2004, **67**, 1685-1689.
279. D. B. Stierle and D. J. Faulkner, *J. Nat. Prod.*, 1991, **54**, 1134-1136.
280. S. Sakemi, L. E. Totton and H. H. Sun, *J. Nat. Prod.*, 1990, **53**, 995-999.
281. R. Talpir, A. Rudi, M. Ilan and Y. Kashman, *Tetrahedron Lett.*, 1992, **33**, 3033-3034.
282. C. A. Volk and M. Köck, *Org. Lett.*, 2003, **5**, 3567-3569.
283. C. A. Volk and M. Köck, *Org. Biomol. Chem.*, 2004, **2**, 1827-1830.
284. C. A. Volk, H. Lippert, E. Lichte and M. Köck, *Eur. J. Org. Chem.*, 2004, **2004**, 3154-3158.
285. C. Cychon, G. Schmidt, T. Mordhorst and M. Köck, *Z. Naturforsch. B*, 2012, **67**, 944-950.
286. C. Timm, C. Volk, F. Sasse and M. Köck, *Org. Biomol. Chem.*, 2008, **6**, 4036-4040.
287. T. Teruya, K. Kobayashi, K. Suenaga and H. Kigoshi, *J. Nat. Prod.*, 2006, **69**, 135-137.
288. V. Damodaran, J. L. Ryan and R. A. Keyzers, *J. Nat. Prod.*, 2013, **76**, 1997-2001.
289. S. Albrizio, P. Ciminiello, E. Fattorusso, S. Magno and J. R. Pawlik, *J. Nat. Prod.*, 1995, **58**, 647-652.
290. K. Sepčić, G. Guella, I. Mancini, F. Pietra, M. D. Serra, G. Menestrina, K. Tubbs, P. Macek and T. Turk, *J. Nat. Prod.*, 1997, **60**, 991-996.
291. S. P. McCormack, Master of Science thesis, The University of Waikato, 2015.
292. M. Łukowiak, *PeerJ*, 2020, **8**, e10601.
293. B. E. Picton and C. C. Morrow, *Nudibranchs of the British Isles*, Immel Publishing, http://www.seaslug.org.uk/nudibranchs/index.html, 1994.
294. R. A. Hoover, R. Armour, I. Dow and J. E. Purcell, *Hydrobiologia*, 2012, **690**, 199-213.
295. R. Ritson-Williams, S. S. Sonia and V. J. Paul, *Mar. Ecol. Prog. Ser.*, 2003, **255**, 207-218.
296. S. J. Hall, C. D. Todd and A. D. Gordon, *J. Anim. Ecol.*, 1982, **51**, 907-921.
297. K. Iken, C. Avila, A. Fontana and M. Gavagnin, *Mar. Biol.*, 2002, **141**, 101-109.
298. C. A. Avila, *J. Molluscan Stud.*, 1998, **64**, 215-222.
299. R. A. Hoover, R. Armour, I. Dow and J. E. Purcell, *Hydrobiologia*, 2012, **690**, 199-213.
300. S. J. Hall, C. D. Todd and A. D. Gordon, *J. Anim. Ecol.*, 1982, **51**, 907-921.
301. S. Gemballa and F. Schermutzki, *Mar. Biol.*, 2004, **144**, 1213-1222.
302. J. W. F. Chu and S. P. Leys, *Invertebr. Biol.*, 2012, **131**, 75-81.
303. C. Megina, J. L. Carballo, J. L. Cervera and J. García, *J. Molluscan Stud.*, 2002, **68**, 173-179.
304. T. Belmonte, J. Alvim, V. Padula and G. Muricy, *Spixiana*, 2015, **38**, 187-195.
305. B. K. Penney, *J. Molluscan Stud.*, 2013, **79**, 64-73.
306. S. K. F. Yiu and J.-W. Qiu, *Reg. Stud. Mar. Sci.*, 2023, **61**, 102858.
307. M. C. Pratt and E. W. Grason, *Biol. Invasions*, 2007, **9**, 645-655.

308. World Register of Marine Species, *Austrodoris kerguelenensis* (Bergh, 1884), https://www.marinespecies.org/aphia.php?p=taxdetails&id=197053, accessed on 29, October 2024.
309. P. L. Munday, D. L. Dixson, J. M. Donelson, G. P. Jones, M. S. Pratchett, G. V. Devitsina and K. B. Døving, *Proc. Natl. Acad. Sci. U. S. A.*, 2009, **106**, 1848-1852.
310. R. K. Zimmer-Faust, P. B. O'Neill and D. W. Schar, *Biol. Bull.*, 1996, **190**, 82-87.
311. R. Zitoun, S. D. Connell, C. E. Cornwall, K. I. Currie, K. Fabricius, L. J. Hoffmann, M. D. Lamare, J. Murdoch, S. Noonan, S. G. Sander, M. A. Sewell, N. T. Shears, C. M. G. van den Berg and A. M. Smith, *Marine and Freshwater Research*, 2020, **71**, 321-344.
312. M. Miller, *J. Molluscan Stud.*, 2001, **67**, 491-499.
313. M. C. Miller, Poirieria (Conchology Section Auckland Institute & Museum), 1967, vol. 3(1), pp. 1-11.
314. P. R. Bergquist, *N.Z. Oceanogr. Inst. Mem.*, 1996, **107**, 1-53.
315. L. Gris, C. N. Battershill and M. R. Prinsep, *J. Chem. Ecol.*, 2023, **49**, 599-610.
316. World Register of Marine Species, *Chromodoris aureomarginata* (Cheeseman, 1881), https://www.marinespecies.org/aphia.php?p=taxdetails&id=558429, accessed on 9 October, 2024.
317. L. Forster, PhD thesis, The University of Queensland, 2020.
318. X.-R. Tian, H.-F. Tang, Y.-S. Li, H.-W. Lin, X.-P. Fan, J.-T. Feng and X. Zhang, *Phytochem. Lett.*, 2014, **9**, 1-6.
319. G. R. Pettit, J. F. Day, J. L. Hartwell and H. B. Wood, *Nature*, 1970, **227**, 962-963.
320. G. R. Pettit, C. L. Herald, D. L. Doubek, D. L. Herald, E. Arnold and J. Clardy, *J. Am. Chem. Soc.*, 1982, **104**, 6846-6848.
321. D. L. Alkon, M.-K. Sun, A. J. Tuchman and R. E. Thompson, *J. Alzheimer's Dis.*, 2023, **96**, 759-766.
322. A. E. Trindade-Silva, G. E. Lim-Fong, K. H. Sharp and M. G. Haygood, *Curr. Opin. Biotechnol.*, 2010, **21**, 834-842.
323. G. R. Pettit, C. L. Herald, Y. Kamano, D. Gust and R. Aoyagi, *J. Nat. Prod.*, 1983, **46**, 528-531.
324. D. E. Schaufelberger, G. N. Chmurny, J. A. Beutler, M. P. Koleck, A. B. Alvarado, B. W. Schaufelberger and G. M. Muschik, *J. Org. Chem.*, 1991, **56**, 2895-2900.
325. G. N. Chmurny, M. P. Koleck and B. D. Hilton, *J. Org. Chem.*, 1992, **57**, 5260-5264.
326. G. R. Pettit, Y. Kamano, C. L. Herald and M. Tozawa, *J. Am. Chem. Soc.*, 1984, **106**, 6768-6771.
327. G. R. Pettit, J. E. Leet, C. L. Herald, Y. Kamano, F. E. Boettner, L. Baczynskyj and R. A. Nieman, *J. Org. Chem.*, 1987, **52**, 2854-2860.
328. G. Pettit, F. Gao, D. Sengupta, J. Coll, C. Herald, D. Doubek, J. Schmidt, J. Van Camp, J. Rudloe and R. Nieman, *Tetrahedron*, 1991, **47**, 3601-3610.
329. G. R. Pettit, Y. Kamano and C. L. Herald, *J. Org. Chem.*, 1987, **52**, 2848-2854.
330. G. R. Pettit, F. Gao, P. M. Blumberg, C. L. Herald, J. C. Coll, Y. Kamano, N. E. Lewin, J. M. Schmidt and J.-C. Chapuis, *J. Nat. Prod.*, 1996, **59**, 286-289.
331. N. Lopanik, K. R. Gustafson and N. Lindquist, *J. Nat. Prod.*, 2004, **67**, 1412-1414.
332. H.-B. Yu, F. Yang, Y.-Y. Li, J.-H. Gan, W.-H. Jiao and H.-W. Lin, *J. Nat. Prod.*, 2015, **78**, 1169-1173.
333. G. R. Pettit, Y. Kamano and C. L. Herald, *J. Nat. Prod.*, 1986, **49**, 661-664.
334. B.-F. Ruan and H.-L. Zhu, *Curr. Med. Chem.*, 2012, **19**, 2652-2664.

335. X.-R. Tian, H.-F. Tang, Y.-S. Li, H.-W. Lin, N. Ma, W. Zhang and M.-N. Yao, *J. Asian Nat. Prod. Res.*, 2009, **11**, 1005-1012.
336. X.-R. Tian, H.-F. Tang, J.-T. Feng, Y.-S. Li, H.-W. Lin, X.-P. Fan and X. Zhang, *Mar. Drugs*, 2014, **12**, 1987-2003.
337. F. Farokhi, G. Wielgosz-Collin, M. Clement, J.-M. Kornprobst and G. Barnathan, *Mar. Drugs*, 2010, **8**, 2988-2998.
338. K. Chebaane and U. Guyot, *Tetrahedron Lett.*, 1986, **27**, 1495-1496.
339. J. G. L. Almeida, A. I. V. Maia, D. V. Wilke, E. R. Silveira, R. Braz-Filho, J. J. La Clair, L. V. Costa-Lotufo and O. D. L. Pessoa, *Mar. Drugs*, 2012, **10**, 2846-2860.
340. T. Hattori, K. Adachi and Y. Shizuri, *J. Nat. Prod.*, 1998, **61**, 823-826.
341. U. Anthoni, C. Larsen, P. H. Nielsen, C. Christophersen and G. Lidgren, *Comp Biochem Physiol B Biochem Mol Biol.*, 1989, **92**, 711-713.
342. E. Berdyshev, O. Getmanova, V. Svetashev and A. Kubanin, *Comp Biochem Physiol B Biochem Mol Biol.*, 1992, **102**, 639-641.
343. F. Yang, H.-J. Zhang, J.-T. Chen, H.-F. Tang, S.-J. Piao, W.-S. Chen and H.-W. Lin, *Nat. Prod. Res.*, 2011, **25**, 1505-1511.
344. R. G. Kerr, R. Vicchiarelli and S. S. Kerr, *J. Nat. Prod.*, 1999, **62**, 468-470.
345. World Register of Marine Species, *Polycera* (Cuvier, 1816), https://www.marinespecies.org/aphia.php?p=taxdetails&id=138369,
346. M. Carbone, A. Herrero-Barrencua, M. L. Ciavatta, J. J. Castro, J. L. Cervera and M. Gavagnin, *Biochem. Syst. Ecol.*, 2019, **83**, 62-65.
347. G. E. Lim, PhD thesis, University of California, San Diego, 2004.
348. S. K. Davidson, PhD thesis, University of California, San Diego, 1999.
349. K. Gustafson and R. J. Andersen, *J. Org. Chem.*, 1982, **47**, 2167-2169.
350. E. I. Graziani, PhD thesis, The Univeristy of British Columbia, 1996.
351. E. I. Graziani and R. J. Andersen, *Chem. Commun.*, 1996, 2377-2378.
352. M. R. Prinsep, unpublished work.
353. N. Fathallah, A. Tamer, R. Ibrahim, M. kamal and M. E. Kes, *Futur. J. Pharm. Sci.*, 2023, **9**, 98.
354. M. F. Mehbub, M. V. Perkins, W. Zhang and C. M. M. Franco, *Biotechnology Advances*, 2016, **34**, 473-491.
355. M. S. Agrawal and B. F. Bowden, *Marine Drugs*, 2005, **3**, 9-14.
356. M. D. Unson, C. B. Rose, D. J. Faulkner, L. S. Brinen, J. R. Steiner and J. Clardy, *The Journal of Organic Chemistry*, 1993, **58**, 6336-6343.
357. A. Casapullo, L. Minale, F. Zollo, C. Roussakis and J. F. Verbist, *Tetrahedron letters*, 1995, **36**, 2669-2672.
358. W.-H. Jiao, B.-H. Cheng, G.-D. Chen, G.-H. Shi, J. Li, T.-Y. Hu and H.-W. Lin, *Organic letters*, 2018, **20**, 3092-3095.
359. C. E. McNamara, L. Larsen, N. B. Perry, J. L. Harper, M. V. Berridge, E. W. Chia, M. Kelly and V. L. Webb, *Journal of Natural Products*, 2005, **68**, 1431-1433.
360. R. Sakai, K. Suzuki, K. Shimamoto and H. Kamiya, *The Journal of organic chemistry*, 2004, **69**, 1180-1185.
361. W.-H. Jiao, X.-J. Huang, J.-S. Yang, F. Yang, S.-J. Piao, H. Gao, J. Li, W.-C. Ye, X.-S. Yao and W.-S. Chen, *Organic letters*, 2012, **14**, 202-205.
362. T. F. Molinski and C. M. Ireland, *The Journal of Organic Chemistry*, 1988, **53**, 2103-2105.
363. C. E. Salomon, D. H. Williams and D. J. Faulkner, *Journal of natural products*, 1995, **58**, 1463-1466.

364. R. Hinde, F. Pironet and M. A. Borowitzka, *Mar. Biol.*, 1994, **119**, 99-104.
365. R. W. Thacker and S. Starnes, *Mar. Biol.*, 2003, **142**, 643-648.
366. A. Gauvin, J. Smadja, M. Aknin, R. Faure and E. Gaydou, *Can. J. Chem.*, 2000, **78**, 986-992.
367. Y. Sera, K. Adachi and Y. Shizuri, *J. Nat. Prod.*, 1999, **62**, 152-154.
368. B. Mun, W. Wang, H. Kim, D. Hahn, I. Yang, D. H. Won, E.-H. Kim, J. Lee, C. Han, H. Kim, M. Ekins, S.-J. Nam, H. Choi and H. Kang, *Arch. Pharmacal Res*, 2015, **38**, 18-25.
369. M. B. Ksebati and F. J. Schmitz, *J. Nat. Prod.*, 1988, **51**, 857-861.
370. E. Mollo, M. Gavagnin, M. Carbone, Y.-W. Guo and G. Cimino, *Chemoecology*, 2005, **15**, 31-36.
371. R. Kazlauskas, P. Murphy, R. Wells, J. Daly and P. Schönholzer, *Tetrahedron Lett.*, 1978, **19**, 4951-4954.
372. R. Dunlop, R. Kazlauskas, G. March, P. Murphy and R. Wells, *Aust. J. Chem.*, 1982, **35**, 95-103.
373. R. J. Capon and J. K. MacLeod, *J. Nat. Prod.*, 1987, **50**, 1136-1137.
374. M. R. Prinsep, unpublished work.
375. W. B. Rudman, *Zool. J. Linn. Soc.*, 1988, **93**, 133-185.
376. R. Cambie, P. Craw, P. R. Bergquist and P. Karuso, *J. Nat. Prod.*, 1987, **50**, 948-949.
377. M. Kernan, R. Cambie and P. R. Bergquist, *J. Nat. Prod.*, 1990, **53**, 724-727.
378. A. Rudi, Y. Erez, Y. Benayahu and Y. Kashman, *Tetrahedron Lett.*, 2005, **46**, 8613-8616.
379. A. Sato, T. Morishita, T. Shiraki, S. Yoshioka, H. Horikoshi, H. Kuwano, H. Hanzawa and T. Hata, *J. Org. Chem.*, 1993, **58**, 7632-7634.
380. N. Tran, J. Hooper and R. Capon, *Aust. J. Chem.*, 1995, **48**, 1757-1760.
381. M. Tsuda, Y. Takahashi, J. Fromont, Y. Mikami and J. Kobayashi, *J. Nat. Prod.*, 2005, **68**, 1277-1278.
382. K. Warabi, S. Matsunanga, R. W. M Van Soest and N. Fusetani, *J. Org. Chem.*, 2003, **68**, 2765-2770.
383. R. Cambie, P. R. Bergquist and P. Karuso, *J. Nat. Prod.*, 1988, **51**, 1014-1016.
384. C. P. Ridley, M. V. R. Reddy, G. Rocha, F. D. Bushman and D. J. Faulkner, *Biorg. Med. Chem.*, 2002, **10**, 3285-3290.
385. W. Y. Yoshida, K. K. Lee, A. R. Carroll and P. J. Scheuer, *Helv. Chim. Acta*, 1992, **75**, 1721-1725.
386. A. Rudi, I. Goldberg, Z. Stein, F. Frolow, Y. Benayahu, M. Schleyer and Y. Kashman, *J. Org. Chem.*, 1994, **59**, 999-1003.
387. A. Rudi, T. Evan, M. Aknin and Y. Kashman, *J. Nat. Prod.*, 2000, **63**, 832-833.
388. J. A. Palermo, M. F. Rodríguez Brasco and A. M. Seldes, *Tetrahedron*, 1996, **52**, 2727-2734.
389. A. R. Carroll, P. C. Healy, R. J. Quinn and C. J. Tranter, *J. Org. Chem.*, 1999, **64**, 2680-2682.
390. H. Zhang, M. M. Conte, Z. Khalil, X.-C. Huang and R. J. Capon, *RSC Advances*, 2012, **2**, 4209-4214.
391. J. M. Ryan, PhD thesis, Te Herenga Waka-Victoria University of Wellington, 2007.
392. U. Kang, L. K. Cartner, D. Wang, C.-K. Kim, C. L. Thomas, G. M. Woldemichael, B. E. Gryder, J. F. Shern, J. Khan, C. Castello-Branco, E. C. Sherer, X. Wang, E. L. Regalado and K. R. Gustafson, *J. Nat. Prod.*, 2020, **83**, 3464-3470.
393. H. Zhang, M. M. Conte, X.-C. Huang, Z. Khalil and R. J. Capon, *Org. Biomol. Chem.*, 2012, **10**, 2656-2663.

394. N. Lindquist, W. Fenical, G. D. Van Duyne and J. Clardy, *J. Org. Chem.*, 1988, **53**, 4570-4574.
395. R. A. Davis, A. R. Carroll, G. K. Pierens and R. J. Quinn, *J. Nat. Prod.*, 1999, **62**, 419-424.
396. A. Carroll, B. Bowden and J. Coll, *Aust. J. Chem.*, 1993, **46**, 489-501.
397. S. Malla Reddy, M. Srinivasulu, N. Satyanarayana, A. K. Kondapi and Y. Venkateswarlu, *Tetrahedron*, 2005, **61**, 9242-9247.
398. S. Urban, M. Butler and R. Capon, *Aust. J. Chem.*, 1994, **47**, 1919-1924.
399. S. Urban, L. Hobbs, J. Hooper and R. Capon, *Aust. J. Chem.*, 1995, **48**, 1491-1494.
400. D. Pla, F. Albericio and M. Alvarez, *Anticancer Agents Med. Chem.*, 2008, **8**, 746-760.
401. L. C. Forster, A. M. White, K. L. Cheney and M. J. Garson, *Nat. Prod. Commun.*, 2018, **13**, 1934578X1801300.
402. L. C. Forster, A. E. Winters, K. L. Cheney, P. Dewapriya, R. J. Capon and M. J. Garson, *J. Nat. Prod.*, 2017, **80**, 670-675.
403. A. M. White, A. S. Dewi, K. L. Cheney, A. E. Winters, J. T. Blanchfield and M. J. Garson, *Nat. Prod. Commun.*, 2016, **11**, 921-924.
404. A. M. White, G. K. Pierens, L. C. Forster, A. E. Winters, K. L. Cheney and M. J. Garson, *J. Nat. Prod.*, 2016, **79**, 477-483.
405. A. E. Winters, A. M. White, K. L. Cheney and M. J. Garson, *J. Molluscan Stud.*, 2019, **85**, 133-142.
406. World Register of Marine Species, *Chromodoris obsoleta* (Rüppell & Leuckart, 1831), **https://www.marinespecies.org/aphia.php?p=taxdetails&id=559924**, accessed on 4, November 2024.
407. World Register of Marine Species, *Chromodoris albopunctata* (Garrett, 1879), **https://www.marinespecies.org/aphia.php?p=taxdetails&id=559920**,
408. World Register of Marine Species, *Chromodoris cavae* (Eliot, 1904), **https://www.marinespecies.org/aphia.php?p=taxdetails&id=209590**, accessed on 4, November 2024.
409. World Register of Marine Species, *Chromodoris geminus* (Rudman, 1987), **https://www.marinespecies.org/aphia.php?p=taxdetails&id=209585**, accessed on 8 November, 2024.
410. World Register of Marine Species, *Chromodoris gleniei* (Kelaart, 1858), **https://www.marinespecies.org/aphia.php?p=taxdetails&id=209595**, accessed on November, 9 2024.
411. World Register of Marine Species, *Chromodoris annulata* (Eliot, 1904), **https://www.marinespecies.org/aphia.php?p=taxdetails&id=209592**, accessed on November, 9 2024.
412. E. J. Dumdei, E. D. De Silva, R. J. Andersen, M. I. Choudhary and J. Clardy, *J. Am. Chem. Soc.*, 1989, **111**, 2712-2713.
413. P. L. Katavic, P. Jumaryatno, J. N. A. Hooper, J. T. Blanchfield and M. J. Garson, *Australian Journal of Chemistry*, 2012, **65**, 531.
414. E. D. De Silva, S. A. Morris, S. Miao, E. Dumdei and R. J. Andersen, *J. Nat. Prod.*, 1991, **54**, 993-997.
415. L. C. Forster, G. K. Pierens, A. M. White, K. L. Cheney, P. Dewapriya, R. J. Capon and M. J. Garson, *ACS Omega*, 2017, **2**, 2672-2677.
416. A. E. Winters, N. F. Green, N. G. Wilson, M. J. How, M. J. Garson, N. J. Marshall and K. L. Cheney, *Proc. R. Soc. B: Biol. Sci.*, 2017, **284**, 20170926.

417. Y. Hirayama, P. L. Katavic, A. M. White, G. K. Pierens, L. K. Lambert, A. E. Winters, H. Kigoshi, M. Kita and M. J. Garson, *Aust. J. Chem.*, 2016, **69**, 136.
418. T. Miyamoto, K. Sakamoto, K. Arao, T. Komori, R. Higuchi and T. Sasaki, *Tetrahedron*, 1996, **52**, 8187-8198.
419. L. C. Forster, J. K. Clegg, K. L. Cheney and M. J. Garson, *Mar. Drugs*, 2021, **19**, 680.
420. A. S. Dewi, G. K. Pierens, K. L. Cheney, J. T. Blanchfield and M. J. Garson, *Aust. J. Chem.*, 2018, **71**, 798-803.
421. L. C. Forster, G. K. Pierens, J. K. Clegg and M. J. Garson, *J. Nat. Prod.*, 2020, **83**, 714-719.
422. L. C. Forster, G. K. Pierens and M. J. Garson, *J. Nat. Prod.*, 2019, **82**, 449-455.
423. L. Mayol, V. Piccialli and D. Sica, *Tetrahedron Lett.*, 1985, **26**, 1357-1360.
424. B. C. M. Potts, D. J. Faulkner and R. S. Jacobs, *J. Nat. Prod.*, 1992, **55**, 1701-1717.
425. P. R. Bergquist and S. C. de Cook, in *Systema Porifera: A Guide to the Classification of Sponges*, eds. J. N. A. Hooper, R. W. M. Van Soest and P. Willenz, Springer US, Boston, MA, 2002, pp. 1072-1076.
426. M. M. K. Kumar, J. Devilal Naik, K. Satyavathi, H. Ramana, P. Raghuveer Varma, K. Purna Nagasree, D. Smitha and D. Venkata Rao, *Nat. Prod. Res.*, 2014, **28**, 888-894.
427. M. Karak, T. Oishi and K. Torikai, *Tetrahedron Lett.*, 2018, **59**, 2800-2803.
428. Y. Chen, P. Lan and M. G. Banwell, *Org. Lett.*, 2022, **24**, 2931-2934.
429. G. P. Gardini, in *Adv. Heterocycl. Chem.*, eds. A. R. Katritzky and A. J. Boulton, Academic Press, 1973, vol. 15, pp. 67-98.
430. V. Ji Ram, A. Sethi, M. Nath and R. Pratap, in *The Chemistry of Heterocycles*, eds. V. Ji Ram, A. Sethi, M. Nath and R. Pratap, Elsevier, 2019, pp. 149-478.
431. H. Kotoučová, I. Strnadová, M. Kovandová, J. Chudoba, H. Dvořáková and R. Cibulka, *Org. Biomol. Chem.*, 2014, **12**, 2137-2142.
432. M. Tsuda, K. Nozawa, K. Shimbo and J. Kobayashi, *J. Nat. Prod.*, 2003, **66**, 292-294.
433. J. Kobayashi, J.-F. Cheng, Y. Kikuchi, M. Ishibashi, S. Yamamura, Y. Ohizumi, T. Ohtac and S. Nozoec, *Tetrahedron Lett.*, 1990, **31**, 4617-4620.
434. R. A. Davis, L. V. Christensen, A. D. Richardson, R. M. Da Rocha and C. M. Ireland, *Mar. Drugs*, 2003, **1**, 27-33.
435. H. Kang and W. Fenical, *J. Org. Chem.*, 1997, **62**, 3254-3262.
436. G. W. Chan, T. Francis, D. R. Thureen, P. H. Offen, N. J. Pierce, J. W. Westley, R. K. Johnson and D. J. Faulkner, *J. Org. Chem.*, 1993, **58**, 2544-2546.
437. G. Fan, Z. Li, S. Shen, Y. Zeng, Y. Yang, M. Xu, T. Bruhn, H. Bruhn, J. Morschhäuser, G. Bringmann and W. Lin, *Biorg. Med. Chem.*, 2010, **18**, 5466-5474.
438. A. T. Wang, M. R. Prinsep and R. D. Martinus, *SpringerPlus*, 2016, **5**, 742.